Universidad Autónoma de Madrid

Departamento de Bioquímica

Identificación y análisis de nuevas dianas celulares con efecto neurogénico y neuroprotector

Tesis Doctoral

José Ángel Morales García

Madrid, 2011

Departamento de Bioquímica
Facultad de Medicina
Universidad Autónoma de Madrid

Identificación y análisis de nuevas dianas celulares con efecto neurogénico y neuroprotector

José Ángel Morales García

Licenciado en Biología

Directores de Tesis: Dra. Ana María Pérez Castillo
Dr. Ángel Santos Montes

Instituto de Investigaciones Biomédicas de Madrid "Alberto Sols"
CSIC-UAM

MINISTERIO
DE CIENCIA E
INNOVACIÓN

CSIC

UAM UNIVERSIDAD AUTONOMA DE MADRID

INSTITUTO DE INVESTIGACIONES BIOMÉDICAS
"ALBERTO SOLS"

Ana María Pérez Castillo, Profesora de Investigación del Consejo Superior de Investigaciones Científicas adscrito al Instituto de Investigaciones Biomédicas "Alberto Sols" de Madrid y **Ángel Santos Montes**, Catedrático del Departamento de Bioquímica y Biología Molecular III de la Universidad Complutense de Madrid, certifican que:

José Ángel Morales García, Licenciado en Biología por la Universidad Complutense de Madrid, ha realizado su Tesis Doctoral titulada **"Identificación y análisis de nuevas dianas celulares con efecto neurogénico y neuroprotector"** bajo nuestra dirección, en el Instituto de Investigaciones Biomédicas "Alberto Sols" (CSIC-UAM).

Consideramos que la presente Tesis Doctoral reúne las condiciones de originalidad y rigor necesarios y se encuentra en condiciones de ser presentada y defendida públicamente para optar al grado de Doctor.

Y para que conste donde proceda, firmamos la presente autorización en Madrid a 15 de Abril de dos mil once.

Dra. Ana Mª Pérez Castillo
Directora de la Tesis
Profesora de Investigación, CSIC
CiberNED

Dr. Ángel Santos Montes
Director de la Tesis
Catedrático, UCM

Vº Bº Dr. Jaime Renart Pita
Tutor de la Tesis
Profesor Honorario del Dpto. de Bioquímica
Universidad Autónoma de Madrid

Agradecimientos

Toda mi gratitud y admiración a la Dra. Ana Pérez Castillo y al Dr. Angel Santos Montes por la fabulosa dirección de esta tesis, por su asesoramiento, por su paciencia y por todo lo que me han enseñado sobre ciencia y sobre la vida.

Mi mas sincero agradecimiento al Ministerio de Ciencia e Innovación, al programa Innocash, a Noscira, a Araclon, asi como al Centro de Investigación Biomédica en Red de Enfermedades Neurodegenerativas (CIBERned) por la financiación que ha hecho posible la realización de esta tesis.

Gracias a todo el laboratorio 1.9, por su ayuda científica y personal.

Muchísimas gracias al Dr. Jaime Renart, por tutorizar este trabajo y también a todo el personal del Instituto de Investigaciones Biomédicas A. Sols, por su calidad humana y por hacernos la vida un poco más facil.

Por supuesto a mi familia y amigos por su apoyo emocional.

Gracias a TODOS por TODO.

Resumen

En este trabajo hemos analizado, mediante el uso de inhibidores y activadores específicos, el papel del receptor de proliferadores peroxisomales gamma (PPARγ) y la glucogeno sintasa quinasa-3beta (GSK-3β) en neurogenesis en animales adultos, y el papel de los canales de calcio dependientes de voltaje (CCSV) tipo no-L y la fosfodiesterasa 7 (PDE7) en neuroprotección.

Nuestros resultados muestran claramente que los ligandos de PPARγ, pioglitazona y rosiglitazona, estimulan la proliferación, diferenciación y migración de las células madre neurales *in vitro.* De acuerdo con los resultados observados *in vitro*, ratas adultas tratadas con pioglitazona presentan un aumento en la proliferación de células progenitoras en la zona subventricular de los ventrículos laterales y en la corriente migratoria rostral. Análisis por microscopía electrónica muestran también cambios importantes en la ultraestructura de la zona subventricular en los animales tratados con pioglitazona, incluyendo un aumento en el número de cadenas migratorias. Por otra parte, la inhibición de GSK-3β induce neurogénesis *in vivo* en la zona subgranular del giro dentado del hipocampo. Estudios in vitro con cultivos de neuroesferas demuestran que la inhibición de GSK-3β aumenta la proliferación y migración de las células madre neurales. Esta inhibición tiene también como resultado un aumento en el número de células con un fenotipo neuronal. Estos resultados sugieren que ambas dianas podrían jugar un papel importante en la expansión y diferenciación de las poblaciones de células madres en el cerebro adulto con el consiguiente interés terapéutico de cara a la reparación del daño neurológico.

Con respecto a la neuroprotección, nuestros resultados muestran claramente que el nuevo inhibidor de CCSV tipo no-L, NP04634, tiene un potente efecto anticonvulsivo, antiinflamatorio y neuroprotector en un modelo de daño excitotóxico inducido por kainato en hipocampo. La administración por vía oral de NP04634 redujo el porcentaje de ratas que entraron en *status epilepticus* tras una inyección con kainato, aumentando además la latencia de entrada en dicho *status* y reduciendo la mortalidad en aquellas ratas que finalmente adquirieron dicho estado. El compuesto NP04634 previno además la pérdida neuronal en las capas CA1 y CA3 del hipocampo y redujo la activación glial inducida por kainato. Finalmente, nuestros resultados muestran que inhibidores de PDE7 protegen las neuronas dopaminérgicas y reducen la neuroinflamación *in vitro* frente al daño inducido por ácido kaínico y 6-OHDA. De acuerdo con estos resultados, el tratamiento de ratas adultas con los inhibidores de PDE 7, S14 y BRL50481, disminuyó significtivamente la neurodegeneración dopaminérgica inducida por lipopolisacárido bacteriano y mejoró la función motora de los animales. Estos resultados sugieren que ambas dianas juegan un papel importante en neuroprotección y que por tanto podrían ser relevantes para el desarrollo de nuevas estrategias terapéuticas en procesos neurodegenerativos.

Abstract

This work has analyzed, using specific ligands and inhibitor drugs, the role of the Peroxisome proliferator-activated receptor gamma (PPARγ) and Glycogen synthase kinase 3 beta (GSK-3β) in adult neurogenesis, and the role of non L-type voltage sensitive calcium channel (VSCC) and phosphodiesterase-7 (PDE7) in neuroprotection.

Here we show a novel function for the nuclear receptor PPARγ in controlling stem cell expansion in the adult mammalian brain. We demonstrate that ligands of PPARγ, pioglitazone and rosiglitazone, induce proliferation, differentiation and migration of the neural stem cells *in vitro*. According with these results, adult rats treated with pioglitazone have elevated numbers of proliferating progenitor cells in the subventricular zone and the rostral migratory stream. Electron microscopy analysis also showed important changes in the subventricular zone ultrastructure of pioglitazone-treated animals including an increased number of migratory cell chains. Also, inhibition of the enzyme GSK-3β induces neurogenesis in the dentate gyrus of the hippocampus of adult rats. In addition, in vitro studies demonstrate that inhibition of GSK-3β induces proliferation, migration, and differentiation of neural stem cells towards a neuronal phenotype. These results suggest that PPARγ and GSK-3β could be play an important role in expansion and differentiation of the neural stem cells populations, what can represent a new promising strategy for restoring neurogenesis

Our results also show that intragastrical administration of NP04634, a novel non L-type VSCC inhibitor, could prevent the entrance in *status epilepticus* and the neuronal loss evoked by intraperitoneal injection of KA. Our results show that administration of NP04634 reduced the percentage of rats which entered SE after KA injection, increased the latency of SE entry, and significantly reduced the mortality of rats which entered *status epilepticus*. Also, NP04634 prevented the loss of hippocampal CA1 and CA3 pyramidal neurons and reduced the gliosis induced by KA. These results point to a potential anticonvulsant and neuroprotective role for NP04634. We have also demonstrated that inhibition of PDE7 enhances neurprotection and diminishes neuroinflammation in well-characterized cellular and animal models of Parkinson Disease. Treatment of adult rats with the blood brain barrier permeable PDE7 inhibitor named S14, significantly protects dopaminergic neurodegeneration and improves motor function in lipopolysaccharide-lesioned animals. We also show that S14 effects are mediated by the cAMP/PKA signaling pathway. As such, these findings identify PDE 7 as a potential new therapeutic target for the treatment of Parkinson disease.

Índice

Clave de Abreviaturas

6-OHDA	6-hidroxidopamina
BHE	**B**arrera **H**emato**E**ncefálica
BO	**B**ulbo **O**lfatorio
CCSV	**C**anal de **C**alcio **S**ensible a **V**oltaje
CMR	**C**orriente **M**igratoria **R**ostral
DAB	**D**i**A**mino**B**encidina
DCX	Doblecortina (**D**ouble**C**orte**X**)
DHP	**D**i**H**idro**P**iridina
DS	**D**esviación e**S**tándar
E	Día **E**mbrionario
EA	**E**nfermedad de **A**lzheimer
EP	**E**nfermedad de **P**arkinson
GFAP	Proteína ácida fibrilar glial (**G**lial **F**ibrillary **A**cidic **P**rotein)
KA	Kainato (**K**ainic **A**cid)
LDH	**L**actato **D**es**H**idrogenasa
MTT	3-[4,5-di**M**ethyl**T**hiazol-2-yl]-2,5-diphenyl **T**etrazoliumbromide
NS	**N**euroe**S**fera
P	Día **P**ostnatal
PDE	**P**hospho**D**i**E**sterasa
PF	**P**ara**F**ormaldehído
PGZ	**P**io**G**lita**Z**ona
PKA	Proteína Quinasa A (**P**rotein **K**inase **A**)
PLP	**P**otenciación a **L**argo **P**lazo
PPARγ	**P**eroxisome **P**roliferator-**A**ctivated **R**eceptor **G**amma
PSA-NCAM	Molécula de adhesion celular neural combinada con ácido polisiálico (**P**olysicalic **A**cid-**N**eural **C**ell **A**dhesion **M**olecule)
RGZ	**R**osi**G**lita**Z**ona
SE	**S**tatus **E**pilepticus
ES	**E**rror e**S**tadístico
SNC	**S**istema **N**ervioso **C**entral
SNpc	**S**ustancia **N**egra **p**arte **c**ompacta
TDZD	**T**ia**D**ia**Z**oli**D**inona
TH	**T**irosina **H**idroxilasa
ZSG	Zona subgranular
ZSV	Zona subventricular

Introducción

1.- NEUROGÉNESIS EN EL CEREBRO ADULTO.

En mamíferos la neurogénesis se produce fundamentalmente durante el periodo prenatal aunque también se ha demostrado que el cerebro adulto tiene la capacidad, aunque limitada, de generar nuevas neuronas. La capacidad neurogénica del sistema nervioso central (SNC) adulto, está restringida fundamentalmente a dos nichos neurogénicos: la zona subventricular (ZSV) de los ventrículos laterales y la zona subgranular (ZSG) del giro dentado (Gage, 2002; Luskin et al., 1997). La neurogénesis es un proceso complejo que implica múltiples actividades celulares incluyendo la proliferación de células madre neurales (progenitores), migración y diferenciación, supervivencia, adquisición de destino celular y maduración e integración de las nuevas neuronas formadas, procesos a su vez regulados por múltiples factores (Alvarez-Buylla and Lim, 2004; Zhao et al., 2008). El conocimiento detallado de estos factores y su mecanismo de acción, nos podría proveer de instrumentos que nos permitieran ampliar la limitada capacidad neurogénica del cerebro adulto y consecuentemente abrir nuevos campos para el desarrollo de terapias eficaces en el tratamiento del daño cerebral y de las enfermedades neurodegenerativas.

1.1.- Células madre neurales en el adulto.

Las células madre son células precursoras que se caracterizan por tener un ciclo celular de división lento, capacidad de autorrenovación a largo plazo y multipotencialidad, pudiendo dar lugar de manera constante a distintos tipos celulares (Drapeau and Nora Abrous, 2008; McKay, 1997; Seaberg and van der Kooy, 2002).

En el caso del SNC para que una célula pueda ser considerada célula madre debe tener el potencial de poder diferenciarse a neurona, glia u oligodendrocito, además de tener capacidad de autorrenovación (McKay, 1997). El factor de crecimiento epidérmico (EGF) y el factor de crecimiento de fibroblastos-2 (FGF-2), juegan un papel fundamental en la proliferación de estas células tanto *in vitro* como *in vivo* (Doetsch et al., 2002). Dicho papel es fácilmente observable *in vitro* ya que estos factores promueven la formación de neuroesferas (NS), que son agrupamientos de células madre neurales no diferenciadas que se pueden obtener a partir de las dos principales regiones neurogénicas en el adulto, la ZSV y la ZSG (Figura I). Las NS se forman cuando se crecen las células madre en suspensión, pudiéndose inducir su diferenciación mediante fijación de las mismas a un sustrato. En estas condiciones de cultivo, las células de la neurosfera migran y diferencian hacia los tres tipos celulares característicos del SNC: neuronas, células gliales y oligodendrocitos (Reynolds and Weiss, 1992). Por tanto, las NS constituyen un modelo excelente para el análisis de posibles factores que pudieran tener una incidencia sobre dichos procesos.

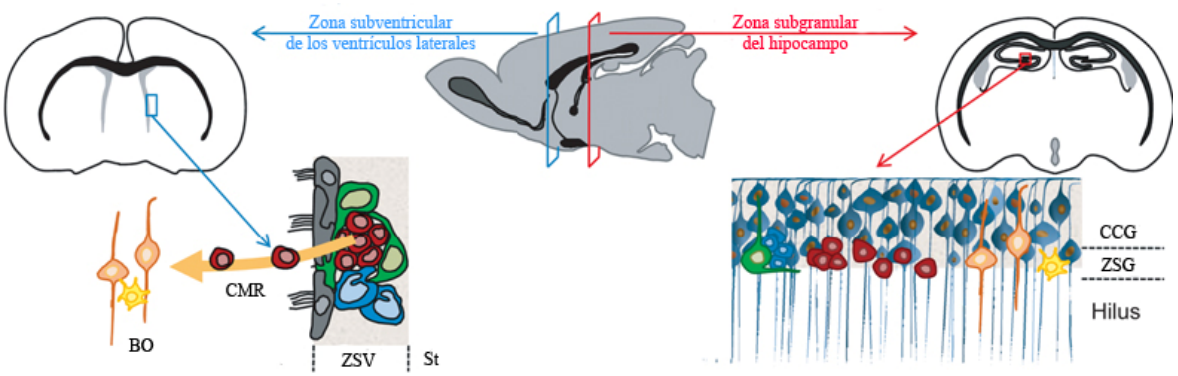

Figura I.- Esquema de los dos principales nichos neurogénicos del cerebro adulto: la zona subventricular de los ventrículos laterales (ZSV) y la zona subgranular del hipocampo (ZSG). BO, bulbo olfatorio; CCG, capa celular granular; CMR, corriente migratoria rostral; St, estriado.

1.2.-Zona subventricular (ZSV) de los ventrículos laterales.

La ZSV se localiza en la pared lateral de los ventrículos laterales, y constituye el mayor nicho neurogénico en el cerebro adulto. Las células madres neurales de la ZSV son capaces de generar nuevas neuronas que migran al bulbo olfatorio (BO) (Lois and Alvarez-Buylla, 1994; Luskin, 1993), aunque también se ha sugerido que podrían migrar a otras regiones del cerebro (Gould et al., 1999; Magavi et al., 2000). Además la ZSV también es fuente de células gliales (Goldman, 1995; Levison and Goldman, 1993; Nait-Oumesmar et al., 1999).

La ZSV se compone de distintos tipos celulares con una serie de características que hacen que sean fácilmente identificables mediante técnicas de microscopía electrónica (Figura II). Los astrocitos (células de tipo B), que *in vivo* funcionan como precursores neurales, se caracterizan por un soma de gran tamaño y por tener el citoplasma poco denso y rico en filamentos intermedios. Pueden ser de dos tipos: células tipo B1, que contactan con la cavidad ventricular y de tipo B2 localizadas basalmente entre el parénquima estriatal y las células tipo A (Doetsch et al., 1997). Las células tipo B2 se caracterizan por tener un contorno irregular, menor cantidad de ribosomas libres en su citoplasma y la cromatina mas compacta (Alonso et al., 2008; Doetsch et al., 1997). Las células B1 poseen un pequeño cilio primario orientado hacia la cavidad, responsable del control de la proliferación celular, y una expansión que contacta con los vasos sanguíneos (Han et al., 2008). Estas células tipo B1 dan lugar a progenitores neurales o células de tipo C, caracterizadas por tener un citoplasma muy denso, donde se diferencia claramente el aparato de Golgi, un núcleo irregular con invaginaciones, cromatina laxa y un gran nucleolo reticulado (Doetsch et al., 1997). Las células tipo C tienen una gran capacidad proliferativa, y se dividen simétricamente para dar lugar a neuroblastos con capacidad migradora (células de tipo A). Estas células A se identifican por su pequeño tamaño y por tener un núcleo denso y escaso citoplasma, características propias de células migradoras.

Doetsch y cols. (Doetsch et al., 1999) observaron que al eliminar las células de tipo A y C, éstas eran capaces de regenerase a partir de las células B, demostrando que las B efectivamente actuaban como células precursoras Además recientemente se ha descrito que las células de tipo B *in vivo* son capaces de dar lugar a oligodendrocitos que migran al cuerpo calloso (Gonzalez-Perez et al., 2009; Menn et al., 2006). Por su parte las células de tipo A (neuroblastos) migran ventralmente a través de la corriente migratoria rostral (CMR) hacia el BO para convertirse en interneuronas (Alvarez-Buylla and Garcia-Verdugo, 2002; Lois and Alvarez-Buylla, 1993; Lois and Alvarez-Buylla, 1994) lo cual es fundamental para el mantenimiento de la capacidad olfativa (So et al., 2008). Otro componente de la ZSV son las células de tipo E (células del epéndimo) que forman una monocapa epitelial que separa la ZSV de la cavidad del ventrículo. También se ha descrito que los vasos sanguíneos de la región tienen gran importancia neurogénica puesto que intervienen en la activación de los nichos neurogénicos (Shen et al., 2008).

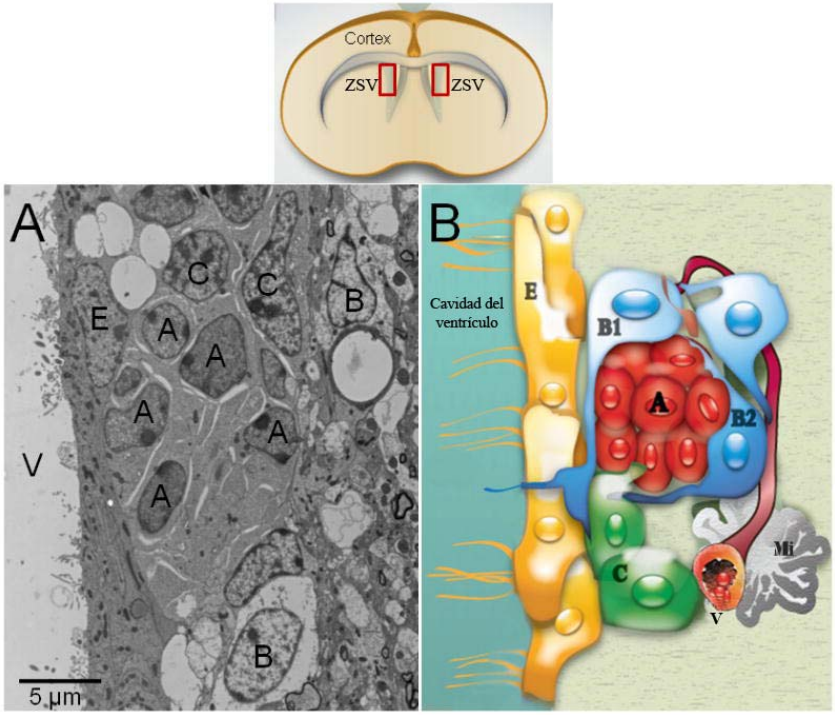

Figura II.- Nicho neurogénico de la zona subventricular (ZSV) en el cerebro adulto. A) Imagen de microscopía electrónica que muestra los distintos tipos celulares, células tipo A (neuroblastos migradores), células de tipo B (astrocitos), células de tipo C (progenitores neurales) y células de tipo E (células del epéndimo). B) Representación esquemática de la organización de la ZSV en el adulto, Mi, microglía; V, vaso sanguíneo. González-Pérez et al., 2009.

La corriente migratoria rostral (CMR) es la ruta a lo largo de la cual los neuroblastos migran desde la zona mas rostral del ventrículo lateral hacia el BO (Figura III), donde se diferencian a neuronas granulares y periglomerulares (Alvarez-Buylla and Lim, 2004; Lois and Alvarez-Buylla, 1994). Los neuroblastos en migración que forman cadenas migratorias hacia el

bulbo olfatorio, se caracterizan por tener una morfología alargada. Estas cadenas incluyen también células gliales que actúan como soporte direccional de los neuroblastos y evitan que se salgan prematuramente de la ruta de migración (Alvarez-Buylla et al., 2002). Que la migración de neuroblastos a los largo de la CMR se realice correctamente depende de múltiples proteínas entre las que se incluyen proteínas de adhesión y de la matriz extracelular. En concreto la forma polisialilada de la molécula de adhesión celular neural (PSA-NCAM), está implicada en el establecimiento de contactos entre los neuroblastos en migración y las células gliales que los soportan, y por tanto, juega un importante papel en la migración. Esta molécula esta presente en los neuroblastos en migración, pero no en otros tipos celulares de la CMR, por lo que se utiliza como marcador específico de neuroblastos en la CMR (Battista and Rutishauser, 2010; Bonfanti and Theodosis, 1994; Rousselot et al., 1995). Otras proteínas que se utilizan como marcadores de neuroblastos son la doblecortina (DCX), marcador endógeno para neuroblastos en división y neuronas inmaduras (Brown et al., 2003; Couillard-Despres et al., 2005) y β-tubulina, marcador de nuevas neuronas (Doetsch and Alvarez-Buylla, 1996).

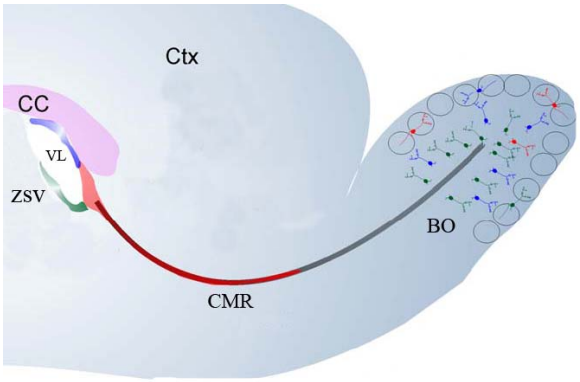

Figura III.- Esquema de la corriente migratoria rostral (CMR) que parte desde la zona subventricular (ZSV) hacia el bulbo olfatorio (BO). CC, cuerpo calloso; Ctx, corteza; VL, ventrículo lateral.

1.3.- Zona subgranular (ZSG) del hipocampo.

La ZSG del giro dentado del hipocampo es una región proliferativa rica en progenitores neuronales que dan lugar a neuronas granulares (Figura IV). Los progenitores de esta región son astrocitos radiales (células tipo B), que se localizan en la parte mas interna de la capa granular, junto al hilus. Estas células han demostrado tener *in vitro* propiedades multipotenciales (Seri et al., 2001; Song et al., 2002). *In vivo* parecen tener capacidad limitada de diferenciación, por lo que algunos autores consideran a las células tipo B como progenitores neuronales en lugar de células madre neurales del adulto. Estas células se dividen asimétricamente para dar lugar a células de tipo D que se diferencian localmente en neuronas granulares maduras. Parece ser que estas neuronas recién formadas están implicadas en procesos relacionados con la memoria, el aprendizaje o la depresión (Aimone et al., 2006). Las células D también expresan PSA-NCAM y

doblecortina, compartiendo similitudes con los neuroblastos de la ZSV (Seri et al., 2004; Seri et al., 2001).

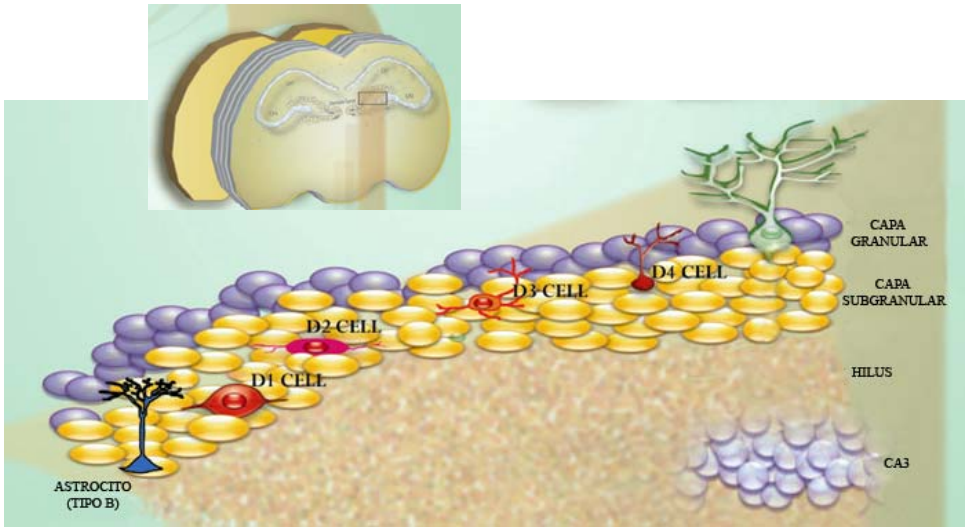

Figura IV.- Esquema de la zona subgranular en el hipocampo. Las células de tipo B (astrocitos) son progenitores primarios que dan lugar a progenitores intermediarios (células D1-D4) las cuales formaran neuronas granulares. González-Pérez et al., 2009.

Las neuronas granulares recién formadas solo migran una corta distancia para integrarse en la capa granular adyacente. A continuación extienden sus dendritas y axones, los cuales llegan hasta la capa CA3 del hipocampo (Zhao et al., 2006).

1.4.- Uso terapéutico de las células madre

Las células madre neurales podría ser de gran utilidad para la reparación del sistema nervioso central tras un daño traumático o enfermedad neurodegenerativa. Múltiples datos indican que la neurogénesis puede estimularse en situaciones de daño cerebral. Por ejemplo se ha descrito la presencia de marcardores neurogénicos en regiones que han sufrido isquemia (Carmichael, 2003; Jin et al., 2001; Zhang et al., 2004), epilepsia o daño traumático (Curtis et al., 2003; Liu et al., 1998; Parent et al., 1997). En ciertos modelos de enfermedades desmielinizantes se ha observado como los progenitores de la ZSV migran hacia aquellas regiones donde la desmielinización es mayor, y se diferencian a células gliales (Brundin et al., 2003; Picard-Riera et al., 2002)

No obstante existen trabajos que demuestran que en determinadas enfermedades neurodegenerativas, se da una disminución de la proliferación celular en las regiones neurogénicas. En modelos experimentales con ratones que reproducen características patológicas de la enfermedad de Alzheimer (EA), se ha descrito una pérdida de capacidad neurogénica en la ZSV (Regan et al., 2006). Esta disminución se observa también en cerebros postmortem de pacientes de Parkinson (EP), sugiriéndose que la perdida de actividad neurogénica es debida a

que la ausencia de dopamina afecta a los precursores neurales en el adulto (Hoglinger et al., 2004). Estos datos sostienen que en enfermedades neurodegenerativas como Alzheimer o Parkinson, no sólo se produce degeneración y muerte de las neuronas maduras, sino que también influye negativamente en el proceso de formación de nuevos progenitores neuronales en el cerebro adulto. De acuerdo con estos datos, la estimulación de aquellas poblaciones de células madre endógenas y progenitores neuronales, podría ser un método prometedor para mejorar la funcionalidad en algunas de las regiones afectadas por patologías neurodegenerativas.

Existen factores extrínsecos e intrínsecos que influyen en el mantenimiento y en la regulación de la neurogénesis *in vivo* (Ostenfeld and Svendsen, 2003). Entre los extrínsecos se encuentran un gran número de factores de crecimiento que han demostrado inducir la proliferación y diferenciación de precursores celulares, entre los que se incluyen el factor de crecimiento similar a insulina de tipo 1 (IGF-1) (Anderson et al., 2002), EGF (Doetsch et al., 2002), FGF-2 (Bartlett et al., 1995; Johe et al., 1996), el factor neurotrópico derivado de cerebro (BDNF) (Larsen et al., 2007) y Noggin (Lim et al., 2000). La neurogénesis en el adulto se ve influida también por la activación de varios factores intrínsecos, entre los que se encuentran de forma destacada los factores de transcripción Pax 6 (Hack et al., 2005; Kohwi et al., 2005), Notch 1 (Lutolf et al., 2002) y Mash 1 (Parras et al., 2004). Entender el mecanismo de acción de estos y otros factores sobre la neurogénesis así como identificar nuevas dianas implicadas en este proceso, constituiría sin duda un gran avance en el uso con fines terapéuticos de los nichos neurogénicos del adulto. De esta manera se podría inducir la producción de nuevas neuronas y células gliales, capaces de reparar el daño producido y servir como terapia en diversos trastornos del SNC como epilepsia, traumatismos, isquemias y enfermedades neurodegenerativas.

2.- MUERTE NEURONAL: DAÑO AGUDO Y NEURODEGENERACIÓN.

El daño neural agudo y las enfermedades neurodegenerativas se caracterizan por una pérdida gradual y selectiva de neuronas en las regiones afectadas del sistema nervioso. Entre las patologías que causan daño neuronal se encuentran la isquemia, traumatismos, epilepsia y enfermedades como Parkinson o Alzheimer. La patogénesis de estos trastornos neurológicos es multifactorial, con una compleja combinación de factores genéticos y ambientales. A pesar de no conocerse en detalle las causas y mecanismos por los cuales se produce la muerte neuronal en estas alteraciones, se sabe que algunos factores juegan un papel primordial. Entre estos factores destacan la generación de especies reactivas de oxígeno, el incremento en la concentración citoplásmica de Ca^{2+}, las disfunciones mitocondriales o los procesos de neuroinflamación y excitotoxidad.

2.1.- Epilepsia.

La epilepsia es un desorden neurológico común caracterizado por la presencia de ataques convulsivos recurrentes (Sander and Shorvon, 1996). Aproximadamente el 40% de las epilepsias son adquiridas, lo que significa que la condición epiléptica se desarrolla como consecuencia de un daño en el sistema nervioso (de Graaf, 1974; Delorenzo et al., 2005; Lothman et al., 1991; McNamara, 1994). El estado epiléptico (SE) se adquiere como consecuencia de una serie de convulsiones repetidas que producen muerte neuronal, por lo que es una causa frecuente de daño cerebral y esta altamente asociado con el desarrollo posterior de epilepsia (de Graaf, 1974; Delorenzo et al., 2005; Lothman et al., 1991; McNamara, 1994; Sander and Shorvon, 1996). Se cree que el SE daña las neuronas a través de un incremento de la liberación de aminoácidos excitatorios, sobre todo glutamato (Olney et al., 1986) que por activación de sus receptores aumenta los niveles intracelulares de calcio y activa las vías de muerte celular (Mody and MacDonald, 1995) proceso que se denomina excitotoxicidad. La lesión neurológica, en la fase inicial, es similar a la originada por la isquemia (Corsellis and Bruton, 1983), mientras que en una fase tardía se desarrolla gliosis y atrofia, convirtiéndose la lesión neurológica en epileptógena. El hipocampo es un área cerebral frecuentemente implicada en epilepsia y en la que se produce daño excitotoxico, siendo las neuronas más afectada las de las capas CA1, CA3 e hilus (Meldrum, 1983). Se ha comprobado además que la inducción experimental de ataques en roedores produce una importante respuesta inflamatoria en el cerebro, responsable del comienzo y propagación de la actividad epiléptica (De Simoni et al., 2000; Jankowsky and Patterson, 2001; Minami et al., 1991; Oprica et al., 2003). A los efectos patofisiológicos de la epilepsia contribuyen directamente los canales de calcio sensibles a voltaje (CCSVs) puesto que al despolarizarse permiten la entrada de calcio y consecuentemente la liberación de neurotransmisores (Verkhratsky, 2005). Por esta razón, los compuestos inhibidores de CCSVs serían buenos candidatos como agentes terapeuticos para enfermedades en las que esta implicado un mecanismo de excitotoxicidad. Los bloqueantes clásicos de los canales de calcio son las dihidropiridinas (DHP), benzotiacepinas, fenilalquilaminas y ciertos péptidos (toxinas) procedentes de serpientes, arañas o especies marinas (Lewis and Garcia, 2003; Olivera, 1997; Olivera et al., 1994; Uchitel, 1997). La aplicación terapéutica de las toxinas basada en sus propiedades selectivas ha sido extensamente revisada (Livett et al., 2004). Estas toxinas bloquean los CCSVs mediante la oclusión física del poro del canal, acción que realizan toxinas como la ω-conotoxina GVIA, MVIIA y MIIC; o bien modificando la cinética de apertura y cierre del canal, como hace la ω-agatoxina IVA. Hasta el momento no se conoce totalmente en detalle la estructura de los CCSVs, así como la naturaleza exacta de los mecanismos moleculares que regulan la acción de sus bloqueantes, lo que hace mas difícil la síntesis de compuestos eficaces (Triggle, 2003; Triggle, 2007). Además el problema de compuestos como las conotoxinas es que su naturaleza peptídica hace que sean más lábiles y no atraviesen la barrera

hematoencefálica (BHE). Por esta razón la síntesis de nuevas moléculas más estables y capaces de cruzar la barrera hematoencefálica e inhibir CCSVs podría llevar al desarrollo de nuevos fármacos más eficaces en el tratamiento de enfermedades como la epilepsia donde el mecanismo excitotóxico juega un papel central.

2.2.- Enfermedad de Parkinson.

La enfermedad de Parkinson es una de las enfermedades neurodegenerativas mas comunes, afectando aproximadamente al 2% de la población mayor de 60 años (Jankovic et al., 2007). La enfermedad de Parkinson se caracteriza por una pérdida masiva de neuronas dopaminérgicas y la subsecuente disminución en los niveles de dopamina, en la *substantia nigra pars compacta* (SNpc) con presencia frecuente, aunque no siempre, de acúmulos proteicos llamados cuerpos de Lewy (Schapira, 2008). La dopamina se sintetiza en las neuronas dopaminérgicas de la *sustancia nigra* y es liberada en gran cantidad al cuerpo estriado, modulando la actividad de las neuronas de dicho área lo que promueve la ejecución de movimientos controlados e intencionados. La pérdida de dopamina en EP, por tanto, produce disfunciones motoras importantes como bradiquinesa, temblor, rigidez, inestabilidad postural y problemas cognitivos (Lesage and Brice, 2009). La mayoría de los pacientes con Parkinson han perdido entre un 60-80% de neuronas dopaminérgicas en el momento de la aparición de los síntomas. Entre las posibles causas que contribuyen a la muerte de las células dopaminérgicas se encuentra la disfunción mitocondrial y el estrés oxidativo, aunque su etiología es aún desconocida (Rantham Prabhakara et al., 2008).

Los procesos inflamatorios contribuyen en gran manera al daño neuronal que se observa en EP. De hecho el análisis postmorten de cerebros de pacientes con EP muestra activación microglial en la SNpc y el estriado. También se observa activación microglial en modelos animales de EP (Cicchetti et al., 2002; McGeer et al., 2003; Orr et al., 2005). Las células gliales activadas producen citoquinas proinflamatorias tales como la interleuquina-1β (IL-1β), IL-6 y el factor de necrosis tumoral (TNF-α), que en grandes concentraciones inducen daño en las neuronas cercanas. Este daño neuronal a su vez reactiva el proceso inflamatorio, estimulando de nuevo a las células gliales, lo cual mantiene la inflamación en la zona y favorece el desarrollo de la enfermedad. De acuerdo con este esquema parece bastante lógico pensar que bloqueando las vías de activación de las células gliales se conseguiría que la neuroinflamación no se mantuviera, lo que repercutiría en una menor muerte de las neuronas dopaminérgicas. A pesar de los avances existentes en el descubrimiento de los factores responsables del desarrollo de la enfermedad de Parkinson ninguna terapia hasta la fecha ha demostrado ser capaz de parar o revertir el curso de la enfermedad. La mayoría de las terapias actuales van encaminadas hacia el tratamiento sintomático de la enfermedad. Por todo ello es necesario encontrar nuevas dianas capaces de prevenir la activación glial y la muerte neuronal que se produce en el desarrollo de esta enfermedad. El uso de estas

nuevas dianas terapéuticas que reduzcan la inflamación y sean capaces de inducir neuroprotección, combinado con tratamientos paliativos ya existentes mejoraría por tanto la calidad de vida de los afectados de enfermedad de Parkinson.

3.- MECANISMOS DE DAÑO NEUROLÓGICO

Son múltiples los mecanismos que causan daño neural, aquí abordaremos dos de ellos, la excitotoxicidad y la neuroinflamación que consideramos los mas pertinentes de cara a entender los resultados obtenidos en este trabajo.

3.1.- Excitotoxicidad.

La excitotoxicidad hace referencia al efecto tóxico que sobre las neuronas tiene el exceso de activación, excitación. En condiciones fisiológicas el glutamato es liberado en la hendidura sináptica, alcanzando sus receptores y transmitiendo el impulso nervioso a la neurona postsináptica. Este proceso es de muy corta duración ya que el glutamato es rápidamente retirado mediante transportadores que están presentes tanto en las neuronas como en los astrocitos. Sin embargo una persistencia de niveles elevados de este neurotransmisor en el espacio extracelular, y la constante activación de sus receptores resulta finalmente tóxico para las neuronas. Olney (Olney and Sharpe, 1969) propuso que la muerte neuronal inducida por este aminoácido se debía a una despolarización prolongada de las neuronas, y le dio el nombre de excitotoxicidad. La excitotoxicidad se ha implicado en múltiples desórdenes neurodegenerativos y viene marcada por tres eventos principales: 1) la liberación excesiva del correspondiente neurotransmisor excitatorio; 2) la unión de dicho neurotransmisor a sus receptores, lo que despolariza la neurona; 3) activación de una serie de mecanismos celulares que desencadenan una disfunción celular y producen finalmente la muerte neuronal (Choi, 1988).

El glutamato es el principal agente neurotransmisor usado en las sinapsis excitatorias del SNC de los mamíferos (Meldrum, 2000) y por tanto está implicado en prácticamente todos los procesos que tienen lugar en el cerebro, tanto en los de desarrollo del sistema nervioso, la migración o la diferenciación de las neuronas, así como en la función cerebral normal, como la cognición, la memoria y el aprendizaje. El glutamato actúa mediante la activación de diversos receptores (Meldrum, 1983; Meldrum, 2000; Nakanishi, 1992) que se han dividido en dos grandes grupos, receptores ionotrópicos y receptores metabotrópicos. Los receptores ionotrópicos son canales iónicos regulados por ligando y los metabotrópicos pertenecen a la superfamilia de receptores acoplados a proteínas G. Nos centraremos en los receptores ionotrópicos ya que son los más relevantes para entender el mecanismo de excitotoxicidad.

Los receptores ionotrópicos son proteínas integrales de membrana formadas por 4 ó 5 subunidades (Dingledine and Conn, 2000) y se clasifican en tres grupos en función de sus

propiedades farmacológicas, fundamentalmente en función del agonista sintético capaz de activarlo de forma especifica: 1) receptores activados por acido α-amino-3-hidroxi-5-metil-4-isoxazolpropiónico (receptores AMPA, AMPARs), 2) receptores activados por N-metil-D-aspartato (receptores NMDA, NMDARs) y 3) receptores activados por kainato (receptores KA, KARs).

Los receptores AMPA son codificados por una familia de 4 genes que dan origen a 4 subunidades denominadas GluR1- 4. En función de la subunidad que se exprese, los cambios post-transcripciones y las diferentes modificaciones que sufren, este tipo de receptores están implicados en un amplio abanico de actividades funcionales. Participan en la transmisión rápida de la información sináptica y se les ha implicado también en algunas formas de plasticidad sináptica como la potenciación a largo plazo (PLP) (Bliss and Collingridge, 1993; Song and Huganir, 2002) así como en procesos de aprendizaje, memoria, excitotoxicidad y neuroprotección (Malinow and Malenka, 2002). La unión del glutamato a este receptor provoca la apertura del canal iónico asociado, lo que resulta en un potencial excitatorio postsináptico. Los receptores de AMPA se distribuyen por todo el cerebro y su expresión es muy alta en hipocampo y en las capas superficiales de la corteza (Song and Huganir, 2002).

Los receptores de NMDA son heterómeros constituidos por dos tipos de subunidades: NR1 y NR2 (Healy and Meador-Woodruff, 2000) con diferentes propiedades farmacológicas. NR1 es el producto de un gen a partir del cual se originan múltiples isoformas por corte y empalme alternativo y es imprescindible para la formación del canal iónico. Las subunidades NR2 son codificadas en 4 genes diferentes y tienen el sitio de unión para glutamato. Además de estas subunidades se han clonado dos subunidades NR3. Estos receptores son permeables para Na^+, K^+ y Ca^{2+} y están involucrados en la transmisión normal de la información y son necesarios para la generación de determinadas formas de PLP. Dada su alta permeabilidad a Ca^{2+}, estos receptores participan de forma muy activa en el proceso de excitotoxicidad (Sanchez-Prieto et al., 2004; Seeburg et al., 2001).

Los receptores KA están formados por dos subfamilias de subunidades: las de baja afinidad, en la que se incluyen GlutR5-7, y las de alta afinidad, KA1 y KA2 codificadas todas ellas por genes diferentes que se expresan ampliamente en el sistema nervioso, incluyendo el hipocampo, la corteza y el sistema límbico (Egebjerg et al., 1991; Frerking and Nicoll, 2000). Estos receptores se han implicado en epileptogénesis (Lerma, 2003).

3.1.1.- Mecanismos de excitotoxicidad.

La primera etapa en el proceso de excitotoxicidad se produce por una excesiva activación por glutamato de sus receptores, etapa que puede denominarse de *inducción,* siendo por tanto la excitotoxicidad un proceso dependiente de receptor. La activación excesiva de los receptores de

glutamato propicia la entrada del calcio extracelular en la neurona fundamentalmente por dos vías, a través de los canales de calcio dependientes de voltaje, que se abrirían como consecuencia de la despolarización, y a través de los receptores de NMDA permeables a calcio, que requieren para su apertura la despolarización de la neurona y la unión de glutamato. Además de la entrada masiva de calcio extracelular, también se han implicado los depósitos intracelulares de calcio en el proceso de excitotoxicidad (Mahy et al., 1995; Nitsch and Scotti, 1992; Robledo et al., 1999).

La última etapa en el proceso de excitotoxicidad incluye procesos directamente responsables de la degeneración neuronal, es decir, las consecuencias finales de la activación de las cascadas citotóxicas por enzimas catabólicas. La producción de radicales libres puede ser otra vía importante de muerte neuronal por interferir en la homeostasis del calcio, activar alguna de las cadenas anteriormente mencionadas e iniciar algunos de los procesos destructivos como la peroxidación de lípidos.

El mecanismo de excitotoxicidad se ha implicado en múltiples procesos de daño cerebral como son el daño isquémico, daño cerebral por trauma (Friberg and Wieloch, 2002; Mody and MacDonald, 1995; Norenberg and Rao, 2007; Starkov et al., 2004), epilepsia (DeLorenzo et al., 1998; Pal et al., 1999; Sombati and Delorenzo, 1995; Sun et al., 2002) así como en las enfermedades de EA, EP y Huntington (Bezprozvanny, 2009; Choi, 1988; Choi, 1994; Doble, 1999; Gibson et al.; Meldrum and Garthwaite, 1990; Wang et al., 2005).

3.1.2.- Modelo animal de excitotoxicidad.

La administración a animales de experimentación de ácido kaínico (KA) provoca daños neurológicos que se han comparado con los daños observados en el análisis postmorten del cerebro de pacientes con epilepsia de lóbulo temporal, por lo que se ha usado ampliamente como un modelo animal de dicha patología (Ben-Ari and Cossart, 2000; Ben-Ari et al., 1980; Choi, 1988). La administración de KA constituye un modelo clásico de excitotoxicidad, produciendo una secuencia de estados alterados del comportamiento que se caracterizan por la aparición de ataques epilépticos que desemboca finalmente en la entrada en "*status epilepticus*" (Ben-Ari et al., 1980; Sperk, 1994). Estos ataques vienen seguidos de neurodegeneración en regiones específicas del cerebro, como la corteza piriforme, la amígdala, el tálamo y el hipocampo, donde las zonas más afectadas son las capas CA1, CA3 y las interneuronas del hilus (Coyle, 1983; Oprica et al., 2003; Sperk, 1994; Sperk et al., 1985; Tauck and Nadler, 1985). Esto es debido a que en la capa CA3 y en el hilus del hipocampo existe una gran cantidad de receptores para kainato y en las dendritas apicales y basales de la capa CA1 existe una alta densidad de receptores AMPA y NMDA (Contractor et al., 2000; Lauri et al., 2001; Le Meur et al., 2007; Qiu and Knopfel, 2007; Ulas et al., 1990). La muerte neuronal inducida por KA *in vivo* se debe a la liberación masiva de glutamato

inducida por esta excitotoxina (Sperk, 1994), aunque en cultivos neuronales el KA es también capaz de inducir muerte celular (Brorson et al., 1994; Courtney et al., 1995).

El KA al activar de manera directa y constante los receptotes de glutamato no solo da lugar a muerte neuronal sino que además produce la activación de células gliales, la cuales juegan un papel muy importante en la neurodegeneración inducida por esta toxina. La razón de esto es que al activarse las células gliales se incrementa la expresión de genes implicados en la producción de óxido nítrico y citoquinas, los cuales contribuyen a la expansión del daño neuronal producido, contribuyendo por su parte a la muerte neuronal (del Zoppo et al., 2000; Sharma et al., 2009).

3.2.- Neuroinflamación. Papel de astrocitos y microglia.

En los procesos inflamatorios que se producen en el SNC tienen un papel fundamental las células gliales: astrocitos y células de microglia. La inflamación en este tejido se considera uno de los principales factores implicados en la patología de enfermedades neurodegenerativas como la esclerosis múltiple (revisado en Comabella and Khoury, 2011), la EA o la EP (Akiyama, 1994; McGeer and McGeer, 2007; Tansey et al., 2007), así como desórdenes epilépticos (revisado en Vezzani and Granata, 2005). Las citoquinas liberadas en estos procesos tanto por las células gliales como por las propias neuronas, son proteínas producidas fundamentalmente por las células del sistema inmune y pueden ser pro- y anti-inflamatorias (Rothwell et al., 2001). Juegan un papel esencial en la defensa del organismo frente a infecciones, inflamación, traumatismos e isquemias. Las citoquinas que inician la respuesta inflamatoria son fundamentalmente la IL-1β, IL-6 y el TNF-α, que pueden actuar conjuntamente con otras citoquinas como la IL-8, IL-10, IL-12, IL-18 y el interferón gamma (IFN-γ) para llevar a cabo la respuesta inflamatoria (Wang et al., 2002).

Los astrocitos son las células más abundantes del cerebro constituyendo el 50% del total de las células de la corteza cerebral. Son células con forma estrellada y fáciles de identificar gracias a la expresión de la proteína acídica fibrilar glial (GFAP) que forma parte de su citoesqueleto. Esta células juegan un papel esencial en el funcionamiento del sistema nervioso y entre sus funciones están las de unir las neuronas a los capilares sanguíneos y mantener una concentración equilibrada de nutrientes entre el medio extracelular e intracelular previniendo la entrada de determinadas sustancias nocivas. Por ello los astrocitos ejercen una acción muy importante formando parte de la BHE. En este sentido, existen muchas evidencias que indican que la función de la BHE se encuentra alterada en muchas neuropatologías, como epilepsia, EA y EP, como consecuencia de la alteración de la astroglía (Abbott et al., 2006). Por último la astroglía también ayuda a mantener una concentración correcta de iones potasio en el espacio extracelular de las neuronas, captan neurotransmisores de las zonas sinápticas después de su liberación, y de este modo, ayudan a regular las actividades sinápticas (Leis et al., 2005; Binder & Steinhäuser, 2006).

Las células de microglia son macrófagos residentes en el SNC y constituyen el tipo celular más importante de cuantos intervienen en la inflamación de este tejido, controlando el microambiente que rodea al resto de células y produciendo factores capaces de influir sobre astrocitos y neuronas. En condiciones fisiológicas la microglia, que presenta un fenotipo no activado, produce factores neurotróficos y agentes antiinflamatorios (Streit, 2002) como el factor de crecimiento nervioso (NGF), factor de crecimiento derivado de glía (GDNF), factor de crecimiento derivado de cerebro (BDNF), neurotrofina-4 (NT-4) e IL-10. Cuando la microglia se activa, en respuesta a un patógeno o daño tisular, promueve el inicio de una respuesta inflamatoria que sirve para activar el sistema inmune e iniciar la reparación del tejido dañado. Como consecuencia de su activación cambia su morfología, y pasa de tener múltiples ramificaciones a tener un aspecto ameboide y redondeado (Gerhard et al., 2006; Streit, 1999) produciendo mediadores proinflamatorios como TNF-α, ciclooxigenasa-2 (COX-2), IL-1β e IL-6 (Akiyama et al., 2000) que actúan directamente sobre las neuronas, induciendo degeneración neuronal (McCoy and Tansey, 2008; Simi et al., 2007).

En condiciones patológicas puede ocurrir que la inflamación se mantenga en el tiempo, debido a que el estimulo pro-inflamatorio no desaparece, lo que mantiene el sistema inmune activado. Los astrocitos también participan en la inflamación y su activación se manifiesta por un aumento en el número, tamaño y motilidad de estas células (Braak et al., 2007; Damier et al., 1993), así como por un aumento de la proteína GFAP tanto en el soma como en las prolongaciones. Además se puede observar que el tamaño de las prolongaciones es menor y el soma aparece ensanchado. Muchos de los factores producidos tanto por los astrocitos como por las células microgliales, como TNF-α o IL1β, intervienen en los procesos inflamatorios que aumentan el daño neuronal que se produce en el daño cerebral (Saijo et al., 2009).

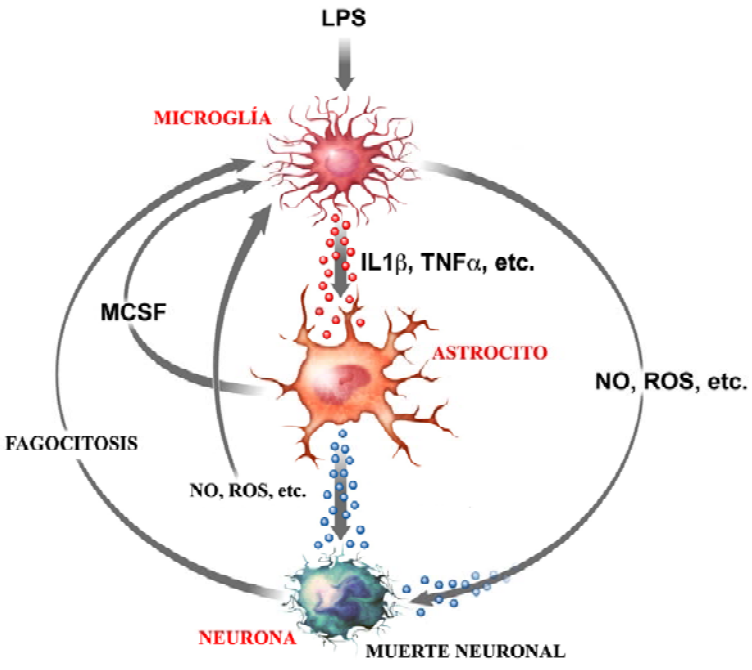

Figura V.- Neuroinflamación y neurodegeneración. Cuando la microglía se hiperactiva ante un estímulo proinflamatorio produce factores neurotóxicos como IL-1β y TNF-α que activan de forma paracrina a la astroglía. Esta activación promueve la producción de mediadores tóxicos, como NO y ROS. Estos mediadores además de activar a la microglía pueden actuar sinergísticamente con los factores neurotóxicos producidos por la microglía y conducir a la muerte neuronal. A su vez, como consecuencia de la degeneración neuronal se producen activadores microgliales que continúan activando a la microglía. De esta manera se entra en un ciclo inflamatorio que contribuye al avance de la enfermedad. IL1β, interleuquina 1β; LPS, lipopolisacárido; MCSF, factor estimulante de macrófagos; NO, óxido nítrico; ROS, radicales libres de óxigeno; TNF-α, factor de necrósis tumoral.

Existen varios modelos animales que reproducen en mayor o menor medida la enfermedad de Parkinson. Entre estos se encuentra el tratamiento de los animales con lipopolisacárido bacteriano (LPS), el cual es capaz de inducir la degeneración de las células dopaminérgicas fundamentalmente a través de una activación glial, especialmente de células de microglia (Gao et al., 2002). TLR4, el principal receptor de LPS, se expresa fundamentalmente en microglía, aunque también en menor cantidad en astrocitos (Kim et al., 2000), a través de él, el LPS es capaz de aumentar la producción de mediadores inflamatorios, fundamentalmente en la microglia como acabamos de comentar (Hunter et al., 2007). La neuroinflamación contribuye en gran medida a la muerte de las neuronas dopaminérgicas que se observa en EP (Hirsch and Hunot, 2009). La inyección intracraneal de LPS en la SNpc es por tanto un modelo experimental de EP (Castano et al., 1998; Gao et al., 2008) que reproduce los episodios de muerte celular dopaminérgica que se producen como consecuencia de una excesiva liberación de agentes proinflamatorios por parte de las células gliales hiperactivadas.

Otro modelo experimental de EP es el uso de 6-hidroxidopamina (6-OHDA) (Gomez-Lazaro et al., 2008; Ikeda et al., 2008; Mu et al., 2009). Al tener una estructura similar a la dopamina, la 6-OHDA tiene gran afinidad por los transportadores de dopamina y por eso penetra en las neuronas dopaminergicas a las que destruye selectivamente (Lehmensiek et al., 2006). El acumulo de 6-OHDA desencadena una auto-oxidación no enzimática que promueve la formación de radicales libres principal mecanismo por el que la 6-OHDA induce muerte neuronal, aunque la inhibición de la respiración mitocondrial también esta implicada (Schober, 2004). El tratamiento con 6-OHDA de células SH-SY5Y se utiliza también frecuentemente como modelo de EP *in vitro*, puesto que estas células tienen características de neuronas dopaminérgicas y la 6-OHDA induce su muerte (Hwang and Jeong, 2008; Lev et al., 2008). Aunque *in vitro* la muerte de las células SH-SY5Y inducida por 6-OHDA es independiente de la vía inflamatoria (Shih et al., 2009), *in vivo* la administración de 6-OHDA parece ser tóxica para las neuronas dopaminérgicas en parte por activación de los mecanismos de inflamación.

4.- DIANAS TERAPÉUTICAS.

4.1.- RECEPTOR ACTIVADO POR PROLIFERADORES PEROXISOMALES GAMMA (PPARγ).

Los PPAR son un pequeño grupo de factores de transcripción dependientes de ligando que pertenecen a la superfamilia de receptores nucleares, en la que se incluyen también los receptores de hormonas esteroideas, tiroideas, vitamina D y retinoides entre otros. Los PPARs funcionan formando heterodímeros con el receptor del ácido 9-cis retinoico (RXR) y se unen a secuencias especificas de ADN que denominamos elementos de respuesta a PPAR (PPREs) presentes en los genes diana (Figura VI). Inicialmente los PPARs se implicaron en la regulación del metabolismo

de lípidos. Controlan la expresión de genes que participan en la síntesis y oxidación de ácidos grasos, y están involucrados en el almacenamiento de ácidos grasos en diferentes tejidos.

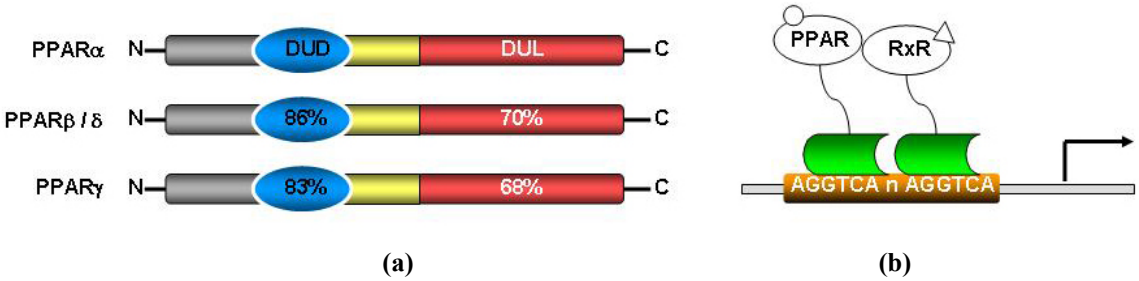

Figura VI.- a) Estructura de los miembros de la subfamilia PPAR. DUD, dominio de unión a DNA; DUL, dominio de unión a ligando. Los números representan el porcentaje de homología con el PPARα; b) El complejo PPAR/RXR se une a las regiones promotoras, los PPRE, e induce la expresión génica.

Centrándonos en concreto en PPARγ, son numerosos los ligandos capaces de activarlo, como los leucotrienos y algunas prostaglandinas, que son ligandos naturales (Forman et al., 1995; Jiang et al., 1998; Paruchuri et al., 2008). También numerosos ligandos sintéticos como las tiazolidinedionas (TZDs), (pioglitazona, rosiglitazona y troglitazona) y ciertos derivados similares a la tirosina (Blaschke et al., 2006; Desvergne and Wahli, 1999; Rosen and Spiegelman, 2001) activan este receptor. PPARγ participa en diversos procesos biológicos como la diferenciación de adipocitos y la homeóstasis de lipidos y glucosa (Desvergne and Wahli, 1999; Rosen and Spiegelman, 2001; Tontonoz et al., 1994), siendo muy abundante en el tejido adiposo (Debril et al., 2001; Dreyer et al., 1992; Kliewer et al., 1994; Michalik et al., 2006). También se ha implicado en la regulación de procesos inflamatorios (Ricote et al., 1999; Szeles et al., 2007). Datos más recientes sugieren que PPARγ actúa también como regulador de la inflamación en el sistema nervioso central (Heneka et al., 2005) y que podría ser una posible diana farmacológica en la lucha contra la neurodegeneración (Heneka and Landreth, 2007). En este sentido resultados obtenidos con animales de experimentación indican que los ligandos de PPARγ confieren neuroproteccion y mejora neurológica tras un daño cerebral (Abdelrahman et al., 2005; Bernardo et al., 2000; Landreth and Heneka, 2001; Townsend and Pratico, 2005). Nuestro grupo ha demostrado que miembros de una familia de compuestos denominados tiadiazolidinonas (TDZDs), los cuales poseen cierta homología estructural con la familia TZDs, son capaces también de activar PPARγ y, probablemente a través de esta activación, inhiben la activación de microglía y astroglía *in vitro* tras un daño inducido con LPS. Estos compuestos son también potentes antiinflamatorios y neuroprotectores en un modelo de excitotoxicidad *in vivo* por inyección de KA (Luna-Medina et al., 2005; Luna-Medina et al., 2007).

4.2.- GLUCÓGENO SINTASA-QUINASA 3β (GSK-3β)

GSK-3 es una proteina quinasa implicada en múltiples vías de señalización y que fue inicialmente identificada como enzima clave en la regulación del metabolismo de la glucosa (Woodgett and Cohen, 1984). Existen dos isoformas, GSK-3α y GSK-3β, con un 95% de homología en el dominio quinasa (Figura VII). Las regiones con menor homología en la secuencia corresponden al extremo C-terminal, con tan sólo un 36%, y el extremo N-terminal en el que sólo la isoforma α posee una cola de aminoácidos rica en glicinas (Woodgett, 1990).

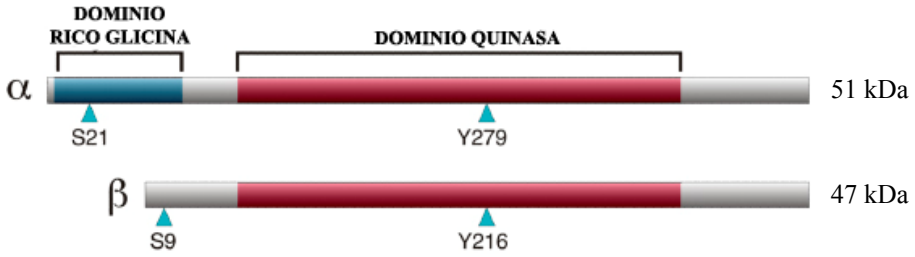

Figura VII.- Representación esquemática de las dos isoformas de GSK-3, GSK-3α y GSK-3β. Ambas isoformas presentan un dominio quinasa con una homología de secuencia del 98%. La isoforma GSK-3α presenta en el extremo N-terminal un dominio rico en glicina. Las flechas azules indican los sitios de fosforilación en serina 21 y 9 (inhibición) y en tirosina 279 y 216 (activación).

En roedores y humanos existe una variante de GSK-3β, GSK-3β2, que se expresa específicamente en el sistema nervioso y durante el desarrollo (Mukai et al., 2002) estando implicada en procesos de morfogénesis neuronal *in vivo* (Castano et al. 2010; Wood-Kaczmar et al., 2009). GSK3 actúa de mediador en la ruta de Wnt (wingless) (Woodgett, 2001) interviniendo en diversos procesos en el SNC como neurogénesis, migración neuronal, polarización neuronal y crecimiento axonal. La razón por la que los GSK3s están implicados en tan amplia variedad de rutas celulares es por la gran cantidad de sustratos sobre los que actúan. Entre esos sustratos destacan la proteína de unión a elementos de respuesta a AMPc (CREB) (Grimes and Jope, 2001a), proteínas de la familia del factor nuclear de células T activadas (Nfat) (Beals et al., 1997; Neal and Clipstone, 2001), neurogenina-2 (Ma et al., 2008), SMAD-1 (Fuentealba et al., 2007), c-Jun (de Groot et al., 1993) y β-catenina. Todos estos factores de transcripción juegan un papel importante en la regulación de la expresión génica (Aberle et al., 1997).

GSK-3β en concreto se ha implicado en procesos relacionados con la supervivencia celular, formación del citoesqueleto, crecimiento celular (Frame and Cohen, 2001; Jope and Johnson, 2004; Woodgett, 2001). También se ha implicado en procesos de inflamación (Cohen and Frame, 2001; Jope and Johnson, 2004; Kockeritz et al., 2006) así como en el desarrollo de la enfermedad de Alzheimer (Hooper et al., 2008). La regulación de la actividad de GSK-3β es

compleja, se inactiva por fosforilación de serina en posición 9. Numerosas quinasas, como Akt, PKC, quinasa p70 S6 y PKA son capaces de fosforilar GSK-3β en su serina 9 y por tanto inactivarla (Grimes and Jope, 2001b; Kaytor and Orr, 2002). GSK-3β también puede ser inhibida por las vias de señalización de la insulina y de wnt (Kockeritz et al., 2006). La inhibición de GSK-3β mediante administración de inhibidores tales como TDZD-8 y SB disminuye la disfunción orgánica provocada tras la inyección de LPS y peptidoglicano, sugiriéndose el uso de inhibidores de este enzima como terapias en endotoxemia asociada a sepsis, shocks y alteraciones relacionadas con inflamación local o sistémica (Dugo et al., 2005). La inhibición de GSK-3β también ha demostrado ser eficaz frente a la inflamación crónica en un modelo animal de artritis (Cuzzocrea et al., 2006).

GSK-3β es muy abundante en el cerebro y, en los últimos años, se ha sugerido que podría jugar un papel importante en procesos de neurodegeneración, sugieriéndose un posible efecto de su inhibición en protección neuronal. Los inhibidores de GSK-3β se han propuesto como posibles candidatos para el tratamiento del Alzheimer (Martinez et al., 2002b) existiendo una clara relación entre la activación de GSK-3β y esta enfermedad (Hooper et al., 2008). Esto es debido a que GSK-3β está implicado en la hiperfosforilación de la proteína tau, en el aumento de la formación de Aβ y la progresión de la neurodegeneración que favorece los déficits de memoria y aprendizaje propios de esta enfermedad. El tratamiento con cloruro de litio, inhibidor de GSK-3β, de ratones transgénicos que sobreexpresan tau, así como el uso de ratones *GSK-3β* $^{-/-}$, revirtió la fosforilación de la proteína favoreciendo que no se formaran agregados y redujo la formación de placa β-amiloide, mejorando así los síntomas de la enfermedad (Noble et al., 2005; Rockenstein et al., 2007). La actividad de GSK-3β se ha asociado también con la enfermedad de Parkinson, puesto que la inhibición de esta enzima disminuye la expresión de α-sinucleína en modelos celulares de Parkinson (Kozikowski et al., 2006).

Uno de los inconvenientes del uso de litio como inhibidor de GSK3 es que el litio también inhibe otras moléculas como inositol polifosfato 1-fosfatasa (IPPasa), inositol monofosfato fosfatasa (IMPasa), fructosa 1,6-bisfosfatasa (FBPasa), bisfosfato nucleotidasa (BPNasa) y fosfoglucomutasa (PGM) (Gould et al., 2006). Esto ha llevado a que en la actualidad se estén haciendo grandes esfuerzos en la búsqueda de nuevos inhibidores de GSK-3 más potentes y selectivos.

4.3.- CANALES DE CALCIO SENSIBLES A VOLTAJE (CCSVs).

Los CCSVs son estructuras proteicas complejas formadas por cuatro subunidades diferentes (α1, β, α2δ, γ), siendo las tres primeras indispensables para que el canal sea funcional (Figura VIII). La subunidad α1 es la de mayor tamaño y contiene el poro iónico, el sensor de voltaje, el mecanismo de compuerta y la mayoría de los sitios conocidos de regulación del canal por segundos mensajeros, fármacos y toxinas. En los mamíferos, la subunidad α1 está codificada por al menos 10 genes distintos de ahí la diversidad farmacológica y electrofisiológica de los CCSVs (Hofmann et al., 1994). La subunidad β es una subunidad auxiliar esencial ubicada intracelularmente que se coexpresa con la subunidad α1; la subunidad α2δ tiene un papel modulador de los canales y al igual que la subunidad β modifica la interacción con los bloqueadores; la subunidad γ es una proteína integral de membrana que modula los CCSVs e interacciona con otras proteínas de membrana (Arikkath and Campbell, 2003; Lacinova, 2005).

Los CCSVs son mediadores clave de la entrada de calcio en las neuronas como respuesta a una despolarización de la membrana. La entrada de calcio regula multitud de respuestas neuronales, como la activación de enzimas dependientes de calcio, la expresión de genes (Clark et al., 2006; Dolmetsch et al., 2001; Sutton et al., 1999), la liberación de neurotransmisores por los terminales presinapticos (Seagar and Takahashi, 1998; Spafford et al., 2004; Wheeler et al., 1996) y la regulación de la excitabilidad neuronal (Perez-Reyes, 1998). El sistema nervioso expresa diferentes tipos de CCSVs con diferentes tipos de localización celular y funciones fisiológicas específicas. Los CCSVs se clasifican en función de su estructura y propiedades electrofisiológicas y farmacológicas en seis subtipos: P, Q, N, L T y R (Dolphin, 2006; Khosravani and Zamponi, 2006). Se han descrito cambios en la expresión de los canales de calcio dependientes de voltaje en enfermedades como el dolor neuropático, la epilepsia y el fallo cardíaco congestivo. El uso de fármacos capaces de inhibir algunos tipos de canales de calcio dependientes de voltaje esta extendido en diversas patologías (Elmslie, 2004), de hecho los inhibidores de calcio han demostrado ser potentes agentes neuroprotectores y anticonvulsivos y potencian la eficacia anticonvulsiva de los fármacos antiepilépticos convencionales (Czuczwar et al., 1990; De Sarro et al., 1988; Dolin et al., 1988; Kaminski et al., 2001; Vezzani et al., 1988). Los subtipos N y P/Q se encuentran fundamentalmente en los terminales presinapticos y controlan la liberación de neurotransmisor. Por tanto, estos inhibidores podrían inhibir la liberación de glutamato y ser compuestos eficaces como anticonvulsivos y antiexcitotóxicos. De hecho el bloqueo de estos canales en animales de experimentación han demostrado ejercer efectos neuroprotectores (Asakura et al., 1997; Huang et al., 1997; Lee et al., 2004), y ser eficaces para el tratamiento de enfermedades como isquemia, dolor y epilepsia (Cox, 2000; Lukyanetz et al., 2002; Miljanich, 2004; Takahara et al., 2004).

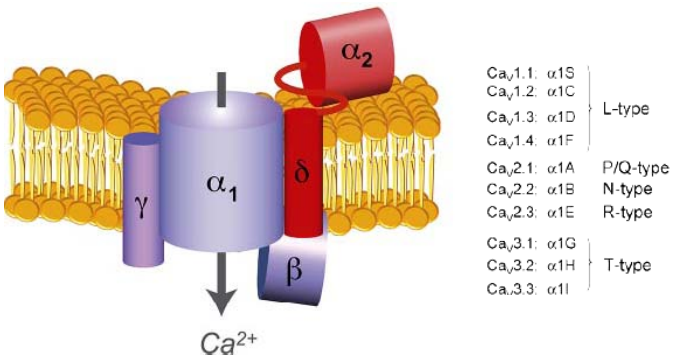

Figura VIII.- Tipos de canales de calcio. **Los canales de calcio son complejos heteroméricos constituidos por distintas subunidades que constituyen el poro a través del cual circula el calcio. En función de la subunidad α1 que contengan se distinguen varias tipos de canales: tipo L, P/Q, N, R y T.**

4.4.- FOSFODIESTERASA 7 (PDE7).

Las PDEs son enzimas que hidrolizan AMPc y GMPc. La familia de las PDEs esta constituida por 21 miembros clasificados en 11 grupos de acuerdo con la homología de secuencia, su distribución celular y la sensibilidad que presentan ante distintos inhibidores (Bender and Beavo, 2006; Conti and Beavo, 2007). La principal diana del AMPc es la proteína quinasa A (PKA) (Torgersen et al., 2002), entre cuyas acciones destaca la fosforilación de los factores de transcripción CREB (cyclic AMP response element binding protein) (Shaywitz and Greenberg, 1999), que se unen a elementos de DNA en los promotores de genes que responden a AMPc (Figura IX). Dado el relevante papel que el AMPc juega en múltiples funciones en el cerebro, los inhibidores de PDEs han adquirido relevancia como posibles diana terapéuticas para el tratamiento de enfermedades neurológicas como la depresión y el Alzheimer (Menniti et al., 2006). Diversos estudios han sugerido que los niveles de AMPc son importantes en neuroprotección y neuroinflamación (Lonze and Ginty, 2002; Volakakis et al. 2010). Por ello el control de los niveles de AMPc podría ser importante para regular los procesos neuroinflamatorios y consecuentemente tener un efecto sobre el desarrollo de enfermedades neurodegenerativas donde la inflamación juega un importante papel, entre las que se incluirían enfermedades como el Parkinson. Una manera de controlar los niveles de dicho mensajero es controlando su hidrólisis, acción que realizan las PDEs como se ha indicado. En concreto la PDE7, que hidroliza AMPc, se ha utilizado como diana en el control de la neuroinflamación (Giembycz and Smith, 2006). La familia de las PDE7 se compone de dos genes, PDE7A y PDE7B, que se expresan abundantemente en el sistema nervioso central de rata y en numerosos tejidos periféricos. En concreto, en el cerebro de rata, PDE7A es abundante en el bulbo olfatorio, hipocampo y varios núcleos cerebrales (Miro et al., 2001). La mayor cantidad de PDE7B en el cerebro se ha descrito en el cerebelo, giro dentado del hipocampo y estriado (Reyes-Irisarri et al., 2005; Sasaki et al., 2002). Aunque no existe mucha información acerca de las funciones fisiológicas reguladas por PDE7, se ha demostrado que su acción está implicada en procesos proinflamatorios y que es necesaria para la inducción de la proliferación de las células T del sistema inmune (Nakata et al., 2002).

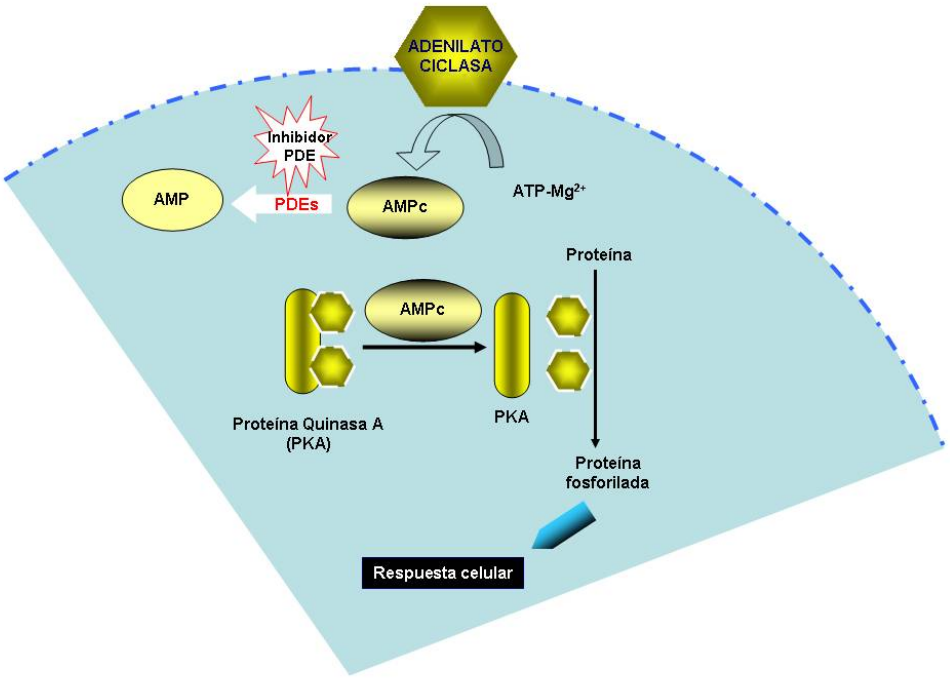

Figura IX.- Esquema resumido de la acción de las fosfodiesterasas en el control de los niveles de AMPc intracelulares.

Objetivos

En la actualidad, las terapias existentes frente a enfermedades neurodegenerativas son fundamentalmente paliativas y han demostrado ser poco eficaces. Es necesario por tanto, el desarrollo de nuevos fármacos con propiedades neuroprotectoras, antiinflamatorias y antiexcitotóxicas que eviten la progresión de la enfermedad. A esto se une la necesidad de encontrar compuestos con capacidad neurogénica, capaces de inducir la formación de un linaje neuronal específico que pueda reemplazar las neuronas que se pierden en este tipo de enfermedades.

El objetivo principal de esta tesis es, por tanto, identificar y analizar nuevas dianas celulares con efecto neuroprotector y neurogénico.

Para ello nos planteamos los siguientes objetivos:

1. Analizar el posible efecto de los activadores del receptor activado por proliferadores peroxisomales gamma (PPARγ) sobre proliferación, migración y diferenciación de células progenitoras neurales.

2. Analizar el posible efecto de los inhibidores de GSK-3β como inductores de neurogénesis.

3. Analizar el posible efecto neuroprotector del inhibidor de canales de calcio dependientes de voltaje (CCSVs) tipo no L, NP04634, en un modelo de daño cerebral por excitotoxicidad.

4. Analizar el posible efecto neuroprotector de nuevas dianas, en concreto PDE7, en modelos celulares y animales de enfermedad de Parkinson.

Materiales y Métodos

1.- ESTUDIOS *IN VIVO*.

1.1.- Animales.

Se han utilizado ratas Wistar macho de entre 8 y 12 semanas de edad procedentes del animalario del Instituto de Investigaciones Biomédicas de Madrid, donde fueron criados en condiciones óptimas de temperatura y humedad, en ciclos de 12 horas de luz-oscuridad y con agua y comida *ad libitum*. Todo lo concerniente al trato de los animales y a los protocolos experimentales usados fue previamente aprobado por la Comisión de Bioética para la Investigación Animal del Consejo Superior de Investigaciones Científicas, según lo recogido por las normativas española (RD. 1201/2005, del 10 de Octubre) y europea (normativa 86/609). Los procedimientos utilizados fueron diseñados con el fin de reducir al máximo el número de animales a utilizar, adoptándose en todo momento las medidas pertinentes para minimizar el sufrimiento de los mismos.

1.2.- Modelo de daño excitotóxico.

Se utilizó como modelo de daño excitotóxico la administración de ácido kaínico (KA; Sigma). La administración de esta excitotoxina provoca la aparición de convulsiones en los animales y daño neurológico en diversas áreas del cerebro, particularmente en el hipocampo (Holopainen, 2008; Ravizza et al., 2008). En concreto, el daño causado reproduce muchos de los aspectos que se observan en el hipocampo de pacientes con epilepsia de lóbulo temporal (Ben-Ari, 1985), por lo que la administración de KA se considera modelo eficaz para el estudio de esta forma de epilepsia.

El KA, a una dosis de 10 mg/kg diluido en suero salino, se administró por vía intraperitoneal. Se dividieron los animales en tres grupos. El grupo I fue el grupo control, a los cuales se les inyectó salino mientras que a los grupos II y III se les inyectó KA. Al grupo III se le administró además NP04634 (Noscira S.A.), por vía intragástrica, dos dosis de 100 mg/kg, 12 y 4 horas antes de la inyección de KA.

1.2.1. -Estudio del comportamiento.

Tras la inyección de KA los animales se colocaron en jaulas de plástico individuales, donde fueron monitorizados y grabados en video, analizándose su comportamiento en las siguientes 4 horas. El estado convulsivo de los animales se clasificó de acuerdo con la escala de Racine y Sperk (Racine, 1972; Sperk et al., 1985) como sigue: Valor 0 = no se observaron cambios; 0.5 = sacudidas de "*secado*", que denominaremos simplemente sacudidas; 1 = movimientos faciales y orales; 2 = asentimiento; 3 = *clonus* extremidades delanteras; 4 = clonus y levantamiento; 5 = levantamiento y caída; 6 = muerte. Se considera que los animales han entrado en SE cuando sufren

un ataque continuo o intermitente sin recuperación completa de la consciencia (Fase 4-5) durante al menos 30 minutos.

1. 3. - Neurogénesis.

Se analizó el potencial neurogénico de los compuestos pioglitazona (PGZ; Actos, Lilly) y NP031112 (Noscira) administrados por vía intragástrica. La administración de PGZ (20 mg/kg/día) se hizo durante 3 días consecutivos y la de NP031112 (50 mg/kg/día) durante 7 o 14 días. Al grupo de animales control se le administró PBS. Para analizar la formación de nuevas células en el cerebro de animales adultos, se inyectó como marcador de división celular 5-bromo-2-deoxyuridina (BrdU) por vía intraperitoneal. Los animales recibieron una única dosis de BrdU (50 mg/kg) y 24 horas después fueron sacrificados, con excepción de un grupo de animales tratados con PGZ que fueron mantenidos durante 21 días tras la inyección con BrdU para estudiar migración celular desde la región subventricular (ZSV) hasta el bulbo olfatorio (BO).

1.4.- Modelo de enfermedad de Parkinson.

Como modelo experimental de Parkinson (EP) hemos utilizado la administración de lipopolisacárido bacteriano (LPS; Sigma), que es un potente inductor de inflamación y que al ser inyectado en la parte compacta de la sustancia negra (SNpc) provoca una notable pérdida de neuronas dopaminérgicas (Herrera et al., 2000). Los animales previamente anestesiados con una mezcla de ketamina (60mg/kg) y medetomidina (5μg/kg) se colocaron sobre un aparato estereotáxico (Kopf Instruments, CA) donde se les inyectó en la SNpc, unilateral e intracerebralmente, 10μg de LPS en un volumen final de 2.5 μl, según las coordenadas de Paxinos y Watson (1998): desde bregma: 4.8 mm posterior, 1.7 mm lateral y 8.2 mm profundidad. Los compuestos, S14 y BRL50481 (BRL), analizados como posibles neuroprotectores se inyectaron a la vez que el LPS en cantidades de 20 y 60 nanomoles respectivamente. El compuesto S14 fue sintetizado y suministrado por el grupo de la Profesora Ana Martínez del Instituto de Química Médica de Madrid (CSIC) y BRL fue adquirido en Tocris. Los animales control se inyectaron con vehículo (2.5 μl de PBS). Para la inyección se utilizó una microbomba (KD Scientific, Holliston, MA). Una vez terminada la operación, los animales fueron estabulados individualmente para su correcta recuperación y mantenidos en el animalario. Una parte de los animales se mantuvieron durante 3 semanas al cabo de las cuales se testó el daño neurológico mediante test rotacional. El resto de los animales se perfundieron a las 72 horas con paraformaldehido 4% y se preservaron los cerebros para posteriores análisis (ver apartado 1.6).

1.4.1.- Test rotacional.

La inyección subcutánea de apomorfina (0.1mg/kg, Sigma) induce un movimiento rotatorio en aquellas ratas con un lado de la SNpc lesionada, produciéndose el giro en el sentido contrario al lado lesionado (Jerussi and Glick, 1975). Las ratas se observaron durante 30 minutos después de la inyección de apomorfina, contándose el número de giros realizados. Previamente a la inducción del daño en la SNpc, todas las ratas pasaron este test, para evitar animales con problemas motores de base.

1.5.- Extracción de proteína de tejidos y Western blot.

La extracción de tejidos para Western blot se llevó a cabo mediante procedimiento estándar. Tras el sacrificio de los animales se extrajo y diseccionó el cerebro, almacenándose las diferentes áreas de interés a -80ºC hasta su posterior uso. Para la extracción de proteínas, las muestras se homogeneizaron, con ayuda de un homogenizador de émbolo de vidrio a 4ºC en tampón RIPA (1% NP 40 Igepal, 0.5% deoxicolato sódico y 0.1% docecil sulfato sódico (SDS) en PBS), conteniendo inhibidores de proteasas y fosfatasas (1mM fenilmetilsulfonil fluoruro (PMSF), 1mM ortovanadato de sodio y 10 mM pirofosfato sódico). La concentración de proteína total se determinó por el método Bradford (Bio-Rad Hércules, CA) utilizando como patrón seroalbúmina bovina (BSA, Sigma).

Se separaron las proteínas (20µg por muestra) mediante electroforesis en geles de poliacrilamida al 10% bajo condiciones desnaturalizantes (SDS) y reductoras (PAGE-SDS) y se transfirieron a una membrana de nitrocelulosa (Protran, Whatman, Dassel, Germany). Las membranas se bloquearon durante 1h a temperatura ambiente en T-TBS (Tris-HCl 20 mM pH 7.5, NaCl 150 mM, Tween-20 0.05%) con un 5% de leche en polvo desnatada o con un 1% BSA, en función del anticuerpo primario. A continuación se incubaron con el correspondiente anticuerpo primario (ver Tabla I) en el medio de bloqueo durante 15 horas a 4ºC. Tras lavarse las membranas con T-TBS durante 15 minutos se incubaron con el correspondiente anticuerpo secundario anti-IgG de ratón o de conejo acoplado a peroxidasa (Sta. Cruz Biotech) durante 1 hora a temperatura ambiente en el medio de bloqueo. Los inmunocomplejos se visualizaron utilizando el sistema de quimioluminiscencia ECL (Amersham) siguiendo las indicaciones del fabricante. En todos los casos se utilizó el anticuerpo anti-α-tubulina (Sigma) como control de carga.

Anticuerpo	Origen	Dilución	Fabricante
α-PDE7A	Conejo	1/1000	Santa Cruz
α-PDE7B	Cabra	1/1000	Santa Cruz
α-tubulina (alfa)	Ratón	1/5000	Sigma

Tabla I. Listado de anticuerpos usados para WB en tejido.

1.6.- Estudios histoquímicos.

1.6.1.- Obtención de muestras.

Los animales previamente anestesiados se perfundieron transcardíacamente con una solución de paraformaldehido (PF) al 4% en PBS. Los cerebros se postfijaron a 4ºC durante 24h en la misma solución, y crioprotegieron en dicha solución con sacarosa al 30%. Finalmente se congelaron en hielo seco y mantuvieron a -80ºC. Los cerebros se cortaron en un criostato (Cryocut 1900, Leica) en secciones de 30µm que se conservaron en un tampón de congelación (30 % glicerol, 30% etilenglicol y 40% de tampón fosfato (PB) 0.1M) y almacenaron a -80ºC hasta su uso. Se hicieron cortes coronales y sagitales en función de las áreas a analizar.

1.6.2.- Tinción histológica de Nissl.

Se utilizo para teñir y cuantificar neuronas. Las secciones, previamente montadas sobre portas gelatinizados, se sumergieron en etanol al 70% durante 24 h, se tiñeron con violeta de cresilo (0.1% en tampón acetato (2.7% de acetato sódico, 1.3% ácido acético, en agua)) durante 5 minutos y se lavaron en alcoholes de gradación ascendente para finalmente ser diferenciados con alcohol y ácido acético. Tras una hora en xilol los portas fueron cubiertos con DePeX (Serva, Heidelbert, Alemania) y fotografiados. Para cuantificar el numero de neuronas se contó con el soporte informático analySIS (Soft Imaging System). El numero de células teñidas en el hilus y las regiones CA1 y CA3 del hipocampo se contaron en cinco campos independientes/corte y tres cortes por animal a 400 aumentos.

1.6.3.- Tinción histológica con hematoxilina.

Esta tinción se utilizo como contratinción para un análisis histológico mas preciso. Para ello las secciones coronales de hipocampo previamente inmunoteñidas con BrdU, fueron montadas en portas gelatinizados y sumergidos en una solución con hematoxilina (1mg/ml en agua) durante 2 minutos. A continuación se deshidrataron en concentraciones ascendentes de alcoholes y tras un paso final por xilol fueron cubiertas con DePeX para posteriormente ser analizados.

1.6.4.- Tinción con Fluoro-Jade B.

Esta tinción se utilizó para marcar neuronas dañadas, en proceso de degeneración (Schmued et al. 1997). Secciones montadas en portas gelatinizados se sumergieron en baños sucesivos con alcohol 100%, alcohol 70% y agua destilada para después preincubar durante 15 minutos en agitación con una disolución acuosa con 0.06% de permanganato. Tras incubar con la solución de tinción (0.001% de Fluoro-Jade B (Chemicon) en ácido acético) durante 30 minutos a temperatura ambiente (TA), las secciones fueron lavadas en agua destilada, secadas a temperatura

ambiente y montadas con DePeX. Las muestras fueron fotografiadas con un microscopio confocal Radiance 2100 (Bio-Rad, Hercules, CA).

1.6.5.- Inmunohistoquímica.

Se utilizaron secciones en flotación que se incubaron con el correspondiente anticuerpo primario y en las condiciones especificadas, en función de si iban a ser visualizadas con diaminobencidina o con fluorescencia. La especificidad de los anticuerpos utilizados se verificó mediante la ausencia total de señal al omitir el anticuerpo primario. En los experimentos de detección de BrdU, antes de iniciar la incubación con el correspondiente anticuerpo, las secciones fueron incubadas con HCl 2M a 37ºC durante 30 minutos y luego neutralizadas con borato sódico 0.1M. La tabla II muestra los anticuerpos utilizados.

Anticuerpo	Origen	Dilución	Fabricante
α - BrdU	Ratón	1/400	Dako
α - CD11b (OX-42)	Ratón	1/100	Serotec
α - doublecortin (DCX)	Cabra	1/200	St. Cruz
α - GFAP	Ratón	1/300	Sigma
α - Neu N	Conejo	1/100	Chemicon
α-PDE7A	Conejo	1/100	Santa Cruz
α-PDE7B	Cabra	1/100	Santa Cruz
α - PPARγ	Ratón	1/200	Santa Cruz
α - PSA-NCAM	Ratón	1/100	Chemicon
α - TH	Conejo	1/300	Chemicon
α - (β-III)-tubulina	Ratón	1/200	Sigma

Tabla II. Listado de anticuerpos usados para inmunohistoquímica en tejido.

1.6.5.1.- Revelado con diaminobencidina (DAB).

El primer paso fue la inhibición de la actividad peroxidasa endógena mediante la incubación con 1.5% de H_2O_2 en PBS durante 30 minutos. A continuación las muestras se bloquearon con 5% suero normal (de cabra o caballo, según corresponda), con 0.1M de lisina y 0.1% de Triton X-100. Los cortes se incubaron toda la noche a 4ºC con los anticuerpos primarios correspondientes diluidos en la misma solución de bloqueo y después se lavaron 3 veces en PBS. Los anticuerpos primarios fueron visualizados usando anticuerpos secundarios biotinilados, con los que se incubaron las muestras durante 1 hora a temperatura ambiente, seguido de un tratamiento con el kit Vectastain elite ABC complex de Vector. Todas las secciones se montaron sobre portas gelatinizados para posteriormente ser fotografiadas con un microscopio Zeiss Axiophot acoplado a una cámara Olympus DP-50 digital o un estereomicroscopio modular Leica MZ6.

En el análisis de la respuesta glial se cuantificaron dos parámetros: 1) el número de células gliales activadas, y 2) la intensidad de tinción. Para ello se identificaron los cuerpos celulares uno a uno, normalizándose su intensidad de tinción en función del fondo existente en cada preparación. Se asignaron valores arbitrarios en una escala de 1 (fondo de tinción) a 256. Para determinar la

activación de astrocitos se utilizó como marcador un anticuerpo anti-GFAP (Glial Fibrillary Acidic Protein) y un anticuerpo contra CD11b (OX-42) para determinar la activación de la microglia. Las células BrdU positivas se contaron a lo largo del hipocampo usándose 1 sección cada 60 µm y analizándose a 400 aumentos.

1.6.5.2.- Fluorescencia.

La incubación con los anticuerpos primarios se llevo a cabo de manera similar a lo expuesto en el apartado 1.6.5.1, excepto por la omisión de la inactivación de las peroxidasas endógenas. La visualización se llevó a cabo mediante el uso de anticuerpos conjugados a Alexa-488 (fluoróforo verde) y Alexa 647 (fluoróforo rojo), todos de Molecular Probes (OR, USA). Todas las secciones se montaron sobre portas y posteriormente se fotografiaron con un microscopio confocal Radiance 2100. Las células BrdU positivas se contaron a lo largo de toda la SVZ y la RMS, usándose 1 sección cada 60µm y analizándose a 400 aumentos. Para evaluar el número de células $BrdU^+/NeuN^+$ en el bulbo olfatorio, se contaron 5 campos independientes (400 aumentos) en 5 secciones diferentes por animal (n=5).

1.6.6.- Microscopía electrónica de transmisión.

Los animales fueron perfundidos siguiendo el procedimiento detallado en el apartado 1.6.1, pero en esta ocasión usando una mezcla de paraformaldehido al 2% con glutaraldehído al 2.5% en tampón fosfato 0.1M. Los cerebros postfijados en sacarosa al 30% en la misma solución de perfusión se lavaron con PB y se cortaron coronalmente a 200 µm en un vibrátomo. A continuación las secciones se trataron con tetróxido de osmio al 2% en PB 0.1M durante 2 horas y luego deshidratadas en alcoholes a concentraciones crecientes. Tras 20 minutos en óxido de propileno a temperatura ambiente y 12 horas en una mezcla de propileno-resina (1:1) las muestras fueron incluidas en resina (Durcupan™, Fluka, Buchs, Switzerland) y mantenidas a 60ºC hasta la completa polimerización de la misma. Se realizaron a continuación cortes semifinos seriados de 1.5 µm de espesor con un ultramicrotomo, que se tiñeron con una solución al 1% de azul de toluidina, para estudiar la organización de la SVZ y la RMS. Con el fin de identificar los diferentes tipos celulares de la SVZ se realizaron cortes ultrafinos (70 nm) en un ultramicrotomo Reichert, que se montaron sobre unas rejillas de cobre y se tiñeron con una solución de acetato de uranilo y citrato (Electron Microscopy Science, Hatfield, UK) diluida al 2% en una solución de hidróxido de potasio y a temperatura ambiente. Por último las preparaciones se observaron y fotografiaron en un microscopio electrónico Fei (Tecnai-Spirit) acoplado a una cámara digital (Morada, Soft-imaging System).

2.- ESTUDIOS *IN VITRO.*

2.1.- Cultivos celulares.

2.1.1.-Cultivos primarios de células gliales.

Este tipo de cultivos se inició a partir de la corteza cerebral de ratas de dos días de edad postnatal (P2). Una vez decapitados los animales se procedió a extraer el cerebro, eliminar las meninges y diseccionar la corteza cerebral, la cual se disgregó con una pipeta Pasteur de vidrio en medio de cultivo DMEM frío. El homogeneizado obtenido se centrifugó durante 10 minutos a 1050 rpm y tras eliminar el sobrenadante se resuspendió el pellet en DMEN 10:10:1 (DMEM con 10% de suero fetal bovino, 10% de suero de caballo y 1% de penicilina/estreptomicina) y se sembraron las células en frascos de cultivo. Tras 7 días de cultivo en condiciones estándar (95% de humedad, 37ºC de temperatura y 5% de CO_2), los frascos fueron agitados en un agitador orbital durante 4 horas a 230 rpm a 37ºC, permitiendo así separar las células microgliales no adherentes del resto de tipos celulares: astrocitos y oligodendrocitos. A continuación los botes de cultivo fueron agitados durante toda la noche a 260 rpm a 37ºC para separar oligodendrocitos de astrocitos. De esta manera se consiguió aislar la astroglía, que fue sembrada en placas de 24 pocillos sobre cristales previamente tratados con poli-D-lisina (20µg/ml en agua). Tras 2 días en cultivo los astrocitos fueron tratados con NP04634 (Noscira, 25 µM) 1 hora antes de inducir daño mediante exposición a LPS (10 µg /ml), tras lo cual se dejaron 24h en cultivo para a continuación evaluar la expresión de distintos marcadores de citotoxicidad (ver sección 2.3).

2.1.2.- Cultivo de células madre neurales.

Los cultivos de células madre neurales se iniciaron a partir de las dos áreas neurogénicas del cerebro adulto, la zona subventricular (SVZ) y la zona subgranular del hipocampo (SGZ). Para ello se diseccionó el cerebro obteniéndose la SVZ y el hipocampo, que se disgregaron en medio DMEN, con 1% glutamina, 0.05% gentamicina y 0.3% fungizona. Después de tratar con 0.05% tripsina-EDTA, 0.3 mg/ml de hialuronidasa y 0.5 U/ml DNAsa en DMEM, se procedió a eliminar los restos de mielina con DPBS (Invitrogen). Las células se sembraron en placas de 6 pocillos y se cultivaron con DMEN/F12 (1:1, Invitrogen) con antibióticos y suplementado con 2% B27 (Gibco), 10 ng/ml de factor de crecimiento epidérmico (EGF, Peprotech, London, UK) y 10 ng/ml de factor de crecimiento de fibroblastos (FGF, Peprotech). En estas condiciones las células proliferan en flotación y forman grupos esféricos, las neurosferas (NS) primarias. Tras 3 días en cultivo en condiciones estándar, las NS se trataron según el tipo de diana celular a estudiar. A partir de las NS primarias se obtienen las NS secundarias. Para ello, después de 7 días de cultivo, las NS primarias se disocian y las células se vuelven a cultivar en las mismas condiciones obteniéndose nuevas neurosferas. El estudio de la posible respuesta de las células madre neurales a los diferentes

tratamientos se llevó a cabo tanto con NS primarias como secundarias. En la tabla III se indican los productos utilizados, su origen y las concentraciones a las que se utilizaron.

Compuestos				
Producto	**Abreviatura**	**Tipo Compuesto**	**Proveedor**	**Dosis**
Alsterpaulona	Alst	Inhibidor GSK-3β	Sigma	10 μM
GW9662	GW	Inhibidor PPARγ	Cayman	10, 30 μM
NP031111	NP11	Inhibidor GSK-3β	IQM*	10 μM
NP031112	NP12	Inhibidor GSK-3β	IQM*	2,5 μM
NP031115	NP15	Inhibidor GSK-3β	IQM*	10 μM
Pioglitazona	PGZ	Ligando PPARγ	Actos. Lilly	5, 10, 30 μM
Rosiglitazona	RGZ	Ligando PPARγ	Cayman	5, 10, 30 μM
T0070907	T	Inhibidor PPARγ	Cayman	25, 50 μM
VII	VII	Inhibidor GSK-3β	Sigma	10 μM
VIII	VIII	Inhibidor GSK-3β	Sigma	10 μM
VPs. 2.51, 2.54, 3.16, 3.31, 3.35	----	Inhibidor GSK-3β	IQM*	10 μM
*** Prof. Ana Martínez. Instituto de Química Médica. CSIC.**				

Tabla III. Listado de compuestos usados en cultivos de neuroesferas.

2.1.2.1.- Diferenciación de cultivos.

Con el fin de determinar la capacidad de las células madre neurales de generar los distintos tipos celulares del SN, neuronas, astrocitos u oligodendrocitos, se sembraron las NS, previamente cultivadas durante 10 días, sobre cristales tratados con poli-L-lisina (100μg/ml), en ausencia de factores exógenos de crecimiento. Tras 24h en cultivo se fijaron las NS con paraformaldehido al 4% en PBS y se conservaron en PBS con 0.05% de azida sódica a 4ºC hasta su análisis inmunocitoquímico.

2.1.2.2.- Ensayo de migración celular.

Se utilizaron NS en crecimiento, las cuales fueron recogidas del cultivo de una en una y pegadas en pocillos de 35mm previamente tratados con poli-L-lisina. A las 48h se examinó el crecimiento de la NS con un microscopio de contraste de fases, adquiriéndose las imágenes con un equipo Nikon Digital Sight, SD-L1. La distancia de migración celular se calculó desde el límite de la esfera.

2.1.2.3.- Medidas de crecimiento y proliferación celular.

El número de neuroesferas primarias y secundarias así como su tamaño fue analizado con ayuda de un microscopio Nikon Digital Sight, SD-L1 (Nikon, Japan). Los ensayos de proliferación se llevaron con NS primarias, en ausencia o presencia de los distintos tratamientos ya mencionados, cultivadas durante 7 días. Tras este periodo, se sembraron las NS sobre cristales previamente tratados con poli-L-lisina y se dejaron durante 24h. Pasado ese tiempo se fijaron y conservaron tal como se indica en el apartado 2.1.2.1.

2.1.3.- Cultivo de células de neuroblastoma humano SH-SY5Y.

Las celulas SH-SY5Y (Sigma) se cultivaron en condiciones estándar en medio Ham′s F12:EMEM (EBSS) (1:1) con 2 mM glutamina y 15% de suero fetal bovino (FBS). En la tabla IV se resumen los compuestos utilizados con esta línea celular.

Compuestos				
Producto	**Abreviatura**	**Tipo**	**Proveedor**	**Dosis**
BRL50481	BRL	Inhibidor de PDE7	Tocris Bioscience	30 µM
H-89	----	Inhibidor de PKA	Calbiochem	20 µM
Rolipram	Rol	Inhibidor de PDE4	Tocris Bioscience	30 µM
Rp-cAMP	Rp	Análogo de AMPc	BioLog	100 µM
S14	----	Inhibidor de PDE7	IQM*	10 µM
*Prof. Ana Martínez. Instituto de Química Médica. CSIC.				
Agente Citotóxico				
6-hidroxidopamina	6-OHDA		Sigma	30 µM

Tabla IV. Listado de compuestos usados en cultivos de SH-SY5Y.

2.1.4.- Cultivos primarios de células de mesencéfalo ventral.

Los cultivos celulares se obtuvieron a partir del mesencéfalo ventral de embriones de rata de 14 días de edad (E14). Las madres gestantes se sacrificaron por dislocación cervical y se extrajeron los sacos embrionarios, que se diseccionaron en medio HBSS sin Ca^{++} ni Mg^{++} (Gibco). Se aisló el mesencéfalo ventral que fue triturado mecánicamente usando una micropipeta en medio HBSS. Se centrifugó el homogeneizado obtenido a 1200xg durante 5 minutos, siendo el pellet resultante resuspendido en medio MEM suplementado con 10% FBS, 10% HS, 1g/l de glucosa, glutamina 2mM, piruvato sódico 1mM, aminoácidos no esenciales 100 µM, penicilina 50U/ml y estreptomicina 50 µg/ml. Las células obtenidas se sembraron en placas de 24 pocillos a una densidad de 5.10^5 células/pocillo o bien en placas de 96 pocillos a 10^5 células/pocillo y se mantuvieron en condiciones estándar. Después de una semana en cultivo, las células se trataron con LPS (10 µg/ml) o con 6-OHDA (35 µM, Sigma), solos o en combinación con S14 (10 µM). Tras 24 horas en cultivo se procesaron las muestras para inmunocitoquímica o para medición de los niveles de nitritos en el medio.

2.2.- Extracción de proteína total de cultivos celulares y Western blot.

Los cultivos de SH-SY5Y previamente tratados con Rol, BRL o S14 durante 1 hora fueron mantenidos en presencia de 6-OHDA durante 16h, para finalmente ser lavados 2 veces con PBS y proceder a la extracción de proteína total. Para extraer las proteínas, las células se lisaron en

tampón de lisis (NaF 50mM, $Na_4P_2O_7$ 10mM, EDTA 5mM, Tris-HCl 50 mM pH 7.5, Triton X-100 0.5%, NaPPi 10 mM) y en presencia de inhibidores de fosfatasa y proteasas (ortovanadato sódico 0.2mM, ditiotreitol 1mM, 2µg/ml de leupeptina, 2µg/ml de aprotinina, 2µg/ml de pepstatina A y PMSF 0.4mM). La concentración de proteína total se determinó por el método Bradford utilizando como patrón BSA. Las proteínas se separaron en geles PAGE-SDS, se transfirieron a membranas de nitrocelulosa y se incubaron con los anticuerpos primarios (tabla V) y secundarios tal como se indica en el apartado 1.5.

En todos los casos se utilizó el anticuerpo anti-α-tubulina como control de carga, con excepción de aquellos experimentos en los que se uso un anticuerpo anti-P-CREB, en los que el control de carga se hizo usando un anticuerpo anti-CREB.

Anticuerpo	Origen	Dilución	Fabricante
α - CREB	Ratón	1/1000	ABcam
α - CREB (fosforilada)	Ratón	1/1000	ABcam
α-PDE7A	Conejo	1/1000	Santa Cruz
α-PDE7B	Cabra	1/1000	Santa Cruz
α - PPARγ	Ratón	1/1000	Santa Cruz
α-tubulina (alfa)	Ratón	1/5000	Sigma

Tabla V. Listado de anticuerpos usados para WB en células.

2.3.- Inmunocitoquímica.

Para los estudios inmunocitoquímicos se utilizaron células adheridas a cristales. Para ello las células se cultivan en placas de 24 pocillos, con el correspondiente cubreobjetos de cristal tratado con poli-L-lisina (100µg/ml), donde se realizan los correspondientes tratamientos. A continuación se fijan las células sumergiendo los cristales durante 20 minutos a temperatura ambiente en una solución de paraformaldehido 4%. Los cristales se lavan varias veces con PBS para a continuación ser permeabilizados con 0.1% Triton X-100 en PBS durante 30 minutos a 37ºC. Seguidamente fueron incubados con el correspondiente anticuerpo primario a 37ºC durante 1 hora. Tras 3 lavados de 5 minutos con PBS se incubaron con el correspondiente anticuerpo secundario fluorescente durante 45 minutos a 37ºC. Una vez montados los cristales sobre portas con Vectashield, se obtuvieron las imágenes con microscopía confocal. Para los experimentos de cuantificación se utilizo el soporte informático analySIS. El número de células consideradas positivas para un marcador específico se refirió al número total de núcleos (DAPI) contados. Estas cuantificaciones se realizaron con aumento de 400x sobre al menos cinco campos independientes elegidos al azar.

Los anticuerpos utilizados en inmunocitoquímica se resumen en la tabla VI.

Anticuerpo	Origen	Dilución	Fabricante
Primario			
α - (β-III)-Tubulina (TuJ-1)	Conejo	1/200	Covance
α - Caspasa 3	Conejo	1/200	R&D Systems
α - CD11b (OX-42)	Ratón	1/400	Serotec
α - COX-2	Conejo	1/100	St. Cruz
α - GFAP	Ratón	1/300	Sigma
α - Ki67	Conejo	1/100	Novocastra
α - MAP-2	Ratón	1/200	Sigma
α - Neu N	Conejo	1/100	Chemicon
α-PDE7A	Conejo	1/100	Santa Cruz
α-PDE7B	Cabra	1/100	Santa Cruz
α - TH	Ratón	1/100	Sigma
α - TNFα	Cabra	1/100	Santa Cruz
Secundario			
Alexa - 488	Cabra, Conejo, Ratón	1/400	Molec. Probes
Alexa - 546	Cabra, Conejo	1/400	Molec. Probes
Alexa - 647	Ratón, Conejo	1/400	Molec. Probes

Tabla VI. Listado de anticuerpos usados para inmunohistoquímica en células.

2.4.- Ensayo de viabilidad celular (MTT).

La viabilidad celular de las células SH-SY5Y, se midió mediante un ensayo colorimétrico con sal de tretazolium (3-[4,5-dimethylthiazol-2-yl]-2,5-diphenyl tetrazoliumbromide (MTT)) de Roche Diagnostic, basado en la capacidad de las células viables para reducir el MTT (amarillo) a formazán (azul). Para ello se sembraron 30.000 células/pocillo en placas multipocillo de 96 y a las 24 horas se trataron con los correspondientes compuestos en las condiciones indicadas. Tras 24h en condiciones estándar de cultivo, se incubaron las células con MTT (0.5mg/ml) durante 4 horas para a continuación solubilizar en 10% de SDS / 0.01 M HCl en oscuridad durante 12 horas. La reducción del MTT por parte de las células se cuantificó mediante medición de la absorbancia a 550nm, según las indicaciones del fabricante. Los datos se expresaron como porcentaje de células viables.

2.5.- Determinación de nitritos.

Los niveles de nitritos en el medio de cultivo como medida de la producción de óxido nítrico, se evaluaron en el sobrenadante de células SH-SY5Y y de cultivos mesencefálicos cultivados en placas de 96 pocillos. Estos cultivos fueron tratados con diversos compuestos 2 horas antes de su exposición a 6-OHDA (los cultivos de SH-SY5Y) o a LPS (los cultivos mesencefálicos). La medición de los niveles de nitrito producidos se realizó, tras 24 horas en contacto con el agente citotóxico. Para ello se mezcló la misma cantidad de sobrenadante que de reactivo de Griess (40mg/ml agua) y tras 15 minutos de incubación a temperatura ambiente se midió la absorbancia a 540nm con un lector de placas. La concentración de nitrito se determinó a partir de una curva patrón con concentraciones conocidas de nitrito de sodio.

2.6.- Medición de lactato deshidrogenasa (LDH).

Para estimar el daño celular se midieron los niveles de lactato deshidrogenasa (LDH) liberado por las células SH-Y5Y dañadas, en el medio de cultivo, 24 horas después de su exposición a 6-OHDA. Se utilizó un método colorimétrico que mide la cantidad de sal de formazán que se forma tras la conversión de lactato a piruvato, puesto que la reducción de la sal de formazán es proporcional a la actividad LDH existente. Se tomó el sobrenadante de los cultivos y se incubó con el correspondiente reactivo de acuerdo con las instrucciones del fabricante (Kit de detección de citotoxicidad de Roche) durante 1h a temperatura ambiente. La intensidad del color obtenido en el ensayo, medido en un lector de placas a 490nm, fue proporcional a la actividad LDH y por tanto al número de células dañadas. Los datos se expresaron como porcentaje de daño citotóxico.

2.7.- Medición de los niveles de AMPc.

Los niveles intracelulares de AMPc se midieron en cultivos de SH-SY5Y con un sistema inmunoenzimático (GE Healthcare, Amersham, UK). Las células previamente sembradas durante 24 horas en placas multipocillo de 96 (30.000 células /pocillo) fueron tratadas durante 1h con S14, BRL y Rol. A continuación se lisaron y se midieron los niveles de AMPc siguiendo las instrucciones del fabricante. La lectura colorimétrica se realizó en un lector de placas a 450 nm. Todas las lecturas se normalizaron con la correspondiente curva patrón con niveles de AMPc conocidos. Se hicieron al menos tres experimentos independientes, cada uno de ellos por triplicado, y la cantidad de AMPc se expresó en fmol/pocillo.

2.8.- Medición de la muerte celular por apoptosis.

Se utilizaron para ello dos procedimientos estándar, determinar por un lado la presencia de fosfatidilserina en la cara externa de la membrana celular y por otro la cantidad de caspasa 3 activa, ambos métodos claramente reconocidos como marcadores de apoptosis. La cantidad de fosfatidilserina se midió con inmunotinción con anexina V acoplada a FITC (Bender MedSystems) y observación con microscopio confocal. Los niveles de caspasa-3 activada se determinaron por inmunocitoquimica usando un anticuerpo especifico anti caspasa-3 activada (R&D Systems). La cuantificación de células positivas para ambos marcadores de apoptosis se realizó en 20 campos independientes a 400x aumentos.

3.- ANÁLISIS ESTADÍSTICO.

Los análisis estadísticos fueron llevados a cabo mediante el soporte informático SPSS (Inc., Chicago, IL). Las comparaciones de medias entre variables continuas de distribución normal ser realizó utilizando el test *t* de *Student*. Las comparaciones entre diferentes grupos de animales se realizaron mediante un análisis ANOVA seguido de un test Newman-Keuls óptimo para comparaciones múltiples. Los datos ofrecidos se expresan como la media ± desviación estándar (ds) o como media ± error estándar (es). Todos los *p-valores* indicados son de dos colas, estableciéndose la significancia estadística como $p \leq 0.05$.

Resultados

1. -EFECTO NEUROGÉNICO DE LOS LIGANDOS DE PPARγ.

1.1.- Efecto de la pioglitazona sobre la proliferación celular en la zona subventricular.

Inicialmente analizamos la expresión PPARγ en el cerebro adulto, prestando especial interés a las zonas neurogénicas. Los resultados se muestran en la figura 1. Como puede observarse esta proteína esta ampliamente distribuida en el cerebro tal como muestra el análisis por Western blot de diversas áreas cerebrales (figura 1A). También es abundante en los dos principales nichos neurogénicos del adulto, el giro dentado del hipocampo y la zona subventricular (ZSV), como muestra el análisis inmunohistoquímico (figura 1B). Además, encontramos también expresión de PPARγ a lo largo de toda la corriente migratoria rostral (CMR) desde la ZSV hasta el bulbo olfatorio (BO), tal y como muestra la sección sagital de en la figura 1B (panel central).

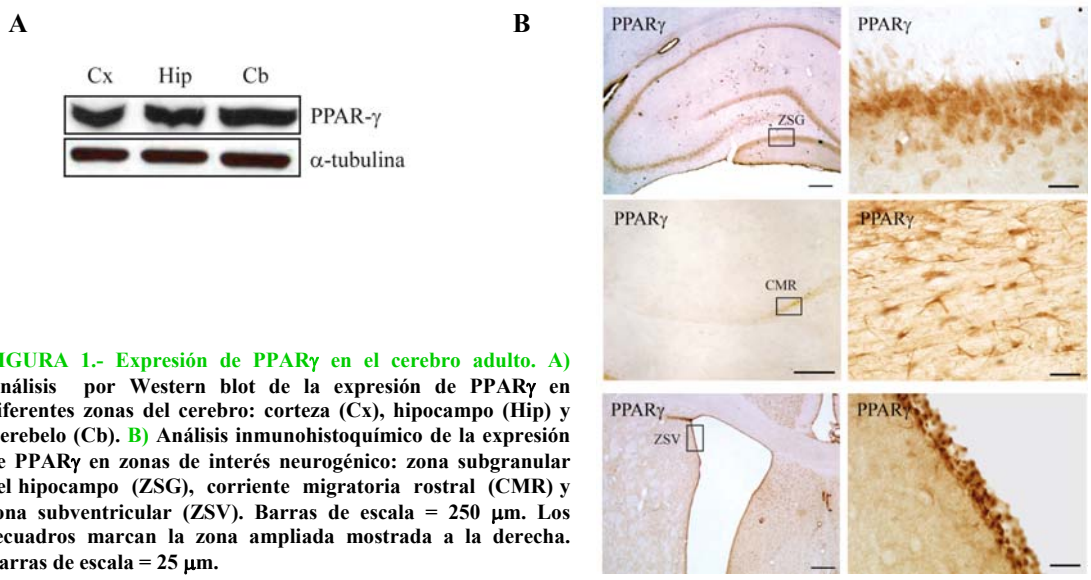

FIGURA 1.- Expresión de PPARγ en el cerebro adulto. A) Análisis por Western blot de la expresión de PPARγ en diferentes zonas del cerebro: corteza (Cx), hipocampo (Hip) y Cerebelo (Cb). B) Análisis inmunohistoquímico de la expresión de PPARγ en zonas de interés neurogénico: zona subgranular del hipocampo (ZSG), corriente migratoria rostral (CMR) y zona subventricular (ZSV). Barras de escala = 250 µm. Los recuadros marcan la zona ampliada mostrada a la derecha. Barras de escala = 25 µm.

A continuación analizamos el efecto de la pioglitazona, un ligando específico de PPARγ, sobre la proliferación en la ZSV y la CMR. Se eligió pioglitazona para el estudio *in vivo*, frente a otros ligandos de este receptor, por su capacidad para atravesar la barrera hematoencefálica (Brodbeck et al., 2008; Maeshiba et al., 1997). La pioglitazona, administrada oralmente durante 3 días, claramente aumentó el número de células positivas para BrdU en la ZSV y la CMR (figura 2). En la ZSV se observó un aumento de un 35% en el número de células $BrdU^+$ tras el tratamiento con pioglitazona (figuras 2B, 2E). En la CMR este aumento fue de un 40 % (figuras 2D, 2F). Los resultados de la tinción histológica también permitieron observar un aumento en el tamaño de la ZSV (figura 2A) así como una mayor dispersión de la CMR (figura 2C) en los animales tratados con pioglitazona.

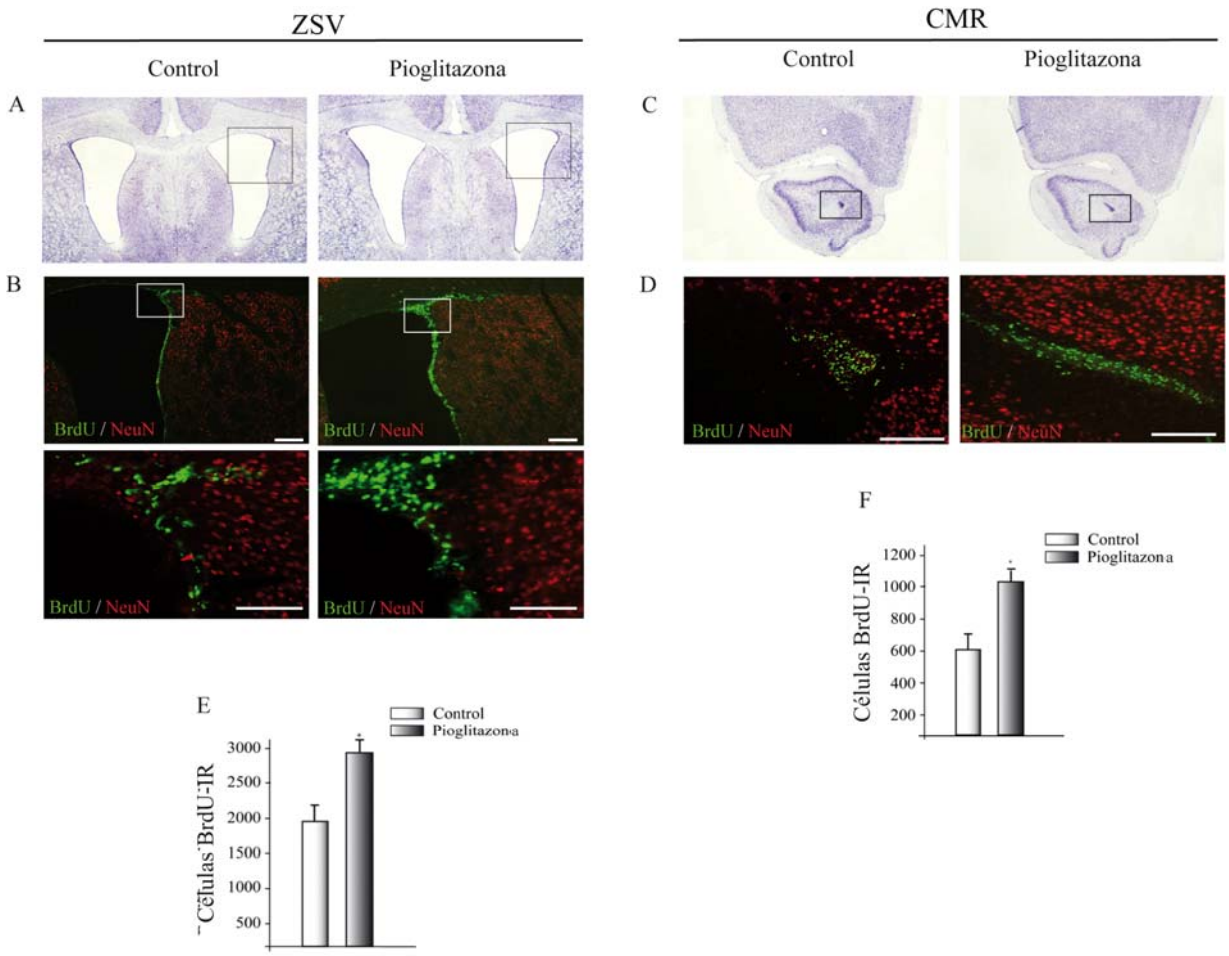

FIGURA 2.- Efecto de la pioglitazona sobre la proliferación celular en la zona subventricular y la corriente migratoria rostral. Secciones coronales de animales control y tratados con pioglitazona se tiñeron con violeta de cresilo (Nissl) o se inmunotiñeron con anticuerpos anti-BrdU (verde) y anti-NeuN (rojo). Los recuadros en A y C muestran las zonas ampliadas en B y D. Los recuadros en B muestran la zona ampliada debajo. E y F muestran la cuantificación del número de células BrdU inmunoreactivas (IR) en la ZSV y la CMR. Los valores representan la media ± ds correspondiente a cinco animales distintos. *P<0.05. Barra de escala en B y D = 200 µm y en las ampliaciones 100 µm.

Para una mejor caracterización del efecto de la pioglitazona en la ZSV y la CMR se realizó un análisis inmunohistoquímico, sobre secciones coronales y sagitales, con distintos marcadores: doblecortina (DCX), como marcador endógeno de neuroblastos y neuronas inmaduras (Brown et al., 2003; Couillard-Despres et al., 2005); la forma polisialilada de la molécula de adhesión celular neural (PSA-NCAM), como marcador específico de neuroblastos en la CMR (Battista and Rutishauser; Bonfanti and Theodosis, 1994; Rousselot et al., 1995) y β-tubulina III como marcador de nuevas neuronas en migración (Doetsch and Alvarez-Buylla, 1996).

Nuestros resultados muestran que la pioglitazona en la CMR aumentó significativamente el número de células DCX^+ (figura 3A) particularmente en algunas zonas como el brazo anterior y el "*codo*" de la CMR. Lo mismo se observó en el caso de PSA-NCAM, que se expresaba de manera abundante a lo largo de toda la CMR, existiendo mayor inmunoreactividad en los animales tratados con pioglitazona (figura 3C). La administración de pioglitazona también promovió un aumento en la expresión de DCX en la ZSV, con la presencia de un mayor número de cadenas migratorias (figura 3B). Por último nuestros resultados muestran un aumento en la expresión de β-tubulina en la ZSV de los animales tratados con pioglitazona (figura 3D).

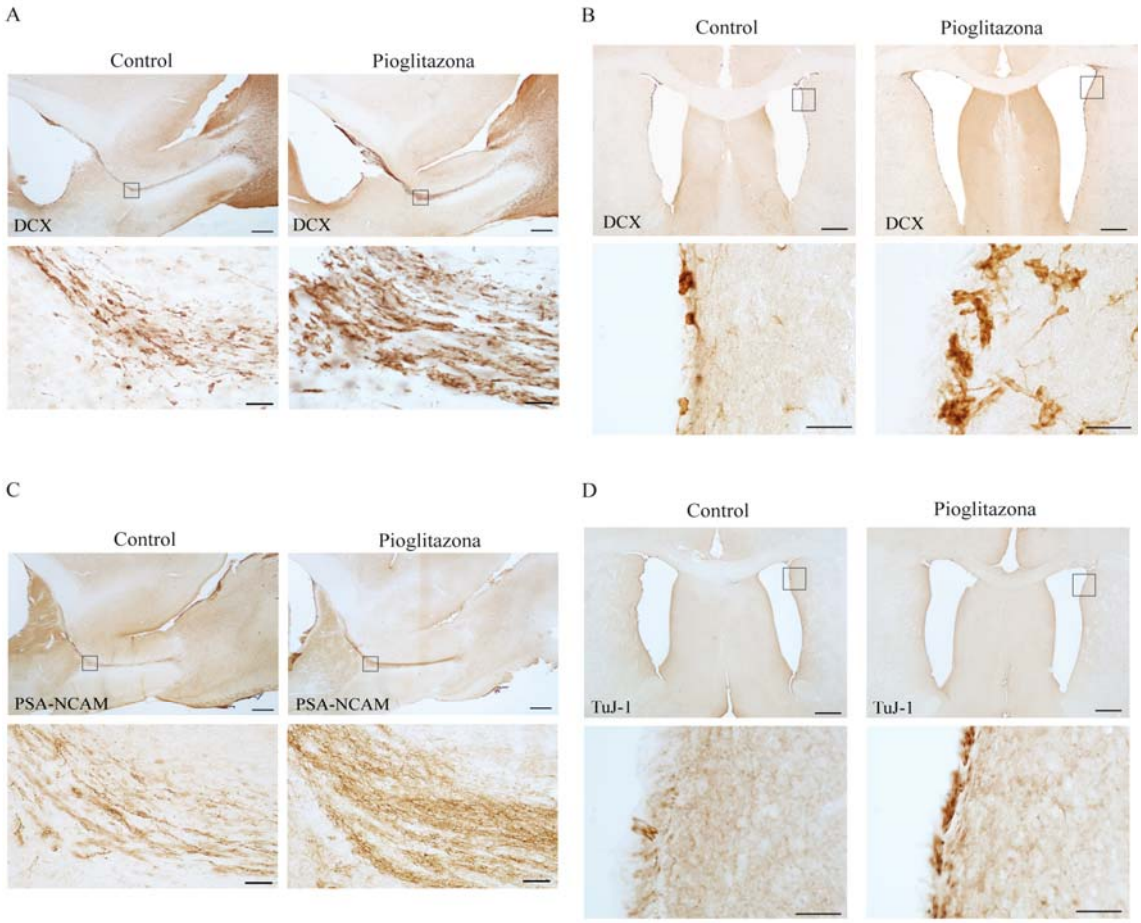

FIGURA 3.- Efecto de la pioglitazona sobre los precursores neurales y su capacidad migratoria en la zona subventricular (ZSV) y la corriente migratoria rostral (CMR). (A, B) Expresión de DCX en la CMR y en la ZSV mediante tinción inmunohistoquímica en animales control y tratados con pioglitazona. Los recuadros en A y B muestran la zona ampliada en la imagen inferior (C) Imágenes representativas de la inmunotinción de PSA-NCAM en la CMR. Los recuadros muestran la zona ampliada en la imagen inferior. (D) Imágenes representativas de la inmunotinción de β-III-tubulina (TuJ-1) en la ZSV de animales control y tratados con pioglitazona. Los recuadros muestran la zona ampliada en la imagen inferior. Barras de escala en A, B, C y D = 250 µm y en las ampliaciones 25 µm.

1.2.- Efecto de la pioglitazona sobre la migración celular desde la ZSV.

Se analizaron las características morfológicas de la ZSV en animales controles y tratados con pioglitazona mediante microscopía electrónica de transmisión (MET). Esta técnica nos permitió identificar y caracterizar los diferentes tipos de células en la ZSV en base a sus características ultraestructurales (Danilov et al., 2009; Doetsch et al., 1997). Inicialmente se tiñeron con azul de toluidina secciones coronales semifinas de la pared lateral de la ZSV, lo que nos permitió ver la composición de las células que componen la ZSV. En la figura 4A pueden verse, en los animales control, cadenas de neuroblastos próximas al límite entre el epéndimo de la ZSV y el neuropilo subyacente. Los animales tratados con pioglitazona (figura 4B) presentaban una ZSV con un área ependimaria mas desarrollada y un mayor número de neuroblastos migrando (flechas en figura 4B), localizados mas profundamente en el neuropilo.

En los animales controles se observó la típica estructura de la ZSV, con una zona ependimaria en cuyo límite aparecían cadenas de células migradoras de tipo A (figura 4C, área punteada). Estas células se identificaron por su pequeño tamaño y por tener un núcleo denso y escaso citoplasma, características propias de células migradoras. Los astrocitos o células de tipo B se identificaron por su soma de mayor tamaño y su citoplasma menos denso, rico en filamentos intermedios. El tratamiento con pioglitazona alteró la estructura de la ZSV (figura 4D). Se observó un aumento del número de neuroblastos que, en comparación con los animales control (figura 4C), poseían una morfología irregular y se localizaban en un área más alejada de la línea basal que separa el área ependimaria. Otro cambio observado con respecto a los controles (figura 4E) fue que los espacios intercelulares entre las células migradoras eran mayores en los animales tratados con pioglitazona (flechas en figura 4F). Con respecto a la CMR, pudo observarse que en los animales tratados con pioglitazona había un mayor número de células formando parte de las cadenas de neuroblastos migrando (figura 4H). Estas células presentaban una mayor dispersión, tendiendo a formar una CMR mas expandida, en comparación con el control (figura 4G).

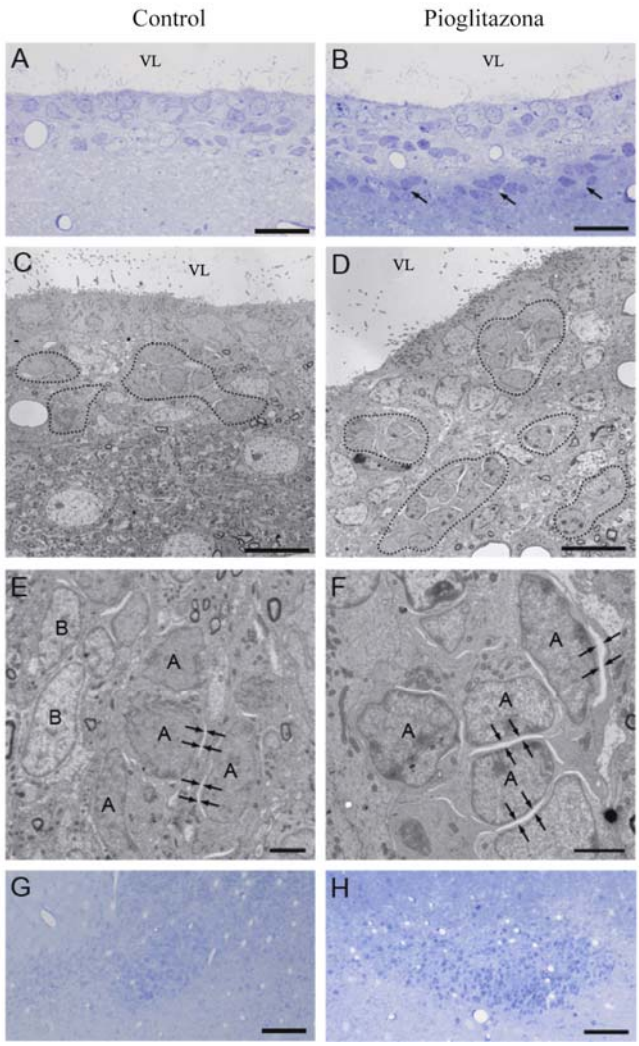

Figura 4.- Efecto de la pioglitazona sobre la migración celular en la zona subventricular (ZSV) y en la corriente migratoria rostral (CMR). (A) Sección semifina teñida con azul de toluidina mostrando la ZSV de animales control su citoarquitectura típica. (B) Los animales tratados intragástricamente con pioglitazona presentan mayor número de neuroblastos migrando (flechas) en la ZSV. (C) Ultraestructura de la ZSV de un animal control. El área punteada junto al epéndimo muestra cadenas de células tipo A migrando. (D) El tratamiento con pioglitazona incrementa el número de cadenas de neuroblastos migrando (zona punteada), las cuales además se localizan en zonas mas profundas con respecto al epéndimo. (E) Típica cadena de neuroblastos migrando. Las flechas marcan los espacios intercelulares entre las células en migración. También se observan grupos de células tipo B (astrocitos) formando parte de esas cadenas migradoras. (F) Detalle de cadenas migradoras de animales tratados con pioglitazona en los que se observan mayores espacios intercelulares entre los neuroblastos en migración (flechas). (G) Sección semifina teñida con azul de toluidina mostrando la CMR de un animal control, caracterizada por la presencia de cadenas migradoras formando masas celulares densas y compactas. (H) CMR de un animal tratado con pioglitazona donde se observan grandes grupos con gran densidad de células y una mayor distribución en comparación con el control. VL: ventrículo lateral. Barras de escala en A y B = 20 µm; C y D = 10 µm; E y F = 2 µm; G y H = 50 µm.

1.3.- Efecto de la pioglitazona sobre la formación de nuevas neuronas en el bulbo olfatorio.

Dado que la pioglitazona estimula la proliferación y migración de los neuroblastos en la ZSV, estudiamos si éstos completaban su ciclo llegando al bulbo olfatorio para finalmente diferenciarse. Para ello realizamos un análisis inmunohistoquímico 21 días después del tratamiento con pioglitazona y de la inyección de BrdU. Tras ese tiempo, la mayoría de las células BrdU positivas ya han llegado a la capa celular granular del bulbo olfatorio a través de la CMR y expresan un fenotipo neuronal (Winner et al., 2002). Determinamos la cantidad de células BrdU y NeuN positivas en el bulbo olfatorio de animales controles e inyectados con pioglitazona. Nuestros resultados muestran que el número de células doblemente marcadas ($BrdU^+/NeuN^+$) aumentaba en la capa glomerular del bulbo olfatorio tras el tratamiento con pioglitazona (figura 5A y B).

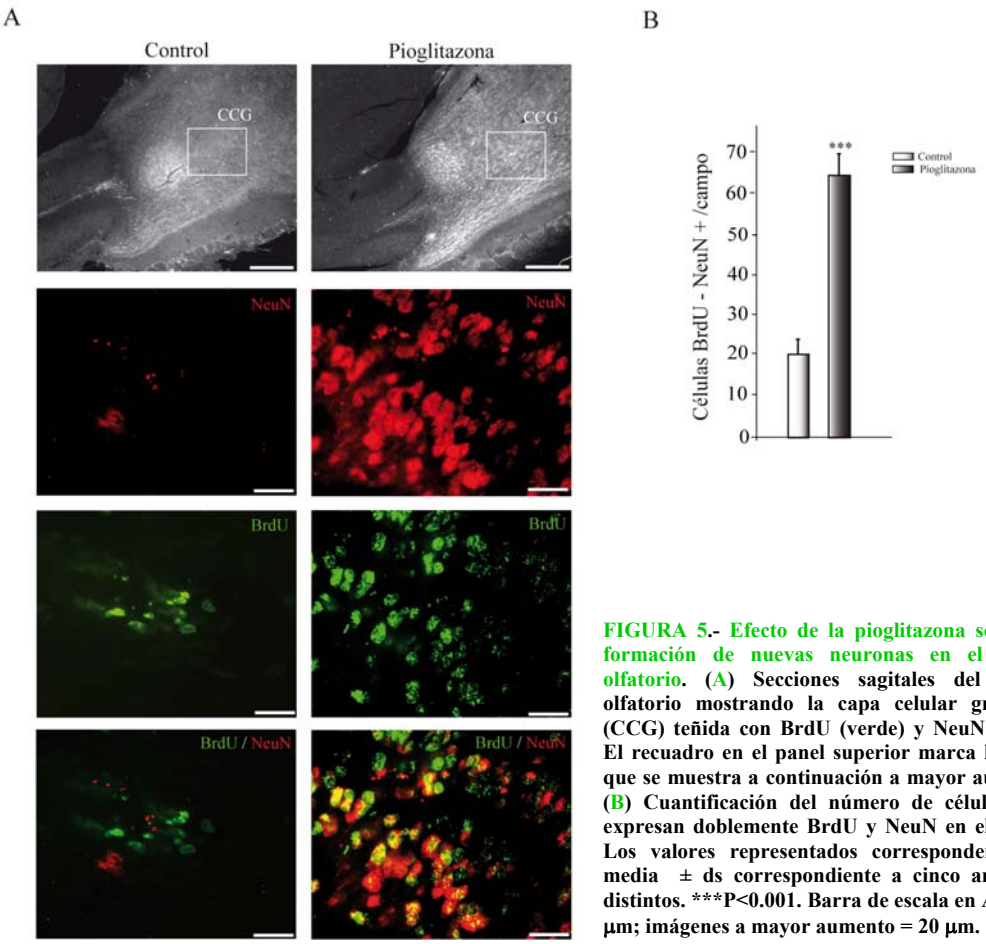

FIGURA 5.- Efecto de la pioglitazona sobre la formación de nuevas neuronas en el bulbo olfatorio. (A) Secciones sagitales del bulbo olfatorio mostrando la capa celular granular (CCG) teñida con BrdU (verde) y NeuN (rojo). El recuadro en el panel superior marca la zona que se muestra a continuación a mayor aumento (B) Cuantificación del número de células que expresan doblemente BrdU y NeuN en el CCG. Los valores representados corresponden a la media ± ds correspondiente a cinco animales distintos. ***P<0.001. Barra de escala en A = 100 µm; imágenes a mayor aumento = 20 µm.

1.4.- Efecto de pioglitazona y rosiglitazona sobre la neurogenesis *in vitro*.

En vista de los resultados observados, nos propusimos estudiar a continuación el mecanismo de acción de pioglitazona y rosiglitazona (otro ligando específico de PPARγ) como agentes neurogénicos y en qué medida se encuentra implicado PPARγ en todo el proceso. Para ello llevamos a cabo estudios *in vitro*, utilizando un modelo experimental de cultivo con neuroesferas (NS) primarias y secundarias derivadas de células madre neurales. Inicialmente estudiamos si estas células expresan PPARγ mediante análisis de Western blot. Tal y como muestra la figura 6, PPARγ se expresa en neuroesferas, independientemente de su estado de diferenciación.

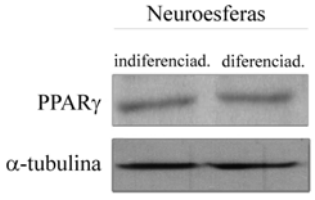

FIGURA 6.- Expresión de PPARγ en neuroesferas. Western blot representativo de la expresión de PPARγ en neurosferas indiferenciadas (crecidas en flotación durante 7 días) y diferenciadas (crecidas en medio de adhesión durante 2 dias).

A continuación descartamos que las concentraciones usadas de estos compuestos tuvieran efecto tóxico. Para ello analizamos por inmunocitoquímica los niveles de caspasa-3 activada. Como puede observarse en la figura 7, no observamos efecto tóxico de estos compuestos a las concentraciones utilizadas.

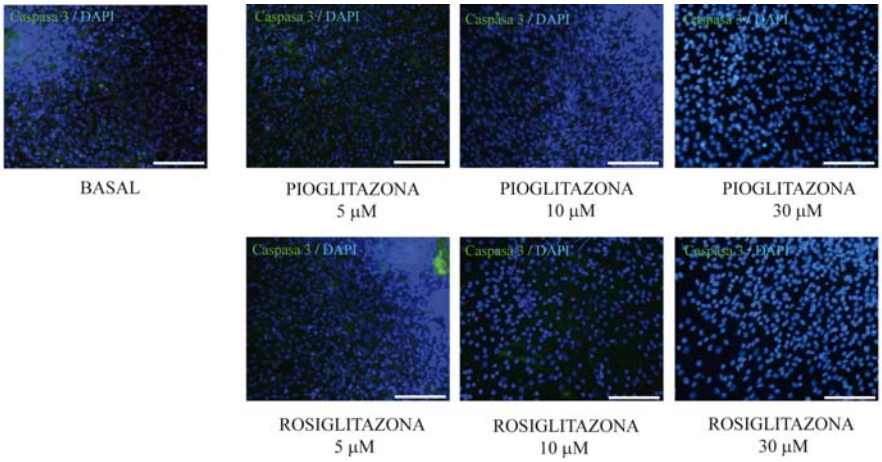

FIGURA 7.- Efecto de la pioglitazona y rosiglitazona sobre la viabilidad celular. Análisis inmunocitoquímico de la activación de caspasa 3. Se tiñeron las células madre después de 7 dias de cultivo con un anticuerpo anti-caspasa 3 activada (verde). Los núcleos se tiñeron con DAPI (azul). Barra de escala = 100 µm.

Evaluamos el efecto de ambos ligandos sobre la capacidad de formación de NS, determinando el número de NS formadas y el tamaño de las mismas. Tras 10 días de cultivo en presencia de pioglitazona y rosiglitazona, encontramos un aumento significativo tanto en el número como en el diámetro de NS primarias (figura 8A y B). En el caso de la pioglitazona obtuvimos 310±12 NS primarias con un diámetro medio de 212±6 µm y de 323±10 NS con un diámetro medio de 219±9 µm en el caso de la rosiglitazona, frente a las 183±14 NS con un diámetro medio de 94±7 µm de los controles. Ambos compuestos también aumentaron la capacidad de formación de neurosferas secundarias, como puede observarse en la figura 8. En presencia de pioglitazona se obtuvieron 341±15 NS con un diámetro medio de 219±5 µm y en el caso de rosiglitazona 336±12 NS con un diámetro medio de 198±5 µm, frente a las 210±10 NS con un diámetro medio de 96±5 µm de los controles. Nuestros resultados *in vitro* concuerdan con los resultados obtenidos previamente in vivo y sugieren claramente que estos compuestos tienen un importante efecto promotor de la neurogenesis y autorenovación de las células madres. A continuación analizamos si la acción de pioglitazona y rosiglitazona estaba mediada por PPARγ. Para ello utilizamos dos antagonistas específicos de PPARγ, GW9662 (GW) y T0070907 (T). Los resultados se muestran en la figura 8A y B. Como puede observarse, ambos antagonistas bloquearon el efecto de la pioglitazona y la rosiglitazona en las neuroesferas primarias. No se observó ningún efecto sobre el número y tamaño de las neuroesferas cuando se cultivaron solamente en presencia de GW y T

(figura 8A, B). Resultados similares se obtuvieron en el caso de la formación de NS secundarias con el uso de GW, datos mostrados en la figura 8B. Estos resultados por tanto sugieren que tanto la pioglitazona como la rosiglitazona ejercen su acción a través de PPARγ.

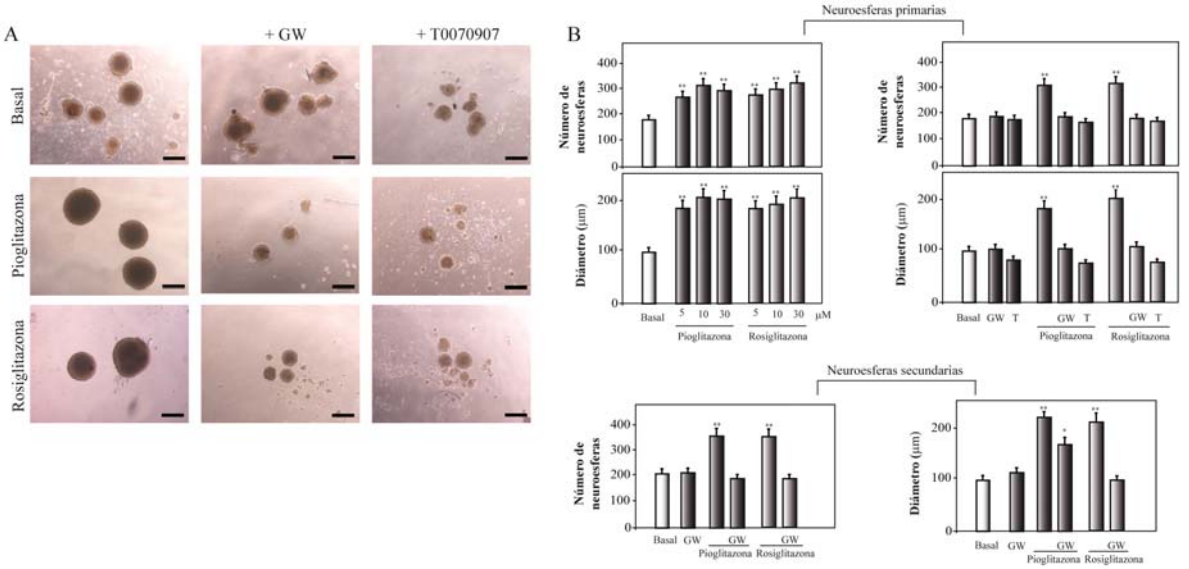

FIGURA 8.- Efecto de piotglitazona y rosiglitazona sobre la formación y crecimiento de neuroesferas. (A) Fotografías representativas del tamaño de las NS crecidas en flotación durante 7 días en presencia o ausencia de pioglitazona (10 µM) y de rosiglitazona (30 µM). Algunos de los cultivos fueron pre-incubados durante 1h con 30 µM GW9663 (GW) o con 50 µM T0070907 (T) antes de la adición de los ligandos de PPARγ. Barra de escala = 50 µm; (B) Cuantificación del efecto de las diferentes dosis de pioglitazona y rosiglitazona (5, 10 y 30 µM) sobre el crecimiento de las neuroesferas primarias. Se evaluó también el número de NS secundarias formadas así como su diámetro y el efecto de los antagonistas GW y T, sobre la acción de pioglitazona y rositglitazona. Los valores representados corresponden a la media±ds correspondiente a tres experimentos distintos, realizados por triplicado. *P < 0.05; **P<0.01, con respecto al basal.

Puesto que la pioglitazona y la rosiglitazona indujeron la formación de NS y aumentaron su tamaño, el siguiente paso fue estudiar su efecto sobre un marcador específico de células en división, como es la proteina Ki67. Tras 7 días de tratamiento de los cultivos con pioglitazona y rosiglitazona, observamos un claro aumento en el numero de células que expresaban Ki67 en las NS primarias, (figura 9). Estos datos indican un claro efecto de estos compuestos sobre la proliferación celular.

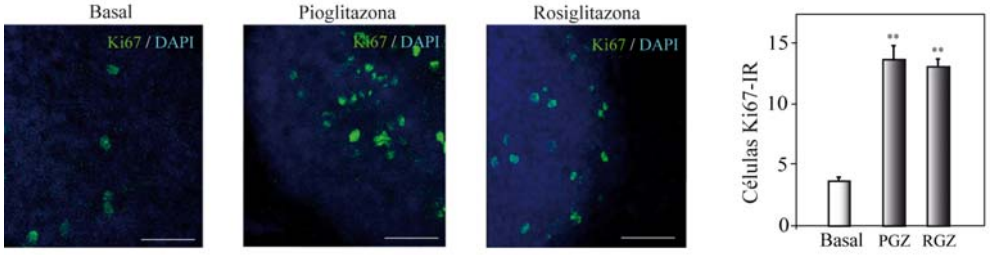

FIGURA 9.- Efecto de pioglitazona y rosiglitazona sobre la expresión de Ki67. Imágenes representativas de microscopía confocal mostrando la expresión de Ki67 (verde) en neuroesferas primarias. Los núcleos se tiñeron con DAPI (azul). Se muestra también la cuantificación de dichas células Ki67 inmunoreactivas (IR) en cultivos de NS tratados con pioglitazona (PGZ) y rosiglitazona (RGZ). Barra de escala = 100 µm Los resultados reflejan la media ± ds correspondiente a tres experimentos independientes realizados por triplicado.

1.5.- Efecto de la pioglitazona y la rosiglitazona sobre la migración celular en cultivos de neuroesferas.

El posible efecto de los ligandos de PPARγ sobre la migración de células madres neurales se analizó tratando las NS, previamente pegadas sobre cristal, con pioglitazona y rosiglitazona durante 48h. Los resultados obtenidos muestran que el tratamiento con ambos ligandos (figura 10A) durante ese tiempo producía un aumento en la migración de las células fuera de la NS. La pioglitazona y la rosiglitazona indujeron un incremento de la migración de 1.6 y 1.5 veces, respectivamente, en comparación con el control, (figura 10B). En el grupo control, las células permanecían formando grupos siempre cercanos al núcleo de la NS (figura 10A). Por el contrario, en los cultivos tratados con los ligandos de PPARγ las células migraron notablemente, alejándose del núcleo de la NS (figura 10A) incluso llegándose a solapar las áreas de migración entre NS adyacentes.

Analizamos de nuevo si este efecto sobre la migración celular estaba mediado por la activación de PPARγ, para lo cual utilizamos un antagonista selectivo, GW9662. Los resultados obtenidos muestran que GW9662 bloquea el efecto de la pioglitazona y la rosiglitazona sobre la migración de células fuera de la NS (Figura 10). Estos resultados sugieren la implicación del receptor de PPARγ en los efectos pro-migratorios observados con pioglitazona y rosiglitazona. Por tanto, la activación de PPARγ jugaría un papel regulador en la formación y migración de neuroblastos en cerebro de rata adulta.

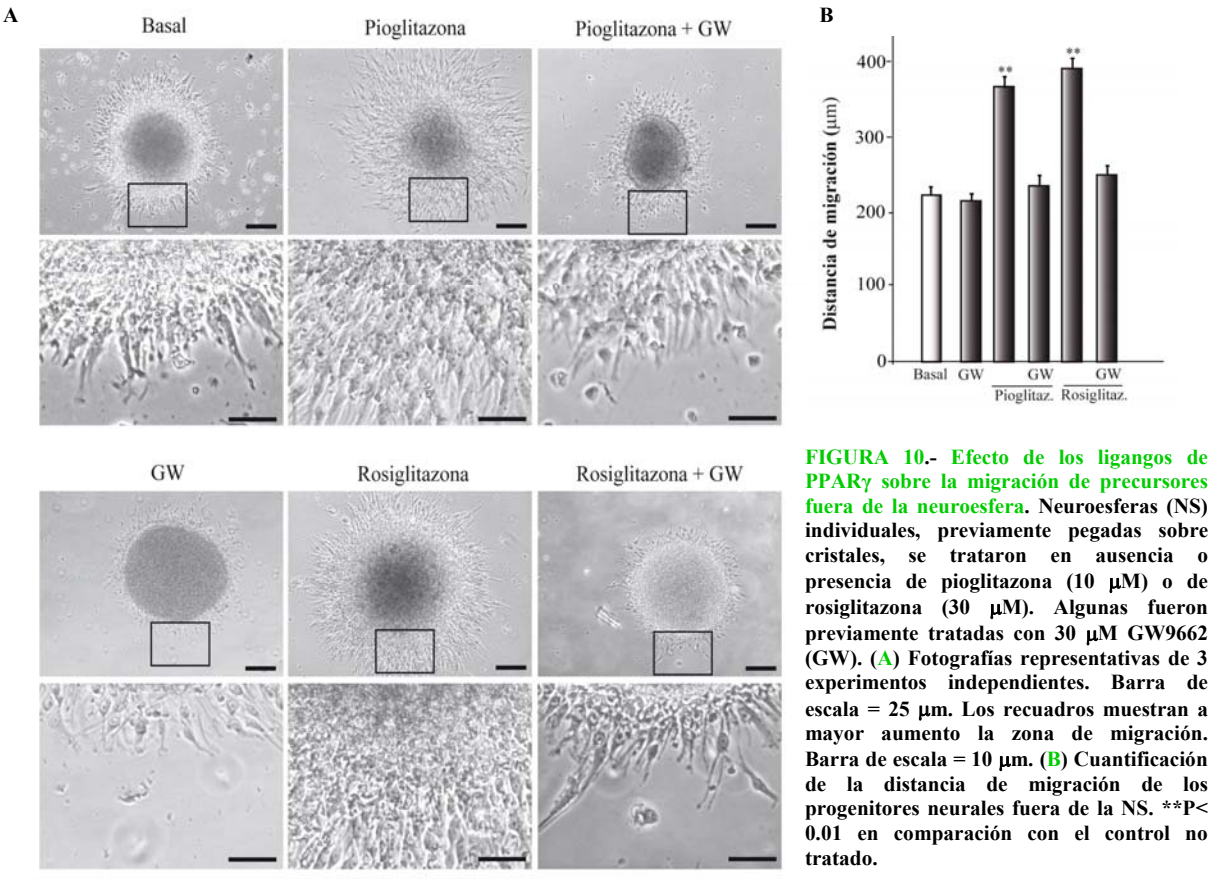

FIGURA 10.- Efecto de los ligangos de PPARγ sobre la migración de precursores fuera de la neuroesfera. Neuroesferas (NS) individuales, previamente pegadas sobre cristales, se trataron en ausencia o presencia de pioglitazona (10 µM) o de rosiglitazona (30 µM). Algunas fueron previamente tratadas con 30 µM GW9662 (GW). (A) Fotografías representativas de 3 experimentos independientes. Barra de escala = 25 µm. Los recuadros muestran a mayor aumento la zona de migración. Barra de escala = 10 µm. (B) Cuantificación de la distancia de migración de los progenitores neurales fuera de la NS. **P< 0.01 en comparación con el control no tratado.

1.6.- Efecto de la pioglitazona y la rosiglitazona sobre la diferenciación de células madre neurales.

Nuestro siguiente objetivo fue determinar si dichos compuestos regulaban la diferenciación celular en cultivos de neuroesferas. Para ello, analizamos mediante inmunocitoquímica la presencia de los diferentes tipos de células del sistema nervioso central, dentro y fuera de la NS. Utilizamos MAP-2 como marcador de neuronas y GFAP como marcador de astrocitos. Nuestros resultados mostraron que había muy pocas células marcadas con GFAP y MAP-2 en los cultivos de NS control (figura 11). Sin embargo, el tratamiento con los ligandos de PPARγ produjo un aumento notable en el número de células que expresan MAP-2 y GFAP, fundamentalmente en las células que salen de la NS (figura 11). El aumento en la inmunoreactividad para GFAP, (figura 11A), no solo afectaba al número de células sino también al tamaño de las prolongaciones que salían de las células, que eran mas gruesas y largas (imágenes ampliadas en figura 11A). Resultados similares se obtuvieron en el análisis con MAP-2.

La incubación con GW previa al tratamiento con pioglitazona y rosiglitazona inhibió el efecto de estos dos compuestos sobre la diferenciación celular. Estos datos indican que el efecto tanto de pioglitazona como rosiglitazona sobre la diferenciación de células madre neurales se debe a su unión a PPARγ, promoviendo su activación.

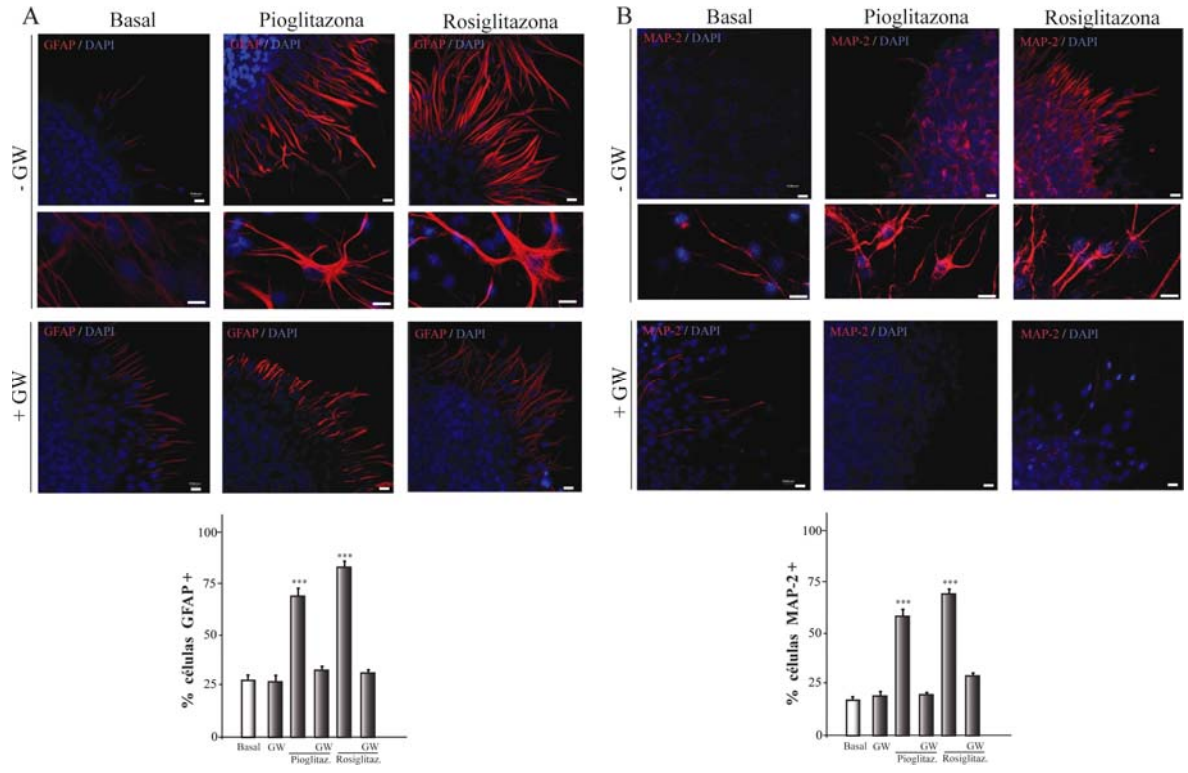

FIGURA 11.- Efecto de rosiglitazona y pioglitazona sobre la diferenciación celular en neuroesferas. Las NS fueron tratadas o no con pioglitazona (10 µM) y rosiglitazona (30 µM) durante 7 días y pegadas sobre cristales para que diferenciasen durante 48h. Algunos cultivos se incubaron con GW9662 (GW, 30 µM que se añadió 1h antes que rosiglitazona o pioglitazona. (A) Expresión de GFAP (rojo) y cuantificación del número de células GFAP$^+$. (B) Expresión del marcador neuronal MAP-2 (rojo) y cuantificación del número de células MAP2$^+$. En ambos casos se tiñeron los núcleos con DAPI (azul). Las fotografías a mayor aumento muestran en detalle algunas de las células localizadas en los extremos de la neuroesfera. Los resultados reflejan la media ± ds correspondiente a tres experimentos independientes realizados por triplicado. Barra de calibración = 10 µm. ***P<0.001.

2.- EFECTO NEUROGÉNICO DE LOS INHIBIDORES DE GSK-3β.

La inhibición selectiva de GSK-3β se ha realizado mediante el uso de tres inhibidores clásicos: Alsterpaulona, inhibidor VII e inhibidor VIII, así como de nuevos inhibidores sintetizados en el Instituto de Química Médica de Madrid (CSIC) por el grupo de la Dra. Ana Martínez. En concreto estos compuestos son NP031111, NP031112 y NP031115 que pertenecen a la familia de las tiadiazolidinonas (TDZDs) y se describieron como los primeros fármacos capaces de inhibir a GSK-3β de manera no competitiva con el ATP (Martinez et al., 2002a). Por su parte los compuestos denominados VPs (VP 2.51, VP2.54, VP3.16, VP3.31, VP3.35) son inhibidores estructurales de GSK-3β. VP 2.51 y VP 2.54 pertenecen a la familia de los tiazoles; VP 3.16 es una maleimida, mientras que VP 3.31 y VP3.35 son benzimidazoles.

2.1.- Efecto de la inhibición de GSK-3β sobre el crecimiento y supervivencia de células madre neurales en cultivo (neuroesferas).

Después de tratar las neuroesferas durantes 7 días con los inhibidores de GSK-3β indicados, observamos que tanto el número de neuroesferas formadas como el diámetro de las mismas era significativamente mayor después del tratamiento con todos los inhibidores utilizados (figura 12) en comparación con los cultivos control. Para evaluar la capacidad de formación de NS secundarias, y basándonos en los resultados obtenidos con las NS primarias, seleccionamos alsterpaulona, un inhibidor clásico de GSK-3β, y NP031112. Los resultados mostrados en la figura 12B demuestran como la inhibición de GSK-3β por parte de alsterpaulona y NP031112 promovía también una mayor formación de NS secundarias, en comparación con el control.

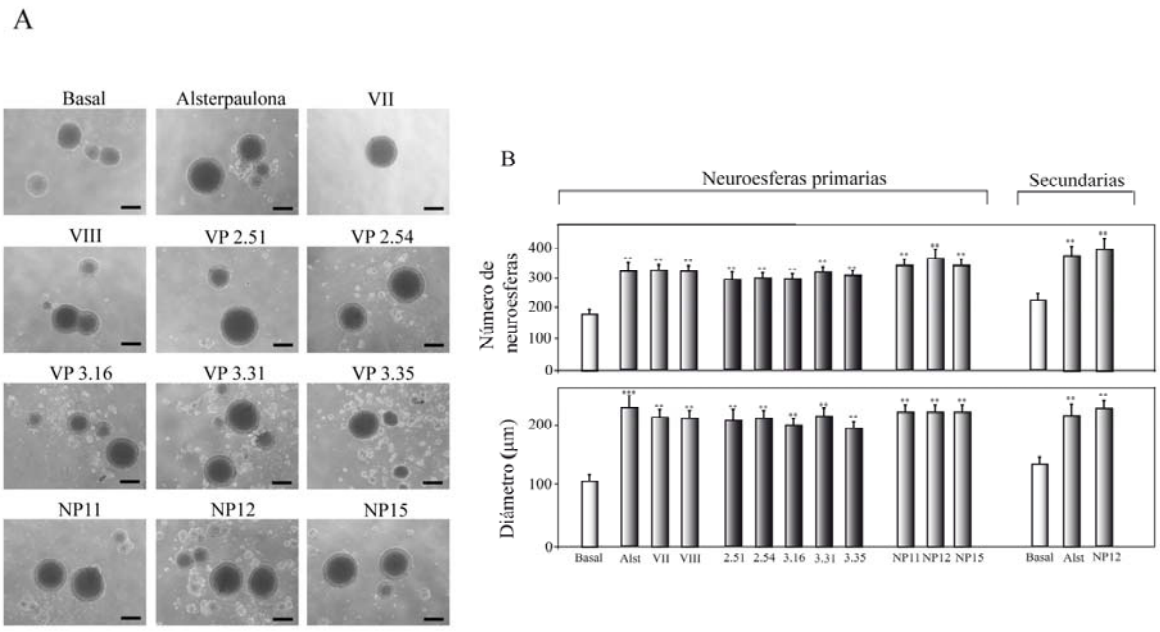

La figura 12 continúa en la página siguiente

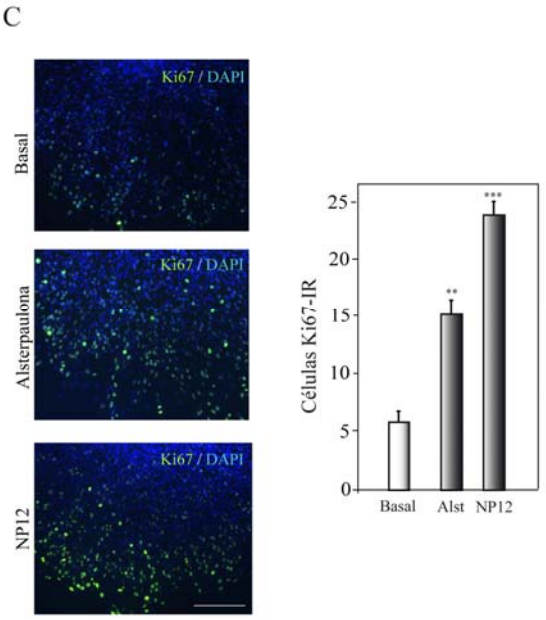

FIGURA 12.- Efecto de la inhibición de GSK-3β sobre la formación y crecimiento de neuroesferas en cultivo. (A) Imágenes representativas del tamaño de las NS en presencia de los distintos inhibidores de GSK-3β (todos a una concentración de 10μM). (B) Efecto de los inhibidores de GSK-3β (10 μM) sobre el crecimiento de las NS. Se evaluaron dos parámetros: 1) número de NS formadas y 2) diámetro de las NS. Dos de los inhibidores de GSK-3β más potentes, Alsterpaulona y NP12 (10 μM) se utilizaron para evaluar el efecto de la inhibición de GSK-3β sobre la formación y crecimiento de NS secundarias. Barra de escala = 50 μm. (C) Expresión de Ki67 (verde) y cuantificación de las células inmunoreactivas (IR) en NS primarias tratadas con Alsterpaulona y NP12. Los núcleos se tiñeron con DAPI (azul). Barra de escala = 75 μm. Los resultados de las cuantificaciones reflejan la media ± ds correspondiente a tres experimentos independientes realizados por triplicado. **P<0,01; ***P<0.001, con respecto al basal.

Una vez comprobado que la inhibición de GSK-3β inducía la formación de un mayor número de NS, y de mayor tamaño, a continuación evaluamos si ese aumento era debido a un aumento de la proliferación en los progenitores neurales. Para ello utilizamos Ki67 como marcador específico de células en división. Tras 7 días de tratamiento de los cultivos con los inhibidores de GSK-3β, encontramos que el numero de células Ki67+ aumentaba significativamente en comparación con los cultivos controles sin tratar, (figura 12D), lo que indica un claro efecto inductor de la proliferación por parte de estos compuestos.

2.2.-Efecto de la inhibición de GSK-3β sobre la migración celular en cultivos de neuroesferas.

Para evaluar si la inhibición de GSK-3β era capaz de modular la migración de células fuera de la propia NS, tratamos las NS, previamente pegadas sobre cristal, con alsterpaulona y NP031112 durante 48h. Nuestros resultados mostraron que ambos compuestos (figura 13A) indujeron la migración de las células fuera de la NS. La migración, medida por la máxima distancia desde el borde de la neurofera, fue 3 veces superior en presencia de NP031112 comparada con el control, mientras que con la alsterpaulona el incremento fue de 2 veces (figura 13B). En el grupo control, las células permanecieron formando grupos siempre cercanos al núcleo de la NS (figura 13A).

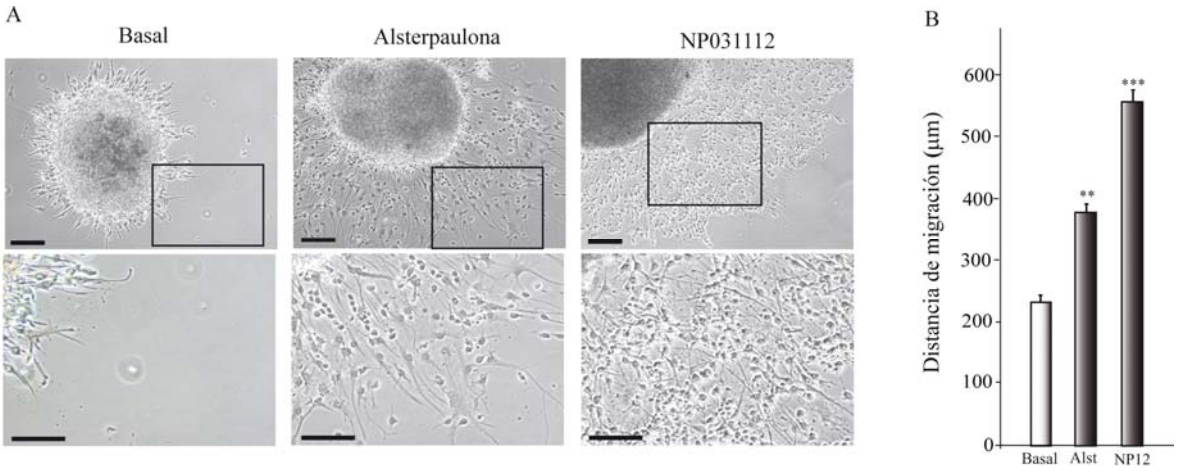

FIGURA 13.- Efecto de alsterpaulona y NP12 sobre la migración de células fuera de la neuroesfera (NS). NS individuales, previamente pegadas sobre cristales, se trataron en ausencia o presencia de 10 µM alsterpaunola (Alst) o de NP031112 (10 µM), midiéndose después la distancia de migración fuera de la NS. (A) Fotografías representativas de 3 experimentos independientes. Barra de escala = 25 µm. Los recuadros muestran a mayor aumento la zona de migración. Barra de escala fotos a mayor aumento = 10 µm. (B) Cuantificación de la distancia de migración de los progenitores neurales, expresados como la media ± ds correspondiente a tres experimentos independientes realizados por triplicado. **P< 0.01; ***P<0.001 en comparación con el control no tratado.

2.3.- Efecto de la inhibición de GSK-3β sobre la diferenciación de células madre neurales.

Puesto que la inhibición de GSK-3β parecía inducir la proliferación y migración de precursores neurales en cultivos de NS, evaluamos a continuación si dicha inhibición tenía algún efecto sobre la diferenciación celular en NS primarias. Analizamos mediante inmunocitoquímica la presencia de los diferentes tipos de células del sistema nervioso central, dentro y fuera de la NS, utilizando β-tubulina (TuJ), como marcador de neuronas y GFAP como marcador de astrocitos. Mientras que en los cultivos control solo se observaron algunas células aisladas positivas para β-tubulina y GFAP (figuras 14 y 15) el tratamiento con los inhibidores de GSK-3β indicados produjo un aumento en el número de células que expresaban β-tubulina (figura 14 y 15) migrando fuera de la NS.

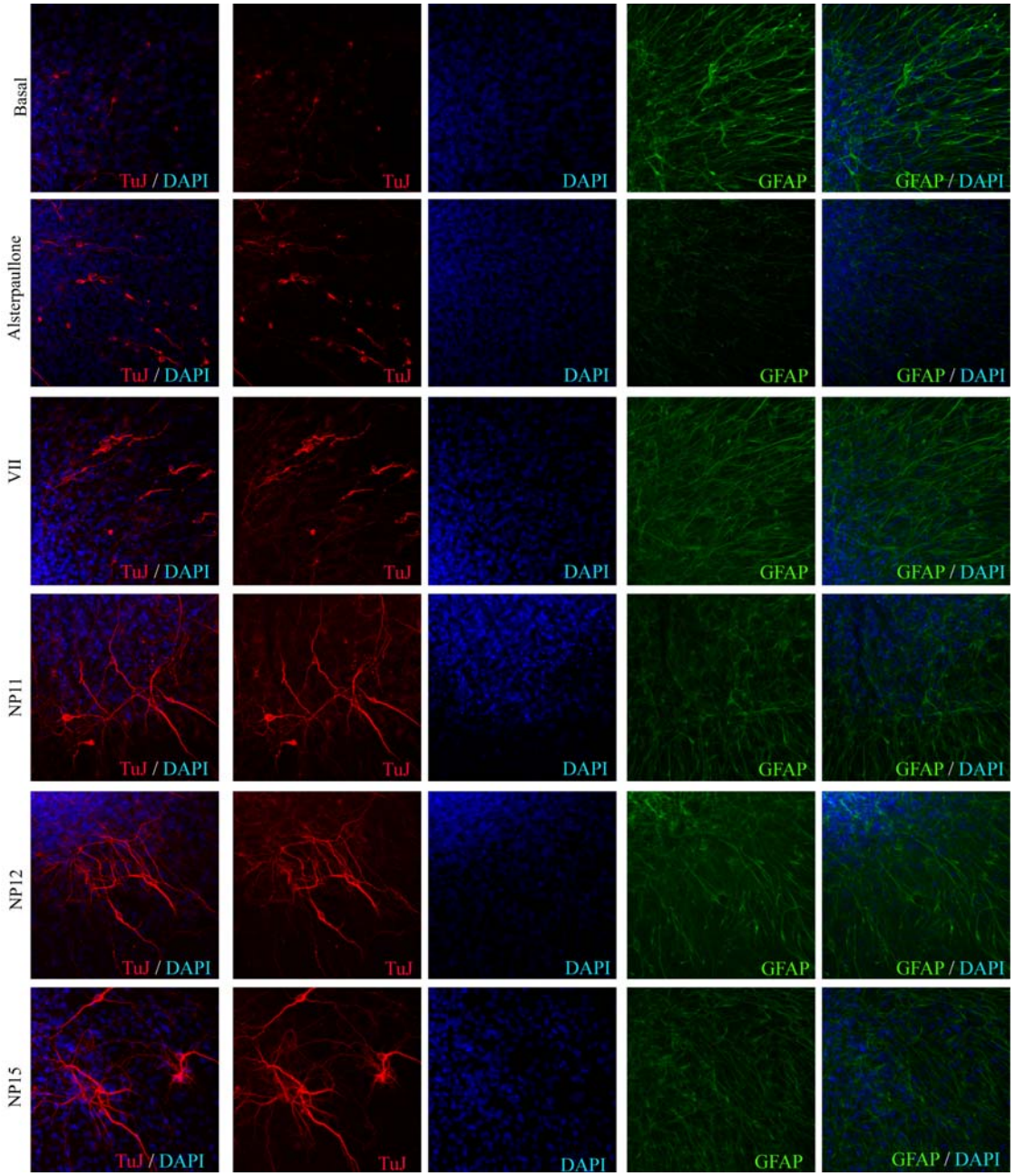

FIGURA 14.- Efecto de la inhibición de GSK-3β sobre la diferenciación celular en neuroesferas (NS). Las NS fueron tratadas con diferentes inhibidores de GSK-3β (10 µM) durante 7 días y pegadas sobre cristales para que diferenciasen durante 2 días. A continuación se evaluó por inmunocitoquímica la expresión de β-tubulina (rojo) o GFAP (verde) en las NS. Los núcleos se tiñeron con DAPI (azul). Barra de calibración = 20 µm.

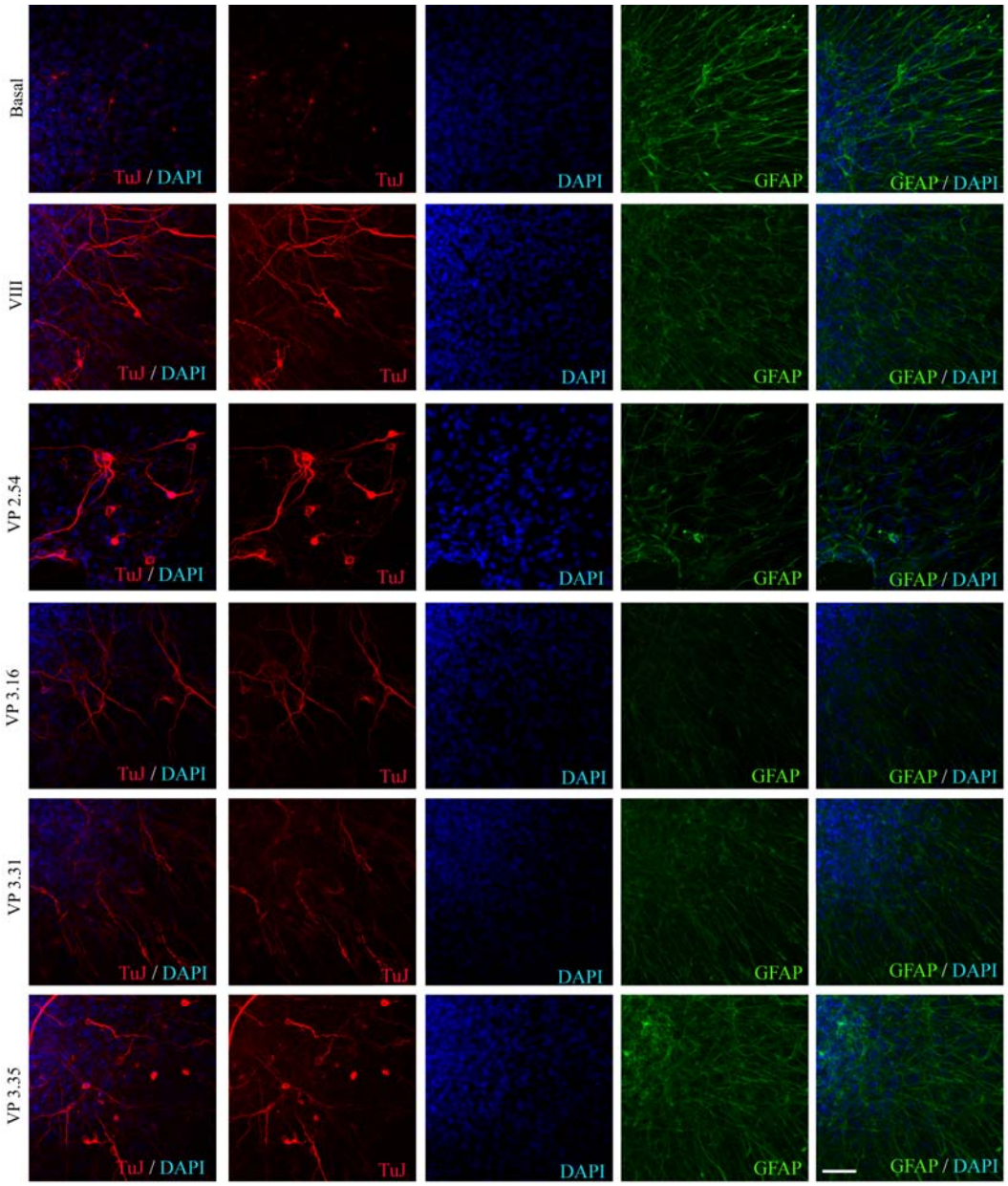

FIGURA 15.- Efecto de la inhibición de GSK-3β sobre la diferenciación celular en neuroesferas (NS). Las neuroesferas fueron tratadas con diferentes inhibidores de GSK-3β (10 μM) durante 7 días y pegadas sobre cristales para que diferenciasen durante 2 días. A continuación se evaluó por inmunocitoquímica la expresión de β-tubulina (rojo) o GFAP (verde) en las NS. Los núcleos se tiñeron con DAPI (azul). Barra de calibración = 20 μm.

2.4.- Efecto de NP031112 sobre la proliferación celular en la ZSG del hipocampo.

Como se ha mostrado en los apartados anteriores, la inhibición de GSK3-β *in vitro* indujo la proliferación, migración y diferenciación celular *in vitro* de NS procedentes de hipocampo. Para determinar el efecto que dicha inhibición pudiera tener *in vivo* utilizamos uno de los inhibidores de esta enzima, NP03112, que es capaz de atravesar la barrera hematoencefálica. Este compuesto fue administrado mediante sonda intragástrica durante 7 o 14 días antes del sacrificio. Un día antes del sacrificio de los animales se les inyectó BrdU para medir las nuevas células generadas. El efecto de NP031112 sobre la proliferación celular en el giro dentado del hipocampo se estudió en secciones coronales teñidas con un anticuerpo anti-BrdU. Los resultados obtenidos mostraron un incremento significativo en el número de células marcadas en el giro dentado (GD, figura 16) de los animales tratados con NP031112. A los 7 días de tratamiento, los animales tratados tenían un 46 % mas de células BrdU positivas en el giro dentado del hipocampo que los animales controles tratados con vehículo (figura 16). Tras 14 días de tratamiento, el incremento de las células proliferando en los animales tratados (figura 16) era de un 57% más con respecto al control.

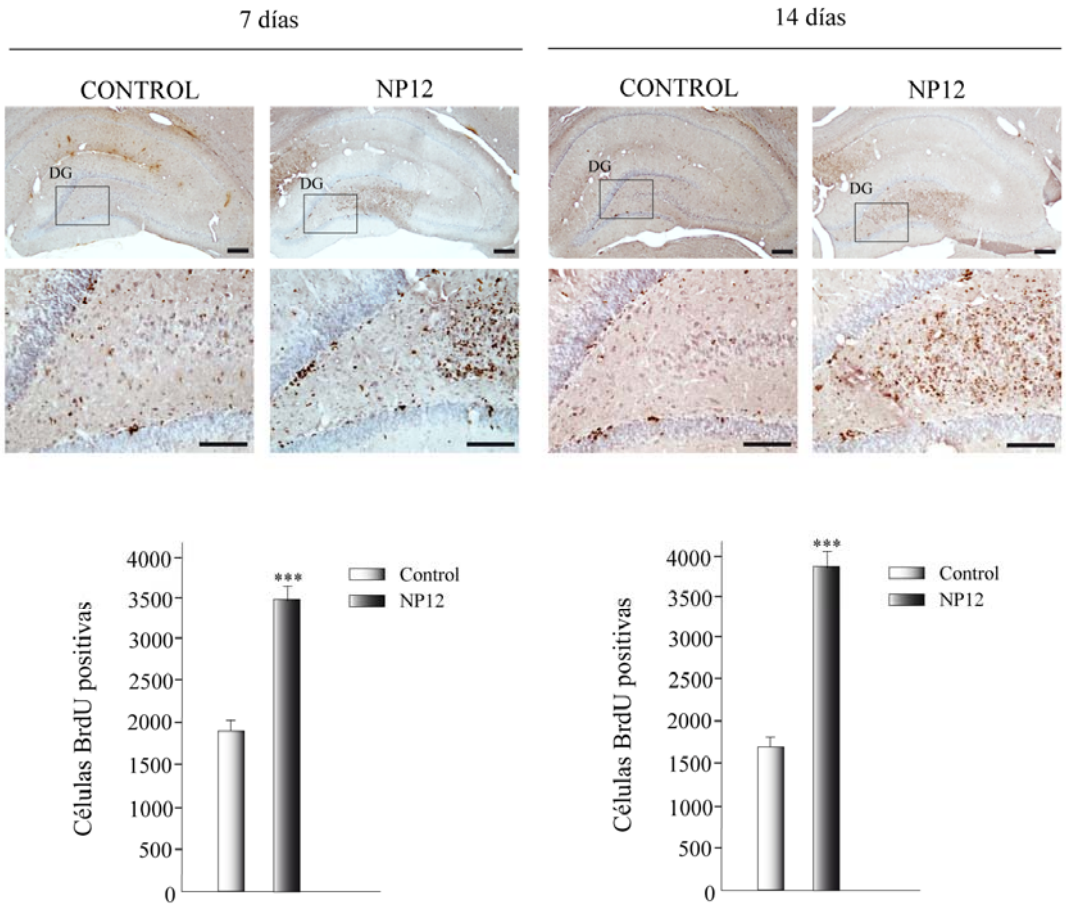

FIGURA 16.- Efecto de NP12 sobre la proliferación celular en el giro dentado (GD) del hipocampo. (A) Secciones coronales de animales control y tratados con NP12, que se tiñeron con un anticuerpo anti-BrdU y contratiñeron con hematoxilina. Las fotos ampliadas muestran con mas detalle la zona del GD. (B) Cuantificación del número de células BrdU positivas en el GD del hipocampo. Los valores representan la media ± ds correspondiente a cinco animales distintos. ***P<0.001. Barra de escala = 250 µm. Imágenes ampliadas = 100 µm.

2.5.- Efecto de la inhibición de GSK-3β sobre la migración celular en la ZSG del hipocampo.

El estudio inmunohistoquímico se realizó en secciones coronales utilizando DCX y PSA-NCAM. En el hipocampo, el tratamiento con NP031112 durante 7 días, claramente aumentaba el número de células que expresan DCX principalmente en el giro dentado, aunque también en otras capas del hipocampo como la CA1 y la CA3 (figura 17). Resultados similares se obtuvieron en los animales tratados durante 14 días (figura 17). Con respecto a PSA-NCAM, a los 7 y 14 días de tratamiento con NP12, se observó un aumento de su expresión en las células del giro dentado y de la CA3 (figura 18).

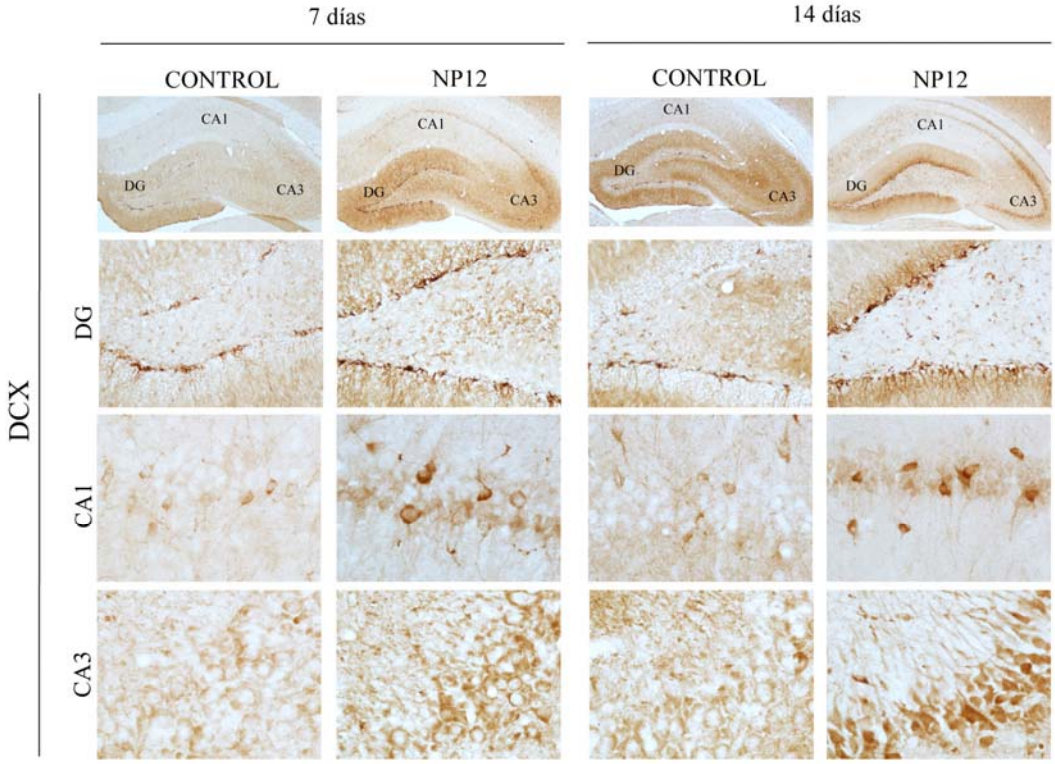

FIGURA 17.- Efecto del NP12 sobre la capacidad de migración de precursores neurales en el hipocampo. Se evaluó la expresión de DCX y de PSA-NCAM mediante tinción inmunohistoquímica en secciones coronales de hipocampo de animales control y animales tratados intragástricamente con NP12. Los imágenes a mas aumento muestran las zonas ampliadas del giro dentado (GD) y las capas CA1 y CA3 del hipocampo. Barra de escala = 250 µm. Imágenes ampliadas = 100 µm.

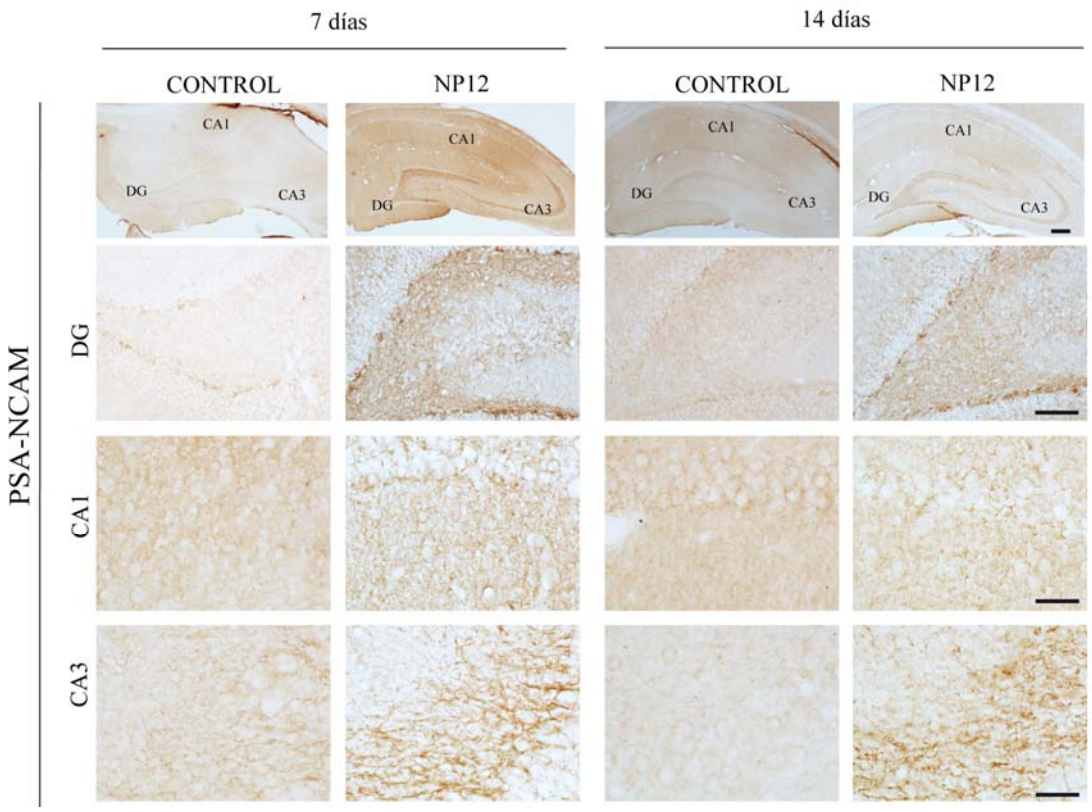

FIGURA 18.- Efecto del NP12 sobre la capacidad de migración de precursores neurales en el hipocampo. Se evaluó la expresión de DCX y de PSA-NCAM mediante tinción inmunohistoquímica en secciones coronales de hipocampo de animales control y animales tratados intragástricamente con NP12. Los imágenes a mas aumento muestran las zonas ampliadas del giro dentado (GD) y las capas CA1 y CA3 del hipocampo. Barra de escala = 250 µm. Imágenes ampliadas = 100 µm.

3.- EFECTO ANTIINFLAMATORIO, NEUROPROTECTOR Y ANTICONVULSIVO DE NP04634.

La desregulación de la homeostasis del calcio es un mecanismo fundamental en la neurotoxicidad excitatoria que a su vez esta implicada en diversas enfermedades neurodegenerativas (Sattler and Tymianski, 2000). El control del flujo de calcio a través de sus canales dependientes de voltaje puede ser considerado, por tanto, una buena diana para el desarrollo de fármacos que puedan controlar el aumento intracelular del calcio, y por tanto prevenir la muerte neuronal. Por esta razón hemos estudiado el posible efecto neuroprotector del NP04634 (figura 19), compuesto que en células cromafines bovinas ha demostrado ser un inhibidor de canales de Ca^{2+} dependientes de voltaje tipo no L (Valero et al., 2009).

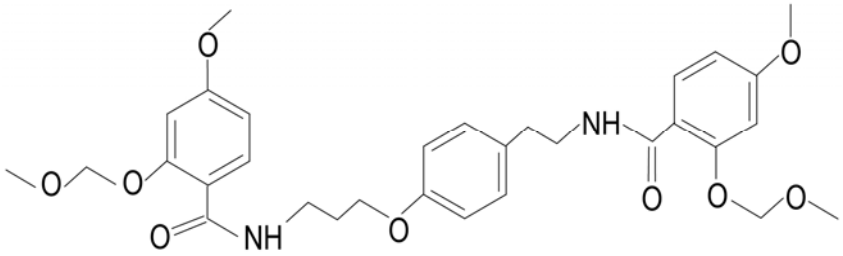

FIGURA 19.- Estructura del compuesto NP04634.

.1.-Efecto del NP04634 sobre la actividad convulsiva inducida por kainato.

Como se ha comentado en la introducción, la administración de kainato induce una secuencia de alteraciones del comportamiento que finalmente desemboca en un estado de convulsiones generalizadas o "*status epilepticus*" (SE) (Sperk, 1994). Tras la inyección intraperitoneal de KA, el 80% de los animales entraron en SE. Dicho porcentaje disminuyó hasta un 30% en aquellas ratas previamente tratadas con NP04634, tal y como se muestra en la figura 20A. Además de disminuir el porcentaje de animales que entraron en SE, NP04634 incrementó el tiempo en el que los animales alcanzaban el SE, disminuyendo además la severidad de los ataques. El tiempo medio que tardaron las ratas inyectadas con kainato en entrar en SE fue de 84.6±10.5 minutos (figura 20B), mientras que la latencia en el caso de animales tratados con NP04634 fue aproximadamente el doble (145.32±9.3 minutos ***p<0.001). Las ratas inyectadas con KA presentaron un número mayor de sacudidas, en comparación con los animales tratados con NP04634 (ver figura 20C). Finalmente, la mortalidad fue de aproximadamente el 25% en las ratas inyectadas solo con KA y que alcanzaron el SE, mientras que la mortalidad se redujo al 13% en aquellas tratadas con NP04634.

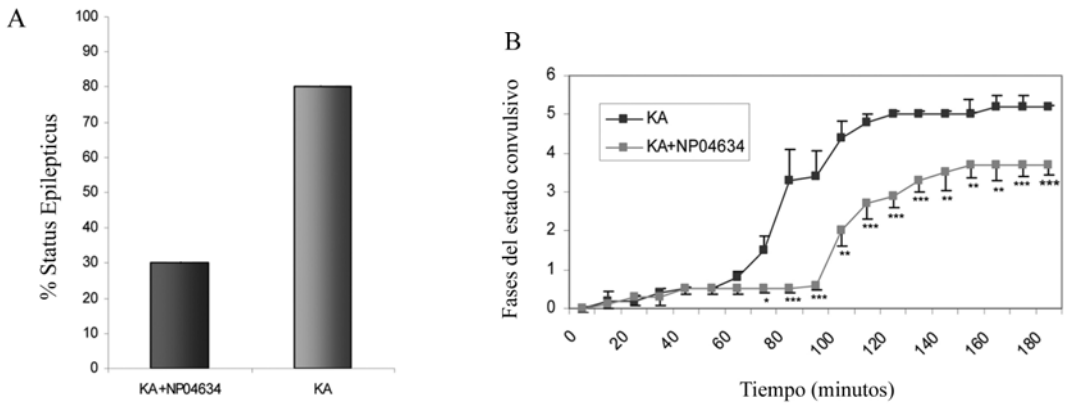

La figura 20 continúa en la página siguiente.

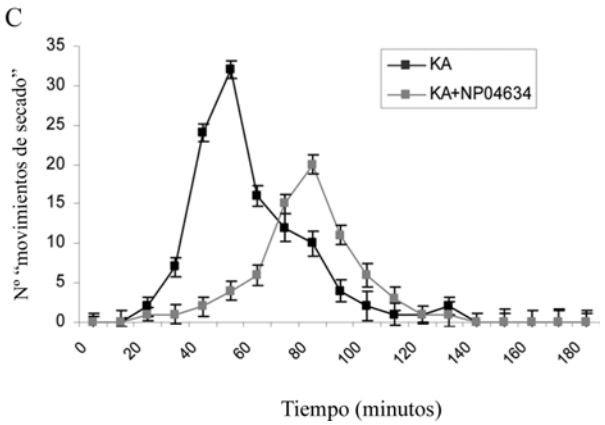

FIGURA 20.- Efecto del NP04634 sobre la actividad convulsiva inducida por kainato. El NP04634 fue administrado intragástricamente 12 y 4 horas antes de la inyección intraperitoneal de kainato. (A) Porcentaje de ratas que entraron en estado epiléptico (SE). (B) Fases del estado convulsivo. *P<0.05, **P<0.01, ***P<0.001. (C) Número de "sacudidas de secado" previos a la entrada en SE. Los valores representan la media ± error estándar de al menos 7 animales por gurpo.

3.2.- Efecto neuroprotector de NP04634 frente a daño cerebral inducido por kainato in vivo.

Como consecuencia del estado epiléptico se produce un proceso neurodegenerativo en determinadas regiones del cerebro, especialmente en el hipocampo, donde las células piramidales de la capa CA3, las interneuronas del giro dentado y las células piramidales de la CA1 son las mas vulnerables (Coyle, 1983; Sperk et al., 1985; Tauck and Nadler, 1985). Dados los resultados obtenidos, estudiamos a continuación la eficacia del compuesto NP04634 como agente neuroprotector frente a la neurodegeneración inducida por KA. Para ello evaluamos el daño en el hipocampo, 72h después de la inyección de KA, en animales controles e inyectados con NP04634 que alcanzaron SE. La figura 21A muestra como el tratamiento previo con NP04634 resulta en una total protección de las neuronas del hipocampo, comparada con la pérdida neuronal abundante que se produce en las capas CA1, CA3 e hilus, tras la inyección de KA en los controles. El análisis cuantitativo de la integridad celular en dichas capas mostró una pérdida neuronal del 94% (CA1), 87% (CA3) y 90% (hilus), al compararse con los animales control. No se observó una pérdida neuronal significativa en dichas capas en aquellos animales previamente tratados con NP04634. Este efecto neuroprotector del compuesto NP04634 se confirmó con la tinción con Fluoro-Jade B, que indica degeneración neuronal, (figura 21A) donde se observa una ausencia total de fluorescencia en las regiones CA1, CA3 e hilus del hipocampo en los animales tratados con el compuesto, de manera similar a lo que se observa en el grupo control. Por el contrario, los animales inyectados con KA (figura 21A, panel central) presentan una fuerte señal en dichas regiones, coincidiendo con aquellas zonas en las que se observaba una pérdida neuronal en la tinción de Nissl.

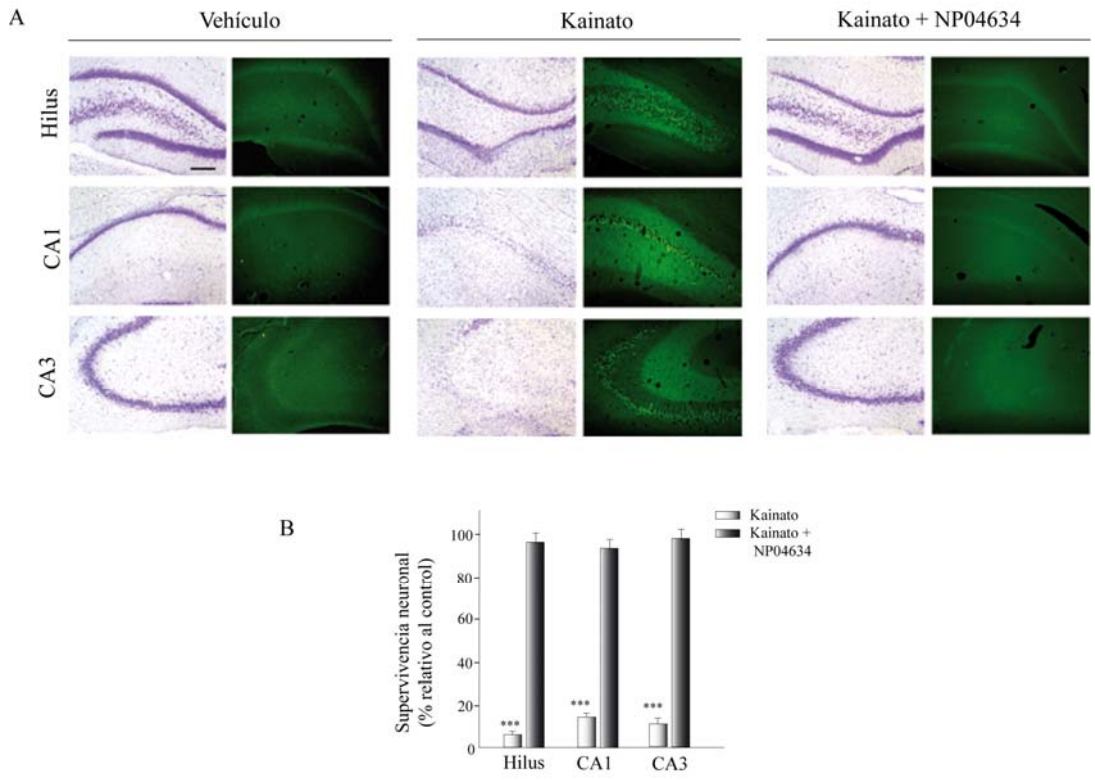

FIGURA 21.- Efecto de NP04634 sobre la muerte neuronal inducida por kainato. (A) Secciones coronales de hipocampo de animales inyectados con vehículo, kainato o kainato-previo tratamiento con NP04634. Las muestras se tiñeron con violeta de cresilo (Nissl) o con Fluoro-Jade B. (B) Cuantificación del daño celular en hilus y capas CA1 y CA3 del hipocampo. Los datos, normalizados con respecto al control se representan como la media ± ds (5 secciones / animal y 5 animales diferentes de los que entraron en SE). ***P<0.001 vs. control (inyectados con vehículo). Barra de escala = 10 µm.

3.3.- Efecto anti-inflamatorio de NP04634 *in vivo e in vitro.*

Una de las acciones mas notables que tiene lugar en el hipocampo tras un daño excitotóxico es la consiguiente activación glial. 72 h después de la inyección con KA en el hipocampo puede observarse un incremento importante en la activación de astrocitos y microglía. La activación de los astrocitos se pone de manifiesto por el aumento en la expresión de GFAP en todas las regiones del hipocampo (figura 22A). Esta hiperactivación astroglial se manifiesta tanto por un aumento considerable del número de células inmunoreactivas como por la intensidad de las mismas, tal y como puede observarse en la figura 22B.

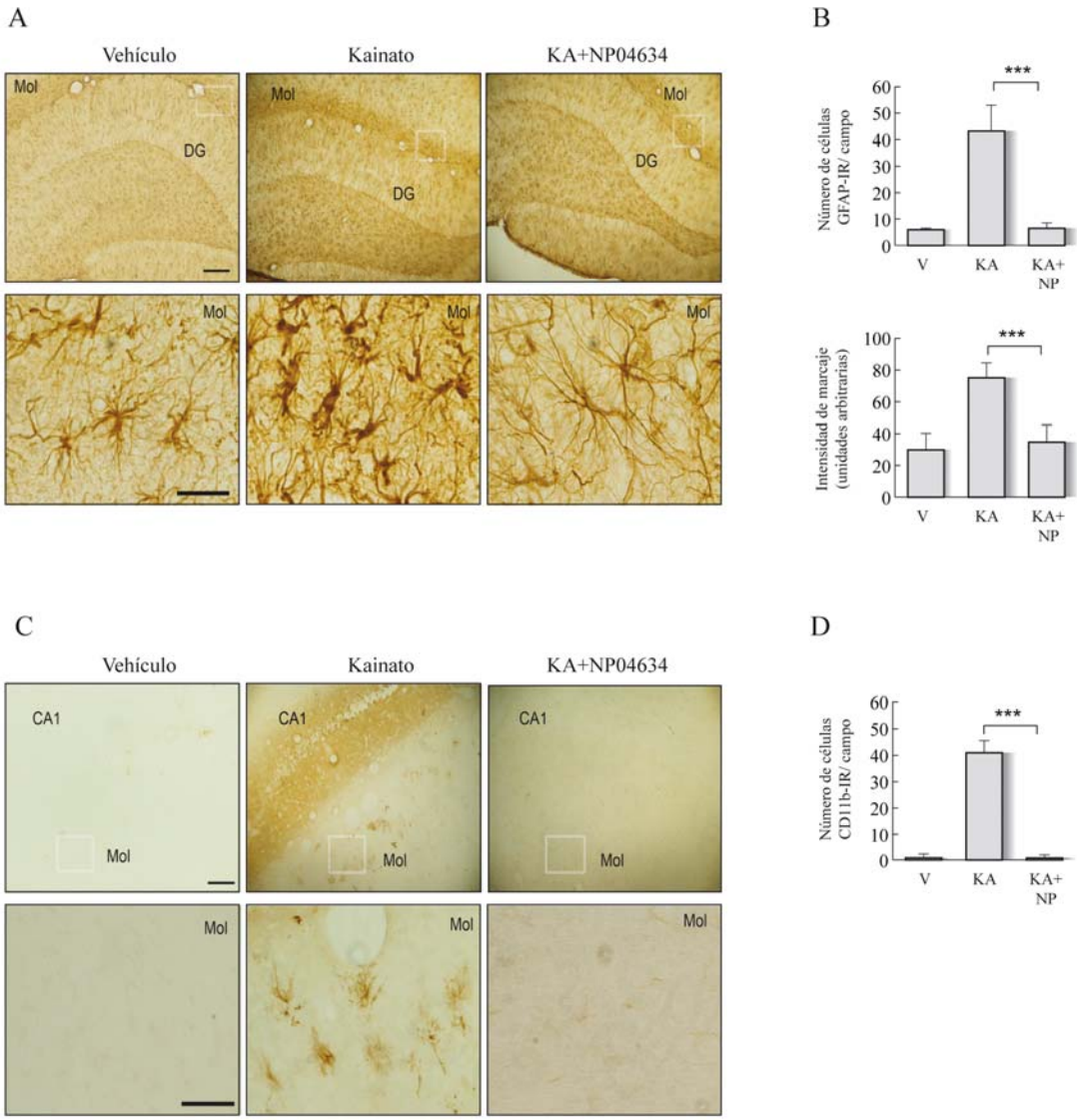

FIGURA 22.- Efecto del NP04634 sobre gliosis inducida por kainato. Secciones coronales de hipocampo de animales inyectados con vehículo, kainato o kainato-previo tratamiento con NP04634. (A) Expresión de GFAP marcando astroglía hiper-activada. (B) Cuantificación del número de astrocitos inmunoreactivos (IR) así como de la intensidad de marcaje en la capa molecular del hipocampo. (C) Expresión de CD11b (OX-42) para detectar microglía reactiva. (D) Cuantificación del número de microglía reactiva. Los valores representan la media ± ds (5 secciones / animal y 5 animales diferentes). ***P<0.001. Los recuadros en A y C marcan la zona de la capa molecular ampliada que se muestra a continuación. Barra de escala = 250 µm. Ampliaciones = 25 µm.

Por el contrario, 72h después de la inyección de KA, aquellos animales pre-tratados con NP04634, mostraban una expresión de GFAP similar a la que se observaba en los animales control, presentando astrocitos con una morfología típica de células no activadas. Con respecto a las células microgliales, 72h después de la inyección de KA se produce una hiperactivación de las mismas, lo que se traduce en un aumento de la expresión de CD11b (OX-42), y por tanto de un aumento del número de células inmunoreactivas, sobre todo en la capa molecular del hipocampo (fig. 22C). También se producen cambios importantes en la morfología microglial, lo que incluye un aumento del tamaño de los cuerpos somáticos, así como un adelgazamiento y retracción de sus procesos celulares, características propias de la microglía reactiva (Jorgensen et al., 1993; Ladeby et al.,

2005). El tratamiento con NP04634 bloqueó completamente la activacion por KA de la microglia (Figura 22C y D).

Finalmente, con el fin de confirmar los resultados anti-inflamatorios obtenidos *in vivo*, estudiamos la implicación del NP04634 en la respuesta inflamatoria *in vitro* en cultivos primarios de astrocitos. Para ello evaluamos la producción por parte de estas células, previamente estimuladas con LPS, de sustancias neurotóxicas y de factores pro-inflamatorios, tales como COX-2 o TNF-α (figura 23). El pre-tratamiento de los cultivos primarios de astrocitos con NP04634 bloquea por completo la producción de dichos agente pro-inflamatorios tras su exposición a LPS, confirmándose el efecto anti-inflamatorio observado por este compuesto *in vivo*.

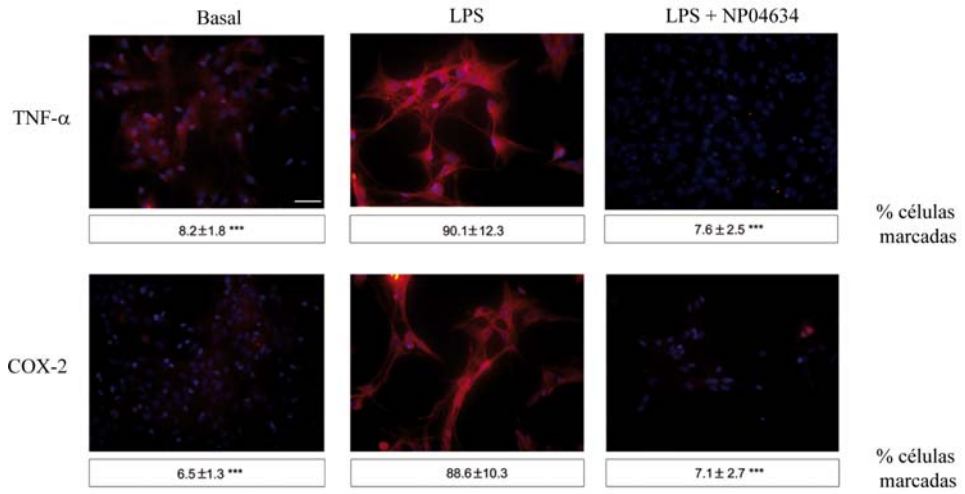

FIGURA 23.- Efecto del NP04634 sobre la inducción por LPS de factores pro-inflamatorios en cultivos primarios de astrocitos. Los astrocitos se estimularon con LPS en ausencia o presencia de NP04634 para a continuación evaluar por inmufluorescencia la expresión de factores pro-inflamatorios: TNF-α y COX-2 (rojo). Los núcleos aparecen teñidos con DAPI (azul). La figura muestra los resultados representativos correspondientes a tres experimentos diferentes. Los valores representados bajo las imágenes corresponden a la media ± SD de tres experimentos diferentes y 5 campos independientes (>50 células/campo) por cultivo. ***P<0.001. Barra de escala = 10 µm.

4.- EFECTO NEUROPROTECTOR DE LOS INHIBIDORES DE FOSFODIESTERASA-7.

La inhibición selectiva de la enzima fosfodiesterasa 7 (PDE7) se ha llevado a cabo mediante la utilización de una molécula heterocíclica denominada S14, sintetizada en el Instituto de Química Médica de Madrid (CSIC) y cuya estructura se representa en la figura 24.

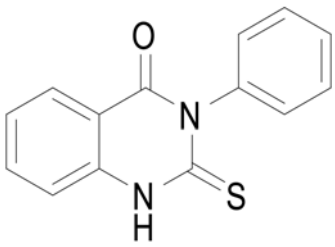

FIGURA 24.- Estructura del S14, inhibidor de PDE7.

4.1.- Expresión de PDE7.

Inicialmente analizamos la expresión de PDE7 en el sistema nervioso central de rata adulta. Mediante WB medimos los niveles de las dos isoformas de PDE7, PDE7A y PDE7B, encontrado que ambas se encontraban ampliamente distribuidas en el cerebro. Como puede observarse están presentes en corteza, hipocampo y estriado (figura 25). También se expresa en la línea celular de neuroblastoma humano SH-SY5Y.

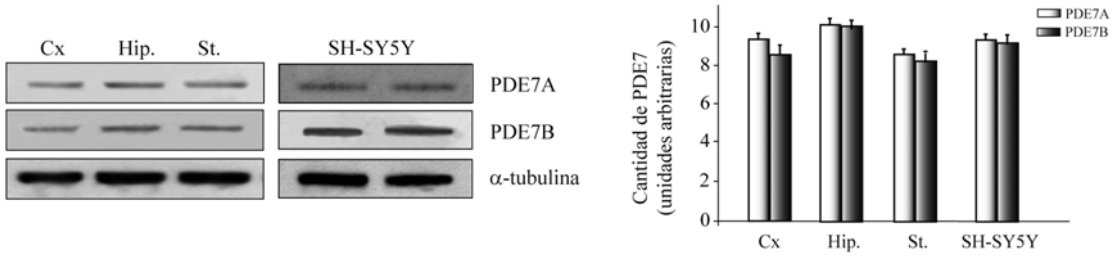

FIGURA 25.- Análisis por western blot y cuantificación de la expresión de PDE7A y PDE7B en diferentes zonas del cerebro: corteza (Cx), hipocampo (Hip) y estriado (St) y en la línea celular dopaminérgica SH-SY5Y.

Tambien encontramos, mediante análisis inmunohistoquímico, que PDE7A y B se expresan en la SNpc (figura 26). Los niveles de PDE7A y B en este área son bajos en animales controles. Por el contrario, en los animales inyectados intracerebralmente con LPS la expresión de ambas isoformas aumentaba notablemente en la SNpc.

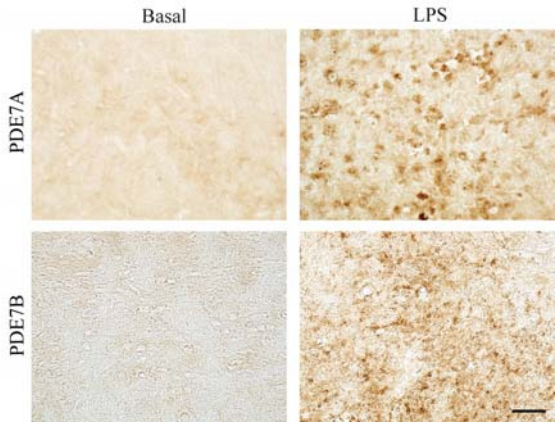

FIGURA 26.- Expresión de PDE7A Y PDE7B en la parte compacta de la sustancia negra (SNpc) de ratas adultas. Se muestra también la expresión de ambas isoenzimas 72h después de inyectar LPS intracerebralmente en dicha región. Barra de escala = 25 µm.

Por inmunocitoquimica confirmamos la expresión de PDE7A y B en células SH-SY5Y, así como en cultivos primarios de células de mesencéfalo embrionario de rata (figura 27). El doble marcaje inmunocitoquímico realizado mostró como las células TH^+ co-expresaban PDE7A y PDE7B.

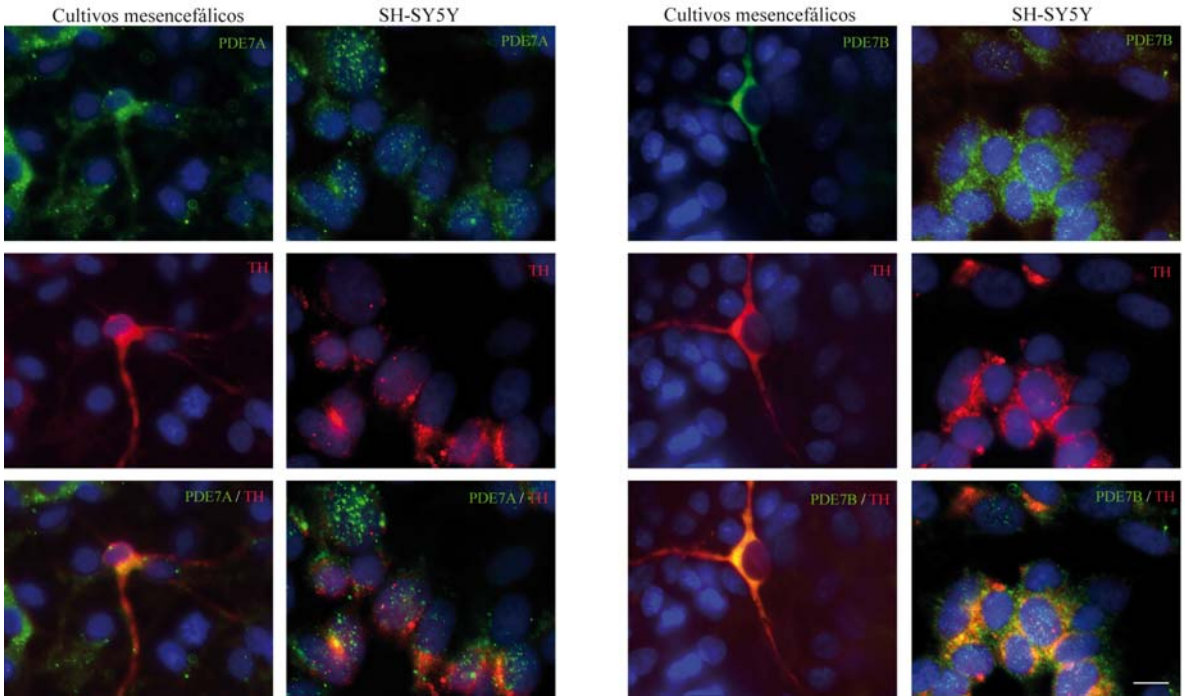

FIGURA 27.- Análisis inmunocitoquímico de la expresión de PDE7A y PDE7B (verde) junto con tirosina-hidroxilasa (rojo) en cultivos embrionarios de mesencéfalo y en células SH-SY5Y. Los núcleos se tiñeron con DAPI (azul). Barras de escala = 10 µm.

4.2.- La inhibición de PDE7 protege a las células SH-SY5Y frente al daño inducido por 6-hidroxidopamina (6-OHDA).

La línea neuronal dopaminérgica humana SH-SY5Y se usa habitualmente como modelo experimental en estudios de neurodegeneración dopaminérgica empleándose 6-OHDA como agente neurotóxico. Como consecuencia de la toxicidad inducida por 6-OHDA se produce un aumento en la producción de lactato deshidrogenasa (LDH) así como un aumento de la cantidad de nitritos generados. S14 inhibe PDE7 con una IC50 de 5,5 µM, aunque también es capaz de inhibir PDE4, pero con una IC50 de 22µM, es decir, una capacidad inhibitoria cinco veces menos potente que la que ejerce sobre PDE7. Como controles usamos los inhibidores clásicos BRL50481 (BRL), inhibidor de PDE7 y Rolipram (Rol), inhibidor de PDE4.

Nuestros resultados mostraron que el tratamiento con S14 prevenía la muerte neuronal producida por la 6-OHDA (figura 28A). Además, la incubación con S14 disminuyó los niveles de LDH hasta en un 50%, en comparación con los niveles detectados frente a la exposición con 6-OHDA (figura 28B). Con respecto a los niveles de nitrito producidos, tal y como muestra la figura 28C, el tratamiento con S14 disminuyó dichos niveles hasta casi niveles basales. Estos resultados sugieren que S14, a través de la inhibición de PDE7, protege a las células SH-SY5Y de la muerte inducida por 6-OHDA. Además S14 parecía contribuir a la reducción del estrés oxidativo inducido por 6-OHDA al reducir la producción de radicales libres.

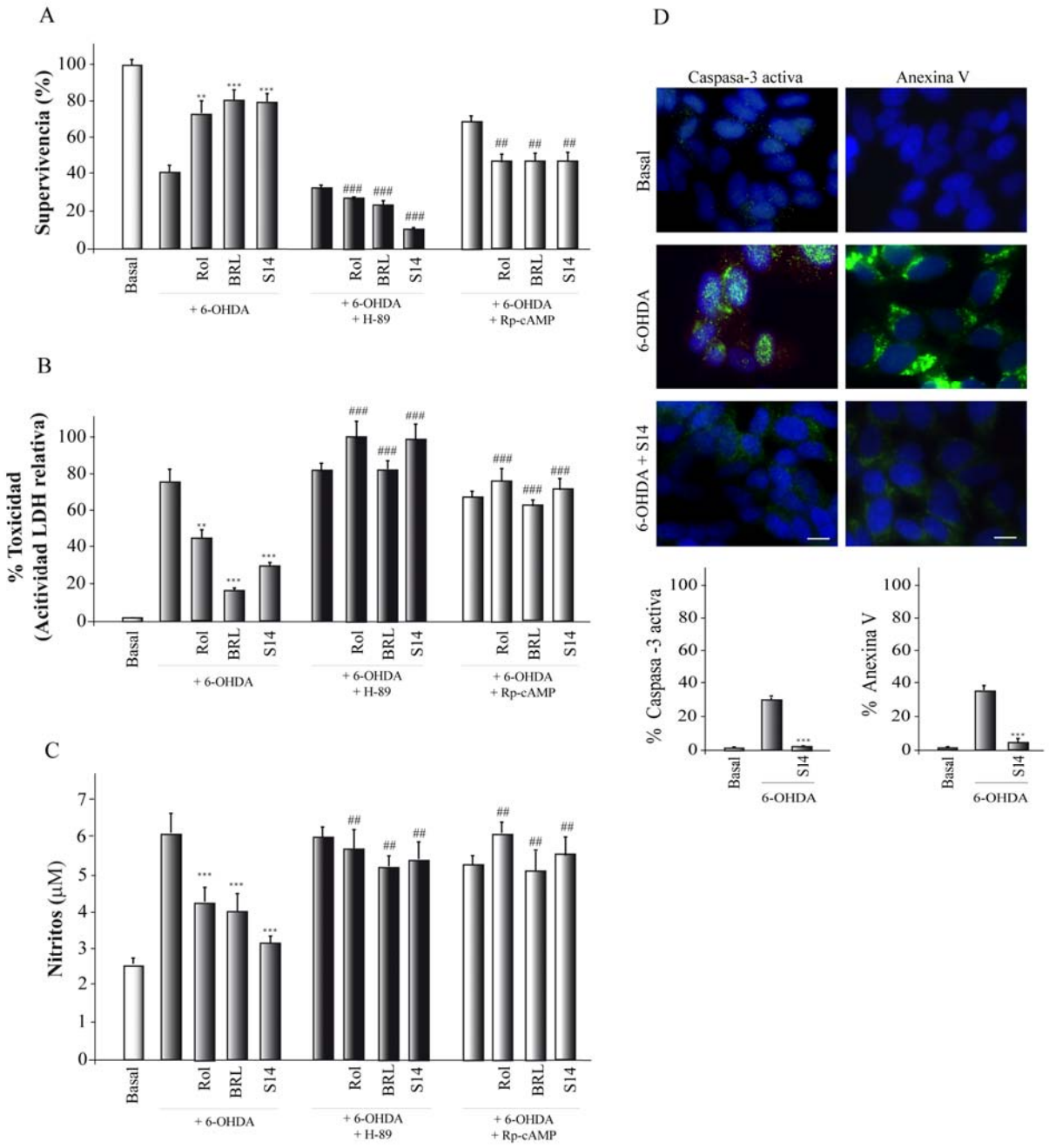

FIGURA 28.- Efecto neuroprotector del S14 en cultivos de SH-SY5Y. Las células SH-SY5Y fueron expuestas a 6-hidroxidopamina (6-OHDA, 35 µM) durante 16 h en presencia o ausencia de Rolipram (Rol, 30 µM), BRL50481 (BRL, 30 µM) o S14 (10 µM). (A) Ensayo de viabilidad celular por MTT. (B) Determinación de la actividad LDH. (C) Evaluación de los niveles de nitrito producidos (ensayo de Griess). Algunos de los cultivos fueron tratados con H89, inhibidor de la proteína quinasa A o con Rp-cAMP, antagonista de AMPc. Los valores representan la media±ds de tres experimentos independientes determinados por sextuplicado. ** P<0.01, *** P<0.001 en comparación con las células tratadas con 6-OHDA; ## P<0.01, ### P<0.001 en comparación con los valores obtenidos por cada tratamiento en ausencia de H89 o Rp-cAMP. (D) Niveles de apoptosis medidos por inmunodetección de caspasa-3 activa (verde) o Anexina V-FITC (verde). Se muestras imágenes representativas de al menos tres experimentos independientes. Los núcleos se tiñeron con DAPI (azul). Barra de escala = 10 µm. Se muestra también la cuantificación correspondiente al número de células inmunoreactivas para caspasa-3 activa y Anexina V-FITC. *** P<0.001 en comparación con las células tratadas con 6-OHDA.

Para completar estos resultados analizamos por inmunocitoquímica los niveles de los marcadores de apoptosis caspasa 3 activa y de Anexina V. Las fotografías de la figura 28D muestran que el 27% de las células SH-SY5Y, tras 16h de cultivo en presencia de 6-OHDA, eran positivas para caspasa 3 activa, y el 34% se teñian con Anexina V. El tratamiento con S14 revertía casi por completo este efecto, lo que indica que S14 es capaz de rescatar a las células SH-SY5Y de la apoptosis inducida por 6-OHDA.

4.3.- Implicacion de la via AMPc-PKA en la acción neuroprotectora de S14 en células SH-SY5Y.

Dado que el S14 es un inhibidor selectivo de PDE7, inicialmente evaluamos su efecto sobre los niveles de AMPc en las células SH-SY5Y. Tratamos por tanto los cultivos de SH-SY5Y durante 1h con S14 o con Rol y BRL y determinamos mediante ELISA la cantidad de AMPc en los cultivos (figura 29A). Nuestros resultados muestran que el tratamiento con S14 aumentaba los niveles de AMPc en cultivos celulares de SH-SY5Y (figura 29 A).

La diana intracelular mas común sobre la que actúa el AMPc, provocando múltiples acciones, es la Proteina Quinasa A (PKA) (Houslay and Kolch, 2000). No obstante el AMPc es también responsable de otras actividades que no están mediadas por esta quinasa (Charles et al., 2003; Lastres-Becker et al., 2008). Por esta razón evaluamos si el efecto neuroprotector del S14, estaba mediado por PKA. Las células SH-SY5Y fueron tratadas con 6-OHDA, previa incubación con Rol, BRL o S14. Algunos cultivos fueron pre-tratados con H89, un inhibidor de PKA, o con Rp-cAMP, un analógo de AMPc que actúa como inhibidor competitivo de AMPc. El ensayo de supervivencia celular y citotoxicidad (figura 28A y B) mostró como la acción neuroprotectora que ejercía el S14 frente al daño con 6-OHDA disminuía en aquellos cultivos pre-tratados con los dos inhibidores, H-89 y Rp-cAMP. Resultados similares se obtuvieron al medir los niveles de nitrito producidos (figura 28C), lo que sugería que la ruta AMPc/PKA estaba mediando el efecto que el S14 tenía sobre las células SH-SY5Y. Con el fin de corroborar estos resultados, estudiamos el estado de fosforilación de la proteína CREB, una diana conocida de PKA (figura 29B). Como consecuencia del tratamiento con los inhibidores de PDEs se produjo un aumento en el contenido de CREB-fosforilada. Estos resultados están de acuerdo con la hipótesis de que la vía de señalización de S14 implica AMPc-PKA.

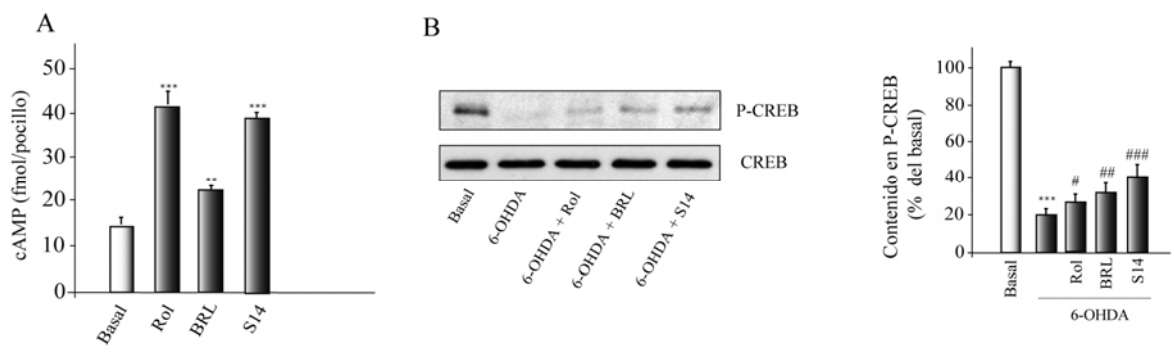

FIGURA 29.- Implicacion de la via AMPc-PKA en el efecto neuroprotector de S14 en cultivos de SH-SY5Y. (A) Niveles intracelulares de AMPc en células tratadas durante 1h con los compuestos indicados. **P<0.01; ***P<0.001 en comparación con las células basal (no tratadas). (B) Western blot representativo y cuantificación mostrando la fosforilación de CREB tras la incubación de los cultivos con 6-OHDA en presencia o ausencia de los compestos indicados: Rolipram (Rol, 30 µM), BRL50481 (BRL, 30 µM) o S14 (10 µM). El uso de un anticuerpo que no discrimina entre CREB y su forma fosforilada indica que los distintos tratamientos no afectaron los niveles totales de CREB. ***P<0.001 en comparación con las células basal; # P<0.05 ;## P<0.01, ### P<0.001 en comparación con los cultivos tratados con 6-OHDA.

4.4.- La inhibición de PDE7 protege a los cultivos mesencefálicos embrionarios frente a la muerte celular inducida por lipopolisacárido.

Visto los efectos neuroprotectores de S14 en SH-Y5Y nos propusimos a continuación estudiar su acción en un sistema más fisiológico como son los cultivos primarios procedentes de mesencéfalo embrionario de rata. Los cultivos mesencefálicos embrionarios, son ricos en neuronas dopaminérgicas y en células gliales (astrocitos y microglía) y por tanto sensibles al tratamiento con LPS, puesto que en su presencia las células gliales son sobreestimuladas y como consecuencia de ese estado de hiperactivación producen agentes pro-inflamatorios, lo que se traduce en una pérdida en la viabilidad neuronal (Chen et al., 2008). Lo que hicimos primero fue analizar si el tratamiento con S14 afectaba a la producción de dos de esos agentes pro-inflamatorios: TNF-α y COX-2. Para ello analizamos por doble inmunofluorescencia la co-expresión de marcadores gliales (GFAP para astrocitos y OX-42 para microglía) junto con TNF-α y COX-2 en cultivos mesencefálicos tratados con LPS o LPS+S14.

Los resultados obtenidos se muestran en la figura 30. Como puede observarse LPS induce la expresión de TNFα y COX-2 tanto en las células $GFAP^+$ (astrocitos) como las $OX\text{-}42^+$ (microglía) y el tratamiento con S14 bloquea casi por completo dicha inducción. La posterior cuantificación del número de células $TNF\alpha^+$ y $COX\text{-}2^+$ (figura 31) muestra que el tratamiento con S14 reduce la expresión de ambos agente proinflamatorios en un 80% y un 72% respectivamente

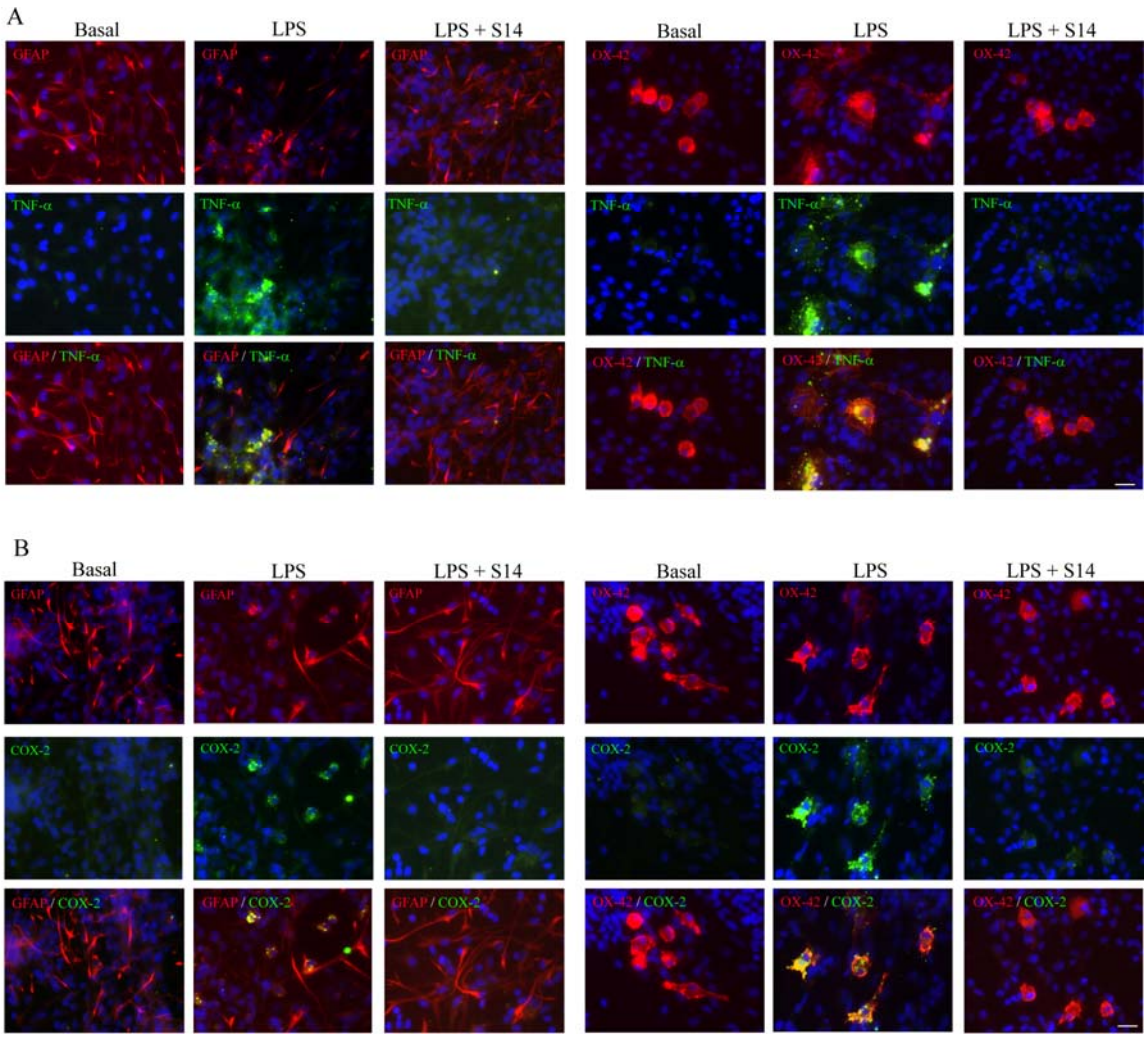

FIGURA 30.- Efecto de S14 sobre la inflamación inducida por LPS en cultivos mesencefálicos. **Los cultivos mesencefálicos embrionarios de rata se trataron con LPS (1 µg/ml) en presencia o ausencia de S14 (10 µM). (A) Expresión de TNF-a (verde) en astrocitos marcados con GFAP (rojo) y en microglía marcada con CD11b (OX-42, rojo). (B) Expresión de COX-2 (verde) en astrocitos marcados con GFAP (rojo) y en microglía marcada con CD11b (OX-42, rojo). Los núcleos se tiñeron con DAPI (azul). Barra de escala = 25 µm.**

.

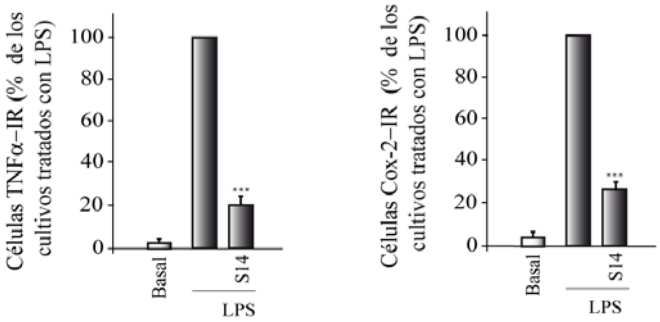

FIGURA 31.- Efecto del S14 en la prevención de la inflamación inducida por LPS en cultivos mesencefálicos. **Cuantificación del número de células inmunoreactivas (IR) para cada anticuerpo utilizado. Los valores representan la media de al menos tres experimentos distintos y 20 campos independientes (> 50 células /campo) por condición. ***P<0.001 en comparación con los cultivos tratados con LPS.**

A continuación determinamos el efecto de S14 sobre la viabilidad de las neuronas dopaminérgicas de los cultivos mediante la cuantificación del número de células que expresaban tirosina hidroxilasa (TH). Tal y como se muestra en la figura 32A, el efecto del LPS se tradujo en una disminución del 42% en el número de neuronas TH-inmunoreactivas. El compuesto S14, añadido a estos cultivos, protegió de forma significativa frente a la toxicidad producida por LPS. También medimos la cantidad de nitritos liberados tras exponer los cultivos mesencefálicos a la acción citotóxica del LPS en presencia o ausencia de S14. Como puede observarse en la figura 32B, LPS provoca un aumento en el contenido de nitritos. Este aumento se bloqueó completamente cuando los cultivos eran tratados con S14 e incluso se obtuvieron niveles más bajos en los cultivos tratados con S14 que en los controles (figura 32B). Todos estos datos sugieren que la acción neuroprotectora del S14 podría deberse, al menos en parte, a un efecto anti-inflamatorio, puesto que inhibe la activación de las células gliales presentes en los cultivos, evitando la producción de agente pro-inflamatorios. Finalmente analizamos el posible efecto neuroprotector de S14 en la toxicidad inducida por 6-OH. Nuestros resultados muestran que esta toxina provoca la muerte del 80% de las células dopaminérgicas (figura 32C). El tratamiento con S14 de los cultivos supuso un aumento considerable en la supervivencia de las neuronas TH^+ frente al daño ocasionado por 6-OHDA.

4.5.- Efecto neuroprotector de la inhibición de PDE7 en un modelo animal de Parkinson.

A la vista de los resultados obtenidos *in vitro*, nos propusimos a continuación ver si el S14 ejercía los mismos efectos neuroprotectores en un modelo animal de Parkinson. El LPS inyectado en la *subtantia nigra pars compacta* (SNpc) en roedores, induce la pérdida de células dopaminérgicas así como la activación de la microglía colindante (Kim et al., 2000; McCoy et al., 2006). Por tanto inyectamos unilateralmente en la SNpc de ratas adultas vehículo, LPS o una combinación de LPS con S14. Como control de la inhibición de PDE7, un grupo de animales fueron inyectados con LPS y BRL50481, un inhibidor comercial con capacidad de inhibir específicamente a este enzima. Al cabo de 72h de la inyección intracerebral, los animales fueron sacrificados. Para evaluar los efectos del S14 se llevó a cabo un estudio histológico con secciones coronales previamente tenidas con azul de toulidina. Los resultados obtenidos mostraron una pérdida neuronal relevante en la SNpc tras la inyección de LPS (85%), presumiblemente de neuronas dopaminérgicas (figura 33A). El tratamiento conjunto con S14, protegió notablemente a las neuronas del daño con LPS, como ilustra la figura 33, donde pudo observarse un abundante número de somas celulares, en una situación muy similar a la que se apreciaba en los animales control. Para corroborar nuestra hipótesis de que el S14 está protegiendo a las neuronas dopaminérgicas de la SNpc, realizamos una inmunotinción con un anticuerpo anti tirosina-hidroxilasa (TH). La figura 33B muestra unos resultados similares a los observados con la tinción

histológica, es decir, una pérdida importante de neuronas TH^+ a los 3 días tras la inyección con LPS. Dicha pérdida era mucho menos acusada, alrededor del 25%, en el caso de los animales tratados conjuntamente con S14. Estos resultados son concordantes con los resultados previamente obtenidos *in vitro*, reforzando la idea de que el S14 protege a las neuronas dopaminérgicas.

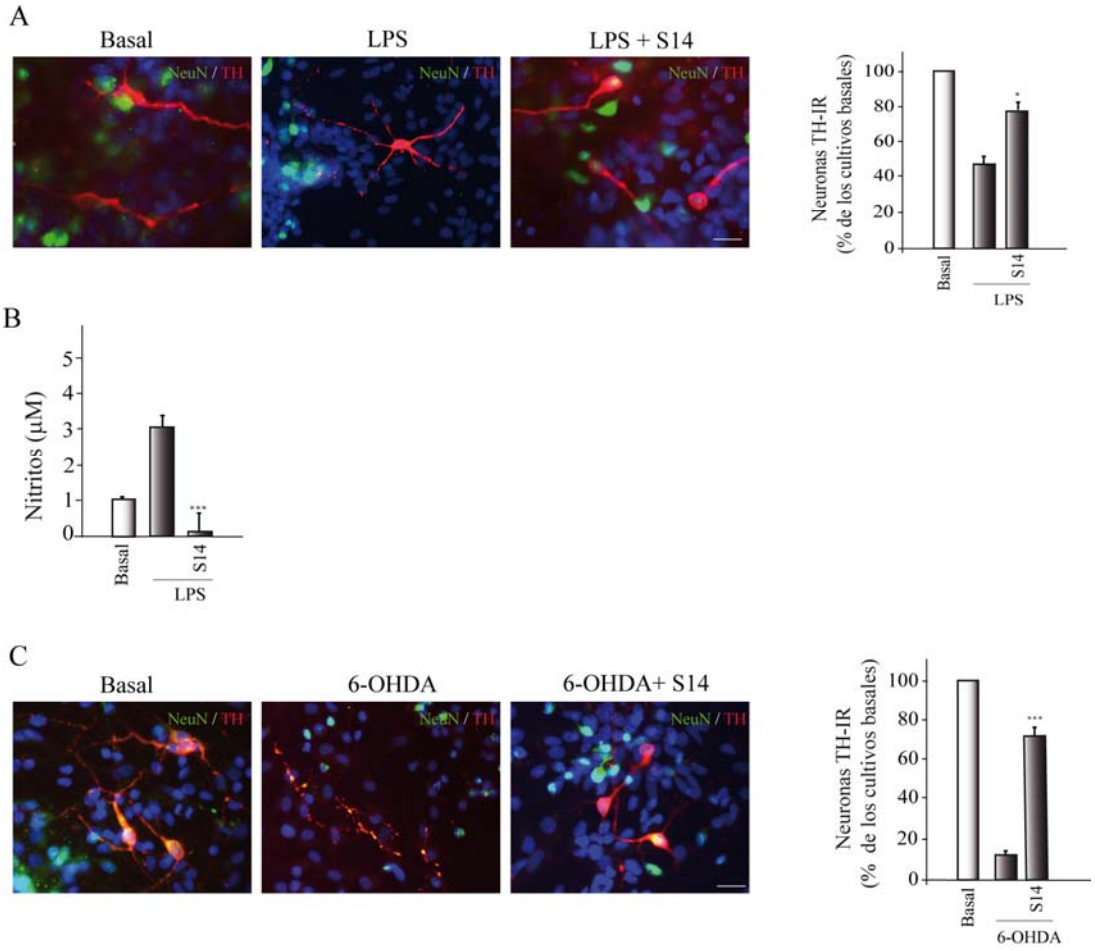

FIGURA 32.- Efecto neuroprotector de S14 en cultivos mesencefálicos. (A) Los cultivos se trataron con LPS (1 µg/ml) en presencia o ausencia de S14 (10 µM). La expresión de tirosina hidroxilasa (TH, rojo) y NeuN (verde) se evaluó por inmunofluorescencia usando anticuerpos específicos. Los núcleos se tiñeron con DAPI (azul). Barra de escala = 20 µm. A la derecha de las fotos se muestra la cuantificación del número de células inmunoreactivas (IR) para cada anticuerpo utilizado. Los valores representan la media de al menos tres experimentos distintos y 20 campos independientes (> 50 células /campo) por condición.*P<0.05; ***P<0.001 en comparación con los cultivos tratados con LPS. (B) Evaluación de la producción de nitritos mediante la reacción de Griess. Los valores representan la media ± ds de seis replicas en tres experimentos distintos.*P<0.001 en comparación con los cultivos tratados con LPS. (C) Cultivos primarios procedentes de mesencéfalo embrionario tratados con 6-OHDA en presencia o ausencia de S14. Se evaluó la expresión de TH por inmunofluorescenica y posteriormente se cuantificó, expresándose los resultados como la media ± ds de al menos tres experimentos distintos y 20 campos independientes (> 50 células /campo) por condición.***P<0.001 en comparación el tratado con 6-OHDA.**

Al igual que lo que ocurría *in vitro,* la inyección *in vivo* de LPS en la SNpc activó las células microgliales, mientras que la inyección de S14 bloqueó este efecto de LPS. Como puede observarse en la figura 34, no había prácticamente células $OX\text{-}42^+$ en los animales control ni en el hemisferio contralateral de los animales inyectados con LPS. Sin embargo, el hemisferio inyectados con LPS mostraba una zona con una clara inmunoreactividad para OX-42. Este signo claro de microgliosis estaba prácticamente ausente en aquellos animales inyectados además de con LPS, con S14.

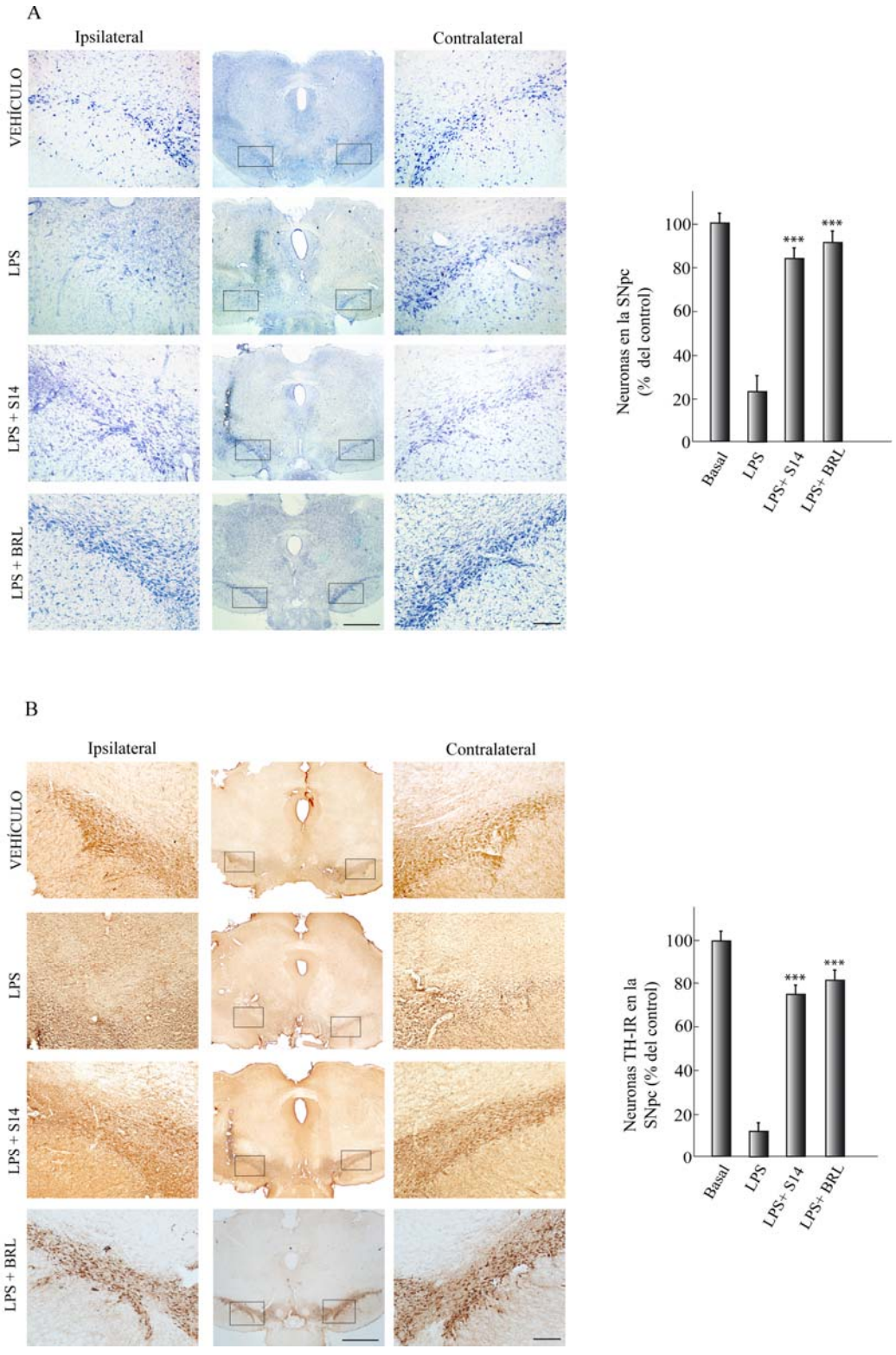

FIGURA 33.- Efecto neuroprotector de S14 en un modelo de Parkinson. Ratas adultas fueron inyectadas unilateralmente en la sustancia negra parte compacta (SNpc) con vehículo o LPS (10µg) sólo o combinado con S14 (20nmol) o con BRL50481 (60nmol). A las 72h los cerebros fueron extraídos y secciones coronales analizadas por inmunohistoquímica. (A) Tinción con violeta de cresilo (Nissl) de la SNpc con la correspondiente cuantificación (B) Inmunohistoquímica que muestra la expresón de TH en la SNpc. A la derecha se muestra la cuantificación del número de neuronas dopaminérgicas. Barra de escala = 500 µm. En ambas figuras los recuadros muestran la zona de la SNpc ampliada. Barra de escala = 100 mm. Las cuantificaciones corresponden a la media ± ds de tres experimentos diferentes, con 4 animales por grupo experimental y cinco secciones independientes por animal, expresados como porcentaje relativo al grupo de animales control. ***P<0.001 en comparación con los animales tratados con LPS.

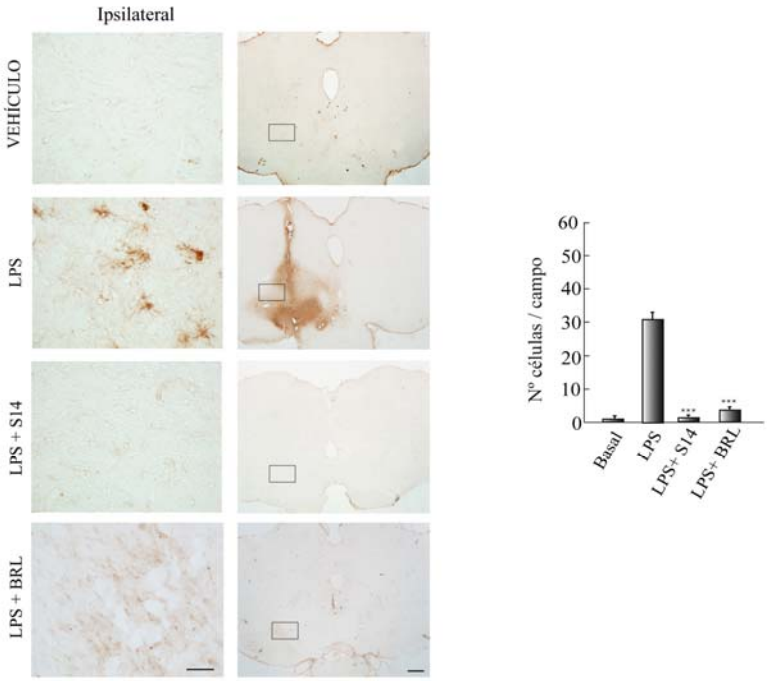

FIGURA 34.- Efecto antiinflamatorio de S14 en un modelo de Parkinson. Se inyectaron Ratas adultas unilateralmente en la substantia nigra pars compacta (SNpc) con vehículo o LPS (10µg) sólo o combinado con S14 (20nmol) o con BRL50481 (60nmol). A las 72h los cerebros fueron extraídos y secciones coronales analizadas por inmunohistoquímica que muestra la expresión de CD11b (OX-42) en la SNpc. A la derecha se muestra la cuantificación del número de células reactivas expresadas como la media ± ds de tres experimentos diferentes, con 4 animales por grupo experimental y cinco secciones independientes por animal. ***P<0.001 en comparación con los animales tratados con LPS. Barra de escala = 500 µm. Los recuadros muestran la zona de la SNpc ampliada a continuación. Barra de escala = 100 µm.

El uso como control de otro inhibidor de PDE7, BRL50481 nos permitió comprobar que dicho inhibidor poseía un efecto neuroprotector y anti-inflamatorio similar al observado con el S14. Su inyección conjunta con LPS hacía que sólo disminuyera en un 20% el número de neuronas dopaminérgicas (figura 33B), valor significativamente inferior al 85% de pérdida neuronal dopaminérgica observada en los animales inyectados solo con LPS. Igualmente el BRL50481 disminuía la hiperactivación de la microglía observada en el grupo de ratas tratadas con LPS (figura 34). Estos resultados refuerzan nuestra hipótesis de que PDE7 pudiera ser una excelente diana en el campo de la neuroprotección de neuronas dopaminérgicas.

Finalmente analizamos desde un punto de vista del comportamiento el efecto neuroprotector de S14. Para ello realizamos un test de comportamiento rotacional tres semanas después de lesionar la SNpc con LPS. Para ello administramos a los animales apomorfina y analizamos el número de giros que realiza el animal. La apomorfina, al ser un agonista dopaminérgico, induce de manera contralateral un comportamiento rotatorio en los animales hemi-parkinsonianos. Los animales lesionados, tras la inyección de apomorfina, comenzaron a realizar movimientos rotatorios, girando como mínimo 7 veces por minuto contralateralmente al hemisferio

lesionado (figura 35), en contraposición a la ausencia de vueltas de los animales control. Los animales inyectados con S14 solo realizaron un giro por minuto, lo que sugiere una elevada integridad de la SNpc.

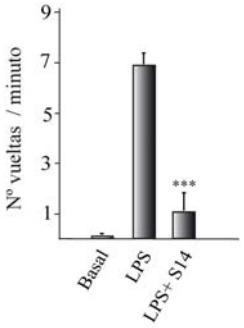

FIGURA 35.- Test de comportamiento rotacional. Ratas adultas fueron inyectadas unilateralmente en la *substantia nigra pars compacta* (SNpc) con vehículo o LPS (10µg) sólo o combinado con S14 (20nmol). Tres semanas después de la inyección a los animales se les indujo un comportamiento rotatorio mediante una inyección con apomorfina. Los valores representan la media ± ds de tres experimentos diferentes, con 12 animales/grupo experimental. ***P<0.001 en comparación con los animales inyectados con LPS.

Discusión

1.- NEUROGÉNESIS

La presencia en el cerebro adulto de células madres neurales, concretamente en la zona subventricular de los ventrículos laterales (ZSV) y en la zona subgranular del hipocampo (ZSG), está bien establecida. Sin embargo, nuestro conocimiento de los factores y mecanismos que promueven y regulan la proliferación, migración, diferenciación y supervivencia de dichas células madre es limitado. En este trabajo hemos analizado el papel que ejercen PPARγ y GSK3-β sobre la neurogénesis en ratas adultas, valorando su importancia como posibles dianas celulares en el tratamiento de enfermedades neurodegenerativas. Nuestros resultados muestran que ligandos capaces de activar PPARγ estimulan la neurogénesis en la zona subventricular e inhibidores de GSK3β estimulan la neurogénesis en la zona subgranular del giro dentado del hipocampo, sugiriendo que ambas dianas podrían jugar un papel importante en la expansión y diferenciación de estas poblaciones de células madres en el cerebro adulto. Esto sin duda es de gran interés clínico ya que podrían representar dos dianas terapéuticas importantes en procesos de reparación del daño neurológico donde se produce una gran pérdida de neuronas.

1.1.- Efecto neurogénico de los ligandos de PPARγ.

Nuestros estudios *in vivo* muestran claramente que la pioglitazona promueve en ratas adultas: 1) la proliferación de neuroblastos en la ZSV, 2) su migración a través de la CMR y 3) su diferenciación a neuronas granulares y periglomerulares en el BO. De forma congruente con estos estudios *in vivo*, hemos observado que tanto pioglitazona como rosiglitazona, promueven la expansión y diferenciación de células madre neurales en cultivo, puesto que aumentan la formación de neuroesferas primarias y secundarias. Confirmamos además *in vitro* que este efecto de pioglitazona y rosiglitazona está muy probablemente mediado por PPARγ, puesto que GW9662 y T0070907, dos inhibidores específicos de este receptor, consiguen bloquear el efecto de ambos ligandos. Estos resultados son la primera demostración de que ligandos de PPARγ inducen neurogénesis en adultos, sugiriendo que este receptor podría ser una diana terapéutica importante en procesos de reparación del sistema nervioso. De interés es que la ZSV, donde se han estudiado estos efectos, es la mayor fuente de progenitores neurales que posee el cerebro adulto (Lois and Alvarez-Buylla, 1993; Morshead et al., 1994), los cuales migran hacia el bulbo olfatorio a través de la corriente migratoria rostral (CMR), donde diferencian a neuronas (Alvarez-Buylla and Garcia-Verdugo, 2002; Doetsch et al., 1997; Gage, 2002; Garcia-Verdugo et al., 1998).

La pioglitazona induce también la migración de células progenitoras de la ZSV. En los animales tratados con este ligando de PPARγ hemos observado más cadenas de neuroblastos, que se localizan en capas mas profundas de la ZSV, en el neuropilo. Las cadenas de neuroblastos observadas en los animales tratados presentan grandes espacios intercelulares, los cuales están

relacionados con las necesidades de movimiento de las células (Doetsch et al., 1997). Estos resultados son similares a los descritos por Doetsch et al. (2002), en ratones tratados con factor de crecimiento epidérmico (EGF) administrado intraventricularmente mediante una bomba osmótica. A pesar de que el EGF posee un efecto neurogénico más potente que pioglitazona y rosiglitazona, los ligandos de PPARγ tendrían la ventaja de ser moléculas pequeñas, estables y que se pueden administrar por vía gástrica, ya que, por lo menos, pioglitazona es capaz de atravesar la barrera hematoencefálica. El aumento de células en fase de migración en los animales tratados con pioglitazona que sugieren estos resultados, se confirma por el elevado numero de células DCX^+ que encontramos en la ZSV y de células PSA-$NCAM^+$ que encontramos en la ZSV y CMR de los animales tratados. Ya hemos apuntado que las neuronas generadas en la ZSV migran a través de la CMR y se integran finalmente en el BO como interneuronas granulares y periglomerulares (Bayer, 1983; Kaplan and Hinds, 1977; Pencea et al., 2001). Dado que el tratamiento con pioglitazona produce un aumento en la proliferación y migración celular seria de esperar también, si el proceso se completa de forma adecuada, un aumento de nuevas interneuronas en el BO de los animales tratados. Efectivamente nuestros resultados muestran que existe un aumento de células marcadas con NeuN y BrdU en la capa granular del BO. En este trabajo no hemos analizado las consecuencias funcionales del aumento de la neurogénesis en los animales inyectados con pioglitazona. Sin embargo, en base a los datos de la literatura científica, seria razonable suponer que el tratamiento con pioglitazona mejoraría la memoria olfativa. Se ha demostrado que la neurogénesis es esencial en el mantenimiento del número de neuronas del BO (Drapeau and Nora Abrous, 2008; Lazarini et al., 2009; Zhao et al., 2008), mejora los procesos de aprendizaje relacionados con el olfato (Romero-Grimaldi et al., 2006), regula la memoria olfativa a corto plazo en ratones adultos (Breton-Provencher et al., 2009; Kermen et al.; Rochefort et al., 2002; Sultan et al., 2010) y es fundamental para el reconocimiento parental de las crías (Mak and Weiss, 2010).

Los resultados que hemos obtenidos *in vitro* confirman los resultados observados *in vivo* y sugieren claramente que dichos efectos podrían estar mediados de forma directa por el receptor PPARγ. Pioglitazona y rosiglitazona inducen proliferación, diferenciación y migración de células madre neurales en cultivo y dichos efectos se bloquean cuando además de con estos ligandos las células se incuban con los antagonistas de PPARγ, GW9662 y T0070907. De acuerdo con estos resultados hemos observado que los cultivos de células madre procedentes de la ZSV expresan PPARγ, al igual que la ZSV en animales adultos. Todo ello es compatible con la hipótesis de que las células madre tienen receptores PPARγ a través de los cuales se producirían los efectos observados. Es interesante en este sentido señalar que células madre neurales obtenidas de embriones transgénicos con un solo alelo de este receptor ($PPAR\gamma^{+/-}$), y por tanto con menor contenido del mismo, crecen de forma mucho mas lenta y con una morfología alterada (Wada et

al., 2006). Lo mismo se observa en células madre neurales en cultivo, al silenciar la expresión de PPARγ mediante el uso de lentivirus con RNA de interferencia para este factor de transcripción (Wada et al., 2006).

La formación de neuroesferas secundarias permite evaluar el potencial expansivo y la capacidad autorrenovadora de las células madre, puesto que a partir de las células disociadas de una neurosfera primaria se pueden originar múltiples neurosferas secundarias sin perder su actividad proliferativa ni su potencial de generar los diversos tipos de células neurales. La propia formación de neuroesferas secundarias es un indicador de la división de las células madre neurales por autorrenovación. (Reynolds and Weiss, 1996). El incremento significativo observado en el número de neuroesferas secundarias formadas tras el tratamiento con pioglitazona y rosiglitazona sugiere que los ligandos de PPARγ estimulan la capacidad de división celular asimétrica o autorrenovadora de las células madre neurales, lo que conduce a su expansión.

Las células madre neurales son capaces de diferenciarse a neuronas, astrocitos y oligodendrocitos (Gage, 2000; Temple, 2001). Nuestros resultados muestran cómo la activación de PPARγ induce la diferenciación de las células madre hacia neuronas y astrocitos. Esto contrasta con los estudios publicados por Wada y cols. (2006) donde observan que ligandos de PPARγ en cultivos de células madre neurales de origen embrionario estimulan la proliferación pero inhiben la diferenciación. Esta discrepancia podría deberse a razones metodológicas o a diferencias en las condiciones experimentales, puesto que este grupo utiliza neuroesferas procedentes de cerebros completos de embriones mientras que en este trabajo hemos utilizado neuroesferas aisladas de ZSV de ratas adultas.

Nuestros resultados muestran también que pioglitazona y rosiglitazona promueven la migración de células madre neurales en cultivo. Cuando las condiciones experimentales cambian y se pasa de cultivos de neuroesferas en flotación a neuroesferas adheridas a sustrato, las células son capaces de migrar fuera de la neuroesfera (Ocbina et al., 2006). Nuestros resultados reflejan claramente como el tratamiento con ligandos de PPARγ aumenta el número de células que salen de la neurosfera y la distancia a la que se alejan, confirmándose los resultados que habíamos obtenido *in vivo*. Se observa una cierta tendencia por parte de las células a migrar de manera individual, en lugar de hacerlo formando cadenas como ocurre *in vivo* o tal y como han descrito otros autores en cultivo (Wichterle et al., 1997). Esta diferencia podría ser debida a las condiciones de cultivo utilizadas por Wichterle y col. y las que hemos utilizado en este trabajo.

En resumen nuestros resultados sugieren claramente que los ligandos de PPARγ, posiblemente por la activación de este receptor, son capaces de mantener la población de células madre neurales y de inducir la diferenciación y migración de estas células en la ZSV de animales adultos. Estos datos sugieren que el factor de transcripción PPARγ, podría representar una nueva

diana capaz de promover correctamente el proceso de neurogénesis, a través de su activación por diversos ligandos capaces de atravesar la barrera hematoencefálica, y por tanto con nuevas posibilidades terapéuticas en enfermedades del sistema nervioso central, como enfermedades neurodegenerativas, donde se produce una muerte neuronal masiva. Un hecho interesante a destacar es la capacidad de inducir migración por parte de estos ligandos, ya que cuando se produce un daño neuronal es importante no sólo que se produzcan nuevas neuronas capaces de reparar el daño, sino también que éstas sean capaces de migrar hacia el sitio dañado.

1.2.- Efecto neurogénico de los inhibidores de GSK-3β.

La ZSG es uno de los grandes nichos neurogénicos en el cerebro adulto (Altman and Das, 1965; Kuhn et al., 1996) estimándose que unas 9000 nuevas células nacen diariamente en el hipocampo de rata (Cameron and McKay, 2001). Nuestros resultados muestran claramente que la administración *in vivo* de NP031112, un inhibidor de GSK3β, aumenta la proliferación celular en el hipocampo. Igualmente los experimentos realizados *in vitro* confirman que la inhibición de GSK3-β promueve la expansión y mantenimiento de las células madre neurales procedentes de hipocampo aumentando el número y el tamaño de las neuroesferas formadas y la expresión de un marcador de proliferación como Ki67. La mayoría de las células formadas en la ZSG migran una pequeña distancia hasta integrarse en la capa granular donde diferencian a neuronas granulares que proyectan sus axones hasta la región CA3 (Jessberger and Kempermann, 2003; Kempermann et al., 2004, Toni, 2008 #1145; van Praag et al., 2002). La inhibición de GSK3-β, tal y como muestran nuestros resultados, promueve la migración celular en esta zona *in vivo*, y favorece, *in vitro,* el movimiento de las células fuera del núcleo de la neuroesfera, cuando se cultivan en condiciones de adherencia. En estas condiciones de adherencia la inhibición de GSK3-β también estimula la formación de nuevas neuronas puesto que incrementa el número de células positivas para β-tubulina. Estos resultados sugieren que GSK3-β podría ser una diana terapéutica cuya inhibición promovería correctamente el proceso de neurogenesis lo que sin duda es de gran interés clínico en un contexto de daño cerebral de origen traumático o neurodegenerativo.

Nuestros resultados mostrando un aumento de proliferación *in vitro* en presencia de inhibidores de GSK3-β están de acuerdo con datos previos que muestran la importancia de GSK3-β en el mantenimiento de las características de las células madre. La inhibición de GSK3-β mediante 6-bromoindirubin-3'-oxime (BIO) mantiene la capacidad pluripotencial y favorece la auto-renovación de las poblaciones de células madre embrionarias en humanos y roedores (Sato et al., 2004; Storm et al., 2007; Tateishi et al., 2007). Otra manera de silenciar este enzima es mediante el uso de células madre embrionarias de ratón con el gen de GSK3-β truncado. En este sistema, la deleción de GSK-3β condujo a un aumento masivo en la expresión de fosfo-histona-3 y BrdU,

demostrando que la inactivación de GSK-3β induce la proliferación de progenitores neurales (Doble and Woodgett, 2007; Kim et al., 2009b).

Hasta el momento no había datos acerca del efecto de la inhibición de GSK3-β sobre precursores neurales del hipocampo, aunque es sabido que GSK-3β se expresa en el citoplasma, núcleo y mitocondria de las neuronas granulares del giro dentado del hipocampo (Bijur and Jope, 2003; Hong et al., 2009). Nuestros resultados muestran que la inhibición de GSK3-β induce *in vitro* la proliferación y expansión de células madre neurales procedentes de hipocampo de animales adultos. Estos resultados en hipocampo concuerdan con los descritos por Maurer y cols. (2007) en neurosferas de la ZSV de ratas adultas. Dicho estudio muestra como la inactivación de GSK-3β, mediante el uso del inhibidor SB216763, aumenta la proliferación y neurogénesis en células madre neurales de esa región (Maurer et al., 2007).

El posible papel de GSK3-β en la migración celular no se ha descrito en células madre neurales, existiendo tan sólo dos estudios que sugieren que la inhibición de GSK-3β aumenta la migración celular en cultivos de astrocitos (Etienne-Manneville and Hall, 2003) y de fibroblastos (Bianchi et al., 2005). El trabajo de Etienne-Manneville y cols. (2003) mostró que los niveles de GSK3-β fosforilado en serina 9 (GSK3-β inactiva) eran mucho mayores en aquellos astrocitos en migración. Confirmó además estos resultados mediante el uso de inhibidores como LiCl y SB216763, tratamientos que potenciaban la capacidad de migración de astrocitos. Por su parte Bianchi y cols (2005) silenciaron la expresión de GSK3-β mediante el uso de un RNA de interferencia, comprobando que dicha inactivación del enzima favorecía la capacidad migratoria de los fibroblastos. Nuestros resultados muestran por primera vez que la inhibición de GSK3-β induce la migración de precursores neurales del hipocampo fuera de la neuroesfera cuando esta se crece en adhesión.

Con respecto al papel de GSK-3β en la diferenciación, se ha descrito que la inhibición de dicho enzima induce la diferenciación de precursores neuronales dopaminérgicos de mesencéfalo embrionario a neuronas dopaminérgicas adultas (Castelo-Branco et al., 2004). Lo mismo ocurre en cultivos de células del cerebelo, donde el tratamiento con cloruro de litio, inhibidor clásico de GSK-3, contribuye a la maduración de las neuronas granulares cerebelares (Lucas et al., 1998). Desde un abordaje experimental opuesto, los resultados son similares. Por ejemplo, Spittaels y cols. (2002) han demostrado que la sobreexpresión de GSK-3β en ratones transgénicos se correlaciona con una disminución del volumen cerebral, sobre todo en la región de la corteza, debido a una disminución de la población neuronal y alteraciones en la ramificación de las terminaciones nerviosas (Spittaels et al., 2002). Nuestros resultados siguen esta línea puesto que encontramos también que la inhibición de GSK-3β induce diferenciación de precursores neurales del hipocampo. Aún así existe cierta discrepancia con los resultados obtenidos en el grupo del Dr.

Doble, que describen como en células madre embrionarias de animales GSK3-$\beta^{-/-}$, la ausencia del enzima produce una pérdida en la capacidad de diferenciación de estas células (Doble et al., 2007; Kim et al., 2009b), disminuyendo la capacidad neurogénica de las mismas, tal y como vieron al estudiar la expresión de marcadores como β-tubulina, MAP2, SMI32 y NeuN. Esta discrepancia podría deberse al sistema biológico estudiado, puesto que estos investigadores utilizan células madre embrionarias de corteza cerebral, procedentes de ratones con mutación doble, en el gen de GSK3-α y GSK3-β.

En nuestro trabajo, la diferenciación inducida por la inhibición de GSK-3β que observamos es fundamentalmente hacia un linaje neuronal. Cabe recordar que los precursores neurales recién formados diferencian hacia un linaje neuronal o un linaje glial inmediatamente después de su formación (Steiner et al., 2004; Steiner et al., 2008). Por eso la diferenciación a un linaje u otro, es un proceso altamente sensible a cambios patológicos y fisiológicos. De hecho los procesos inflamatorios que suponen el elemento común en muchas enfermedades neurodegenerativas conducen a una mayor diferenciación hacia un fenotipo glial (Ekdahl et al., 2003; Monje et al., 2003) en detrimento de un fenotipo neuronal. Se ha postulado que la neurogénesis adulta pueda ser un mecanismo compensatorio a la perdida neuronal en desordenes neurológicos o como consecuencia del envejecimiento. Esta afirmación viene avalada por el aumento de neurogénesis observada en algunas enfermedades neurodegenerativas (Curtis et al., 2003; Jin et al., 2006), incluida la enfermedad de Alzheimer (Jin et al., 2004). Nuestros resultados mostrando que la inhibición de GSK-3β aumenta el potencial neurogénico en el hipocampo, y promueve la diferenciación hacia un linaje neuronal sugieren que GSK-3β podría ser una diana terapéutica en enfermedades neurodegenerativas como el Alzheimer o la enfermedad de Parkinson.

Finalmente experimentos *in vivo* confirman nuestros resultados *in vitro*. Hemos observado como la administración *in vivo* de un inhibidor de GSK-3β, NP031112, aumenta la proliferación celular en el giro dentado del hipocampo. Este aumento de la proliferación podría explicar el incremento en el número de precursores celulares, tal y como se ha sugerido en otros estudios (Couillard-Despres et al., 2005; Kim et al., 2009a). Estos resultados, obtenidos con marcaje con BrdU, se ven confirmados por el aumento de células marcadas con DCX y PSA-NCAM. DCX se expresa transitoriamente en precursores neuronales y en neuronas inmaduras, por lo cual es utilizado habitualmente como marcador de neurogénesis (Brown et al., 2003). Además existe una relación directa entre aumento del número de células que expresan DCX con el incremento de la capacidad neurogénica en hipocampo (Couillard-Despres et al., 2005). PSA-NCAM, que se expresa en el hipocampo de roedores adultos, fundamentalmente en neuronas recién formadas de la capa granular (Seki and Arai, 1993), actua como regulador de la plasticidad neuronal y sináptica (revisado en Bonfanti, 2006; Gascon et al., 2007; Rutishauser, 2008). Nuestros resultados muestran

claramente que la inhibición de GSK-3β *in vivo* no solo produce un aumento de la proliferación celular en el giro dentado del hipocampo sino que además se observa un incremento del número de células DCX^+ y $PSA\text{-}NCAM^+$, lo que efectivamente sugiere que la administración oral del compuesto NP031112 es capaz de inducir neurogénesis en el hipocampo.

El aumento del número de células PSA-NCAM inmunoreactivas en la capa granular del giro dentado del hipocampo es un hecho característico en modelos animales de daño cerebral (Emery et al., 2000), relacionándose el aumento de expresión de PSA-NCAM con un aumento en la plasticidad neuronal de la zona dañada, con un aumento en el número de neuronas regenerándose o bien con un aumento en el número de nuevas neuronas formadas. Por tanto el uso de NP031112 como inhibidor de GSK-3β pudiera ser un agente eficaz como inductor de neurogénesis en aquellas enfermedades que, como el Alzheimer o Parkinson, cursan con una importante pérdida neuronal. Finalmente, no podemos descartar que lo efectos descritos para NP031112 *in vivo* puedan deberse también a mecanismos diferentes de la inhibición de GSK3-β, ya que nuestro laboratorio ha descrito que este compuesto es capaz de activar PPARγ (Luna-Medina et al., 2007).

2.- NEUROPROTECCIÓN.

Las enfermedades neurodegenerativas se caracterizan por una pérdida gradual progresiva y selectiva de neuronas. El deterioro funcional dependerá de las células que se pierden y del área afectada. En este trabajo hemos analizado el efecto neuroprotector de dos moléculas que actúan sobre dos dianas distintas, NP04634, un inhibidor novel de canales de calcio sensibles a voltaje (CCSVs) tipo no-L y S14, un nuevo inhibidor de fosfodiesterasa 7 (PDE7). El posible efecto neuroprotector de cada uno de ellos se analizó en un modelo distinto de neurodegeneración. NP04634 en daño excitotóxico en hipocampo inducido por KA y S14 en daño inflamatorio en SNpc inducido por LPS. Nuestros resultados muestran que ambos compuestos tienen un potente efecto neuroprotector y antiinflamatorio sugiriendo que ambas dianas podrían ser relevantes para el desarrollo de nuevas estrategias terapéuticas.

2.1.- Efecto neuroprotector de NP04634.

Los análisis de comportamiento muestran que NP04634 disminuye el porcentaje de animales que entran en *status epilepticus* (SE) tras la inyección de KA y aumenta el tiempo de latencia en aquellos animales que alcanzan dicho SE. Todo ello sugiere que este compuesto ejerce un efecto anticonvulsivo. El análisis histológico muestra que NP04634 previene en gran medida la muerte neuronal en las capas CA1 y CA3 del hipocampo producida como consecuencia de daño excitotóxico. También observamos una disminución de la inflamación en el hipocampo.

Finalmente, los resultados obtenidos en el estudio *in vitro* refuerzan estos resultados, ya que muestran un potente efecto anti-inflamatorio de NP04634 en cultivos primarios de astrocitos.

Los CCSVs son la principal vía de entrada de calcio como consecuencia de la despolarización de la neurona por acción del glutamato, expresándose en el hipocampo los seis subtipos de CCSVs: L, N, P, Q, R y T (Lee et al., 2004; Leitch et al., 2009; Talley et al., 1999). Nosotros hemos utilizado el modelo animal de excitotoxicidad inducida por kainato puesto que estudios fisiológicos previos habían demostrado que los CCSVs, presentes en las células del hipocampo, aumentaban su actividad en las neuronas CA1 y células granulares del giro dentado en comparación con los animales control (Beck et al., 1998; Faas et al., 1996). En concreto en las neuronas CA1 esa actividad es debida fundamentalmente a los canales tipo P/Q, L y R. (Hendriksen et al., 1997). Nuestro trabajo se ha basado también en datos previos que demostraban la capacidad del compuesto NP04634 para inhibir los CCSVs en células cromafines. Según estos datos NP04634 tendría efectos citoprotectores en un modelo de citotoxicidad mediada por Ca^{2+} (Valero et al., 2009).

Por otra parte la inyección de KA afecta particularmente al hipocampo puesto que esta zona del cerebro posee una alta concentración de receptores de kainato, por lo que el daño observado en este modelo experimental reproduce en parte las alteraciones características de la epilepsia del lóbulo temporal en humanos, debido a la entrada masiva de calcio, lo que contribuye a la aparición de daño neuronal (Pal et al., 1999; Sombati and Delorenzo, 1995; Sun et al., 2002). Puesto que la activación excesiva de los CCSVs es una vía importante de entrada de calcio y contribuye notablemente al daño excitotóxico (Verkhratsky, 2005), diversos estudios apuntan al uso de inhibidores de CCSVs en terapia anticonvulsiva y antiexcitotóxica. Por ejemplo, se ha descrito el efecto neuroprotector de toxinas bloqueantes de canales de tipo N y P/Q en modelos experimentales de daño isquémico (Asakura et al., 1997; Huang et al., 1997; Lee et al., 2004). Nuestros resultados muestran que la administración de NP04634 previa a la administración de KA tiene un claro efecto anticonvulsivo ya que reduce notablemente el número de "sacudidas de secado", retrasa el tiempo necesario para alcanzar el SE y reduce claramente el número de animales que entran en SE. Los efectos del NP04634 que hemos descrito concuerdan con trabajos previos donde se muestran los efectos antiepilépticos de las sustancias que actúan como bloqueantes de los CCSVs neuronales, como es el caso del antiepilético lamotrigina, que inhibe los canales de tipo no L (Stefani et al., 1996), tal y como se ha propuesto para NP04634. Del mismo modo las toxinas que bloquean los canales de tipo N y P/Q previenen el desarrollo de epilepsia en modelos de estimulación eléctrica repetida (Gasior et al., 2007; Wang et al., 2007) y poseen efectos antiepilépticos en modelos animales de ataques inducidos por sonidos de alta intensidad (Jackson and Scheideler, 1996). Estos datos concuerdan con el hecho de que los canales de calcio sensibles a voltaje de tipo N y P/Q son muy abundantes en los terminales presinápticos (Sabria et al., 1995) y

que el calcio juega un papel importante en la liberación de neurotransmisores. Ya hemos apuntado con anterioridad que el calcio a altas concentraciones citosólicas es extremadamente tóxico para las células del SN (Choi, 1988; Doble, 1999; Meldrum and Garthwaite, 1990; Wang et al., 2005), razón por la cual aquellas moléculas con capacidad para bloquear los canales de calcio han sido objeto de estudio debido a su potencial neuroprotector. Los efectos farmacológicos de bloqueo de los CCSVs de tipo no-L se realizan en concreto mediante el uso de toxinas como la ω-agatoxina IVA para los estudios de canales P/Q y ω-conotoxina GVIA y ω-conotoxina MVIIA para canales tipo N. Sus efectos neuroprotectores han sido ampliamente estudiados en diferentes modelos animales de daño cerebral en los que esta implicado el glutamato, como la isquemia (Asakura et al., 1997; Berman et al., 2000; Buchan et al., 1994; Lee et al., 2004; Samii et al., 1999; Valentino et al., 1993; Yamada et al., 1994; Zhao et al., 1994). Sin embargo estos péptidos aunque son considerados bloqueantes selectivos de CCSVs, han resultado no ser tan específicos como se pensaba siendo además sus efectos de duración y eficacia limitada (Cohen & Kraus, 2004). Además de estas toxinas se han descrito también un pequeño número de bloqueantes de CCSVs neuronales mas adecuados para tratamiento oral. Estas moléculas, como el LY042826 y LY393615 (Hicks et al., 2000) o el NNC 09-0026 y CNS 1237 (O'Neill et al., 1997) aunque han demostrado tener cierta capacidad neuroprotectora *in vivo* en diferentes modelos de isquemia cerebral son también menos específicas (Asakura et al., 2000; Hu et al., 1999; Huang et al., 1997; Menzler et al., 2000; Schelkun et al., 1999). Existe también cierta controversia con el uso de inhibidores de tipo L, puesto que los resultados obtenidos tanto en modelos experimentales como en ensayos clínicos parecen no ser muy homogéneos (Gotoh et al., 1986; Horn et al., 2001; Kawaguchi et al., 1999; Mohr et al., 1994; Roda et al., 995; Snape et al., 1993; Wahlgren et al., 1994 ; Clark et al., 1997, 1999, 2001; Schabitz et al., 1996; Tazaki et al., 1988).

La neuroinflamación, como ya hemos comentado, participa de forma notable como agente causal del daño neuronal que acontece en diversas patologías (Buffo et al.). En este sentido existen múltiples trabajos que asocian el daño causado por KA con una activación significativa de las células gliales lo cual conduce a una mayor muerte neuronal (Jung et al., 2006; Kawaguchi et al., 2005; Rappold et al., 2006). Nuestros resultados muestran que las alteraciones morfológicas que sufren los astrocitos junto con el importante incremento en la expresión de GFAP, síntomas típicos de hiperactivación astroglial, se encuentran notablemente reducidos en aquellos animales tratados con NP04634. La microglía también se vé afectada como consecuencia de la acción del KA, activación que queda de igual modo bloqueada por acción del NP04634. Esa hiperactivación de las células gliales es fundamental en el desarrollo de la neurodegeneración del hipocampo inducida por KA puesto que inducen la expresión de genes proinflamatorios que contribuyen a la iniciación del proceso de degeneración neuronal. En este sentido el análisis *in vitro* del posible efecto antiinflamatorio de NP04634 muestra claramente que este compuesto, en células gliales, bloquea

directamente la activación de la cascada inflamatoria inducida por LPS. Esto se traduce en una disminución en la producción de TNF-α y COX-2, dos potentes agentes proinflamatorios, en cultivos primarios de astrocitos tratados con NP04634. Estos resultados concuerdan con los obtenidos previamente *in vivo*, indicando que la activación glial queda significativamente disminuida en los animales tratados con NP04634. Por tanto es evidente que NP04634 inhibe directamente la inducción de mediadores proinflamatorios en las células gliales. La regulación de los mediadores proinflamatorios se considera como un mecanismo clave en el control de la muerte celular. COX-2 esta implicado en la patogénesis de múltiples alteraciones neurológicas (Giovannini et al., 2003; Teismann et al., 2003), y el aumento de su expresión se ha asociado con isquemia y epilepsia (Minghetti, 2007; Nogawa et al., 1997; Oliveira et al., 2008). Otro de los factores proinflamatorios, TNF-α, se sobreexpresa en modelos experimentales basados en convulsiones (Vezzani et al., 2008). La disminución de la actividad proinflamatoria que induce el tratamiento con NP04634 se encuentra asociada a una importante disminución en la muerte de las neuronas de las capas CA1 y CA3 del hipocampo. Por el contrario, los animales inyectados con KA presentan una gran perdida neuronal en dicha zona. Por tanto la supresión por parte del NP04634 tanto de la expresión de COX-2 como de TNF-α en respuesta a un daño cerebral puede ser la responsable de la reducción en la pérdida neuronal del hipocampo observada *in vivo*. Estos resultados prueban que el compuesto NP04634 ejerce un potente efecto neuroprotector en un modelo establecido de daño excitotóxico inducido por KA. Resulta de interés el hecho de que la prevención de la muerte neuronal por parte de este compuesto se produce independientemente de si el animal alcanza el SE o no. Aunque se sabe que la pérdida neuronal es el resultado de la intensa actividad convulsiva producida, se ha descrito que los ataques breves pero intermitentes también inducen daño neuronal (Bengzon et al., 1997). A pesar de estos datos nosotros no observamos una pérdida neuronal significativa en el hipocampo de los animales tratados con NP04634 que han alcanzado el SE lo que sugiere que este compuesto actúa como un potente agente neuroprotector.

Respecto al mecanismo de acción por el cual el compuesto NP04634 estaría ejerciendo su actividad, existen evidencias que sugieren que dicho compuesto pudiera actuar bloqueando los CCSVs de tipo no-L, aunque sería necesario realizar un estudio electrofisiológico en detalle. Por un lado, el compuesto NP04634 posee una gran capacidad para bloquear la entrada de calcio en experimentos de despolarización celular realizados en células cromafines bovinas (Valero et al., 2009), células que comparten con las neuronas muchas características, como por ejemplo la expresión de los mismos CCSVs. En dichas células, los canales de calcio de tipo no-L constituyen la mayoría de los canales CCSVs, contribuyendo aproximadamente al 80% de las corrientes globales de calcio (Garcia et al., 2006), bloqueando el compuesto NP04634 a bajas concentraciones (<10 μM) fundamentalmente a los subtipos P/Q (Valero et al., 2009). Por otro lado nuestros

resultados demuestran una potente acción antiinflamatoria del compuesto NP04634, reduciendo notablemente la hiperactivación glial tanto *in vivo* como *in vitro*. Curiosamente este tipo de canales se encuentran en mayor grado en cultivos primarios de astrocitos (D'Ascenzo et al., 2004; Latour et al., 2003) siendo además el calcio uno de los principales mensajeros secundarios implicados en la producción de citoquinas en las células gliales (Hoffmann et al., 2003; Robbins et al., 1987).

Nuestros resultados muestran que NP04634 posee un notable efecto anti-inflamatorio, neuroprotector y anti-convulsivo, en un modelo de daño cerebral excitotóxico inducido por KA. Además este compuesto es capaz de disminuir la inducción de agentes pro-inflamatorios tales como COX-2 y TNF-α en cultivos primarios de astrocitos tratados con LPS. Puesto que el NP04634 es un bloqueante eficaz de los CCSVs no de tipo L, resulta razonable especular que su acción estaá mediada por inhibición de este tipo de canales, aunque no nos es posible excluir la posibilidad de que NP04634 pueda actuar a través de algún otro mecanismo. NP04634 puede ser considerado por tanto como una nueva droga con acción antiinflamatoria, neuroprotectora y anticonvulsiva a tener en cuenta por su posible potencial terapéutico para el tratamiento de patologías relacionadas con excitotoxicidad por calcio, como es el caso de la epilepsia y otros desórdenes neurodegenerativos.

2.2.- Efecto neuroprotector de la inhibición de fosfodiesterasa 7.

Nuestros resultados muestran claramente que la inhibición de PDE7 tiene un efecto neuroprotector en células dopaminérgicas tanto *in vivo* como *in vitro.* En el caso de los estudios *in vitro* hemos observado que la inhibición de PDE7 protege de la muerte inducida por 6-OHDA tanto en la línea neuronal dopaminérgica humana SH-SY5Y como en cultivos primarios de mesencéfalo embrionario. Además atenúa la producción de nitritos y la producción de agentes proinflamatorios. Estos resultados podrían ser de gran interés en relación con la enfermedad de Parkinson si tenemos en cuenta que el efecto neurotóxico de 6-OHDA, en modelos animales tanto *in vitro* como *in vivo*, comparte muchas similitudes con lo que se piensa que ocurre en las neuronas dopaminérgicas que degeneran en pacientes con Parkinson (Ouyang and Shen, 2006). En concreto 6-OHDA altera la actividad mitocondrial y aumenta la producción de especies reactivas de oxigeno que se consideran finalmente las causantes de la muerte de las células dopaminérgicas (Blum et al., 2001). Ya que S14 actúa como inhibidor de PDE7, hemos analizado los niveles de esta enzima en los sistemas que hemos utilizado tanto *in vitro* como in vivo. Con respecto a la expresión de PDE7 en células SH-SY5Y, es muy poco lo que se conoce hasta el momento. Sólo un trabajo, mediante PCR a tiempo real ha descrito la presencia de RNA mensajero (mRNA) de PDE7 en estas células (Hoffmann et al., 1998). En este trabajo hemos mostrado que la proteína PDE7 esta presente en células SH-SY5Y y también en precursores dopaminérgicos embrionarios ya que hemos observado que, en cultivos de estas células, se coexpresa con tirosina-hidroxilasa (TH).

De acuerdo con la neuroprotección observada *in vitro* por S14 los resultados obtenidos en un modelo de Parkinson *in vivo* han demostrado que el tratamiento con el compuesto S14 protege notablemente de la degeneración neuronal dopaminérgica y reduce la activación glial. Estos efectos de S14 sobre la población de células dopaminérgicas y la disminución de los proceso inflamatorios se tradujo en una notable mejoría de la función motora de las ratas lesionadas tratadas con este compuesto.

De igual manera que lo observado *in vitro* en cultivos de células, tanto en la línea celular SH-SY5Y como en cultivos mesencefálicos, hemos comprobado que PDE 7 se expresa en la SNpc, tal como sugieren nuestros estudios de inmunohistoquímica. Estos resultados confirman y amplían resultados previos que describían la presencia de la isoforma PDE7B por hibridación in situ en secciones de cerebro de rata (Reyes-Irisarri et al., 2005). Nuestros resultados describen por primera vez la presencia de proteína de las dos isoformas de PDE7 en la SNpc de rata. Además no solo demostramos que PDE7A y B estan presentes en la SNpc, sino que su expresión aumenta notablemente tras la inyección de LPS, sugiriendo que un aumento de la actividad de PDE7 podría ser un factor a considerar a la hora de entender como se produce el daño en las neuronas dopaminergicas. El hecho de que los inhibidores de PDE7 resulten tan eficaces en modelos de daño diferentes como los analizados *in vivo* e *in vitro* sugieren que PDE7 podría ser una diana muy importante de cara al desarrollo de nuevas terapias para EP.

Con respecto al mecanismo de acción de S14, los resultados obtenidos en este trabajo demuestran que este compuesto ejerce su acción a través de la vía de señalización de AMPc /PKA. La incubación de células SH-SY5Y con S14 provoca un aumento en el contenido de AMPc intracelular. El AMPc es capaz de activar al menos tres vías distintas de señalización en las células. La primera que se caracterizó y la que más se ha estudiado es la vía de PKA, la cual conlleva la fosforilación de diferentes sustratos entre los que se encuentran varios factores de transcripción, fundamentalmente CREB. La segunda vía de señalización sería aquella por la que AMPc actúa sobre Epac, que a su vez activa a la GTPasa Rap-1 (Bos, 2003). Por último, AMPc sería capaz de activar Ras, gracias a la activación previa de CNrasGEF (Pham et al., 2000). Nuestros resultados mostrando que los inhibidores de PKA bloquean el efecto neuroprotector de S14 tanto en células SY5 como en cultivos mesencefálicos embrionarios estarían de acuerdo con la hipótesis de que esta vía es la utilizada por S14. El efecto neuroprotector que supone la inhibición de PDE7 concuerda con los resultados obtenidos por otros grupos en los que se describe como la activación de la vía de señalización de AMPc inhibe la muerte celular característica de algunas enfermedades neurodegenerativas, implicando a PKA en procesos de neuroprotección (Lee et al., 2005; Stetler et al.). Además la activación de PKA inducida por AMPc es fundamental para un desarrollo y funcionamiento adecuado de las neuronas (Song et al., 1997). Resulta interesante señalar el aumento generalizado de la muerte celular durante el desarrollo del SNC en los animales carentes

de CREB, lo cual también es patente durante el periodo postnatal, lo que favorece un incremento progresivo de la degeneración del SNC (Lonze et al., 2002; Mantamadiotis et al., 2002). Es importante mencionar también que la inhibición de la vía de señalización de AMPc se ha asociado con el desarrollo de la enfermedad de Alzheimer (Yamamoto-Sasaki et al., 1999) sugiriéndose que la reducción de los niveles de AMPc asociado a una disminución de la fosforilación de CREB, observado en cerebros humanos post-mortem, contribuye al mayor desarrollo de dicha enfermedad. En este sentido cabe recordar que la vía PKA/CREB es de vital importancia en procesos relacionados con la memoria a largo plazo, y que el péptido precursor amiloide actúa directamente sobre esta ruta, disminuyendo los niveles de AMPc, inhibiendo PKA por tanto inhibiendo la fosforilación de CREB (Vitolo et al., 2002) Otras de las patologías asociadas a la inhibición de la via de AMPc es la enfermedad de Hungtinton, donde la disminución de los niveles de AMPc suprime la activación transcripcional dependiente de CREB, lo cual a su vez afecta a la supervivencia neuronal (Jiang et al., 2003; Nucifora et al., 2001; Shimohata et al., 2000). Nuestros resultados añaden nuevos datos importantes demostrando que el aumento de los niveles intracelulares de AMPc *in vitro* como consecuencia de la inhibición de PDE7 favorece la protección de las neuronas dopaminérgicas y ejerce una acción anti-inflamatoria, al igual que lo descrito en otros sistema celulares que revelan que un incremento en los niveles de AMPc como consecuencia de la inhibición de la actividad fosfodiesterasa aumenta la supervivencia de las neuronas motoras medulares (Hanson, 1998), regula la formación de mielina en oligodendrocitos (Bolton & Butt, 2006) y atenúa la activación de las células gliales (Zhang et al., 2002). Aunque nuestros datos indican que AMPc estaría activando PKA, no podemos descartar que otras vías de acción del AMPc hayan sido igualmente inhibidas y que también jueguen un papel importante en los procesos de neuroprotección observados.

Hemos descrito también que el tratamiento *in vitro* con S14 de cultivos primarios embrionarios mesencefálicos disminuye significativamente los niveles de dos potentes agentes proinflamatorios, como TNF-α y COX-2. Durante los últimos años se ha descrito el papel que tienen los procesos neuroinflamatorios en la degeneración nigroestriatal, que constituye la base de la enfermedad de Parkinson. Ya hemos comentado que cuando las células gliales se activan liberan sustancias citotóxicas y agentes proinflamatorios que están directamente implicados en el desarrollo de múltiples patologías neurodegenerativas (Glass et al. 2010). Por tanto, controlando dichos procesos neuroinflamatorios podemos evitar el avance de la degeneración neuronal. De hecho estudios epidemiológicos han sugerido que el tratamiento crónico con antiinflamatorios no esteroideos puede proteger contra enfermedades neurodegenerativas como el Alzheimer y el Parkinson (Chen et al., 2003; Hald and Lotharius, 2005; Townsend and Pratico, 2005). En nuestro modelo *in vivo* de Parkinson, mediante la administración LPS, reproducimos al menos en parte los

procesos neuroinflamatorios que caracterizan esta enfermedad (Dutta et al., 2008; Kim et al., 2000; Liu et al., 2000)

Finalmente, de acuerdo con el efecto neuroprotector descrito, la administración de S14 reduce la perdida de neuronas dopaminérgicas de la SNpc de un 80 a un 20%, observándose además una clara mejoría de la actividad motora en las ratas inyectadas con S14. Las ratas que recibieron LPS sufrían una pérdida de un 80% en el número de neuronas TH-inmunoreactivas, acompañado de la aparición de alteraciones de la función motora. Esto es debido a que la lesión unilateral en la via dopaminérgica nigroestriatal produce un desequilibrio de dopamina entre la zona lesionada del estriado y la que no, por lo que el animal presenta un movimiento rotatorio hacia el lado lesionado (Anden et al., 1966; Ungerstedt and Arbuthnott, 1970). Al tratar a estos animales con un agonista de la dopamina, como la apomorfina, se induce un movimiento rotatorio contralateral a la zona lesionada (Schwarting and Huston, 1996). Este comportamiento rotatorio coincide con el daño a las neuronas dopaminérgicas en la SN y por tanto con la disminución de dopamina en el estriado (Toledo-Aral et al., 2002). Los resultados obtenidos en la prueba de comportamiento pusieron de manifiesto las diferencias significativas existentes entre los animales tratados y los inyectados con LPS, proporcionando el tratamiento con S14 una total protección frente al daño inducido como demuestra la ausencia de rotación en los animales tratados

En resumen hemos demostrado que la inhibición de PDE7 protege a las neuronas dopaminérgicas de la muerte celular y evita una excesiva hiper activación de las células gliales en un modelo *in vitro* e *in vivo* de enfermedad de Parkinson. El mecanismo celular por el cual estos efectos se estarían produciendo indica un incremento del AMPc intracelular, lo que activaría la vía de PKA/CREB. Estos resultados muestran por primera vez que la inhibición de PDE7 conduce a la protección neuronal dopaminérgica y por tanto podría considerarse como nueva diana terapéutica para enfermedades neurodegenerativas.

Conclusiones

1. Los ligandos de PPARγ actúan como reguladores de la neurogénesis en el cerebro adulto, induciendo *in vitro* e *in vivo* la proliferación, migración y diferenciación de la población de células madre neurales en la zona subventricular.

2. Esta acción se bloquea casi totalmente por dos inhibidores específicos de PPARγ, GW9662 y T0070907, sugiriendo que los ligandos de PPARγ actúan fundamentalmente a través de este receptor.

3. La inhibición *in vitro* de GSK-3β en células madre neurales de ratas adultas tiene un potente efecto neurogénico, promoviendo la proliferación, migración y diferenciación a neuronas de estas poblaciones.

4. Estudios *in vivo* muestran que el compuesto NP031112, inhibidor de GSK-3β, tiene efectos neurogénicos en induce migración en la zona subgranular del giro dentado.

5. El inhibidor de canales de calcio dependiente de voltaje tipo no L, NP04634, tiene efectos antiinflamatorios, neuroprotectores y anticonvulsivos en un modelo *in vivo* de daño excitotóxico inducido por ácido kaínico.

6. En cultivos primarios de astrocitos NP04634 inhibe la producción de agentes pro-inflamatorios inducida por LPS.

7. La inhibición de PDE7 *in vitro* protege a las neuronas dopaminérgicas de la muerte celular inducida por diferentes sustancias citotóxicas, disminuyendo la activación de las células gliales y la producción, por tanto, de agentes proinflamatorios. Esta acción probablemente se realice a través de un mecanismo que implica la vía de AMPc-PKA.

8. En estudios *in vivo* los inhibidores de PDE7, S14 y BRL, protegen a las neuronas dopaminérgicas de la SNpc del daño inducido por LPS, mejorando notablemente la respuesta motora de los animales lesionados.

Bibliografía

Abbott, N. J., Ronnback, L., and Hansson, E. (2006). Astrocyte-endothelial interactions at the blood-brain barrier. Nat Rev Neurosci *7*, 41-53.

Abdelrahman, M., Sivarajah, A., and Thiemermann, C. (2005). Beneficial effects of PPAR-gamma ligands in ischemia-reperfusion injury, inflammation and shock. Cardiovasc Res *65*, 772-781.

Aberle, H., Bauer, A., Stappert, J., Kispert, A., and Kemler, R. (1997). beta-catenin is a target for the ubiquitin-proteasome pathway. EMBO J *16*, 3797-3804.

Aimone, J. B., Wiles, J., and Gage, F. H. (2006). Potential role for adult neurogenesis in the encoding of time in new memories. Nat Neurosci *9*, 723-727.

Akiyama, H. (1994). Inflammatory response in Alzheimer's disease. Tohoku J Exp Med *174*, 295-303.

Akiyama, H., Arai, T., Kondo, H., Tanno, E., Haga, C., and Ikeda, K. (2000). Cell mediators of inflammation in the Alzheimer disease brain. Alzheimer Dis Assoc Disord *14 Suppl 1*, S47-53.

Alonso, M., Ortega-Perez, I., Grubb, M. S., Bourgeois, J. P., Charneau, P., and Lledo, P. M. (2008). Turning astrocytes from the rostral migratory stream into neurons: a role for the olfactory sensory organ. J Neurosci *28*, 11089-11102.

Altman, J., and Das, G. D. (1965). Autoradiographic and histological evidence of postnatal hippocampal neurogenesis in rats. J Comp Neurol *124*, 319-335.

Alvarez-Buylla, A., and Garcia-Verdugo, J. M. (2002). Neurogenesis in adult subventricular zone. J Neurosci *22*, 629-634.

Alvarez-Buylla, A., and Lim, D. A. (2004). For the long run: maintaining germinal niches in the adult brain. Neuron *41*, 683-686.

Alvarez-Buylla, A., Seri, B., and Doetsch, F. (2002). Identification of neural stem cells in the adult vertebrate brain. Brain Res Bull *57*, 751-758.

Anden, N. E., Dahlstrom, A., Fuxe, K., and Larsson, K. (1966). Functional role of the nigro-neostriatal dopamine neurons. Acta Pharmacol Toxicol (Copenh) *24*, 263-274.

Anderson, M. F., Aberg, M. A., Nilsson, M., and Eriksson, P. S. (2002). Insulin-like growth factor-I and neurogenesis in the adult mammalian brain. Brain Res Dev Brain Res *134*, 115-122.

Arikkath, J., and Campbell, K. P. (2003). Auxiliary subunits: essential components of the voltage-gated calcium channel complex. Curr Opin Neurobiol *13*, 298-307.

Asakura, K., Kanemasa, T., Minagawa, K., Kagawa, K., Yagami, T., Nakajima, M., and Ninomiya, M. (2000). alpha-eudesmol, a P/Q-type Ca(2+) channel blocker, inhibits neurogenic vasodilation and extravasation following electrical stimulation of trigeminal ganglion. Brain Res *873*, 94-101.

Asakura, K., Matsuo, Y., Kanemasa, T., and Ninomiya, M. (1997). P/Q-type Ca2+ channel blocker omega-agatoxin IVA protects against brain injury after focal ischemia in rats. Brain Res *776*, 140-145.

Bartlett, P. F., Richards, L. R., Kilpatrick, T. J., Talman, P. T., Bailey, K. A., Brooker, G. J., Dutton, R., Koblar, S. A., Nurcombe, V., Ford, M. O., and et al. (1995). Factors regulating the differentiation of neural precursors in the forebrain. Ciba Found Symp *193*, 85-99; discussion 117-126.

Battista, D., and Rutishauser, U. (2010). Removal of polysialic acid triggers dispersion of subventricularly derived neuroblasts into surrounding CNS tissues. J Neurosci *30*, 3995-4003.

Bayer, S. A. (1983). 3H-thymidine-radiographic studies of neurogenesis in the rat olfactory bulb. Exp Brain Res *50*, 329-340.

Beals, C. R., Sheridan, C. M., Turck, C. W., Gardner, P., and Crabtree, G. R. (1997). Nuclear export of NF-ATc enhanced by glycogen synthase kinase-3. Science *275*, 1930-1934.

Beck, H., Steffens, R., Elger, C. E., and Heinemann, U. (1998). Voltage-dependent Ca2+ currents in epilepsy. Epilepsy Res *32*, 321-332.

Ben-Ari, Y. (1985). Limbic seizure and brain damage produced by kainic acid: mechanisms and relevance to human temporal lobe epilepsy. Neuroscience *14*, 375-403.

Ben-Ari, Y., and Cossart, R. (2000). Kainate, a double agent that generates seizures: two decades of progress. Trends Neurosci *23*, 580-587.

Ben-Ari, Y., Tremblay, E., and Ottersen, O. P. (1980). Injections of kainic acid into the amygdaloid complex of the rat: an electrographic, clinical and histological study in relation to the pathology of epilepsy. Neuroscience *5*, 515-528.

Bender, A. T., and Beavo, J. A. (2006). Cyclic nucleotide phosphodiesterases: molecular regulation to clinical use. Pharmacol Rev *58*, 488-520.

Bengzon, J., Kokaia, Z., Elmer, E., Nanobashvili, A., Kokaia, M., and Lindvall, O. (1997). Apoptosis and proliferation of dentate gyrus neurons after single and intermittent limbic seizures. Proc Natl Acad Sci U S A *94*, 10432-10437.

Berman, R. F., Verweij, B. H., and Muizelaar, J. P. (2000). Neurobehavioral protection by the neuronal calcium channel blocker ziconotide in a model of traumatic diffuse brain injury in rats. J Neurosurg *93*, 821-828.

Bernardo, A., Levi, G., and Minghetti, L. (2000). Role of the peroxisome proliferator-activated receptor-gamma (PPAR-gamma) and its natural ligand 15-deoxy-Delta12, 14-prostaglandin J2 in the regulation of microglial functions. Eur J Neurosci *12*, 2215-2223.

Bezprozvanny, I. (2009). Calcium signaling and neurodegenerative diseases. Trends Mol Med *15*, 89-100.

Bianchi, M., De Lucchini, S., Marin, O., Turner, D. L., Hanks, S. K., and Villa-Moruzzi, E. (2005). Regulation of FAK Ser-722 phosphorylation and kinase activity by GSK3 and PP1 during cell spreading and migration. Biochem J *391*, 359-370.

Bijur, G. N., and Jope, R. S. (2003). Glycogen synthase kinase-3 beta is highly activated in nuclei and mitochondria. Neuroreport *14*, 2415-2419.

Binder DK, Steinhäuser C. (2006). Functional changes in astroglial cells in epilepsy. Glia 54, 358-68.

Blaschke, F., Takata, Y., Caglayan, E., Law, R. E., and Hsueh, W. A. (2006). Obesity, peroxisome proliferator-activated receptor, and atherosclerosis in type 2 diabetes. Arterioscler Thromb Vasc Biol *26*, 28-40.

Bliss, T. V., and Collingridge, G. L. (1993). A synaptic model of memory: long-term potentiation in the hippocampus. Nature *361*, 31-39.

Blum, D., Torch, S., Lambeng, N., Nissou, M., Benabid, A. L., Sadoul, R., and Verna, J. M. (2001). Molecular pathways involved in the neurotoxicity of 6-OHDA, dopamine and MPTP: contribution to the apoptotic theory in Parkinson's disease. Prog Neurobiol *65*, 135-172.

Bolton S, Butt AM. (2006). Cyclic AMP-mediated regulation of the resting membrane potential in myelin-forming oligodendrocytes in the isolated intact rat optic nerve. Exp Neurol *202*, 36-43.

Bonfanti, L. (2006). PSA-NCAM in mammalian structural plasticity and neurogenesis. Prog Neurobiol *80*, 129-164.

Bonfanti, L., and Theodosis, D. T. (1994). Expression of polysialylated neural cell adhesion molecule by proliferating cells in the subependymal layer of the adult rat, in its rostral extension and in the olfactory bulb. Neuroscience *62*, 291-305.

Bos, J. L. (2003). Epac: a new cAMP target and new avenues in cAMP research. Nat Rev Mol Cell Biol *4*, 733-738.

Braak, H., Sastre, M., and Del Tredici, K. (2007). Development of alpha-synuclein immunoreactive astrocytes in the forebrain parallels stages of intraneuronal pathology in sporadic Parkinson's disease. Acta Neuropathol *114*, 231-241.

Breton-Provencher, V., Lemasson, M., Peralta, M. R., 3rd, and Saghatelyan, A. (2009). Interneurons produced in adulthood are required for the normal functioning of the olfactory bulb network and for the execution of selected olfactory behaviors. J Neurosci *29*, 15245-15257.

Brodbeck, J., Balestra, M. E., Saunders, A. M., Roses, A. D., Mahley, R. W., and Huang, Y. (2008). Rosiglitazone increases dendritic spine density and rescues spine loss caused by apolipoprotein E4 in primary cortical neurons. Proc Natl Acad Sci U S A *105*, 1343-1346.

Brorson, J. R., Manzolillo, P. A., and Miller, R. J. (1994). Ca2+ entry via AMPA/KA receptors and excitotoxicity in cultured cerebellar Purkinje cells. J Neurosci *14*, 187-197.

Brown, J. P., Couillard-Despres, S., Cooper-Kuhn, C. M., Winkler, J., Aigner, L., and Kuhn, H. G. (2003). Transient expression of doublecortin during adult neurogenesis. J Comp Neurol *467*, 1-10.

Brundin, L., Brismar, H., Danilov, A. I., Olsson, T., and Johansson, C. B. (2003). Neural stem cells: a potential source for remyelination in neuroinflammatory disease. Brain Pathol *13*, 322-328.

Buchan, A. M., Gertler, S. Z., Li, H., Xue, D., Huang, Z. G., Chaundy, K. E., Barnes, K., and Lesiuk, H. J. (1994). A selective N-type Ca(2+)-channel blocker prevents CA1 injury 24 h following severe forebrain ischemia and reduces infarction following focal ischemia. J Cereb Blood Flow Metab *14*, 903-910.

Buffo, A., Rolando, C., and Ceruti, S. Astrocytes in the damaged brain: molecular and cellular insights into their reactive response and healing potential. Biochem Pharmacol *79*, 77-89.

Cameron, H. A., and McKay, R. D. (2001). Adult neurogenesis produces a large pool of new granule cells in the dentate gyrus. J Comp Neurol *435*, 406-417.

Carmichael, S. T. (2003). Gene expression changes after focal stroke, traumatic brain and spinal cord injuries. Curr Opin Neurol *16*, 699-704.

Castano, A., Herrera, A. J., Cano, J., and Machado, A. (1998). Lipopolysaccharide intranigral injection induces inflammatory reaction and damage in nigrostriatal dopaminergic system. J Neurochem *70*, 1584-1592.

Castano, Z., Gordon-Weeks, P. R., and Kypta, R. M. (2010). The neuron-specific isoform of glycogen synthase kinase-3beta is required for axon growth. J Neurochem *113*, 117-130.

Castelo-Branco, G., Rawal, N., and Arenas, E. (2004). GSK-3beta inhibition/beta-catenin stabilization in ventral midbrain precursors increases differentiation into dopamine neurons. J Cell Sci *117*, 5731-5737.

Cicchetti, F., Brownell, A. L., Williams, K., Chen, Y. I., Livni, E., and Isacson, O. (2002). Neuroinflammation of the nigrostriatal pathway during progressive 6-OHDA dopamine degeneration in rats monitored by immunohistochemistry and PET imaging. Eur J Neurosci *15*, 991-998.

Clark, M. E., He, Q., He, Z., Huang, K. H., Alm, E. J., Wan, X. F., Hazen, T. C., Arkin, A. P., Wall, J. D., Zhou, J. Z., and Fields, M. W. (2006). Temporal transcriptomic analysis as Desulfovibrio vulgaris Hildenborough transitions into stationary phase during electron donor depletion. Appl Environ Microbiol *72*, 5578-5588.

Cohen, C. & Kraus, R. (2004). The therapeutic utility of targeting Cav2 channels. In *Calcium Channel Pharmacology*. ed McDonough, S.I. pp. 73-93. New York: Kluwer Acdemic/Plenum Publisher.

Cohen, P., and Frame, S. (2001). The renaissance of GSK3. Nat Rev Mol Cell Biol *2*, 769-776.

Comabella, M., and Khoury, S. J. (2011). Immunopathogenesis of multiple sclerosis. Clin Immunol. In press.

Conti, M., and Beavo, J. (2007). Biochemistry and physiology of cyclic nucleotide phosphodiesterases: essential components in cyclic nucleotide signaling. Annu Rev Biochem *76*, 481-511.

Contractor, A., Swanson, G. T., Sailer, A., O'Gorman, S., and Heinemann, S. F. (2000). Identification of the kainate receptor subunits underlying modulation of excitatory synaptic transmission in the CA3 region of the hippocampus. J Neurosci *20*, 8269-8278.

Corsellis, J. A., and Bruton, C. J. (1983). Neuropathology of status epilepticus in humans. Adv Neurol *34*, 129-139.

Couillard-Despres, S., Winner, B., Schaubeck, S., Aigner, R., Vroemen, M., Weidner, N., Bogdahn, U., Winkler, J., Kuhn, H. G., and Aigner, L. (2005). Doublecortin expression levels in adult brain reflect neurogenesis. Eur J Neurosci *21*, 1-14.

Courtney, M. J., Enkvist, M. O., and Akerman, K. E. (1995). The calcium response to the excitotoxin kainate is amplified by subsequent reduction of extracellular sodium. Neuroscience *68*, 1051-1057.

Cox, B. (2000). Calcium channel blockers and pain therapy. Curr Rev Pain *4*, 488-498.

Coyle, J. T. (1983). Neurotoxic action of kainic acid. J Neurochem *41*, 1-11.

Curtis, M. A., Penney, E. B., Pearson, A. G., van Roon-Mom, W. M., Butterworth, N. J., Dragunow, M., Connor, B., and Faull, R. L. (2003). Increased cell proliferation and neurogenesis in the adult human Huntington's disease brain. Proc Natl Acad Sci U S A *100*, 9023-9027.

Cuzzocrea, S., Mazzon, E., Di Paola, R., Muia, C., Crisafulli, C., Dugo, L., Collin, M., Britti, D., Caputi, A. P., and Thiemermann, C. (2006). Glycogen synthase kinase-3beta inhibition attenuates the degree of arthritis caused by type II collagen in the mouse. Clin Immunol *120*, 57-67.

Czuczwar, S. J., Chodkowska, A., Kleinrok, Z., Malek, U., and Jagiello-Wojtowicz, E. (1990). Effects of calcium channel inhibitors upon the efficacy of common antiepileptic drugs. Eur J Pharmacol *176*, 75-83.

Charles, M. P., Adamski, D., Kholler, B., Pelletier, L., Berger, F., and Wion, D. (2003). Induction of neurite outgrowth in PC12 cells by the bacterial nucleoside N6-methyldeoxyadenosine is mediated through adenosine A2a receptors and via cAMP and MAPK signaling pathways. Biochem Biophys Res Commun *304*, 795-800.

Chen, H., Zhang, S. M., Hernan, M. A., Schwarzschild, M. A., Willett, W. C., Colditz, G. A., Speizer, F. E., and Ascherio, A. (2003). Nonsteroidal anti-inflammatory drugs and the risk of Parkinson disease. Arch Neurol *60*, 1059-1064.

Chen, H. Q., Jin, Z. Y., Wang, X. J., Xu, X. M., Deng, L., and Zhao, J. W. (2008). Luteolin protects dopaminergic neurons from inflammation-induced injury through inhibition of microglial activation. Neurosci Lett *448*, 175-179.

Choi, D. W. (1988). Glutamate neurotoxicity and diseases of the nervous system. Neuron *1*, 623-634.

Choi, D. W. (1994). Calcium and excitotoxic neuronal injury. Ann N Y Acad Sci *747*, 162-171.

D'Ascenzo, M., Vairano, M., Andreassi, C., Navarra, P., Azzena, G. B., and Grassi, C. (2004). Electrophysiological and molecular evidence of L-(Cav1), N- (Cav2.2), and R- (Cav2.3) type Ca2+ channels in rat cortical astrocytes. Glia *45*, 354-363.

Damier, P., Hirsch, E. C., Zhang, P., Agid, Y., and Javoy-Agid, F. (1993). Glutathione peroxidase, glial cells and Parkinson's disease. Neuroscience *52*, 1-6.

Danilov, A. I., Gomes-Leal, W., Ahlenius, H., Kokaia, Z., Carlemalm, E., and Lindvall, O. (2009). Ultrastructural and antigenic properties of neural stem cells and their progeny in adult rat subventricular zone. Glia *57*, 136-152.

de Graaf, A. S. (1974). Epidemiological aspects of epilepsy in northern Norway. Epilepsia *15*, 291-299.

de Groot, R. P., Auwerx, J., Bourouis, M., and Sassone-Corsi, P. (1993). Negative regulation of Jun/AP-1: conserved function of glycogen synthase kinase 3 and the Drosophila kinase shaggy. Oncogene *8*, 841-847.

De Sarro, G. B., Meldrum, B. S., and Nistico, G. (1988). Anticonvulsant effects of some calcium entry blockers in DBA/2 mice. Br J Pharmacol *93*, 247-256.

De Simoni, M. G., Perego, C., Ravizza, T., Moneta, D., Conti, M., Marchesi, F., De Luigi, A., Garattini, S., and Vezzani, A. (2000). Inflammatory cytokines and related genes are induced in the rat hippocampus by limbic status epilepticus. Eur J Neurosci *12*, 2623-2633.

Debril, M. B., Renaud, J. P., Fajas, L., and Auwerx, J. (2001). The pleiotropic functions of peroxisome proliferator-activated receptor gamma. J Mol Med *79*, 30-47.

del Zoppo, G., Ginis, I., Hallenbeck, J. M., Iadecola, C., Wang, X., and Feuerstein, G. Z. (2000). Inflammation and stroke: putative role for cytokines, adhesion molecules and iNOS in brain response to ischemia. Brain Pathol *10*, 95-112.

DeLorenzo, R. J., Pal, S., and Sombati, S. (1998). Prolonged activation of the N-methyl-D-aspartate receptor-Ca2+ transduction pathway causes spontaneous recurrent epileptiform discharges in hippocampal neurons in culture. Proc Natl Acad Sci U S A *95*, 14482-14487.

Delorenzo, R. J., Sun, D. A., and Deshpande, L. S. (2005). Cellular mechanisms underlying acquired epilepsy: the calcium hypothesis of the induction and maintainance of epilepsy. Pharmacol Ther *105*, 229-266.

Desvergne, B., and Wahli, W. (1999). Peroxisome proliferator-activated receptors: nuclear control of metabolism. Endocr Rev *20*, 649-688.

Dingledine, R., and Conn, P. J. (2000). Peripheral glutamate receptors: molecular biology and role in taste sensation. J Nutr *130*, 1039S-1042S.

Doble, A. (1999). The role of excitotoxicity in neurodegenerative disease: implications for therapy. Pharmacol Ther *81*, 163-221.

Doble, B. W., Patel, S., Wood, G. A., Kockeritz, L. K., and Woodgett, J. R. (2007). Functional redundancy of GSK-3alpha and GSK-3beta in Wnt/beta-catenin signaling shown by using an allelic series of embryonic stem cell lines. Dev Cell *12*, 957-971.

Doble, B. W., and Woodgett, J. R. (2007). Role of glycogen synthase kinase-3 in cell fate and epithelial-mesenchymal transitions. Cells Tissues Organs *185*, 73-84.

Doetsch, F., and Alvarez-Buylla, A. (1996). Network of tangential pathways for neuronal migration in adult mammalian brain. Proc Natl Acad Sci U S A *93*, 14895-14900.

Doetsch, F., Caille, I., Lim, D. A., Garcia-Verdugo, J. M., and Alvarez-Buylla, A. (1999). Subventricular zone astrocytes are neural stem cells in the adult mammalian brain. Cell *97*, 703-716.

Doetsch, F., Garcia-Verdugo, J. M., and Alvarez-Buylla, A. (1997). Cellular composition and three-dimensional organization of the subventricular germinal zone in the adult mammalian brain. J Neurosci *17*, 5046-5061.

Doetsch, F., Petreanu, L., Caille, I., Garcia-Verdugo, J. M., and Alvarez-Buylla, A. (2002). EGF converts transit-amplifying neurogenic precursors in the adult brain into multipotent stem cells. Neuron *36*, 1021-1034.

Dolin, S. J., Hunter, A. B., Halsey, M. J., and Little, H. J. (1988). Anticonvulsant profile of the dihydropyridine calcium channel antagonists, nitrendipine and nimodipine. Eur J Pharmacol *152*, 19-27.

Dolmetsch, R. E., Pajvani, U., Fife, K., Spotts, J. M., and Greenberg, M. E. (2001). Signaling to the nucleus by an L-type calcium channel-calmodulin complex through the MAP kinase pathway. Science *294*, 333-339.

Dolphin, A. C. (2006). A short history of voltage-gated calcium channels. Br J Pharmacol *147 Suppl 1*, S56-62.

Drapeau, E., and Nora Abrous, D. (2008). Stem cell review series: role of neurogenesis in age-related memory disorders. Aging Cell *7*, 569-589.

Dreyer, C., Krey, G., Keller, H., Givel, F., Helftenbein, G., and Wahli, W. (1992). Control of the peroxisomal beta-oxidation pathway by a novel family of nuclear hormone receptors. Cell *68*, 879-887.

Dugo, L., Collin, M., Allen, D. A., Patel, N. S., Bauer, I., Mervaala, E. M., Louhelainen, M., Foster, S. J., Yaqoob, M. M., and Thiemermann, C. (2005). GSK-3beta inhibitors attenuate the organ injury/dysfunction caused by endotoxemia in the rat. Crit Care Med *33*, 1903-1912.

Dutta, G., Zhang, P., and Liu, B. (2008). The lipopolysaccharide Parkinson's disease animal model: mechanistic studies and drug discovery. Fundam Clin Pharmacol *22*, 453-464.

Egebjerg, J., Bettler, B., Hermans-Borgmeyer, I., and Heinemann, S. (1991). Cloning of a cDNA for a glutamate receptor subunit activated by kainate but not AMPA. Nature *351*, 745-748.

Ekdahl, C. T., Claasen, J. H., Bonde, S., Kokaia, Z., and Lindvall, O. (2003). Inflammation is detrimental for neurogenesis in adult brain. Proc Natl Acad Sci U S A *100*, 13632-13637.

Elmslie, K. S. (2004). Calcium channel blockers in the treatment of disease. J Neurosci Res *75*, 733-741.

Emery, D. L., Raghupathi, R., Saatman, K. E., Fischer, I., Grady, M. S., and McIntosh, T. K. (2000). Bilateral growth-related protein expression suggests a transient increase in regenerative potential following brain trauma. J Comp Neurol *424*, 521-531.

Etienne-Manneville, S., and Hall, A. (2003). Cdc42 regulates GSK-3beta and adenomatous polyposis coli to control cell polarity. Nature *421*, 753-756.

Faas, G. C., Vreugdenhil, M., and Wadman, W. J. (1996). Calcium currents in pyramidal CA1 neurons in vitro after kindling epileptogenesis in the hippocampus of the rat. Neuroscience *75*, 57-67.

Forman, B. M., Tontonoz, P., Chen, J., Brun, R. P., Spiegelman, B. M., and Evans, R. M. (1995). 15-Deoxy-delta 12, 14-prostaglandin J2 is a ligand for the adipocyte determination factor PPAR gamma. Cell *83*, 803-812.

Frame, S., and Cohen, P. (2001). GSK3 takes centre stage more than 20 years after its discovery. Biochem J *359*, 1-16.

Frerking, M., and Nicoll, R. A. (2000). Synaptic kainate receptors. Curr Opin Neurobiol *10*, 342-351.

Friberg, H., and Wieloch, T. (2002). Mitochondrial permeability transition in acute neurodegeneration. Biochimie *84*, 241-250.

Fuentealba, L. C., Eivers, E., Ikeda, A., Hurtado, C., Kuroda, H., Pera, E. M., and De Robertis, E. M. (2007). Integrating patterning signals: Wnt/GSK3 regulates the duration of the BMP/Smad1 signal. Cell *131*, 980-993.

Gage, F. H. (2000). Mammalian neural stem cells. Science *287*, 1433-1438.

Gage, F. H. (2002). Neurogenesis in the adult brain. J Neurosci *22*, 612-613.

Gao, H. M., Jiang, J., Wilson, B., Zhang, W., Hong, J. S., and Liu, B. (2002). Microglial activation-mediated delayed and progressive degeneration of rat nigral dopaminergic neurons: relevance to Parkinson's disease. J Neurochem *81*, 1285-1297.

Gao, H. M., Kotzbauer, P. T., Uryu, K., Leight, S., Trojanowski, J. Q., and Lee, V. M. (2008). Neuroinflammation and oxidation/nitration of alpha-synuclein linked to dopaminergic neurodegeneration. J Neurosci *28*, 7687-7698.

Garcia-Verdugo, J. M., Doetsch, F., Wichterle, H., Lim, D. A., and Alvarez-Buylla, A. (1998). Architecture and cell types of the adult subventricular zone: in search of the stem cells. J Neurobiol *36*, 234-248.

Garcia, A. G., Garcia-De-Diego, A. M., Gandia, L., Borges, R., and Garcia-Sancho, J. (2006). Calcium signaling and exocytosis in adrenal chromaffin cells. Physiol Rev *86*, 1093-1131.

Gascon, E., Vutskits, L., Jenny, B., Durbec, P., and Kiss, J. Z. (2007). PSA-NCAM in postnatally generated immature neurons of the olfactory bulb: a crucial role in regulating p75 expression and cell survival. Development *134*, 1181-1190.

Gasior, M., White, N. A., and Rogawski, M. A. (2007). Prolonged attenuation of amygdala-kindled seizure measures in rats by convection-enhanced delivery of the N-type calcium channel antagonists omega-conotoxin GVIA and omega-conotoxin MVIIA. J Pharmacol Exp Ther *323*, 458-468.

Gerhard A, Pavese N, Hotton G, Turkheimer F, Es M, Hammers A, Eggert K, Oertel W, Banati RB, Brooks DJ. (2006). In vivo imaging of microglial activation with [11C](R)-PK11195 PET in idiopathic Parkinson's disease. Neurobiol Dis *21*, 404-12

Gibson, G. E., Starkov, A., Blass, J. P., Ratan, R. R., and Beal, M. F. Cause and consequence: mitochondrial dysfunction initiates and propagates neuronal dysfunction, neuronal death and behavioral abnormalities in age-associated neurodegenerative diseases. Biochim Biophys Acta *1802*, 122-134.

Giembycz, M. A., and Smith, S. J. (2006). Phosphodiesterase 7A: a new therapeutic target for alleviating chronic inflammation? Curr Pharm Des *12*, 3207-3220.

Giovannini, M. G., Scali, C., Prosperi, C., Bellucci, A., Pepeu, G., and Casamenti, F. (2003). Experimental brain inflammation and neurodegeneration as model of Alzheimer's disease: protective effects of selective COX-2 inhibitors. Int J Immunopathol Pharmacol *16*, 31-40.

Glass, C. K., Saijo, K., Winner, B., Marchetto, M. C., and Gage, F. H. (2010). Mechanisms underlying inflammation in neurodegeneration. Cell *140*, 918-934.

Goldman, J. E. (1995). Lineage, migration, and fate determination of postnatal subventricular zone cells in the mammalian CNS. J Neurooncol *24*, 61-64.

Gomez-Lazaro, M., Bonekamp, N. A., Galindo, M. F., Jordan, J., and Schrader, M. (2008). 6-Hydroxydopamine (6-OHDA) induces Drp1-dependent mitochondrial fragmentation in SH-SY5Y cells. Free Radic Biol Med *44*, 1960-1969.

Gonzalez-Perez, O., Romero-Rodriguez, R., Soriano-Navarro, M., Garcia-Verdugo, J. M., and Alvarez-Buylla, A. (2009). Epidermal growth factor induces the progeny of subventricular zone type B cells to migrate and differentiate into oligodendrocytes. Stem Cells *27*, 2032-2043.

Gould, E., Reeves, A. J., Graziano, M. S., and Gross, C. G. (1999). Neurogenesis in the neocortex of adult primates. Science *286*, 548-552.

Gould, T. D., Picchini, A. M., Einat, H., and Manji, H. K. (2006). Targeting glycogen synthase kinase-3 in the CNS: implications for the development of new treatments for mood disorders. Curr Drug Targets *7*, 1399-1409.

Grimes, C. A., and Jope, R. S. (2001a). CREB DNA binding activity is inhibited by glycogen synthase kinase-3 beta and facilitated by lithium. J Neurochem *78*, 1219-1232.

Grimes, C. A., and Jope, R. S. (2001b). The multifaceted roles of glycogen synthase kinase 3beta in cellular signaling. Prog Neurobiol *65*, 391-426.

Hack, M. A., Saghatelyan, A., de Chevigny, A., Pfeifer, A., Ashery-Padan, R., Lledo, P. M., and Gotz, M. (2005). Neuronal fate determinants of adult olfactory bulb neurogenesis. Nat Neurosci *8*, 865-872.

Hald, A., and Lotharius, J. (2005). Oxidative stress and inflammation in Parkinson's disease: is there a causal link? Exp Neurol *193*, 279-290.

Han, Y. G., Spassky, N., Romaguera-Ros, M., Garcia-Verdugo, J. M., Aguilar, A., Schneider-Maunoury, S., and Alvarez-Buylla, A. (2008). Hedgehog signaling and primary cilia are required for the formation of adult neural stem cells. Nat Neurosci *11*, 277-284.

Hanson MG Jr, Shen S, Wiemelt AP, McMorris FA, Barres BA. (1998). Cyclic AMP elevation is sufficient to promote the survival of spinal motor neurons in vitro. J Neurosci *18*, 7361-71

Healy, D. J., and Meador-Woodruff, J. H. (2000). Ionotropic glutamate receptor modulation preferentially affects NMDA receptor expression in rat hippocampus. Synapse *38*, 294-304.

Hendriksen, H., Kamphuis, W., and Lopes da Silva, F. H. (1997). Changes in voltage-dependent calcium channel alpha1-subunit mRNA levels in the kindling model of epileptogenesis. Brain Res Mol Brain Res *50*, 257-266.

Heneka, M. T., and Landreth, G. E. (2007). PPARs in the brain. Biochim Biophys Acta *1771*, 1031-1045.

Heneka, M. T., Sastre, M., Dumitrescu-Ozimek, L., Hanke, A., Dewachter, I., Kuiperi, C., O'Banion, K., Klockgether, T., Van Leuven, F., and Landreth, G. E. (2005). Acute treatment with the PPARgamma agonist pioglitazone and ibuprofen reduces glial inflammation and Abeta1-42 levels in APPV717I transgenic mice. Brain *128*, 1442-1453.

Herrera, A. J., Castano, A., Venero, J. L., Cano, J., and Machado, A. (2000). The single intranigral injection of LPS as a new model for studying the selective effects of inflammatory reactions on dopaminergic system. Neurobiol Dis *7*, 429-447.

Hicks, C. A., Ward, M. A., and O'Neill, M. J. (2000). Neuroprotective effects of the neuronal Ca(2+) channel blockers, LY042826 and LY393615 in vivo. Eur J Pharmacol *408*, 241-248.

Hirsch, E. C., and Hunot, S. (2009). Neuroinflammation in Parkinson's disease: a target for neuroprotection? Lancet Neurol *8*, 382-397.

Hoffmann, A., Kann, O., Ohlemeyer, C., Hanisch, U. K., and Kettenmann, H. (2003). Elevation of basal intracellular calcium as a central element in the activation of brain macrophages (microglia): suppression of receptor-evoked calcium signaling and control of release function. J Neurosci *23*, 4410-4419.

Hoffmann, R., Abdel'Al, S., and Engels, P. (1998). Differential distribution of rat PDE-7 mRNA in embryonic and adult rat brain. Cell Biochem Biophys *28*, 103-113.

Hofmann, F., Biel, M., and Flockerzi, V. (1994). Molecular basis for Ca2+ channel diversity. Annu Rev Neurosci *17*, 399-418.

Hoglinger, G. U., Rizk, P., Muriel, M. P., Duyckaerts, C., Oertel, W. H., Caille, I., and Hirsch, E. C. (2004). Dopamine depletion impairs precursor cell proliferation in Parkinson disease. Nat Neurosci *7*, 726-735.

Holopainen, I. E. (2008). Seizures in the developing brain: cellular and molecular mechanisms of neuronal damage, neurogenesis and cellular reorganization. Neurochem Int *52*, 935-947.

Hong, X. P., Peng, C. X., Wei, W., Tian, Q., Liu, Y. H., Yao, X. Q., Zhang, Y., Cao, F. Y., Wang, Q., and Wang, J. Z. (2009). Essential role of tau phosphorylation in adult hippocampal neurogenesis. Hippocampus.

Hooper, C., Killick, R., and Lovestone, S. (2008). The GSK3 hypothesis of Alzheimer's disease. J Neurochem *104*, 1433-1439.

Houslay, M. D., and Kolch, W. (2000). Cell-type specific integration of cross-talk between extracellular signal-regulated kinase and cAMP signaling. Mol Pharmacol *58*, 659-668.

Hu, L. Y., Ryder, T. R., Rafferty, M. F., Feng, M. R., Lotarski, S. M., Rock, D. M., Sinz, M., Stoehr, S. J., Taylor, C. P., Weber, M. L., *et al.* (1999). Synthesis of a series of 4-benzyloxyaniline analogues as neuronal N-type calcium channel blockers with improved anticonvulsant and analgesic properties. J Med Chem *42*, 4239-4249.

Huang, C. S., Song, J. H., Nagata, K., Yeh, J. Z., and Narahashi, T. (1997). Effects of the neuroprotective agent riluzole on the high voltage-activated calcium channels of rat dorsal root ganglion neurons. J Pharmacol Exp Ther *282*, 1280-1290.

Hunter, R. L., Dragicevic, N., Seifert, K., Choi, D. Y., Liu, M., Kim, H. C., Cass, W. A., Sullivan, P. G., and Bing, G. (2007). Inflammation induces mitochondrial dysfunction and dopaminergic neurodegeneration in the nigrostriatal system. J Neurochem *100*, 1375-1386.

Hwang, Y. P., and Jeong, H. G. (2008). The coffee diterpene kahweol induces heme oxygenase-1 via the PI3K and p38/Nrf2 pathway to protect human dopaminergic neurons from 6-hydroxydopamine-derived oxidative stress. FEBS Lett *582*, 2655-2662.

Ikeda, Y., Tsuji, S., Satoh, A., Ishikura, M., Shirasawa, T., and Shimizu, T. (2008). Protective effects of astaxanthin on 6-hydroxydopamine-induced apoptosis in human neuroblastoma SH-SY5Y cells. J Neurochem *107*, 1730-1740.

Jackson, H. C., and Scheideler, M. A. (1996). Behavioural and anticonvulsant effects of Ca2+ channel toxins in DBA/2 mice. Psychopharmacology (Berl) *126*, 85-90.

Jankovic, J., Watts, R. L., Martin, W., and Boroojerdi, B. (2007). Transdermal rotigotine: double-blind, placebo-controlled trial in Parkinson disease. Arch Neurol *64*, 676-682.

Jankowsky, J. L., and Patterson, P. H. (2001). The role of cytokines and growth factors in seizures and their sequelae. Prog Neurobiol *63*, 125-149.

Jerussi, T. P., and Glick, S. D. (1975). Apomorphine-induced rotation in normal rats and interaction with unilateral caudate lesions. Psychopharmacologia *40*, 329-334.

Jessberger, S., and Kempermann, G. (2003). Adult-born hippocampal neurons mature into activity-dependent responsiveness. Eur J Neurosci *18*, 2707-2712.

Jiang, C., Ting, A. T., and Seed, B. (1998). PPAR-gamma agonists inhibit production of monocyte inflammatory cytokines. Nature *391*, 82-86.

Jiang, H., Nucifora, F. C., Jr., Ross, C. A., and DeFranco, D. B. (2003). Cell death triggered by polyglutamine-expanded huntingtin in a neuronal cell line is associated with degradation of CREB-binding protein. Hum Mol Genet *12*, 1-12.

Jin, K., Minami, M., Lan, J. Q., Mao, X. O., Batteur, S., Simon, R. P., and Greenberg, D. A. (2001). Neurogenesis in dentate subgranular zone and rostral subventricular zone after focal cerebral ischemia in the rat. Proc Natl Acad Sci U S A *98*, 4710-4715.

Jin, K., Peel, A. L., Mao, X. O., Xie, L., Cottrell, B. A., Henshall, D. C., and Greenberg, D. A. (2004). Increased hippocampal neurogenesis in Alzheimer's disease. Proc Natl Acad Sci U S A *101*, 343-347.

Jin, K., Wang, X., Xie, L., Mao, X. O., Zhu, W., Wang, Y., Shen, J., Mao, Y., Banwait, S., and Greenberg, D. A. (2006). Evidence for stroke-induced neurogenesis in the human brain. Proc Natl Acad Sci U S A *103*, 13198-13202.

Johe, K. K., Hazel, T. G., Muller, T., Dugich-Djordjevic, M. M., and McKay, R. D. (1996). Single factors direct the differentiation of stem cells from the fetal and adult central nervous system. Genes Dev *10*, 3129-3140.

Jope, R. S., and Johnson, G. V. (2004). The glamour and gloom of glycogen synthase kinase-3. Trends Biochem Sci *29*, 95-102.

Jorgensen, M. B., Finsen, B. R., Jensen, M. B., Castellano, B., Diemer, N. H., and Zimmer, J. (1993). Microglial and astroglial reactions to ischemic and kainic acid-induced lesions of the adult rat hippocampus. Exp Neurol *120*, 70-88.

Jung, K. H., Chu, K., Lee, S. T., Kim, J., Sinn, D. I., Kim, J. M., Park, D. K., Lee, J. J., Kim, S. U., Kim, M., *et al.* (2006). Cyclooxygenase-2 inhibitor, celecoxib, inhibits the altered hippocampal neurogenesis with attenuation of spontaneous recurrent seizures following pilocarpine-induced status epilepticus. Neurobiol Dis *23*, 237-246.

Kaminski, R. M., Mazurek, M., Turski, W. A., Kleinrok, Z., and Czuczwar, S. J. (2001). Amlodipine enhances the activity of antiepileptic drugs against pentylenetetrazole-induced seizures. Pharmacol Biochem Behav *68*, 661-668.

Kaplan, M. S., and Hinds, J. W. (1977). Neurogenesis in the adult rat: electron microscopic analysis of light radioautographs. Science *197*, 1092-1094.

Kawaguchi, K., Hickey, R. W., Rose, M. E., Zhu, L., Chen, J., and Graham, S. H. (2005). Cyclooxygenase-2 expression is induced in rat brain after kainate-induced seizures and promotes neuronal death in CA3 hippocampus. Brain Res *1050*, 130-137.

Kaytor, M. D., and Orr, H. T. (2002). The GSK3 beta signaling cascade and neurodegenerative disease. Curr Opin Neurobiol *12*, 275-278.

Kempermann, G., Jessberger, S., Steiner, B., and Kronenberg, G. (2004). Milestones of neuronal development in the adult hippocampus. Trends Neurosci *27*, 447-452.

Kermen, F., Sultan, S., Sacquet, J., Mandairon, N., and Didier, A. Consolidation of an olfactory memory trace in the olfactory bulb is required for learning-induced survival of adult-born neurons and long-term memory. PLoS One *5*, e12118.

Khosravani, H., and Zamponi, G. W. (2006). Voltage-gated calcium channels and idiopathic generalized epilepsies. Physiol Rev *86*, 941-966.

Kim, J. S., Jung, J., Lee, H. J., Kim, J. C., Wang, H., Kim, S. H., Shin, T., and Moon, C. (2009a). Differences in immunoreactivities of Ki-67 and doublecortin in the adult hippocampus in three strains of mice. Acta Histochem *111*, 150-156.

Kim, W. G., Mohney, R. P., Wilson, B., Jeohn, G. H., Liu, B., and Hong, J. S. (2000). Regional difference in susceptibility to lipopolysaccharide-induced neurotoxicity in the rat brain: role of microglia. J Neurosci *20*, 6309-6316.

Kim, W. Y., Wang, X., Wu, Y., Doble, B. W., Patel, S., Woodgett, J. R., and Snider, W. D. (2009b). GSK-3 is a master regulator of neural progenitor homeostasis. Nat Neurosci *12*, 1390-1397.

Kliewer, S. A., Forman, B. M., Blumberg, B., Ong, E. S., Borgmeyer, U., Mangelsdorf, D. J., Umesono, K., and Evans, R. M. (1994). Differential expression and activation of a family of murine peroxisome proliferator-activated receptors. Proc Natl Acad Sci U S A *91*, 7355-7359.

Kockeritz, L., Doble, B., Patel, S., and Woodgett, J. R. (2006). Glycogen synthase kinase-3--an overview of an over-achieving protein kinase. Curr Drug Targets *7*, 1377-1388.

Kohwi, M., Osumi, N., Rubenstein, J. L., and Alvarez-Buylla, A. (2005). Pax6 is required for making specific subpopulations of granule and periglomerular neurons in the olfactory bulb. J Neurosci *25*, 6997-7003.

Kozikowski, A. P., Gaisina, I. N., Petukhov, P. A., Sridhar, J., King, L. T., Blond, S. Y., Duka, T., Rusnak, M., and Sidhu, A. (2006). Highly potent and specific GSK-3beta inhibitors that block tau phosphorylation and decrease alpha-synuclein protein expression in a cellular model of Parkinson's disease. ChemMedChem *1*, 256-266.

Kuhn, H. G., Dickinson-Anson, H., and Gage, F. H. (1996). Neurogenesis in the dentate gyrus of the adult rat: age-related decrease of neuronal progenitor proliferation. J Neurosci *16*, 2027-2033.

Lacinova, L. (2005). Voltage-dependent calcium channels. Gen Physiol Biophys *24 Suppl 1*, 1-78.

Ladeby, R., Wirenfeldt, M., Garcia-Ovejero, D., Fenger, C., Dissing-Olesen, L., Dalmau, I., and Finsen, B. (2005). Microglial cell population dynamics in the injured adult central nervous system. Brain Res Brain Res Rev *48*, 196-206.

Landreth, G. E., and Heneka, M. T. (2001). Anti-inflammatory actions of peroxisome proliferator-activated receptor gamma agonists in Alzheimer's disease. Neurobiol Aging *22*, 937-944.

Larsen, M. H., Rosenbrock, H., Sams-Dodd, F., and Mikkelsen, J. D. (2007). Expression of brain derived neurotrophic factor, activity-regulated cytoskeleton protein mRNA, and enhancement of adult hippocampal neurogenesis in rats after sub-chronic and chronic treatment with the triple monoamine re-uptake inhibitor tesofensine. Eur J Pharmacol *555*, 115-121.

Lastres-Becker, I., Fernandez-Perez, A., Cebolla, B., and Vallejo, M. (2008). Pituitary adenylate cyclase-activating polypeptide stimulates glial fibrillary acidic protein gene expression in cortical precursor cells by activating Ras and Rap1. Mol Cell Neurosci *39*, 291-301.

Latour, I., Hamid, J., Beedle, A. M., Zamponi, G. W., and Macvicar, B. A. (2003). Expression of voltage-gated Ca2+ channel subtypes in cultured astrocytes. Glia *41*, 347-353.

Lauri, S. E., Bortolotto, Z. A., Bleakman, D., Ornstein, P. L., Lodge, D., Isaac, J. T., and Collingridge, G. L. (2001). A critical role of a facilitatory presynaptic kainate receptor in mossy fiber LTP. Neuron *32*, 697-709.

Lazarini, F., Mouthon, M. A., Gheusi, G., de Chaumont, F., Olivo-Marin, J. C., Lamarque, S., Abrous, D. N., Boussin, F. D., and Lledo, P. M. (2009). Cellular and behavioral effects of cranial irradiation of the subventricular zone in adult mice. PLoS One *4*, e7017.

Le Meur, K., Galante, M., Angulo, M. C., and Audinat, E. (2007). Tonic activation of NMDA receptors by ambient glutamate of non-synaptic origin in the rat hippocampus. J Physiol *580*, 373-383.

Lee, B., Butcher, G. Q., Hoyt, K. R., Impey, S., and Obrietan, K. (2005). Activity-dependent neuroprotection and cAMP response element-binding protein (CREB): kinase coupling, stimulus intensity, and temporal regulation of CREB phosphorylation at serine 133. J Neurosci *25*, 1137-1148.

Lee, L. L., Galo, E., Lyeth, B. G., Muizelaar, J. P., and Berman, R. F. (2004). Neuroprotection in the rat lateral fluid percussion model of traumatic brain injury by SNX-185, an N-type voltage-gated calcium channel blocker. Exp Neurol *190*, 70-78.

Lehmensiek, V., Tan, E. M., Liebau, S., Lenk, T., Zettlmeisl, H., Schwarz, J., and Storch, A. (2006). Dopamine transporter-mediated cytotoxicity of 6-hydroxydopamine in vitro depends on expression of mutant alpha-synucleins related to Parkinson's disease. Neurochem Int *48*, 329-340.

Leitch, B., Szostek, A., Lin, R., and Shevtsova, O. (2009). Subcellular distribution of L-type calcium channel subtypes in rat hippocampal neurons. Neuroscience *164*, 641-657.

Leis JA, Bekar LK, Walz W. (2005). Potassium homeostasis in the ischemic brain. Glia *50*, 407-16.

Lerma, J. (2003). Roles and rules of kainate receptors in synaptic transmission. Nat Rev Neurosci *4*, 481-495.

Lesage, S., and Brice, A. (2009). Parkinson's disease: from monogenic forms to genetic susceptibility factors. Hum Mol Genet *18*, R48-59.

Lev, N., Ickowicz, D., Melamed, E., and Offen, D. (2008). Oxidative insults induce DJ-1 upregulation and redistribution: implications for neuroprotection. Neurotoxicology *29*, 397-405.

Levison, S. W., and Goldman, J. E. (1993). Both oligodendrocytes and astrocytes develop from progenitors in the subventricular zone of postnatal rat forebrain. Neuron *10*, 201-212.

Lewis, R. J., and Garcia, M. L. (2003). Therapeutic potential of venom peptides. Nat Rev Drug Discov *2*, 790-802.

Lim, D. A., Tramontin, A. D., Trevejo, J. M., Herrera, D. G., Garcia-Verdugo, J. M., and Alvarez-Buylla, A. (2000). Noggin antagonizes BMP signaling to create a niche for adult neurogenesis. Neuron *28*, 713-726.

Liu, B., Du, L., and Hong, J. S. (2000). Naloxone protects rat dopaminergic neurons against inflammatory damage through inhibition of microglia activation and superoxide generation. J Pharmacol Exp Ther *293*, 607-617.

Liu, J., Solway, K., Messing, R. O., and Sharp, F. R. (1998). Increased neurogenesis in the dentate gyrus after transient global ischemia in gerbils. J Neurosci *18*, 7768-7778.

Livett, B. G., Gayler, K. R., and Khalil, Z. (2004). Drugs from the sea: conopeptides as potential therapeutics. Curr Med Chem *11*, 1715-1723.

Lois, C., and Alvarez-Buylla, A. (1993). Proliferating subventricular zone cells in the adult mammalian forebrain can differentiate into neurons and glia. Proc Natl Acad Sci U S A *90*, 2074-2077.

Lois, C., and Alvarez-Buylla, A. (1994). Long-distance neuronal migration in the adult mammalian brain. Science *264*, 1145-1148.

Lonze, B. E., and Ginty, D. D. (2002). Function and regulation of CREB family transcription factors in the nervous system. Neuron *35*, 605-623.

Lonze, B. E., Riccio, A., Cohen, S., and Ginty, D. D. (2002). Apoptosis, axonal growth defects, and degeneration of peripheral neurons in mice lacking CREB. Neuron *34*, 371-385.

Lothman, E. W., Bertram, E. H., 3rd, and Stringer, J. L. (1991). Functional anatomy of hippocampal seizures. Prog Neurobiol *37*, 1-82.

Lucas, F. R., Goold, R. G., Gordon-Weeks, P. R., and Salinas, P. C. (1998). Inhibition of GSK-3beta leading to the loss of phosphorylated MAP-1B is an early event in axonal remodelling induced by WNT-7a or lithium. J Cell Sci *111 (Pt 10)*, 1351-1361.

Lukyanetz, E. A., Shkryl, V. M., and Kostyuk, P. G. (2002). Selective blockade of N-type calcium channels by levetiracetam. Epilepsia *43*, 9-18.

Luna-Medina, R., Cortes-Canteli, M., Alonso, M., Santos, A., Martinez, A., and Perez-Castillo, A. (2005). Regulation of inflammatory response in neural cells in vitro by thiadiazolidinones derivatives through peroxisome proliferator-activated receptor gamma activation. J Biol Chem *280*, 21453-21462.

Luna-Medina, R., Cortes-Canteli, M., Sanchez-Galiano, S., Morales-Garcia, J. A., Martinez, A., Santos, A., and Perez-Castillo, A. (2007). NP031112, a thiadiazolidinone compound, prevents inflammation and neurodegeneration under excitotoxic conditions: potential therapeutic role in brain disorders. J Neurosci *27*, 5766-5776.

Luskin, M. B. (1993). Restricted proliferation and migration of postnatally generated neurons derived from the forebrain subventricular zone. Neuron *11*, 173-189.

Luskin, M. B., Zigova, T., Soteres, B. J., and Stewart, R. R. (1997). Neuronal progenitor cells derived from the anterior subventricular zone of the neonatal rat forebrain continue to proliferate in vitro and express a neuronal phenotype. Mol Cell Neurosci *8*, 351-366.

Lutolf, S., Radtke, F., Aguet, M., Suter, U., and Taylor, V. (2002). Notch1 is required for neuronal and glial differentiation in the cerebellum. Development *129*, 373-385.

Ma, Y. C., Song, M. R., Park, J. P., Henry Ho, H. Y., Hu, L., Kurtev, M. V., Zieg, J., Ma, Q., Pfaff, S. L., and Greenberg, M. E. (2008). Regulation of motor neuron specification by phosphorylation of neurogenin 2. Neuron *58*, 65-77.

Maeshiba, Y., Kiyota, Y., Yamashita, K., Yoshimura, Y., Motohashi, M., and Tanayama, S. (1997). Disposition of the new antidiabetic agent pioglitazone in rats, dogs, and monkeys. Arzneimittelforschung *47*, 29-35.

Magavi, S. S., Leavitt, B. R., and Macklis, J. D. (2000). Induction of neurogenesis in the neocortex of adult mice. Nature *405*, 951-955.

Mahy, N., Bendahan, G., Boatell, M. L., Bjelke, B., Tinner, B., Olson, L., and Fuxe, K. (1995). Differential brain area vulnerability to long-term subcortical excitotoxic lesions. Neuroscience *65*, 15-25.

Mak, G. K., and Weiss, S. (2010). Paternal recognition of adult offspring mediated by newly generated CNS neurons. Nat Neurosci *13*, 753-758.

Malinow, R., and Malenka, R. C. (2002). AMPA receptor trafficking and synaptic plasticity. Annu Rev Neurosci *25*, 103-126.

Mantamadiotis, T., Lemberger, T., Bleckmann, S. C., Kern, H., Kretz, O., Martin Villalba, A., Tronche, F., Kellendonk, C., Gau, D., Kapfhammer, J., *et al.* (2002). Disruption of CREB function in brain leads to neurodegeneration. Nat Genet *31*, 47-54.

Martinez, A., Alonso, M., Castro, A., Perez, C., and Moreno, F. J. (2002a). First non-ATP competitive glycogen synthase kinase 3 beta (GSK-3beta) inhibitors: thiadiazolidinones (TDZD) as potential drugs for the treatment of Alzheimer's disease. J Med Chem *45*, 1292-1299.

Martinez, A., Castro, A., Dorronsoro, I., and Alonso, M. (2002b). Glycogen synthase kinase 3 (GSK-3) inhibitors as new promising drugs for diabetes, neurodegeneration, cancer, and inflammation. Med Res Rev *22*, 373-384.

Maurer, M. H., Bromme, J. O., Feldmann, R. E., Jr., Jarve, A., Sabouri, F., Burgers, H. F., Schelshorn, D. W., Kruger, C., Schneider, A., and Kuschinsky, W. (2007). Glycogen synthase kinase 3beta (GSK3beta) regulates differentiation and proliferation in neural stem cells from the rat subventricular zone. J Proteome Res *6*, 1198-1208.

McCoy, M. K., Martinez, T. N., Ruhn, K. A., Szymkowski, D. E., Smith, C. G., Botterman, B. R., Tansey, K. E., and Tansey, M. G. (2006). Blocking soluble tumor necrosis factor signaling with dominant-negative tumor necrosis factor inhibitor attenuates loss of dopaminergic neurons in models of Parkinson's disease. J Neurosci *26*, 9365-9375.

McCoy, M. K., and Tansey, M. G. (2008). TNF signaling inhibition in the CNS: implications for normal brain function and neurodegenerative disease. J Neuroinflammation *5*, 45.

McGeer, E. G., and McGeer, P. L. (2007). The role of anti-inflammatory agents in Parkinson's disease. CNS Drugs *21*, 789-797.

McGeer, P. L., Schwab, C., Parent, A., and Doudet, D. (2003). Presence of reactive microglia in monkey substantia nigra years after 1-methyl-4-phenyl-1,2,3,6-tetrahydropyridine administration. Ann Neurol *54*, 599-604.

McKay, R. (1997). Stem cells in the central nervous system. Science *276*, 66-71.

McNamara, J. O. (1994). Cellular and molecular basis of epilepsy. J Neurosci *14*, 3413-3425.

Meldrum BS. (2000). Glutamate as a neurotransmitter in the brain: review of physiology and pathology. J Nutr *130* (4S Suppl), 1007S-15S.

Meldrum, B., and Garthwaite, J. (1990). Excitatory amino acid neurotoxicity and neurodegenerative disease. Trends Pharmacol Sci *11*, 379-387.

Meldrum, B. S. (1983). Endocrine consequences of status epilepticus. Adv Neurol *34*, 399-403.

Menn, B., Garcia-Verdugo, J. M., Yaschine, C., Gonzalez-Perez, O., Rowitch, D., and Alvarez-Buylla, A. (2006). Origin of oligodendrocytes in the subventricular zone of the adult brain. J Neurosci *26*, 7907-7918.

Menniti, F. S., Faraci, W. S., and Schmidt, C. J. (2006). Phosphodiesterases in the CNS: targets for drug development. Nat Rev Drug Discov *5*, 660-670.

Menzler, S., Bikker, J. A., Suman-Chauhan, N., and Horwell, D. C. (2000). Design and biological evaluation of non-peptide analogues of omega-conotoxin MVIIA. Bioorg Med Chem Lett *10*, 345-347.

Michalik, L., Auwerx, J., Berger, J. P., Chatterjee, V. K., Glass, C. K., Gonzalez, F. J., Grimaldi, P. A., Kadowaki, T., Lazar, M. A., O'Rahilly, S., *et al.* (2006). International Union of Pharmacology. LXI. Peroxisome proliferator-activated receptors. Pharmacol Rev *58*, 726-741.

Miljanich, G. P. (2004). Ziconotide: neuronal calcium channel blocker for treating severe chronic pain. Curr Med Chem *11*, 3029-3040.

Minami, M., Kuraishi, Y., and Satoh, M. (1991). Effects of kainic acid on messenger RNA levels of IL-1 beta, IL-6, TNF alpha and LIF in the rat brain. Biochem Biophys Res Commun *176*, 593-598.

Minghetti, L. (2007). Role of COX-2 in inflammatory and degenerative brain diseases. Subcell Biochem *42*, 127-141.

Miro, X., Perez-Torres, S., Palacios, J. M., Puigdomenech, P., and Mengod, G. (2001). Differential distribution of cAMP-specific phosphodiesterase 7A mRNA in rat brain and peripheral organs. Synapse *40*, 201-214.

Mody, I., and MacDonald, J. F. (1995). NMDA receptor-dependent excitotoxicity: the role of intracellular Ca2+ release. Trends Pharmacol Sci *16*, 356-359.

Monje, M. L., Toda, H., and Palmer, T. D. (2003). Inflammatory blockade restores adult hippocampal neurogenesis. Science *302*, 1760-1765.

Morshead, C. M., Reynolds, B. A., Craig, C. G., McBurney, M. W., Staines, W. A., Morassutti, D., Weiss, S., and van der Kooy, D. (1994). Neural stem cells in the adult mammalian forebrain: a relatively quiescent subpopulation of subependymal cells. Neuron *13*, 1071-1082.

Mu, X., He, G., Cheng, Y., Li, X., Xu, B., and Du, G. (2009). Baicalein exerts neuroprotective effects in 6-hydroxydopamine-induced experimental parkinsonism in vivo and in vitro. Pharmacol Biochem Behav *92*, 642-648.

Mukai, F., Ishiguro, K., Sano, Y., and Fujita, S. C. (2002). Alternative splicing isoform of tau protein kinase I/glycogen synthase kinase 3beta. J Neurochem *81*, 1073-1083.

Nait-Oumesmar, B., Decker, L., Lachapelle, F., Avellana-Adalid, V., Bachelin, C., and Van Evercooren, A. B. (1999). Progenitor cells of the adult mouse subventricular zone proliferate, migrate and differentiate into oligodendrocytes after demyelination. Eur J Neurosci *11*, 4357-4366.

Nakanishi S. 1992. Molecular diversity of glutamate receptors and implications for brain function. Science *258*, 597-603.

Nakata, A., Ogawa, K., Sasaki, T., Koyama, N., Wada, K., Kotera, J., Kikkawa, H., Omori, K., and Kaminuma, O. (2002). Potential role of phosphodiesterase 7 in human T cell function: comparative effects of two phosphodiesterase inhibitors. Clin Exp Immunol *128*, 460-466.

Neal, J. W., and Clipstone, N. A. (2001). Glycogen synthase kinase-3 inhibits the DNA binding activity of NFATc. J Biol Chem *276*, 3666-3673.

Nitsch, C., and Scotti, A. L. (1992). Ibotenic acid-induced calcium deposits in rat substantia nigra. Ultrastructure of their time-dependent formation. Acta Neuropathol *85*, 55-70.

Noble, W., Planel, E., Zehr, C., Olm, V., Meyerson, J., Suleman, F., Gaynor, K., Wang, L., LaFrancois, J., Feinstein, B., *et al.* (2005). Inhibition of glycogen synthase kinase-3 by lithium correlates with reduced tauopathy and degeneration in vivo. Proc Natl Acad Sci U S A *102*, 6990-6995.

Nogawa, S., Zhang, F., Ross, M. E., and Iadecola, C. (1997). Cyclo-oxygenase-2 gene expression in neurons contributes to ischemic brain damage. J Neurosci *17*, 2746-2755.

Norenberg, M. D., and Rao, K. V. (2007). The mitochondrial permeability transition in neurologic disease. Neurochem Int *50*, 983-997.

Nucifora, F. C., Jr., Sasaki, M., Peters, M. F., Huang, H., Cooper, J. K., Yamada, M., Takahashi, H., Tsuji, S., Troncoso, J., Dawson, V. L., *et al.* (2001). Interference by huntingtin and atrophin-1 with cbp-mediated transcription leading to cellular toxicity. Science *291*, 2423-2428.

O'Neill, M. J., Bath, C. P., Dell, C. P., Hicks, C. A., Gilmore, J., Ambler, S. J., Ward, M. A., and Bleakman, D. (1997). Effects of Ca2+ and Na+ channel inhibitors in vitro and in global cerebral ischaemia in vivo. Eur J Pharmacol *332*, 121-131.

Ocbina, P. J., Dizon, M. L., Shin, L., and Szele, F. G. (2006). Doublecortin is necessary for the migration of adult subventricular zone cells from neurospheres. Mol Cell Neurosci *33*, 126-135.

Oliveira, M. S., Furian, A. F., Royes, L. F., Fighera, M. R., Fiorenza, N. G., Castelli, M., Machado, P., Bohrer, D., Veiga, M., Ferreira, J., *et al.* (2008). Cyclooxygenase-2/PGE2 pathway facilitates pentylenetetrazol-induced seizures. Epilepsy Res *79*, 14-21.

Olivera, B. M. (1997). E.E. Just Lecture, 1996. Conus venom peptides, receptor and ion channel targets, and drug design: 50 million years of neuropharmacology. Mol Biol Cell *8*, 2101-2109.

Olivera, B. M., Miljanich, G. P., Ramachandran, J., and Adams, M. E. (1994). Calcium channel diversity and neurotransmitter release: the omega-conotoxins and omega-agatoxins. Annu Rev Biochem *63*, 823-867.

Olney, J. W., Collins, R. C., and Sloviter, R. S. (1986). Excitotoxic mechanisms of epileptic brain damage. Adv Neurol *44*, 857-877.

Olney, J. W., and Sharpe, L. G. (1969). Brain lesions in an infant rhesus monkey treated with monsodium glutamate. Science *166*, 386-388.

Oprica, M., Eriksson, C., and Schultzberg, M. (2003). Inflammatory mechanisms associated with brain damage induced by kainic acid with special reference to the interleukin-1 system. J Cell Mol Med *7*, 127-140.

Orr, C. F., Rowe, D. B., Mizuno, Y., Mori, H., and Halliday, G. M. (2005). A possible role for humoral immunity in the pathogenesis of Parkinson's disease. Brain *128*, 2665-2674.

Ostenfeld, T., and Svendsen, C. N. (2003). Recent advances in stem cell neurobiology. Adv Tech Stand Neurosurg *28*, 3-89.

Ouyang, M., and Shen, X. (2006). Critical role of ASK1 in the 6-hydroxydopamine-induced apoptosis in human neuroblastoma SH-SY5Y cells. J Neurochem *97*, 234-244.

Pal, S., Sombati, S., Limbrick, D. D., Jr., and DeLorenzo, R. J. (1999). In vitro status epilepticus causes sustained elevation of intracellular calcium levels in hippocampal neurons. Brain Res *851*, 20-31.

Parent, J. M., Yu, T. W., Leibowitz, R. T., Geschwind, D. H., Sloviter, R. S., and Lowenstein, D. H. (1997). Dentate granule cell neurogenesis is increased by seizures and contributes to aberrant network reorganization in the adult rat hippocampus. J Neurosci *17*, 3727-3738.

Parras, C. M., Galli, R., Britz, O., Soares, S., Galichet, C., Battiste, J., Johnson, J. E., Nakafuku, M., Vescovi, A., and Guillemot, F. (2004). Mash1 specifies neurons and oligodendrocytes in the postnatal brain. EMBO J *23*, 4495-4505.

Paruchuri, S., Jiang, Y., Feng, C., Francis, S. A., Plutzky, J., and Boyce, J. A. (2008). Leukotriene E4 activates peroxisome proliferator-activated receptor gamma and induces prostaglandin D2 generation by human mast cells. J Biol Chem *283*, 16477-16487.

Pencea, V., Bingaman, K. D., Freedman, L. J., and Luskin, M. B. (2001). Neurogenesis in the subventricular zone and rostral migratory stream of the neonatal and adult primate forebrain. Exp Neurol *172*, 1-16.

Perez-Reyes, E. (1998). Molecular characterization of a novel family of low voltage-activated, T-type, calcium channels. J Bioenerg Biomembr *30*, 313-318.

Pham, N., Cheglakov, I., Koch, C. A., de Hoog, C. L., Moran, M. F., and Rotin, D. (2000). The guanine nucleotide exchange factor CNrasGEF activates ras in response to cAMP and cGMP. Curr Biol *10*, 555-558.

Picard-Riera, N., Decker, L., Delarasse, C., Goude, K., Nait-Oumesmar, B., Liblau, R., Pham-Dinh, D., and Evercooren, A. B. (2002). Experimental autoimmune encephalomyelitis mobilizes neural progenitors from the subventricular zone to undergo oligodendrogenesis in adult mice. Proc Natl Acad Sci U S A *99*, 13211-13216.

Qiu, D. L., and Knopfel, T. (2007). An NMDA receptor/nitric oxide cascade in presynaptic parallel fiber-Purkinje neuron long-term potentiation. J Neurosci *27*, 3408-3415.

Racine, R. J. (1972). Modification of seizure activity by electrical stimulation. II. Motor seizure. Electroencephalogr Clin Neurophysiol *32*, 281-294.

Rantham Prabhakara, J. P., Feist, G., Thomasson, S., Thompson, A., Schommer, E., and Ghribi, O. (2008). Differential effects of 24-hydroxycholesterol and 27-hydroxycholesterol on tyrosine hydroxylase and alpha-synuclein in human neuroblastoma SH-SY5Y cells. J Neurochem *107*, 1722-1729.

Rappold, P. M., Lynd-Balta, E., and Joseph, S. A. (2006). P2X7 receptor immunoreactive profile confined to resting and activated microglia in the epileptic brain. Brain Res *1089*, 171-178.

Ravizza, T., Gagliardi, B., Noe, F., Boer, K., Aronica, E., and Vezzani, A. (2008). Innate and adaptive immunity during epileptogenesis and spontaneous seizures: evidence from experimental models and human temporal lobe epilepsy. Neurobiol Dis *29*, 142-160.

Regan, C., Katona, C., Walker, Z., Hooper, J., Donovan, J., and Livingston, G. (2006). Relationship of vascular risk to the progression of Alzheimer disease. Neurology *67*, 1357-1362.

Reyes-Irisarri, E., Perez-Torres, S., and Mengod, G. (2005). Neuronal expression of cAMP-specific phosphodiesterase 7B mRNA in the rat brain. Neuroscience *132*, 1173-1185.

Reynolds, B. A., and Weiss, S. (1992). Generation of neurons and astrocytes from isolated cells of the adult mammalian central nervous system. Science *255*, 1707-1710.

Reynolds, B. A., and Weiss, S. (1996). Clonal and population analyses demonstrate that an EGF-responsive mammalian embryonic CNS precursor is a stem cell. Dev Biol *175*, 1-13.

Ricote, M., Huang, J. T., Welch, J. S., and Glass, C. K. (1999). The peroxisome proliferator-activated receptor(PPARgamma) as a regulator of monocyte/macrophage function. J Leukoc Biol *66*, 733-739.

Robbins, D. S., Shirazi, Y., Drysdale, B. E., Lieberman, A., Shin, H. S., and Shin, M. L. (1987). Production of cytotoxic factor for oligodendrocytes by stimulated astrocytes. J Immunol *139*, 2593-2597.

Robledo, P., Ursu, G., and Mahy, N. (1999). Effects of adenosine and gamma-aminobutyric acid A receptor antagonists on N-methyl-D-aspartate induced neurotoxicity in the rat hippocampus. Hippocampus *9*, 527-533.

Rockenstein, E., Torrance, M., Adame, A., Mante, M., Bar-on, P., Rose, J. B., Crews, L., and Masliah, E. (2007). Neuroprotective effects of regulators of the glycogen synthase kinase-3beta signaling pathway in a transgenic model of Alzheimer's disease are associated with reduced amyloid precursor protein phosphorylation. J Neurosci *27*, 1981-1991.

Rochefort, C., Gheusi, G., Vincent, J. D., and Lledo, P. M. (2002). Enriched odor exposure increases the number of newborn neurons in the adult olfactory bulb and improves odor memory. J Neurosci *22*, 2679-2689.

Romero-Grimaldi, C., Gheusi, G., Lledo, P. M., and Estrada, C. (2006). Chronic inhibition of nitric oxide synthesis enhances both subventricular zone neurogenesis and olfactory learning in adult mice. Eur J Neurosci *24*, 2461-2470.

Rosen, E. D., and Spiegelman, B. M. (2001). PPARgamma : a nuclear regulator of metabolism, differentiation, and cell growth. J Biol Chem *276*, 37731-37734.

Rothwell, L., Hamblin, A., and Kaiser, P. (2001). Production and characterisation of monoclonal antibodies specific for chicken interleukin-2. Vet Immunol Immunopathol *83*, 149-160.

Rousselot, P., Lois, C., and Alvarez-Buylla, A. (1995). Embryonic (PSA) N-CAM reveals chains of migrating neuroblasts between the lateral ventricle and the olfactory bulb of adult mice. J Comp Neurol *351*, 51-61.

Rutishauser, U. (2008). Polysialic acid in the plasticity of the developing and adult vertebrate nervous system. Nat Rev Neurosci *9*, 26-35.

Sabria, J., Pastor, C., Clos, M. V., Garcia, A., and Badia, A. (1995). Involvement of different types of voltage-sensitive calcium channels in the presynaptic regulation of noradrenaline release in rat brain cortex and hippocampus. J Neurochem *64*, 2567-2571.

Saijo, K., Winner, B., Carson, C. T., Collier, J. G., Boyer, L., Rosenfeld, M. G., Gage, F. H., and Glass, C. K. (2009). A Nurr1/CoREST pathway in microglia and astrocytes protects dopaminergic neurons from inflammation-induced death. Cell *137*, 47-59.

Samii, A., Badie, H., Fu, K., Luther, R. R., and Hovda, D. A. (1999). Effects of an N-type calcium channel antagonist (SNX 111; Ziconotide) on calcium-45 accumulation following fluid-percussion injury. J Neurotrauma *16*, 879-892.

Sanchez-Prieto, J., Paternain, A. V., and Lerma, J. (2004). Dual signaling by mGluR5a results in bi-directional modulation of N-type Ca2+ channels. FEBS Lett *576*, 428-432.

Sander, J. W., and Shorvon, S. D. (1996). Epidemiology of the epilepsies. J Neurol Neurosurg Psychiatry *61*, 433-443.

Sasaki, T., Kotera, J., and Omori, K. (2002). Novel alternative splice variants of rat phosphodiesterase 7B showing unique tissue-specific expression and phosphorylation. Biochem J *361*, 211-220.

Sato, N., Meijer, L., Skaltsounis, L., Greengard, P., and Brivanlou, A. H. (2004). Maintenance of pluripotency in human and mouse embryonic stem cells through activation of Wnt signaling by a pharmacological GSK-3-specific inhibitor. Nat Med *10*, 55-63.

Sattler, R., and Tymianski, M. (2000). Molecular mechanisms of calcium-dependent excitotoxicity. J Mol Med *78*, 3-13.

Schapira, A. H. (2008). Mitochondrial dysfunction in neurodegenerative diseases. Neurochem Res *33*, 2502-2509.

Schelkun, R. M., Yuen, P., Malone, T. C., Rock, D. M., Stoehr, S., Szoke, B., and Tarczy-Hornoch, K. (1999). Synthesis and biological activity of substituted bis-(4-hydroxyphenyl)methanes as N-type calcium channel blockers. Bioorg Med Chem Lett *9*, 2447-2452.

Schober, A. (2004). Classic toxin-induced animal models of Parkinson's disease: 6-OHDA and MPTP. Cell Tissue Res *318*, 215-224.

Schwarting, R. K., and Huston, J. P. (1996). The unilateral 6-hydroxydopamine lesion model in behavioral brain research. Analysis of functional deficits, recovery and treatments. Prog Neurobiol *50*, 275-331.

Seaberg, R. M., and van der Kooy, D. (2002). Adult rodent neurogenic regions: the ventricular subependyma contains neural stem cells, but the dentate gyrus contains restricted progenitors. J Neurosci *22*, 1784-1793.

Seagar, M., and Takahashi, M. (1998). Interactions between presynaptic calcium channels and proteins implicated in synaptic vesicle trafficking and exocytosis. J Bioenerg Biomembr *30*, 347-356.

Seeburg, P. H., Single, F., Kuner, T., Higuchi, M., and Sprengel, R. (2001). Genetic manipulation of key determinants of ion flow in glutamate receptor channels in the mouse. Brain Res *907*, 233-243.

Seki, T., and Arai, Y. (1993). Highly polysialylated neural cell adhesion molecule (NCAM-H) is expressed by newly generated granule cells in the dentate gyrus of the adult rat. J Neurosci *13*, 2351-2358.

Seri, B., Garcia-Verdugo, J. M., Collado-Morente, L., McEwen, B. S., and Alvarez-Buylla, A. (2004). Cell types, lineage, and architecture of the germinal zone in the adult dentate gyrus. J Comp Neurol *478*, 359-378.

Seri, B., Garcia-Verdugo, J. M., McEwen, B. S., and Alvarez-Buylla, A. (2001). Astrocytes give rise to new neurons in the adult mammalian hippocampus. J Neurosci *21*, 7153-7160.

Sharma, A. K., Searfoss, G. H., Reams, R. Y., Jordan, W. H., Snyder, P. W., Chiang, A. Y., Jolly, R. A., and Ryan, T. P. (2009). Kainic acid-induced F-344 rat model of mesial temporal lobe epilepsy: gene expression and canonical pathways. Toxicol Pathol *37*, 776-789.

Shaywitz, A. J., and Greenberg, M. E. (1999). CREB: a stimulus-induced transcription factor activated by a diverse array of extracellular signals. Annu Rev Biochem *68*, 821-861.

Shen, Q., Wang, Y., Kokovay, E., Lin, G., Chuang, S. M., Goderie, S. K., Roysam, B., and Temple, S. (2008). Adult SVZ stem cells lie in a vascular niche: a quantitative analysis of niche cell-cell interactions. Cell Stem Cell *3*, 289-300.

Shih, Y. T., Chen, I. J., Wu, Y. C., and Lo, Y. C. (2009). San-Huang-Xie-Xin-Tang Protects Against Activated Microglia- and 6-OHDA-induced Toxicity in Neuronal SH-SY5Y Cells. Evid Based Complement Alternat Med.

Shimohata, T., Nakajima, T., Yamada, M., Uchida, C., Onodera, O., Naruse, S., Kimura, T., Koide, R., Nozaki, K., Sano, Y., *et al.* (2000). Expanded polyglutamine stretches interact with TAFII130, interfering with CREB-dependent transcription. Nat Genet *26*, 29-36.

Simi, A., Tsakiri, N., Wang, P., and Rothwell, N. J. (2007). Interleukin-1 and inflammatory neurodegeneration. Biochem Soc Trans *35*, 1122-1126.

So, K., Moriya, T., Nishitani, S., Takahashi, H., and Shinohara, K. (2008). The olfactory conditioning in the early postnatal period stimulated neural stem/progenitor cells in the subventricular zone and increased neurogenesis in the olfactory bulb of rats. Neuroscience *151*, 120-128.

Sombati, S., and Delorenzo, R. J. (1995). Recurrent spontaneous seizure activity in hippocampal neuronal networks in culture. J Neurophysiol *73*, 1706-1711.

Song, H. J., Ming, G. L., and Poo, M. M. (1997). cAMP-induced switching in turning direction of nerve growth cones. Nature *388*, 275-279.

Song, H. J., Stevens, C. F., and Gage, F. H. (2002). Neural stem cells from adult hippocampus develop essential properties of functional CNS neurons. Nat Neurosci *5*, 438-445.

Song, I., and Huganir, R. L. (2002). Regulation of AMPA receptors during synaptic plasticity. Trends Neurosci *25*, 578-588.

Spafford, J. D., Van Minnen, J., Larsen, P., Smit, A. B., Syed, N. I., and Zamponi, G. W. (2004). Uncoupling of calcium channel alpha1 and beta subunits in developing neurons. J Biol Chem *279*, 41157-41167.

Sperk, G. (1994). Kainic acid seizures in the rat. Prog Neurobiol *42*, 1-32.

Sperk, G., Lassmann, H., Baran, H., Seitelberger, F., and Hornykiewicz, O. (1985). Kainic acid-induced seizures: dose-relationship of behavioural, neurochemical and histopathological changes. Brain Res *338*, 289-295.

Spittaels, K., Van den Haute, C., Van Dorpe, J., Terwel, D., Vandezande, K., Lasrado, R., Bruynseels, K., Irizarry, M., Verhoye, M., Van Lint, J., *et al.* (2002). Neonatal neuronal overexpression of glycogen synthase kinase-3 beta reduces brain size in transgenic mice. Neuroscience *113*, 797-808.

Starkov, A. A., Chinopoulos, C., and Fiskum, G. (2004). Mitochondrial calcium and oxidative stress as mediators of ischemic brain injury. Cell Calcium *36*, 257-264.

Stefani, A., Spadoni, F., Siniscalchi, A., and Bernardi, G. (1996). Lamotrigine inhibits Ca2+ currents in cortical neurons: functional implications. Eur J Pharmacol *307*, 113-116.

Steiner, B., Kronenberg, G., Jessberger, S., Brandt, M. D., Reuter, K., and Kempermann, G. (2004). Differential regulation of gliogenesis in the context of adult hippocampal neurogenesis in mice. Glia *46*, 41-52.

Steiner, B., Zurborg, S., Horster, H., Fabel, K., and Kempermann, G. (2008). Differential 24 h responsiveness of Prox1-expressing precursor cells in adult hippocampal neurogenesis to physical activity, environmental enrichment, and kainic acid-induced seizures. Neuroscience *154*, 521-529.

Stetler, R. A., Gao, Y., Zukin, R. S., Vosler, P. S., Zhang, L., Zhang, F., Cao, G., Bennett, M. V., and Chen, J. Apurinic/apyrimidinic endonuclease APE1 is required for PACAP-induced neuroprotection against global cerebral ischemia. Proc Natl Acad Sci U S A *107*, 3204-3209.

Storm, M. P., Bone, H. K., Beck, C. G., Bourillot, P. Y., Schreiber, V., Damiano, T., Nelson, A., Savatier, P., and Welham, M. J. (2007). Regulation of Nanog expression by phosphoinositide 3-kinase-dependent signaling in murine embryonic stem cells. J Biol Chem *282*, 6265-6273.

Streit WJ, Walter SA, Pennell NA. (1999). Reactive microgliosis. Prog Neurobiol *57*, 563-81

Streit, W. J. (2002). Microglia as neuroprotective, immunocompetent cells of the CNS. Glia *40*, 133-139.

Sultan, S., Mandairon, N., Kermen, F., Garcia, S., Sacquet, J., and Didier, A. (2010). Learning-dependent neurogenesis in the olfactory bulb determines long-term olfactory memory. FASEB J *24*, 2355-2363.

Sun, D. A., Sombati, S., Blair, R. E., and DeLorenzo, R. J. (2002). Calcium-dependent epileptogenesis in an in vitro model of stroke-induced "epilepsy". Epilepsia *43*, 1296-1305.

Sutton, K. G., McRory, J. E., Guthrie, H., Murphy, T. H., and Snutch, T. P. (1999). P/Q-type calcium channels mediate the activity-dependent feedback of syntaxin-1A. Nature *401*, 800-804.

Szeles, L., Torocsik, D., and Nagy, L. (2007). PPARgamma in immunity and inflammation: cell types and diseases. Biochim Biophys Acta *1771*, 1014-1030.

Takahara, A., Konda, T., Enomoto, A., and Kondo, N. (2004). Neuroprotective effects of a dual L/N-type Ca(2+) channel blocker cilnidipine in the rat focal brain ischemia model. Biol Pharm Bull *27*, 1388-1391.

Talley, E. M., Cribbs, L. L., Lee, J. H., Daud, A., Perez-Reyes, E., and Bayliss, D. A. (1999). Differential distribution of three members of a gene family encoding low voltage-activated (T-type) calcium channels. J Neurosci *19*, 1895-1911.

Tansey, M. G., McCoy, M. K., and Frank-Cannon, T. C. (2007). Neuroinflammatory mechanisms in Parkinson's disease: potential environmental triggers, pathways, and targets for early therapeutic intervention. Exp Neurol *208*, 1-25.

Tateishi, K., Ashihara, E., Honsho, S., Takehara, N., Nomura, T., Takahashi, T., Ueyama, T., Yamagishi, M., Yaku, H., Matsubara, H., and Oh, H. (2007). Human cardiac stem cells exhibit mesenchymal features and are maintained through Akt/GSK-3beta signaling. Biochem Biophys Res Commun *352*, 635-641.

Tauck, D. L., and Nadler, J. V. (1985). Evidence of functional mossy fiber sprouting in hippocampal formation of kainic acid-treated rats. J Neurosci *5*, 1016-1022.

Teismann, P., Vila, M., Choi, D. K., Tieu, K., Wu, D. C., Jackson-Lewis, V., and Przedborski, S. (2003). COX-2 and neurodegeneration in Parkinson's disease. Ann N Y Acad Sci *991*, 272-277.

Temple, S. (2001). The development of neural stem cells. Nature *414*, 112-117.

Toledo-Aral, J. J., Mendez-Ferrer, S., Pardal, R., and Lopez-Barneo, J. (2002). Dopaminergic cells of the carotid body: physiological significance and possible therapeutic applications in Parkinson's disease. Brain Res Bull *57*, 847-853.

Tontonoz, P., Hu, E., and Spiegelman, B. M. (1994). Stimulation of adipogenesis in fibroblasts by PPAR gamma 2, a lipid-activated transcription factor. Cell *79*, 1147-1156.

Torgersen, K. M., Vang, T., Abrahamsen, H., Yaqub, S., and Tasken, K. (2002). Molecular mechanisms for protein kinase A-mediated modulation of immune function. Cell Signal *14*, 1-9.

Townsend, K. P., and Pratico, D. (2005). Novel therapeutic opportunities for Alzheimer's disease: focus on nonsteroidal anti-inflammatory drugs. FASEB J *19*, 1592-1601.

Triggle, D. J. (2003). Drug targets in the voltage-gated calcium channel family: why some are and some are not. Assay Drug Dev Technol *1*, 719-733.

Triggle, D. J. (2007). Calcium channel antagonists: clinical uses--past, present and future. Biochem Pharmacol *74*, 1-9.

Uchitel, O. D. (1997). Toxins affecting calcium channels in neurons. Toxicon *35*, 1161-1191.

Ulas, J., Monaghan, D. T., and Cotman, C. W. (1990). Kainate receptors in the rat hippocampus: a distribution and time course of changes in response to unilateral lesions of the entorhinal cortex. J Neurosci *10*, 2352-2362.

Ungerstedt, U., and Arbuthnott, G. W. (1970). Quantitative recording of rotational behavior in rats after 6-hydroxy-dopamine lesions of the nigrostriatal dopamine system. Brain Res *24*, 485-493.

Valentino, K., Newcomb, R., Gadbois, T., Singh, T., Bowersox, S., Bitner, S., Justice, A., Yamashiro, D., Hoffman, B. B., Ciaranello, R., and et al. (1993). A selective N-type calcium channel antagonist protects against neuronal loss after global cerebral ischemia. Proc Natl Acad Sci U S A *90*, 7894-7897.

Valero, T., del Barrio, L., Egea, J., Canas, N., Martinez, A., Garcia, A. G., Villarroya, M., and Lopez, M. G. (2009). NP04634 prevents cell damage caused by calcium overload and mitochondrial disruption in bovine chromaffin cells. Eur J Pharmacol *607*, 47-53.

van Praag, H., Schinder, A. F., Christie, B. R., Toni, N., Palmer, T. D., and Gage, F. H. (2002). Functional neurogenesis in the adult hippocampus. Nature *415*, 1030-1034.

Verkhratsky, A. (2005). Physiology and pathophysiology of the calcium store in the endoplasmic reticulum of neurons. Physiol Rev *85*, 201-279.

Vezzani, A., Balosso, S., and Ravizza, T. (2008). The role of cytokines in the pathophysiology of epilepsy. Brain Behav Immun *22*, 797-803.

Vezzani, A., and Granata, T. (2005). Brain inflammation in epilepsy: experimental and clinical evidence. Epilepsia *46*, 1724-1743.

Vezzani, A., Wu, H. Q., Stasi, M. A., Angelico, P., and Samanin, R. (1988). Effect of various calcium channel blockers on three different models of limbic seizures in rats. Neuropharmacology *27*, 451-458.

Vitolo, O. V., Sant'Angelo, A., Costanzo, V., Battaglia, F., Arancio, O., and Shelanski, M. (2002). Amyloid beta -peptide inhibition of the PKA/CREB pathway and long-term potentiation: reversibility by drugs that enhance cAMP signaling. Proc Natl Acad Sci U S A *99*, 13217-13221.

Volakakis, N., Kadkhodaei, B., Joodmardi, E., Wallis, K., Panman, L., Silvaggi, J., Spiegelman, B. M., and Perlmann, T. (2010). NR4A orphan nuclear receptors as mediators of CREB-dependent neuroprotection. Proc Natl Acad Sci U S A *107*, 12317-12322.

Wada, K., Nakajima, A., Katayama, K., Kudo, C., Shibuya, A., Kubota, N., Terauchi, Y., Tachibana, M., Miyoshi, H., Kamisaki, Y., *et al.* (2006). Peroxisome proliferator-activated receptor gamma-mediated regulation of neural stem cell proliferation and differentiation. J Biol Chem *281*, 12673-12681.

Wang, L. F., Wu, J. T., and Sun, C. C. (2002). Local but not systemic administration of IFN-gamma during the sensitization phase of protein antigen immunization suppress Th2 development in a murine model of atopic dermatitis. Cytokine *19*, 147-152.

Wang, Q., Yu, S., Simonyi, A., Sun, G. Y., and Sun, A. Y. (2005). Kainic acid-mediated excitotoxicity as a model for neurodegeneration. Mol Neurobiol *31*, 3-16.

Wang, S., Ding, M., Wu, D., Zhan, J., and Chen, Z. (2007). omega-Conotoxin MVIIA inhibits amygdaloid kindled seizures in Sprague-Dawley rats. Neurosci Lett *413*, 163-167.

Wheeler, D. B., Randall, A., and Tsien, R. W. (1996). Changes in action potential duration alter reliance of excitatory synaptic transmission on multiple types of Ca2+ channels in rat hippocampus. J Neurosci *16*, 2226-2237.

Wichterle, H., Garcia-Verdugo, J. M., and Alvarez-Buylla, A. (1997). Direct evidence for homotypic, glia-independent neuronal migration. Neuron *18*, 779-791.

Winner, B., Cooper-Kuhn, C. M., Aigner, R., Winkler, J., and Kuhn, H. G. (2002). Long-term survival and cell death of newly generated neurons in the adult rat olfactory bulb. Eur J Neurosci *16*, 1681-1689.

Wood-Kaczmar, A., Kraus, M., Ishiguro, K., Philpott, K. L., and Gordon-Weeks, P. R. (2009). An alternatively spliced form of glycogen synthase kinase-3beta is targeted to growing neurites and growth cones. Mol Cell Neurosci *42*, 184-194.

Woodgett, J. R. (1990). Molecular cloning and expression of glycogen synthase kinase-3/factor A. EMBO J *9*, 2431-2438.

Woodgett, J. R. (2001). Judging a protein by more than its name: GSK-3. Sci STKE *2001*, re12.

Woodgett, J. R., and Cohen, P. (1984). Multisite phosphorylation of glycogen synthase. Molecular basis for the substrate specificity of glycogen synthase kinase-3 and casein kinase-II (glycogen synthase kinase-5). Biochim Biophys Acta *788*, 339-347.

Yamada, K., Teraoka, T., Morita, S., Hasegawa, T., and Nabeshima, T. (1994). Omega-conotoxin GVIA protects against ischemia-induced neuronal death in the Mongolian gerbil but not against quinolinic acid-induced neurotoxicity in the rat. Neuropharmacology *33*, 251-254.

Yamamoto-Sasaki, M., Ozawa, H., Saito, T., Rosler, M., and Riederer, P. (1999). Impaired phosphorylation of cyclic AMP response element binding protein in the hippocampus of dementia of the Alzheimer type. Brain Res *824*, 300-303.

Zhang, B., Yang, L., Konishi, Y., Maeda, N., Sakanaka, M., and Tanaka, J. (2002). Suppressive effects of phosphodiesterase type IV inhibitors on rat cultured microglial cells: comparison with other types of cAMP-elevating agents. Neuropharmacology *42*, 262-269.

Zhang, R., Zhang, Z., Wang, L., Wang, Y., Gousev, A., Zhang, L., Ho, K. L., Morshead, C., and Chopp, M. (2004). Activated neural stem cells contribute to stroke-induced neurogenesis and neuroblast migration toward the infarct boundary in adult rats. J Cereb Blood Flow Metab *24*, 441-448.

Zhao, C., Deng, W., and Gage, F. H. (2008). Mechanisms and functional implications of adult neurogenesis. Cell *132*, 645-660.

Zhao, C., Teng, E. M., Summers, R. G., Jr., Ming, G. L., and Gage, F. H. (2006). Distinct morphological stages of dentate granule neuron maturation in the adult mouse hippocampus. J Neurosci *26*, 3-11.

Zhao, Q., Smith, M. L., and Siesjo, B. K. (1994). The omega-conopeptide SNX-111, an N-type calcium channel blocker, dramatically ameliorates brain damage due to transient focal ischaemia. Acta Physiol Scand *150*, 459-461.

Anexo

Publicaciones derivadas de la Tesis Doctoral:

- **Morales-Garcia, J. A**., Redondo, M., Alonso-Gil, S., Gil, C., Perez, C., Martinez, A., Santos, A., and Perez-Castillo, A. (2011). Phosphodiesterase 7 inhibition preserves dopaminergic neurons in cellular and rodent models of Parkinson disease. PLoS One *6*, e17240.

.

- **Morales-Garcia, J. A**., Luna-Medina, R., Alfaro-Cervello, C., Cortes-Canteli, M., Santos, A., Garcia-Verdugo, J. M., and Perez-Castillo, A. (2011). Peroxisome proliferator-activated receptor gamma ligands regulate neural stem cell proliferation and differentiation in vitro and in vivo. Glia *59*, 293-307

- **Morales-Garcia, J. A**., Luna-Medina, R., Martinez, A., Santos, A., and Perez-Castillo, A. (2009). Anticonvulsant and neuroprotective effects of the novel calcium antagonist NP04634 on kainic acid-induced seizures in rats. J Neurosci Res *87*, 3687-3696.

Otras publicaciones realizadas durante el desarrollo de la Tesis Doctoral:

- Aguilar-Morante, D[*]., **Morales-Garcia, J. A**[*]., Sanz-SanCristobal, M., Garcia-Cabezas, M. A., Santos, A., and Perez-Castillo, A. (2010). Inhibition of glioblastoma growth by the thiadiazolidinone compound TDZD-8. PLoS One *5*, e13879. [*]**Igual contribución**.

- Gine, E., **Morales-Garcia, J. A**., Perez-Castillo, A., and Santos, A. (2010). Developmental hypothyroidism increases the expression of kainate receptors in the hippocampus and the sensitivity to kainic acid-induced seizures in the rat. Endocrinology *151*, 3267-3276.

- Perez Castillo, A., Aguilar-Morante, D., **Morales-Garcia, J. A**., and Dorado, J. (2008). Cancer stem cells and brain tumors. Clin Transl Oncol *10*, 262-267.

- Luna-Medina, R., Cortes-Canteli, M., Sanchez-Galiano, S., **Morales-Garcia, J. A**., Martinez, A., Santos, A., and Perez-Castillo, A. (2007). NP031112, a thiadiazolidinone compound, prevents inflammation and neurodegeneration under excitotoxic conditions: potential therapeutic role in brain disorders. J Neurosci *27*, 5766-5776.

OPEN ACCESS Freely available online

PLoS one

Phosphodiesterase 7 Inhibition Preserves Dopaminergic Neurons in Cellular and Rodent Models of Parkinson Disease

Jose A. Morales-Garcia[1], Miriam Redondo[2], Sandra Alonso-Gil[1], Carmen Gil[2], Concepción Perez[2], Ana Martinez[2], Angel Santos[3], Ana Perez-Castillo[1]*

1 Instituto de Investigaciones Biomédicas, Consejo Superior de Investigaciones Científicas CSIC-UAM, Arturo Duperier, 4 and Centro de Investigación Biomédica en Red sobre Enfermedades Neurodegenerativas (CIBERNED), Madrid, Spain, **2** Instituto de Química Médica, CSIC, Juan de la Cierva, Madrid, Spain, **3** Departamento de Bioquímica y Biología Molecular, Facultad de Medicina, Universidad Complutense de Madrid, Madrid, Spain

Abstract

Background: Phosphodiesterase 7 plays a major role in down-regulation of protein kinase A activity by hydrolyzing cAMP in many cell types. This cyclic nucleotide plays a key role in signal transduction in a wide variety of cellular responses. In the brain, cAMP has been implicated in learning, memory processes and other brain functions.

Methodology/Principal Findings: Here we show a novel function of phosphodiesterase 7 inhibition on nigrostriatal dopaminergic neuronal death. We found that S14, a heterocyclic small molecule inhibitor of phosphodiesterase 7, conferred significant neuronal protection against different insults both in the human dopaminergic cell line SH-SY5Y and in primary rat mesencephalic cultures. S14 treatment also reduced microglial activation, protected dopaminergic neurons and improved motor function in the lipopolysaccharide rat model of Parkinson disease. Finally, S14 neuroprotective effects were reversed by blocking the cAMP signaling pathways that operate through cAMP-dependent protein kinase A.

Conclusions/Significance: Our findings demonstrate that phosphodiesterase 7 inhibition can protect dopaminergic neurons against different insults, and they provide support for the therapeutic potential of phosphodiesterase 7 inhibitors in the treatment of neurodegenerative disorders, particularly Parkinson disease.

Citation: Morales-Garcia JA, Redondo M, Alonso-Gil S, Gil C, Perez C, et al. (2011) Phosphodiesterase 7 Inhibition Preserves Dopaminergic Neurons in Cellular and Rodent Models of Parkinson Disease. PLoS ONE 6(2): e17240. doi:10.1371/journal.pone.0017240

Editor: Thierry Amédée, Centre national de la recherche scientifique, University of Bordeaux, France

Received November 2, 2010; **Accepted** January 24, 2011; **Published** February 24, 2011

Funding: This work was supported by the Ministerio de Ciencia y Tecnología (www.micinn.es) (SAF2007-62811 and SAF 2010-16365 to A.P.-C.), and SAF2009-13015-C02-01 to A.M., and by the Ministerio de Ciencia y Tecnologia (www.micinn.es) and ARACLON (www.araclon.com) in the joint project PET2008-0245 and by Instituto de Salud Carlos III (Red Temática de Investigación en Esclerosis Múltiple (to A.M.)). The funders had no role in study design, data collection and analysis, decision to publish, or preparation of the manuscript.

Competing Interests: The authors state that Araclon Biotech has been a commercial funder, together with the MICINN, for this work, but they have not participated in the experimental design on the manuscript and none of the authors is an employee of the company. This funding does not alter the authors' adherence to the PloS ONE policies on sharing data and materials. Some of the results here presented are protected by patent application P200930189 (owner CSIC). A license transfer agreement has been recently reached with ARACLON.

* E-mail: aperez@iib.uam.es

Introduction

Parkinson disease (PD) is one of the most common progressive neurodegenerative disorder, affecting around 1% of the elderly population. Typical symptoms of this disease are muscle rigidity, bradykinesia, resting tremor and postural instability. At the cellular level, PD is characterized by the loss of dopamine-containing neurons in the substantia nigra pars compacta (SNpc) although neuropathology can extend into other brain regions [1]. The cell death leads to the loss of dopamine in areas where these neurons project, causing the described symptoms. The main known risk factor is age, however susceptibility genes including α-synuclein, leucine rich repeat kinase 2 (LRRK-2), and glucocerebrosidase (GBA) have shown that genetic predisposition is another important causal factor in a 10% of diagnosed patients. There is currently no cure and no effective disease-modifying therapy. The dopamine replacement therapy in clinical use is only palliative; leading to temporarily limited improvement of clinical symptoms, and the chronic treatment with dopaminergic drugs have severe side effects as bradykinesia. Consequently, new approaches to treat Parkinson disease are needed to find disease's modifying agents that may delay or stop the neuronal death.

Neuroinflammation has been increasingly recognized as a primary mechanism involved in PD pathogenesis [2,3]. Loss of dopamine-producing neurons in PD is accompanied by inflammation in surrounding support glial cells. Activation of microglia has been demonstrated in SN and striatum from postmortem PD brains and in PD animal models [4,5,6]. This inflammatory state in glial cells leads to the production of toxic substances, including cytokines such as IL-1β, IL-6, and TNF-α, that further damage neurons, leading to a cycle of inflammatory damage that ultimately worsens the progression of the disease. New evidence in experimental animals indicates that blocking the signaling pathways in glial cells responsible for turning

on neurotoxic genes dramatically decreases damage to dopaminergic neurons. Unfortunately, current therapies do not address this neuroinflammation problem, being focused on ameliorating the symptoms of dopamine loss rather than on the underlying causes of injury to dopaminergic neurons. Targeting the signaling pathways in glial cells responsible for neuroinflammation represents a promising new therapeutic approach designed to preserve remaining neurons in PD patients, thereby extending the window of efficacy of existing symptomatic drugs in order to better maintain quality of life. Given the evidence for neuroinflammation in PD, agents with anti-inflammatory effects have been investigated for their neuroprotective potential [7].

Different studies have suggested that cyclic AMP (cAMP) levels might play an important role in neuroprotection and in the neuroinflammatory response [8,9] thus control of the levels of this nucleotide could trigger the regulation of the pathological neuroinflammatory process and, consequently, to delay the progression of neurodegenerative disorders, such as PD. Intracellular cAMP levels depend on one hand on their synthesis by adenylyl cyclases and, on the other hand, on its degradation by cyclic nucleotide 3′, 5′-phosphodiesterases (PDEs) [10,11]. Hence, PDEs have recently emerged as important drug targets for regulating several diseases [12].

The PDEs comprise a family of 21 members, which have been so far classified into 11 groups, according to their sequence homology, cellular distribution, and sensitivity to different PDE inhibitors [11,12], being some of them expressed on central nervous system [13]. PDE7 is a cAMP-specific PDE, which is insensitive to a PDE4 inhibitor, Rolipram [10,11] and it has been recently demonstrated that can be a target for the control of neuroinflammation [14]. The PDE7 family is composed of two genes, PDE7A and PDE7B. High mRNA concentrations of both PDE7A and PDE7B are expressed in rat brain and in numerous peripheral tissues, although the distribution of these enzymes at the protein levels has not been reported. Within the brain PDE7A mRNA is abundant in the olfactory bulb, hippocampus, and several brain-stem nuclei [15]. The highest concentrations of PDE7B transcripts in the brain are found in the cerebellum, dentate gyrus of the hippocampus and striatum [16,17]. There is very little information regarding the physiological functions regulated by PDE7. It has been shown that PDE7 is involved in pro-inflammatory processes and is necessary for the induction of T-cell proliferation [18]. In addition, specific inhibitors of PDE7 have been recently reported as potential new drugs for the treatment of brain diseases [19]. However, a detailed analysis of the effect of these compounds on normal central nervous system function as well as in pathological conditions have yet to be described.

Several years ago, our research group was the first one in reporting the first PDE7 selective inhibitors [20]. Since then, a lot of efforts have been done to increase potency and selectivity of this kind of compounds, conforming a great variety of diverse chemical compounds with interesting pharmacological profiles [21]. We have recently reported a new and diverse chemical family of PDE7 inhibitors, the quinazolines ones, discovered by using a ligand-based virtual screening [22]. Moreover, the biological profile of these new thioxoquinazolines showed that they are useful compounds to decrease the inflammatory activation in a T-cell line [23].

In the present study, we demonstrate for the first time, that PDE7 inhibition enhances neuroprotection and diminishes neuroinflammation in well-characterized cellular and animal models of PD. In addition, treatment of adult rats with the blood brain barrier permeable PDE7 inhibitor named S14 (Phenyl-2-thioxo-(1H)-quinazolin-4-one, Figure 1) significantly protects dopaminergic neurodegeneration and improves motor function in LPS-lesioned animals. Lastly, we also show that its effects are mediated by the cAMP/PKA signaling pathway. As such, these findings identify PDE7 as a potential therapeutic target for the treatment of Parkinson Disease.

Results

Expression of PDE7

We first analyzed whether PDE7 was expressed throughout the central nervous system of the adult rat. As can be seen in Figure 2A, significant levels of PDE7A and PDE7B were detected in different brain regions including the striatum. In the case of the SNpc, we found, by immunohistochemistry studies, that the levels of PDE7A and PDE7B are low in the basal state. However, they were notably increased after LPS injection (Figure 2B). These results are of interest since these genes have been related to inflammation [18]. Moreover, the increased observed after LPS injury support our data showing an important role for PDE7 inhibitors as neuroprotective agents of dopaminergic neurons. Additionally, both isoforms of PDE7 are expressed in the SH-SY5Y neuroblastoma cell line and in primary rat mesencephalic cultures (Fig. 2C). Besides, double immunocytochemistry studies clearly show that TH positive cells expressed PDE7A and PDE7B.

PDE7 inhibition protects neuronal SH-SY5Y cells from 6-hydroxydopamine (6-OHDA)-induced death

The human dopaminergic neuronal cell line SH-SY5Y possesses many qualities of substantia nigra neurons [24] and is therefore widely used as a model to study the death of dopaminergic neurons. Since S14 has been described as a PDE7 inhibitor, we first analyzed whether this compound could increase cAMP levels on SH-SY5Y cells. To this end, cells were treated for 1 h with S14 and two well-known PDE4 and PDE7 inhibitors, Rolipram and BRL50481, respectively, and cAMP levels were analyzed by ELISA. Figure 3A shows that, as expected, Rolipram and BRL50481, were able to elevate the levels of cAMP in these cultures. Treatment with S14 also resulted in a significant increase in the levels of cAMP. We next analyzed the phosphorylation state

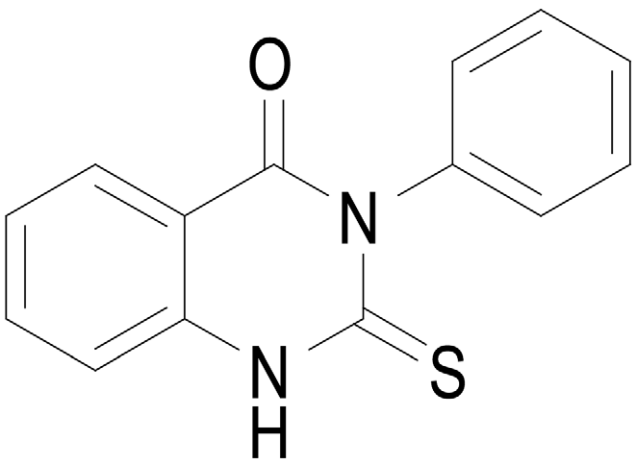

Figure 1. Structure of the PDE7 inhibitor used in the experiments, the quinazoline derivative S14.
doi:10.1371/journal.pone.0017240.g001

A

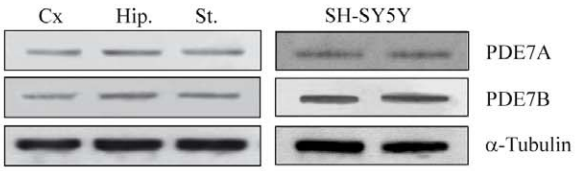
Cx
Hip.
St.
SH-SY5Y
PDE7A
PDE7B
α-Tubulin

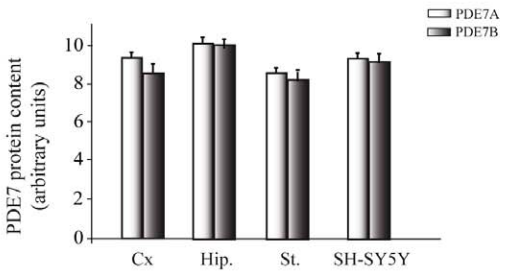
PDE7A
PDE7B
PDE7 protein content (arbitrary units)
10
8
6
4
2
0
Cx
Hip.
St.
SH-SY5Y

B

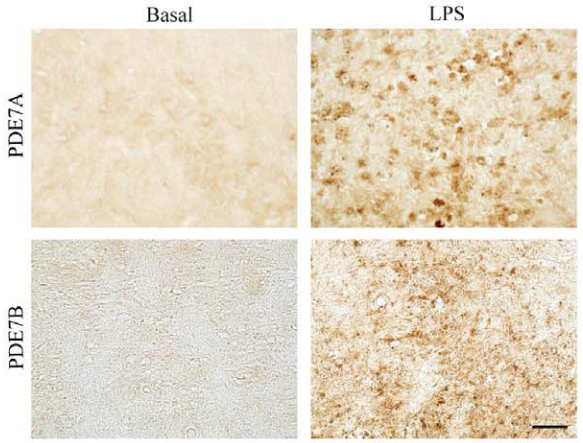
Basal
LPS
PDE7A
PDE7B

C

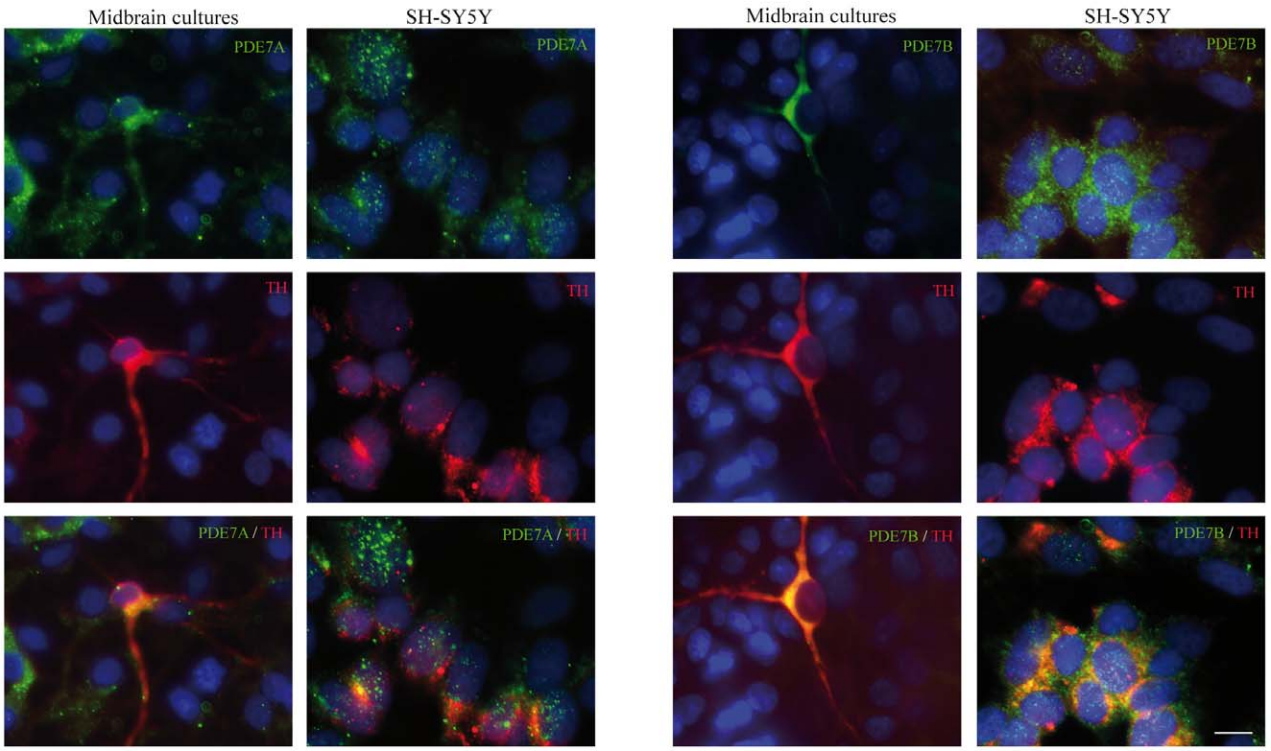
Midbrain cultures
SH-SY5Y
Midbrain cultures
SH-SY5Y
PDE7A
PDE7A
PDE7B
PDE7B
TH
TH
TH
TH
PDE7A / TH
PDE7A / TH
PDE7B / TH
PDE7B / TH

Figure 2. Western blot and immunocytochemical analysis of PDE7A and PDE7B. (**A**) Representative Western blot and quantification analysis showing expression levels of PDE7A and PDE7B in different brain regions and in the dopaminergic cell line SH-SY5Y. Cx, cerebral cortex; Hip, hippocampus; St, striatum. (**B**) Inmunohistochemical analysis of PDE7A and PDE7B expression in the *substantia nigra pars compacta* (SNpc) of adult rats. Figure also shows the expression of both isoenzymes 72 h after lipopolysaccharide (LPS, 10 μg) injection in this area. Scale bar, 25 μm. (**C**) Immunofluorescence analysis of PDE7A and PDE7B expression (green) and tyrosine hydroxylase (TH, red) in the dopaminergic cell line SH-SY5Y and in primary mesencephalic cultures. Representative results of at least three independent experiments are shown. Scale bar, 10 μm. Nuclei were counterstained with DAPI (blue).
doi:10.1371/journal.pone.0017240.g002

of the *cAMP response element-binding protein* (CREB), a known target of the cAMP/PKA signaling pathway. As shown in Figure 3B, treatment of SH-SY5Y with Rolipram, BRL50481 or S14, together with 6-OHDA, resulted in an increase of phosphorylated CREB levels.

We then examined the effect of S14 on the cell death induced by 6-OHDA exposure. As shown in Figure 3C, 6-OHDA treatment resulted in a loss of viability, as assessed by a decline in (3-(4,5-dimethylthiazol-2-yl)-2,5-diphenyl tetrazolium bromide) (MTT) and a significant elevation in lactate dehydrogenase (LDH) level (Fig. 3C), as compared with control untreated cells. Incubation with the PDE7 inhibitor quinazoline compound S14 afforded significant protection against 6-OHDA-induced cell death lowering elevated LDH levels by as much as 50% and reversing the decline in MTT by 22%. This neuroprotective effect was mimicked by BRL50481 and by Rolipram. S14 has an IC50 of 5.5 μM on PDE7A, five times more potent than its inhibition on PDE4D (IC50 = 22 μM) [22]. Quinazoline derivative S14 does not inhibit PDE3 (3% of inhibition at 10 μM) therefore preventing the compound from possible cardio toxic effects. Hence, the results obtained here suggest that S14 protects the human dopaminergic neuronal cell line SH-SY5Y from cell death through an inhibition of the PDE7 enzyme.

Toxicity induced by 6-OHDA was also accompanied by an increase in nitrite production (Fig. 3C, lower panel), and its concentration was brought toward normality after S14 treatment, indicating that this drug blocks 6-OHDA-induced oxidative stress, which leads to free radical generation.

Activation of PKA by cAMP is required for S14-induced neuroprotection of SH-SY5Y

The most common intracellular target of cAMP is PKA. PKA activation is responsible for many of the actions attributed to cAMP [25]. Nonetheless there are other effects of this nucleotide, which are not mediated by PKA [26,27]. We therefore investigated if PKA activation is required for the neuroprotective actions of S14. To this end, SH-SY5Y exposed to 6-OHDA and pretreated or not with Rolipram, BRL50481 or S14, were treated with the PKA inhibitor H89 or the specific membrane-permeable inhibitor of PKA activation adenosine 3′,5′-cyclic monophosphorothioate Rp-isomer (Rp-cAMP). As shown in Figure 3C, both compounds prevented the increase in cell viability and the decrease in nitrite liberation elicited by the three PDE inhibitors, suggesting that the cAMP/PKA pathway mediates their effects on SH-SY5Y cells.

Lastly, apoptosis was determined by measuring the levels of active caspase 3 and Annexin V analysis (Fig. 3D). Our results indicate that 27% of the SH-SY5Y cell population was positive for caspase 3 staining within 16 h after treatment with 6-OHDA and that this effect was almost completely reversed by the treatment with the S14 compound. Annexin V-FITC analysis also showed a significant decrease in the number of apoptotic cells in those cultures treated with S14 (Fig. 3D). These results suggest that S14 is rescuing SH-SY5Y cells from 6-OHDA-induced apoptosis.

PDE7 inhibition protects cultured primary mesencephalic cells from lipopolysaccharide- and 6-OHDA-induced cell death

We next examined whether PDE7 inhibition could also have neuroprotective effects on primary ventral mesencephalic cultures. These cultures are known to be vulnerable to LPS treatment, resulting in a loss of neuronal viability [28]. The viability of mesencephalic cell cultures, known to be rich in dopaminergic neurons, was determined by quantifying tyrosine hydroxylase (TH) immunoreactivity after exposure to LPS. Treatment with this endotoxin decreased the number of TH^+ cells by 42% (Fig. 4A). S14 addition significantly preserved TH^+ cells from LPS toxicity. No significant difference in the number of DAPI-positive nuclei was found among the treated cultures (data not shown). We also analyzed whether S14 affected the LPS-induced expression of TNF-α and COX-2, two well known proinflammatory agents. As shown in Figure 4A, incubation of primary mesencephalic cultures with S14 completely abrogated the induction of TNF-α and COX-2 expression after LPS treatment, suggesting that the protection observed by S14 could be exerted, at least in part, through an effect upon inflammatory reaction of microglial cells present in the cultures. These results were further corroborated by measuring nitrite liberation to the culture medium (Fig. 4B). LPS treatment resulted in an increase in the concentration of nitrites in the cultures medium, which was significantly prevented by S14. In fact the levels of nitrites in the S14-treated cultures were even lower that those detected in control non-treated cells.

The neuroprotective effects of S14 were also tested after exposure to the dopaminergic toxin 6-OHDA. As expected, 6-OHDA significantly decreased TH-positive cells (80%) (Fig. 4C). Addition of S14 to the cultures conferred a robust protection against 6-OHDA-mediated cell loss.

Neuroprotective role of PDE7 inhibition in an *in vivo* model of PD

Given the in vitro anti-inflammatory and neuroprotective effects described above, we then assessed the efficacy of S14 in a well-characterized rodent model of PD. LPS injection into the SNpc of rodents induces dopaminergic cell loss and microglial activation [29,30]. To this end, adult rats were injected unilaterally in the SNpc with vehicle, LPS, or LPS plus S14 and were killed 72 h after injection. Histological analysis were used to evaluate the extend of dopaminergic cell loss and microglial activation in the SNpc of the different groups of animals. A significant preservation of dopaminergic neurons was found in S14-injected rats compared with abundant dopaminergic neuron damage after injection with LPS (Fig. 5). Quantitative studies showed a decrease of 85%, compared with the vehicle-injected rats, in the number of dopaminergic neurons in the SNpc after LPS injection. In contrast, in the S14-treated group, only a moderate decrease (25%) in dopaminergic cell number was observed 3 days after LPS injection. These results extend the observations made in vitro and suggest that treatment of LPS-injected animals with S14 results in an almost complete prevention of dopaminergic injury. In addition, we also analyzed the effect of BRL50481, a well

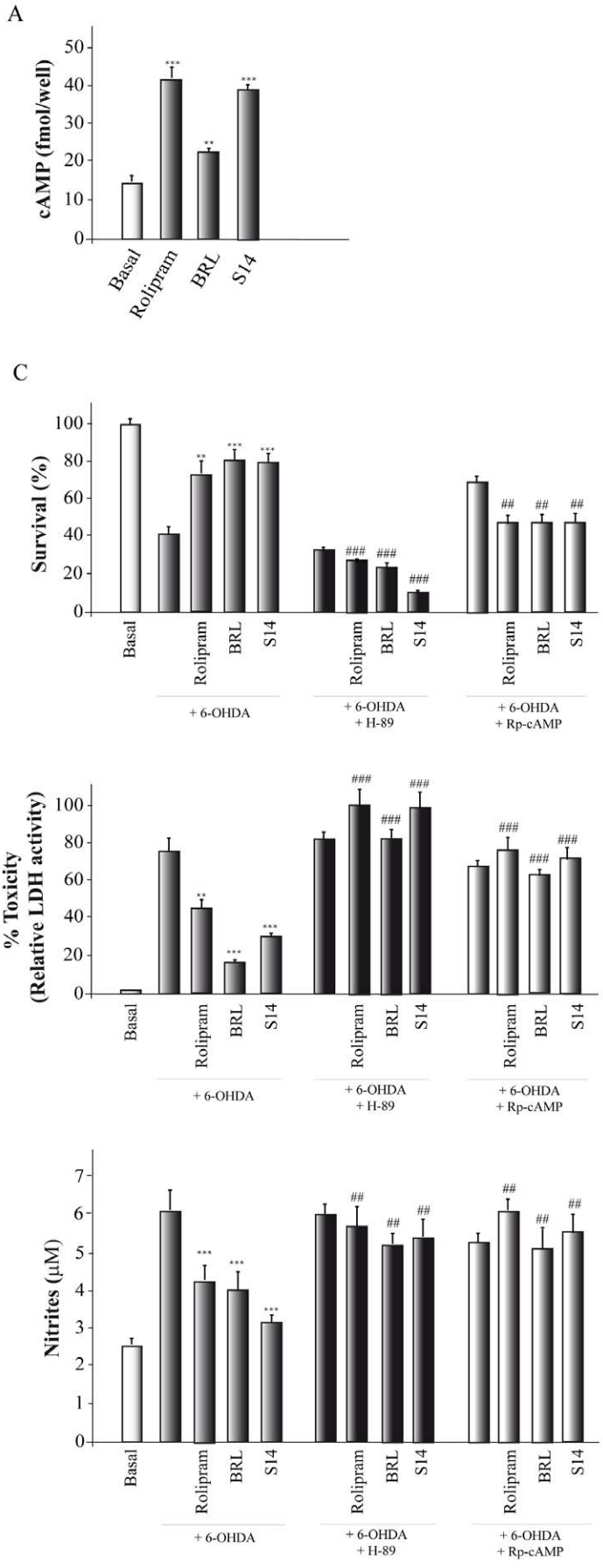
A
cAMP (fmol/well)
Basal
Rolipram
BRL
S14
B
P-CREB
CREB
Basal
6-OHDA
6-OHDA + Rolipram
6-OHDA + BRL
6-OHDA + S14
P-CREB protein content (% of basal cultures)
Rol
6-OHDA
C
Survival (%)
% Toxicity (Relative LDH activity)
Nitrites (μM)
+ 6-OHDA
+ 6-OHDA + H-89
+ 6-OHDA + Rp-cAMP
D
Active Caspase-3
Annexin V
6-OHDA + S14
% Active Caspase -3
% Annexin V

Figure 3. Effect of S14 on 6-OHDA-induced SH-SY5Y cell death. Cells were treated with Rolipram (30 μM), BRL50481 (BRL, 30 μM), or S14 (10 μM) as indicated in Methods. (**A**) Intracellular levels of cAMP in cells treated during 1 hr with the indicated compounds. $^{**}p<0.01$; $^{***}p<0.001$ *versus* non-treated (basal) cells. (**B**) Representative Western blot showing phosphorylation of CREB after incubation of cells with 6-OHDA (35 μM) for 16 h in the presence or absence of the indicated compounds. A specific anti-phospho-CREB antibody was used. The use of an antiserum that does not discriminate between CREB and phospho-CREB (bottom panel) indicates that the total levels of CREB are not affected by the treatments. Quantification analysis are shown. $^{***}p<0.001$ *versus* non-treated (basal) cells; $^{\#}p<0.05$, $^{\#\#}p<0.01$, $^{\#\#\#}p<0.001$ *versus* 6-OHDA-treated cells. Rol, Rolipram (**C**) Cell viability, cytotoxicity and nitrite production were measured as indicated in Methods. Some cultures were pretreated with the protein kinase A inhibitor H89 or the cAMP antagonist Rp-cAMP. Values represent the mean ± SD of six replications in three different experiments. $^{**}p<0.01$; $^{***}p<0.001$, *versus* 6-OHDA-treated cells; $^{\#\#}p<0.01$, $^{\#\#\#}p<0.001$ *versus* the values obtained in the absence of H89 or Rp-cAMP (**D**) Apoptotic levels were determined by active caspase 3 (green) and Annexin V-FITC (green) immunodetection. Representative images of at least three independent experiments are shown. Scale bar, 10 μm. Nuclei were counterstained with DAPI (blue). Quantification of active caspase 3 and Annexin V-FITC-positive cells is shown. $^{***}p<0.001$ *versus* 6-OHDA-treated cells.
doi:10.1371/journal.pone.0017240.g003

characterized PDE7 inhibitor, on this same model of PD. Our results showed that BRL50481 has similar neuroprotective and anti-inflammatory effects as S14. Only a 20% decrease in the number of dopaminergic neurons (Figure 5B) was observed in rats injected with this compound, compared to 85% found in LPS-treated animals.

One of the events that take place in the SNpc after LPS injury is the activation of microglial cells, which is in part responsible for the dopaminergic cell degeneration. Microglial cells (identified as OX-42-positive cells) were very scarce in the contralateral part of LPS-injected animals and in the SNpc of vehicle-injected animals (Figure 6A). Seventy-two hours after LPS injection, a high OX-42 immunoreactive signal was clearly observed in the SNpc. This strong microgliosis was completely absent in the animals treated with the quinazoline PDE7 inhibitor S14. Also, BRL50481 treatment of LPS-injured rats completely abrogated the microgliosis observed in the LPS-treated group (Figure 6A). Altogether, these results reinforce our hypothesis that PDE7 could be an important target for neuroprotection of dopaminergic neurons.

Finally we analyzed the effects of S14 treatment on rotational behavior by assessing the behavioral changes in hemi-parkinsonian rats. To this end, three weeks following LPS lesion rats were injected with apomorphine, which is known to induce contralateral rotational behavior in denervated animals. Figure 6B shows that the LPS-treated rats exhibited 7 contralateral turns per minute following an administration of apomorphine. Rats lesioned with LPS and treated with S14 showed a significant improvement (only 1 turn per minute) after apomorphine. Vehicle-treated animals showed no contralateral rotational behavior. Immunohistochemistry analysis also showed that, three weeks after LPS administration, dopaminergic cell death was significantly attenuated in the group treated with S14 (data not shown).

Discussion

In this study, we have demonstrated, for the first time, that inhibition of PDE7 induces neuroprotection of human dopaminergic neuronal cells SH-SY5Y and of primary mesencephalic cultures and attenuates the production of nitrites and proinflammatory agents. Our data also show that inhibition of PDE7 results in an inhibition of microglial activation and has neuroprotective effects on the nigrostriatal system in an *in vivo* model of PD. In addition, the neuroprotective effect of PDE7 inhibition appears to be mediated by the cAMP/PKA signaling pathway. These results suggest that inhibition of PDE7 can represent a new therapeutic approach for the treatment of PD and other neurodegenerative disorders in which inflammation processes are involved. Thus, PDE7 inhibitors may represent a new generation of valuable drugs.

We initially analyzed the neuroprotective and anti-inflammatory effects of the PDE7 inhibitor S14 in the human dopaminergic cell line SH-SY5Y and in primary mesencephalic cultures. Human neuroblastoma cells exposed to 6-OHDA are used as *in vitro* model for PD, due to similar cellular processes that occur in the degenerating dopaminergic neurons [31]. We show that S14 significantly attenuates 6-OHDA-induced neuronal cell death and nitrite liberation in the SH-SY5Y neuronal cell line and in mesencephalic cultures. These effects are accompanied by an elevation of intracellular cAMP levels, indicating that also in dopaminergic neurons the activity of PDE7 is important in governing cellular cAMP concentration. The mechanism of action of this compound seems to be the inhibition of the PDE7 enzyme, the subsequent activation of the cAMP/PKA signaling pathway and the activation of the transcription factor cAMP response element-binding protein (CREB) by phosphorylation. It is known that cAMP can activate at least three different signaling pathways within cells. The first one to be characterized and the most extensively studied rely on the activation of PKA, which then phosphorylates different substrates including transcription factors such as CREB. However, cAMP can also stimulate the guanine nucleotide exchange protein Epac, which in turn activates the GTPase Rap-1 [32]. Other pathway identified as activated by cAMP includes another guanine nucleotide exchange protein called CNrasGEF, which directly activates Ras [33]. Yet, our results showing a reversion of the anti-inflammatory and neuroprotective effects of S14 by both Rp-cAMP and H89 (a specific inhibitor of PKA activation), support the notion that S14 specifically activates cAMP-dependent PKA activation.

These neuroprotective actions of PDE7 inhibition are in accordance with previous findings showing that cAMP signaling pathway might inhibit cell death in various neurodegenerative disorders. Previous work has demonstrated a clear involvement of PKA in neuroprotection [34,35]. Absence of CREB in developing brain results in generalized cell death, whereas postnatal disruption of this transcription factor triggers progressive neurodegeneration [36]. Also, it has been shown that CREB is necessary for neuronal survival and axonal growth in different neuronal populations [9]. Of note, inhibition of cAMP signaling pathway has been suggested to contribute to Hungtinton disease pathology [37,38,39]. Our results add new and important data establishing that elevation of intracellular cAMP levels through inhibition of PDE7 promotes protection of dopaminergic cells and has potent anti-inflammatory effects.

To evaluate the translational relevance of the aforementioned cellular effects, the anti-inflammatory and neuroprotective actions of direct administration of S14 into the brain were assessed in a classical rodent model of PD. Research in the last years has unveiled an important role for neuroinflammation in the degeneration of the nigrostriatal dopaminergic pathway that constitutes the pathological basis of PD. Neuroinflammation is characterized by the activation of glial cells that release various cytotoxic substances, including pro-inflammatory cytokines, reac-

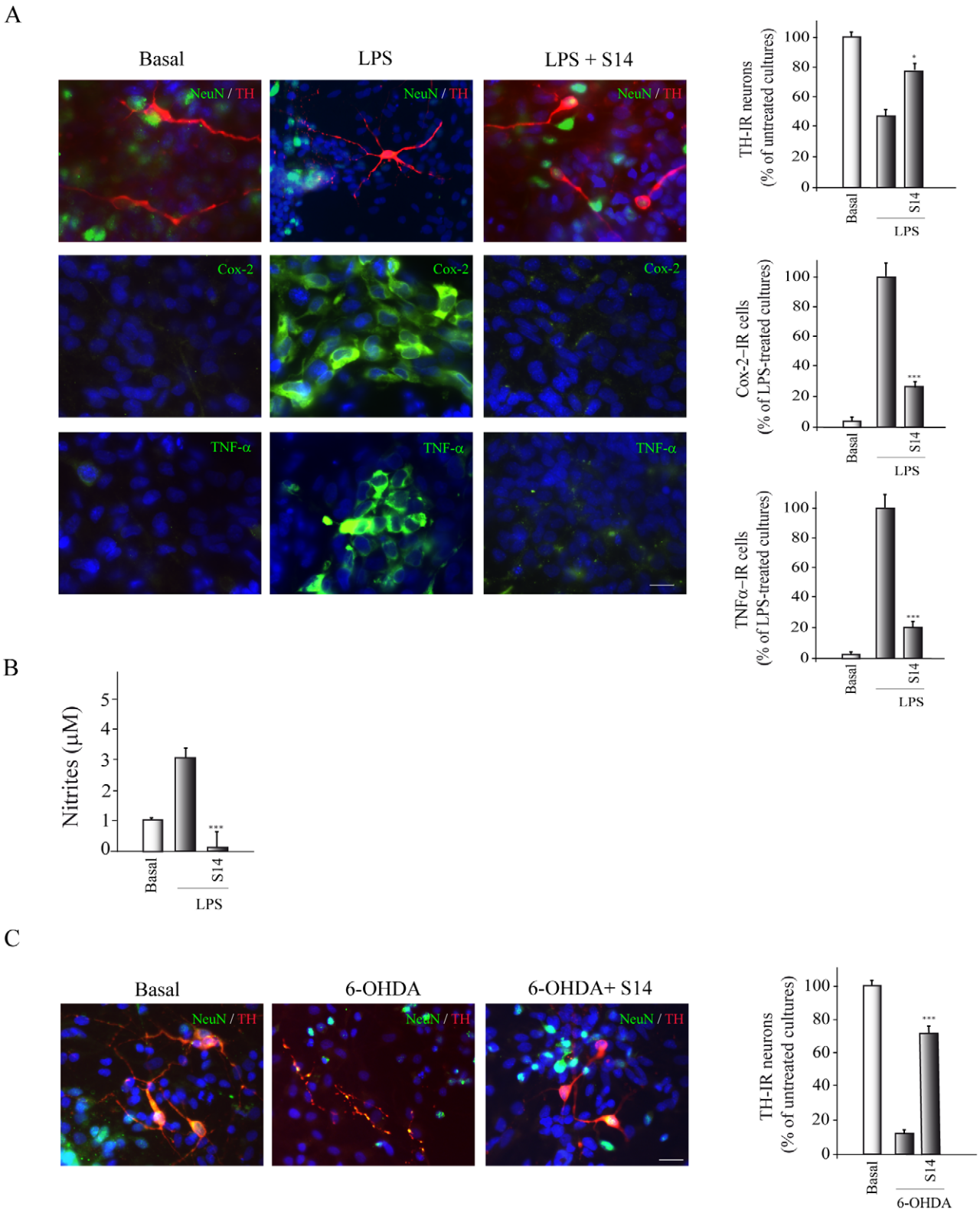

Figure 4. Effect of S14 on cell death and inflammation processes in mesencephalic cell cultures induced by incubation with LPS or 6-OHDA. (**A**) Rat primary mesencephalic cultures were treated with LPS (1 μg/ml) in the absence or presence of S14 (10 μM) and the expression of TH, COX-2 and TNF-α was evaluated by immunofluorescence analysis using specific antibodies, as described in Methods. Representative results of three independent experiments are shown. Scale bars, 20 μm. Nuclei were counterstained with DAPI. Quantification of the numbers of immunoreactive cells was performed as described in Methods. Values represent the mean from three different experiments and twenty independent fields (≥50 cells/field) per culture. $^{*}p<0.05$; $^{***}p<0.001$ *versus* LPS-treated cells. (**B**) Nitrite production was evaluated by the Griess reaction. Values represent the mean ± SD of six replications in three different experiments. $^{***}p<0.001$, *versus* LPS-treated cells (**C**) Rat primary mesencephalic

cultures were treated with 6-OHDA in the absence or presence of S14 and the expression of TH^+ cells was evaluated by immunofluorescence analysis using specific antibodies, as described in Methods. Representative results of three independent experiments are shown. Scale bars, 20 μm. Nuclei were counterstained with DAPI. Quantification of the numbers of immunoreactive cells was performed as described in Methods. Values represent the mean ± SD from three different experiments and twenty independent fields (≥50 cells/field) per culture. $^{***}p<0.001$ versus 6-OHDA-treated cells.
doi:10.1371/journal.pone.0017240.g004

tive oxygen species, and nitric oxide and sustained reactivity of microglia is implicated in the pathology of many neurodegenerative disorders [40]. Inhibition of this process could then protect against neurodegeneration and expansion of brain injury. This view is further supported by epidemiologic data showing that long-term treatment with non-steroidal anti-inflammatory drugs may protect against Alzheimer disease and Parkinson disease [41,42,43]. Administration of the bacterial endotoxin LPS in rats induces a consistent glial activation and a subsequent dopaminergic cell loss that parallels many aspects of PD [29,44,45]. Here, we show that S14 has potent anti-inflammatory effects *in vivo* after LPS injection in the SNpc. Our results indicate that this compound significantly reduces the accumulation of reactive microglia in the striatum of lesioned-rats. The underlying mechanism of this anti-inflammatory effect of S14 may involve the suppression of certain cytokines, e.g. TNF-α. Indeed our *in vitro* results show that treatment of primary mesencephalic cultures with S14 significantly decreased TNF-α and COX-2 levels, two potent pro-inflammatory agents.

Besides this potent anti-inflammatory action of S14, the administration of this compound also causes a significant preservation of dopaminergic cells loss in the SNpc. PD is characterized by selective degeneration of dopaminergic neurons in the SN. Rats receiving LPS presented classic reductions in the number of TH-immunoreactive cells, a marker of dopaminergic cells in the SN. These animals also demonstrated motor function deficits. A unilateral lesion in nigrostriatal dopaminergic pathway produces an imbalance of dopamine between the lesioned and unlesioned striatum leading to circle toward the side of the lesion [46,47]. Treatment of the animals with a dopamine agonist such as apomorphine leads to contralateral rotational behavior in denervated animals [48]. This rotational behavior is consistent with damage to dopaminergic neurons in the SN and the decrease of dopamine in the striatum [49]. Behavioral assessment detected significant differences between the LPS and control animals at 3 weeks after LPS administration. S14 administration provided complete protection, as assessed by TH-positive cell number and motor behavioral. We found that apomorphine-induced turning behavior in the LPS-treated group was significantly inhibited by S14 treatment. Overall, the LPS rats treated with S14 were indistinguishable from controls.

In conclusion, here we have shown that inhibition of PDE7 hinders dopaminergic cell death and glial activation in an animal model of PD. The mechanisms that underlie these effects appear to be an elevation of intracellular cAMP, which acts via the PKA-CREB pathway. These results show for the first time that inhibition of the PDE7 enzyme leads to dopaminergic neuronal protection and therefore its inhibitors may exert useful therapeutic actions in patients with PD, a hypothesis that is amenable to clinical testing.

Materials and Methods

Animal experiments

All procedures with animals were specifically approved by the 'Ethics Committee for Animal Experimentation' of the Instituto de Investigaciones Biomedicas (CSIC-UAM), licence number SAF 2010/16365, and carried out in accordance with the protocols issued which followed National (normative 1201/2005) and International recommendations (normative 86/609 from the European Communities Council). Adequate measures were taken to minimize pain or discomfort of animals.

LPS injection *in vivo*

Adult male Wistar rats (8–12 weeks old) were used in this study. The animals, divided into four groups, with at least six rats in each group, were properly anaesthetized and placed in a stereotaxic apparatus (Kopf Instruments, CA). LPS (10 μg in 2.5 μl PBS) alone or in combination with S14 (20 nmol) or with BRL50481 (60 nmol) were injected into the right side of the SNpc (coordinates from Bregma: posterior - 4.8 mm; lateral + 2.0 mm; ventral: +8.2 mm, according to the atlas of Paxinos and Watson [50]). The dose of LPS was chosen based in previous published data [29,30,51]. The amount of S14 injected was calculated taking into account the distribution volume of this cerebral area and the effective dose observed in the *in vitro* experiments. Control animals of the same age were injected with PBS. Rats were then housed individually to recover and sacrificed 72 h after lesioning.

Histology and Immunohistochemistry

Seventy-two hours after lesioning, the animals were anaesthetized and perfused transcardially with a 4% paraformaldehyde solution. The brains were removed, postfixed in the same solution at 4°C overnight, cryoprotected, frozen, and 30 μm coronal sections were obtained in a cryostat. Free-floating sections were processed for cresyl violet (Nissl stain) or immunohistochemistry using the diaminobenzidine method as previously described [52]. To detect PDE7 in SNpc, rabbit anti-PDE7A and goat anti-PDE7B antibodies (Santa Cruz Biotech) were used. For immunodetection of activated glia and dopaminergic neurons, a mouse anti-CD11b antibody (Serotec, Germany) and a rabbit anti-tyrosine hydroxylase (Chemicon/Millipore, USA) antibody, respectively, were used. After being dehydrated, cleared, and mounted with DePeX (Serva, Heidelberg, Germany), samples were examined with a Zeiss (Oberkochen, Germany) Axiophot microscope, equipped with an Olympus DP-50 digital camera, and a Leica (Nussloch, Germany) MZ6 modular stereomicroscope. Four animals from each experimental group were analyzed. Neuronal integrity and specifically dopaminergic cell death was assessed by counting the percentage of Nissl-stained and TH^+ cells, respectively, in the SNpc in four well-defined high magnification (x400) fields per animal, using a computer-assisted image analySIS software (Soft Imaging System Corp). Microgliosis was quantified similarly.

Behavioural testing. Apomorphine-induced rotational behavioural test was performed 3 weeks following LPS lesioning of the SNpc. Rats were given a subcutaneous injection of apomorphine (0.5 mg/kg in saline), then placed individually in plastic beakers and videotaped for 30 minutes. Analysis of completed (360°) rotations was made offline and expressed as number of turns per minute. Rats showing more than six turns per minute were considered as properly lesioned. Three different experiments with al least 12 animals/experimental group were performed.

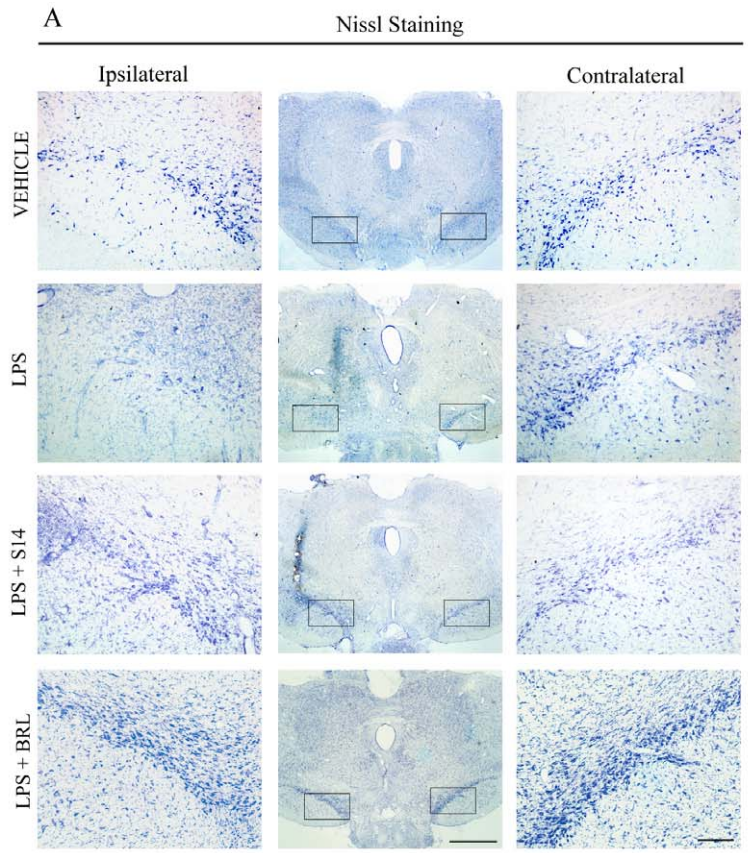
A
Nissl Staining
Ipsilateral
Contralateral
VEHICLE
LPS
LPS + S14
LPS + BRL

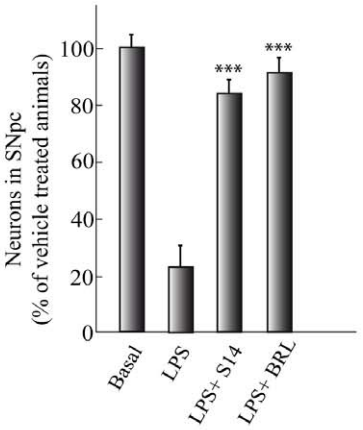
Neurons in SNpc
(% of vehicle treated animals)
100
80
60
40
20
0
***
***
Basal
LPS
LPS+ S14
LPS+ BRL

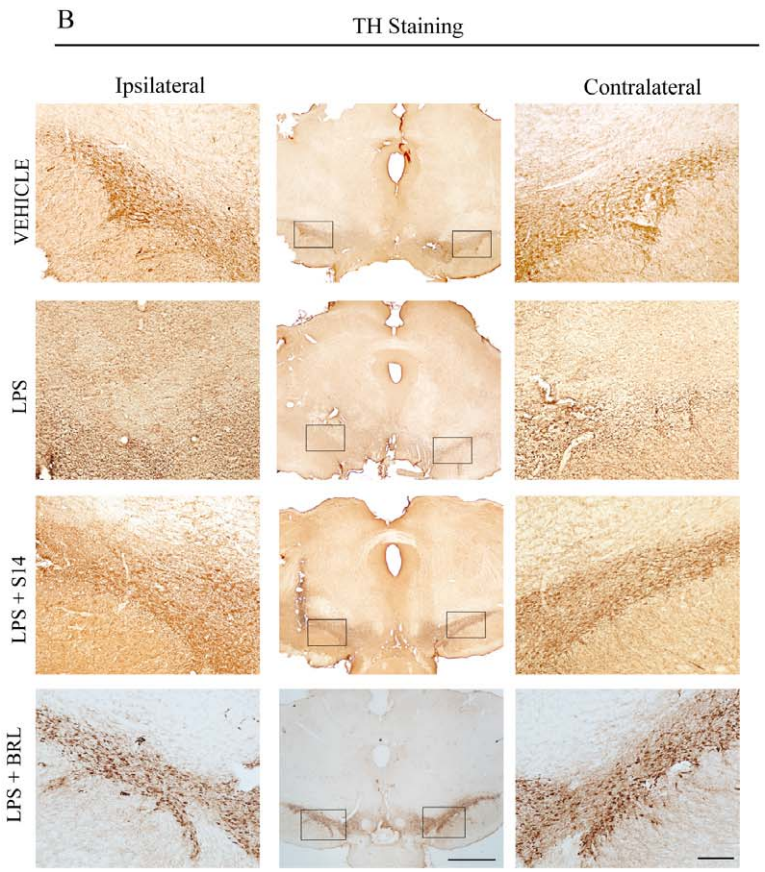
B
TH Staining
Ipsilateral
Contralateral
VEHICLE
LPS
LPS + S14
LPS + BRL

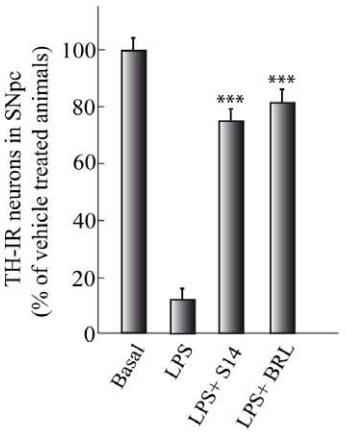
TH-IR neurons in SNpc
(% of vehicle treated animals)
100
80
60
40
20
0
***
***
Basal
LPS
LPS+ S14
LPS+ BRL

Figure 5. Effect of S14 on dopaminergic cell death *in vivo*. LPS (10 μg) or vehicle was injected unilaterally into the adult *substantia nigra pars compacta* (SNpc) of adult rats. A group of animals also received S14 (20 nmol) or BRL50481 (BRL, 60 nmol) together with LPS. After 72 h the brains were removed and tissue sections were processed for (**A**) Nissl staining to label neurons or (**B**) tyrosine hydroxylase (TH) immunoreactivity to label dopaminergic neurons. Scale bars, 500 μm. Insets scale bars, 100 μm. Quantification of the numbers of neurons in A or TH-immunoreactive (IR) cells in B is shown. Values represent the mean ± SD, expressed as a percentage of vehicle-treated animals, from three different experiments, four animals/experiment/experimental group, and five independent sections per animal. $^{***}p<0.001$ versus LPS-treated animals.
doi:10.1371/journal.pone.0017240.g005

Mesencephalic cell cultures

Cultures were derived from the ventral mesencephalon of rat embryos at embryonic day 14. Briefly, rats were killed by cervical dislocation and embryonic sacs dissected and collected in ice-cold HBSS medium (Ca^{2+} and Mg^{2+} free). Ventral mesencephalon was isolated, gently minced and triturated with a micropipette in HBSS medium. Then the supernatant was collected, and centrifuged at 1200 x*g*/5 min. The pellet was resuspended in culture media (MEM supplemented with 10% FBS, 10% HS, glucose 1 g/l glutamine 2 mM, sodium pyruvate 1 mM, non-essential aminoacids 100 μM, penicillin 50 U/ml and streptomycin 50 μg/ml), and cells seeded onto 24-well plates (5×10^5 cells/well) or 96-well plates (1×10^5 cells/well). After 1 week in culture, cells were treated with LPS (1 μg/ml) [53,54,55] or 6-OHDA (35 μM, Sigma), alone or in combination with S14 (10 μM). The effective dose of S14 was determined based on previous studies on EC50 [22]. After 24 h, cultures were processed for immunocytochemistry and nitrite determination.

SH-SY5Y cell culture

The human neuroblastoma SH-SY5Y cell line was obtained from Sigma-Aldrich and propagated in F12 medium/EMEM containing glutamine (2 mM), 1% of non-essential amino acids and 15% of fetal bovine serum (FBS), under humidified 5% CO_2 and 95% air. On attaining semiconfluence, cells were treated or not with 6-OHDA (35 μM, Sigma) for 24 h. Some cultures were pretreated for 1 h with S14 (10 μM), Rolipram (30 μM, Tocris Bioscience) or BRL-50481 (30 μM, Tocris Bioscience). To analyze the role of cAMP, some plates were also preincubated with the PKA inhibitor H-89 (20 μM, BIOMOL Research Laboratories) or the cAMP antagonist Rp-cAMP (100 μM, BIOMOL Research Laboratories) for 24 h before the addition of the different compounds. At different times after treatments, cells were processed for western blot, cell viability assay, LDH measurement, nitrites release, and immunocytochemical analysis.

Cell viability assay

Cell viability was measured using the MTT assay (Roche Diagnostic, GmbH), based on the ability of viable cells to reduce yellow MTT to blue formazan. Briefly, cells were cultured in 96-well plates and treated with the indicated compounds for 16 h, then cells were incubated with MTT (0.5 mg/ml, 4 h) and subsequently solubilized in 10% SDS/0.01 M HCl for 12 h in the dark. The extent of reduction of MTT was quantified by absorbance measurement at 595 nm according to the manufacturer's protocol.

LDH release assay

Cytotoxicity was assessed by measuring the levels of lactate dehydrogenase (LDH) released into the culture medium 16 h after the different treatments. LDH activity was measured using a Cytotoxicity Detection kit (Roche Molecular Biochemicals, Indianapolis, IN, USA) and quantified by measuring absorbance at 490 nm.

Nitrites measurement

Accumulation of nitrites in media was assayed by the standard Griess reaction. After stimulation of cells with the different treatments for 16 hours, supernatants were collected and mixed with an equal volume of Griess reagent (Sigma- Aldrich). Samples were then incubated at room temperature for 15 minutes and absorbance read using a plate reader at 492/540 nm.

cAMP assay

Quantification of cAMP was carried out using the EIA (enzyme immunoassay) kit from GE Healthcare. Briefly, SH-SY5Y cells were seeded at 3×10^4/well in 96-well dishes and incubated overnight before the assay. After 1 h incubation with S14, Rolipram or BRL50481, cAMP intracellular levels were determined following the manufacture's instructions.

Immunoblot analysis

Proteins were isolated from brain tissue or cell cultures by standard methods. Some SH-SY5Y cultures were pre-treated with Rolipram (30 μM), BRL50481 (BRL, 30 μM), or S14 (10 μM) for 1 h before 6-OHDA (35 μM) addition and kept in these conditions for 16 h. A total amount of 30 μg of protein was loaded on a 10% SDS-PAGE gel. After electrophoresis, proteins were transferred to nitrocellulose membranes (Protran, Whatman, Dassel, Germany) and blots were probed with the indicated primary antibodies, as previously described [56]. The antibodies used were the following: rabbit anti-PDE7A (1:1000, Santa Cruz Biotech., USA), goat anti-PDE7B (1:1000; Santa Cruz Biotech., USA), mouse monoclonal anti-α-tubulin (1:5000; Sigma), rabbit anti-p-CREB (1:1000; Cell Signaling) and rabbit anti-CREB (1:1000; Cell Signaling). All incubations with primary antibodies were carried out overnight, with gently shaking at 4°C. Secondary peroxidase-conjugated donkey anti-rabbit and rabbit anti-mouse antibodies were from Amersham Biosciences (GE Healthcare, Buckinghamshire, England) and Jackson Immunoresearch, respectively. Secondary antibodies incubations were done at room temperature for 1 hour. Values in figures are the average of the quantification of at least three independent experiments corresponding to three different samples.

Immunocytochemistry

At the end of the treatment period, SH-SY5Y or primary mesencephalic cultures, grown on glass cover-slips in 24-well cell culture plates, were washed with PBS and fixed for 30 min with 4% paraformaldehyde at 25°C and permeabilized with 0.1% Triton X-100 for 30 min at 37°C. After 1 h incubation with the corresponding primary antibody, cells were washed with PBS and incubated with an Alexa-labeled secondary antibody (Invitrogen, San Diego, CA) for 45 min at 37°C. Images were acquired using a Radiance 2100 confocal microscope (Bio-Rad, Hercules, CA), with a 350 nm diode laser to excite DAPI (4,6,diamidino-2-phenylindole) a 488-Argon laser to excite Alexa 488 and a 647 laser to excite Alexa 647. Confocal microscope settings were adjusted to produce the optimum signal-to-noise ratio. To compare fluorescence signals from different preparations, settings were fixed for all samples within the same analysis. The following antibodies were used: rabbit anti-PDE7A (Santa Cruz Biotech), goat anti-PDE7B (Santa Cruz Biotech), goat anti-Cox-2 (Santa Cruz Biotech), goat anti-TNFα (Santa Cruz Biotech), rabbit anti-

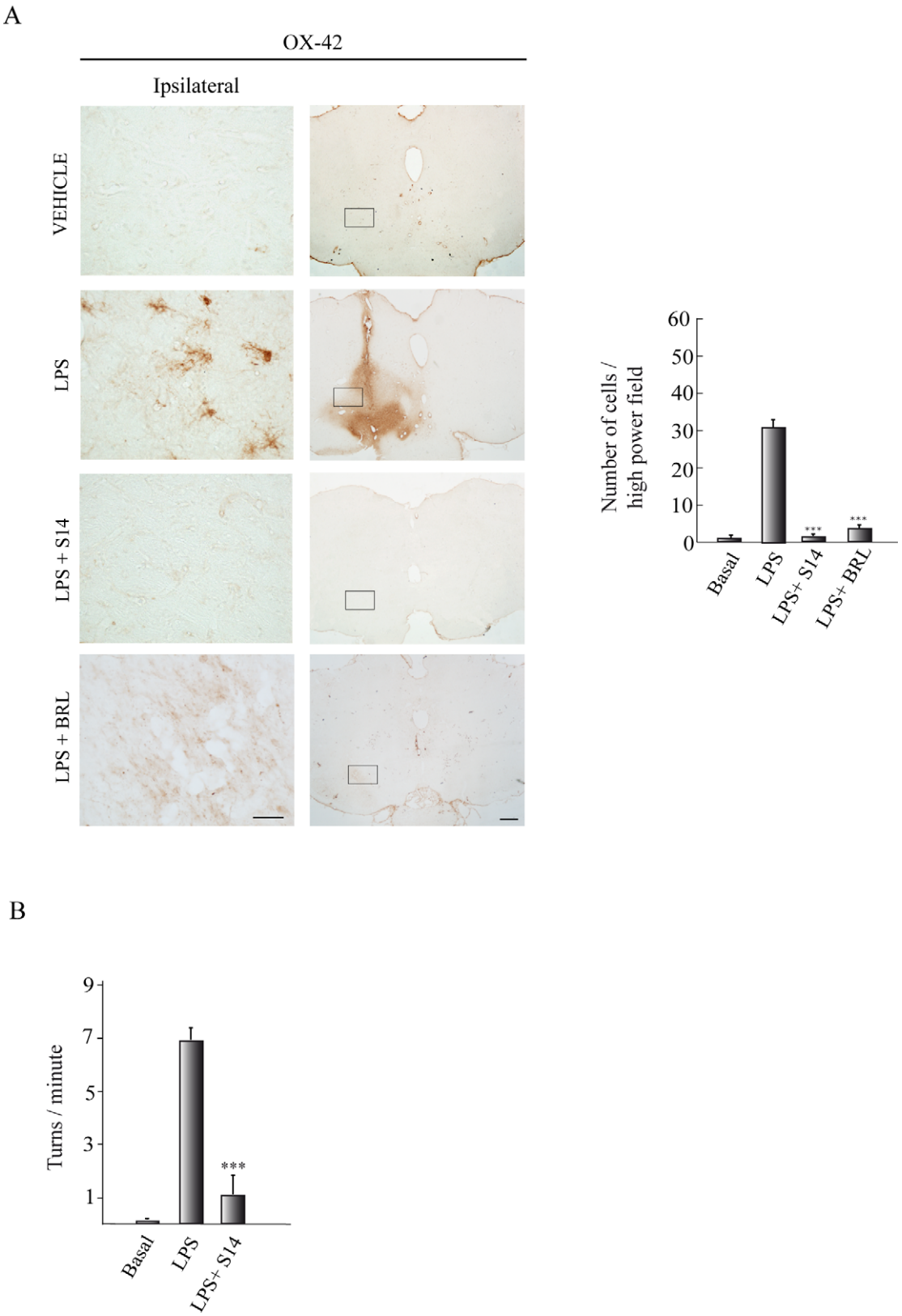

Figure 6. Effect of S14 on *in vivo* inflammation and rotational behavior. Lipopolysaccharide (LPS, 10 μg) or vehicle was injected unilaterally into the adult *substantia nigra pars compacta* (SNpc) of adult rats. A group of animals also received S14 (20 nmol) or BRL50481 (BRL, 60 nmol) together with LPS. (**A**) After 72 h the brains were removed and tissue sections were processed for CD11b (OX-42) immunoreactivity lo label activated microglia. Scale bars, 500 μm. Insets scale bars, 100 μm. Quantification of the reactive cells is expressed as the mean ± SD, from three different experiments, four animals/experiment/experimental group, and five independent sections per animal. $^{***}p<0.001$ versus LPS-treated animals. (**B**) Behavioral analysis. Three weeks after treatment apomorphine-induced rotations were analyzed in control, LPS-injected, and LPS+S14-injected rats. Values represent the means ± SD from three different experiments. $^{***}p<0.001$, *versus* LPS-injected animals.
doi:10.1371/journal.pone.0017240.g006

tyrosine hydroxylase (Chemicon/Millipore), mouse anti-tyrosine hydroxilase (Sigma) and mouse anti-NeuN (Chemicon). For the quantification of COX-2, TNF-α and TH immunoreactive cells, the number of positive cells was quantified in 20 independent random fields at x400 magnification.

Measurement of apoptosis. To calculate the extend of apoptotic cell death, SH-SY5Y cells were treated or not with S14, incubated with 6-OHDA for 16 h, and phosphatydilserine (PS) exposure on the surface of apoptotic cells was detected by confocal microscopy after staining with Annexin V-FITC (Bender MedSystems, Vienna, Austria). Levels of active caspase-3 were also determined using a specific rabbit anti-active caspase-3 antibody (R&D Systems). For the quantification of Annexin-V-positive cells and active caspase-3 immunoreactive cells, the number of positive cells was quantified as described above.

Statistics analysis

Statistical comparisons for significance among differents groups of animals were performed by ANOVA followed by Newman-Keuls'test for multiple comparisons. Student's *t*-test was used to analyze statistical differences between cells. Differences were considered statistically significant at $p<0.05$.

Author Contributions

Conceived and designed the experiments: JAM-G AM AS AP-C. Performed the experiments: JAM-G SA-G CP. Analyzed the data: JAM-G AM AS AP-C. Contributed reagents/materials/analysis tools: MR CG. Wrote the manuscript: JAM-G AS AM AP-C.

References

1. Damier P, Hirsch EC, Agid Y, Graybiel AM (1999) The substantia nigra of the human brain. II. Patterns of loss of dopamine-containing neurons in Parkinson's disease. Brain 122(Pt 8): 1437–1448.
2. Tansey MG, McCoy MK, Frank-Cannon TC (2007) Neuroinflammatory mechanisms in Parkinson's disease: potential environmental triggers, pathways, and targets for early therapeutic intervention. Experimental neurology 208: 1–25.
3. McGeer EG, McGeer PL (2007) The role of anti-inflammatory agents in Parkinson's disease. CNS Drugs 21: 789–797.
4. Orr CF, Rowe DB, Mizuno Y, Mori H, Halliday GM (2005) A possible role for humoral immunity in the pathogenesis of Parkinson's disease. Brain 128: 2665–2674.
5. McGeer PL, Schwab C, Parent A, Doudet D (2003) Presence of reactive microglia in monkey substantia nigra years after 1-methyl-4-phenyl-1,2,3,6-tetrahydropyridine administration. Ann Neurol 54: 599–604.
6. Cicchetti F, Brownell AL, Williams K, Chen YI, Livni E, et al. (2002) Neuroinflammation of the nigrostriatal pathway during progressive 6-OHDA dopamine degeneration in rats monitored by immunohistochemistry and PET imaging. Eur J Neurosci 15: 991–998.
7. Gagne JJ, Power MC (2010) Anti-inflammatory drugs and risk of Parkinson disease: a meta-analysis. Neurology 74: 995–1002.
8. Volakakis N, Kadkhodaei B, Joodmardi E, Wallis K, Panman L, et al. (2010) NR4A orphan nuclear receptors as mediators of CREB-dependent neuroprotection. Proc Natl Acad Sci U S A 107: 12317–12322.
9. Lonze BE, Ginty DD (2002) Function and regulation of CREB family transcription factors in the nervous system. Neuron 35: 605–623.
10. Mehats C, Andersen CB, Filopanti M, Jin SL, Conti M (2002) Cyclic nucleotide phosphodiesterases and their role in endocrine cell signaling. Trends Endocrinol Metab 13: 29–35.
11. Conti M, Beavo J (2007) Biochemistry and physiology of cyclic nucleotide phosphodiesterases: essential components in cyclic nucleotide signaling. Annu Rev Biochem 76: 481–511.
12. Bender AT, Beavo JA (2006) Cyclic nucleotide phosphodiesterases: molecular regulation to clinical use. Pharmacol Rev 58: 488–520.
13. Kleppisch T (2009) Phosphodiesterases in the central nervous system. Handb Exp Pharmacol. pp 71–92.
14. Giembycz MA, Smith SJ (2006) Phosphodiesterase 7A: a new therapeutic target for alleviating chronic inflammation? Curr Pharm Des 12: 3207–3220.
15. Miro X, Perez-Torres S, Palacios JM, Puigdomenech P, Mengod G (2001) Differential distribution of cAMP-specific phosphodiesterase 7A mRNA in rat brain and peripheral organs. Synapse 40: 201–214.
16. Sasaki T, Kotera J, Omori K (2002) Novel alternative splice variants of rat phosphodiesterase 7B showing unique tissue-specific expression and phosphorylation. Biochem J 361: 211–220.
17. Reyes-Irisarri E, Perez-Torres S, Mengod G (2005) Neuronal expression of cAMP-specific phosphodiesterase 7B mRNA in the rat brain. Neuroscience 132: 1173–1185.
18. Nakata A, Ogawa K, Sasaki T, Koyama N, Wada K, et al. (2002) Potential role of phosphodiesterase 7 in human T cell function: comparative effects of two phosphodiesterase inhibitors. Clin Exp Immunol 128: 460–466.
19. Gil C, Campillo N, Perez A, Martinez A (2008) Phosphodiesteresae 7 (PDE7) inhibitors as new drugs for neurological and anti-inflammatory disorders. ExpOpinTherPatents 18: 1127–1139.
20. Martinez A, Castro A, Gil C, Miralpeix M, Segarra V, et al. (2000) Benzyl derivatives of 2,1,3-benzo- and benzothieno[3,2-a]thiadiazine 2,2-dioxides: first phosphodiesterase 7 inhibitors. J Med Chem 43: 683–689.
21. Castro A, Jerez MJ, Gil C, Martinez A (2005) Cyclic nucleotide phosphodiesterases and their role in immunomodulatory responses: advances in the development of specific phosphodiesterase inhibitors. Med Res Rev 25: 229–244.
22. Castro A, Jerez MJ, Gil C, Calderon F, Domenech T, et al. (2008) CODES, a novel procedure for ligand-based virtual screening: PDE7 inhibitors as an application example. Eur J Med Chem 43: 1349–1359.
23. Castano T, Wang H, Campillo NE, Ballester S, Gonzalez-Garcia C, et al. (2009) Synthesis, structural analysis, and biological evaluation of thioxoquinazoline derivatives as phosphodiesterase 7 inhibitors. ChemMedChem 4: 866–876.
24. Takahashi T, Deng Y, Maruyama W, Dostert P, Kawai M, et al. (1994) Uptake of a neurotoxin-candidate, (R)-1,2-dimethyl-6,7-dihydroxy-1,2,3,4-tetrahydroisoquinoline into human dopaminergic neuroblastoma SH-SY5Y cells by dopamine transport system. J Neural Transm Gen Sect 98: 107–118.
25. Houslay MD, Kolch W (2000) Cell-type specific integration of cross-talk between extracellular signal-regulated kinase and cAMP signaling. Mol Pharmacol 58: 659–668.
26. Charles MP, Adamski D, Kholler B, Pelletier L, Berger F, et al. (2003) Induction of neurite outgrowth in PC12 cells by the bacterial nucleoside N6-methyldeoxyadenosine is mediated through adenosine A2a receptors and via cAMP and MAPK signaling pathways. Biochem Biophys Res Commun 304: 795–800.
27. Lastres-Becker I, Fernandez-Perez A, Cebolla B, Vallejo M (2008) Pituitary adenylate cyclase-activating polypeptide stimulates glial fibrillary acidic protein gene expression in cortical precursor cells by activating Ras and Rap1. Mol Cell Neurosci 39: 291–301.
28. Chen HQ, Jin ZY, Wang XJ, Xu XM, Deng L, et al. (2008) Luteolin protects dopaminergic neurons from inflammation-induced injury through inhibition of microglial activation. Neurosci Lett 448: 175–179.
29. Kim WG, Mohney RP, Wilson B, Jeohn GH, Liu B, et al. (2000) Regional difference in susceptibility to lipopolysaccharide-induced neurotoxicity in the rat brain: role of microglia. J Neurosci 20: 6309–6316.
30. McCoy MK, Martinez TN, Ruhn KA, Szymkowski DE, Smith CG, et al. (2006) Blocking soluble tumor necrosis factor signaling with dominant-negative tumor necrosis factor inhibitor attenuates loss of dopaminergic neurons in models of Parkinson's disease. J Neurosci 26: 9365–9375.
31. Ouyang M, Shen X (2006) Critical role of ASK1 in the 6-hydroxydopamine-induced apoptosis in human neuroblastoma SH-SY5Y cells. J Neurochem 97: 234–244.
32. Bos JL (2003) Epac: a new cAMP target and new avenues in cAMP research. Nat Rev Mol Cell Biol 4: 733–738.
33. Pham N, Cheglakov I, Koch CA, de Hoog CL, Moran MF, et al. (2000) The guanine nucleotide exchange factor CNrasGEF activates ras in response to cAMP and cGMP. Current biology 10: 555–558.
34. Stetler RA, Gao Y, Zukin RS, Vosler PS, Zhang L, et al. Apurinic/apyrimidinic endonuclease APE1 is required for PACAP-induced neuroprotection against global cerebral ischemia. Proc Natl Acad Sci U S A 107: 3204–3209.
35. Lee B, Butcher GQ, Hoyt KR, Impey S, Obrietan K (2005) Activity-dependent neuroprotection and cAMP response element-binding protein (CREB): kinase coupling, stimulus intensity, and temporal regulation of CREB phosphorylation at serine 133. J Neurosci 25: 1137–1148.
36. Mantamadiotis T, Lemberger T, Bleckmann SC, Kern H, Kretz O, et al. (2002) Disruption of CREB function in brain leads to neurodegeneration. Nat Genet 31: 47–54.
37. Nucifora FC, Jr., Sasaki M, Peters MF, Huang H, Cooper JK, et al. (2001) Interference by huntingtin and atrophin-1 with cbp-mediated transcription leading to cellular toxicity. Science 291: 2423–2428.
38. Jiang H, Nucifora FC, Jr., Ross CA, DeFranco DB (2003) Cell death triggered by polyglutamine-expanded huntingtin in a neuronal cell line is associated with degradation of CREB-binding protein. Hum Mol Genet 12: 1–12.
39. Shimohata T, Nakajima T, Yamada M, Uchida C, Onodera O, et al. (2000) Expanded polyglutamine stretches interact with TAFII130, interfering with CREB-dependent transcription. Nat Genet 26: 29–36.
40. Glass CK, Saijo K, Winner B, Marchetto MC, Gage FH Mechanisms underlying inflammation in neurodegeneration. Cell 140: 918–934.

41. Townsend KP, Pratico D (2005) Novel therapeutic opportunities for Alzheimer's disease: focus on nonsteroidal anti-inflammatory drugs. Faseb J 19: 1592–1601.
42. Chen H, Zhang SM, Hernan MA, Schwarzschild MA, Willett WC, et al. (2003) Nonsteroidal anti-inflammatory drugs and the risk of Parkinson disease. Arch Neurol 60: 1059–1064.
43. Hald A, Lotharius J (2005) Oxidative stress and inflammation in Parkinson's disease: is there a causal link? Exp Neurol 193: 279–290.
44. Liu B, Du L, Hong JS (2000) Naloxone protects rat dopaminergic neurons against inflammatory damage through inhibition of microglia activation and superoxide generation. J Pharmacol Exp Ther 293: 607–617.
45. Dutta G, Zhang P, Liu B (2008) The lipopolysaccharide Parkinson's disease animal model: mechanistic studies and drug discovery. Fundam Clin Pharmacol 22: 453–464.
46. Anden NE, Dahlstrom A, Fuxe K, Larsson K (1966) Functional role of the nigro-neostriatal dopamine neurons. Acta Pharmacol Toxicol (Copenh) 24: 263–274.
47. Ungerstedt U, Arbuthnott GW (1970) Quantitative recording of rotational behavior in rats after 6-hydroxy-dopamine lesions of the nigrostriatal dopamine system. Brain Res 24: 485–493.
48. Schwarting RK, Huston JP (1996) The unilateral 6-hydroxydopamine lesion model in behavioral brain research. Analysis of functional deficits, recovery and treatments. Prog Neurobiol 50: 275–331.
49. Toledo-Aral JJ, Mendez-Ferrer S, Pardal R, Lopez-Barneo J (2002) Dopaminergic cells of the carotid body: physiological significance and possible therapeutic applications in Parkinson's disease. Brain Res Bull 57: 847–853.
50. Paxinos GaW, C (1998) The Rat Brain in Stereotaxic Coordinates. San-Diego: Academic Press.
51. Heneka MT, Klockgether T, Feinstein DL (2000) Peroxisome proliferator-activated receptor-gamma ligands reduce neuronal inducible nitric oxide synthase expression and cell death in vivo. J Neurosci 20: 6862–6867.
52. Luna-Medina R, Cortes-Canteli M, Sanchez-Galiano S, Morales-Garcia JA, Martinez A, et al. (2007) NP031112, a thiadiazolidinone compound, prevents inflammation and neurodegeneration under excitotoxic conditions: potential therapeutic role in brain disorders. The Journal of neuroscience 27: 5766–5776.
53. Morales-Garcia JA, Luna-Medina R, Martinez A, Santos A, Perez-Castillo A (2009) Anticonvulsant and neuroprotective effects of the novel calcium antagonist NP04634 on kainic acid-induced seizures in rats. J Neurosci Res 87: 3687–3696.
54. Cortes-Canteli M, Luna-Medina R, Sanz-Sancristobal M, Alvarez-Barrientos A, Santos A, et al. (2008) CCAAT/enhancer binding protein beta deficiency provides cerebral protection following excitotoxic injury. J Cell Sci 121: 1224–1234.
55. Luna-Medina R, Cortes-Canteli M, Alonso M, Santos A, Martinez A, et al. (2005) Regulation of Inflammatory Response in Neural Cells in Vitro by Thiadiazolidinones Derivatives through Peroxisome Proliferator-activated Receptor {gamma} Activation. J Biol Chem 280: 21453–21462.
56. Cortes-Canteli M, Wagner M, Ansorge W, Perez-Castillo A (2004) Microarray analysis supports a role for ccaat/enhancer-binding protein-beta in brain injury. J Biol Chem 279: 14409–14417.

GLIA

GLIA 59:293–307 (2011)

Peroxisome Proliferator-Activated Receptor γ Ligands Regulate Neural Stem Cell Proliferation and Differentiation *In Vitro* and *In Vivo*

JOSE A. MORALES-GARCIA,[1,2] ROSARIO LUNA-MEDINA,[1] CLARA ALFARO-CERVELLO,[3,4] MARTA CORTES-CANTELI,[1] ANGEL SANTOS,[4] JOSE M. GARCIA-VERDUGO,[3,4] AND ANA PEREZ-CASTILLO[1,2]*

[1]*Instituto de Investigaciones Biomédicas, CSIC-UAM, Arturo Duperier 4, 28029-Madrid, Spain*
[2]*Centro de Investigación Biomédica en Red sobre Enfermedades Neurodegenerativas (CIBERNED) Spain*
[3]*Unidad Mixta Centro de Investigación Príncipe Felipe - Universidad de Valencia, Spain*
[4]*Departamento de Bioquímica y Biología Molecular, Facultad de Medicina, Universidad Complutense de Madrid, 28040-Madrid, Spain*

KEY WORDS
neurogenesis; pioglitazone; PPAR gamma; RMS; SVZ

ABSTRACT
Peroxisome proliferator-activated receptor gamma (PPARγ) belongs to a family of ligand-activated nuclear receptors and its ligands are known to control many physiological and pathological situations. Its role in the central nervous system has been under intense analysis during the last years. Here we show a novel function for PPARγ in controlling stem cell expansion in the adult mammalian brain. Adult rats treated with pioglitazone, a specific ligand of PPARγ, had elevated numbers of proliferating progenitor cells in the subventricular zone and the rostral migratory stream. Electron microscopy analysis also showed important changes in the subventricular zone ultrastructure of pioglitazone-treated animals including an increased number of migratory cell chains. These results were further confirmed *in vitro*. Neurosphere assays revealed significant increases in the number of neurosphere forming cells from pioglitazone- and rosiglitazone (two specific ligands of PPARγ receptor)-treated cultures that exhibited enhanced capacity for cell migration and differentiation. The effects of pioglitazone were blocked by the PPARγ receptor antagonists GW9662 and T0070907, suggesting that its effects are mediated by a mechanism dependent on PPARγ activation. These results indicate for the first time that activation of PPARγ receptor directly regulates proliferation, differentiation, and migration of neural stem cells *in vivo*.

INTRODUCTION

The ability of the adult central nervous system to produce new neurons is limited, rendering the brain particularly vulnerable to injury and disease. In mammals, the majority of neurons are born by the prenatal period, but it is well established that neurons continue to arise in two niches of the adult brain, the subventricular zone (SVZ) of the lateral ventricle and the subgranular zone (SGZ) of the dentate gyrus (Gage et al., 1998; Luskin et al., 1997). Progenitor cells in the SVZ migrate to the olfactory bulb (OB) through the rostral migratory stream (RMS) where they differentiate into granule and periglomerular neurons. In the hippocampus, new neurons arise in the subgranular zone of the dentate gyrus. Both cell-extrinsic and cell-intrinsic factors have been shown to influence the maintenance and regulation of the neurogenic system *in vivo* (Ostenfeld and Svendsen, 2003). Among the extrinsic factors a number of growth factors have been shown to affect the proliferation and differentiation of precursor cell populations, including insulin-like growth factor-1 (Anderson et al., 2002), epidermal growth factor (EGF) (Doetsch et al., 2002), basic fibroblast growth factor (bFGF) (Bartlett et al., 1995; Johe et al., 1996), and other factors like the brain-derived neurotrophic factor (Larsen et al., 2007) and Noggin (Lim et al., 2000). Additionally, adult neurogenesis has also been shown to be influenced by the activation of several intrinsic transcription factors among which are the transcription factors Pax 6 (Hack et al., 2005; Kohwi et al., 2005), Notch 1 (Lutolf et al., 2002), and Mash 1 (Parras et al., 2004).

Peroxisome proliferator-activated receptor gamma (PPARγ) is a member of the nuclear receptor family of transcription factors, which includes different proteins mediating ligand-dependent transcriptional activation (Debril et al., 2001; Dreyer et al., 1992; Kliewer et al., 1994; Michalik et al., 2006). PPARγ participates in many biological processes including adipocyte differentiation, lipid and glucose homeostasis (Desvergne and Wahli, 1999; Rosen and Spiegelman, 2001; Tontonoz et al., 1994), and regulation of inflammatory responses (Ricote et al., 1999; Szeles et al., 2007). Several natural and synthetic ligands for PPARγ have been described. Among the natural ligands, polyunsaturated fatty acids and some prostaglandins and leukotrienes have been shown to be potent activators of this receptor (Forman et al., 1995; Jiang et al., 1998; Paruchuri et al., 2008).

Additional Supporting Information may be found in the online version of this article.

M. Cortes-Canteli is currently at the Department of Neurobiology and Genetics, The Rockefeller University, New York, NY.

*Correspondence to: Ana Perez-Castillo, Instituto de Investigaciones Biomédicas, Consejo Superior de Investigaciones Científicas-Universidad Autónoma de Madrid. Arturo Duperier, 4. 28029-Madrid, Spain. E-mail: aperez@iib.uam.es

Received 27 April 2010; Accepted 1 October 2010

DOI 10.1002/glia.21101

Published online 1 December 2010 in Wiley Online Library (wileyonlinelibrary.com).

Synthetic ligands include the antidiabetic thiazolidinediones (TZDs) such as troglitazone, pioglitazone, and rosiglitazone (Blaschke et al., 2006; Desvergne and Wahli, 1999; Rosen and Spiegelman, 2001) as well as some new compounds, the aryl-tyorosine derivatives, described as novel PPARγ ligands (Brown et al., 1999).

Beyond these functions, recent data have shown that PPARγ acts as a regulator of central nervous system inflammation (Heneka et al., 2005) and is a powerful pharmacological target for counteracting neurodegeneration, as shown in animal models (e.g. of Parkinson's and Alzheimer's diseases) review in (Heneka and Landreth, 2007). In this context, data from animal experiments strongly indicate that ligands of PPARγ confer neuroprotection and neurological improvement following brain injury (Abdelrahman et al., 2005; Bernardo et al., 2000; Landreth and Heneka, 2001; Townsend and Pratico, 2005) and PPARγ ligands, including the antidiabetic thiazolidinediones (TZDs), have been implicated in anti-inflammatory process in diverse tissues, including the brain (Kielian and Drew, 2003; Ricote et al., 1999). Consistent with this idea, we have recently demonstrated that different members of the thiadiazolidinone (TDZD) family (chemical structure-related derivatives to TZDs) inhibited the activation of astrocytes and microglial cells *in vitro* and are potent anti-inflammatory and neuroprotective agents against kainic acid-induced *in vivo* excitotoxicity, through a mechanism apparently involving PPARγ activation (Luna-Medina et al., 2005; Luna-Medina et al., 2007b). We found a significant preservation of hippocampal cells in TDZD-injected rats compared with abundant neuronal loss in CA1, CA3, and hilus after injection with kainic acid (Luna-Medina et al., 2007b), suggesting a possible neurogenic action of the TDZD compound. Also, we have preliminary data showing that the TDZD compound NP031112, a potent anti-inflammatory and neuroprotective agent, which is currently under Phase II clinical trial for the treatment of Alzheimer's disease, is a powerful inducer of neurogenesis in the two neurogenic niches, subventricular zone and hippocampus, of adult rats (Luna-Medina et al., 2007a).

On the basis of the previous evidence, in this study we were interested in determining whether activation of PPARγ might have a role in the proliferation, differentiation, and migration of neural progenitor cells. Our studies showed that pioglitazone, a specific ligand of PPARγ, is a potent inducer of neuroblasts formation and migration in the SVZ of adult rats. *In vitro*, PPARγ ligands increased the number, differentiation and migration capacity of adult rat neurospheres. Altogether, these findings suggest that ligands of PPARγ regulate neural progenitor cell proliferation and migration and may influence their differentiation in adult forebrain.

MATERIALS AND METHODS

Animals

All animal-related procedures were approved by the Laboratory Animal Care and Use Committee of the Consejo Superior de Investigaciones Científicas and were conducted in accordance with the guidelines of the European Communities Council, directive 86/609/EEC. All efforts were made to minimize animal suffering and to reduce the number of animals used. Adult (8–12 weeks old) Wistar rats were used throughout the study.

Pioglitazone and Bromodeoxyuridine Administration

Adult male Wistar rats ($n = 5$ per group) housed in a 12-hour light-dark cycle animal facility received daily intragastrical administration of pioglitazone (20 mg/kg body weight) for three consecutive days. This dose of pioglitazone was chosen because it has been shown to be effective *in vivo* in different previously published works (Breidert et al., 2002; Ji et al., 2009; Peiris et al., 2007; Saitoh et al., 2007; Schmerbach et al., 2008). To label the entire population of fast proliferating SVZ and RMS cells, rats were intraperitoneally injected with 5-bromo-2-deoxyuridine (BrdU, 50 mg/kg) 24 h or 21 days before sacrifice.

Tissue Preparation, Histology, and Immunohistochemistry

After treatment, the animals were anaesthetized and perfused transcardially with 4% paraformaldehyde solution. The brains were removed, postfixed in the same solution at 4°C overnight, cryoprotected in the paraformaldehyde solution containing 30% sucrose, frozen, and 30 μm coronal and sagital sections were obtained in a cryostat. Free floating sections were processed for cresyl violet (Nissl stain) and immunohistochemistry using immunofluorescence analysis or diaminobenzidine method as previously described (Luna-Medina et al., 2007b). For BrdU detection, samples were first incubated with 2 M HCl for 30 min at 37° before blocking 1 h in PBS containing 5% normal serum, 0.1 M lysine, and 0.1% Triton X-100. Sections were then incubated with anti-BrdU mouse monoclonal (DAKO, Denmark) and anti-neuN rabbit polyclonal (Chemicon) antibodies at 4°C overnight, washed three times and incubated with AlexaFluor 488 and Alexa 647 secondary antibodies for 1 h at room temperature. After rinses, sections were mounted with Vectashield. Images were obtained using a Radiance 2100 confocal microscope (Bio-Rad, Hercules, CA) with a 488 laser line to excite Alexa-488 and a 647 laser line to excite Alexa-647. Confocal microscope settings were adjusted to produce the optimum signal-to-noise ratio. BrdU-positive cells were scored throughout the entire SVZ and RMS. One section every 60 μm was analyzed at high magnification (×40). For the quantification of immunoreactive BrdU/NeuN cells in the olfactory bulb, the number of positive cells was counted in five independent random fields (×400 magnification), in five different sagital sections per animal ($n = 5$ animals). For doublecortin (DCX) and β-III-tubulin detec-

tion floating sections were immersed in 3% H_2O_2 to inactivate endogenous peroxidase, blocked for 2 h at room temperature in 5% normal horse serum in PBS, containing 4% bovine serum albumin, 0.1 M lysine, and 0.1% Triton X-100. Afterwards, the sections were incubated overnight with anti-doublecortin goat (Santa Cruz, CA), anti-PSA-NCAM mouse (Chemicon), and anti- β-III-tubulin mouse (Sigma) antibodies. After several rinses, sections were incubated for 1 h with the corresponding biotinylated secondary antibody and then processed following the avidin-biotin protocol (ABC, Vectastain kit, Vector Labs). Tissues were then mounted onto gelatin-coated slides, dried, dehydrated in xylene, and mounted with DePeX (Serva, Heidelberg, Germany). The slides were examined with a Zeiss Axiophot microscope, equipped with an Olympus DP-50 digital camera, and a Leica MZ6 modular stereomicroscope.

Electron Microscopy

Rats were deeply anesthetized and perfused transcardially with 0.9% saline, followed by Karnovsky's fixative (2% paraformaldehyde, and 2.5% glutaraldehyde). Brains were postfixed overnight in the same fixative and washed in 0.1 M phosphate buffer (PB). Coronal 200 μm sections were cut on a vibratome. Sections were then post-fixed in 2% osmium for 2 h, rinsed, dehydrated and finally embedded in Araldite (Durcupan ACM, Fluka, Switzerland). Serial 1.5 μm semithin sections were cut with a diamond knife and stained with 1% toluidine blue to study the organization of the SVZ and RMS. To identify the different individual cell types in the SVZ, ultrathin (70 nm) sections were cut with a diamond knife. Photomicrographs were obtained under a Fei microscope (Tecnai-Spirit) using a digital camera (Morada, Soft-imaging System).

Neurosphere Cultures

Neurosphere (NS) cultures were derived from adult rats and induced to proliferate using established passaging methods to achieve optimal cellular expansion according to published protocols (Ferron et al., 2007). Briefly, rats were decapitated, brains removed and the subventricular zone was dissected, minced and dissociated with DMEM (Invitrogen) containing glutamine, gentamicin, and fungizone. After treatment with trypsin-EDTA, hialuronidase and DNAse, myelin was removed by using DPBS (Invitrogen). Cells were seeded into 6-well dishes and cultured in Dubecco's Modified Eagle's Medium (DMEM)/F12 (1:1, Invitrogen) containing 10 ng/mL epidermal growth factor (EGF, Peprotech, London, UK), 10 ng/mL fibroblast growth factor (FGF, Peprotech) and N2 medium (Gibco). After three days in culture, some primary NS cultures were treated with pioglitazone (5, 10, and 30 μM, Takeda Europe R&D Centre Ltd., London, UK), rosiglitazone (5, 10 and 30 μM, Cayman, Ann Arbor, MI), or vehicle for another seven days. Some cultures were pretreated for 30 min with GW9662 (10 and 30 μM, Cayman) and T0070907 (25 and 50 μM, Cayman). These primary neurospheres were then dissociated and replated in normal proliferative conditions for another seven to nine days to score the number of secondary neurospheres generated. Six to eight wells per condition tested were counted.

Protein Extraction and Western Blot Analysis

After sacrifice, brains were immediately dissected and cortex, hippocampus and cerebellum isolated and frozen on dry ice and stored at −80°C until protein extraction. For protein extraction, samples were homogenized in ice-cold RIPA buffer and equal quantities of total protein were separated by 10% SDS-PAGE. After electrophoresis, proteins were transferred to nitrocellulose membranes (Protran, Whatman, Dassel, Germany) and blots were probed with anti-PPARγ (Santa Cruz, Santa Cruz, CA) antibody. For each sample, the α-tubulin level expression (Sigma) was determined as a loading control.

Growth and Proliferation Measurements

Primary and secondary NS cells were counted and their size was analyzed using the Nikon Digital Sight, SD-L1 (Nikon, Japan). Proliferation assays were carried out by culturing whole primary NS, in the presence or absence of the indicated stimuli, during 10 days. Afterwards they were plated onto poly-L-lysine coated coverslips for 24 h. Cells were then fixed in cold methanol, stained with anti-Ki67 antibody (Novo Castra Laboratories, Newcastle, UK) and processed for immunocytochemistry as previously described (Luna-Medina et al., 2005).

Differentiation of NS Cultures

To determine the ability of rosiglitazone and pioglitazone to produce neurons, astrocytes or oligodendrocytes, whole neurospheres from 10-day old cultures were plated onto poly-L-lysine coated coverslips in the absence of exogenous growth factors. Cells were allowed to adhere for 24 h and fixed using cold methanol. Cells were then processed for immunocytochemistry.

Assay of Cell Migration

Single spheres were picked up with a pipette and plated onto poly-L-lysine coated 35 mm dishes. At 48 h post-plating, the outgrowth of the neurosphere cells was examined under the phase contrast microscope, and the images were acquired with a Nikon Digital Sight, SD-L1 software. The farthest distance of cell migration was calculated from the edge of the sphere. At least 10 plated neurospheres per situation were analyzed.

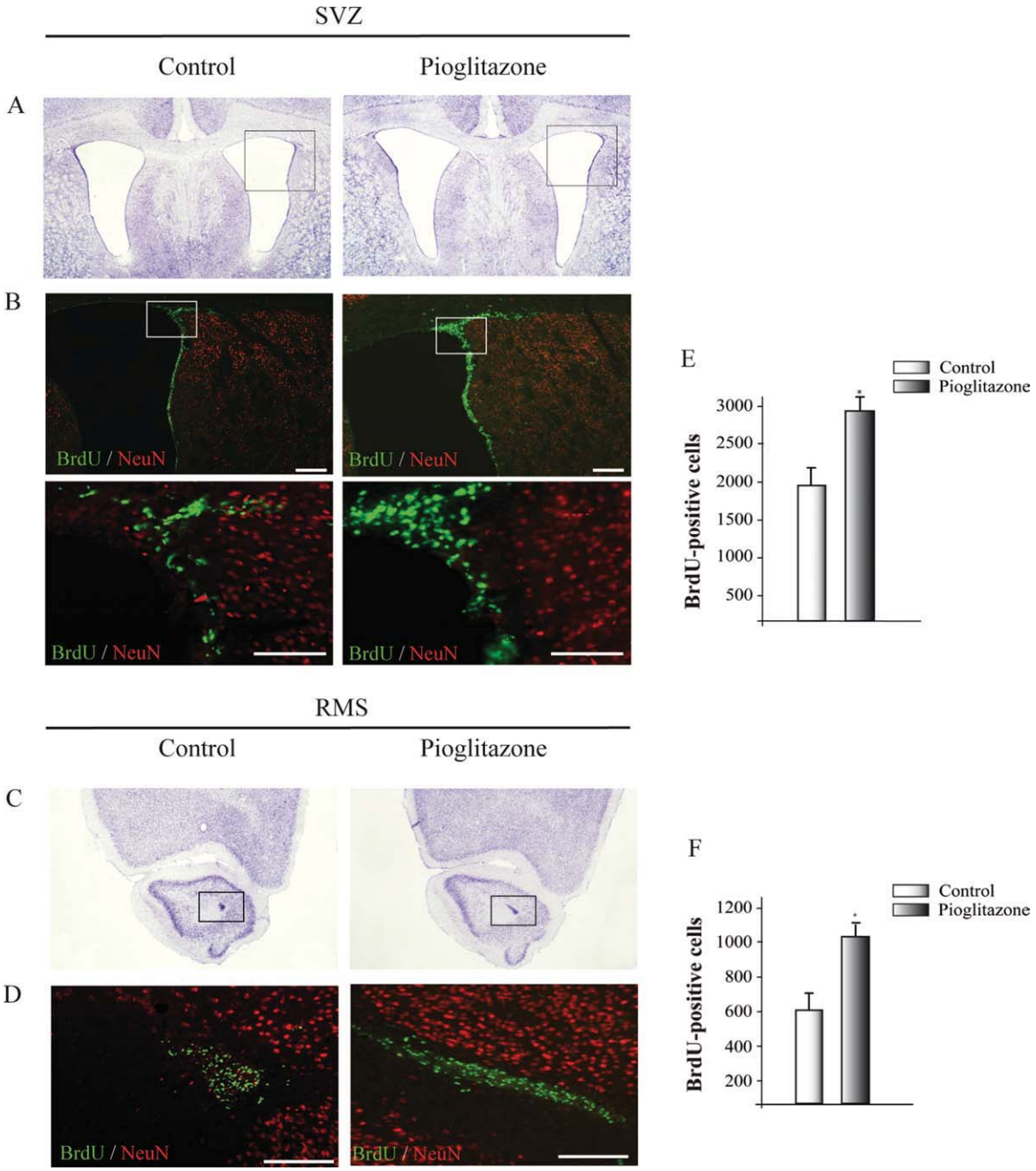

Fig. 1. Pioglitazone action on proliferating cells in the subventricular zone (SVZ) and the rostral migratory stream (RMS). Representative coronal sections showing Nissl staining and micrographs of BrdU-labeled cells (green) and NeuN-stained cells (red) in the SVZ (**A, B**) and in the RMS (**C, D**). Insets show higher magnifications of representative areas in the SVZ. (**E, F**) Quantification of BrdU-positive cells from the SVZ and RMS. Values are the mean ± sd from five different animals. *$P \leq 0.05$. Scale bar in B, D: 200 μm; insets: 100 μm.

Immunocytochemistry

Cells were processed for immunocytochemistry as previously described (Luna-Medina et al., 2005). Briefly, at the end of the treatment period, NS cultures were grown on glass cover-slips in 24-well cell culture plates. Cultures were then washed with phosphate-buffered-saline (PBS) and fixed for 30 min with 4% paraformaldehyde at 25°C, and permeabilized with 0.1% Triton X-100 for 30 min at 37°C. After 1 h incubation with the corresponding primary antibody, cells were washed with phosphate-buffered-saline and incubated with an Alexa-labeled secondary antibody (Molecular Probes; Leiden, The Netherlands) for 45 min at 37°C. Later on, images were obtained using a Radiance 2100 confocal microscope (Bio-Rad, Hercules, CA) as described for immunohistochemistry. Quantification was undertaken using the image analySIS software (Soft Imaging System Corp., Münster, Germany) and normalized to total nuclei. Primary antibodies were directed against the following:

MAP-2 (mouse; Sigma), GFAP (mouse; Sigma), active caspase-3 (rabbit, R&D) and CNPase (mouse, Chemicon, Temecula, CA). Dapi staining was used as a nuclear marker. For quantification of the number of cells producing a given marker, in any given experiment the number of positive cells leaving the neurosphere body were then counted. Cell numbers were estimated from a total of six to eight neurospheres per condition over three independent experiments.

Statistical Determinations

Data are given as the mean ± SD. of at least five different animals per group. Comparisons of different groups were performed using the Student's t test with $P \leq 0.05$ being considered significant.

RESULTS

Since pioglitazone is a specific ligand of the nuclear receptor PPARγ, we first analyzed whether PPARγ was expressed in the adult brain, particularly in neurogenic areas. Western blot and immunohistochemistry (Supp. Info. Fig. 1) analysis demonstrated that PPARγ was expressed throughout the central nervous system of the adult rat. Interestingly, significant levels of PPARγ protein were found in the two neurogenic niches, the SVZ and the hippocampus. PPARgamma expression was found in the SVZ as well as in the RMS. PPARγ is expressed at high levels in the RMS and remains detectable in these cells as they migrate into the OB.

Effect of Pioglitazone on Proliferation of Adult Progenitor Cells *In Vivo* in the Subventricular Zone and Rostral Migratory Stream

We first analyzed whether pioglitazone affected the proliferation kinetics of mitotically active progenitor cells in the SVZ and RMS. For this *in vivo* study we decided to use this PPARγ ligand because of its well known ability to cross the blood brain barrier. To this end, rats were treated during three days with pioglitazone or vehicle followed by one BrdU injection 24 h before sacrifice. Coronal sections were stained with cressyl violet (Nissl staining) or with specific anti-BrdU and anti-NeuN antibodies (see Fig 1). Nissl staining showed an increase in the size of the SVZ in animals treated with pioglitazone (Fig. 1A, right panel), in comparison with controls. No morphological alterations were observed on the rest of the neuropil or in other cortical, septal or striatal structures. Also a widespread distribution of the RMS was observed in pioglitazone-treated animals (Fig. 1C, right panel). Twenty-four hours after the BrdU injection there was a considerable increase in the number of labeled cells both in the SVZ (Fig. 1B, right panel) and RMS (Fig. 1D, right panel) of pioglitazone-treated rats relative to the vehicle-treated control group SVZ (Fig 1B, left panel) and RMS (Fig 1D, left panel). Pioglitazone treatment increased SVZ BrdU-labeled cell numbers by about 35% above control values (Fig. 1E). Similar results were obtained in the RMS where a significant increase in the number of BrdU cells was found in pioglitazone-treated animals in comparison with control ones (Fig. F). Besides a higher number of proliferating cells in the RMS, we also found that pioglitazone-treated animals showed a widespread RMS (Fig 1D, right panel), compared with control rats, in which the RMS usually appeared as a dense cluster of cells (Fig 1D, left panel).

To determine the cell types that were increased in the RMS and the SVZ, rats were treated during three days with pioglitazone or vehicle and sagittal or coronal brain sections were stained for DCX. DCX is a microtubule-associated protein, which is a valuable endogenous marker for dividing neuroblasts and immature neurons (Brown et al., 2003; Couillard-Despres et al., 2005). As shown in Fig. 2A,B, pioglitazone treatment clearly increases the number of DCX^+ cells in the RMS (Fig. 2A), specially in some areas, such as the anterior arm or the elbow (Fig. 2A, right panel). Similar results were observed in the SVZ of pioglitazone-treated animals (Fig. 2B, right panel) with an increase in the migrating chain of cells. The pioglitazone-induced increase in the number of neuroblast was further substantiated by staining with PSA-NCAM, a marker of migrating neuroblasts (Fig. 2C). As happened with the number of DCX^+ cells, animals treated with pioglitazone presented a higher number of PSA-NCAM-stained cells in the RMS. To characterize the cells marked in the SVZ, coronal sections were stained with an specific anti-β tubulin antibody, a molecule present in the migrating neuronal precursors (Doetsch and Alvarez-Buylla, 1996). Our results clearly showed an increase in β-tubulin staining in the pioglitazone-treated animals (Fig. 2D, right panel).

Effect of Pioglitazone on Migrating Cells and the Subventricular Zone

We then analyzed the morphological features of the SVZ in the different groups of animals. To this end, we performed light and electron microscopy (EM) analysis on coronal sections of the ventricular lateral wall of the SVZ. EM allows characterization and identification of SZV cell types through their specific ultrastructural features, which have been well established in rodents (Danilov et al., 2009; Doetsch et al., 1997).

Analyzing toluidine blue-stained semithin sections of the SVZ of control animals, next to the ependymal lining we found chains of neuroblasts (Fig. 3A). However, pioglitazone-treated animals (Fig. 3B) displayed an expanded SVZ, with an increased number of migrating neuroblasts. These cell clusters were located deeply in the neuropil.

EM analysis showed a typical SVZ structure in control animals (Fig. 3C). Close to the ependymal cell lining, we

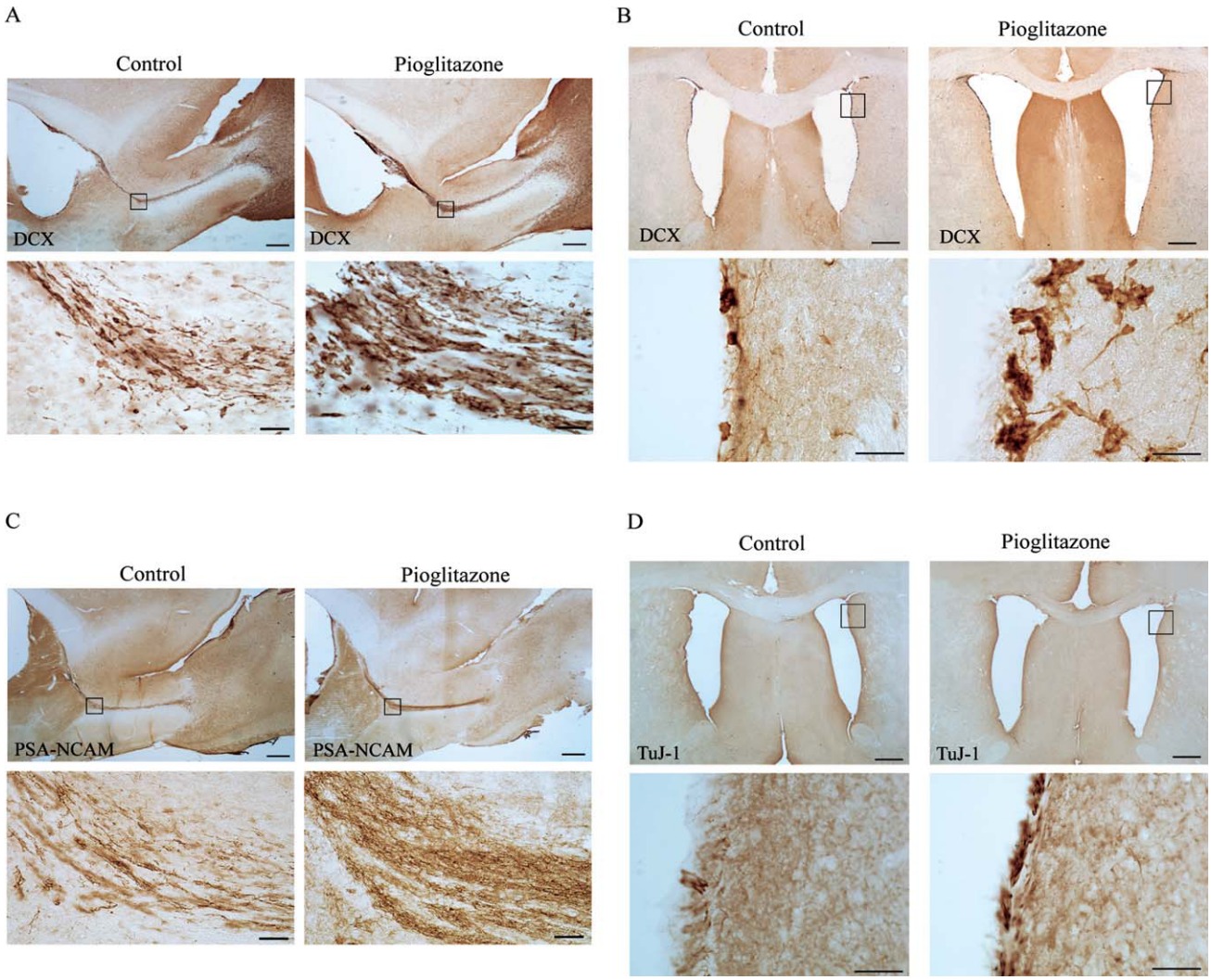

Fig. 2. Effect of PPARγ ligands on neural progenitor cells and their migration in the SVZ and RMS. Representative immunohistochemical images of DCX expression on sagital sections of RMS (**A**) and coronal sections of SVZ (**B**) of control and pioglitazone-treated animals. Insets show higher magnifications of the elbow area of RMS (A) and the SVZ (B). **C:** Representative immunohistochemical images of PSA-NCAM expression on sagital sections of control and pioglitazone-treated animals. Insets show higher magnifications of the elbow area of the RMS (**D**) Representative coronal sections showing staining of the SVZ with an specific anti-β tubulin antibody. Scale bar in A, B, C, D: 250 μm, Insets: 25 μm. [Color figure can be viewed in the online issue, which is available at wileyonlinelibrary.com.]

found chains (Fig. 3C, pointed line) of migrating cells (Type A). These cells were identified by their small size and dark scanty cytoplasm. Astrocytes or type B cells were identified as large, less electrodense cells, rich of intermediate filaments. After pioglitazone treatment, the SVZ showed several ultrastructural changes. First, an increased number of neuroblasts were observed. These neuroblasts, in comparison with control animals, showed an irregular shape (Fig. 3D). Moreover, migrating cell chains were located deeper in the SVZ compared with control rats. Additionally, intercellular spaces characteristic of migrating neuroblasts were more prominent in the pioglitazone-treated animals (Fig. 3F), compared with controls (Fig. 3E). Signs of pathological events or tumoral cells were also absent. Regarding the RMS, migrating type A cells and astrocytes were observed in control animals; these cells accumulated forming a typical dense cell mass (Fig. 3G). The RMS of pioglitazone-treated animals (Fig. 3H) showed dispersed chains of migrating neuroblasts, which tended to spread invading a larger surface.

Effect of Pioglitazone on Newly Generated Cells in the Olfactory Bulb

The neuronal differentiation of newborn cells in the olfactory bulb was assessed using double immunofluorescence labelling for BrdU and NeuN (postmitotic and postmigrational neurons), 21 days after treatment with pioglitazone and BrdU injection (see Fig. 4). At this time most of BrdU-positive cells have reached the granule cell layer via the RMS, and express a neuronal phenotype (Winner et al., 2002). The number of BrdU/NeuN-

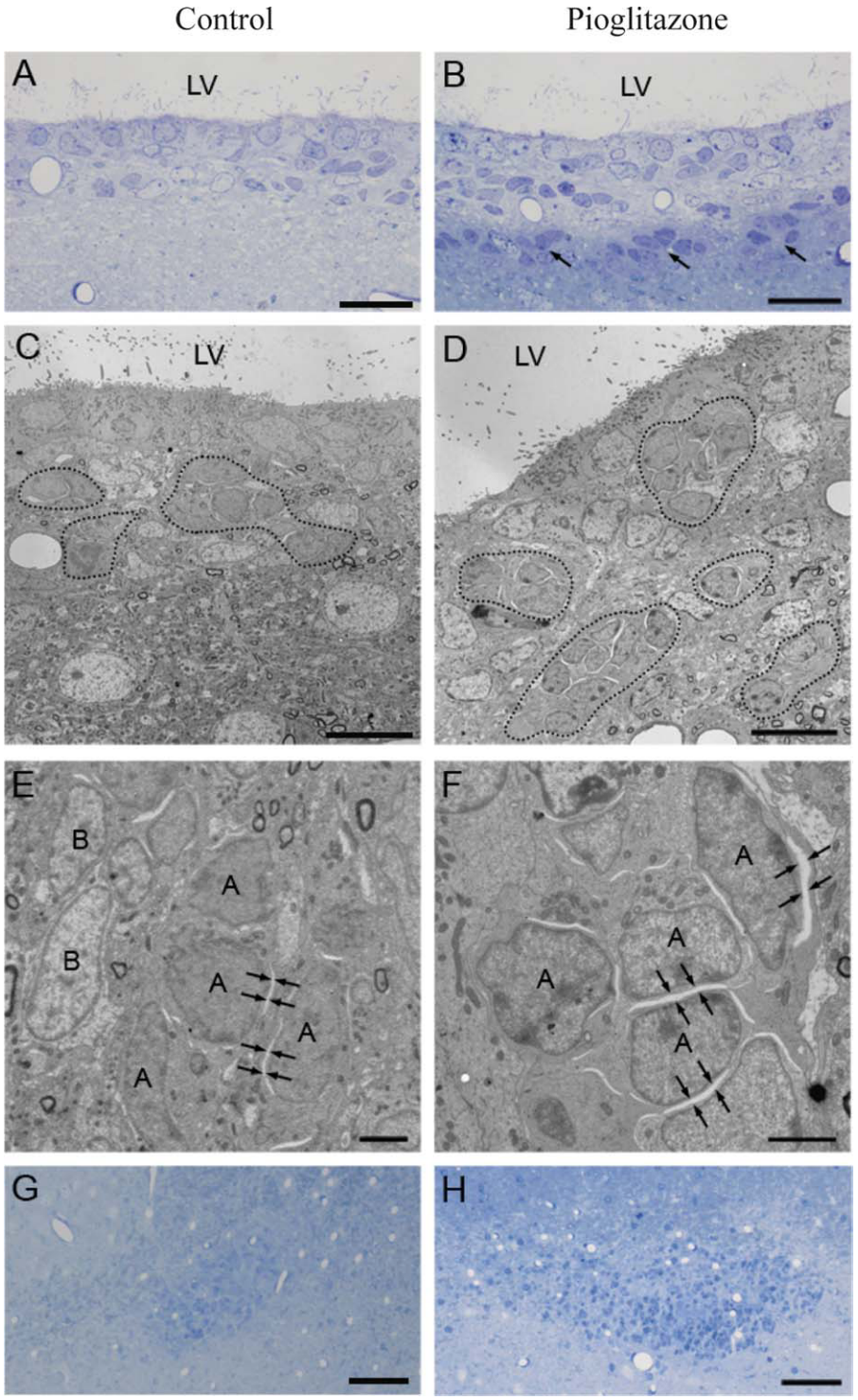

Fig. 3. Effect of PPARγ ligands on migrating cells in the subventricular zone and the rostral migratory stream. **A:** Toluidine blue-stained semithin section of the SVZ of a control rat, with dark round cells forming groups. **B:** The SVZ of pioglitazone-treated rats displayed an increased number of migrating neuroblasts clusters. **C:** Ultrastructure of the SVZ of an untreated rat. Close to the ependymal cell lining, chains of migrating Type A cells (pointed line) showed a dark scanty cytoplasm. Astrocytes (type B cells) were large and less electron-dense and contained abundant intermediate filaments. **D:** After pioglitazone treatment, the number of neuroblasts increased and they showed an irregular shape. Migrating cell chains (pointed line) were deeper located in the SVZ compared with control rats. **E:** Migrating neuroblasts typically displayed intercellular spaces (arrows), indicative of cell movement, in untreated rats. **F:** In pioglitazone-treated mice, intercellular spaces were more prominent than in control animals (arrows). **G:** Rostral migratory stream of a control animal. Migrating cells and astrocytes accumulate forming a dense cell mass. **H:** The rostral migratory stream of pioglitazone-treated mice showed a larger size, with an increased cell number. Scale bar in (A, B) 20 μm; (C, D) 10 μm; (E, F) 2 μm; (G,H) 50 μm. LV, lateral ventricle. [Color figure can be viewed in the online issue, which is available at wileyonlinelibrary.com.]

positive cells in the granule cell layer was quantified as described in Material and Methods. Our results showed that after 21 days, there is a significant increase in the amount of newly generated neurons (BrdU/NeuN immunoreactive cells) in this area, in the animals treated with pioglitazone (Fig. 4A,B). That means that pioglitazone increases the number of new neurons into the olfactory bulb.

The PPARγ Ligands Pioglitazone and Rosiglitazone Control the Growth and Survival of Neurospheres

As a step toward understanding the role of PPARγ ligands on neurogenesis, we used primary and secondary derived neural stem cells as a model system. These studies allow us to better understand the mechanism by

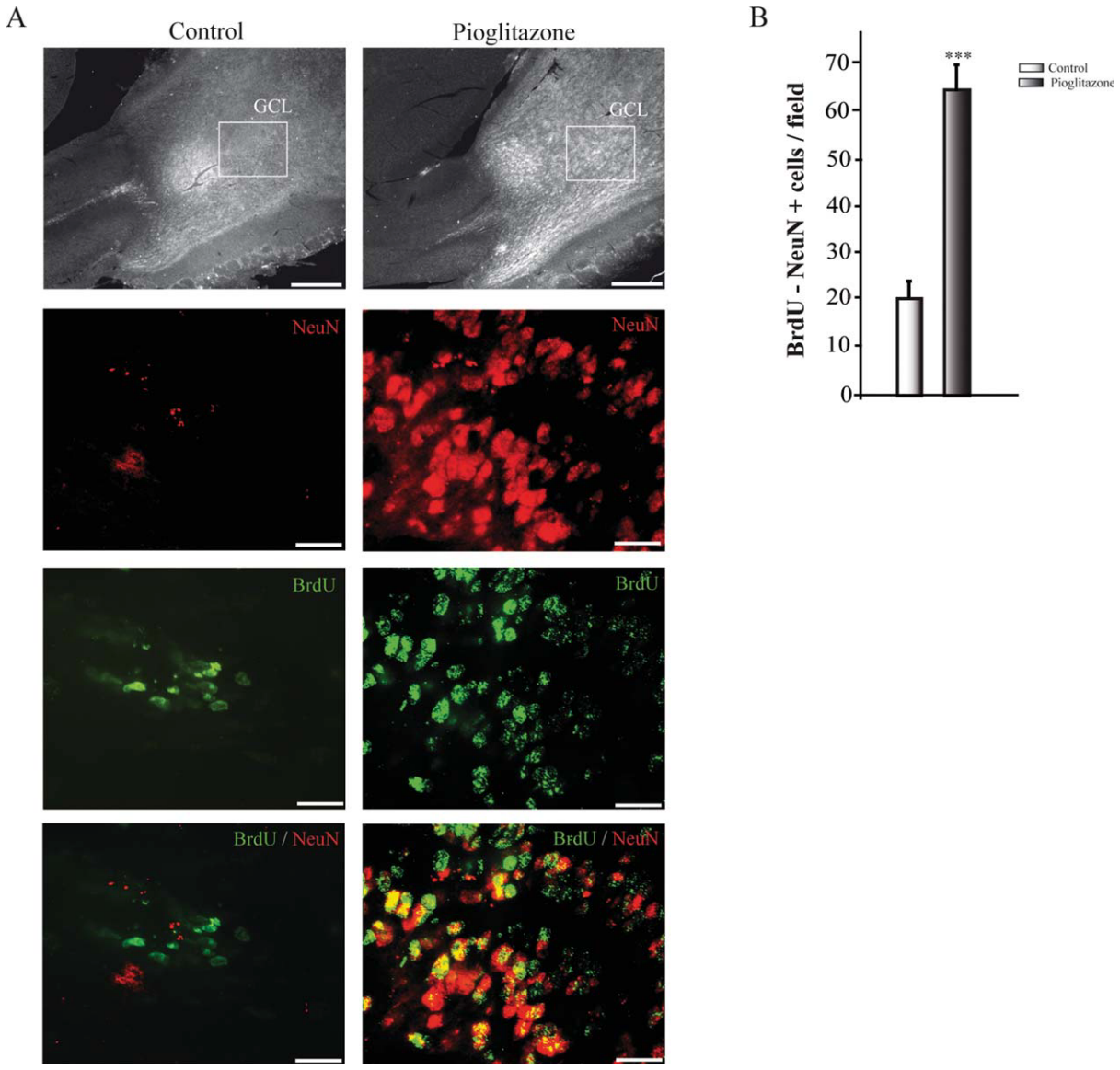

Fig. 4. Effect of PPARγ ligands on newly generated neurons in the olfactory bulb. **A:** Sagital sections showing the granule cell layer (GCL) of the olfactory bulb stained with BrdU (green) and NeuN (red). **B:** Quantification of the number of BrdU/NeuN double stained cells into the GCL. Values are the mean ± SD from five different animals. $^{***}P \leq 0.001$. Scale bar in A 100 μm; insets: 20 μm.

which pioglitazone acts as a neurogenic agent and the possible involvement of the nuclear receptor PPARγ. Primary neurospheres were obtained from adult rats and maintained and expanded as described in Materials and Methods. We first analyzed by Western blotting whether PPARγ was expressed in the neurosphere cultures. As shown in Fig. 5A, PPARγ was notably expressed in NS, regardless of their differentiation state. Next, we investigated whether addition of pioglitazone and rosiglitazone, another well-known and potent PPARγ ligand, to the medium of growing NS would increase their rate of formation and/or their size. To that point, different concentrations of pioglitazone and rosiglitazone on primary NS were used (Fig. 5C).

After 10 days of growth in suspension, there was a significant increase in both the number and diameter of primary NS growing in the presence of both ligands (Fig. 5B,C). Consistent with a role in stem cell regulation suggested by the *in vivo* experiments, pioglitazone- and rosiglitazone-treated NS exhibited an enhanced self-renewal capacity. Primary spheres derived from pioglitazone- and rosiglitazone-treated progenitors formed "secondary" NS when dissociated and replated (Fig. 5C), indicating self-renewal capacity. Specifically, neonatal pioglitazone- and rosiglitazone-treated primary NS produced respectively 341 ± 15.7 and 336 ± 12.2 secondary NS, while non-treated neurospheres only produced 210 ± 10.5 secondary neurospheres. Treatment of

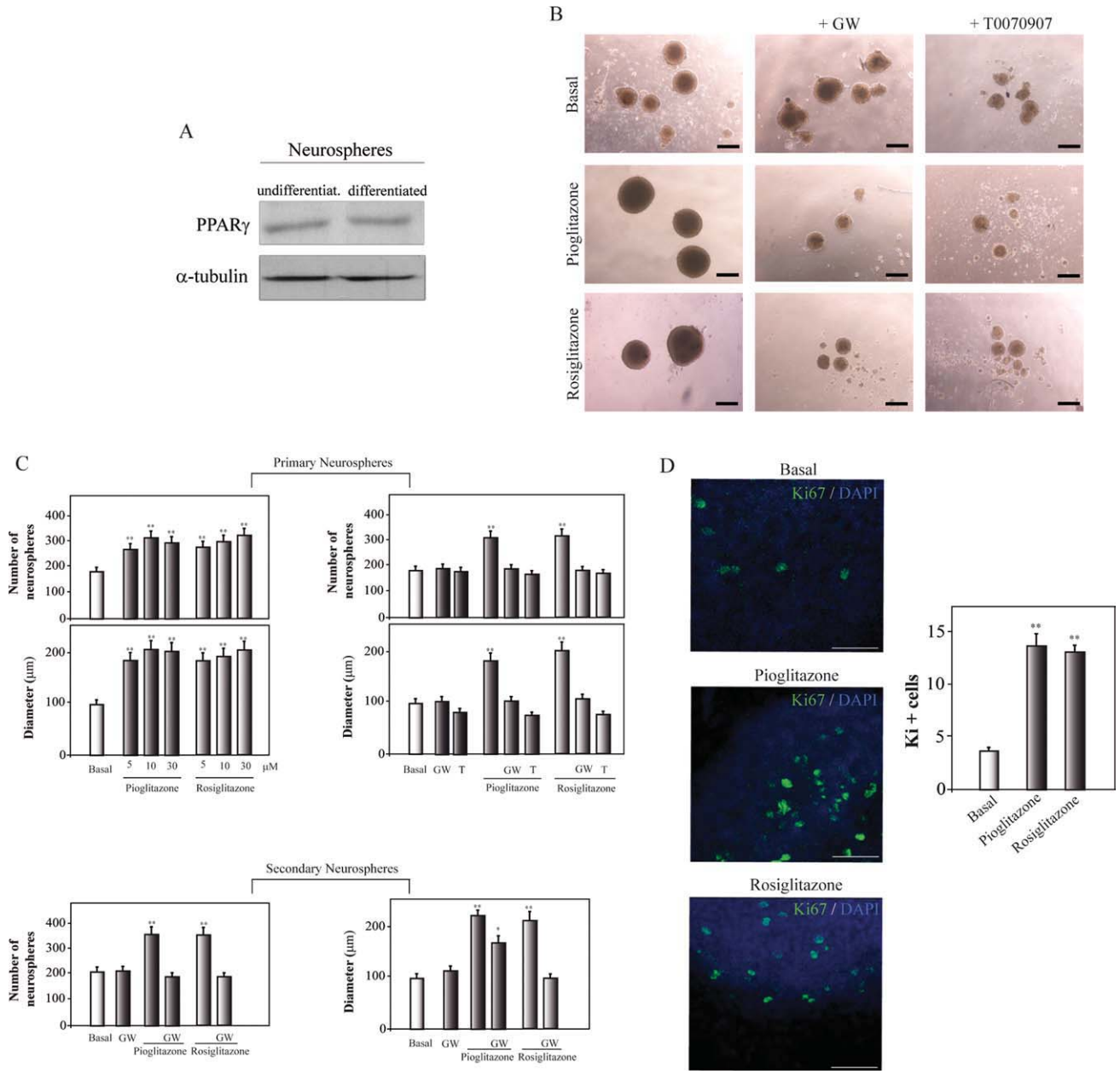

Fig. 5. Effect of PPARγ ligands on neurosphere formation and growth. **A**: Western blot analysis showing expression of PPARγ in neurospheres grown for seven days (undifferentiated) or after an additional two days of adhesion (differentiated cultures). **B:** Representative phase-contrast micrographs showing the size of neurospheres cultures for seven days in the presence or absence of pioglitazone (10 μM) or rosiglitazone (30 μM). Some cultures were preincubated 1 h with 30 μM GW9662 (GW) or 50 μM T0070907 prior to the addition of the compounds. Scale bars, 50 μm. **C:** Effect of different doses of pioglitazone and rosiglitazone (5, 10, and 30 μM) on the growth of primary neurospheres. The number of neurospheres was counted and its diameter measured. The diameter of 50 primary and secondary neurospheres and the total number of neurospheres was determined in control and in pioglitazone- or rosiglitazone- treated cells. Some cultures were preincubated with GW9662 (GW, 30 μM) or with T0070907 (T, 50 μM). The graphs in (**C**) demonstrate a significant increase in the number and diameter of the neurospheres in those cultures treated with pioglitazone or rosiglitazone. **D:** Representative confocal images of Ki67 immunoreactivity (green) in primary neurospheres. Dapi staining (blue) was used as a nuclear marker. Quantification of Ki67+ cells reveals a significant induction of the Ki67+ cells in pioglitazone- and rosiglitazone-treated neurospheres. Results are mean values ± SD from three independent experiments performed in triplicate. $^{**}P \leq 0.01$. [Color figure can be viewed in the online issue, which is available at wileyonlinelibrary.com.]

neurosphere cultures with pioglitazone or rosiglitazone did not alter cell viability, as measured by active caspase-3 staining (Supp. Info. Fig. 2).

Next, we tested the possible implication of the PPARγ receptor in the observed effect of pioglitazone and rosiglitazone. To this end we analyzed whether the specific PPARγ antagonists GW9662 and T0070907 impaired the action of the drugs. As shown in Fig. 5B,C, treatment of primary NS with these antagonists significantly inhibited the effects of the drugs on primary NS formation and size. Similar results were obtained on secondary NS pre-treated with GW (Fig. 5C, lower panel). These

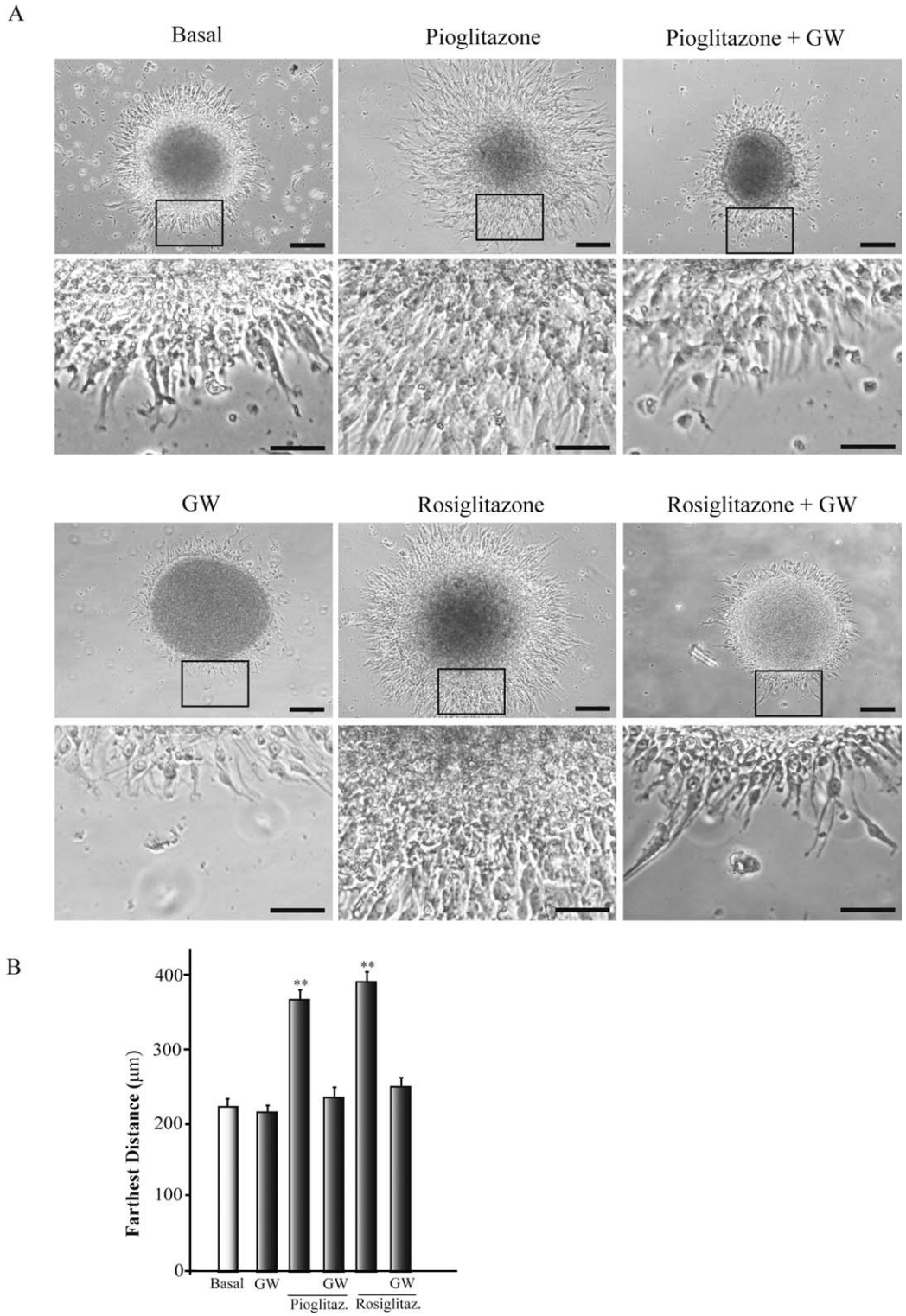

Fig. 6. Effect of PPARγ ligands on cell migration out of the neurosphere. Single neurospheres were plated on a poly-lysine-coated culture Petri dish in the presence or absence of pioglitazone (10 μM) or rosiglitazone (30 μM), and the cell migration out of the sphere was monitored 48 h later. Some cultures were pre-incubated 1 hour with 30 μM GW9662 (GW) prior to the addition of the compounds. **A:** Shown are representative photomicrographs of three independent experiments. Scale bars, 25 μm. Insets show higher magnifications of the migrating area. Scale bars, 10 μM (**B)** Quantitative data of farthest distance of neural progenitor cell migration. $^{**}P \leq 0.01$, versus control nontreated cultures.

results suggest that both rosiglitazone and pioglitazone are acting through a PPARγ-dependent mechanism.

These studies thus far demonstrate that PPARγ is expressed by NS and that their specific ligands pioglitazone and rosiglitazone enhance the number as well as the size of the NS generated from neonatal SVZ, suggesting that PPARγ activation by these factors regulates the proliferation of sphere forming progenitors. Therefore, proliferation of pioglitazone- and rosiglitazone-treated cells was assessed 7 days after treatment by staining for Ki67, a marker of dividing cells. As expected, treatment of adherent primary NSC significantly increased Ki67-staining, indicating a direct effect of pioglitazone and rosiglitazone on proliferation (Fig. 5D).

The PPARγ Ligands Pioglitazone and Rosiglitazone Alter Migration Patterns From Neurospheres

In order to test whether pioglitazone and rosiglitazone modulate migration of NS, we exposed NS to both agents during 48 h. The results summarized in Fig. 6 indicate that migration in the presence of both, pioglitazone and rosiglitazone for 48 h resulted in an increased migration (1.6- and 1.5-fold, respectively of the controls). These cells moved long distances from the centre of the NS to often create overlapping zones of migration between adjacent NS. The cells from control NS remained close to the neurosphere origin and were observed in closely associated groups.

Next, we investigated whether PPARγ activation is involved in the effects upon migration of both pioglitazone and rosiglitazone. To this end, NS cultures were pretreated with the selective PPARγ antagonist GW9662 before exposure to these agents. As shown in Fig. 6, GW9662 suppressed the enhanced migration detected in pioglitazone- and rosiglitazone-treated NS cultures. These results suggest again an involvement of the nuclear receptor PPARγ in the migration effects of both compounds.

Altogether these data implicate the PPARγ receptor as a regulator of neuroblast formation and migration in the adult rat brain.

The PPARγ Ligands Pioglitazone and Rosiglitazone Enhance Differentiation of Neurospheres After Adhesion

To investigate whether PPARγ ligands influence cell differentiation after adhesion of NS, we analyzed by immunocytochemistry the different central nervous system cell types in the inside and the outgrowth of control, pioglitazone- and rosiglitazone-treated NS. Twenty-four hours after plating in the absence of EGF and FGF, NS extended multiple processes, which stained for the uncommitted neural precursor marker nestin. To identify the cell types generated by the effect of pioglitazone and rosiglitazone, cells were stained for immunofluorescence using antibodies against MAP-2 for neurons, GFAP for astrocytes, and CNPase for immature oligodendrocytes. As shown in Fig. 7A,B, in control cultures only scattered cells stained with GFAP or MAP-2 were observed. After treatment with PPARγ ligands the number of MAP-2- and GFAP-positive cells was significantly increased specially in the outgrowth of the NS (see Fig. 7). An increase of the length of GFAP immunoreactive fibers was observed, with long processes extended from the NS (high magnification in figure 7A). Figure 7B also shows in detail an increase of the number of migrating MAP-2 positive cells outside the NS. On the other hand, the number of CNPase positive oligodendrocytes precursors was not significantly altered by either rosiglitazone or pioglitazone (data not shown). Addition of GW9662 completely abolished the effects of both compounds on differentiation.

DISCUSSION

Although its functional effect on brain damage has been recently investigated, there is almost no information about the effect that PPARγ activation has on neurogenesis in the adult brain. In the present study we used the TZD compound pioglitazone to demonstrate that PPARγ activation promotes proliferation, differentiation and migration of neuroblasts in the SVZ and RMS of adult rats. The results of this study demonstrate that PPARγ plays a role in regulating the expansion and differentiation of the stem cell population. This is evident *in vitro* by enhanced numbers of primary neurospheres and by rosiglitazone- and pioglitazone-mediated induction of $GFAP^+$ and $MAP2^+$ cells, and *in vivo* by an increased proliferation and a larger population of neuroblasts that finally integrate into the olfactory bulb as newly generated neurons. Enhancement of neural stem cells proliferation and differentiation by pioglitazone and rosiglitazone is possibly provoked by an activation of PPARγ, as demonstrated by the inhibition of their effects by the PPARγ antagonists GW9662 and T0070907. These studies reveal a novel role for PPARγ and may represent a potential therapeutic strategy for stem cell activation.

Neurogenesis can be regulated at multiple points, such as proliferation, differentiation, and migration, processes that are controlled by a number of extracellular signaling cues (Alvarez-Buylla and Lim 2004; Lie et al., 2004). The SVZ harbors the largest pool of proliferating cells in adult mammals (Lois and Alvarez-Buylla, 1993; Morshead et al., 1994). Pioglitazone-treatment increased cell proliferation in the SVZ and the RMS, as indicated by the changes in the number of BrdU-labeled cells after 3 days of pioglitazone treatment. We also present evidence that PPARγ activation induces expansion of highly migratory SVZ progenitors in the adult rat. The increased proliferation, neuroblast migration in the SVZ and RMS, and subsequent increase of newborn neurons incorporated within the OB can be relevant in olfactory-associated behavior. There is

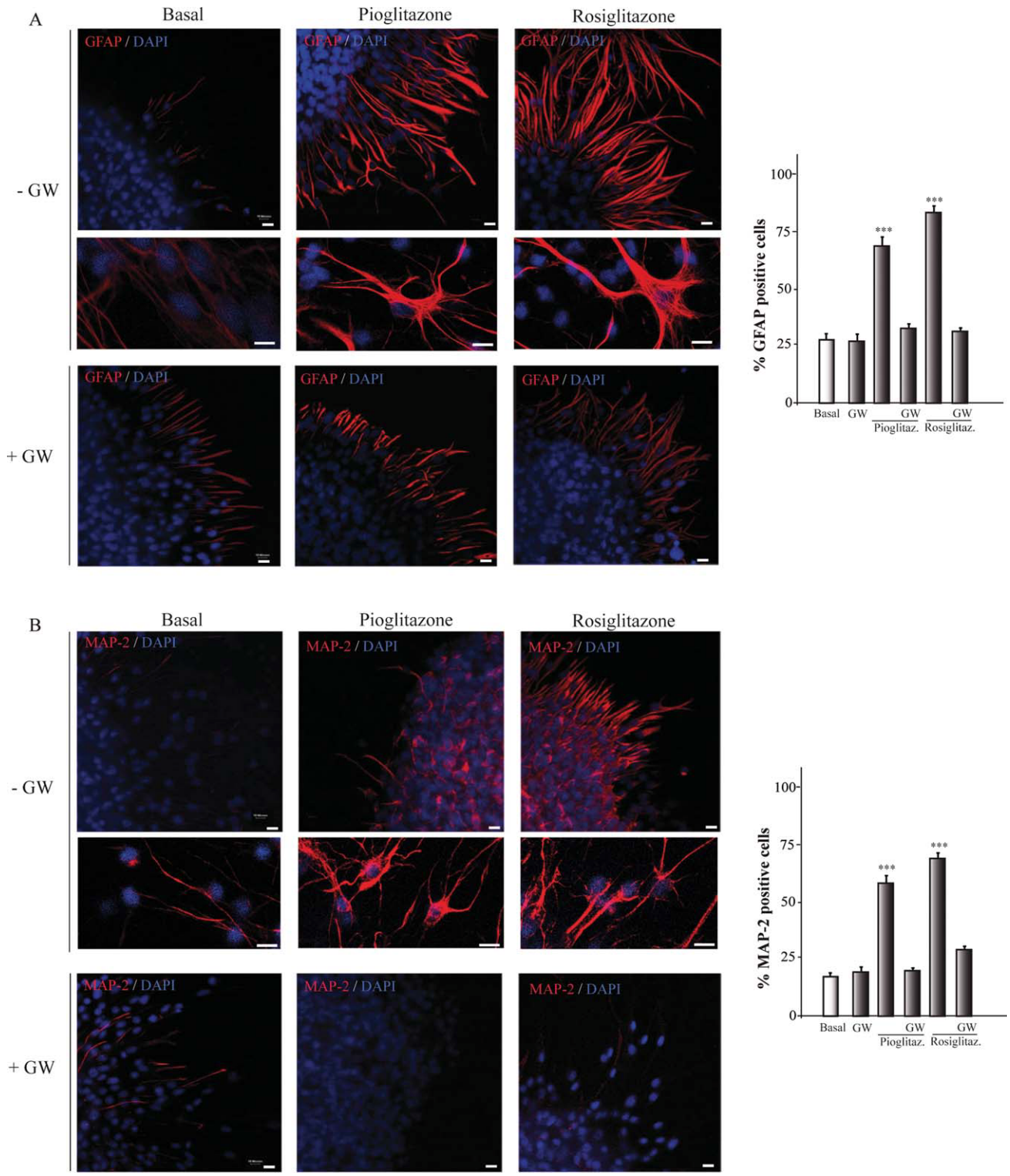

Fig. 7. Effect of PPARγ ligands on neurosphere differentiation. The neurospheres were grown for seven days in the presence or absence of pioglitazone (10 μM) or rosiglitazone (30 μM) and then adhered for two days to allow differentiation. Cultures were labeled with MAP-2 (red, for neuronal cells), or GFAP (red, for astrocytes) antibodies and counterstained with DAPI (blue). Some cultures were preincubated 1 h with 30 μM GW9662 (GW) prior to the addition of pioglitazone. Addition of pioglitazone enhanced the number of GFAP (**A**) and MAP2 (**B**) positive cells inside the neurosphere. High magnification pictures in A and B show in detail some of the GFAP- or MAP-2-immunoreactive cells migrated from the neurosphere in culture. Representative confocal images of at least five independent experiments are shown. Scale bars, 10 μm. $^{*}P \leq 0.05$; $^{***}P \leq 0.001$.

evidence that adult mice short term memory is dependent of neurogenesis. Mice housed in an odor-enriched environment showed an increased survival of progenitor cells in the OB as well as an enhanced olfactory short memory (Rochefort et al., 2002). On the other hand, chemical inhibition of neurogenesis with the antimitotic drug araC, drastically reduced short-term olfactory memory (Breton-Provencher et al., 2009). More recently, also long-term olfactory memory has been shown to be dependent of neurogenesis. Both neurogenesis and long term memory are impaired after treatment with antimitotic drugs and protein synthesis inhibitors (Kermen et al., 2010; Sultan et al., 2010). Irradiation-induced decrease in constitutive neurogenesis in the OB has been shown to decrease olfactory long-term memory but not other olfactory functions (Lazarini et al., 2009). Also, Mak and Weiss (Mak and Weiss, 2010) have shown that paternal-adult offspring recognition depends of OB neurogenesis and implicates prolactin signaling pathway (Mak and Weiss, 2010). Finally, it has been shown that chronic systemic inhibition of nitrite production increases proliferation in the subventricular zone and neurogenesis in the OB associated with a better olfactory learning performance (Romero-Grimaldi et al., 2006). Based on these data, together with our results, we could infer that pioglitazone -induced OB neurogenesis may improve olfactory-associated memory.

We observed large chains of neuroblasts far away from the SVZ, deep in the striatum. This effect reminds to that observed when mice where administered EGF with an intraventricular osmotic pump (Doetsch et al., 2002). Speaking of stimulating neurogenesis, the advantage of pioglitazone is that it can be administered intragastrically for a systemic effect. To our knowledge, this paper is the first direct demonstration of an involvement of PPARγ in the proliferation, migration, and differentiation of neural progenitor cells. Regarding the possible mechanism of action through which PPARγ regulates neural stem cell proliferation and differentiation, since this receptor is a transcription factor we favor the idea that this regulation takes place through direct activation of some genes involved in these processes (Mu et al., 2010).

The data obtained here also show that activation of PPARγ also stimulates neural progenitor cell proliferation in neurospheres *in vitro*. Our results suggest that PPARγ may regulate neural stem cell number by regulating the type of cell division. The formation of secondary neurospheres from primary neurospheres is indicative of self-renewing stem cell division (Reynolds and Weiss, 1996). The higher number of secondary neurospheres in pioglitazone- and rosiglitazone-treated NS cultures, indicate that the neural stem cells generated in presence of these factors underwent a higher proportion of self-renewing or symmetric cell divisions, leading to an expansion of the stem cell pool. This lends support to the view that PPARγ activation might stimulate the capability to maintain stemness.

Neural stem cells differentiate into neurons, astrocytes and oligodendrocytes (Gage, 2000; Temple, 2001). Here, we show that PPARγ is involved in the control of neural stem cell differentiation. Our results indicate that activation of PPARγ causes neural stem cells to differentiate into astrocytes and neurons. The finding that rosiglitazone and pioglitazone are able to induce differentiation of NS cells differs from a previous report indicating that rosiglitazone induced proliferation of embryonic mouse NS cells and concurrently inhibited their differentiation into neurons (Wada et al., 2006b). This discrepancy may simply reflect methodological differences in isolating neural stem cells or different experimental conditions. Additionally, our work was performed with neurospheres isolated from the SVZ of adult rats, whereas the neurospheres by Wada et al. came from whole brain of mice embryos on days 13-14 of gestation, where other factors might be involved.

Our work shows that PPARγ activation has a dual function in neural stem cells proliferation and differentiation, and suggests that ligands of PPARγ are not only mitogens for neural stem cells, but are also inducers of neuronal differentiation. It seems interesting that activation of PPARγ can promote both proliferation and differentiation. However, precedents for this phenomenon are seen in the case of insulin-like growth factor 1 (Arsenijevic and Weiss, 1998) and leukotriene B4 (Wada et al., 2006a). In this respect, we suggest that PPARγ can present a new strategy for restoring neurogenesis.

Cell division in the SVZ is responsible for new neurons being added to the granular and the periglomerular layers of the olfactory bulb. These cells migrate through the RMS, where the majority disperses throughout the granule layer and a small percentage develops into interneurons in the periglomerular layer (Altman, 1969; Doetsch et al., 1997; Lois and Alvarez-Buylla, 1994). The identification of factors that promote neural stem cell division and regulate proliferation, differentiation, and migration of their progeny would facilitate attempts to manipulate the production of new neurons and glia and help in understanding the ongoing maintenance of neural circuitry in the mature central nervous system. Here, we demonstrate an increased capacity of migration of neurosphere-derived cells in response to both pioglitazone and rosiglitazone. This is especially important in a clinical setting since the identification of factors that not only promote neural stem cells proliferation and differentiation but also have a significant effect on their migration capacity might have an important regulatory role in SVZ migratory events in a brain injury context. One important finding in this study is that activation of PPARγ is required for the observed effects of rosiglitazone and pioglitazone. These results lend support to the view that activation of this receptor can have an important regulatory role in neurogenesis in the normal brain as well as after a brain injury or a neurodegenerative disease. In contrast with this, very recently Lee et al. have shown that oral administration of rosiglitazone decreases neurogenesis in the mouse hippocampus (Lee et al., 2010). The reasons for this discrepancy are uncertain, although it could be due to an indirect effect of the long treatment with rosiglitazone

since it is well established that this drug, in contrast with pioglitazone, does not cross the blood brain barrier (Brodbeck et al., 2008; Landreth et al., 2008; Pedersen et al., 2006; Risner et al., 2006; Watson et al., 2005).

In summary these studies clearly demonstrate that ligands of PPARγ play a versatile role, both in maintaining the progenitor pools and in inducing differentiation and migration of various cell types in the central nervous system through activation of this receptor.

ACKNOWLEDGMENTS

This work was supported by the Ministerio de Educacion y Ciencia [SAF2007-62811 to A.P.-C and SAF2008-01274 to J.M.G.-V.] J.A.M-G. is a post-doctoral fellow of Centro de Investigación Biomédica en Red sobre Enfermedades Neurodegenerativas, founded by the Instituto de Salud Carlos III.

REFERENCES

Abdelrahman M, Sivarajah A, Thiemermann C. 2005. Beneficial effects of PPAR-gamma ligands in ischemia-reperfusion injury, inflammation and shock. Cardiovascular Res 65:772–781.

Altman J. 1969. Autoradiographic and histological studies of postnatal neurogenesis. III. Dating the time of production and onset of differentiation of cerebellar microneurons in rats. J Comp Neurol 136:269–293.

Alvarez-Buylla A, Lim DA. 2004. For the long run: Maintaining germinal niches in the adult brain. Neuron 41:683–686.

Anderson MF, Aberg MA, Nilsson M, Eriksson PS. 2002. Insulin-like growth factor-I and neurogenesis in the adult mammalian brain. Brain Res Dev Brain Res 134(1-2):115–122.

Arsenijevic Y, Weiss S. 1998. Insulin-like growth factor-I is a differentiation factor for postmitotic CNS stem cell-derived neuronal precursors: Distinct actions from those of brain-derived neurotrophic factor. J Neurosci 18:2118–2128.

Bartlett PF, Richards LR, Kilpatrick TJ, Talman PT, Bailey KA, Brooker GJ, Dutton R, Koblar SA, Nurcombe V, Ford MO, et al. 1995. Factors regulating the differentiation of neural precursors in the forebrain. Ciba Found Symp 193:85–99; discussion 117–126.

Bernardo A, Levi G, Minghetti L. 2000. Role of the peroxisome proliferator-activated receptor-gamma (PPAR-gamma) and its natural ligand 15-deoxy-Delta12, 14-prostaglandin J2 in the regulation of microglial functions. Eur J Neurosci 12:2215–2223.

Blaschke F, Takata Y, Caglayan E, Law RE, Hsueh WA. 2006. Obesity, peroxisome proliferator-activated receptor, and atherosclerosis in type 2 diabetes. Arteriosclerosis, thrombosis, and vascular biology 26:28–40.

Breidert T, Callebert J, Heneka MT, Landreth G, Launay JM, Hirsch EC. 2002. Protective action of the peroxisome proliferator-activated receptor-gamma agonist pioglitazone in a mouse model of Parkinson's disease. J Neurochem 82:615–624.

Breton-Provencher V, Lemasson M, Peralta MR III, Saghatelyan A. 2009. Interneurons produced in adulthood are required for the normal functioning of the olfactory bulb network and for the execution of selected olfactory behaviors. J Neurosci 29:15245–15257.

Brodbeck J, Balestra ME, Saunders AM, Roses AD, Mahley RW, Huang Y. 2008. Rosiglitazone increases dendritic spine density and rescues spine loss caused by apolipoprotein E4 in primary cortical neurons. Proc Natl Acad Sci USA 105:1343–1346.

Brown JP, Couillard-Despres S, Cooper-Kuhn CM, Winkler J, Aigner L, Kuhn HG. 2003. Transient expression of doublecortin during adult neurogenesis. J Comp Neurol 467:1–10.

Brown KK, Henke BR, Blanchard SG, Cobb JE, Mook R, Kaldor I, Kliewer SA, Lehmann JM, Lenhard JM, Harrington WW, others. 1999. A novel N-aryl tyrosine activator of peroxisome proliferator-activated receptor-gamma reverses the diabetic phenotype of the Zucker diabetic fatty rat. Diabetes 48:1415–1424.

Couillard-Despres S, Winner B, Schaubeck S, Aigner R, Vroemen M, Weidner N, Bogdahn U, Winkler J, Kuhn HG, Aigner L. 2005. Doublecortin expression levels in adult brain reflect neurogenesis. Eur J Neurosci 21:1–14.

Danilov AI, Gomes-Leal W, Ahlenius H, Kokaia Z, Carlemalm E, Lindvall O. 2009. Ultrastructural and antigenic properties of neural stem cells and their progeny in adult rat subventricular zone. Glia 57:136–152.

Debril MB, Renaud JP, Fajas L, Auwerx J. 2001. The pleiotropic functions of peroxisome proliferator-activated receptor gamma. J Mol Med 79:30–47.

Desvergne B, Wahli W. 1999. Peroxisome proliferator-activated receptors: Nuclear control of metabolism. Endocr Rev 20:649–688.

Doetsch F, Alvarez-Buylla A. 1996. Network of tangential pathways for neuronal migration in adult mammalian brain. Proc Natl Acad Sci USA 93:14895–14900.

Doetsch F, Garcia-Verdugo JM, Alvarez-Buylla A. 1997. Cellular composition and three-dimensional organization of the subventricular germinal zone in the adult mammalian brain. J Neurosci 17:5046–5061.

Doetsch F, Petreanu L, Caille I, Garcia-Verdugo JM, Alvarez-Buylla A. 2002. EGF converts transit-amplifying neurogenic precursors in the adult brain into multipotent stem cells. Neuron 36:1021–1034.

Dreyer C, Krey G, Keller H, Givel F, Helftenbein G, Wahli W. 1992. Control of the peroxisomal beta-oxidation pathway by a novel family of nuclear hormone receptors. Cell 68:879–887.

Ferron SR, Andreu-Agullo C, Mira H, Sanchez P, Marques-Torrejon MA, Farinas I. 2007. A combined ex/in vivo assay to detect effects of exogenously added factors in neural stem cells. Nat Protoc 2:849–859.

Forman BM, Tontonoz P, Chen J, Brun RP, Spiegelman BM, Evans RM. 1995. 15-Deoxy-delta 12, 14-prostaglandin J2 is a ligand for the adipocyte determination factor PPAR gamma. Cell 83:803–812.

Gage FH. 2000. Mammalian neural stem cells. Science 287:1433–1438.

Gage FH, Kempermann G, Palmer TD, Peterson DA, Ray J. 1998. Multipotent progenitor cells in the adult dentate gyrus. J Neurobiol 36:249–266.

Hack MA, Saghatelyan A, de Chevigny A, Pfeifer A, Ashery-Padan R, Lledo PM, Gotz M. 2005. Neuronal fate determinants of adult olfactory bulb neurogenesis. Nat Neurosci 8:865–872.

Heneka MT, Landreth GE. 2007. PPARs in the brain. Biochimica et biophysica acta 1771:1031–1045.

Heneka MT, Sastre M, Dumitrescu-Ozimek L, Hanke A, Dewachter I, Kuiperi C, O'Banion K, Klockgether T, Van Leuven F, Landreth GE. 2005. Acute treatment with the PPARgamma agonist pioglitazone and ibuprofen reduces glial inflammation and Abeta1-42 levels in APPV717I transgenic mice. Brain 128(Part 6):1442–1453.

Ji S, Kronenberg G, Balkaya M, Farber K, Gertz K, Kettenmann H, Endres M. 2009. Acute neuroprotection by pioglitazone after mild brain ischemia without effect on long-term outcome. Exp Neurol 216:321–328.

Jiang C, Ting AT, Seed B. 1998. PPAR-gamma agonists inhibit production of monocyte inflammatory cytokines. Nature 391:82–86.

Johe KK, Hazel TG, Muller T, Dugich-Djordjevic MM, McKay RD. 1996. Single factors direct the differentiation of stem cells from the fetal and adult central nervous system. Genes Dev 10:3129–3140.

Kermen F, Sultan S, Sacquet J, Mandairon N, Didier A. 2010. Consolidation of an olfactory memory trace in the olfactory bulb is required for learning-induced survival of adult-born neurons and long-term memory. PLoS One 5:e12118.

Kielian T, Drew PD. 2003. Effects of peroxisome proliferator-activated receptor-gamma agonists on central nervous system inflammation. J Neurosci Res 71:315–325.

Kliewer SA, Forman BM, Blumberg B, Ong ES, Borgmeyer U, Mangelsdorf DJ, Umesono K, Evans RM. 1994. Differential expression and activation of a family of murine peroxisome proliferator-activated receptors. Proc Natl Acad Sci USA 91:7355–7359.

Kohwi M, Osumi N, Rubenstein JL, Alvarez-Buylla A. 2005. Pax6 is required for making specific subpopulations of granule and periglomerular neurons in the olfactory bulb. J Neurosci 25:6997–7003.

Landreth G, Jiang Q, Mandrekar S, Heneka M. 2008. PPARgamma agonists as therapeutics for the treatment of Alzheimer's disease. Neurotherapeutics 5:481–489.

Landreth GE, Heneka MT. 2001. Anti-inflammatory actions of peroxisome proliferator-activated receptor gamma agonists in Alzheimer's disease. Neurobiol Aging 22:937–944.

Larsen MH, Rosenbrock H, Sams-Dodd F, Mikkelsen JD. 2007. Expression of brain derived neurotrophic factor, activity-regulated cytoskeleton protein mRNA, and enhancement of adult hippocampal neurogenesis in rats after sub-chronic and chronic treatment with the triple monoamine re-uptake inhibitor tesofensine. Eur J Pharmacol 555(2-3):115–121.

Lee CH, Choi JH, Yoo KY, Park OK, Moon JB, Sohn Y, Cho JH, Hwang IK, Won MH. 2010. Rosiglitazone, an agonist of peroxisome proliferator-activated receptor gamma, decreases immunoreactivity of

markers for cell proliferation and neuronal differentiation in the mouse hippocampus. Brain Res 1329:30–35.
Lie DC, Song H, Colamarino SA, Ming GL, Gage FH. 2004. Neurogenesis in the adult brain: New strategies for central nervous system diseases. Annu Rev Pharmacol Toxicol 44:399–421.
Lim DA, Tramontin AD, Trevejo JM, Herrera DG, Garcia-Verdugo JM, Alvarez-Buylla A. 2000. Noggin antagonizes BMP signaling to create a niche for adult neurogenesis. Neuron 28:713–726.
Lois C, Alvarez-Buylla A. 1993. Proliferating subventricular zone cells in the adult mammalian forebrain can differentiate into neurons and glia. Proc Natl Acad Sci USA 90:2074–2077.
Lois C, Alvarez-Buylla A. 1994. Long-distance neuronal migration in the adult mammalian brain. Science 264:1145–1148.
Luna-Medina R, Cortes-Canteli M, Alonso M, Santos A, Martinez A, Perez-Castillo A. 2005. Regulation of inflammatory response in neural cells in vitro by thiadiazolidinones derivatives through peroxisome proliferator-activated receptor γ activation. J Biol Chem 280:21453–21462.
Luna-Medina R, Cortes-Canteli M, Morales-Garcia JA, Martinez A, Santos A, Perez-Castillo A. 2007a. Effect of GSK-3β inhibition on neural stem cell proliferation and differentiation. In: Neurochemistry Jo, editor. Salamanca, Spain. Oxford ox4 2dq, Oxon, England: Blackwell Publishing, 9600 Garsington Rd. p56.
Luna-Medina R, Cortes-Canteli M, Sanchez-Galiano S, Morales-Garcia JA, Martinez A, Santos A, Perez-Castillo A. 2007b. NP031112, a thiadiazolidinone compound, prevents inflammation and neurodegeneration under excitotoxic conditions: Potential therapeutic role in brain disorders. J Neurosci 27:5766–5776.
Luskin MB, Zigova T, Soteres BJ, Stewart RR. 1997. Neuronal progenitor cells derived from the anterior subventricular zone of the neonatal rat forebrain continue to proliferate in vitro and express a neuronal phenotype. Mol Cell Neurosci 8:351–366.
Lutolf S, Radtke F, Aguet M, Suter U, Taylor V. 2002. Notch1 is required for neuronal and glial differentiation in the cerebellum. Development 129:373–385.
Mak GK, Weiss S. 2010. Paternal recognition of adult offspring mediated by newly generated CNS neurons. Nat Neurosci 13:753–758.
Michalik L, Auwerx J, Berger JP, Chatterjee VK, Glass CK, Gonzalez FJ, Grimaldi PA, Kadowaki T, Lazar MA, O'Rahilly S, et al. 2006. International Union of Pharmacology. LXI. Peroxisome proliferator-activated receptors. Pharmacol Rev 58:726–741.
Morshead CM, Reynolds BA, Craig CG, McBurney MW, Staines WA, Morassutti D, Weiss S, van der Kooy D. 1994. Neural stem cells in the adult mammalian forebrain: A relatively quiescent subpopulation of subependymal cells. Neuron 13:1071–1082.
Mu Y, Lee SW, Gage FH. 2010. Signaling in adult neurogenesis. Curr Opin Neurobiol 20:416–423
Ostenfeld T, Svendsen CN. 2003. Recent advances in stem cell neurobiology. Adv Tech Stand Neurosurg 28:3–89.
Parras CM, Galli R, Britz O, Soares S, Galichet C, Battiste J, Johnson JE, Nakafuku M, Vescovi A, Guillemot F. 2004. Mash1 specifies neurons and oligodendrocytes in the postnatal brain. EMBO J 23:4495–4505.
Paruchuri S, Jiang Y, Feng C, Francis SA, Plutzky J, Boyce JA. 2008. Leukotriene E4 activates peroxisome proliferator-activated receptor gamma and induces prostaglandin D2 generation by human mast cells. J Biol Chem 283:16477–16487.
Pedersen WA, McMillan PJ, Kulstad JJ, Leverenz JB, Craft S, Haynatzki GR. 2006. Rosiglitazone attenuates learning and memory deficits in Tg2576 Alzheimer mice. Exp Neurol 199:265–273.
Peiris M, Monteith GR, Roberts-Thomson SJ, Cabot PJ. 2007. A model of experimental autoimmune encephalomyelitis (EAE) in C57BL/6 mice for the characterisation of intervention therapies. J Neurosci Methods 163:245–254.
Reynolds BA, Weiss S. 1996. Clonal and population analyses demonstrate that an EGF-responsive mammalian embryonic CNS precursor is a stem cell. Dev Biol 175:1–13.
Ricote M, Huang JT, Welch JS, Glass CK. 1999. The peroxisome proliferator-activated receptor(PPARgamma) as a regulator of monocyte/macrophage function. J Leukoc Biol 66:733–739.
Risner ME, Saunders AM, Altman JF, Ormandy GC, Craft S, Foley IM, Zvartau-Hind ME, Hosford DA, Roses AD. 2006. Efficacy of rosiglitazone in a genetically defined population with mild-to-moderate Alzheimer's disease. Pharmacogenomics J 6:246–254.
Rochefort C, Gheusi G, Vincent JD, Lledo PM. 2002. Enriched odor exposure increases the number of newborn neurons in the adult olfactory bulb and improves odor memory. J Neurosci 22:2679–2689.
Romero-Grimaldi C, Gheusi G, Lledo PM, Estrada C. 2006. Chronic inhibition of nitric oxide synthesis enhances both subventricular zone neurogenesis and olfactory learning in adult mice. Eur J Neurosci 24:2461–2470.
Rosen ED, Spiegelman BM. 2001. PPARgamma: A nuclear regulator of metabolism, differentiation, and cell growth. J Biol Chem 276:37731–37734.
Saitoh Y, Liu R, Ueno H, Mizuta M, Nakazato M. 2007. Oral pioglitazone administration increases food intake through ghrelin-independent pathway in Zucker fatty rat. Diabetes Res Clin Pract 77:351–356.
Schmerbach K, Schefe JH, Krikov M, Muller S, Villringer A, Kintscher U, Unger T, Thoene-Reineke C. 2008. Comparison between single and combined treatment with candesartan and pioglitazone following transient focal ischemia in rat brain. Brain Res 1208:225–233.
Sultan S, Mandairon N, Kermen F, Garcia S, Sacquet J, Didier A. 2010. Learning-dependent neurogenesis in the olfactory bulb determines long-term olfactory memory. FASEB J 24:2355–2363.
Szeles L, Torocsik D, Nagy L. 2007. PPARgamma in immunity and inflammation: cell types and diseases. Biochimica et biophysica acta 1771:1014–1030.
Temple S. 2001. The development of neural stem cells. Nature 414:112–117.
Tontonoz P, Hu E, Spiegelman BM. 1994. Stimulation of adipogenesis in fibroblasts by PPAR gamma 2, a lipid-activated transcription factor. Cell 79:1147–1156.
Townsend KP, Pratico D. 2005. Novel therapeutic opportunities for Alzheimer's disease: Focus on nonsteroidal anti-inflammatory drugs. FASEB J 19:1592–1601.
Wada K, Arita M, Nakajima A, Katayama K, Kudo C, Kamisaki Y, Serhan CN. 2006a. Leukotriene B4 and lipoxin A4 are regulatory signals for neural stem cell proliferation and differentiation. FASEB J 20: 1785–1792.
Wada K, Nakajima A, Katayama K, Kudo C, Shibuya A, Kubota N, Terauchi Y, Tachibana M, Miyoshi H, Kamisaki Y, et al. 2006b. Peroxisome proliferator-activated receptor gamma-mediated regulation of neural stem cell proliferation and differentiation. J Biol Chem 281:12673–12681.
Watson GS, Cholerton BA, Reger MA, Baker LD, Plymate SR, Asthana S, Fishel MA, Kulstad JJ, Green PS, Cook DG, et al. 2005. Preserved cognition in patients with early Alzheimer disease and amnestic mild cognitive impairment during treatment with rosiglitazone: A preliminary study. Am J Geriatr Psychiatry 13:950–958.
Winner B, Cooper-Kuhn CM, Aigner R, Winkler J, Kuhn HG. 2002. Long-term survival and cell death of newly generated neurons in the adult rat olfactory bulb. Eur J Neurosci 16:1681–1689.

Journal of Neuroscience Research 87:3687–3696 (2009)

Anticonvulsant and Neuroprotective Effects of the Novel Calcium Antagonist NP04634 on Kainic Acid-Induced Seizures in Rats

Jose A. Morales-Garcia,[1] Rosario Luna-Medina,[1] Ana Martinez,[2] Angel Santos,[3]⋆ and Ana Perez-Castillo[1]⋆

[1]Instituto de Investigaciones Biomédicas, Consejo Superior de Investigaciones Científicas-Universidad Autónoma de Madrid, and Centro de Investigación Biomédica en Red sobre Enfermedades Neurodegenerativas (CIBERNED), Madrid, Spain
[2]Neuropharma, S.A., Madrid, Spain
[3]Departamento de Bioquímica y Biología Molecular, Facultad de Medicina, Universidad Complutense de Madrid, Madrid, Spain

Kainic acid (KA)-induced status epilepticus (SE) is a well-characterized model of excitotoxic neuronal injury. Excitotoxicity results from activation of specific glutamate receptors, with resultant elevation of intracellular Ca^{2+}. The CA1 and CA3 subregions of the hippocampus are especially vulnerable to KA, and this pattern of neuronal injury resembles that occurring in patients with temporal lobe epilepsy. Calcium plays an essential role in excitotoxicity, and accordingly calcium channel inhibitors have been shown to have protective effects in various experimental models of epilepsy and brain injury. Moreover, they also potentiate the antiseizure efficacy of conventional antiepileptic drugs. This study was undertaken to determine whether NP04634, a novel compound, reported as a non-L-type voltage-sensitive calcium channel (VSCC) inhibitor, could prevent the entrance in SE and the neuronal loss evoked by intraperitoneal injection of KA. Our results show that intragastrical administration of NP04634 reduced the percentage of rats that entered SE after KA injection, increased the latency of SE entry, and significantly reduced the mortality of rats that entered SE. Also, NP04634 prevented the loss of hippocampal CA1 and CA3 pyramidal neurons and reduced the gliosis induced by KA. These results point to a potential anticonvulsant and neuroprotective role for NP04634.

Key words: excitotoxicity; hippocampus; kainic acid; neuroprotection; status epilepticus

Epilepsy is a common neurological disorder characterized by spontaneous recurrent seizures (Sander and Shorvon, 1996). Approximately 40% of epilepsies are acquired, meaning that the epileptic condition is acquired through an injury to the nervous system (de Graaf, 1974; Lothman et al., 1991; McNamara, 1994; DeLorenzo et al., 2005). Status epilepticus (SE) is a frequent cause of brain injury and is tightly associated with the development of epilepsy (de Graaf, 1974; Lothman et al., 1991; McNamara, 1994; Sander and Shorvon, 1996; DeLorenzo et al., 2005). SE is thought to damage neural cells through an increased liberation of excitatory amino acids, mostly glutamate, and the subsequent intense activation of ionotropic receptors (a phenomenon known as *excitoxicity*; Olney et al., 1986).

Systemic administration of the AMPA/kainate receptors agonist kainic acid (KA) is known to induce a sequence of altered behavioral events characterized by epileptiform seizures, which finally develop into SE (Ben-Ari et al., 1980; Sperk, 1994). This is followed by neurodegeneration in specific brain regions, such as the hippocampus, piriform cortex, thalamus, and amygdala. A well-characterized pattern of neurodegeneration in response to KA occurs in the hippocampus, where the CA3 pyramidal cells and interneurons in the hilus of dentate gyrus are the most vulnerable, followed by CA1 pyramidal cells (Coyle, 1983; Sperk et al., 1985; Tauck and Nadler, 1985). KA-induced neuronal death in vivo is due partially

The first two authors contributed equally to this work.

Ana Martinez's current address is Instituto de Química Médica, Consejo Superior de Investigaciones Científicas, 28029-Madrid, Spain

Contract grant sponsor: Ministerio de Educacion y Ciencia; Contract grant number: SAF2007-62811 (to A.P.-C); Contract grant sponsor: CIBERNED (CIBERNED is funded by the Instituto de Salud Carlos III; to J.M.-G.).

⋆Correspondence to: Ana Perez-Castillo, Instituto de Investigaciones Biomédicas, Consejo Superior de Investigaciones Científicas-Universidad Autónoma de Madrid, Arturo Duperier 4, 28029-Madrid, Spain.
E-mail: aperez@iib.uam.es or Angel Santos, Departamento de Bioquímica y Biología Molecular, Facultad de Medicina, Universidad Complutense, Madrid, Spain. E-mail: piedras3@med.ucm.es

Received 24 March 2009; Revised 8 May 2009; Accepted 19 May 2009

Published online 29 June 2009 in Wiley InterScience (www.interscience.wiley.com). DOI: 10.1002/jnr.22165

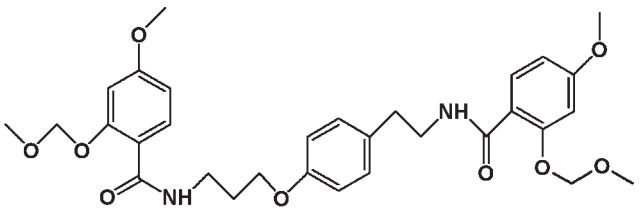

Fig. 1. Structure of the Ca^{2+} channel antagonist NP04634.

to the massive release of glutamate induced by this excitotoxin (Sperk, 1994), although in neurons in culture KA can directly induce cell death (Brorson et al., 1994; Courtney et al., 1995). Based on the similarities of these alterations to the clinical and neuropathological manifestations in humans, KA administration has been widely used as the animal model that mirrors aspects of human temporal lobe epilepsy (Nadler, 1981; Leite et al., 1990).

An essential event in excitotoxicity is the abnormal increase in intracellular calcium as a consequence of the activation of ionotropic glutamate receptors by the massive release of this neurotransmitter. Elevated free cytosolic calcium concentrations have been implicated in various cell death scenarios (Choi, 1988, 1994; Meldrum and Garthwaite, 1990; Doble, 1999; Wang et al., 2005) and in the development of epilepsy (Sombati and DeLorenzo, 1995; DeLorenzo et al., 1998; Pal et al., 1999; Sun et al., 2002). Calcium influx occurs largely through direct activation of NMDA receptors, which under sufficiently depolarized conditions become permeable to Ca^{2+}, and indirectly through voltage-sensitive calcium channels (VSCCs). In addition to this, intracellular calcium channels have been shown to contribute to the pathophysiological effects of calcium (Verkhratsky, 2005). VSCCs have been classified according to their protein structure and electrophysiological and pharmacological features into six different subtypes: P, Q, N, T, L, and R types (Dolphin, 2006; Khosravani and Zamponi, 2006).

Consistently with the excitotoxic hypothesis, calcium inhibitors have been shown to be potent neuroprotective and anticonvulsive agents and are known to potentiate the antiseizure efficacy of conventional antiepileptic drugs (Vezzani et al., 1988; De Sarro et al., 1988; Dolin et al., 1988; Czuczwar et al., 1990; Kaminski et al., 2001). N and P/Q VSCCs subtypes are located predominantly in nerve terminals and control various intracellular calcium-dependent events, such as neurotransmitter release. From these collective data, it could be inferred that inhibitors targeting these VSCC subtypes could be effective anticonvulsive and antiexcitotoxic compounds. In fact, blockage of these channels in experimental animals by specific peptide toxins has been shown to exert strong neuroprotective effects (Asakura et al., 1997; Huang et al., 1997; Lee et al., 2004) and may be useful for treating diverse neurological diseases, including ischemia, pain, and epilepsy (Cox, 2000; Lukyanetz et al., 2002; Miljanich, 2004; Takahara et al., 2004). However, these peptides are labile and usually do not cross the blood–brain barrier, so the synthesis of small molecules able to cross the blood–brain barrier and inhibit VSCC could lead to the development of new therapeutic products.

Here we have analyzed, in an in vivo excitotoxic model of brain injury, the possible anticonvulsive and neuroprotective effects of NP04634. This compound is a novel molecule, which has been reported to be a reversible antagonist of non-L-type VSCCs in bovine chromaffin cells (Valero et al., 2009; Fig. 1). Our results clearly demonstrate that NP04634-treated animals showed a diminished susceptibility to KA, which included an attenuation of seizure activity and a strong neuroprotective effect.

MATERIALS AND METHODS

Materials

NP04634 was obtained from Noscira (Tres Cantos, Madrid, Spain); kainic acid (KA) and general reagents were purchased from Sigma-Aldrich (St. Louis, MO). Stocks solutions of NP04634 were first dissolved in dimethylsulfoxide (DMSO) and then in phosphate-buffered saline (PBS) to the desired concentrations. Mouse anti-cd11b (OX-42) and anti-GFAP monoclonal antibodies were purchased from Serotec (Duesseldorf, Germany) and Sigma-Aldrich, respectively. Polyclonal anti-TNF-α and anti-COX-2 antibodies were from Santa Cruz Biotechnologies (Santa Cruz, CA).

Animals and Seizure Induction

Adult male Wistar rats (8–12 weeks old) were used in this study. The animals were divided into three groups. Group I rats (controls) were injected i.p. with normal saline and groups II and III with KA (10 mg/kg). Group III rats were pretreated with NP04634 (100 mg/kg BW, orally administered via an intragastric tube) 12 and 4 hr before KA injection. Groups I and II were pretreated with vehicle (PBS and DMSO mixture). Adequate measures were taken to minimize pain or discomfort of animals. Experiments were carried out in accordance with the European Communities Council, directive 86/609/EEC.

Behavioral observations were performed for a period of 4 hr. After KA injection, the animals were placed in individual plastic cages and monitored for 4 hr. Video recordings were made with a black-and-white video camera. The convulsive behavior was classified according to the accumulative scale of Racine and Sperk (Racine, 1972; Sperk et al., 1985) as follows: stage 0 = no changes; stage 0.5 = wet dog shakes (WDS); stage 1 = mouth and facial movements; stage 2 = head nodding; stage 3 = forelimbs clonus; stage 4 = rearing; stage 5 = rearing and falling; stage 6 = death. SE was defined as continuous or intermittent behavioral seizure activity without recovery of complete consciousness (stage 4–5) for at least 30 min. Behavioral seizures were scored by their latency (minutes) to onset of SE following KA injection. The number of WDS prior to SE was also counted.

Immunohistochemistry

Seventy-two hours after KA injection, the animals were anesthetized and perfused transcardially with 4% paraformalde-

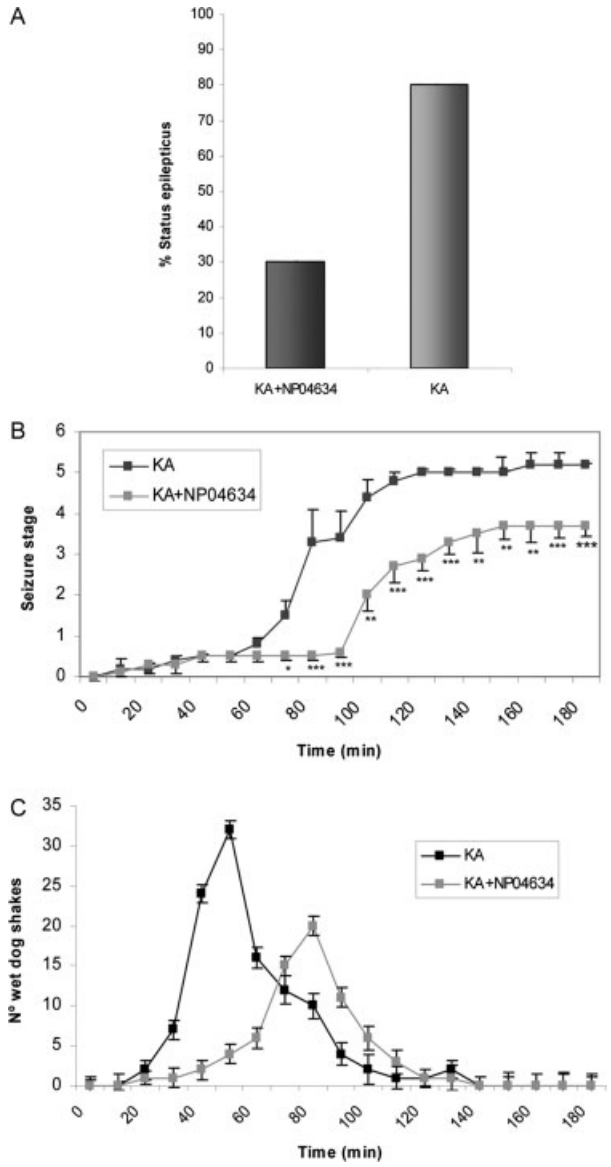

Fig. 2. Effect of NP04634 on behavioral activity after injection of KA. NP04634 (100 mg/kg) was administered intragastrically 12 and 4 hr before intraperitoneal injection of KA (10 mg/kg BW), and the behavioral activity was analyzed as indicated in Materials and Methods. Values represent the mean ± SE. **A:** Percentage of status epilepticus (SE; animals per group ≥ 25). In response to the same dose of KA, the percentage of rats that enter SE in the NP04634-treated group was nearly threefold less than that in the group injected only with KA. **B:** Effects of NP04634 on behavioral seizures induced by KA in rats. The data correspond to animals that entered SE (animals per group = 7). Animals that died during the experiment were assigned stage 6. $*P < 0.05$, $**P \leq 0.01$, and $***P \leq 0.001$. **C:** Comparison of the number of wet dog shakes prior to onset of SE. NP04634-treated rats exhibited a significantly lower total number of wet dog shakes prior to SE than KA-injected animals (animals per group ≥ 7).

hyde solution. The brains were removed, postfixed in the same solution at 4°C overnight, cryoprotected in the paraformaldehyde solution containing 30% sucrose, and frozen, and 30-μm coronal sections were obtained in a cryostat. Free-floating sections were processed for cresyl violet (Nissl stain) or immunohistochemistry with the diaminobenzidine method. Floating sections were immersed for 15 min in 3% H_2O_2 to inactivate endogenous peroxidase and then blocked for 2 hr at room temperature (RT) in 5% normal goat serum (NGS; Vector, Burlingame, CA) in phosphate-buffered saline, containing 4% bovine serum albumin, 0.1 M lysine, and 0.1% Triton X-100. Afterward, the sections were incubated overnight with the corresponding primary antibodies. After several rinses, sections were incubated for 1 hr with a biotinylated secondary antibody. Finally, the sections were processed following the avidin-biotin protocol (ABC Vectastain kit; Vector). Tissues were mounted onto gelatin-coated slides and allowed to dry. Finally, the slides were dehydrated, cleared in xylene, and mounted with DePeX (Serva, Heidelberg, Germany). The slides were examined with a Zeiss Axiophot microscope (equipped with an Olympus DP-50 digital camera) and a Leica MZ6 modular stereomicroscope. Neuronal integrity was assessed by counting the percentage of Nissl-positive cells in the hilus, CA1, and CA3 regions of the hippocampus in five independent, well-defined high-magnification (×400) fields per animal using computer-assisted image analySIS software (Soft Imaging System). The extent of microgliosis was quantified by counting the number of OX-42-positive cells in five independent, well-defined high-magnification (×400) fields per animal, as described above. To evaluate astrogliosis, two different parameters were quantified: number of activated cells, based on the calculation of highly immunostained cell body profiles, and immunosignal intensity, based on the measurement of optical density. Individual cell bodies were manually traced, and their mean staining intensity was normalized against the background of the section, defined as tissue devoid of specific immunostaining. The procedure resulted in arbitrary values on a scale from 1 (background staining) to 256.

Fluoro-Jade Staining

To evaluate neuronal degeneration, Fluoro-Jade B staining was used (Schmued et al., 1997). The sections were mounted on gelatin-coated slides and then dried at RT. After that, the slides were immersed in 100% alcohol, followed by 70% alcohol and distilled water. Then, the slides were incubated shaking gently for 15 min in 0.06% potassium permanganate solution followed by 30 min in dark in the staining solution (0.001% Fluoro-Jade B dye; Chemicon, Temecula, CA). After staining, the sections were rinsed in distilled water, and when dried, immersed in xylene and mounted with DePeX (Serva). Images were analyzed by confocal microscope, as detailed above.

Primary Cultures of Glial Cells

Rat primary cell cultures were established as previously described (Luna-Medina et al., 2005). Astrocytes were prepared from neonatal (P2) rat cerebral cortex. Briefly, after removal of the meninges, the cerebral cortex was dissected, dissociated, and incubated with 0.25% trypsin/EDTA at 37°C for 1 hr. After centrifugation, the pellet was washed three times with HBSS (Gibco, Grand Island, NY), and the cells were plated on non-coated flasks and maintained in Ham's/DMEM (1:1) containing

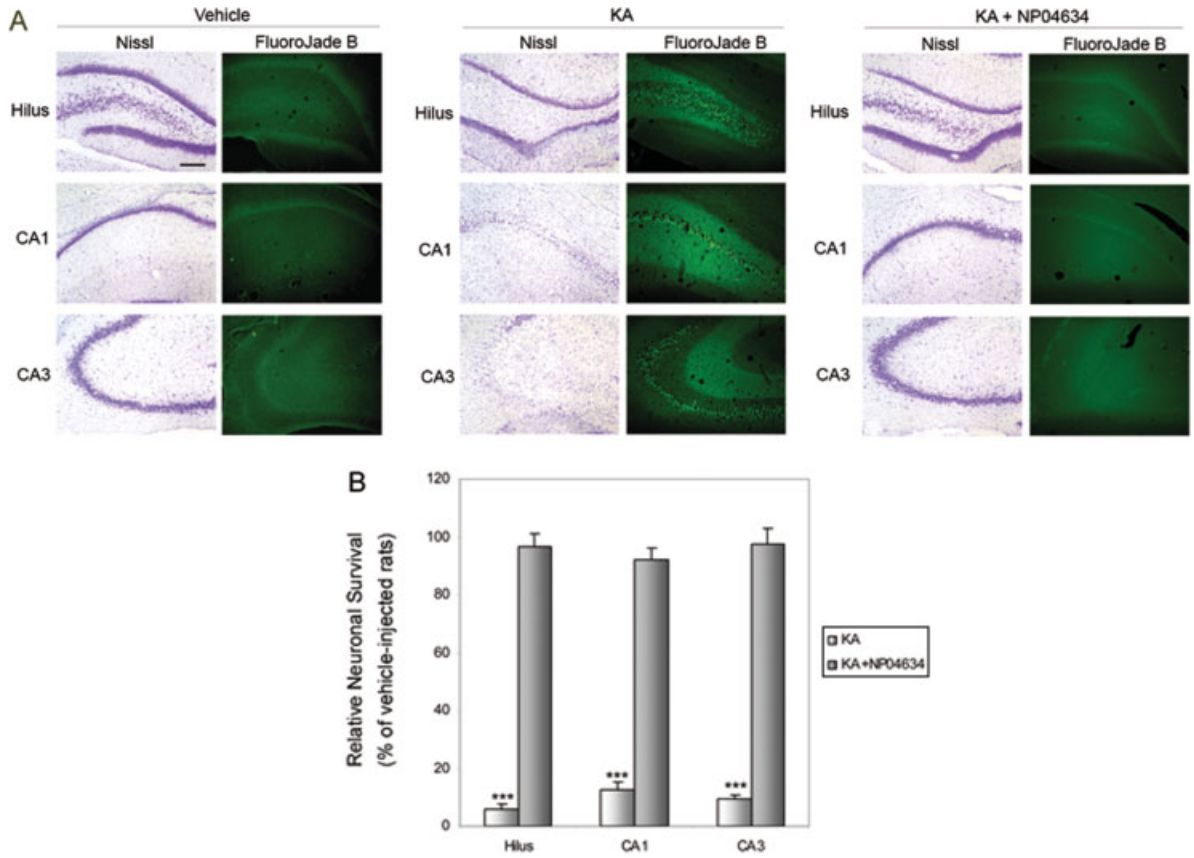

Fig. 3. Effect of NP04634 treatment on KA-induced neuronal damage. **A:** Rats were injected with KA or with KA and previously pretreated with NP04634 and sacrificed 72 hr postinjection. Coronal sections (30 μm) were stained with Fluoro-Jade B and Nissl. NP04634-treated rats exhibited virtually no detectable neuronal degeneration, as detected by Fluoro-Jade B staining, and a negligible loss of neurons in the hilus, CA1, and CA3 regions, as shown by Nissl staining, compared with KA-injected rats. **B:** Extent of neuronal damage in the hilus, CA1, and CA3 areas of the hippocampus was quantified as described in Materials and Methods. Data were normalized against the mean values from vehicle-injected rats. Values represent the mean ± SD from five different animals that entered SE and five independent sections per animal. $^{***}P \leq 0.001$ vs. vehicle-injected rats at each time point. Scale bar = 10 μm. [Color figure can be viewed in the online issue, which is available at www.interscience.wiley.com.]

10% FBS. After 15 days, the flasks were agitated on an orbital shaker for 12 hr at 250 rpm at 37°C, and the nonadherent oligodendrocytes and microglial cells were removed. After 7 days, the flasks were agitated again to remove any remaining microglia cells and then trypsinized and expanded at a 1:5 ratio in complete medium. The purity of the cultures was >95%, as determined by immunofluorescence analysis using anti-GFAP to identify astrocytes. NP04634 (25 μM) was added to the culture medium of astrocytes 1 hr before exposure to lipopolysaccharide (LPS; 10 μg/ml), and cells were harvested 24 hr later for evaluation of tumor necrosis factor-α (TNF-α) and cyclooxygenase type 2 (COX-2) expression.

Immunocytochemistry

At the end of the treatment period, the cultures, grown on glass coverslips in 24-well cell culture plates, were washed with phosphate-buffered saline and fixed for 30 min with 4% paraformaldehyde at 25°C and permeabilized with 0.1% Triton X-100 for 30 min at 37°C. After 1 hr of incubation with the corresponding primary antibody, cells were washed with PBS and incubated with an Alexa-labeled secondary antibody (Molecular Probes, Leiden, The Netherlands) for 45 min at 37°C. Images were acquired using a Radiance 2100 confocal microscope (Bio-Rad, Hercules, CA), with a 350-nm diode laser to excite DAPI and a 647-nm laser line to excite Alexa 647. Confocal microscope settings were adjusted to produce the optimal signal-to-noise ratio. To compare fluorescence signals from different preparations, settings were fixed for all samples within the same analysis. Fluorescence analysis was performed in LaserPix software (Bio-Rad). A quantitative analysis of labeled cells was undertaken in the image analySIS software and normalized to total nuclei. Areas to be counted were traced at high power (×400), and at least five different counting fields were selected at random per culture.

Statistical Analysis

Statistical comparisons for significance among the different groups of animals were performed by ANOVA followed by Newman-Keuls' test for multiple comparisons. $P \leq 0.05$ was considered to be statistically significant. Statistical comparisons for significance between cells were performed via Stu-

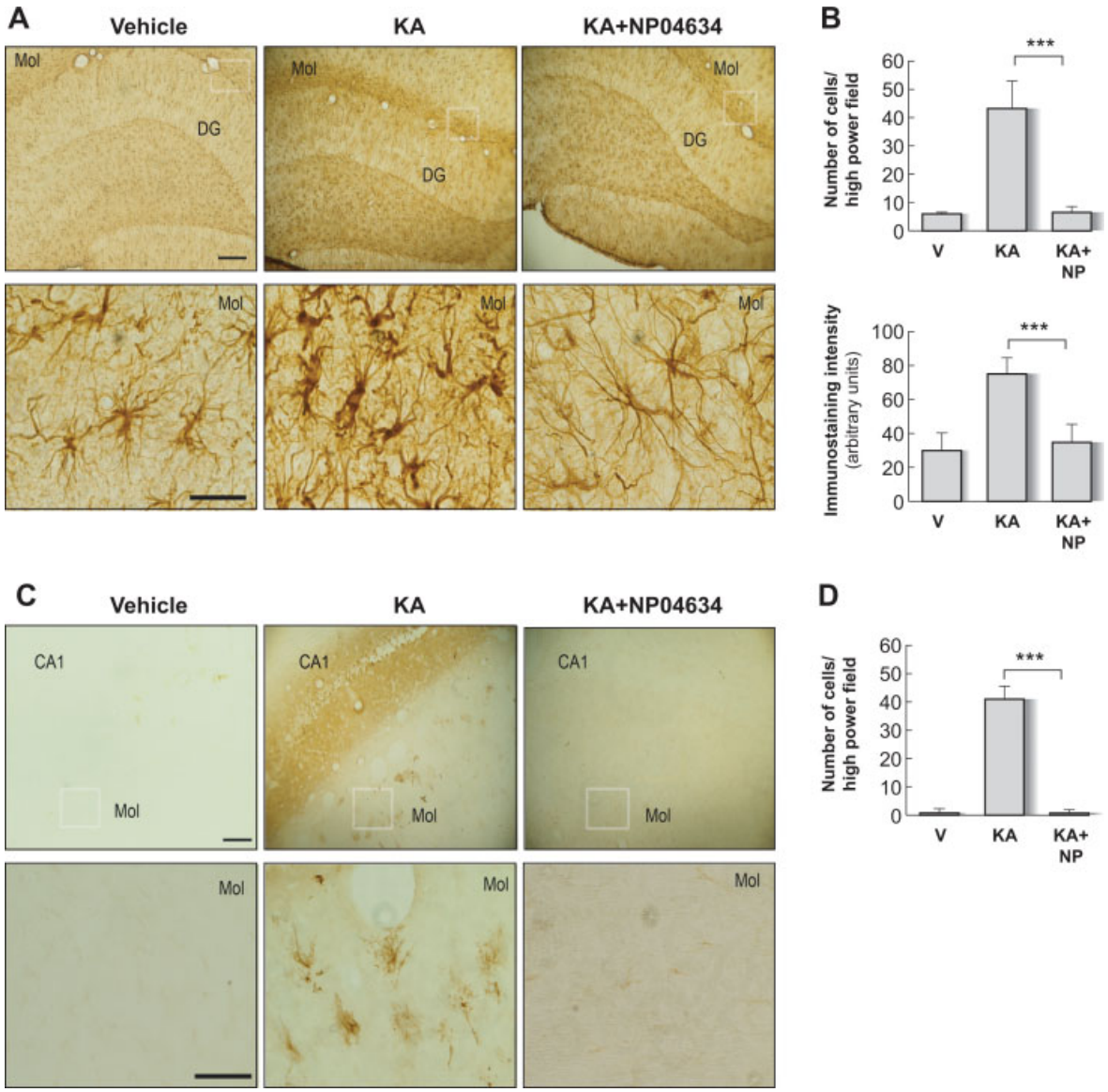

Fig. 4. Effect of NP04634 on KA-induced gliosis. Rats were injected with KA or with KA and previously pretreated with NP04634 (NP) and sacrificed 72 hr postinjection. Coronal sections (30 μm) were stained with mouse monoclonal antibodies directed against either GFAP (**A**) or CD11b (OX-42; **C**) to detect astrocytes or microglial cells, respectively. **Insets** ×1,000. A significant decrease in gliosis was observed in the group treated with NP04634. **B:** Quantification of the number of reactive astrocytes and their mean immunostaining intensity evaluated in the molecular layer of the hippocampus. **D:** Quantification of the number of reactive microglial cells. Values represent the mean ± SD from five different animals and five independent sections per animal. ***$P \leq 0.001$. [Color figure can be viewed in the online issue, which is available at www.interscience.wiley.com.]

dent's test, with $P \leq 0.05$. Data are given as the mean ± SD (Figs. 3–5) or mean ± SE (Fig. 2).

RESULTS

Effect of NP04634 on Convulsive Activity Induced by KA Injection

As expected, KA administration (10 mg/kg BW) induced SE in ~80% of rats. In contrast, this percentage decreased to 30% when the rats were previously treated with NP04634 (Fig. 2A). Also, intragastrical administration of NP04634 both increased the latency of SE entry and reduced the apparent severity of seizures. Specifically, the mean latency for KA-injected rats to SE onset was 84.6 ± 10.5 min, whereas the latency for NP04634-treated rats was approximately two times longer (145.32 ± 9.3 min; $P \leq 0.001$; Fig. 2B). During the latency period, KA-injected rats displayed a much higher number of WDS than NP04634-treated rats (Fig. 2C). Thus, in response to the same dose of KA, NP04634-treated rats exhibited a delayed progression to SE that was associated with a significantly smaller number of

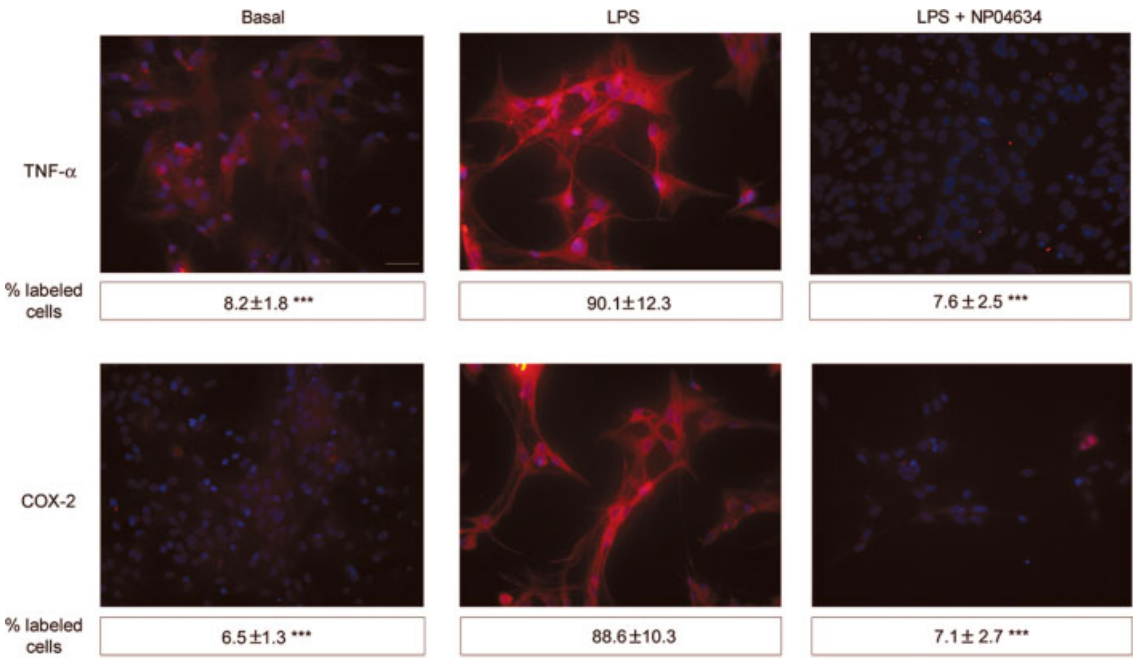

Fig. 5. Induction of proinflammatory mediators in astrocyte primary cultures after treatment with LPS. Primary astrocyte cultures were treated with LPS (10 μg/ml) in the absence or presence of NP04634, and the expression of TNF-α and COX-2 was evaluated by using immunofluorescent detection and confocal microscopy with specific antibodies, as described in Materials and Methods. Representative results from three experiments are shown. Nuclei were counterstained by DAPI (blue). LPS, lipopolysaccharide. Values shown under images represent the mean ± SD from three different experiments and five independent fields (≥50 cells/field) per culture. ***$P \leq 0.001$. Scale bar = 10 μm. [Color figure can be viewed in the online issue, which is available at www.interscience.wiley.com.]

WDS and endured less episodes of severe seizures. Finally, KA administration caused mortality in ~25% of the rats that showed SE, whereas that mortality was reduced to 13% in the NP04634-treated rats that had entered in SE by 24 hr after injection (data not shown).

Neuroprotective Role of NP04634 Following KA-Induced Brain Injury

Given the behavioral results described above, we next assessed the efficacy of NP04634 as a neuroprotector factor against KA-induced neurodegeneration. To this end, hippocampal sections were stained with Fluoro-Jade B (Schmued et al., 1997) to detect degenerating neurons or Nissl to detect surviving neurons. A complete preservation of hippocampal neurons was found in NP04634-treated rats compared with abundant neuronal loss in CA1, CA3, and hilus 72 hr after injection with KA (Fig. 3A). Quantitative studies (Fig. 3B) showed decreases of 94%, 87%, and 90%, compared with the vehicle-injected rats, in the number of neurons in the hilus, CA1, and CA3 subfield of the hippocampus, respectively, after KA injection. In contrast, in the NP04634-treated group, no significant decrease in the number of neurons was observed in the aforementioned areas 72 hr after KA injection. This resistance to injury was also supported by the almost complete absence of Fluoro-Jade B fluorescence in both the CA1 and the CA3 subfields of the hippocampus in the NP04634 group, compared with the strong fluorescence signal displayed by the nontreated animals (Fig. 3A). Interestingly, this neuronal preservation was observed in the NP04634-treated rats, independently of whether or not they reached SE, suggesting that, in addition to its anticonvulsant activity, NP04634 has a neuroprotective effect.

Effect of NP04634 on Glial Activation

One of the events that takes place in the hippocampus following excitotoxic injury is the sequential activation of microglia and astroglia. Astrocytes and microglial cells are considered to be key players in the induction of the neuronal damage following excitotoxic injury. With regard to astrogliosis, resting astrocytes were distributed throughout the entire hippocampus (Fig. 4A). Seventy-two hours after KA injection, an important increase in GFAP immunoreactivity was detected in all regions of the hippocampus (Fig. 4A). We could observe an increase in both the number and the intensity of GFAP-expressing cells. In contrast, 72 hr after KA injection, NP04634 rats displayed less staining for GFAP, and the morphology of the astrocytes was similar to that of resting cells. In addition, after KA injection, numerous reactive microglial cells appeared mainly in the molecular layers of the hippocampus (Fig. 4B). KA treatment resulted in morphological changes in microglial cells, which included swelling of the cell somas and thickening and retraction of the cell processes,

two characteristic features of reactive microglia (Jorgensen et al., 1993; Ladeby et al., 2005). Treatment with NP04634 together with KA completely blocked microglial activation.

NP04634 Inhibits Glial Activation In Vitro

Recent findings in experimental models highlight the possibility that inflammatory processes in the brain contribute to the development of seizures. Therefore, to substantiate further the role of NP04634 in the inflammatory response in neural cells, we next performed in vitro experiments with primary cultures of astrocytes. We then tested the effect of NP04634 on the production of proinflammatory and neurotoxic products from LPS-treated astrocyte cultures. Figure 5 shows that treatment of astrocytes with NP04634 completely abrogated the induction of two proinflammatory agents, TNF-α and COX-2, after LPS treatment. These results further confirm the antiinflammatory effects of NP04634 shown in the in vivo studies.

DISCUSSION

In the present study, we have shown that the new molecule NP04634, reported to be a calcium antagonist, administered before KA injection attenuated the development of SE and prevented both the glial activation and the neuronal cell death that occur in the hippocampus as a consequence of this excitotoxic insult. These results in an intact animal model of SE are further support for the in vitro studies that directly demonstrate the antiinflammatory effects of this compound.

We initially compared the behavioral activity after KA injection between NP04634-treated and control animals. KA injection induced typical behavioral seizures, such as WDS and limbic seizures, and eventually reached SE. NP04634 administered intragastrically before KA injection resulted in an anticonvulsive effect, reducing the percentage of rats that developed SE and increasing the latencies to onset of SE. Results of this study also show that NP04634-treated rats exhibited a significant lower number of WDS during the latency period prior to the onset of SE. The anticonvulsive effect elicited by NP04634 described here is in agreement with previous reports showing antiepileptic effects of drugs that block neuronal VSCCs. It has been shown that the broadly used antiepileptic drug lamotrigine inhibits non-L-type VSCCs (Stefani et al., 1996). Also, specific polypeptide toxins of animal origin, which block P/Q- and N-type VSCCs, prevent amygdaloid kindling (Gasior et al., 2007; Wang et al., 2007) and have antiepileptic effects in the DBA/2 mouse model of audiogenic seizure (Jackson and Scheideler, 1996). These data are in accordance with the fact that N- and P/Q-type VSCC are abundant in presynaptic terminals (Sabria et al., 1995) and that calcium is a key player in neurotransmitter release. Also, high cytosolic calcium levels are extremely toxic for neural cells (Choi, 1988, 1994; Meldrum and Garthwaite, 1990; Doble, 1999; Wang et al., 2005); consequently, neuroprotective agents have been sought among neuronal calcium channel blockers in addition to other molecular design families, such as glutamate antagonists, antiinflammatory drugs, and various sterol compounds.

In fact, the neuroprotective effects of peptide toxins of animal origin, which specifically inhibit N- or P/Q type VSCC blockers, are well documented in different models of brain injury in which glutamate is implicated, such as ischemia and traumatic brain injury (Valentino et al., 1993; Yamada et al., 1994; Zhao et al., 1994; Buchan et al., 1994; Asakura et al., 1997; Samii et al., 1999; Berman et al., 2000; Lee et al., 2004). In addition to peptide toxins, only small numbers of small nonpeptide neuronal VSCC blockers, more suitable for oral therapy, have been shown to provide some degree of neuroprotection in vivo in different models of brain injury (Hicks et al., 2000; O'Neill et al., 1997), although these molecules are usually less specific (Huang et al., 1997; Schelkun et al., 1999; Hu et al., 1999; Asakura et al., 2000; Menzler et al., 2000).

In agreement with all these data, we show here that NP04634 exerts a strong neuroprotective effect in a well-established model of KA-induced excitotoxic injury. Interestingly, the prevention of neuronal cell death by this compound was observed irrespective of whether the animals reached SE. Although it is known that neuronal cell loss is the result of intense seizure activity, it has been also reported that single and intermittent, brief seizures also induce neuronal damage (Bengzon et al., 1997). However, we did not observe any significant neuronal loss in the hippocampus of NP04634-treated rats that had developed SE (Fig. 3), suggesting that this compound acts as a potent neuroprotective agent in addition to its anticonvulsant activity.

There is considerable evidence suggesting that KA treatment is associated with a significant activation of astrocytes and microglial cells. Our data show that the increase in GFAP staining, as well as the morphological changes, associated with astrocytes activation are markedly reduced in animals treated with NP04634. Moreover, the strong microglial activation observed in KA-injected animals was almost completely absent in NP04634-treated rats. The regulation of glial activation is generally considered as a key mechanism in neuronal cell death. It is known that glial cells, as mediators of the inflammatory response, play an important role in the course of KA-induced hippocampal neurodegeneration. Activated astrocytes and microglia cells proliferate and increase the expression of genes implicated in the production of nitric oxide, COX-2, and cytokines, which are mainly responsible for the observed neuronal death. This is in accordance with our results showing a prominent decrease in the number of neurons in the CA1 and CA3 fields of the hippocampus of KA-injected animals, which is blocked by NP04634 administration.

The in vitro studies presented here demonstrate that NP04634 directly blocks the inflammatory activation of astrocytes induced by LPS. The production of

TNF-α and the expression of COX-2, two potent proinflammatory agents, are markedly reduced in primary astrocytes cultures treated with NP04634. These findings are consistent with the in vivo studies indicating that glial activation is significantly attenuated in KA-injected animals previously treated with NP04634. These findings provide evidence that NP04634 directly inhibits the induction of proinflammatory mediators in glial cells. Regulation of proinflammatory mediators is generally considered a key mechanism in neuronal cell death. COX-2 is involved in the pathogenesis of multiple neurological disorders (Giovannini et al., 2003; Teismann et al., 2003), and local increases in COX-2 expression have been associated with ischemia and seizures (Nogawa et al., 1997; Minghetti, 2007; Oliveira et al., 2008). In addition, TNF-α has been shown to be overexpressed in experimental models of seizures (Vezzani et al., 2008). Therefore, the suppression by NP04634 of both COX-2 and TNF-α in response to injury may be directly responsible for the observed reduction in hippocampal neuronal loss in vivo. Finally, these data suggest that NP04634 may work through its blocking effect on non-L-type VSCC, insofar as the presence of these channels in primary astrocyte cultures is well established (Latour et al., 2003; D'Ascenzo et al., 2004) and calcium is an important second messenger for cytokine production in glial cells (Robbins et al., 1987; Hoffmann et al., 2003).

In summary, our results demonstrate that NP04634 has a significant anticonvulsant, antiinflammatory, and neuroprotective effect in KA-injected rats, a well-characterized model of temporal lobe epilepsy. In addition, NP04634 diminished the induction of the proinflammatory markers TNF-α and COX2 in astrocyte cultures after LPS treatment. Because NP04634 is an efficient non-L-type VSCC blocker, it is reasonable to speculate that its actions are mediated via the inhibition of these channels, although we cannot exclude the possibility that NP04634 might also act through other mechanisms. Hence, NP0463 may be a promising new therapeutic drug deserving further attention for the treatment of temporal lobe epilepsy and other neurodegenerative disorders.

ACKNOWLEDGMENTS

The authors have no financial interest in the NP04634 product.

REFERENCES

Asakura K, Matsuo Y, Kanemasa T, Ninomiya M. 1997. P/Q-type Ca^{2+} channel blocker omega-agatoxin IVA protects against brain injury after focal ischemia in rats. Brain Res 776:140–145.

Asakura K, Kanemasa T, Minagawa K, Kagawa K, Yagami T, Nakajima M, Ninomiya M. 2000. Alpha-eudesmol, a P/Q-type Ca^{2+} channel blocker, inhibits neurogenic vasodilation and extravasation following electrical stimulation of trigeminal ganglion. Brain Res 873:94–101.

Ben-Ari Y, Tremblay E, Ottersen OP. 1980. Injections of kainic acid into the amygdaloid complex of the rat: an electrographic, clinical and histological study in relation to the pathology of epilepsy. Neuroscience 5:515–528.

Bengzon J, Kokaia Z, Elmer E, Nanobashvili A, Kokaia M, Lindvall O. 1997. Apoptosis and proliferation of dentate gyrus neurons after single and intermittent limbic seizures. Proc Natl Acad Sci U S A 94:10432–10437.

Berman RF, Verweij BH, Muizelaar JP. 2000. Neurobehavioral protection by the neuronal calcium channel blocker ziconotide in a model of traumatic diffuse brain injury in rats. J Neurosurg 93:821–828.

Brorson JR, Manzolillo PA, Miller RJ. 1994. Ca^{2+} entry via AMPA/KA receptors and excitotoxicity in cultured cerebellar Purkinje cells. J Neurosci 14:187–197.

Buchan AM, Gertler SZ, Li H, Xue D, Huang ZG, Chaundy KE, Barnes K, Lesiuk HJ. 1994. A selective N-type Ca^{2+}-channel blocker prevents CA1 injury 24 hr following severe forebrain ischemia and reduces infarction following focal ischemia. J Cereb Blood Flow Metab 14:903–910.

Choi DW. 1988. Glutamate neurotoxicity and diseases of the nervous system. Neuron 1:623–634.

Choi DW. 1994. Calcium and excitotoxic neuronal injury. Ann N Y Acad Sci 747:162–171.

Courtney MJ, Enkvist MO, Akerman KE. 1995. The calcium response to the excitotoxin kainate is amplified by subsequent reduction of extracellular sodium. Neuroscience 68:1051–1057.

Cox B. 2000. Calcium channel blockers and pain therapy. Curr Rev Pain 4:488–498.

Coyle JT. 1983. Neurotoxic action of kainic acid. J Neurochem 41:1–11.

Czuczwar SJ, Chodkowska A, Kleinrok Z, Malek U, Jagiello-Wojtowicz E. 1990. Effects of calcium channel inhibitors upon the efficacy of common antiepileptic drugs. Eur J Pharmacol 176:75–83.

D'Ascenzo M, Vairano M, Andreassi C, Navarra P, Azzena GB, Grassi C. 2004. Electrophysiological and molecular evidence of L (Cav1)-, N (Cav2.2)-, and R (Cav2.3)-type Ca^{2+} channels in rat cortical astrocytes. Glia 45:354–363.

de Graaf AS. 1974. Epidemiological aspects of epilepsy in northern Norway. Epilepsia 15:291–299.

De Sarro GB, Meldrum BS, Nistico G. 1988. Anticonvulsant effects of some calcium entry blockers in DBA/2 mice. Br J Pharmacol 93:247–256.

DeLorenzo RJ, Pal S, Sombati S. 1998. Prolonged activation of the N-methyl-D-aspartate receptor-Ca^{2+} transduction pathway causes spontaneous recurrent epileptiform discharges in hippocampal neurons in culture. Proc Natl Acad Sci U S A 95:14482–14487.

DeLorenzo RJ, Sun DA, Deshpande LS. 2005. Cellular mechanisms underlying acquired epilepsy: the calcium hypothesis of the induction and maintainance of epilepsy. Pharmacol Ther 105:229–266.

Doble A. 1999. The role of excitotoxicity in neurodegenerative disease: implications for therapy. Pharmacol Ther 81:163–221.

Dolin SJ, Hunter AB, Halsey MJ, Little HJ. 1988. Anticonvulsant profile of the dihydropyridine calcium channel antagonists, nitrendipine and nimodipine. Eur J Pharmacol 152:19–27.

Dolphin AC. 2006. A short history of voltage-gated calcium channels. Br J Pharmacol 147(Suppl 1):S56–S62.

Gasior M, White NA, Rogawski MA. 2007. Prolonged attenuation of amygdala-kindled seizure measures in rats by convection-enhanced delivery of the N-type calcium channel antagonists omega-conotoxin GVIA and omega-conotoxin MVIIA. J Pharmacol Exp Ther 323:458–468.

Giovannini MG, Scali C, Prosperi C, Bellucci A, Pepeu G, Casamenti F. 2003. Experimental brain inflammation and neurodegeneration as model of Alzheimer's disease: protective effects of selective COX-2 inhibitors. Int J Immunopathol Pharmacol 16(Suppl 2): 31–40.

Hicks CA, Ward MA, O'Neill MJ. 2000. Neuroprotective effects of the neuronal Ca^{2+} channel blockers, LY042826 and LY393615 in vivo. Eur J Pharmacol 408:241–248.

Hoffmann A, Kann O, Ohlemeyer C, Hanisch UK, Kettenmann H. 2003. Elevation of basal intracellular calcium as a central element in the activation of brain macrophages (microglia): suppression of receptor-evoked calcium signaling and control of release function. J Neurosci 23:4410–4419.

Hu LY, Ryder TR, Rafferty MF, Feng MR, Lotarski SM, Rock DM, Sinz M, Stoehr SJ, Taylor CP, Weber ML, Bowersox SS, Miljanich GP, Millerman E, Wang YX, Szoke BG. 1999. Synthesis of a series of 4-benzyloxyaniline analogues as neuronal N-type calcium channel blockers with improved anticonvulsant and analgesic properties. J Med Chem 42:4239–4249.

Huang CS, Song JH, Nagata K, Yeh JZ, Narahashi T. 1997. Effects of the neuroprotective agent riluzole on the high voltage-activated calcium channels of rat dorsal root ganglion neurons. J Pharmacol Exp Ther 282:1280–1290.

Jackson HC, Scheideler MA. 1996. Behavioural and anticonvulsant effects of Ca^{2+} channel toxins in DBA/2 mice. Psychopharmacology 126:85–90.

Jorgensen MB, Finsen BR, Jensen MB, Castellano B, Diemer NH, Zimmer J. 1993. Microglial and astroglial reactions to ischemic and kainic acid-induced lesions of the adult rat hippocampus. Exp Neurol 120:70–88.

Kaminski RM, Mazurek M, Turski WA, Kleinrok Z, Czuczwar SJ. 2001. Amlodipine enhances the activity of antiepileptic drugs against pentylenetetrazole-induced seizures. Pharmacol Biochem Behav 68: 661–668.

Khosravani H, Zamponi GW. 2006. Voltage-gated calcium channels and idiopathic generalized epilepsies. Physiol Rev 86:941–966.

Ladeby R, Wirenfeldt M, Garcia-Ovejero D, Fenger C, Dissing-Olesen L, Dalmau I, Finsen B. 2005. Microglial cell population dynamics in the injured adult central nervous system. Brain Res Brain Res Rev 48:196–206.

Latour I, Hamid J, Beedle AM, Zamponi GW, Macvicar BA. 2003. Expression of voltage-gated Ca^{2+} channel subtypes in cultured astrocytes. Glia 41:347–353.

Lee LL, Galo E, Lyeth BG, Muizelaar JP, Berman RF. 2004. Neuroprotection in the rat lateral fluid percussion model of traumatic brain injury by SNX-185, an N-type voltage-gated calcium channel blocker. Exp Neurol 190:70–78.

Leite JP, Bortolotto ZA, Cavalheiro EA. 1990. Spontaneous recurrent seizures in rats: an experimental model of partial epilepsy. Neurosci Biobehav Rev 14:511–517.

Lothman EW, Bertram EH 3rd, Stringer JL. 1991. Functional anatomy of hippocampal seizures. Prog Neurobiol 37:1–82.

Lukyanetz EA, Shkryl VM, Kostyuk PG. 2002. Selective blockade of N-type calcium channels by levetiracetam. Epilepsia 43:9–18.

Luna-Medina R, Cortes-Canteli M, Alonso M, Santos A, Martinez A, Perez-Castillo A. 2005. Regulation of inflammatory response in neural cells in vitro by thiadiazolidinones derivatives through peroxisome proliferator-activated receptor γ activation. J Biol Chem 280:21453–21462.

McNamara JO. 1994. Cellular and molecular basis of epilepsy. J Neurosci 14:3413–3425.

Meldrum B, Garthwaite J. 1990. Excitatory amino acid neurotoxicity and neurodegenerative disease. Trends Pharmacol Sci 11:379–387.

Menzler S, Bikker JA, Suman-Chauhan N, Horwell DC. 2000. Design and biological evaluation of nonpeptide analogues of omega-conotoxin MVIIA. Bioorg Med Chem Lett 10:345–347.

Miljanich GP. 2004. Ziconotide: neuronal calcium channel blocker for treating severe chronic pain. Curr Med Chem 11:3029–3040.

Minghetti L. 2007. Role of COX-2 in inflammatory and degenerative brain diseases. Subcell Biochem 42:127–141.

Nadler JV. 1981. Minireview. Kainic acid as a tool for the study of temporal lobe epilepsy. Life Sci 29:2031–2042.

Nogawa S, Zhang F, Ross ME, Iadecola C. 1997. Cyclo-oxygenase-2 gene expression in neurons contributes to ischemic brain damage. J Neurosci 17:2746–2755.

O'Neill MJ, Bath CP, Dell CP, Hicks CA, Gilmore J, Ambler SJ, Ward MA, Bleakman D. 1997. Effects of Ca^{2+} and Na^{+} channel inhibitors in vitro and in global cerebral ischemia in vivo. Eur J Pharmacol 332:121–131.

Oliveira MS, Furian AF, Royes LF, Fighera MR, Fiorenza NG, Castelli M, Machado P, Bohrer D, Veiga M, Ferreira J, Cavalheiro EA, Mello CF. 2008. Cyclooxygenase-2/PGE2 pathway facilitates pentylenetetrazol-induced seizures. Epilepsy Res 79:14–21.

Olney JW, Collins RC, Sloviter RS. 1986. Excitotoxic mechanisms of epileptic brain damage. Adv Neurol 44:857–877.

Pal S, Sombati S, Limbrick DD Jr, DeLorenzo RJ. 1999. In vitro status epilepticus causes sustained elevation of intracellular calcium levels in hippocampal neurons. Brain Res 851:20–31.

Racine RJ. 1972. Modification of seizure activity by electrical stimulation. II. Motor seizure. Electroencephalogr Clin Neurophysiol 32:281–294.

Robbins DS, Shirazi Y, Drysdale BE, Lieberman A, Shin HS, Shin ML. 1987. Production of cytotoxic factor for oligodendrocytes by stimulated astrocytes. J Immunol 139:2593–2597.

Sabria J, Pastor C, Clos MV, Garcia A, Badia A. 1995. Involvement of different types of voltage-sensitive calcium channels in the presynaptic regulation of noradrenaline release in rat brain cortex and hippocampus. J Neurochem 64:2567–2571.

Samii A, Badie H, Fu K, Luther RR, Hovda DA. 1999. Effects of an N-type calcium channel antagonist (SNX 111; Ziconotide) on calcium-45 accumulation following fluid-percussion injury. J Neurotrauma 16:879–892.

Sander JW, Shorvon SD. 1996. Epidemiology of the epilepsies. J Neurol Neurosurg Psychiatry 61:433–443.

Schelkun RM, Yuen P, Malone TC, Rock DM, Stoehr S, Szoke B, Tarczy-Hornoch K. 1999. Synthesis and biological activity of substituted bis-(4-hydroxyphenyl)methanes as N-type calcium channel blockers. Bioorg Med Chem Lett 9:2447–2452.

Schmued LC, Albertson C, Slikker W Jr. 1997. Fluoro-Jade: a novel fluorochrome for the sensitive and reliable histochemical localization of neuronal degeneration. Brain Res 751:37–46.

Sombati S, DeLorenzo RJ. 1995. Recurrent spontaneous seizure activity in hippocampal neuronal networks in culture. J Neurophysiol 73:1706–1711.

Sperk G. 1994. Kainic acid seizures in the rat. Prog Neurobiol 42:1–32.

Sperk G, Lassmann H, Baran H, Seitelberger F, Hornykiewicz O. 1985. Kainic acid-induced seizures: dose-relationship of behavioural, neurochemical and histopathological changes. Brain Res 338:289–295.

Stefani A, Spadoni F, Siniscalchi A, Bernardi G. 1996. Lamotrigine inhibits Ca^{2+} currents in cortical neurons: functional implications. Eur J Pharmacol 307:113–116.

Sun DA, Sombati S, Blair RE, DeLorenzo RJ. 2002. Calcium-dependent epileptogenesis in an in vitro model of stroke-induced "epilepsy." Epilepsia 43:1296–1305.

Takahara A, Konda T, Enomoto A, Kondo N. 2004. Neuroprotective effects of a dual L/N-type Ca^{2+} channel blocker cilnidipine in the rat focal brain ischemia model. Biol Pharm Bull 27:1388–1391.

Tauck DL, Nadler JV. 1985. Evidence of functional mossy fiber sprouting in hippocampal formation of kainic acid-treated rats. J Neurosci 5:1016–1022.

Teismann P, Tieu K, Choi D-K, Wu D-C, Naini A, Hunot S, Vila M, Jackson-Lewis V, Przedborski S. 2003. Cyclooxygenase-2 is instrumental in Parkinson's disease neurodegeneration. Proc Natl Acad Sci USA 100:5473–5478.

Valentino K, Newcomb R, Gadbois T, Singh T, Bowersox S, Bitner S, Justice A, Yamashiro D, Hoffman BB, Ciaranello R, et al. 1993. A

selective N-type calcium channel antagonist protects against neuronal loss after global cerebral ischemia. Proc Natl Acad Sci U S A 90:7894–7897.

Valero T, Del Barrio L, Egea J, Cañas N, Martinez A, Garcia A, Villarroya M, Garcia-Lopez M. 2009. NP04634 prevents cell damage caused by calcium overload and mitochondrial disruption in bovine chromaffin cells. Eur J Pharmacol (in press).

Verkhratsky A. 2005. Physiology and pathophysiology of the calcium store in the endoplasmic reticulum of neurons. Physiol Rev 85: 201–279.

Vezzani A, Wu HQ, Stasi MA, Angelico P, Samanin R. 1988. Effect of various calcium channel blockers on three different models of limbic seizures in rats. Neuropharmacology 27:451–458.

Vezzani A, Balosso S, Ravizza T. 2008. The role of cytokines in the pathophysiology of epilepsy. Brain Behav Immun 22:797–803.

Wang Q, Yu S, Simonyi A, Sun GY, Sun AY. 2005. Kainic acid-mediated excitotoxicity as a model for neurodegeneration. Mol Neurobiol 31:3–16.

Wang S, Ding M, Wu D, Zhan J, Chen Z. 2007. Omega-conotoxin MVIIA inhibits amygdaloid kindled seizures in Sprague-Dawley rats. Neurosci Lett 413:163–167.

Yamada K, Teraoka T, Morita S, Hasegawa T, Nabeshima T. 1994. Omega-conotoxin GVIA protects against ischemia-induced neuronal death in the Mongolian gerbil but not against quinolinic acid-induced neurotoxicity in the rat. Neuropharmacology 33:251–254.

Zhao Q, Smith ML, Siesjo BK. 1994. The omega-conopeptide SNX-111, an N-type calcium channel blocker, dramatically ameliorates brain damage due to transient focal ischemia. Acta Physiol Scand 150:459–461.

OPEN ACCESS Freely available online

PLoS one

Inhibition of Glioblastoma Growth by the Thiadiazolidinone Compound TDZD-8

Diana Aguilar-Morante[1☯], Jose Angel Morales-Garcia[1☯], Marina Sanz-SanCristobal[1], Miguel Angel Garcia-Cabezas[3], Angel Santos[2], Ana Perez-Castillo[1]*

1 Instituto de Investigaciones Biomédicas, Consejo Superior de Investigaciones Científicas-Universidad Autónoma de Madrid, and Centro de Investigación Biomédica en Red sobre Enfermedades neurodegenerativas (CIBERNED), Madrid, Spain, **2** Departamento de Bioquímica y Biología Molecular, Facultad de Medicina, Universidad Complutense de Madrid, Madrid, Spain, **3** Departamento de Anatomía Patológica, Hospital Universitario "La Paz", Madrid, Spain

Abstract

Background: Thiadiazolidinones (TDZD) are small heterocyclic compounds first described as non-ATP competitive inhibitors of glycogen synthase kinase 3β (GSK-3β). In this study, we analyzed the effects of 4-benzyl-2-methyl-1,2,4-thiadiazolidine-3,5-dione (TDZD-8), on murine GL261 cells growth *in vitro* and on the growth of established intracerebral murine gliomas *in vivo*.

Methodology/Principal Findings: Our data show that TDZD-8 decreased proliferation and induced apoptosis of GL261 glioblastoma cells *in vitro*, delayed tumor growth *in vivo*, and augmented animal survival. These effects were associated with an early activation of extracellular signal-regulated kinase (ERK) pathway and increased expression of EGR-1 and p21 genes. Also, we observed a sustained activation of the ERK pathway, a concomitant phosphorylation and activation of ribosomal S6 kinase (p90RSK) and an inactivation of GSK-3β by phosphorylation at Ser 9. Finally, treatment of glioblastoma stem cells with TDZD-8 resulted in an inhibition of proliferation and self-renewal of these cells.

Conclusions/Significance: Our results suggest that TDZD-8 uses a novel mechanism to target glioblastoma cells, and that malignant progenitor population could be a target of this compound.

Citation: Aguilar-Morante D, Morales-Garcia JA, Sanz-SanCristobal M, Garcia-Cabezas MA, Santos A, et al. (2010) Inhibition of Glioblastoma Growth by the Thiadiazolidinone Compound TDZD-8. PLoS ONE 5(11): e13879. doi:10.1371/journal.pone.0013879

Editor: Maciej Lesniak, The University of Chicago, United States of America

Received July 1, 2010; **Accepted** October 19, 2010; **Published** November 8, 2010

Funding: This work was supported by the Ministerio de Educacion y Ciencia grant SAF2007-62811 (to A.P.-C.). CIBERNED is funded by the Instituto de Salud Carlos III. JA.M.-G. and M.S.-S. are fellows of CIBERNED. D.A.-M. is a fellow of the Consejo Superior de Investigaciones Cienti-ficas. The funders had no role in study design, data collection and analysis, decision to publish, or preparation of the manuscript.

Competing Interests: The authors have declared that no competing interests exist.

* E-mail: piedras3@med.ucm.es

☯ These authors contributed equally to this work.

Introduction

Glioblastomas (GBM) are the most frequent and aggressive neoplasm among human primary brain tumors [1]. Despite many efforts to overcome this aggressive disease the median survival of patients with GBM remains less than 12 months from the time of diagnosis [1,2]. Advances in glioma modeling in the mouse have made the disease amenable to *in vivo* functional and molecular studies [3]. Although there have been important advances in our understanding of malignant gliomas and progress in treating them, the mechanisms underlying GBM pathogenesis and poor response to conventional therapy are yet unclear.

GSK-3β is a serine/threonine kinase which activity is regulated by site-specific phosphorylation. Full activity of this enzyme generally requires phosphorylation at Tyr-216, and conversely, phosphorylation at Ser-9 inhibits GSK-3β activity. Different studies have shown that GSK-3β is involved in many biological processes, including cell cycle progression, apoptosis and viability, cytoskeletal organization, cellular metabolism and tumorigenesis [4,5]. Several of these pathways, are implicated in disease pathogenesis, which has prompted efforts to develop GSK-3β inhibitors for therapeutic applications. GSK-3β plays an important role in glucose metabolism and it is thought to facilitate the development of non-insulin-dependent diabetes [6]. Also, GSK-3β has an important role in promoting inflammatory processes through its activation of the transcription factor NF-κB [7]. This kinase has also been implicated in the development of Alzheimer disease and other neurodegenerative disorders [8]. Lastly, several studies have identified a specific role for GSK-3β on proliferation and apoptosis of cancer cells. GSK-3β activation has been associated with prostate cancer progression [9], and inactivation of this enzyme activates a p53-dependent apoptosis pathway resulting in a diminished colorectal cancer cell growth [10].

The thiadiazolidinone compound TDZD-8 belongs to a family of molecules, which was originally described as non-ATP competitive inhibitors of glycogen synthase kinase 3β (GSK-3β) [11,12]. In line with the implication of GSK-3β-activated pathways in disease pathogenesis, TDZD-8 has been shown to be a protective agent in multiple murine models of disease such as arthritis, spinal cord injury, colitis, and septic shock [13,14,15,16,17]. More recently, TDZD-8 has been shown to selectively induce death of several major forms of leukemia cells,

including malignant myeloid stem and progenitor populations, while sparing normal hematopoietic tissue [18].

In an effort to expand strategies for targeting glioblastoma cells, we have explored the effects of TDZD-8 on glioblastoma development. We demonstrate that TDZD-8 is a potent anti-proliferative and pro-apoptotic agent of glioma cells *in vitro* and *in vivo*. These effects are associated with an early activation of extracellular signal-regulated kinase (ERK), which is followed by an increased expression of the early growth response-1 (EGR-1) and p21. TDZD-8 also elicited a sustained activation of ERK which lead to a phosphorylation of p90RSK and a concomitant inhibition of GSK-3β through phosphorylation of Ser-9. We also demonstrate that TDZD-8 inhibits the growth and neurosphere formation and self-renewal capacity of GL261 cells. As such, these findings identify TDZD-8 as a potential therapeutic agent for the treatment of high grade gliomas.

Results

TDZD-8 treatment reduces glioblastoma development *in vivo*

To analyze the effects of TDZD-8 on glioblastoma growth *in vivo*, we orthotopically implanted GL261 glioma cells into adult mice brains to generate tumors. The murine glioma GL261 model has been the most common used syngeneic transplant model for both subcutaneous and intracranial experimental glioma tumors [19,20,21]. This particular intracranial animal model recapitulates many of the histopathological and biological features of human glioma including necrosis with pseudopalisading, blood vessels infiltration and presence of giant multinucleated cells [22]. First, we monitored tumor growth *in vivo* by magnetic resonance imaging (MRI) at different times after implantation. Animals treated with TDZD-8 1 day after GL261 cell implantation showed a delayed onset and progression of tumors compared to control animals (Fig. 1A, B). Also, tumor volume, as assessed by T_1-weighed images after gadolinium contrast administration, was significantly reduced in mice treated with TDZD-8 (Fig. 1A). About 84% reduction in tumor volume was observed in tumors derived from TDZD-8-treated animals at 13 days post-injection (Fig. 1C). This strong reduction in the tumor growth potential induced by the compound was also observed 20 days post-injection. Both the log-rank test and Kaplan-Meier analysis of the survival data demonstrated a significant survival advantage for the mice treated with TDZD-8 when compared to their controls (40 *versus* 30 days) (Fig. 1D). Log-rank analysis of the data yielded a p value of 0.006. Of note, this delayed tumor growth was also detected when the TDZD-8 treatment was started 6 days after GL261 cell injection (Fig. S1).

We next performed histological examination of tumor tissues 12 and 24 days after treatment (Fig. 2A). Microscopically all the tumors were made of sheets of malignant cells that leaved some microcysts among them. These cells showed highly atypical nuclei with prominent nucleoli and an eosinophilic cytoplasm with filamentous elongations. Many multinucleated malignant cells were also seen (Fig. 2A, asterisks in insets). Altogether these features are characteristic of a typical human high-grade glioma. The grade of pleomorphism and nuclear atipia and the mitotic activity were reminiscent of that found in human glioblastoma multiforme. Tumors from control animals presented more mixoid matrices (Fig. 2A, arrows in insets) and a higher mitotic activity with more than 5 mitotic figures per high power field (Fig. 2A, arrowheads in insets), as compared with TDZD-8-treated animals.

To further understanding on tumors characteristics we performed PCNA and active caspase-3 immunohistochemistry 12 days after implantation to assess the effect of TDZD-8 on proliferation and apoptosis. Quantification of the data revealed that TDZD-8-treated animals showed a significant reduction of PCNA expression (Fig. 2B), suggesting a growth-suppressing action of this compound *in vivo*. Figure 2B also shows that mice treated during 12 days with TDZD-8 presented tumors with elevated active caspase-3 expression, compared with vehicle-treated animals, indicating that TDZD-8 promoted apoptosis of glioma cells *in vivo*.

TZDZ-8 decreases cell proliferation and survival *in vitro*

To understand the mechanism by which TDZD-8 inhibits tumor growth, we initially tested its antiproliferative effect on GL261 glioblastoma cells analyzing BrdU incorporation. Exponentially growing GL261 cells were exposed to 20 μM TDZD-8 for 24 and 48 h, and their proliferation was monitored. A significant decreased in proliferation was observed in cells treated for both 24 and 48 h with 20 μM TDZD-8 compared with untreated control cells (Fig. 3A). Additionally, cell viability, measured by the MTT assay, was significantly diminished in TDZD-8-treated cells (Fig. 3B), compared to controls. Thus, TDZD-8 has an antiproliferative effect on GL261 glioblastoma cells. This anti-proliferative effect of TDZD-8 was also observed in other two human glioblastoma cell lines, A172 (Fig. 3C, D) and U373 (Fig. 3E, F).

To further investigate the role of TDZD-8 in cell growth inhibition, cell death was evaluated by active caspase-3 and TUNEL analysis (Fig. 4). Treatment of GL261 cells at different times with TDZD-8 resulted in an increase of apoptosis that was evident by an increase in the abundance of cleaved caspase-3 (Fig. 4A). Yet again, this proapoptotic effect was also observed in the A172 and U373 glioma cell lines. TUNEL analysis of GL261 cells showed a significant increase in the number of apoptotic cells after TDZD8 treatment (Fig. 4C). Addition of the caspase inhibitor N-benzoylcarbanyl-Val-Ala-Asp-fluoro methylketone (zVAD-fmk) inhibited TDZD-8-induced caspase activation and cell death (Fig. 4B, C). Altogether, these results indicate that TDZD-8 treatment led to a growth arrest of glioblastoma cells by a diminution of cell proliferation and an induction of apoptosis.

Effects of TDZD-8 on the mitogen-activated protein kinase (MAPK) pathway and NF-κB activation

We next investigated possible signaling pathways involved in the TDZD-8 anti-proliferative effects on glioblastoma cells. Activation of ERK has been associated with a diminution of cell survival in different tumor cell lines, including glioblastoma cell lines [23,24,25]. Therefore, we next investigated the possible involvement of this pathway in the anti-proliferative and pro-apoptotic effects of TDZD-8 described here. First, we evaluated the phosphorylation status of ERK1/2. As can be seen in Figure 5A, ERK1/2 become rapidly phosphorylated after TDZD-8 treatment. Next, we examined the expression of two genes known to play an important role in cell growth and which are downstream targets of the ERK cascade [26], the early growth response -1 (EGR-1) gene and p21. An increase in the expression of both genes was observed 1 and 2 hours after TDZD-8 addition to GL261 cells (Fig. 5A). In addition to this rapid effect, we also detected a sustained activation of ERK1/2 and a sustained increase of p21 (Fig. 5B, C). Since the ribosomal S6 kinase (p90RSK) is a well-known target of ERK [27,28] and activated p90RSK can inactivate GSK-3β by phosphorylation at Ser9, we then analyzed the effect of TDZD-8 treatment on the phosphorylation status of these enzymes. As shown in Figure 5B an increase in phosphorylation of p90RSK at Ser380 and GSK-3β at Ser9 was detected 24 hours after TDZD-8 treatment. Noteworthy, although the increase in phosphorylation of ERK1/2 is not as high as the one observed at shorter time points (Fig. 5A) this enhancement is consistent and sufficient to initiate the signaling cascade leading to activation of their target p90RSK and

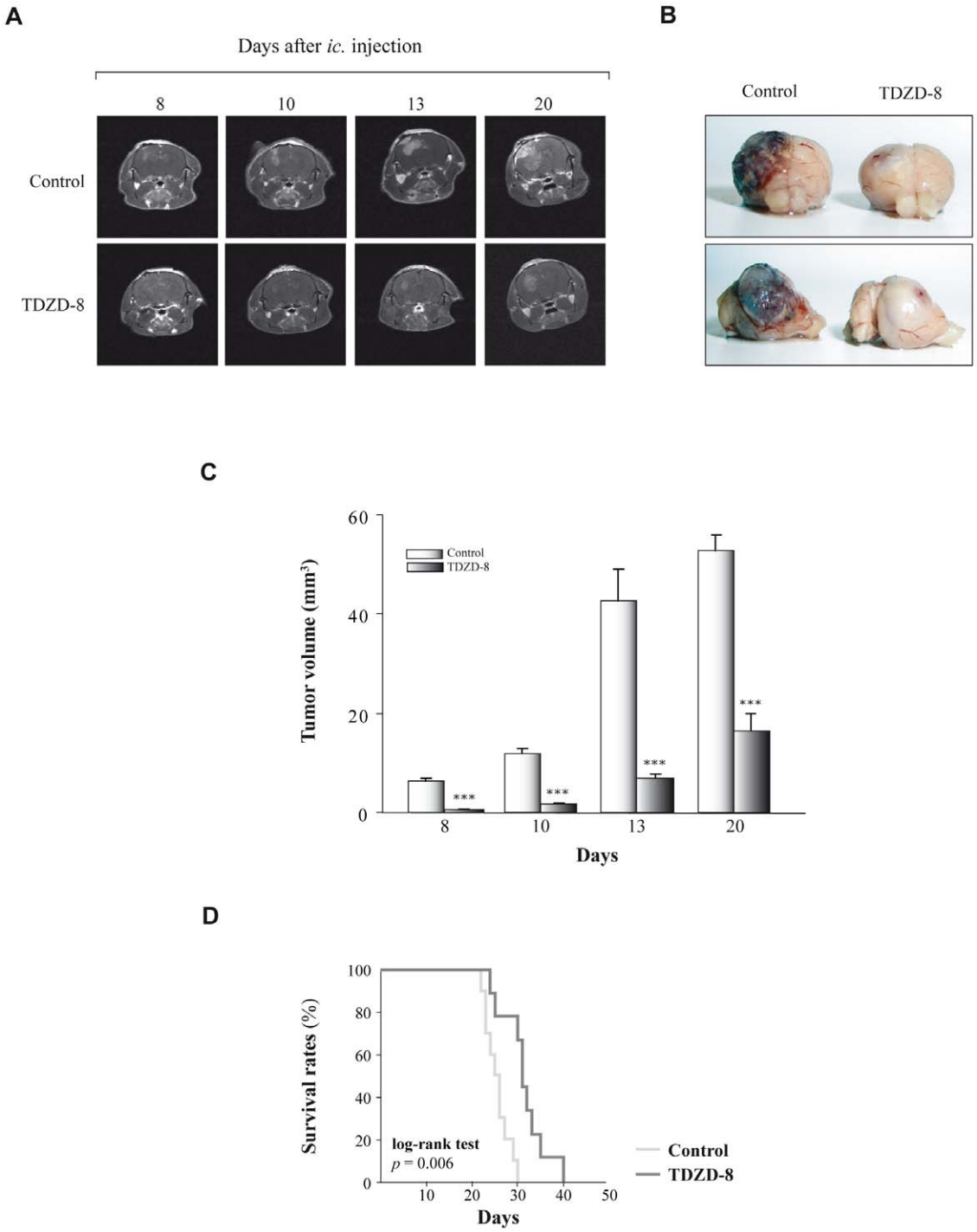

Figure 1. Effects of TDZD-8 treatment on tumor growth *in vivo*. (A) Representative T_1 magnetic resonance imaging (MRI) pictures obtained form mice injected with GL261 and treated with TDZD-8 (5 mg/Kg). T_1-weighted imaging was performed at 7 Tesla as described in Materials and Methods at different times after injection. (B) Representative photographs of GL261 tumors 24 days after implantation are shown. (C) Quantitative analysis of total tumor volumes. Values represent the mean ± SD from five different animals. (D) Kaplan-Meier plots and log-rank statistics analysis of overall survival reveal that TDZD-8 treatment significantly improves survival of tumor-bearing mice compared with their non-treated controls (log-rank test $p = 0.006$).
doi:10.1371/journal.pone.0013879.g001

subsequent inactivation of GSK-3β. To further substantiate the notion that the ERK/p90RSK pathway is involved in the phosphorylation of GSK-3β after TDZD-8 treatment, we used the PD98059 inhibitor to block this pathway. Our results show that addition of PD98059 significantly inhibited the phosphorylation of GSK-3β at Ser9, suggesting that activation of the ERK pathway plays a major role in the phosphorylation and concomitant inactivation of this enzyme [29].

Since it has been also shown that GSK-3β regulates tumor cell survival through a NF-κB-dependent pathway [7,30] we next tested whether GSK-3β inhibition by TDZD-8 could affect NF-κB activity in GL261 cells. To this end, we performed transient

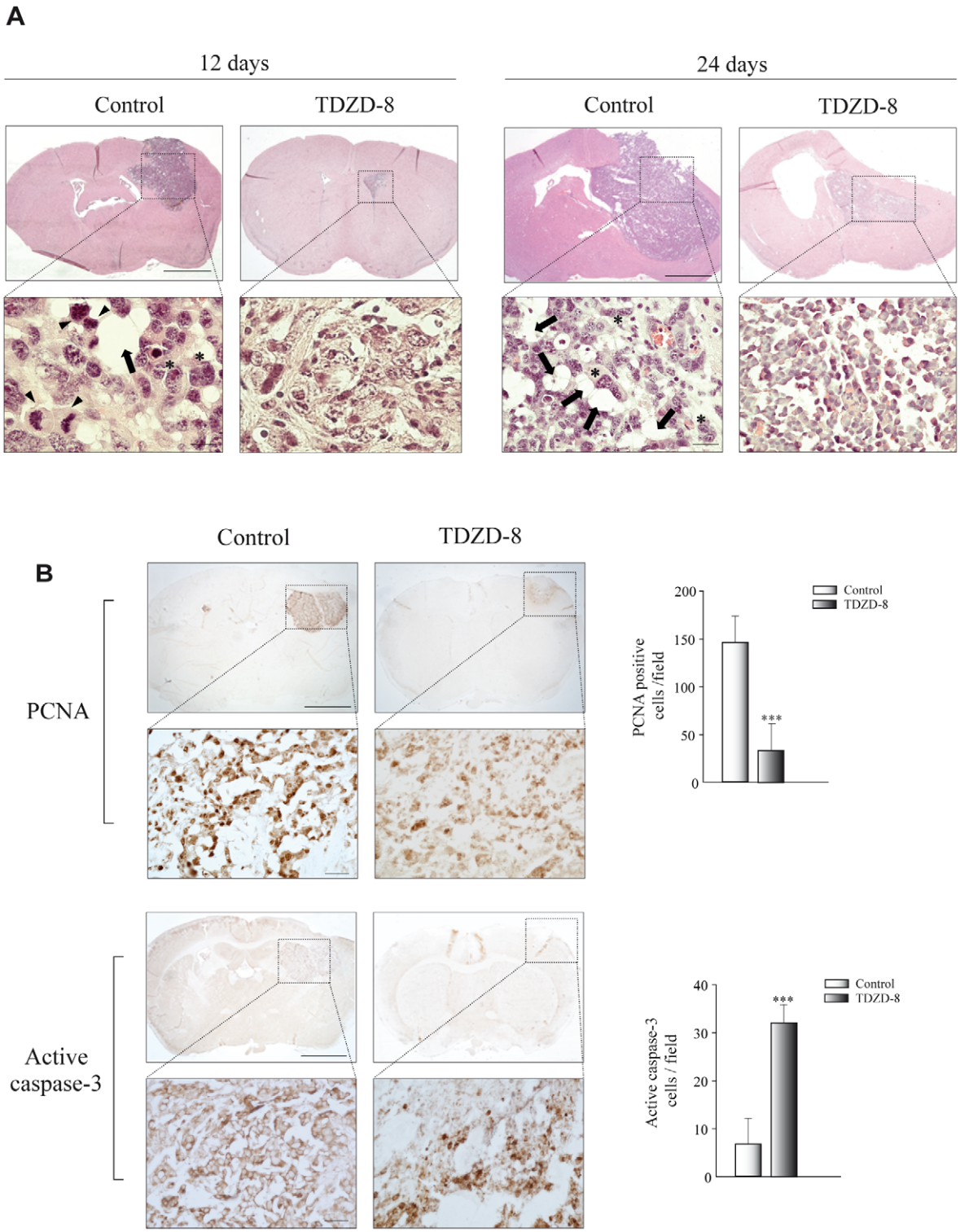

Figure 2. Histological and immunohistochemical analysis of tumors induced by GL261 glioblastoma cells. (A) Representative hematoxylin-eosin stained sections of tumors at 12 and 24 days after injection. Insets show higher magnifications of images shown in the upper panels. Tumors derived from control animals showed clear mixoid matrices (arrows), multinucleated malignant and pleomorphic cells (asterisks), and numerous mitotic figures (arrowheads). (B) Immunohistochemical study of tumor sections for PCNA and active caspase-3 detection 12 days after injection of GL261 cells. Insets show a higher magnification of the images shown in the upper panels. Scale bars, 300 μm. Insets scale bars, 25 μm. Quantification of the number of active caspase-3 and PCNA positive cells was evaluated in tumor sections and values expressed as mean ± SD. positive cells/field. ***$p \leq 0.001$.

doi:10.1371/journal.pone.0013879.g002

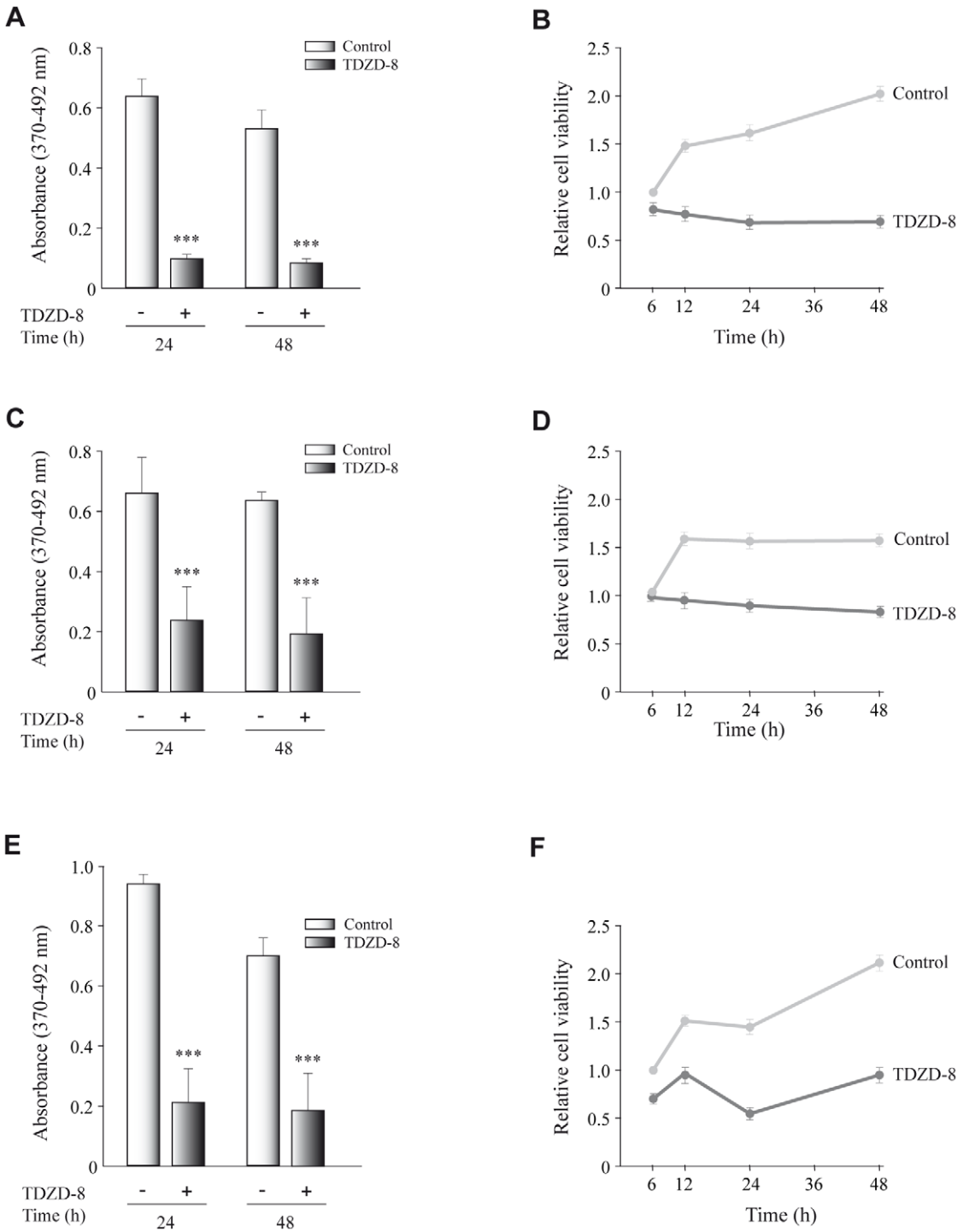

Figure 3. Effect of TDZD-8 treatment on cell proliferation and survival in different glioblastoma cell lines. GL261 (A, B), A172 (C, D) and U373 (E, F). (A, C, E) Proliferation rates determined by a BrdU incorporation assay. Tumoral cells were seeded into individual wells of a 96-well plate and cultivated for 24 and 48 h in the presence or absence of TDZD-8 after which BrdU was added to the culture medium. Cells were harvested 16 h after BrdU addition. Indicated are the means ± SD measured. (B, D, F) Cells were seeded in a 96-well plate and at different times after plating cell viability was determined by the MTT assay, as indicated in Materials and Methods. Values are the means ± SD of at least three different experiments.
doi:10.1371/journal.pone.0013879.g003

transfection assays using a reporter construct that contains three copies of the consensus NF-κB response element (3xKBtk-luc) to determine NF-κB activity in control and TDZD-8-treated cells. As shown in Figure 5D, TDZD-8 inhibited NF-κB activity, which is in accordance with previously published data [31,32].

Effect of TDZD-8 on glioblastoma stem cells

The emerging cancer stem cell model suggests that tumors are organized in a hierarchy with a subpopulation of cancer stem cells (CSCs) responsible for tumor maintenance and progression. Therefore, we determined whether TDZD-8 could also exert an

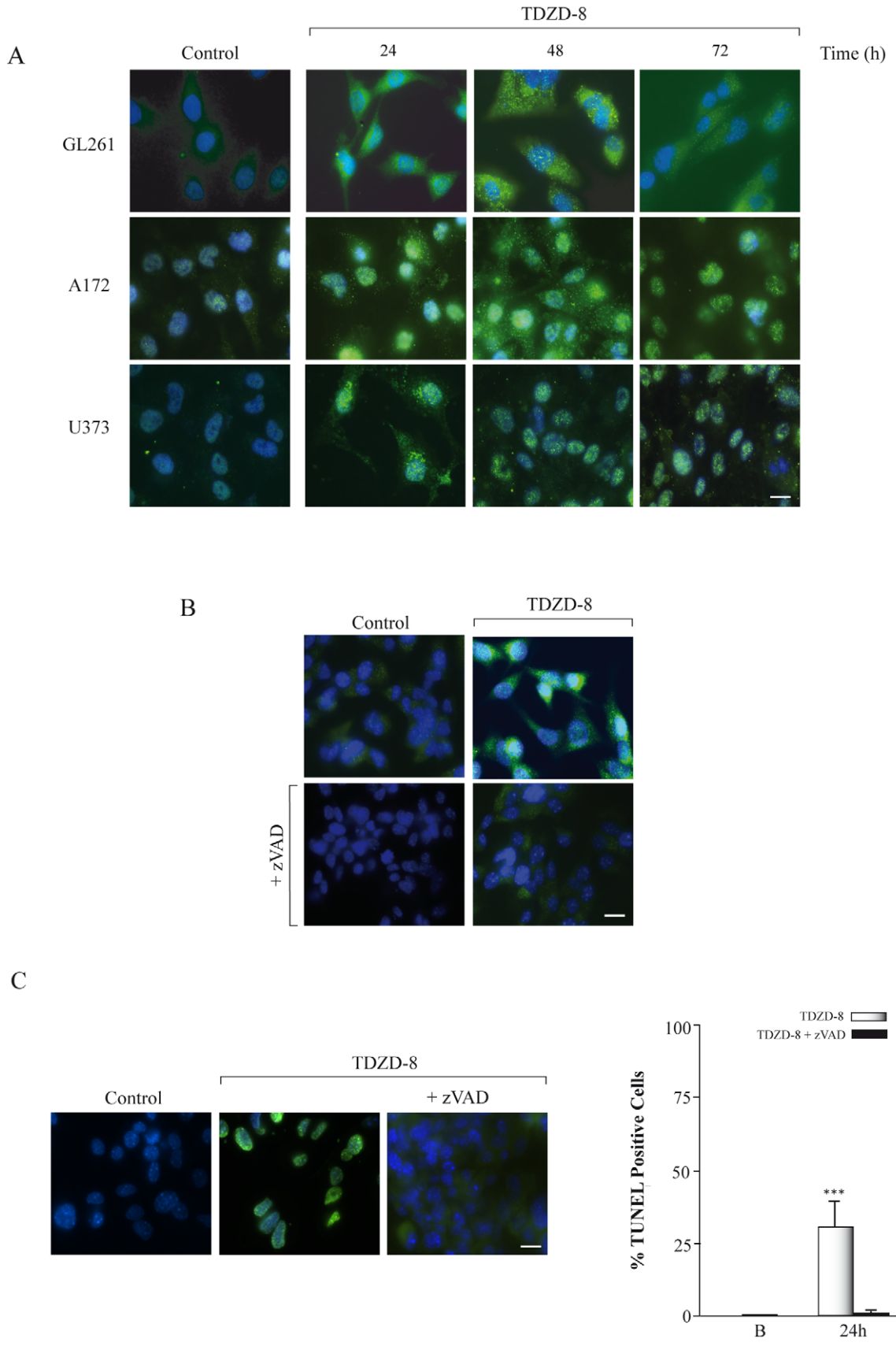

Figure 4. Effect of TDZD-8 treatment on apoptosis. (A) Different glioblastoma cell lines were grown on glass coverslips, treated with TDZD-8 for different times and active caspase-3 was analyzed by immunofluorescence using a specific anti-active caspase-3 antibody. (B) GL261 glioblastoma cells were grown for 24 h on glass coverslips, treated with TDZD-8 or TDZD-8 plus zVAD-fmk and active caspase-3 was analyzed by

immunofluorescence using a specific anti-active caspase-3 antibody. Scale bar, 25 μm. (C) GL261 glioblastoma cells were grown for 24 h on glass coverslips, treated with TDZD-8 or TDZD-8 plus zVAD-fmk and TUNEL analysis was performed. Representative immunofluorescence images are shown. Scale bar, 25 μm. Quantification of TUNEL-positive cells 24 h after TDZD-8 treatment is shown in the right panel. B, basal non-treated cells. Values are the means ± SD of at least three different experiments.
doi:10.1371/journal.pone.0013879.g004

antiproliferative effect on progenitor glioblastoma stem cells by analyzing its effect in GBM-derived neurospheres. It has been shown that the major intermediate filament protein Nestin could be used as a marker of brain CSCs as well as normal neural stem and precursor cells [33,34,35,36]. Therefore, as a first step to establish if TDZD-8 could affect the CSC population in GL261 glioblastoma cells, we examined its effect on the expression of Nestin in adherent cultures of GL261 cells. The results shown in Figure 6A reveal a significant reduction in the protein levels of Nestin in those cultures treated with TDZD-8, which could

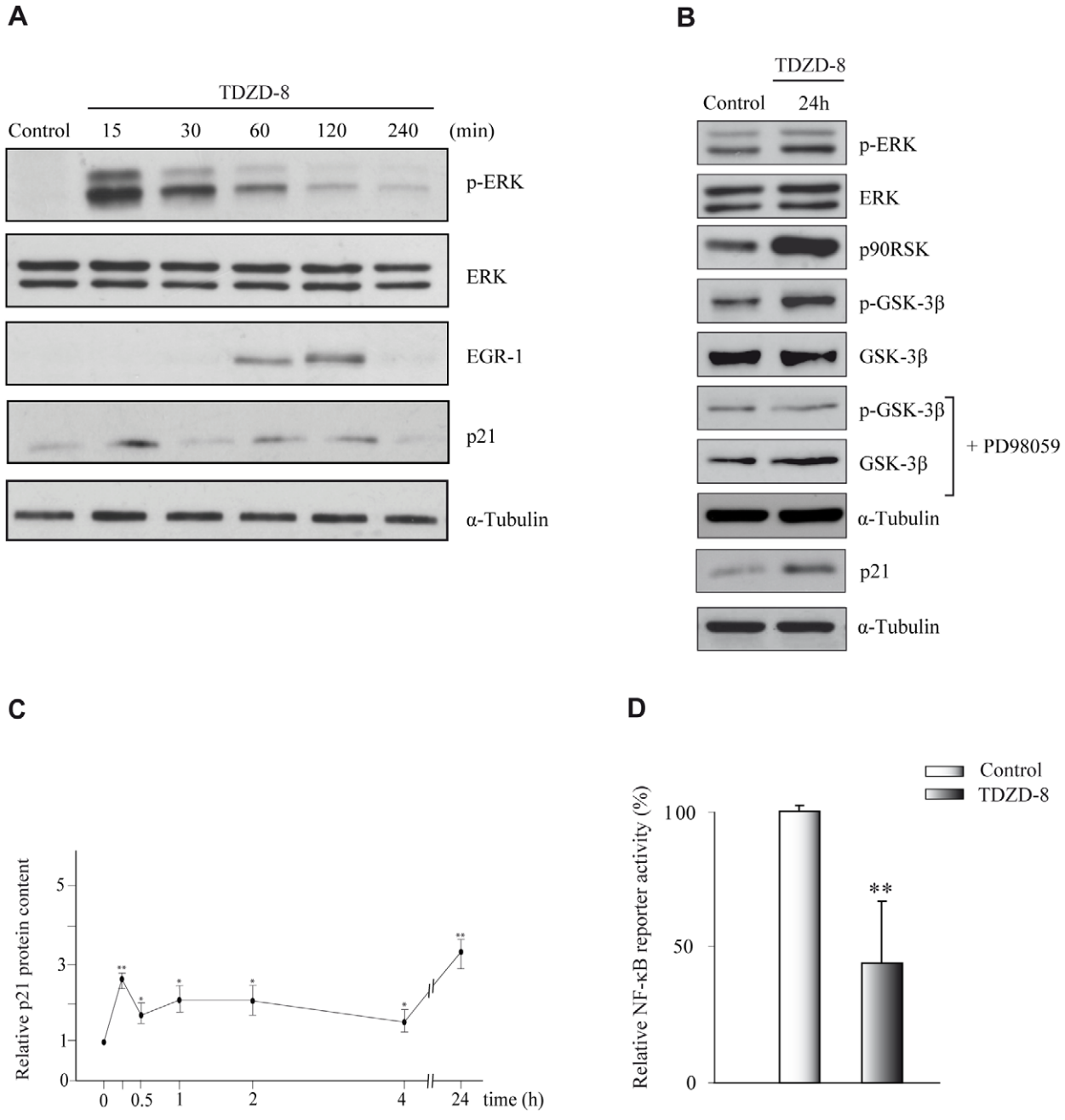

Figure 5. TDZD-8 activates the ERK signaling pathway. (A, B) GL261 cells were treated or not with TDZD-8 for different times and then stained with the corresponding primary antibodies. Some cultures were pretreated for 1 h with the ERK inhibitor PD98059. (C) Quantification of the kinetic induction of p21 by TDZD8. (D) A reporter assay was performed to measure the transcriptional activity of NF-κB. GL261 cells were transfected with 3xNF-tk-luc reporter construct for 48 h in the presence or absence of TDZD-8 and luciferase activity was measured.
doi:10.1371/journal.pone.0013879.g005

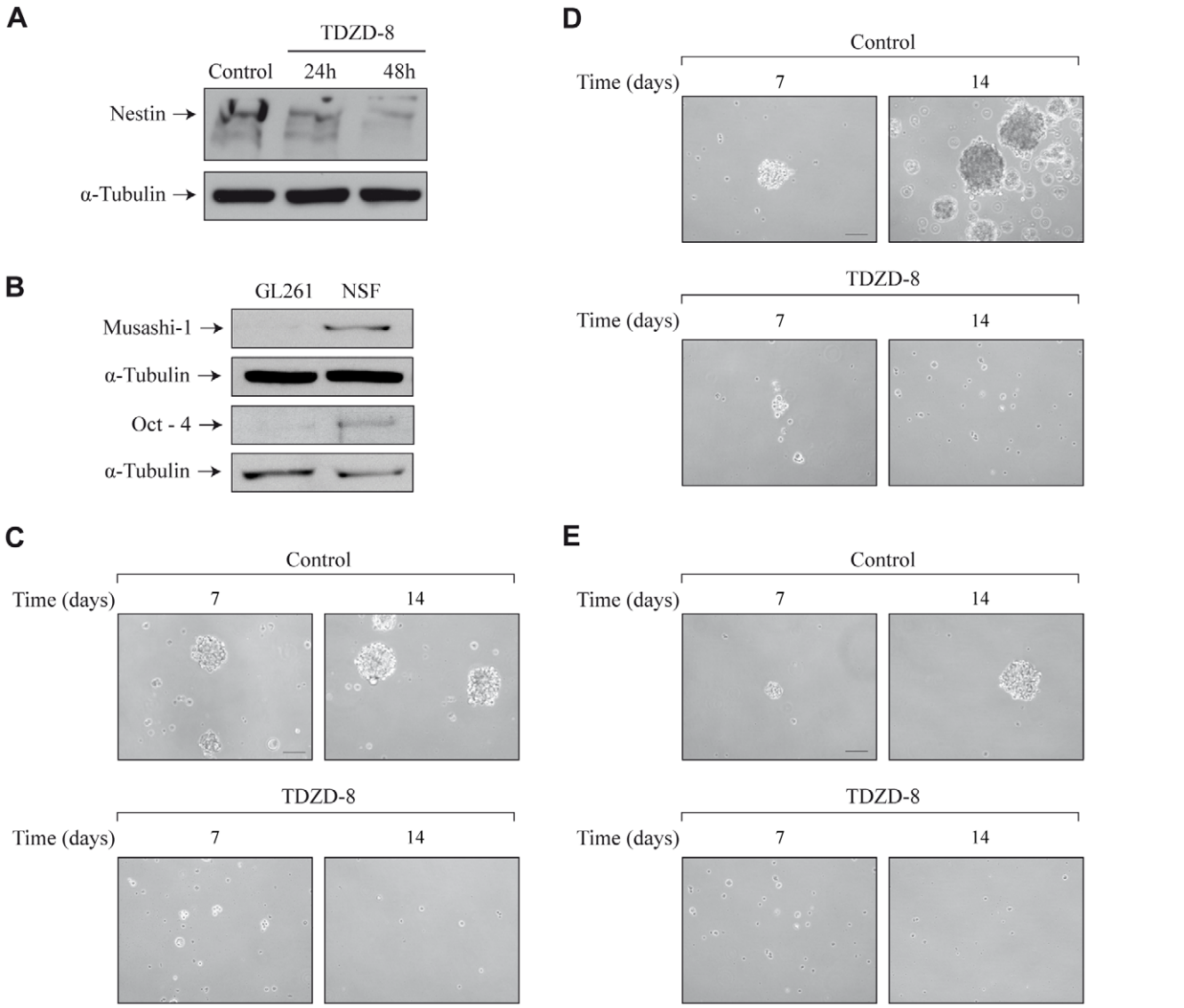

Figure 6. Effect of TDZD-8 on neurosphere formation. (A) Representative Western blot showing Nestin expression in adherent GL261 cells treated with TDZD-8. (B) Representative Western blot of stem cells markers musashi-1 and oct-4 in adherent GL261 and neurospheres cultures 7 days after plating. (C) Representative microphotographs of primary neurosphere cultures 7 and 14 days after plating in neurosphere medium. D) Primary neurospheres were dissociated and plated to analyze secondary neurosphere formation. Representative microphotographs are shown. (E) Representative microphotographs showing self-renewal capacity of neurosphere cultures growing in the presence or absence of TDZD-8. Scale bar, 100 μm.
doi:10.1371/journal.pone.0013879.g006

indicate a loss of stem cells induced by this compound. To further elucidate this point, we examined the effects of TDZD-8 on the formation and growth of GL261-derived neurospheres (primary neurospheres). First, we analyzed the levels of two well-known stem cell markers such as musashi-1 and oct-4 in adherent GL261 cells and neurosphere cultures. As shown in Figure 6B an increased amount of these proteins was observed in the neurospheres indicating an increased population of stem cells in these cultures, compared with attached GL261 cells. Next, we studied if TDZD-8 could affect the CSC population in GL261 glioblastoma cells. Figure 6C shows that TDZD-8 inhibited the formation of primary neurospheres. We observed a significant decrease, at both 7 and 14 days of culture, in the number and volume of TDZD-8-treated neurospheres, compared with controls. To more stringently test the effect of TDZD-8 on the ability of GBM cells to generate new spheres, actively growing 7 day-old GL261-derived primary neurosphere cultures were dissociated, and equal numbers of viable cells were replated in fresh neurosphere medium to generate new neurospheres (secondary neurospheres). Treatment of these cultures with TDZD-8 almost completely blocked the formation of secondary neurospheres (Fig. 6D). Additionally, when primary TDZD-8-treated cultures were dissociated and cultured again for 7 days in the absence of TDZD-8, no formation of secondary neurospheres was observed (data not shown). Finally, to test for the effect of TDZD-8 on the self-renewal of the neurosphere cultures, we dissociated established 7 day-old primary neurosphere cultures, plated them at a very low density [37], and analyzed the capacity to form secondary spheres. As shown in Figure 6E cultures treated with TDZD-8 did not give rise to secondary neurospheres 7 and 14 days after plating, indicating that these cultures did not contain self-renewing stem cells.

Discussion

In this study, we show for the first time that TDZD-8 suppresses the growth of glioma tumors *in vivo* and exerts anti-proliferative and pro-apoptotic activities in glioma cells *in vitro*. These effects were accompanied by an activation of the ERK/p90RSK pathway, a concomitant phosphorylation and inactivation of GSK-3β, and an inhibition of NF-κB activity. Finally, our data showing that TDZD-8 decreases the formation of neurospheres, both at low and high cell density, suggest that this drug could have an inhibitory effect on glioblastoma stem cells proliferation and self-renewal. Collectively, our findings suggest that TDZD-8 might be of therapeutic importance for the treatment of high-grade gliomas.

Previous studies have implicated GSK-3β in tumorigenesis. GSK-3β activation has been associated with prostate cancer progression and TDZD-8 has an inhibitory effect in these tumor cells [9]. Also, GSK-3β inactivation induces a p53-dependent apoptotic pathway resulting in a diminished colorectal cancer cell growth [10,38]. More recently, it has been shown that TDZD-8 inhibits proliferation and induces death of myeloma cell lines [39] and of malignant myeloid progenitors, while sparing normal hematopoietic tissue [18]. In the case of tumors from the central nervous system, contradictory results have been reported. Kotliarova et al. using different glioma cell lines have shown that GSK-3β activation promotes cell survival [30], whereas Ma et al. [40] have shown that GSK-3β activation is required for the induction of apoptosis in SK-N-MC neuroblastoma cells. Our data are in agreement with the results obtained by Kotliarova et al, here we clearly show that the inactivation of GSK-3β by TDZD-8 inhibits glioblastoma tumor growth in vivo. Thus, tumor development was significantly delayed and animal survival improved ($p = 0.006$) in mice injected with this compound. Moreover, TDZD-8 tumors lacked the aggressiveness of control tumors, including necrotic foci and a higher mitotic activity.

In view of the pleiotropic effects of TDZD-8, it is very likely that different mechanisms can be underlying its action. Initially TDZD-8 was synthesized as a high affinity ATP-non-competitive inhibitor of GSK-3β [11,12]. However, recently, several lines of evidence indicate that a GSK-3β-independent mechanism may be involved in TDZD-8 actions. Guzman et al have suggested that the activity of TDZD-8 can be independent of this inhibition since other known GSK-3β inhibitors fail to induce leukemia-specific cell death [18]. In this regard, we have shown that other TDZD compounds exert anti-inflammatory and neuroprotective effects in the brain through activation of the nuclear receptor PPARγ [41,42]. Here, we show that TDZD-8 rapidly activates ERK signaling pathway, which promotes EGR1 expression and an increase in p21 levels. Given the fact that this activation is very fast, it is very unlikely that it could be mediated trough activation of PPARγ. Our findings further corroborate other studies showing that an activation of MAPK signaling pathway in U-87MG glioma cells leads to a proliferation arrest mediated by an increase in EGR-1 expression which concomitantly stimulates p21 transcription [26]. In addition, we also show a delayed activation of ERKs in response to TDZD-8, which is followed by a phosphorylation and activation of p90RSK, a well-known target of these kinases [27,28]. This activation results in a phosphorylation and inactivation of GSK-3β [29]. These results are in agreement with previously published data showing that an activation of ERK is associated with a diminution of cell survival in different tumor cell lines, including glioblastoma cell lines [23,24,25]. Our results therefore suggest that TDZD-8 can inhibit GSK-3β activity not only by directly interacting with this enzyme but also through its phosphorylation at Ser9 via MAPK pathway activation.

It has been reported that inhibition of GSK-3β by different compounds, including TDZD-8, causes an inactivation of NF-κB activity [31,32] and Kotliarova et al have shown that several small molecular inhibitors of GSK-3β activity inhibit glioma cell survival in part through a decrease in intracellular NF-κB activity [30]. Consistent with these data we also show here that treatment of GL261 glioma cells with TDZD-8 led to a decrease in NF-κB activity within these cells. In this regard, other groups have shown that survival of different tumor cells depends on GSK-3β activity trough a NF-κB-dependent pathway [7,43,44].

There is mounting evidence that neural stem cells can be transformed into cancer stem cells and give rise to malignant gliomas by escaping the mechanisms that control proliferation and programmed differentiation [45,46,47]. Several data implicate glioma stem cells in tumor maintenance and therapeutic resistance [48,49,50], in consequence the discovery of putative brain tumor stem cells identifies a new cellular target that might be susceptible to novel treatments. Our results suggest that, in addition to have an inhibitory effect upon the bulk of glioblastomas, TDZD-8 could also inhibit cancer stem cell growth. Treatment with TDZD-8 resulted in an inhibition of neurosphere formation in culture. TDZD-8 inhibited the proliferation and expansion of these neurospheres and hampered their capacity of self-renewal. One feature that contributes to the ability of a stem cell to survive is its inherent resistance to drugs; in this regard our results are particularly important since they suggest that TDZD-8 could reduce the tumor-initiating cells. Our results provide compelling evidence that TDZD-8 is able to both inhibit the bulk of the tumor, characterized by actively cycling cells, and to hinder the growth of neural stem cells characterized by a low rate of division.

In summary, we have presented here the first evidence that TDZD-8 inhibits gliomagenesis and targets glioma stem-like cells and thus may hold promise for treatment of human gliomas.

Materials and Methods

Animal Experiments

Adult male C57BL/6 mice ($n = 10$ per group) were anaesthetized by intraperitoneal injection of ketamine (60 mg/Kg) and medetomidine (0.125 mg/Kg) and positioned in a stereotaxic apparatus (Kopf Instruments, CA). To establish intracranial tumors GL261 cells (125,000 cells) were implanted unilaterally into the right hemisphere using the following coordinates from Bregma: posterior −1.06 mm; lateral 3 mm and a depth of 3 mm, according to the atlas of Paxinos and Franklin [51]. The mice were then housed individually to recover. One day after implantation of GL261 cells, two groups of mice were injected daily intraperitoneally with 5 mg/Kg of TDZD-8 (Sigma) or DMSO (control group) during 22 days. In other group of animals, treatment with TDZD-8 was started 6 days after implantation of GL261 cells, during 7 days. All procedures with animals were specifically approved by the 'Ethics Committee for Animal Experimentation' of the Instituto de Investigaciones Biomedicas (CSIC-UAM), permit number PN 2007/108, and carried out in accordance with the protocols issued which followed National (normative 1201/2005) and International recommendations (normative 86/609 from the European Communities Council). Special care was taken to minimize animal suffering.

Magnetic Resonance Imaging

Magnetic Resonance Imaging (MRI) was performed using an MRI scanner (Bruker PharmaScan 7.0T, 16 cm; Bruker Medical Gmbh, Ettlingen, Germany). Mice brain MRI was performed with a 90 mm gradient insert and a concentrical 38 mm birdcage

resonator, using Paravision v4.0 software (Bruker Medical Gmbh, Ettlingen, Germany) as implemented in a Hewlett-Packard console, operating on a Linux platform. MRI examinations used adult male C57BL/6 mice ($n \geq 10$ per group) anaesthetized through a plastic mask with 2% isofluorane in 99.9% O_2. Animals were allowed to breath spontaneously during the experiment and were placed in a heated cradle to maintain the core body temperature at approx. 37°C. The physiological state of the animal was monitored throughout MRI acquisition through the respiratory rate using a Biotrig physiological monitor (Brucker). Gadolinium-DTPA-enhanced T_1-weighted spin-echo images were acquired at 8, 10, 13 and 20 days after injection with a Rapid Acquisition with Relaxation Enhancement (RARE) [52] sequence in axial orientations (TR: 350 ms, TE: 10.6 ms, averages: 4, FOV: 2.30 cm, acquisition matrix: 256×256, slice thickness: 1.00 mm, number of slices: 16). The *in vivo* spectroscopy protocol acquired two 3x3x3 mm voxels in the striatal area, using a Point-Resolved Spatially Spectroscopy (PRESS) [53] protocol, combined with VAPOR water suppression, [54](TR: 3000 ms, TE: 35 ms, averages: 128). Tumor area was calculated from T_1-weighted images using Image J Software. Tumor volume was estimated from the summation of tumor areas on each slice, multiplied by slice thickness. Average lesion volume was calculated for each condition.

Histology and Immunohistochemistry

Brains were dissected and embedded in paraffin. Sections of 10 μm thickness were prepared and stained with haematoxylin and eosin. Paraffin embedded sections, were also used for detecting proliferation and apoptosis in tumors. First, sections were deparaffinized in xylene and rehydrated in graded concentrations of ethanol. Endogenous peroxidase activity was blocked by incubation in H_2O_2 and after several rinses in PBS, antigen retrieval was performed by microwaving slides in citrate buffer. Once non-specific binding sites were blocked for 1 hour at room temperature, sections were incubated in humid chamber at 4°C overnight with anti-active caspase-3 (1:200, R&D Systems) and anti-PCNA (1:50, Signet Laboratories). After several rinses, sections were incubated for 1 h with a biotinylated secondary antibody and finally processed following the avidin-biotin protocol (Vectastain ABC kit; Vector Laboratories). Tissues were mounted onto gelatin-coated slides, dehydrated, cleared in xylene, and mounted with DePeX (Serva, Heidelberg, Germany). The slides were examined under a Zeiss (Oberkochen, Germany) Axiophot microscope, equipped with an Olympus Optical (Tokyo, Japan) DP-50 digital camera, and a Leica (Nussloch, Germany) MZ6 modular stereomicroscope. For the quantification of active caspase-3 and PCNA expression, the number of positive cells was quantified in 20 random fields at x400 magnification. Data were expressed as mean ± SD positive cells/field.

Cell culture and treatment

GL261 murine glioblastoma cells were obtained from the NCI-Frederick Cancer Research Tumor Repository (Frederick, MD) and propagated in RPMI medium with 10% fetal bovine serum as described [55]. A172 and U373 human glioblastoma cell lines were obtained from Dr. Manuel Guzman (Complutense University, Madrid, Spain) and propagated in DMEM with 10% FBS. On attaining semiconfluence, and based in dose-response analysis (see Fig. S2), cells were treated with 20 μM TDZD-8, a dose widely used in the literature [18,56], for different time intervals. Following treatment cells were processed for western blot and immunocytochemical analysis.

For neurosphere formation GL261 cells were plated and grown in regular medium (RPMI, 10% FBS, glutamine, gentamicine and fungizone). Two days after plating, supernatant was collected and replated in a defined serum-free tumor sphere medium formed by Ham's F-12/Dulbecco's modified Eagle's medium (1:1) supplemented with B27 (Invitrogen, Carlsbad, CA), 20 ng/ml epidermal growth factor (EGF, Peprotech, EC) and 20 ng/ml fibroblast growth factor (FGF, Peprotech, EC). After 1 week in culture some primary neurosphere cultures were treated with TDZD-8 (10 μM) for another 1 week. These primary neurospheres were then dissociated, and 50,000 cells/ml were replated in proliferative conditions, in the absence or presence of TDZD-8, for another 7 or 14 days to score the number of secondary neurospheres generated. For self-renewing experiments, primary neurospheres were dissociated and plated at a density of 2,000 cells/ml for another 7 or 14 days in proliferative medium containing or not TDZD-8. These assays were repeated at least three times in triplicate.

Proliferation assays

The effect of TDZD-8 on cell proliferation was determined using the non-radioactive BrdU-based cell proliferation assay (Roche) according to the manufacturer's protocol. Cells were seeded in triplicate onto 96-well plates at a density of 2,000 cells/well. After 24 h of growth, cells were treated with 20 μM TDZD-8, 16 h later 10 μM BrdU was added and cells were cultured for another 16 h. BrdU incorporation into the DNA was determined by measuring the absorbance at both 370 and 492 nm on an ELISA plate reader.

Cell viability was measured using the MTT assay (Roche Diagnostic, GmbH), based on the ability of viable cells to reduce yellow MTT to blue formazan. Briefly, cells were cultured in 96-well microlitre plates for various periods of time in the presence or absence of 20 μM TDZD-8, then cells were incubated with MTT (0.5 mg/ml, 4 h) and subsequently solubilized in 10% SDS/0.01 M HCl for 12 h in the dark. The extent of reduction of MTT was quantified by absorbance measurement at 550 nm according to the manufacturer's protocol.

Immunoblot analysis

Cultured cells, both adherent and floating cancer stem cells, were harvested and lysed in ice-cold RIPA buffer and equal quantities of total protein were separated by 10% SDS-PAGE. After electrophoresis, proteins were transferred to nitrocellulose membranes (Protran, Whatman, Dassel, Germany) and blots were probed with the indicated primary antibodies, as previously described [57]. The antibodies used were the following: rabbit polyclonal anti-p-ERK1/2 (1:1000, Cell Signaling), rabbit polyclonal anti-ERK1/2 (Cell Signaling), rabbit polyclonal anti-p90RSK (1:1000, Cell Signaling), rabbit polyclonal anti-p-GSK-3β (1:500, Cell Signaling), mouse monoclonal anti-GSK-3β (1:250, BD Transduction), rabbit polyclonal anti-EGR-1 (1:1000, Santa Cruz Biotechnology), rabbit polyclonal anti-p21 (1:1000, Abcam), rabbit polyclonal anti-Musashi 1 (1:1000, Abcam), rabbit polyclonal anti-Oct-4 (1:500, Santa Cruz Biotechnology), rabbit polyclonal anti-Nestin (1:2000; kindly provided by Dr. M. Vallejo, Instituto de Investigaciones Biomédicas, Madrid, Spain), and mouse monoclonal anti-α-tubulin (1:5000, Sigma). Secondary peroxidase-conjugated donkey anti-rabbit and rabbit anti-mouse antibodies were from Amersham Biosciences (GE Healthcare, Buckinghamshire, England) and Jackson Immunoresearch, respectively.

Immunocytochemical staining

At the end of the treatment period the cultures, grown on glass cover-slips in 24-well cell culture plates, were washed with PBS

and fixed for 30 min with 4% paraformaldehyde at 25°C and permeabilized with 0.1% Triton X-100 for 30 min at 37°C. After 1 h incubation with the corresponding primary antibody: anti-active caspase-3 (1:500, R&D Systems) cells were washed with PBS and incubated with an Alexa-labeled secondary antibody (Invitrogen, San Diego, CA) for 45 min at 37°C. Images were acquired using a Radiance 2100 confocal microscope (Bio-Rad, Hercules, CA), with a 350 nm diode laser to excite DAPI (4,6,diamidino-2-phenylindole) and a 488-Argon laser to excite Alexa 488. Confocal microscope settings were adjusted to produce the optimum signal-to-noise ratio. To compare fluorescence signals from different preparations, settings were fixed for all samples within the same analysis.

Determination of apoptotic cells

To calculate the extend of cell death, cells were treated or not with TDZD-8 and TUNEL analysis were performed following the manufacturer's recommendations. Caspase-3 activation was analyzed by immunofluorescence analysis using a specific anti-active caspase-3 antibody. Some cultures were treated with the caspase inhibitor z-VAD-fmk.

Transient transfections

For transient transfection experiments, semi-confluent GL261 cells were transfected with the 3xNFtk-luc reporter plasmid as previously described [58]. Forty-eight hours after transfection, cells were harvested for luciferase and-β-galactosidase (to determine transfection efficiency) activities by using a reporter assay system (Promega, Madison, WI). Each transient transfection experiment was repeated at least three times in triplicate.

Statistics

Other than the survival experiments, Student's test was used to analyze statistical differences between the different groups. Survival curves were plotted with Kaplan-Meier method and survival for the two groups of animals was studied using log-rank test. Differences were considered statistically significant at $p<0.05$.

Supporting Information

Figure S1 Effects of TDZD-8 administered after tumor is established. Representative T_1 magnetic resonance imaging (MRI) pictures obtained from mice treated with TDZD-8 from day 6 after GL261 cells injection. T_1-weighted imaging was performed at 7 Tesla as described in Materials and Methods. The arrow indicates the day the treatment was initiated.
Found at: doi:10.1371/journal.pone.0013879.s001 (1.16 MB TIF)

Figure S2 Cell viability in TDZD-8-treated cells. GL261 glioblastoma cells were incubated with various concentrations of TDZD-8 and viability was assessed by the MTT assay, as indicated in Materials and Methods. Values are the means ± SD of at least three different experiments.
Found at: doi:10.1371/journal.pone.0013879.s002 (0.07 MB TIF)

Author Contributions

Conceived and designed the experiments: AS APC. Performed the experiments: DAM JAMG MSS. Analyzed the data: DAM JAMG MAGC AS APC. Wrote the paper: APC.

References

1. DeAngelis LM (2001) Brain tumors. N Engl J Med 344: 114–123.
2. Benedetti S, Pirola B, Pollo B, Magrassi L, Bruzzone MG, et al. (2000) Gene therapy of experimental brain tumors using neural progenitor cells. Nat Med 6: 447–450.
3. Fomchenko EI, Holland EC (2006) Mouse models of brain tumors and their applications in preclinical trials. Clin Cancer Res 12: 5288–5297.
4. Jope RS, Johnson GV (2004) The glamour and gloom of glycogen synthase kinase-3. Trends Biochem Sci 29: 95–102.
5. Kim L, Kimmel AR (2000) GSK3, a master switch regulating cell-fate specification and tumorigenesis. Curr Opin Genet Dev 10: 508–514.
6. Kaidanovich O, Eldar-Finkelman H (2002) The role of glycogen synthase kinase-3 in insulin resistance and type 2 diabetes. Expert Opin Ther Targets 6: 555–561.
7. Hoeflich KP, Luo J, Rubie EA, Tsao MS, Jin O, et al. (2000) Requirement for glycogen synthase kinase-3beta in cell survival and NF-kappaB activation. Nature 406: 86–90.
8. De Ferrari GV, Inestrosa NC (2000) Wnt signaling function in Alzheimer's disease. Brain Res Brain Res Rev 33: 1–12.
9. Sun A, Shanmugam I, Song J, Terranova PF, Thrasher JB, et al. (2007) Lithium suppresses cell proliferation by interrupting E2F-DNA interaction and subsequently reducing S-phase gene expression in prostate cancer. Prostate 67: 976–988.
10. Ghosh JC, Altieri DC (2005) Activation of p53-dependent apoptosis by acute ablation of glycogen synthase kinase-3beta in colorectal cancer cells. Clin Cancer Res 11: 4580–4588.
11. Martinez A, Alonso M, Castro A, Perez C, Moreno FJ (2002) First non-ATP competitive glycogen synthase kinase 3 beta (GSK-3beta) inhibitors: thiadiazolidinones (TDZD) as potential drugs for the treatment of Alzheimer's disease. J Med Chem 45: 1292–1299.
12. Martinez A, Castro A, Dorronsoro I, Alonso M (2002) GSK-3 inhibitors as promising drugs for the treatment of Alzheimer disease, cancer, diabetes, and inflammation. MedResRev 22: 373–384.
13. Chin PC, Majdzadeh N, D'Mello SR (2005) Inhibition of GSK3beta is a common event in neuroprotection by different survival factors. Brain Res Mol Brain Res 137: 193–201.
14. Dugo L, Abdelrahman M, Murch O, Mazzon E, Cuzzocrea S, et al. (2006) Glycogen synthase kinase-3beta inhibitors protect against the organ injury and dysfunction caused by hemorrhage and resuscitation. Shock 25: 485–491.
15. Cuzzocrea S, Mazzon E, Di Paola R, Muia C, Crisafulli C, et al. (2006) Glycogen synthase kinase-3beta inhibition attenuates the degree of arthritis caused by type II collagen in the mouse. Clin Immunol 120: 57–67.
16. Cuzzocrea S, Genovese T, Mazzon E, Crisafulli C, Di Paola R, et al. (2006) Glycogen synthase kinase-3 beta inhibition reduces secondary damage in experimental spinal cord trauma. J Pharmacol Exp Ther 318: 79–89.
17. Whittle BJ, Varga C, Posa A, Molnar A, Collin M, et al. (2006) Reduction of experimental colitis in the rat by inhibitors of glycogen synthase kinase-3beta. Br J Pharmacol 147: 575–582.
18. Guzman ML, Li X, Corbett CA, Rossi RM, Bushnell T, et al. (2007) Rapid and selective death of leukemia stem and progenitor cells induced by the compound 4-benzyl, 2-methyl, 1,2,4-thiadiazolidine, 3,5 dione (TDZD-8). Blood 110: 4436–4444.
19. Edwards E, Geng L, Tan J, Onishko H, Donnelly E, et al. (2002) Phosphatidylinositol 3-kinase/Akt signaling in the response of vascular endothelium to ionizing radiation. Cancer Res 62: 4671–4677.
20. Kjaergaard J, Tanaka J, Kim JA, Rothchild K, Weinberg A, et al. (2000) Therapeutic efficacy of OX-40 receptor antibody depends on tumor immunogenicity and anatomic site of tumor growth. Cancer Res 60: 5514–5521.
21. Miyatake S, Martuza RL, Rabkin SD (1997) Defective herpes simplex virus vectors expressing thymidine kinase for the treatment of malignant glioma. Cancer Gene Ther 4: 222–228.
22. Zagzag D, Miller DC, Chiriboga L, Yee H, Newcomb EW (2003) Green fluorescent protein immunohistochemistry as a novel experimental tool for the detection of glioma cell invasion in vivo. Brain Pathol 13: 34–37.
23. Goulet AC, Chigbrow M, Frisk P, Nelson MA (2005) Selenomethionine induces sustained ERK phosphorylation leading to cell-cycle arrest in human colon cancer cells. Carcinogenesis 26: 109–117.
24. Tang D, Wu D, Hirao A, Lahti JM, Liu L, et al. (2002) ERK activation mediates cell cycle arrest and apoptosis after DNA damage independently of p53. J Biol Chem 277: 12710–12717.
25. Tewari R, Sharma V, Koul N, Sen E (2008) Involvement of miltefosine-mediated ERK activation in glioma cell apoptosis through Fas regulation. J Neurochem 107: 616–627.
26. Choi BH, Kim CG, Bae YS, Lim Y, Lee YH, et al. (2008) p21 Waf1/Cip1 expression by curcumin in U-87MG human glioma cells: role of early growth response-1 expression. Cancer Res 68: 1369–1377.
27. Wang Z, Zhang B, Wang M, Carr BI (2003) Persistent ERK phosphorylation negatively regulates cAMP response element-binding protein (CREB) activity via recruitment of CREB-binding protein to pp90RSK. J Biol Chem 278: 11138–11144.
28. Roux PP, Richards SA, Blenis J (2003) Phosphorylation of p90 ribosomal S6 kinase (RSK) regulates extracellular signal-regulated kinase docking and RSK activity. Mol Cell Biol 23: 4796–4804.

29. Eldar-Finkelman H (2002) Glycogen synthase kinase 3: an emerging therapeutic target. Trends Mol Med 8: 126–132.
30. Kotliarova S, Pastorino S, Kovell LC, Kotliarov Y, Song H, et al. (2008) Glycogen synthase kinase-3 inhibition induces glioma cell death through c-MYC, nuclear factor-kappaB, and glucose regulation. Cancer Res 68: 6643–6651.
31. Collino M, Aragno M, Castiglia S, Tomasinelli C, Thiemermann C, et al. (2009) Insulin reduces cerebral ischemia/reperfusion injury in the hippocampus of diabetic rats: a role for glycogen synthase kinase-3beta. Diabetes 58: 235–242.
32. Gao HK, Yin Z, Zhou N, Feng XY, Gao F, et al. (2008) Glycogen synthase kinase 3 inhibition protects the heart from acute ischemia-reperfusion injury via inhibition of inflammation and apoptosis. J Cardiovasc Pharmacol 52: 286–292.
33. Galli R, Binda E, Orfanelli U, Cipelletti B, Gritti A, et al. (2004) Isolation and characterization of tumorigenic, stem-like neural precursors from human glioblastoma. Cancer Res 64: 7011–7021.
34. Palmer TD, Willhoite AR, Gage FH (2000) Vascular niche for adult hippocampal neurogenesis. J Comp Neurol 425: 479–494.
35. Singh SK, Clarke ID, Hide T, Dirks PB (2004) Cancer stem cells in nervous system tumors. Oncogene 23: 7267–7273.
36. Taylor MD, Poppleton H, Fuller C, Su X, Liu Y, et al. (2005) Radial glia cells are candidate stem cells of ependymoma. Cancer Cell 8: 323–335.
37. Kong H, Fan Y, Xie J, Ding J, Sha L, et al. (2008) AQP4 knockout impairs proliferation, migration and neuronal differentiation of adult neural stem cells. J Cell Sci 121: 4029–4036.
38. Tan J, Zhuang L, Leong HS, Iyer NG, Liu ET, et al. (2005) Pharmacologic modulation of glycogen synthase kinase-3beta promotes p53-dependent apoptosis through a direct Bax-mediated mitochondrial pathway in colorectal cancer cells. Cancer Res 65: 9012–9020.
39. Zhou Y, Uddin S, Zimmerman T, Kang JA, Ulaszek J, et al. (2008) Growth control of multiple myeloma cells through inhibition of glycogen synthase kinase-3. Leuk Lymphoma 49: 1945–1953.
40. Ma C, Bower KA, Chen G, Shi X, Ke ZJ, et al. (2008) Interaction between ERK and GSK3beta mediates basic fibroblast growth factor-induced apoptosis in SK-N-MC neuroblastoma cells. J Biol Chem 283: 9248–9256.
41. Luna-Medina R, Cortes-Canteli M, Alonso M, Santos A, Martinez A, et al. (2005) Regulation of Inflammatory Response in Neural Cells in Vitro by Thiadiazolidinones Derivatives through Peroxisome Proliferator-activated Receptor {gamma} Activation. J Biol Chem 280: 21453–21462.
42. Luna-Medina R, Cortes-Canteli M, Sanchez-Galiano S, Morales-Garcia JA, Martinez A, et al. (2007) NP031112, a thiadiazolidinone compound, prevents inflammation and neurodegeneration under excitotoxic conditions: potential therapeutic role in brain disorders. The Journal of neuroscience 27: 5766–5776.
43. Takada Y, Fang X, Jamaluddin MS, Boyd DD, Aggarwal BB (2004) Genetic deletion of glycogen synthase kinase-3beta abrogates activation of IkappaBalpha kinase, JNK, Akt, and p44/p42 MAPK but potentiates apoptosis induced by tumor necrosis factor. J Biol Chem 279: 39541–39554.
44. Deng J, Xia W, Miller SA, Wen Y, Wang HY, et al. (2004) Crossregulation of NF-kappaB by the APC/GSK-3beta/beta-catenin pathway. Mol Carcinog 39: 139–146.
45. Singh SK, Clarke ID, Terasaki M, Bonn VE, Hawkins C, et al. (2003) Identification of a cancer stem cell in human brain tumors. Cancer Res 63: 5821–5828.
46. Singh SK, Hawkins C, Clarke ID, Squire JA, Bayani J, et al. (2004) Identification of human brain tumour initiating cells. Nature 432: 396–401.
47. Sanai N, Alvarez-Buylla A, Berger MS (2005) Neural stem cells and the origin of gliomas. N Engl J Med 353: 811–822.
48. Bao S, Wu Q, McLendon RE, Hao Y, Shi Q, et al. (2006) Glioma stem cells promote radioresistance by preferential activation of the DNA damage response. Nature 444: 756–760.
49. Phillips TM, McBride WH, Pajonk F (2006) The response of CD24(-/low)/CD44+ breast cancer-initiating cells to radiation. J Natl Cancer Inst 98: 1777–1785.
50. Woodward WA, Chen MS, Behbod F, Alfaro MP, Buchholz TA, et al. (2007) WNT/beta-catenin mediates radiation resistance of mouse mammary progenitor cells. Proc Natl Acad Sci U S A 104: 618–623.
51. Paxinos G, Franklin K (2001) The mouse brain in stereotaxic coordinates. San Diego: Academic Press.
52. Hennig J, Nauerth A, Friedburg H (1986) RARE imaging: a fast imaging method for clinical MR. Magn Reson Med 3: 823–833.
53. Bottomley PA (1987) Spatial localization in NMR spectroscopy in vivo. Ann N Y Acad Sci 508: 333–348.
54. Tkac I, Starcuk Z, Choi IY, Gruetter R (1999) In vivo 1H NMR spectroscopy of rat brain at 1 ms echo time. Magn Reson Med 41: 649–656.
55. El Andaloussi A, Sonabend AM, Han Y, Lesniak MS (2006) Stimulation of TLR9 with CpG ODN enhances apoptosis of glioma and prolongs the survival of mice with experimental brain tumors. Glia 54: 526–535.
56. Kim SD, Yang SI, Kim HC, Shin CY, Ko KH (2007) Inhibition of GSK-3beta mediates expression of MMP-9 through ERK1/2 activation and translocation of NF-kappaB in rat primary astrocyte. Brain Res 1186: 12–20.
57. Cortes-Canteli M, Wagner M, Ansorge W, Perez-Castillo A (2004) Microarray analysis supports a role for ccaat/enhancer-binding protein-beta in brain injury. J Biol Chem 279: 14409–14417.
58. Pignatelli M, Sanchez-Rodriguez J, Santos A, Perez-Castillo A (2005) 15-Deoxy-{Delta}-12,14-prostaglandin J2 induces programmed cell death of breast cancer cells by a pleiotropic mechanism. Carcinogenesis 26: 81–92.

Developmental Hypothyroidism Increases the Expression of Kainate Receptors in the Hippocampus and the Sensitivity to Kainic Acid-Induced Seizures in the Rat

Elena Giné, Jose Angel Morales-Garcia, Ana Perez-Castillo, and Angel Santos

Departamento de Biología Celular (E.G.) and Departamento de Bioquímica y Biología Molecular (E.G., A.S.), Facultad de Medicina, Universidad Complutense de Madrid, 28040 Madrid, Spain; and Instituto de Investigaciones Biomédicas (J.A.M.-G., A.P.-C.), Consejo Superior de Investigaciones Cientificas-Universidad Autónoma de Madrid and Centro de Investigación Biomédica en Red Sobre Enfermedades Neurodegenerativas, 28029 Madrid, Spain

Thyroid hormones are essential for normal brain development, and multiple alterations at behavioral, cognitive, cellular, and molecular levels have been described in animals made hypothyroid during development. Here we analyzed the effect of developmental hypothyroidism in the rat on the sensitivity to kainic acid-induced limbic seizures and the expression of kainate receptors in the hippocampus. Our results show that hypothyroid rats are extremely sensitive to the proconvulsant and neurotoxic effects of kainic acid (KA). Hypothyroid rats entered in status epilepticus at a dose of KA three times lower than that required to reach status epilepticus in control animals. In accordance with this, high levels of glial activation and neuronal loss after low KA dose injections were observed only in the hippocampus of hypothyroid rats. These effects correlated with an increased expression of kainate receptor subunits, excluding GluR5, in the hippocampus of hypothyroid animals. The concentrations of GluR6, GluR7, KAR1, and KAR2 (ionotropic glutamate receptor subunits of the kainic acid subtype) mRNAs were increased between 50 and 250% in hypothyroid animals relative to the values in controls. In agreement with these results, Western blot and immunohistochemical analysis showed a clear increase in the hippocampal content of GluR6/7 proteins in hypothyroid animals. **(*Endocrinology* 151: 3267–3276, 2010)**

Thyroid hormones (T_4 and T_3) play an important role in the development and metabolism of many mammalian tissues. Most of their actions are mediated by the binding of T_3 to specific nuclear receptors that are ligand-dependent transcription factors that bind to specific DNA sequences in target genes, called thyroid hormone-response elements, and regulate transcription initiation (1, 2). Hence, the regulation by thyroid hormone of the expression of a limited number of genes in the target tissues represents the main mechanism of action of these hormones. Thyroid hormone receptors belong to the nuclear receptor superfamily that is one of the largest families of transcription factors, which include, among others, the receptors for steroid hormones, retinoids, vitamin D_3, peroxisomal proliferators, and many other transcription factors without known ligand (orphan receptors) (1). The transcriptional activity of this family of proteins is regulated by ligand-dependent and ligand-independent mechanisms (3) and participate in a broad range of physiological and cellular functions.

The brain is an important target for thyroid hormone action, as shown by numerous clinical and experimental data (4, 5). The expression of thyroid hormone receptors in the rat brain increases rapidly after birth, reaching the highest value by d 6 of postnatal life (6, 7). In agreement with this, it is during the perinatal period that the conse-

ISSN Print 0013-7227 ISSN Online 1945-7170
Printed in U.S.A.

doi: 10.1210/en.2010-0070 Received January 19, 2010. Accepted April 1, 2010.
First Published Online April 21, 2010

Abbreviations: BW, Body weight; GABAergic, secretion of γ-aminobutyric acid; GFAP, glial fibrillary acidic protein; GluR5-7 and KAR1-2, ionotropic glutamate receptor subunits of the kainic acid subtype; KA, kainic acid; PTZ, pentylenetetrazole; SE, status epilepticus.

quences of hypothyroidism are more dramatic and results in numerous alterations, such as reduction in dendritic arborization of cerebellar Purkinje cells; impairment of nerve process development; poor connectivity among neurons; changes in microtubule content; and impaired myelin deposition, cell migration, and synaptogenesis (5). Many of these alterations become permanent unless an appropriate replacement therapy with thyroid hormones is started very soon after birth. Not all the areas in the brain are equally sensitive to the action of these hormones, and this sensitivity depends on the developmental stage of the animals. Therefore, marked differences, in the response to thyroid hormones, have been observed in different areas and at different developmental ages (8–10).

The hippocampus is indeed an area sensitive to the action of thyroid hormones, both during development and in adults, as shown by numerous clinical and experimental data. In humans, when hypothyroidism occurs during the developmental period, irreversible and severe cognitive deficits and morphological alterations in the hippocampus are observed (11, 12). These effects are less severe when hypothyroidism arises in the adult life, during which minor and reversible cognitive deficits and mood disorders are observed (13). Related with these symptoms, a decrease in glucose metabolism in diverse brain areas, including the hippocampus, has been described in adult hypothyroid patients (14). All these symptoms are reversed by an appropriate thyroid hormone therapy. In experimental animals, developmental hypothyroidism has been associated with morphological, electrophysiological, and biochemical alterations in the hippocampus. A reduction in the number and maturation of both glial and neuronal populations have been described in specific layers of the hippocampus of hypothyroid rats (4, 15, 16) together with marked alterations of synaptic transmission and plasticity and gene expression (17–20). Many of these changes become permanent unless an appropriate therapy is applied. In adult-onset hypothyroidism, diverse neurological alterations also have been described in the rat hippocampus. Memory deficits in hypothyroid animals have been associated with long-term potentiation impairment in CA1 (21) and decreased hippocampal neurogenesis could contribute to depressive-like behavior (22).

A possible role of thyroid hormones in rendering the brain more susceptible to alterations similar to epilepsies derives from clinical cases of dysthyroidism associated with seizures (23–28). Experimental evidence also indicates that dysthyroidism lowers the seizure threshold (29, 30). Additionally, genetically epilepsy-prone rats are hypothyroid (31), and mice prone to audiogenic seizures have postnatal levels of thyroid hormone higher than control mice; treatment with antithyroid drugs improves this condition and T_3 worsens it (32).

The neurotoxin kainic acid (KA) is a potent agonist of the kainate receptors, although also can act through other ionotropic glutamate receptors. Systemic or brain administration of this toxin produces convulsion and can render animals susceptible to unprovoked recurrent seizures, resembling some of the features of human temporal lobe epilepsia such as hippocampal sclerosis (33). Besides KA, other pharmacological agents, frequently used to induce limbic seizures and extensive hippocampal damage, include the cholinergic agonist pilocarpine, probably the most frequently used model of temporal lobe epilepsy, and the secretion of γ-aminobutyric acid (GABAergic) antagonist pentylenetetrazole (PTZ) (34).

In this work, we analyzed, in adult rats, the effect of developmentally induced hypothyroidism on hippocampal sensitivity to this neurotoxin and its possible causes. Our results show a higher sensitivity of hypothyroid animals to KA-induced limbic seizures and neurological damage together with a parallel increase in the amount of ionotropic glutamate receptor of the kainate type in the hippocampus. These effects were not reversed by thyroid hormone treatment because only minor improvements were observed in hypothyroid rats treated with physiological doses of thyroid hormones.

Materials and Methods

Materials

Methyl mercaptoimidazole, T_4, T_3, KA, pilocarpine, scopolamine, lithium chloride, and pentylenetetrazole were obtained from Sigma Chemical Co. (St. Louis, MO). All other chemicals were reagent grade or molecular biology grade.

Animal treatment

Female Wistar rats were mated and the day of appearance of the vaginal plug was considered as d 0 of fetal age. To induce fetal and neonatal hypothyroidism, dams were given 0.02% methyl mercaptoimidazole in the drinking water at d 12 of gestation. This protocol ensures that the animals are hypothyroid, as shown by the decrease growth rate and circulating levels of T_3 (35). Methyl mercaptoimidazole treatment was continued throughout the whole experimental period, and all studies were conducted in adult-age rats. To determine the reversibility of the effects caused by hypothyroidism, hypothyroid rats were daily treated with a physiological combination of T_4 [0.9 μg per 100 g body weight (BW)] and T_3 (0.2 μg per 100 g BW) during 1 wk. The corresponding hypothyroid controls received an equivalent volume of physiological saline.

All animal related procedures were approved by the Laboratory Animal Care and Use Committee of the Universidad Complutense de Madrid and were conducted in accordance with the guidelines of the European Communities Council, Directive 86/609/EEC. All efforts were made to minimize animal suffering and reduce the number of animals used.

Seizure induction

KA was sc injected at the indicated doses and the animals were placed in individual plastic cages and monitored for 3 h. Video recordings were made with a black-and-white video camera. The convulsive behavior was classified according to the accumulative scale of Racine (36) and Sperk *et al.* (33), as follows: stage 0, no changes; stage 0.5, wet dog shakes; stage 1, mouth and facial movements; stage 2, head nodding; stage 3, forelimbs clonus; stage 4, rearing; stage 5, rearing and falling; stage 6, death. Status epilepticus (SE) was defined as continuous or intermittent behavioral seizure activity without recovery of complete consciousness (stages 4–5) for at least 30 min. Behavioral seizures were scored by their latency (minutes) to onset of SE after KA injection.

Seizure induction by lithium-pilocarpine was as follows: the day before the experiment the animals were ip injected with 128 mg/kg LiCl; 30 min before the first pilocarpine injection, the animals were ip injected with scopolamine (1 mg/kg), and pilocarpine (10 mg/kg) was injected every 30 min (up to four injections maximum) until the animal reached SE (37). SE was stopped after 1 h with ip injection of diazepam (4 mg/kg). Finally, the proconvulsant drug pentylenetetrazole was ip injected at a subthreshold dose (35 mg/kg) and the convulsive behavior of animals monitored as indicated.

Real-time PCR

Total RNA from the hippocampus was purified according to the method of Chomczynski and Sacchi (38), and samples (2 μg) were used for the synthesis of cDNA with the RETRoscript kit (Ambion, Austin, TX) using pd(N)6 random hexamer as primers. Real-time PCR was performed in ABI Prism equipment using the SYBR Green PCR master mix (Applied Biosystems, Warrington, UK) and 300-nm concentrations of specific primers. In all samples, each specific sequence was measured at least twice in triplicate. The primers used for the determination of the concentration of the different transcripts were as follows: GluR5: TCA AAA TCC GCC AGC TTC C and TGA GCA GAG GTT TGG CGT CT; *GluR6*: CAG TCC ATC TGC AAC TGT CT and TTC CAG CGG GTC TGT ATG TG; *GluR7*: CCG CAA GTC TGA TAG GAC CC and CAG TAG CCC TCG AAC CGG T; *KAR1* (ionotropic glutamate receptor subunits of the kainic acid subtype) : CAG CCC AGT GTG TTT GTG A and AAC ACC CTG GCA ATT CCC TC; and *KAR2*: TCT TGG GCT TTT CCA TGT TCA and CAA ACT CCG GGT AGA AGG GAT. All of them synthesized DNA fragments of 51 bp. Amplification of the 18S rRNA was used for normalization of cDNA loading in the PCR as previously described (39).

In control hippocampus, random primer cDNA (dilution 1:10) gave cycle threshold values of around 26, 21, 22, 23, and 24 for *GluR5*, *GluR6*, *GluR7*, *KAR1*, and *KAR2* transcripts, respectively. In the case of 18S rRNA, a dilution of 1:1000 gave cycle threshold values between 20 and 21.

Western blot analysis

Hippocampal tissues were homogenized in radioimmunoprecipitation assay buffer and equal quantities of total protein separated by 10% SDS-PAGE and transferred to nitrocellulose membranes (Protran; Whatman, Dassel, Germany). Blots were probed with anti-GluR6/7 polyclonal antibody (Millipore, Bedford, MA) and monoclonal anti-α-tubulin (Sigma). Immunoreactive bands were visualized using the ECL detection kit (Amersham Biosciences, Inc., Buckinghamshire, UK) according to the manufacturer's instructions and quantified by densitometry using ImagePro Plus software (Media Cybernetics, Carlsbad, CA).

Immunohistochemistry

The animals were anesthetized and perfused transcardially with 4% paraformaldehyde solution. The brains were removed, postfixed in the same solution at 4 C overnight, cryoprotected in the paraformaldehyde solution containing 30% sucrose, and kept at −70 C until used. Coronal sections (30 μm) were obtained in a cryostat and processed for cresyl violet (Nissl stain) or immunohistochemistry using the diaminobenzidine method. For the diaminobenzidine method, the sections were immersed for 15 min in 3% H_2O_2 to inactivate endogenous peroxidase and then blocked for 2 h at room temperature in 5% normal goat serum (Vector Laboratories, Burlingame, CA) in PBS containing 4% BSA, 0.1 M lysine, and 0.1% Triton X-100. Afterward the sections were incubated overnight with the corresponding primary antibodies. After several rinses, sections were incubated for 1 h with a biotinylated secondary antibody. Finally, the sections were processed after the avidin-biotin protocol (Vectastain ABC kit; Vector Laboratories). Tissues were mounted onto gelatin-coated slides and were let to dry. Finally, the slides were dehydrated, cleared in xylene and mounted with DePeX (Serva, Heidelberg, Germany). The slides were examined with a Zeiss (Oberkochen, Germany) Axiophot microscope, equipped with an Olympus Optical (Tokyo, Japan) DP-50 digital camera and a Leica (Nussloch, Germany) MZ6 modular stereomicroscope. Neuronal integrity was assessed by counting the number of Nissl-positive cells in the CA3 region of the hippocampus in four independent well defined high-magnification (×400) fields per section and in five sections per animal using computer-assisted image analysis software (Soft Imaging System, Münster, Germany).

Astrogliosis was evaluated by quantifying the number of activated cells [high glial fibrillary acidic protein (GFAP) immunostaining] as described above and the intensity of GFAP staining in at least 100 cell bodies per animal. For this, randomly chosen cells were manually traced and their mean staining intensity was determined using computer-assisted image analySIS software (Soft Imaging System).

The extent of microgliosis was quantified by counting the number of OX-42-positive cells in four independent well-defined high-magnification (×400) fields per section and in four sections per animal as described above.

The following primary antibodies were used: monoclonal anti-cd11b (OX-42) and anti-GFAP antibodies (Serotec, Duesseldorf, Germany) and Sigma, respectively, and polyclonal anti-GluR6/7 antibody. Before immunostaining with anti GluR6/7, tissue sections were boiled in 10 mM citrate buffer according to the manufacturer's instructions.

Statistical analysis

Data were analyzed by ANOVA, followed by Newman-Keul's test as *post hoc* or Student *t* test. The threshold of statistical significance was set at $P < 0.05$.

Results

Behavioral effects of KA in hypothyroid rats

We first analyzed in the three groups of rats (control, hypothyroid, and hypothyroid treated with T_4/T_3) the be-

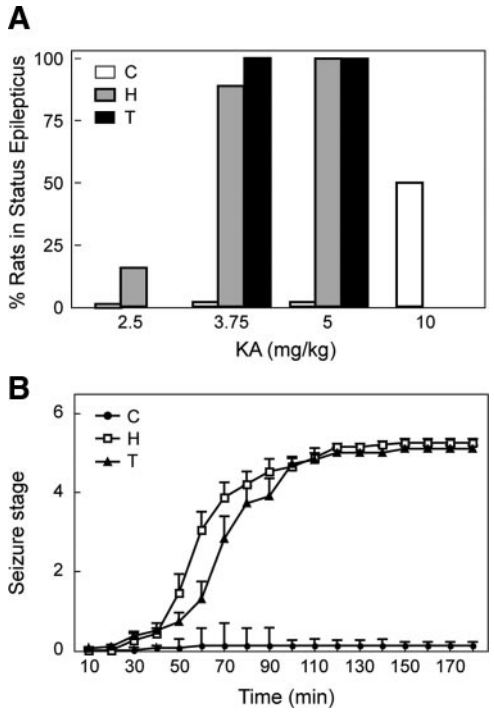

FIG. 1. Effect of hypothyroidism on KA-induced behavioral response. Control (C), hypothyroid (H), and hypothyroid treated with T_4/T_3 (T) rats were sc injected with the indicated doses of KA. The behavioral response was observed for the following 3 h and rated as indicated in *Materials and Methods*. A, Dose-response curve. B, Time-course response to KA (3.75 mg/kg). Values represent the mean ± SE from 15 different animals.

havioral response to KA administration. As shown in Fig. 1A, the hypothyroid animals showed an increased sensitivity to KA-induced limbic seizures, and almost all the animals enter in SE at a dose as low as 3.75 mg/kg BW. On the contrary, at that dose none of the control animals entered in SE, and only some animals showed early symptoms of KA action such as wet dog shakes. A time-course response to a dose of 3.75 mg/kg of KA is shown in Fig. 1B, in which the difference between control and hypothyroid animals is clearly observed. To test whether this higher sensibility of hypothyroid animals to KA could be reversed by the administration of thyroid hormones, hypothyroid rats were treated with T_4/T_3 during 1 wk as indicated in *Materials and Methods*. This treatment has been previously shown to revert the effects of hypothyroidism on different biochemical and behavioral parameters in these hypothyroid adult rats (39). As can be observed in Fig. 1, this treatment had no effect on the sensitivity to KA, as determined by the dose-response curve (Fig. 1A). However, a longer latency to reach SE was observed in the T_4/T_3-treated hypothyroid rats (76 ± 7.5 min in hypothyroid and 97 ± 7.0 min in treated animals, $P < 0.01$), indicating a higher resistance to entrance in SE in these animals.

Effect of hypothyroidism on KA-induced neurological damage in the hippocampus

The KA-induced neurodegeneration was analyzed 72 h after injection of the excitotoxin at a dose of 3.75 mg/kg. Our results clearly show a dramatic reduction in the number of neurons, particularly in the CA3 subfield of the hippocampus, in the hypothyroid animals (Fig. 2). In hypothyroid animals an 80% reduction in the number of neurons was observed in CA3 (Fig. 2B). In contrast, at this concentration, KA did not cause any neuronal damage in the control animals. In hypothyroid animals treated with T_4/T_3, the loss of neurons after KA injection was slightly lower (69%) than the one observed in the hypothyroid group. These results are essentially in accordance with the behavioral results described in Fig. 1. In rats not injected with KA, the same number of neurons were observed in the CA3 field among the three groups of animals analyzed (data not shown), indicating that there are no differences in the number of CA3 hippocampal neurons due to the thyroidal state of the animal, which it is in agreement with previously reported data (16).

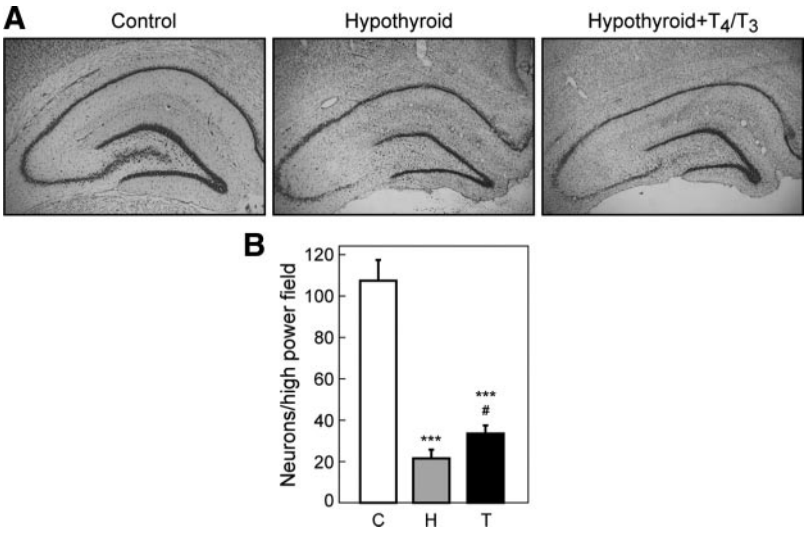

FIG. 2. Effect of hypothyroidism on KA-induced neuronal loss in the hippocampus. Control (C), hypothyroid (H), and hypothyroid treated with T_4/T_3 (T) rats were injected with KA (3.75 mg/kg) and 72 h later perfused transcardially with paraformaldehyde and processed as indicated in *Materials and Methods*. A, Nissl staining. B, Quantification analysis. Values represent the mean ± SE from five different animals. ***, $P \leq 0.001$ *vs.* control; #, $P \leq 0.05$ *vs.* hypothyroid rats.

Effect of hypothyroidism on KA-induced glial activation in the hippocampus

Glial activation was analyzed 72 h after KA (3.75 mg/kg) injection by determining the number and intensity of GFAP-positive cells and the number of cells stained with anti-CD11b (OX-42). As can be seen in Fig. 3A, a

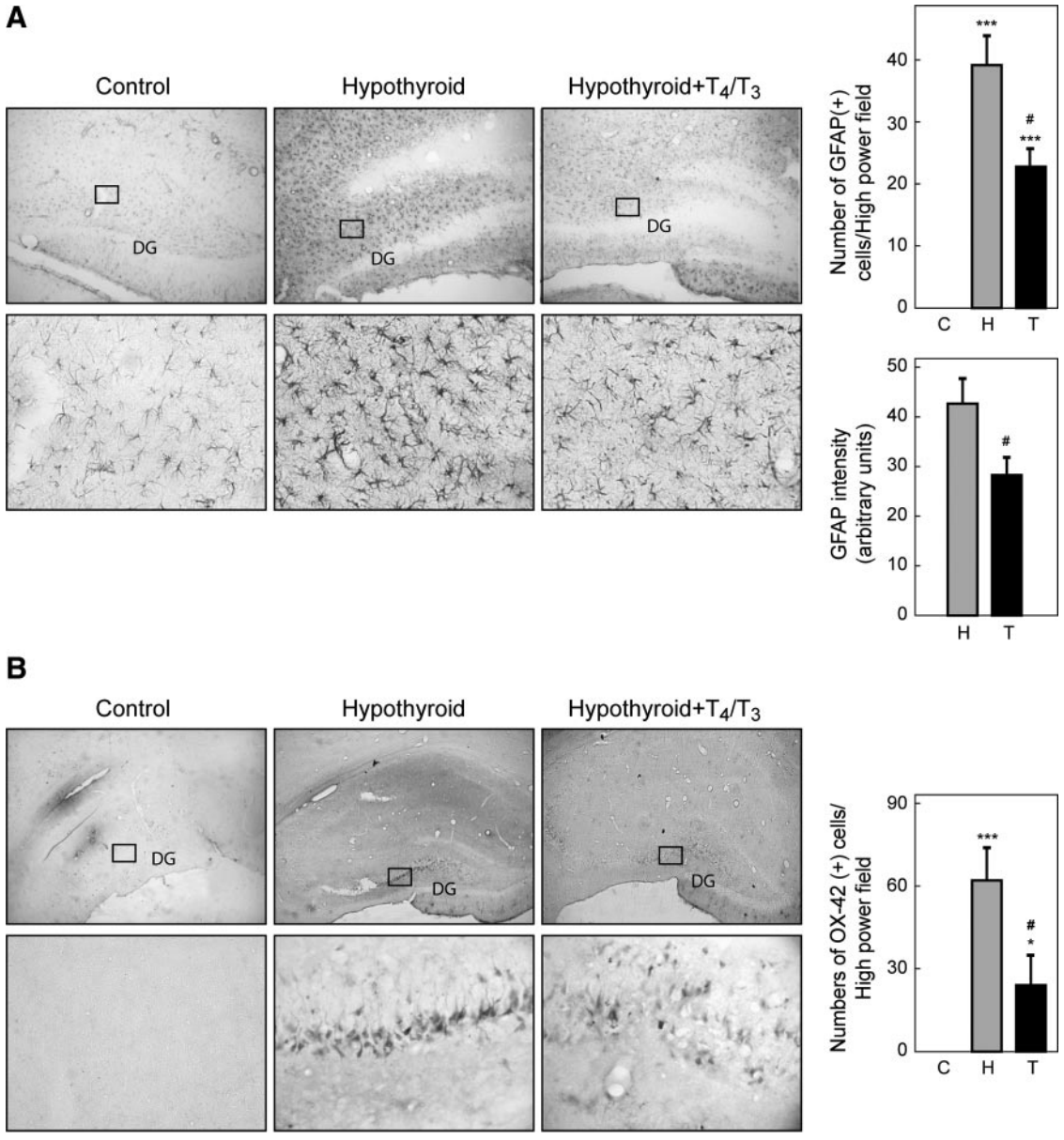

FIG. 3. Effect of hypothyroidism on KA-induced glial activation in the hippocampus. Control (C), hypothyroid (H), and hypothyroid treated with T_4/T_3 (T) rats were injected with KA (3.75 mg/kg) and 72 h later perfused transcardially with paraformaldehyde and processed as indicated in *Materials and Methods*. A, Coronal sections stained with an anti-GFAP antibody and quantification of the number and staining intensity of reactive astrocytes. B, Coronal sections stained with anti-OX-42 antibody and quantification of the number of reactive microglial cells. Values represent the mean ± SE in five different animals. *, $P \leq 0.05$; ***, $P \leq 0.001$ *vs.* control; #, $P \leq 0.05$ *vs.* hypothyroid rats. DG, Denate gyrus.

high number of cells became intensively stained with GFAP antibody as a consequence of the injection of KA in the hypothyroid animals. This strong astrogliosis was absent in the control group. Previous treatment of the hypothyroid animals with T_4/T_3 significantly reduced the number of GFAP-positive cells after KA injection (Fig. 3A). In addition to the decrease in the number of GFAP-positive cells, also a decrease in the intensity of staining of individual astrocytes was observed after T_4/T_3 treatment. In the treated group, the intensity of GFAP staining was 65% of the average value observed in untreated hypothyroid animals. Similar results were observed for OX-42 staining (Fig. 3B). In control animals no OX-42-positive cells were observed after the injection of KA. In contrast, hypothyroid rats showed a high number of OX-42-positive cells. This dramatic increase in the number of activated microglial cells was clearly reduced when hypothyroid animals were previously treated with T_4/T_3. The number of OX-42-positive cells in the treated groups was 45% of the number found in the untreated group.

Effect of hypothyroidism on the expression of kainate receptor subunits

Because the action of KA is mainly mediated through its binding to ionotropic glutamate receptors of the kainate

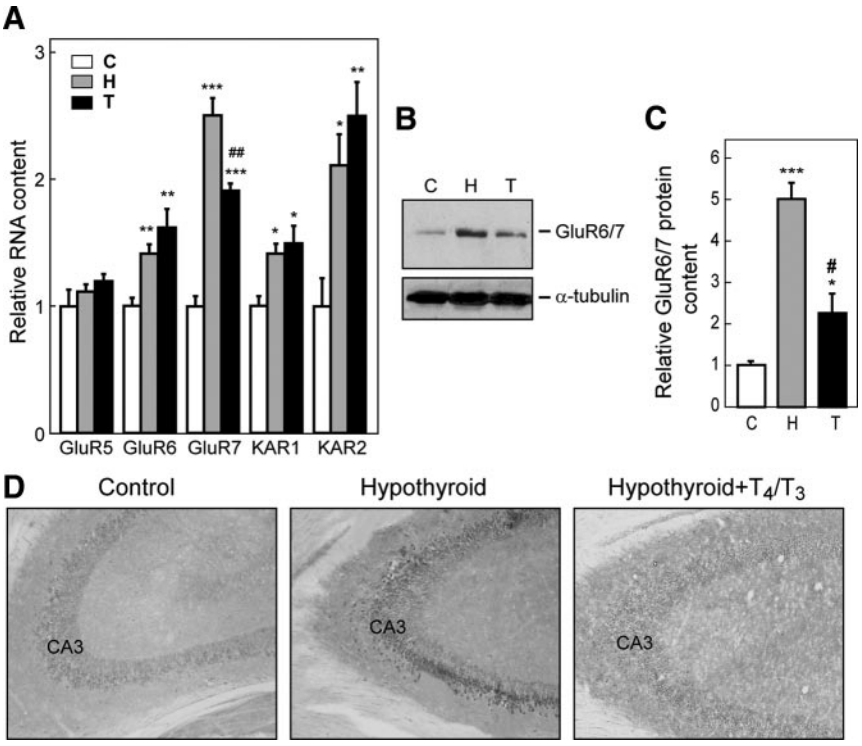

FIG. 4. Effect of hypothyroidism on the expression of kainate receptor subunits in the hippocampus. Total RNA and proteins were extracted from the hippocampus of control (C), hypothyroid (H), and hypothyroid treated with T_4/T_3 (T). Panel A, The amount of the corresponding kainate receptor subunits was determined by quantitative PCR. Panel B, Representative Western blots of GluR6/7. Panel C, Quantification of GluR6/7 protein by Western blot. Panel D, Representative immunohistochemical staining of the hippocampus with anti GluR6/7 antibody. Values represent the mean ± SE from 10 and four different samples in A and C, respectively. ***, $P \leq 0.001$, **, $P \leq 0.01$, *, $P \leq 0.05$ *vs.* control; #, $P \leq 0.05$, ##, $P \leq 0.01$ *vs.* hypothyroid rats.

subtype, we analyzed the possible effect of congenital hypothyroidism on the expression of genes coding for subunits of these receptors. As shown in Fig. 4A, with the exception of GluR5, the amount of all the transcripts of kainate receptor subunits were increased in the hippocampus of hypothyroid animals. This increase was more patent for subunits GluR7 and KAR2 (Fig. 4A). The treatment with T_4/T_3 did not normalize transcript concentration, suggesting that the effect of hypothyroidism cannot be reversed by this late treatment with thyroid hormones. Only a partial decrease in GluR7 transcript was observed after treatment. In line with the increase in kainate receptor transcripts, an increase in the amount of GluR6/7 protein was observed by Western blot and immunohistochemistry in the hippocampus of hypothyroid animals (Fig. 4, B and C). After quantification of the Western blot data (Fig. 4C), a 5-fold increase in the amount of GluR6/7 protein was observed, which was partially reverted by thyroid hormone treatment. In accordance with the Western blot results, immunohistochemistry analysis (Fig. 4D) revealed an increase in the expression of GluR6/7 proteins in the hypothyroid rats, which was partially reverted by thyroid hormone treatment. No major differences in the localization of these proteins were observed among the three groups of animals.

Effect of hypothyroidism on behavioral effects and neurological damage induced by pilocarpine and PTZ

Finally, we analyzed the effect of lithium-pilocarpine and PTZ on seizure induction and neuronal damage in control and hypothyroid rats. Our results show that hypothyroid animals are less sensitive to the proconvulsant effect of pilocarpine than the control ones. As shown in Fig. 5A, 40% of the control rats entered in SE after two injections of pilocarpine; in contrast, none of the hypothyroid rats entered in SE at that dose. When the latency time (the time from the first injection of pilocarpine to SE) was calculated, a clear difference was observed between both groups. Control rats needed 79 ± 4.5 min and a mean of 2.7 injections of pilocarpine to reach SE, whereas hypothyroid animals required 110 ± 7.5 min and an average of 3.7 injections ($P < 0.001$). In the case of PTZ, the hypothyroid rats were more sensitive to the action of this drug. As shown in Fig. 5B, all the hypothyroid rats reached convulsive stage 4–5 after a single injection of a subthreshold dose of PTZ (35 mg/kg); in contrast, none of the control animals showed convulsive behavior. Regarding neuronal loss in the hippocampus, lithium-pilocarpine-induced SE caused extensive damage of pyramidal neurons in both control and hypothyroid animals (Fig. 5C). On the other hand, a single subthreshold dose of PTZ caused some disorganization in pyramidal cells layers only in the hypothyroid animals, and no effect was observed in controls (Fig. 5C). This is in agreement with the fact that only hypothyroid animals showed convulsive behavior after a single subthreshold dose of PTZ and that this effect was brief and transitory and therefore insufficient to cause major neuronal damage.

Discussion

In this work, we have shown that hypothyroid rats are more sensitive to the KA-induced limbic seizures. This was accompanied by a higher expression, in the hippocampus, of genes coding for kainate receptor subunits. Both effects

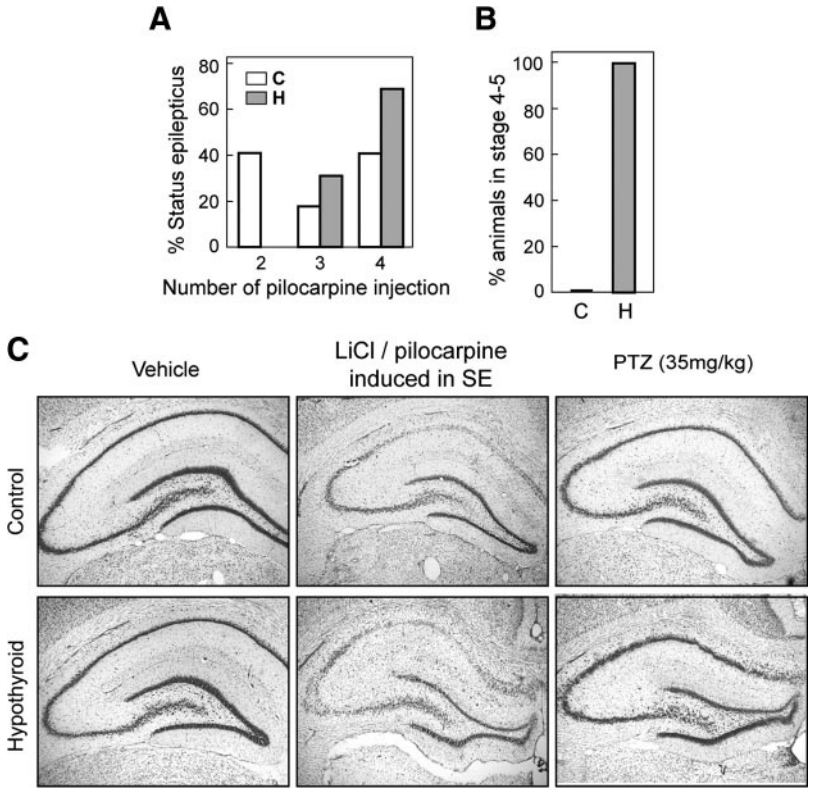

FIG. 5. Effect of hypothyroidism on behavioral and neurotoxic effects of pilocarpine and PTZ. Control (C) and hypothyroid (H) rats were treated with successive injections of pilocarpine (maximum four injections) or a single injection of PTZ and behavioral and neurotoxic effects analyzed as indicated in *Materials and Methods*. Panel A, Percentage of rats in SE after the indicated dose of pilocarpine. Panel B, Behavioral score after PTZ injection. Panel C, Representative Nissl staining of the hippocampus 72 h after the indicated treatments.

are basically irreversible because the administration of physiological amounts of thyroid hormones to these animals has only a modest effect on the sensitivity to KA and the expression of kainate receptor subunits. These results suggest that an increased expression of kainate receptors in the hippocampus could be the cause, or at least play an important role, of the increased sensitivity to KA observed in developmental hypothyroid rats.

Multiple pharmacological, biochemical, and electrophysiological data implicate kainate receptors, particularly those present in the mossy fibers terminal, in the induction of limbic seizures. KA facilitates excitatory synaptic transmission at the mossy fibers (40), and this facilitation is GluR6 dependent, being absent in GluR6$^{-/-}$ mice (41). Forced overexpression of the fully edited GluR6 subunit in the hippocampus of the rat induces limbic seizures (42). Conversely, the lesion of mossy fibers in rats prevents the development of electrographic SE in response to KA administration (43). In addition, other kainate receptor subunits could also play an important role in the epilectogenic action of KA (34).

Our results, indicating that an increase in the expression of kainate receptors in the hippocampus could decrease the threshold of seizure induction, are in agreement with results previously reported by other authors. It has been broadly described that antipsychotic medications can reduce seizure threshold in some patients (44). Interestingly, Meador-Woodruff *et al.* (45) have shown that treatment of rats with clozapine, the second-generation antipsychotic drug most frequently associated with seizures in humans, notably increases the expression of GluR6 in all areas of the hippocampus. Also, Rangel *et al.* (46) have shown that mice lacking the cellular prion protein expressed higher levels of GluR6 and GluR7 in the hippocampus and showed enhanced susceptibility to KA-induced damage.

The induction of limbic seizures is a complex process, and, besides ionotropic GluRs, numerous genes have been implicated in their development. Marked differences in KA sensitivity have been described among different mouse strains (47), and multiple genes have been suggested to play a facilitatory or inhibitory effect on KA-induced limbic seizures (48, 49). One of these genes is neuropilin 2, the semaphorin 3 receptor. The null mutant mice for this gene have a reduced hippocampal population of GABAergic interneurons and are more prone to limbic seizure induction (50). In this regard, it is interesting to note that the hippocampus of rats deprived of thyroid hormones from gestational d 6 until postnatal d 30 have a decreased density of the parvalbumin subpopulation of GABAergic interneurons and that this deficit persisted in adulthood (4). Thus, it is likely that both effects, a decreased population of parvalbumin neurons and an increased expression of kainate receptors, could contribute to the increased sensitivity to KA observed in hypothyroid rats.

Relative to the possible effect of thyroid hormones on the expression of kainate receptors, previous studies have shown that an excess of thyroid hormones during the neonatal period induced an aberrant growth of mossy fiber projections, in both the CA3 subfield and dentate gyrus of the hippocampus, with a parallel increase in the number of high-affinity binding sites for KA (51). Conversely, neonatal hypothyroidism reduced 43% high-affinity binding of KA in the stratum lucidum, specifically in the ventral hippocampus (52). These results are clearly in contrast with ours because we observed an increase in the protein levels of GluR6/7 in the hippocampus of hypothyroid animals, including the stratum lucidum. The reasons for

this discrepancy are unclear, but it has to be pointed out that in the study by Savage *et al.* (52), the rats were made hypothyroid from gestational d 18 until postnatal d 31 and then allow to recover until adulthood, whereas our animals were permanently hypothyroid since gestational d 12.

Our results show that hypothyroidism induces the expression of all kainate receptor subunits with the exception of GluR5. This is certainly an interesting observation, and further detailed studies to assess the molecular mechanisms by which thyroid hormones specifically regulate the expression of kainate receptor subunits are warranted. This generalized induction of kainate receptors in the hippocampus of hypothyroid rats is quite specific for this subfamily of ionotropic GluRs because it was not observed when *N*-methyl-D-aspartate and 2-amino-3-hydroxy-5-methyl-4-isoxazol propionic acid receptor subunits were analyzed, and only the expression of a few subunits was altered (data not shown). Regarding these results, it is important to mention that GluR5, the only subunit not affected by hypothyroidism, has a distinct cellular expression in the hippocampus because it is expressed only in GABAergic neurons, in contrast with the other kainate receptor subunits, which are mainly expressed in glutamatergic neurons (53).

The cholinergic agonist, pilocarpine, and the GABAergic antagonist, pentylenetetrazole, are drugs frequently used to induce limbic seizures. Here we show that congenital hypothyroid rats are more sensitive to PTZ, and consequently, subthreshold doses of this drug, which have no effect on control animals, are able to induce seizure activity in hypothyroid rats. In contrast, hypothyroid animals are less sensitive to pilocarpine administration, as shown by an increase in latency. This lower sensitivity to pilocarpine in hypothyroid animals could be the consequence of the well-established depressing effect of developmental hypothyroidism on cholinergic activity (54, 55).

Interestingly, Grigorenko *et al.* (56) suggested an implication of GluR6 in human epilepsy. An increase in the expression of GluR6 and the percentage of the edited form of this protein have been described in the hippocampus of patients with refractory epilepsy (57). Also, it has been shown that GluR6 mRNA is increased in the temporal cortex of patients with hemimeganencephaly, which is characterized by unilateral hemispheric enlargement, severe cytoarchitectural abnormalities, and intractable epilepsy (58). Moreover, in children with the rare Sturge-Weber neurological syndrome, which courses with seizure activity, a high incidence of central hypothyroidism and a positive response to T_4 therapy have been described (59).

In summary, our results suggest that hypothyroidism, through the regulation of kainate receptors, could favor KA-induced limbic seizures and neurological damage.

Acknowledgments

Address all correspondence and requests for reprints to: A. Santos, Departamento de Bioquímica y Biología Molecular, Facultad de Medicina, Universidad Complutense, 28040 Madrid, Spain. E-mail: piedras3@med.ucm.es; or A. Perez-Castillo, Instituto de Investigaciones Biomedicas, Consejo Superior de Investigaciones Cientificas, Universidad Autonoma, Arturo Duperier 4, 28029 Madrid, Spain. E-mail: aperez@iib.uam.es.

This work was supported by Ministerio de Educacion y Ciencia Grants SAF2004-06263-CO2-02 (to A.S.), SAF2004-06263-CO2-01, and SAF2007-62811 and Comunidad de Madrid Grant GR/SAL/0033/2004 (to A.P.-C.). Centro de Investigación Biomédica en Red Sobre Enfermedades Neurodegenerativas is funded by the Instituto de Salud Carlos III.

Disclosure Summary: The authors have nothing to disclose.

References

1. **Aranda A, Pascual A** 2001 Nuclear hormone receptors and gene expression. Physiol Rev 81:1269–1304
2. **Zhang J, Lazar MA** 2000 The mechanism of action of thyroid hormones. Annu Rev Physiol 62:439–466
3. **Beekum O, Fleskens V, Kalkhoven E** 2009 Posttranslational modifications of PPAR-γ: fine-tuning the metabolic master regulator. Obesity (Silver Spring) 17:213–219
4. **Gilbert ME, Sui L, Walker MJ, Anderson W, Thomas S, Smoller SN, Schon JP, Phani S, Goodman JH** 2007 Thyroid hormone insufficiency during brain development reduces parvalbumin immunoreactivity and inhibitory function in the hippocampus. Endocrinology 148:92–102
5. **Bernal J** 2007 Thyroid hormone receptors in brain development and function. Nat Clin Pract Endocrinol Metab 3:249–259
6. **Perez-Castillo A, Bernal J, Ferreiro B, Pans T** 1985 The early ontogenesis of thyroid hormone receptor in the rat fetus. Endocrinology 117:2457–2461
7. **Strait KA, Schwartz HL, Perez-Castillo A, Oppenheimer JH** 1990 Relationship of c-erbA mRNA content to tissue triiodothyronine nuclear binding capacity and function in developing and adult rats. J Biol Chem 265:10514–10521
8. **Mellström B, Pipaón C, Naranjo JR, Perez-Castillo A, Santos A** 1994 Differential effect of thyroid hormone on NGFI-A gene expression in developing rat brain. Endocrinology 135:583–588
9. **Dowling AL, Martz GU, Leonard JL, Zoeller RT** 2000 Acute changes in maternal thyroid hormone induce rapid and transient changes in gene expression in fetal rat brain. J Neurosci 20:2255–2265
10. **Martinez B, del Hoyo P, Martin MA, Arenas J, Perez-Castillo A, Santos A** 2001 Thyroid hormone regulates oxidative phosphorylation in the cerebral cortex and striatum of neonatal rats. J Neurochem 78:1054–1063
11. **Zoeller RT, Rovet J** 2004 Timing of thyroid hormone action in the developing brain: clinical observations and experimental findings. J Neuroendocrinol 16:809–818
12. **Wang J** 1993 [A morphologic study on hippocampus in endemic cretinism]. Zhonghua Bing Li Xue Za Zhi 22:143–145

13. **Samuels MH, Schuff KG, Carlson NE, Carello P, Janowsky JS** 2007 Health status, mood, and cognition in experimentally induced subclinical hypothyroidism. J Clin Endocrinol Metab 92: 2545–2551
14. **Bauer M, Silverman DH, Schlagenhauf F, London ED, Geist CL, van Herle K, Rasgon N, Martinez D, Miller K, van Herle A, Berman SM, Phelps ME, Whybrow PC** 2009 Brain glucose metabolism in hypothyroidism: a positron emission tomography study before and after thyroid hormone replacement therapy. J Clin Endocrinol Metab 94:2922–2929
15. **Rami A, Rabié A** 1988 Effect of thyroid deficiency on the development of glia in the hippocampal formation of the rat: an immunocytochemical study. Glia 1:337–345
16. **Madeira MD, Sousa N, Lima-Andrade MT, Calheiros F, Cadete-Leite A, Paula-Barbosa MM** 1992 Selective vulnerability of the hippocampal pyramidal neurons to hypothyroidism in male and female rats. J Comp Neurol 322:501–518
17. **Vara H, Martínez B, Santos A, Colino A** 2002 Thyroid hormone regulates neurotransmitter release in neonatal rat hippocampus. Neuroscience 110:19–28
18. **Gilbert ME, Sui L** 2006 Dose-dependent reductions in spatial learning and synaptic function in the dentate gyrus of adult rats following developmental thyroid hormone insufficiency. Brain Res 1069:10–22
19. **Kobayashi K, Akune H, Sumida K, Saito K, Yoshioka T, Tsuji R** 2009 Perinatal exposure to PTU decreases expression of Arc, Homer 1, Egr 1 and Kcna 1 in the rat cerebral cortex and hippocampus. Brain Res 1264:24–32
20. **Royland JE, Parker JS, Gilbert ME** 2008 A genomic analysis of subclinical hypothyroidism in hippocampus and neocortex of the developing rat brain. J Neuroendocrinol 20:1319–1338
21. **Alzoubi KH, Gerges NZ, Aleisa AM, Alkadhi KA** 2009 Levothyroxin restores hypothyroidism-induced impairment of hippocampus-dependent learning and memory: behavioral, electrophysiological, and molecular studies. Hippocampus 19:66–78
22. **Montero-Pedrazuela A, Venero C, Lavado-Autric R, Fernández-Lamo I, García-Verdugo JM, Bernal J, Guadaño-Ferraz A** 2006 Modulation of adult hippocampal neurogenesis by thyroid hormones: implications in depressive-like behavior. Mol Psychiatry 11: 361–371
23. **Bismilla Z, Sell E, Donner E** 2007 Hashimoto encephalopathy responding to risperidone. J Child Neurol 22:855–857
24. **Impallomeni MG** 1977 Unusual presentation of myxoedema coma in the elderly. Age Ageing 6:71–76
25. **Jabbari B, Huott AD** 1980 Seizures in thyrotoxicosis. Epilepsia 21: 91–96
26. **Kulig K, Golightly LK, Rumack BH** 1985 Levothyroxine overdose associated with seizures in a young child. JAMA 254:2109–2110
27. **Su YH, Izumi T, Kitsu M, Fukuyama Y** 1993 Seizure threshold in juvenile myoclonic epilepsy with Graves disease. Epilepsia 34: 488–492
28. **Tsutaoka BT, Kim S, Santucci S** 2005 Seizure in a child after an acute ingestion of levothyroxine. Pediatr Emerg Care 21:857–859
29. **Sundaram MB, Hill A, Lowry N** 1985 Thyroxine-induced petit mal status epilepticus. Neurology 35:1792–1793
30. **Meisami E, Valcana T, Timiras PS** 1970 Effects of neonatal hypothyroidism on the development of brain excitability in the rat. Neuroendocrinology 6:160–167
31. **Mills SA, Savage DD** 1988 Evidence of hypothyroidism in the genetically epilepsy-prone rat. Epilepsy Res 2:102–110
32. **Seyfried TN, Glaser GH, Yu RK** 1979 Thyroid hormone influence on the susceptibility of mice to audiogenic seizures. Science 205: 598–600
33. **Sperk G, Lassmann H, Baran H, Seitelberger F, Hornykiewicz O** 1985 Kainic acid-induced seizures: dose-relationship of behavioural, neurochemical and histopathological changes. Brain Res 338:289–295
34. **Vincent P, Mulle C** 2009 Kainate receptors in epilepsy and excitotoxicity. Neuroscience 158:309–323
35. **Pipaon C, Santos A, Perez-Castillo A** 1992 Thyroid hormone upregulates NGFI-A gene expression in rat brain during development. J Biol Chem 267:21–23
36. **Racine RJ** 1972 Modification of seizure activity by electrical stimulation. II. Motor seizure. Electroencephalogr Clin Neurophysiol 32:281–294
37. **Hellier JL, Dudek FE** 2005 Chemoconvulsant model of chronic spontaneous seizures. Curr Protoc Neurosci Chapter 9:Unit 9, 19
38. **Chomczynski P, Sacchi N** 1987 Single-step method of RNA isolation by acid guanidinium thiocyanate-phenol-chloroform extraction. Anal Biochem 162:156–159
39. **Asúa T, Bilbao A, Gorriti MA, Lopez-Moreno JA, Del Mar Alvarez M, Navarro M, Rodríguez de Fonseca F, Perez-Castillo A, Santos A** 2008 Implication of the endocannabinoid system in the locomotor hyperactivity associated with congenital hypothyroidism. Endocrinology 149:2657–2666
40. **Schmitz D, Mellor J, Nicoll RA** 2001 Presynaptic kainate receptor mediation of frequency facilitation at hippocampal mossy fiber synapses. Science 291:1972–1976
41. **Breustedt J, Schmitz D** 2004 Assessing the role of GLUK5 and GLUK6 at hippocampal mossy fiber synapses. J Neurosci 24: 10093–10098
42. **Telfeian AE, Federoff HJ, Leone P, During MJ, Williamson A** 2000 Overexpression of GluR6 in rat hippocampus produces seizures and spontaneous nonsynaptic bursting *in vitro*. Neurobiol Dis 7:362–374
43. **Okazaki MM, Aitken PG, Nadler JV** 1988 Mossy fiber lesion reduces the probability that kainic acid will provoke CA3 hippocampal pyramidal cell bursting. Brain Res 440:352–356
44. **Hedges D, Jeppson K, Whitehead P** 2003 Antipsychotic medication and seizures: a review. Drugs Today (Barc) 39:551–557
45. **Meador-Woodruff JH, King RE, Damask SP, Bovenkerk KA** 1996 Differential regulation of hippocampal AMPA and kainate receptor subunit expression by haloperidol and clozapine. Mol Psychiatry 1:41–53
46. **Rangel A, Burgaya F, Gavín R, Soriano E, Aguzzi A, Del Río JA** 2007 Enhanced susceptibility of Prnp-deficient mice to kainate-induced seizures, neuronal apoptosis, and death: role of AMPA/kainate receptors. J Neurosci Res 85:2741–2755
47. **McKhann 2nd GM, Wenzel HJ, Robbins CA, Sosunov AA, Schwartzkroin PA** 2003 Mouse strain differences in kainic acid sensitivity, seizure behavior, mortality, and hippocampal pathology. Neuroscience 122:551–561
48. **Dzhala VI, Talos DM, Sdrulla DA, Brumback AC, Mathews GC, Benke TA, Delpire E, Jensen FE, Staley KJ** 2005 NKCC1 transporter facilitates seizures in the developing brain. Nat Med 11: 1205–1213
49. **Noé F, Frasca A, Balducci C, Carli M, Sperk G, Ferraguti F, Pitkänen A, Bland R, Fitzsimons H, During M, Vezzani A** 2009 Neuropeptide Y overexpression using recombinant adeno-associated viral vectors. Neurotherapeutics 6:300–306
50. **Gant JC, Thibault O, Blalock EM, Yang J, Bachstetter A, Kotick J, Schauwecker PE, Hauser KF, Smith GM, Mervis R, Li Y, Barnes GN** 2009 Decreased number of interneurons and increased seizures in neuropilin 2 deficient mice: implications for autism and epilepsy. Epilepsia 50:629–645
51. **Represa A, Tremblay E, Ben-Ari Y** 1987 Aberrant growth of mossy fibers and enhanced kainic acid binding sites induced in rats by early hyperthyroidism. Brain Res 423:325–328
52. **Savage DD, Montano CY, Otero MA, Paxton LL** 1990 Perinatal hypothyroidism decreases hippocampal 3H-vinylidene kainic acid binding in rats. Neuroendocrinology 51:38–44
53. **Paternain AV, Herrera MT, Nieto MA, Lerma J** 2000 GluR5 and GluR6 kainate receptor subunits coexist in hippocampal neurons and coassemble to form functional receptors. J Neurosci 20:196–205

54. **Patel AJ, Hayashi M, Hunt A** 1988 Role of thyroid hormone and nerve growth factor in the development of choline acetyltransferase and other cell-specific marker enzymes in the basal forebrain of the rat. J Neurochem 50:803–811
55. **Gould E, Butcher LL** 1989 Developing cholinergic basal forebrain neurons are sensitive to thyroid hormone. J Neurosci 9:3347–3358
56. **Grigorenko E, Glazier S, Bell W, Tytell M, Nosel E, Pons T, Deadwyler SA** 1997 Changes in glutamate receptor subunit composition in hippocampus and cortex in patients with refractory epilepsy. J Neurol Sci 153:35–45
57. **Grigorenko EV, Bell WL, Glazier S, Pons T, Deadwyler S** 1998 Editing status at the Q/R site of the GluR2 and GluR6 glutamate receptor subunits in the surgically excised hippocampus of patients with refractory epilepsy. Neuroreport 9:2219–2224
58. **Baybis M, Lynch D, Lee A, Patel A, McKhann 2nd G, Chugani D, J Kupsky W, Aronica E, Crino PB** 2004 Altered expression of neurotransmitter-receptor subunit and uptake site mRNAs in hemimeganencephaly. Epilepsia 45:1517–1524
59. **Comi AM, Bellamkonda S, Ferenc LM, Cohen BA, Germain-Lee EL** 2008 Central hypothyroidism and Sturge-Weber syndrome. Pediatr Neurol 39:58–62

Clin Transl Oncol (2008) 10:000-000
DOI

Cancer stem cells and brain tumors

Ana Pérez-Castillo · Diana Aguilar-Morante · José A. Morales-García · Jorge Dorado

Received: 14 February 2008 / Accepted: 19 March 2008

Abstract Besides the role of normal stem cells in organogenesis, cancer stem cells are thought to be crucial for tumorigenesis. Most current research on human tumors is focused on molecular and cellular analysis of the bulk tumor mass. However, evidence in leukemia and, more recently, in solid tumors suggests that the tumor cell population is heterogeneous. In recent years, several groups have described the existence of a cancer stem cell population in different brain tumors. These neural cancer stem cells (NCSC) can be isolated by cell sorting of dissociated suspensions of tumor cells for the neural stem cell marker CD133. These $CD133^+$ cells –which also express nestin, an intermediate filament that is another neural stem cell marker– represent a small fraction of the entire brain tumor population. The stem-like cancer cells appear to be solely responsible for propagating the disease in laboratory models. A promising new approach to treating glioblastoma proposes targeting cancer stem cells. Here, we summarize progress in delineating NCSC and the implications of the discovery of this cell population in human brain tumors.

Q1 **Keywords**

Ana Pérez-Castillo (✉) · Diana Aguilar-Morante ·
José A. Morales-García · Jorge Dorado
Instituto de Investigaciones Biomédicas
CSIC-UAM and Centro de Investigación Biomédica en Red
sobre Enfermedades Neurodegenerativas (CIBERNED)
Arturo Duperier, 4
28029 Madrid, Spain
e-mail: aperez@iib.uam.es

Introduction

The cancer stem cell hypothesis proposes that cancers derive from a small fraction of cancer cells that constitute a reservoir of self-sustained cells with the exclusive ability to self-renew and maintain the tumor. There is increasing evidence that malignant tumors such as leukemias, breast cancers, and brain cancers contain cells that maintain the characteristics of tissue-specific stem cells. These stem-like tumor cells are bestowed with dysregulated potential for self-renewal, excessive proliferation, and aberrant differentiation into a heterogeneous progeny of cancer cells culminating in the intratumor heterogeneity. Rapidly accumulating evidence from various laboratories indicates that in several forms of human cancer, only a minority subpopulation of cancer cells are able to form new tumors when transplanted into immunodeficient mice. The population of cells selectively endowed with tumorigenic capacity can be purified from whole tumor tissues by virtue of a surface marker expression profile and is defined as the "cancer stem cell" population. Cancer stem cells have been identified from various solid tumors, including breast ($CD44^+$ and $CD24^{-/low}$), colorectal ($CD133^+$), ependymoma ($CD133^+$, nestin+, and $BLBP^+$), and glioblastoma ($CD133^+$) [1–4]. An intense debate is ongoing as to whether cancer stem cells originate from adult stem cells or from mature, committed progenitors and/or even terminally differentiated cells that have abnormally acquired self-renewal capacity [2]. It is also suggested that niche cells could be a primary target for carcinogenic insult to adult stem cells, thereby inciting a tumorigenic response [5]. Thus, the molecular mechanisms underlying the genesis of cancer stem cells remain obscure, and identifying unique cell-surface markers for cancer stem cell isolation could provide new tools to address these questions and allow for further molecular and functional characterizations.

High-grade gliomas, which include glioblastoma

(GBM) and anaplastic astrocytoma, are among the most common intrinsic brain tumors in adults and are nearly uniformly fatal. Whereas there has been progress in understanding the molecular genetics of these tumors [6], the cell types of origin are still uncertain, and the molecular determinants of disease aggressiveness are not well understood. A better understanding of the cellular origin and molecular pathogenesis of these tumors may identify new targets for treating these neoplasms. Until recently, GBMs were presumed to arise from glial cells residing within the brain parenchyma However, recent evidence suggests that neural stem cells can be an alternate cellular origin of gliomas [7–9]. In fact, recent evidence demonstrates that neural stem cells can give rise to neoplasms that recapitulate the histopathological hallmarks of human gliomas [10, 11].

Adult neural stem cells are cells in the adult nervous system that can self-renew and differentiate into all types of neural cells, including neurons, astrocytes, and oligodendrocytes [12]. In the adult human forebrain, the majority of neurons are created by the early postnatal period. However, it has been demonstrated that neurons continue to arise in two niches of the adult brain: the subventricular zone (SVZ) of the lateral ventricle and the subgranular zone (SGZ) of the dentate gyrus [13, 14]. In the hippocampus, granule neurons arise in the SGZ of the dentate gyrus. Progenitor cells in the SVZ migrate to the olfactory bulb (OB) through the rostral migratory stream (RMS), where they differentiate into granule and periglomerular neurons of the OB (Fig. 1). Both cell-extrinsic and cell-intrinsic factors have been shown to influence maintenance and regulation of the neurogenic system in vivo [15]. A number of factors, including brain-derived neurotrophic factor (BDNF), insulin-like growth factor-1 (IGF-1), epidermal growth factor (EGF), and basic fibroblast growth factor (bFGF), have been shown to affect proliferation and differentiation of precursor-cell populations [16, 17]. This population of neural stem cells has distinct features such as the capacity of self-renewal, multipotency, asymmetric division, and express characteristics markers such as nestin, a cystoskeletal protein; CD133, a cell-surface marker of normal neural ítem cells; and Notch. The demonstration that the adult human brain contains an abundant source of neural stem cells and that GBMs contain tumorigenic neural stem-like cells indicate that neural stem cells are a plausible origin of human gliomas. This has given rise to speculation that more effective therapies will result from approaches aimed at targeting the stem-cell-like component of GBM [18–21].

Glioblastoma tumor stem cells possess the capacity to self-renewal that leads to daughter cells with the same predisposition for replication as the parental cells, as well as the capacity to recapitulate the generation of a growing tumor [22]. These capacities have been shown for $CD133^+$ cells isolated from glioblastoma [23]. A small number of $CD133^+$ cells are sufficient for formation of glioblastoma in immunodeficient mice. The resulting primary xenograph consisting of a minority of $CD133^+$ cells and a majority of $CD133^+$ cells is a phenocopy of the patient's tumor [2].

In addition to possessing the fundamental stem cell properties of self-renewal and multipotency, glioblastoma stem cells share other characteristics with neural stem cells. They were first isolated from tumors by virtue of CD133 expression, which marks neural stem and progenitor cells [2]. The similarities in gene expression suggest that common cell-signaling systems might operate in normal and malignant neural stem cells. These phenotypic and functional similarities suggest that glioblastoma stem cells might arise from normal neural stem cells that retain self-renewal properties but acquire mutations necessary for tumorigenicity. Indeed, deletion of *Nf1* and *Trp53* from neural stem cells in mice initiates gliomagenesis in the SVZ, where neural stem cells reside [9]. However, whether human glioblastoma stem cells arise from mutated neural stem cells or a more mature cell type that acquires self-renewal capacity remains to be determined.

The stem cell niche

It has been long recognized that normal stem cells of various tissues are tightly regulated by the immediate microenvironment, or stem cell niche [24]. Consequently, an important question is whether glioblastoma stem cells also depend on cues from the environment for survival. Stem cell niches are not merely repositories for stem cells but are complex dynamic entities that actively control stem cell function [25] regulating stem cell renewal and fate. This microenvironment of stem cells is known to help maintain the cells in a quiescent state and preserve their potential to proliferate and differentiate [26, 27]. Direct genetic alterations or dysregulated crosstalk between signaling pathways of the cancer stem cells (CSCs) and cells of their microenvironment have been implicated as important determinants of functional tumor microenvironment preceding cancer development [28, 29].

As commented upon in the "Introduction," studies conducted over recent years have identified stem cells with regenerative capacity in the SVZ and the SGZ of the dentate gyrus. The central structural element of the neural stem cell niche is provided by capillaries within those zones. This organization places the stem cells in close proximity with endothelial and other vascular cells, facilitating communication among these cell types. The existence of niches extends to tumor cells as well. The tumor microenvironment, composed of nonepithelial stromal cells, is increasingly shown to be essential for tumor growth (Fig. 2) [30]. Neural cancer stem cells (NCSC) have been shown to lie within a vascular microenvironment. In this regard, Calabrese et al. recently provided convincing evidence that stem cells from various brain tumors, including glioblastoma, are indeed maintained within vascular niches that mimic the neural stem cell niche [31]. Using coimmunofluorescence and

multiphoton laser scanning microscopy, they showed first that $CD133^+$/$nestin^+$ tumor cells are closely associated with vasculature. Furthermore, increasing the number of endothelial cells and blood vessels in xenografts augmented the NCSC population and the rate of tumor growth. Clinical trials of the antiangiogenic drug bevacizumab [32] have demonstrated a potent antitumor effect in patients with glioblastoma. This effect could be the result of a depletion of the tumor blood supply. However, the presence of a glioblastoma stem cell niche would imply that this drug might also function to disrupt stem cell maintenance. In this regard, Calabrese and colleagues showed that treating glioblastoma-bearing mice with bevacizumab depleted tumor blood vessels and caused a significant reduction both in the NCSC population and tumor growth rate. Interestingly, this treatment did not alter the proliferation or survival of most of the tumor cells, suggesting that the drug was specifically acting on the cancer stem cells.

The notion that cancer stem cells exist in aberrant cell niches is an attractive one. A recent study of human gliomas suggests that bone morphogenic proteins (BMPs), which are niche-derived regulators of neural stem cell fate, might also regulate the differentiation status of cancer stem cells [33]. Therefore, the tumor microenvironment offers a novel approach to treatment through the targeting of cells inside the tumor niche.

Identifying glioblastoma stem cells

Correctly identifying stem cells *in vivo* remains the biggest obstacle to progress in understanding stem cell biology. Identification of reliable markers will allow prospective isolation and characterization of a pure population of CSCs, not just a population of cells containing CSCs. Normal stem cells and their neighboring cells within tissues can rarely be located by histological methods. Some properties that have been widely assumed to mark stem cells, such as preferential bromodeoxyuridine (BrdU) label retention (caused by an expected tendency of stem cells to divide more slowly than many of their progeny), have frequently proven to be unreliable without the use of other markers [34–36]. The "side population" (SP) is defined by Hoechst dye exclusion in flow cytometry and has been commonly used as one of the methods of enriching for cancer stem cells in glioblastomas [37] as well as in other types of tumor cells. Goodell et al. and Hirschmann-Jax et al. demonstrated that the exclusion of Hoechst 33342 dye by SP cells is a dynamic process involving multidrug-resistance transporter 1 (MDR1), a member of the adenosine-triphosphate-binding cassette (ABC) transporter transmembrane proteins [38, 39]. However, MDR1 cannot be taken as a single marker to identify and isolate SP cells, and additional transporters should be analyzed.

Much work has been carried out on brain tumor stem cells enriched by the cell-surface marker CD133. It is unclear at this time whether the SP overlaps with the CD133 population, but both markers have been shown to be highly enriched in neurosphere-forming capacity [40, 41], one of the defining characteristics of neural stem cells and progenitors (Fig. 3). Recently, several groups have isolated NCSC from glioblastomas [7]. They cultured dissociated tumor samples and expanded the cells on a defined, serum-free medium containing fibroblast growth factor and epidermal growth factor. These cells form floating aggregates (neurospheres), just as normal neural stem cells do in the same conditions. These neurospheres retain the self-renewing capacity and expressed neural stem cell markers, such as nestin, CD133, and Notch. Such aggregates, highly enriched in long-term, self-renewing multipotent cells in vitro, formed malignant tumors when transplanted in vivo in immunodeficient mice. These findings indicate that glioblastomas contain cancer-initiating neural stem-like cells, which can be identified by their staining with CD133 [2, 7]. Furthermore, it has been recently shown that CD133 expression correlates with survival in patients with gliomas, lending support to the current cancer stem cell hypothesis [42]. These authors found, using a large panel of human glioma samples, frequencies of $CD133^+$ cells to increase with tumor grade, with many glioblastomas containing > 25% positive cells. In contrast, tissue sections of many World Health Organization (WHO)-grade tumors were devoid of immunoreactive cells, probably indicating a low frequency of CSCs in these less malignant tumors. These findings provide strong and valuable evidence for the CSC hypothesis and the clinical relevance of the $CD133^+$ cell population in glioblastomas.

Another important trait of brain tumor stem cells is the signaling trough Notch receptor. Notch signaling is strongly activated in primary human gliomas and in several glioma cell lines [43] where its depletion reduces tumor proliferation [44]. Moreover, transfection of downstream mediators of the Notch pathway results in an increase in the growth and sphere formation of human glioma CD133+ cells, indicating that Notch signaling is essential for maintenance and proliferation of the tumor stem cell population [45]. A similar effect has been observed in medulloblastoma stem cells, where loss of tumor-forming capacity is attributed to depletion of cancer stem cells in response to Notch signaling blockade [46]. These data are in agreement with the studies in nonneoplastic stem cells that attribute to Notch signaling the role of inhibiting neuronal differentiation and maintaining the neural progenitor pool [47].

Neural cancer stem cells as therapeutic targets

Primary malignant brain tumors are characterized by a short median patient survival and almost 100% tumor-related mortality. Therefore, this brain tumor remains one of the most lethal forms of human cancer. Glial neoplasms are

the most frequent primary intracranial neoplasms in humans, accounting for > 60% of all primary brain tumors. Although glioblastomas, the most malignant of these, rarely spread outside the nervous system, they infiltrate crucial structures in the brain, preventing curative surgical resection. Radiation and chemotherapy offer only modest benefits and remain essentially palliative [48].

Conventional chemotherapy and/or radiation therapies are not usually designed to target a specific cell subpopulation, and their clinical efficacy is measured by their capacity to induce regression of bulk tumor lesions. It is therefore difficult to know whether traditional antitumor treatments are able to target cancer stem cells, which are thought to be resistant to such treatments [49, 50]. If glioblastomas are maintained by NCSCs, cells that are characterized by low rates of division and proliferation, it is clear that therapies such as chemotherapy or radiation, which target actively cycling cells, are doubtful to be effective. Therefore, it is unlikely that existing treatments will ever cure most patients with glioblastoma. Thus, the concept of cancer stem cells provides an interesting conceptual framework to interpret the phenomenon of tumor relapse as well as the heterogeneity found inside tumors in terms of aberrant cell proliferation and differentiation [51].

Cancer treatment has traditionally been based on the implicit assumption that human cancer populations are homogeneous. Cancer is resilient to treatment because malignant cells survive chemotherapy and radiation or avoid immune surveillance of endogenous cytotoxic T cells and natural killer (NK) cells. As cancer stem cells have a capacity for unlimited self-renewal and the ability to initiate and drive tumor progression in an animal model [2, 4] they would seem the most probable candidates responsible for tumor chemoresistance and recurrence.

In fact, recent investigations in the field of brain and breast cancers implicate cancer stem cells in radiation resistance [50, 52, 53]. Bao et al. demonstrated that radiation resistance in highly malignant gliomas (GBM) is most likely mediated by tumor stem cells [50]. This work shows that radiation treatment fails in the long run because it cannot kill the subpopulation of $CD133^+$ tumor-initiating cells. They showed that $CD133^+$ cancer stem cells contributed to glioma resistance through preferential activation of DNA damage checkpoint response and an increase in DNA repair capacity compared with $CD133^+$ tumor cells. The radioresistance of CD133 glioma stem cells could be reversed with a specific inhibitor of Chk1 and Chk2 checkpoint kinases, which are closely associated with cellular resistance to radiation, thereby providing a therapeutic advantage to reducing brain tumor occurrence. As the cell cycle of a normal stem cell is tightly controlled by the checkpoint to maintain genomic stability and integrity, the defective checkpoint responses associated with early cancer development [54, 55] point to an abnormal checkpoint control as a potential contributor to the transformation of normal cells into cancer stem cells. Therefore, targeting the checkpoint response in $CD133^+$ glioblastoma cells may help to overcome the radioresistance of this tumor. Further studies may confirm a rate-limiting role of DNA repair for the functionality of glioblastoma cells.

Also, Liu et al. demonstrated an increased resistance of CD133-positive brain tumor stem cells in response to treatment with chemotherapeutic agents such as carboplatin, paclitaxel, and etoposide compared with $CD133^-$ cells [56]. These studies revealed a higher expression of the multidrug resistance gene BCRP1 and genes that inhibit apoptosis in the CD133-expressing cancer stem cells. The work also showed that CD133 expression was significantly higher in recurrent glioblastomas compared with their respective newly diagnosed tumors. These results suggest that although chemotherapy kills most of the cells in a tumor, NCSCs remain viable and can reappear due to their enhanced chemoresistance.

Regarding the clinical implications of cancer stem cells, Piccirillo et al. were the first to show that human glioblastoma cells expressed BMPs and their cell surface receptors – BMPs being the soluble factors that normally induce neural precursor cells to differentiate into mature astrocytes, a subtype of brain cells called glial cells [33]. These authors showed that BMPs could also promote the differentiation of $CD133^+$ brain tumor stem cells, seriously weakening their tumor-forming ability. The results further imply that tumor populations at least partially retain a developmental hierarchy based on stem cells and remain able to respond to the normal signals that induce them to mature. These findings should lead to renewed interest in devising therapies that promote the differentiation of cancer cells.

Future directions

In conclusion, although major questions remain unanswered concerning the origin and function of NCSCs, their existence in glioblastomas is a widely accepted hypothesis. How these NCSCs control cell growth and cell-cycle progression of glioblastomas, however, is not yet clear. Nor is it clear whether there exists a stem-cell-specific machinery that controls growth and proliferation in a variety of stem cell lineages and why stem cell proliferation gets out of control when asymmetric cell division is compromised. Furthermore, the molecular events that occur when such a compromised stem cell becomes unresponsive to growth control signals remain unknown. The striking discovery of stem cell lineages in many tumors, including glioblastomas, might lead to identification of entirely new mechanisms for stem cell control. All data obtained so far suggest that in the coming years, NCSCs will be identified as a powerful new potential therapeutic target, and knowledge of the detailed biology and clinical significance of this noticeably defined population will provide further support for the NCSC hypothesis. Additionally, efforts now focus on the evaluation of target expression profiles in NCSCs in

glioblastomas and on the potential of these cells to resist therapy. Ultimately, focusing research efforts on the NCSC may drive important advances in our understanding of glioblastoma biology and in developing potential cures for this devastating disease.

Acknowledgments
Work in our laboratory is supported by the Ministerio de Educacion y Ciencia grants SAF2004-06263-CO2-01 and SAF2007-62811 and the Comunidad de Madrid grant GR/SAL/0033/2004.

References

1. Al-Hajj M, Wicha MS, Benito-Hernandez A et al (2003) Prospective identification of tumorigenic breast cancer cells. Proc Natl Acad Sci U S A 100:3983–3988
2. Singh SK, Hawkins C, Clarke ID et al (2004) Identification of human brain tumour initiating cells. Nature 432:396–401
3. Taylor MD, Poppleton H, Fuller C et al (2005) Radial glia cells are candidate stem cells of ependymoma. Cancer Cell 8:323–335
4. O'Brien CA, Pollett A, Gallinger S, Dick JE (2007) A human colon cancer cell capable of initiating tumour growth in immunodeficient mice. Nature 445:106–110
5. Tlsty TD, Hein PW (2001) Know thy neighbor: stromal cells can contribute oncogenic signals. Curr Opin Genet Dev 11:54–59
6. Kitange GJ, Templeton KL, Jenkins RB (2003) Recent advances in the molecular genetics of primary gliomas. Curr Opin Oncol 15:197–203
7. Singh SK, Clarke ID, Terasaki M et al (2003) Identification of a cancer stem cell in human brain tumors. Cancer Res 63:5821–5828
8. Caussinus E, Gonzalez C (2005) Induction of tumor growth by altered stem-cell asymmetric division in Drosophila melanogaster. Nat Genet 37:1125–1129
9. Zhu Y, Guignard F, Zhao D et al (2005) Early inactivation of p53 tumor suppressor gene cooperating with NF1 loss induces malignant astrocytoma. Cancer Cell 8:119–130
10. Bachoo RM, Maher EA, Ligon KL et al (2002) Epidermal growth factor receptor and Ink4a/Arf: convergent mechanisms governing terminal differentiation and transformation along the neural stem cell to astrocyte axis. Cancer Cell 1:269–277
11. Uhrbom L, Dai C, Celestino JC et al (2002) Ink4a-Arf loss cooperates with KRas activation in astrocytes and neural progenitors to generate glioblastomas of various morphologies depending on activated Akt. Cancer Res 62:5551–5558
12. Gage FH (2000) Mammalian neural stem cells. Science 287:1433–1438
13. Luskin MB, Zigova T, Soteres BJ, Stewart RR (1997) Neuronal progenitor cells derived from the anterior subventricular zone of the neonatal rat forebrain continue to proliferate in vitro and express a neuronal phenotype. Mol Cell Neurosci 8:351–366
14. Gage FH, Kempermann G, Palmer TD et al (1998) Multipotent progenitor cells in the adult dentate gyrus. J Neurobiol 36:249–266
15. Ostenfeld T, Svendsen CN (2003) Recent advances in stem cell neurobiology. Adv Tech Stand Neurosurg 28:3–89
16. Bartlett PF, Richards LR, Kilpatrick TJ et al (1995) Factors regulating the differentiation of neural precursors in the forebrain. Ciba Found Symp 193:85–99; discussion 117–126
17. Johe KK, Hazel TG, Muller T et al (1996) Single factors direct the differentiation of stem cells from the fetal and adult central nervous system. Genes Dev 10:3129–3140
18. Ignatova TN, Kukekov VG, Laywell ED et al (2002) Human cortical glial tumors contain neural stem-like cells expressing astroglial and neuronal markers in vitro. Glia 39:193–206
19. Berger F, Gay E, Pelletier L et al (2004) Development of gliomas: potential role of asymmetrical cell division of neural stem cells. Lancet Oncol 5:511–514
20. Oliver TG, Wechsler-Reya RJ (2004) Getting at the root and stem of brain tumors. Neuron 42:885–888
21. Fomchenko EI, Holland EC (2005) Stem cells and brain cancer. Exp Cell Res 306:323–329
22. Clarke MF (2004) Neurobiology: at the root of brain cancer. Nature 432:281–282
23. Galli R, Binda E, Orfanelli U et al (2004) Isolation and characterization of tumorigenic, stem-like neural precursors from human glioblastoma. Cancer Res 64:7011–7021
24. Moore KA, Lemischka IR (2006) Stem cells and their niches. Science 311:1880–1885
25. Scadden DT (2006) The stem-cell niche as an entity of action. Nature 441:1075–1079
26. Fuchs E, Tumbar T, Guasch G (2004) Socializing with the neighbors: stem cells and their niche. Cell 116:769–778
27. Ailles LE, Weissman IL (2007) Cancer stem cells in solid tumors. Curr Opin Biotechnol 18:460–466
28. Moinfar F, Man YG, Arnould L et al (2000) Concurrent and independent genetic alterations in the stromal and epithelial cells of mammary carcinoma: implications for tumorigenesis. Cancer Res 60:2562–2566
29. Lopez-Otin C, Matrisian LM (2007) Emerging roles of proteases in tumour suppression. Nat Rev Cancer 7:800–808
30. Kenny PA, Lee GY, Bissell MJ (2007) Targeting the tumor microenvironment. Front Biosci 12:3468–3474
31. Calabrese C, Poppleton H, Kocak M et al (2007) A perivascular niche for brain tumor stem cells. Cancer Cell 11:69–82
32. Vredenburgh JJ, Desjardins A, Herndon JE 2nd et al (2007) Phase II trial of bevacizumab and irinotecan in recurrent malignant glioma. Clin Cancer Res 13:1253–1259
33. Piccirillo SG, Reynolds BA, Zanetti N et al (2006) Bone morphogenetic proteins inhibit the tumorigenic potential of human brain tumour-initiating cells. Nature 444:761–765
34. Crittenden SL, Leonhard KA, Byrd DT, Kimble J (2006) Cellular analyses of the mitotic region in the Caenorhabditis elegans adult germ line. Mol Biol Cell 17:3051–3061
35. Barker N, van Es JH, Kuipers J, Kujala P et al (2007) Identification of stem cells in small intestine and colon by marker gene Lgr5. Nature 449:1003–1007
36. Kiel MJ, He S, Ashkenazi R et al (2007) Haematopoietic stem cells do not asymmetrically segregate chromosomes or retain BrdU. Nature 449:238–242
37. Kondo T, Setoguchi T, Taga T (2004) Persistence of a small subpopulation of cancer stem-like cells in the C6 glioma cell line. Proc Natl Acad Sci U S A 101:781–786
38. Goodell MA, Brose K, Paradis G et al (1996) Isolation and functional properties of murine hematopoietic stem cells that are replicating in vivo. J Exp Med 183:1797–1806
39. Hirschmann-Jax C, Foster AE, Wulf GG et al (2004) A distinct "side population" of cells with high drug efflux capacity in human tumor cells. Proc Natl Acad Sci U S A 101:14228–14233
40. Yuan X, Curtin J, Xiong Y et al (2004) Isolation of cancer stem cells from adult glioblastoma multiforme. Oncogene 23:9392–9400
41. Beier D, Hau P, Proescholdt M et al (2007) CD133(+) and CD133(–) glioblastoma-derived cancer stem cells show differential growth characteristics and molecular profiles. Cancer Res 67:4010–4015
42. Zeppernick F, Ahmadi R, Campos B et al (2008) Stem cell marker CD133 affects clinical outcome in glioma patients. Clin Cancer Res 14:123–129
43. Pahlman S, Stockhausen MT, Fredlund E, Axelson H (2004) Notch signaling in neuroblastoma. Semin Cancer Biol 14:365–373
44. Purow BW, Haque RM, Noel MW et al (2005) Expression of Notch-1 and its ligands, Delta-like-1 and Jagged-1, is critical for glioma cell survival and proliferation. Cancer Res 65:2353–2363
45. Zhang XP, Zheng G, Zou L et al (2008) Notch activation promotes cell proliferation and the formation of neural stem cell-like colonies in human glioma cells. Mol Cell Biochem 307:101–108
46. Fan X, Matsui W, Khaki L et al (2006) Notch pathway inhibition depletes stem-like cells and blocks engraftment in embryonal brain tumors. Cancer Res 66:7445–7452
47. Yoon K, Gaiano N (2005) Notch signaling in the mammalian central nervous system: insights from mouse mutants. Nat Neurosci 8:709–715
48. Stupp R, Mason WP, van den Bent MJ et al (2005) Radiotherapy plus concomitant and adjuvant temozolomide for glioblastoma. N Engl J Med 352:987–996
49. Guzman ML, Swiderski CF, Howard DS et al (2002) Preferential induction of apoptosis for primary human leukemic stem cells. Proc Natl Acad Sci U S A 99:16220–16225
50. Bao S, Wu Q, McLendon RE et al (2006) Glioma stem cells promote radioresistance by preferential activation of the DNA damage response. Nature 444:756–760
51. Reya T, Morrison SJ, Clarke MF, Weissman IL (2001) Stem cells, cancer, and cancer stem cells. Nature 414:105–111
52. Phillips TM, McBride WH, Pajonk F (2006) The response of CD24(-/low)/CD44+ breast cancer-initiating cells to radiation. J Natl Cancer Inst 98:1777–1785
53. Woodward WA, Chen MS, Behbod F et al (2007) WNT/beta-catenin mediates radiation resistance of mouse mammary progenitor cells. Proc Natl Acad Sci U S A 104:618–623
54. Bartkova J, Horejsi Z, Koed K et al (2005) DNA damage response as a candidate anti-cancer barrier in early human tumorigenesis. Nature 434:864–870
55. Gorgoulis VG, Vassiliou LV, Karakaidos Pet al (2005) Activation of the DNA damage checkpoint and genomic instability in human precancerous lesions. Nature 434:907–913
56. Liu G, Yuan X, Zeng Zet al (2006) Analysis of gene expression and chemoresistance of CD133+ cancer stem cells in glioblastoma. Mol Cancer 5:67

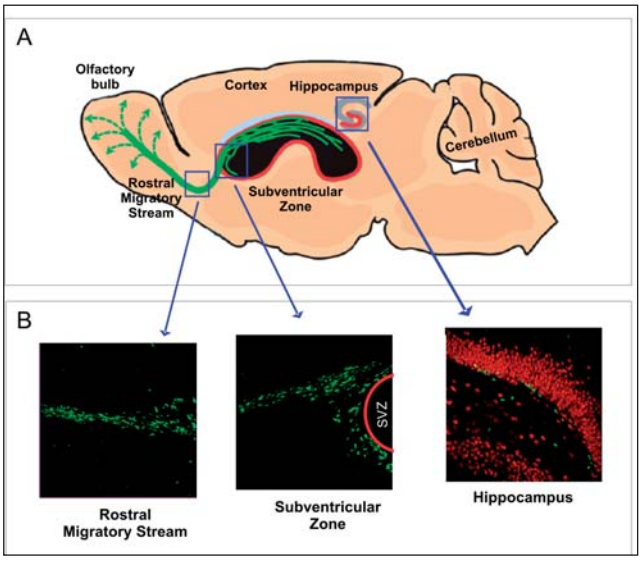

Fig. 1 Neural stem cells niches in the adult human brain. **a** Schematic of a sagittal brain section showing areas in the human brain where neurogenesis takes place. These germinal zones, the subgranular zone (SGZ) of the dentate gyrus in the hippocampus and the subventricular zone (SVZ) of the lateral ventricle, are marked in *red*. Neurons formed in the SVZ that migrate to the olfactory bulb (OB) through the rostral migratory stream (RMS) are shown in green. **b** Neurogenesis in the adult brain revealed by BrdU incorporation *(green)* in RMS, SVZ, and SGZ. In the SGZ of the hippocampus, granular neurons are stained in *red*

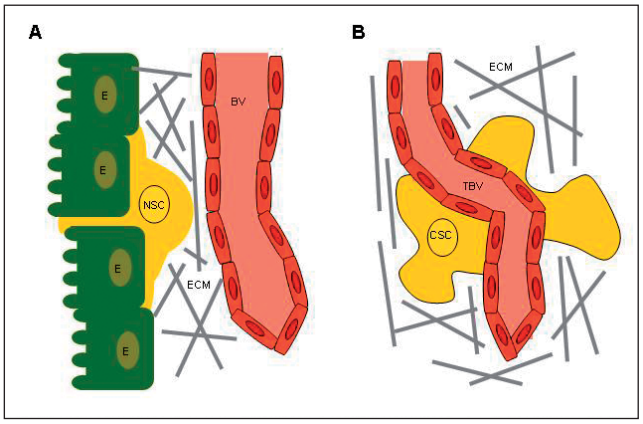

Fig. 2 Normal and tumoral stem cell niche. **a** Schematic of the subventricular zone (SVZ) neural stem cell (NSC) niche. NSCs locate adjacent to ependymal cells (E) and blood vessels (BV). **b** Similarly, glioblastoma cancer stem cells (CSC) are found in contact with tumoral blood vessels (TBV) attracted to the niche by secretion to the extracellular matrix (ECM) of diffusible factors such as vascular endothelial growth factor (VEGF)

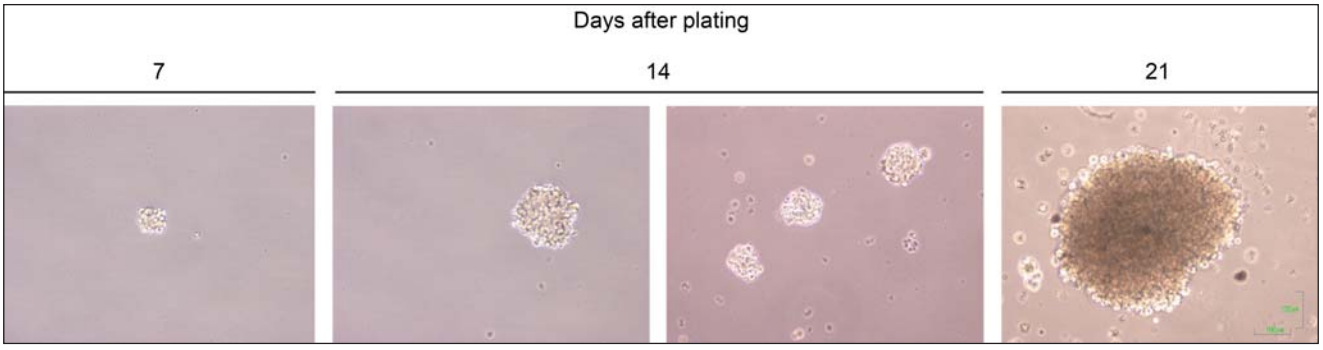

Fig. 3 Neurosphere-forming capacity. Neural cancer stem cells were seeded on low-adherent plates and grown for 21 days in serum-free medium containing basic fibroblast growth factor (bFGF) and epidermal growth factor (EGF)

Neurobiology of Disease

NP031112, a Thiadiazolidinone Compound, Prevents Inflammation and Neurodegeneration under Excitotoxic Conditions: Potential Therapeutic Role in Brain Disorders

Rosario Luna-Medina,[1] Marta Cortes-Canteli,[1] Susana Sanchez-Galiano,[1] Jose A. Morales-Garcia,[1] Ana Martinez,[2] Angel Santos,[3] and Ana Perez-Castillo[1]

[1]Instituto de Investigaciones Biomédicas, Consejo Superior de Investigaciones Científicas, Universidad Autónoma de Madrid, 28029 Madrid, Spain, [2]Neuropharma, S.A. Avenida de la Industria, 28760 Madrid, Spain, and [3]Departamento de Bioquímica y Biología Molecular, Facultad de Medicina, Universidad Complutense de Madrid, 28040 Madrid, Spain

Inflammation and neurodegeneration coexist in many acute damage and chronic CNS disorders (e.g., stroke, Alzheimer's disease, Parkinson's disease). A well characterized animal model of brain damage involves administration of kainic acid, which causes limbic seizure activity and subsequent neuronal death, especially in the CA1 and CA3 pyramidal cells and interneurons in the hilus of the hippocampus. Our previous work demonstrated a potent anti-inflammatory and neuroprotective effect of two thiadiazolidinones compounds, NP00111 (2,4-dibenzyl-[1,2,4]thiadiazolidine-3,5-dione) and NP01138 (2-ethyl-4-phenyl-[1,2,4]thiadiazolidine-3,5-dione), in primary cultures of cortical neurons, astrocytes, and microglia. Here, we show that injection of NP031112, a more potent thiadiazolidinone derivative, into the rat hippocampus dramatically reduces kainic acid-induced inflammation, as measured by edema formation using T_2-weighted magnetic resonance imaging and glial activation and has a neuroprotective effect in the damaged areas of the hippocampus. Last, NP031112-induced neuroprotection, both *in vitro* and *in vivo*, was substantially attenuated by cotreatment with GW9662 (2-chloro-5-nitrobenzanilide), a known antagonist of the nuclear receptor peroxisome proliferator-activated receptor γ, suggesting that the effects of NP031112 can be mediated through activation of this receptor. As such, these findings identify NP031112 as a potential therapeutic agent for the treatment of neurodegenerative disorders.

Key words: **excitotoxicity; neurodegenerative diseases; neuroinflammation; neuroprotection; peroxisome proliferator-activated receptor; thiadiazolidinones**

Introduction

Excitotoxic brain damage is considered one of the major mechanisms by which neurons die in the adult CNS (Choi, 1988; Lipton and Nicotera, 1998). Studies using kainic acid (KA), an analog of glutamate, have provided major contributions to the understanding of neuronal cell death caused by excitotoxicity. Administration of KA in rats is known to induce a sequence of altered behavioral events characterized by epileptiform seizures (Ben-Ari et al., 1980; Sperk, 1994), which are followed by neurodegeneration in specific brain regions, such as the hippocampus, piriform cortex, thalamus, and amygdala. In the hippocampus, the CA3 pyramidal cells and interneurons in the hilus of the dentate gyrus are the most vulnerable, followed by CA1 pyramidal cells (Coyle, 1983; Sperk et al., 1985; Tauck and Nadler, 1985). An essential event in excitotoxicity is the direct and constant activation by KA of specific glutamate receptors, which results in neuronal cell death (Choi, 1988; Doble, 1999; Wang et al., 2005). In addition, glial cells, as mediators of the inflammatory response, also play an important role in the course of KA-induced hippocampal neurodegeneration. Activated astrocytes and microglial cells proliferate and increase the expression of genes implicated in the production of nitric oxide and cytokines. These agents, when released from activated glia, can contribute noticeably to the expansion of brain injury and the delayed loss of neurons (Barone and Feuerstein, 1999; del Zoppo et al., 2000).

Neuroprotection involves the use of agents to prevent disease or injury of the nervous system by inhibiting one or more events leading to neuronal death. Brain injury, as a consequence of vascular or traumatic accidents or neurodegenerative diseases, is a common event, and therefore, neuroprotection has emerged as an increasingly important segment of the biopharmaceutical

Received Oct. 6, 2006; revised April 18, 2007; accepted April 18, 2007.

This work was supported by Ministerio de Educacion y Ciencia Grants SAF2004-06263-C02-01 and 95-0764.OP (A.P.-C.) and SAF2004-06263-C02-02 (A.S.) and Comunidad de Madrid Grant GR/SAL/0033/2004 (A.P.-C.). R.L.-M. is a fellow from the Ministerio de Educación y Ciencia. M.C.-C. is a postdoctoral fellow of the Consejo Superior de Investigaciones Científicas. We thank Marina Sanz-SanCristobal for excellent technical assistance and Ricardo Uña for helping with the quantification analysis. We are indebted to Dr. Sebastián Cerdán for helpful comments and critical reading of this manuscript and to Dr. Pilar López for expert handling of the nuclear magnetic resonance (NMR) instrumentation, as provided by Servicio de Imagen y Espectroscopía por Resonancia Magnética de Alto Campo, the core NMR Facility for small animal imaging of the Institute of Biomedical Research.

Correspondence should be addressed to either of the following: Ana Perez-Castillo, Instituto de Investigaciones Biomédicas, Consejo Superior de Investigaciones Científicas, Universidad Autónoma de Madrid, Arturo Duperier, 4, 28029 Madrid, Spain, E-mail: aperez@iib.uam.es; or Angel Santos, Departamento de Bioquímica y Biología Molecular, Facultad de Medicina, Universidad Complutense de Madrid, 28040 Madrid, Spain, E-mail: piedras3@med.ucm.es.

DOI:10.1523/JNEUROSCI.1004-07.2007

 0270-6474/07/275766-11$15.00/0

market over the last years, representing a major source of untapped potential for development of new therapeutic products and strategies. Formerly, most therapy for neurological disorders was directed at symptoms; however, as the understanding of the molecular basis of neurological disease and injury increases, opportunities for new approaches appear. The peroxisome proliferator-activated receptor γ (PPARγ) has recently emerged as a therapeutic target for neuroprotection (Petrova et al., 1999; Bernardo et al., 2000; Landreth and Heneka, 2001; Diab et al., 2002; Townsend and Pratico, 2005). PPARγ ligands, including the antidiabetic thiazolidinediones (TZDs), nonsteroidal anti-inflammatory drugs (NSAIDs), such as indomethacin, and the prostaglandin derivative 15-deoxy-Δ-^{12,14}-prostaglandin J_2, have been implicated in the anti-inflammatory process in diverse tissues, including the brain (Ricote et al., 1999; Kielian and Drew, 2003). In line with these results, we have recently shown that two thiadiazolidinone (TDZD) compounds, NP00111 (2,4-dibenzyl-[1,2,4]thiadiazolidine-3,5-dione) and NP01138 (2-ethyl-4-phenyl-[1,2,4]thiadiazolidine-3,5-dione), inhibited the activation of astrocytes and microglial cells and were neuroprotective *in vitro* through a mechanism apparently involving PPARγ activation (Luna-Medina et al., 2005), suggesting that TDZDs may act as anti-inflammatory and neuroprotective agents in the CNS.

In the present study, we demonstrate that NP031112, another TDZD compound, which is presently being developed for the treatment of Alzheimer's disease, is a potent anti-inflammatory and neuroprotective agent against KA-induced *in vivo* excitotoxicity. TDZD compounds have been shown to be non-ATP competitive inhibitors of glycogen synthase kinase 3β (GSK-3β) (Martinez et al., 2002a,b). It has also been shown that inactivation of GSK-3β protects against KA-induced neurotoxicity *in vivo* (Goodenough et al., 2004), and therefore this pathway could be involved in the NP031112 response to the excitotoxin *in vivo*. However, our results suggest that NP031112 may act as well through its ability to activate the PPARγ nuclear receptor.

Materials and Methods

Cell culture, transfection, and treatment. Rat primary astrocytes, microglia, and neurons were harvested and cultured as described previously (Luna-Medina et al., 2005). The purity of the cultures was >95%, as determined by immunofluorescence analysis using anti-cd11b (OX-42) to detect microglial cells, glial fibrillary acidic protein (GFAP) to identify astrocytes, and anti-microtubule-associated protein 2 (MAP2) to identify neurons. NP031112 (2.5 μM) was added to the culture medium of astrocytes and microglia 1 h before exposure to glutamate (500 μM), cells were incubated for 24 h before tissue culture medium was collected, and the cells were evaluated for tumor necrosis factor-α (TNF-α) and cyclooxygenase type 2 (COX-2) expression. For transient transfection experiments, primary cultures of astrocytes were transfected with the reporter plasmid pPPRE-tk-luc, containing three PPARγ consensus binding sites upstream of a minimal promoter using Transfast (Promega, Madison, WI) according to the manufacturer's guidelines. Typically, cells received 0.2 μg of luciferase reporter plasmid and were harvested 24 h after treatment with different concentrations of NP031112 for determination of luciferase and β-galactosidase (to determine transfection efficiency) activities. Each transient transfection experiment was repeated at least three times in triplicate.

Antibodies. Mouse monoclonal antibodies to MAP2 and GFAP were from Sigma (St. Louis, MO). Mouse OX-42 and anti-neuN monoclonal antibodies were purchased from Serotec (Duseldorf, Germany), Millipore (Bedford, MA), respectively. Polyclonal anti-TNF-α and anti-COX-2 antibodies were from Santa Cruz Biotechnology (Santa Cruz, CA).

Immunocytochemistry. At the end of the treatment period, the cultures, grown on glass coverslips in 24-well cell culture plates, were washed with PBS and fixed for 30 min with 4% paraformaldehyde at 25°C and permeabilized with 0.1% Triton X-100 for 30 min at 37°C. After 1 h incubation with the corresponding primary antibody, cells were washed with PBS and incubated with an Alexa-labeled secondary antibody (Invitrogen, San Diego, CA) for 45 min at 37°C. Images were acquired using a Radiance 2100 confocal microscope (Bio-Rad, Hercules, CA), with a 350 nm diode laser to excite DAPI (4,6,diamidino-2-phenylindole) and 647 nm laser line to excite Alexa 647. Confocal microscope settings were adjusted to produce the optimum signal-to-noise ratio. To compare fluorescence signals from different preparations, settings were fixed for all samples within the same analysis. Fluorescence analysis was performed using LaserPix software (Bio-Rad). A quantitative analysis of labeled cells was undertaken using the image analySIS software (Soft Imaging System, Münster, Germany) and normalized to total nuclei. Areas to be counted were traced at high power (400×), and at least four different counting fields were selected at random per culture.

Measurement of apoptosis. To calculate the extent of apoptotic cell death, cortical neuronal cultures were treated or not with NP031112 and incubated with glutamate (100 μM), and phosphatydilserine exposure on the surface of apoptotic cells was detected by confocal microscopy after staining with Annexin V-FITC (Bender MedSystems, Vienna, Austria). Neuronal cell death was assessed by counting the percentage of Annexin-V-positive cells in four independent high-magnification (200×) fields per culture, as described above.

KA administration. Adult male Wistar rats (8–12 weeks old) were used in this study. Adequate measures were taken to minimize pain or discomfort of animals. Experiments were performed in accordance with the European Communities Council, directive 86/609/EEC. Rats ($n \geq 5$ per group) were anesthetized by intraperitoneal injection of ketamine (60 mg/kg) and Domtor (5 μg/kg) and placed into a stereotaxic apparatus (David Kopf Instruments, Tujunga, CA). KA (1 μg in 2.5 μl PBS) alone or in combination with NP031112 (2 ng in 2.5 μl PBS) was injected into the hippocampus [coordinates from bregma: posterior, −3.0 mm; lateral, −2.0 mm; depth, 3.5 mm; according to the atlas of Paxinos and Watson (1998)]. Control animals of the same age were injected with vehicle. Two groups of animals also received 0.7 μg of the PPARγ antagonist GW9662 (2-chloro-5-nitrobenzanilide), either alone or in combination with KA. Each injection was performed for >2.5 min using a micropump (KD Scientific, Holliston, MA). The amounts of NP031112 and GW9662 used were calculated based on the *in vitro* results to reach active concentrations within the hippocampus. Lithium chloride (LiCl), a potent inhibitor of GSK-3β activity, was administered (40 mg/kg/d) by intraperitoneal injection to a further two groups of animals, either alone or in combination with KA. The rats were then housed individually to recover.

Seizures were induced by intraperitoneal administration of rats with KA (10 mg/kg) in PBS. Control animals received saline only. Behavioral analysis was monitored for a period of 3 h by trained observers blind to the treatment of the rats. The convulsive behavior was classified according to Racine (1972) and Sperk et al. (1985) as follows: stage 0, no changes; stage 0.5, wet dog shakes (WDS); stage 1, mouth and facial movements; stage 2, head nodding; stage 3, forelimbs clonus; stage 4, rearing; stage 5, rearing and falling; stage 6, death. Status epilepticus (SE) was defined as continuous behavioral seizure activity (stage 5) for ≥5 min. The number of WDS before SE was also examined. In trials using NP031112, the TDZD was administered intragastrically (50 mg/kg) 1 h before KA injection.

Magnetic resonance imaging. Magnetic resonance imaging (MRI) was performed using a 7.0 tesla horizontal bore (16 cm) magnet interfaced with a Bruker Pharmascan console (Bruker Medical, Ettlingen, Germany). Rat brain MRI was performed with a 90 mm gradient insert and a concentrical 38 mm birdcage resonator, using Paravision version 3.1 software (Bruker Medical), as implemented in a Hewlett-Packard (Palo Alto, CA) Linux platform. MRI examinations used adult male Wistar rats ($n = 5$; 250 g) anesthetized through a plastic mask with 2% isoflurane in 99.9% O_2. Animals were allowed to breath spontaneously during the experiment and were placed in a heated cradle to maintain the core body temperature at ~37°C. The physiological state of the animal was monitored throughout MRI acquisition through the respiratory rate and body

temperature, as monitored by a rectal probe. T_2-weighted spin-echo images were acquired at 1, 2, 3, and 9 d after KA injection with a rapid acquisition with relaxation enhancement (Hennig et al., 1986) sequence in axial orientations [repetition time (TR), 2500 ms; echo time (TE), 60 ms; averages, 3; field of view, 2.65 cm; acquisition matrix, 256 × 256; slice thickness, 1.50 mm; number of slices, 15]. The *in vivo* spectroscopy protocol acquired two 4 × 4 × 4 mm voxels in the hippocampal area, using a point-resolved spatially spectroscopy (Bottomley, 1987) protocol, combined with VAPOR water suppression (Tkac et al., 1999) (TR, 3000 ms; TE, 35 ms; averages, 128). The lesion area was calculated from T_2-weighted images using image analySIS software (Soft Imaging System). Lesion volume was estimated from the summation of areas of hyperintensity on each slice, multiplied by slice thickness. Average lesion volume was calculated for each treatment.

Immunohistochemistry. At different times after stereotaxic injection, the animals were anesthetized and perfused transcardially with 4% paraformaldehyde solution. The brains were removed, postfixed in the same solution at 4°C overnight, cryoprotected in the paraformaldehyde solution containing 30% sucrose, frozen, and 30 μm coronal sections were obtained in a cryostat. Free-floating sections were processed for cresyl violet (Nissl stain) or immunohistochemistry using the diaminobenzidine method or double-immunofluorescence analysis. For the diaminobenzidine method, floating sections were immersed for 15 min in 3% H_2O_2 to inactivate endogenous peroxidase, and then blocked for 2 h at room temperature (RT) in 5% normal goat serum (NGS; Vector Laboratories Burlingame, CA) in PBS, containing 4% bovine serum albumin, 0.1 M lysine, and 0.1% Triton X-100. Afterward, the sections were incubated overnight with the corresponding primary antibodies. After several rinses, sections were incubated for 1 h with a biotinylated secondary antibody. Finally, the sections were processed after the avidin-biotin protocol (Vectastain ABC kit; Vector Laboratories). Tissues were mounted onto gelatin-coated slides and were let to dry. Finally, the slides were dehydrated, cleared in xylene, and mounted with DePeX (Serva, Heidelberg, Germany). The slides were examined with a Zeiss (Oberkochen, Germany) Axiophot microscope, equipped with an Olympus Optical (Tokyo, Japan) DP-50 digital camera, and a Leica (Nussloch, Germany) MZ6 modular stereomicroscope. Neuronal integrity was assessed by counting the percentage of Nissl-positive cells in the CA3 region of the hippocampus in five independent well defined high-magnification (400×) fields per animal using a computer-assisted image analySIS software (Soft Imaging System). The extent of microgliosis was quantified by counting the number of OX-42-positive cells in five independent well defined high-magnification (400×) fields per animal, as described above. To evaluate astrogliosis, two different parameters were quantified: number of activated cells, based on the calculation of highly immunostained cell body profiles, and immunosignal intensity, based on the measurement of optical density. Individual cell bodies were manually traced, and their mean staining intensity was normalized against the background of the respective section, defined as tissue devoid of specific immunostaining. The procedure resulted in arbitrary values on a scale from 1 (background staining) to 256.

For the double-immunofluorescence, the protocol was similar to the one described above with some modifications. Briefly, the floating sections were blocked for 1 h in PBS containing 0.25% Triton X-100 and 3% NGS and incubated overnight with the corresponding primary antibodies. Then, AlexaFluor 647 and AlexaFluor 488 secondary antibodies were added for 1 h at RT. Finally, the tissue was mounted with mowiol and the sections were examined as described for immunocytochemistry. The sequential mode was used to acquire fluorescence images to avoid any interference from overlapping fluorescence. The images were obtained using a series of 0.5-μm (depth)-spaced cell fluorescent slices (*z*-axis).

Statistical determinations. The data shown are the means ± SD of at least three independent experiments. Statistical comparisons for significance between cells with different treatments were performed using the Student's test, with $p \leq 0.05$. ANOVA was used to analyze the data of Figures 2–6.

Results

NP031112 inhibits glutamate-induced glial activation and protects cortical neurons from cell death *in vitro*

We first analyzed whether NP031112 affected the glutamate-induced expression of TNF-α and COX-2, two well known proinflammatory agents, in primary glial cultures. As shown in Figure 1*a*, incubation of both astrocyte and microglial cultures with NP031112 completely abrogated the induction of TNF-α and COX-2 expression after glutamate treatment. These effects of NP031112 were not caused by a loss of cell viability, because the 24 h exposure of astrocyte and microglial cells to this TDZD did not modify cell viability (data not shown).

TDZD compounds were originally described as GSK-3β inhibitors (Martinez et al., 2002a,b) and, more recently, we have shown that their effects on neural cells *in vitro* seems to be mediated through activation of the PPARγ nuclear receptor (Luna-Medina et al., 2005). Therefore, we next tested whether LiCl (an inhibitor of GSK-3β) mimicked the effect of NP031112 and whether the specific PPARγ antagonist GW9662 impaired the action of this TDZD. As shown in Figure 1*a*, treatment of astrocyte and microglial cultures with LiCl did not have a major effect on the increase in TNF-α and COX-2 expression elicited by treatment with glutamate. On the contrary, GW9662 significantly inhibited the blocking effects of NP031112 on TNF-α and COX-2 expression after glutamate treatment of glial cultures, suggesting an involvement of PPARγ in the protective effects of NP031112 against the response of glial cultures to glutamate treatment.

In addition to its blocking effect in glial activation after an excitotoxic insult triggered by glutamate treatment, NP031112 was also able to exert a potent neuroprotective effect on cortical neurons from glutamate-induced excitotoxicity (Fig. 1*b*). Treatment of neuronal cultures with NP031112 resulted in a significant reduction in the number of Annexin-V-positive cells compared with untreated cells. As observed with glial cultures, the PPARγ antagonist GW9662 attenuated the neuroprotective effects of NP031112, whereas the GSK-3β inhibitor LiCl did not have any effect on glutamate-induced cell death or inflammatory response.

To further analyze the possible involvement of PPARγ on NP031112 actions, we next examined whether this compound could activate a reporter construct containing three consensus PPARγ response elements (PPRE-tk-luc) in primary cultures of astrocytes. Figure 1*c* shows a dose–response of the induction by NP031112 of PPRE-tk-luc reporter construct. Half-maximal stimulation was reached at 1.16 μM and maximal stimulation (23-fold) at 25 μM NP031112. No bigger induction was observed with higher doses of the compound. These results further suggest that NP031112 can be acting through a PPARγ-dependent mechanism.

Neuroprotective role of NP031112 after excitotoxic brain injury

Given the *in vitro* anti-inflammatory and neuroprotective effects described above, we then assessed the efficacy of NP031112 in an established focal excitotoxic model *in vivo*. To this end, adult rats received intrahippocampal injections of vehicle, KA, or KA plus NP031112 and were killed at different times after injection. Because brain edema is a common pathological trait of brain injury, we first used MRI to determine the neuroprotective efficacy of NP031112 *in vivo*. T_2-weighted MRI allows the visualization of areas of brain edema as hyperintense regions. Indeed, areas of hyperintensity in T_2-weighted images, reflecting cerebral edema or neurodegeneration, were found in the ipsilateral hemisphere

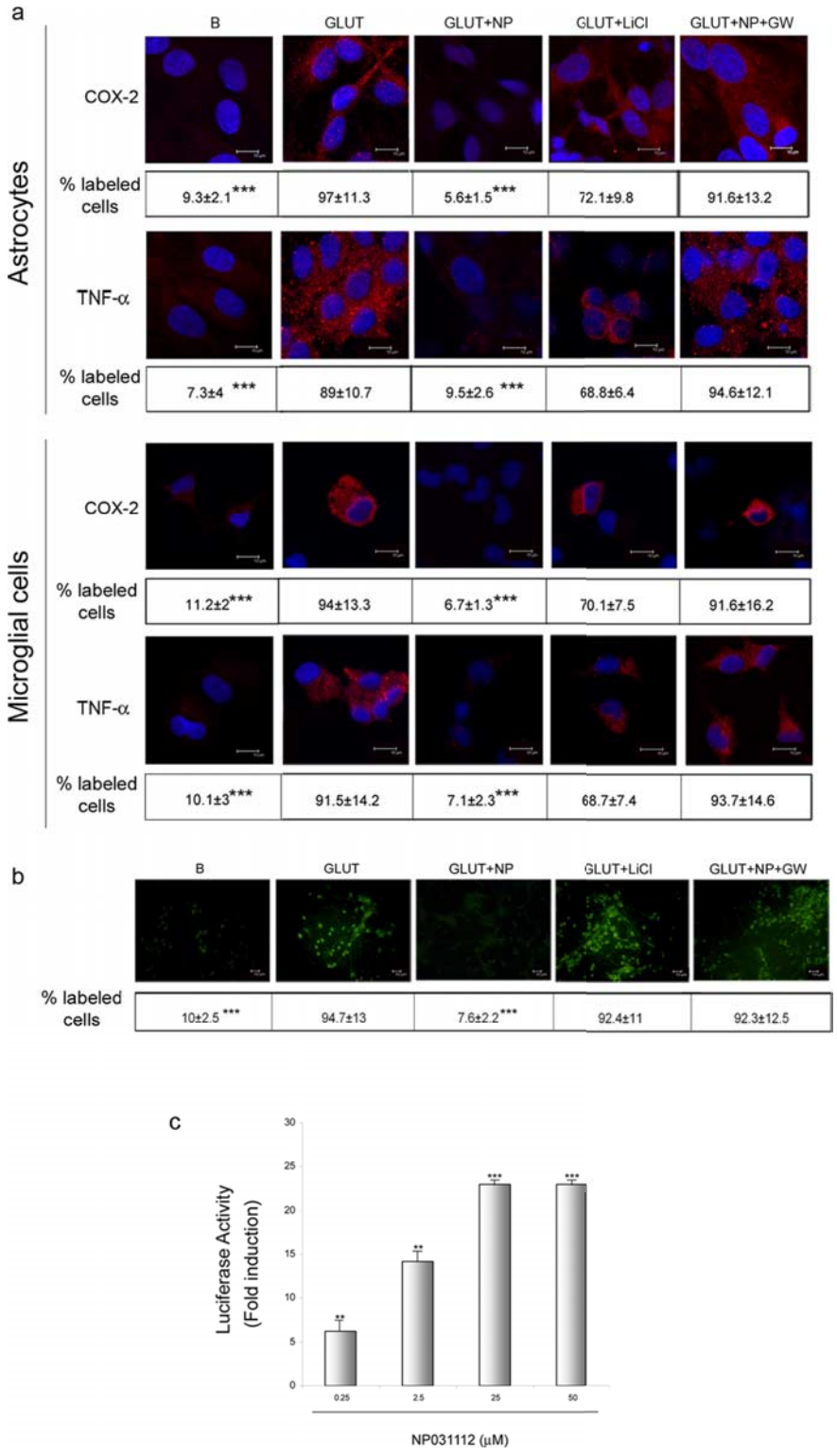

Figure 1. Effects of NP031112 on excitotoxic neural injury *in vitro*. ***a***, Rat primary astrocyte or microglial cultures were treated for 24 h with glutamate (500 μM) in the absence or presence of NP031112 (2.5 μM), and the expression of TNF-α and COX-2 was evaluated by immunofluorescence analysis and confocal microscopy using specific antibodies, as described in Materials and Methods. Some cultures were preincubated 1 h with 30 μM GW9662 before the addition of NP031112 or with 20 mM LiCl before the addition of glutamate. Representative results of three different experiments are shown. Scale bars, 10 μm. Nuclei were counterstained with DAPI (blue). ***b***, Rat primary neuronal cultures were treated for 24 h with glutamate (100 μM) in the absence or presence of NP031112 (2.5 μM). Some cultures were preincubated 1 h with 30 μM GW9662 before the addition of NP031112 or with 20 mM LiCl before the addition of glutamate, and apoptosis was assessed by Annexin-V-FITC staining as described in Materials and Methods. Representative confocal images of three independent experiments are shown. Scale bars, 10 μm. Values in ***a*** and ***b*** represent the mean ± SD from three different experiments and five independent fields ($\geq$ 50 cells/field) per culture. ***$p \leq 0.001$. ***c***, Activation of a PPRE (peroxisome proliferator response element) reporter gene by NP031112. Rat primary astrocytes were transfected with 0.2 μg of the PPRE-tk-luc reporter plasmid, cells were harvested 24 h after treatment with NP031112 at the indicated concentrations, and luciferase activity of cell lysates was determined. Data are expressed relative to the basal values and represent the mean ± SD luciferase activity determined in triplicate in three independent experiments. **$p \leq 0.01$; ***$p \leq 0.001$, versus control nontreated cultures. GLUT, Glutamate; B, basal; GW, GW9662; NP, NP031112.

of KA-injected rats 24 h after KA injection, their hyperintensity becoming further enhanced after 2, 3, and 9 d (Fig. 2*a*). Coinjection of NP031112 resulted in a significant decrease in the hyperintensity of T_2-weighted images, compared with the untreated KA-injected animals. Lesion volume was significantly reduced at all of the times studied after KA injection in the NP031112-treated group. By day 9, the damage in NP031112-treated animals was almost completely absent (98% reduction relative to KA-injected animals) (Fig. 2*b*). Single-voxel proton nuclear magnetic resonance spectra from the hippocampal region of vehicle-, KA, and KA plus NP031112-injected animals are shown in Figure 2*c*. The spectral patterns between the vehicle- and the KA-injected rats were considerably different (Fig. 2*d*). In particular, KA administration was associated with a progressive and significant decrease of *N*-acetyl-aspartate (NAA)/creatine ratio and an increase in lactate/creatine ratio in the ipsilateral hippocampus, suggesting neuronal loss. On the contrary, the spectra observed in NP031112-injected rats were very similar to those found in vehicle-treated animals. These findings indicate that NP031112 protects the brain against KA-induced damage.

The MRI results were further confirmed by histological analysis of the hippocampus. Nissl staining was used to evaluate the extent of neuronal loss in the hippocampus of vehicle-, KA-, and KA plus NP031112-injected rats. A significant preservation of hippocampal cells was found in NP031112-injected rats compared with abundant neuronal loss in the CA1, CA3, and hilus after injection with KA (Fig. 3*a*). Three days after the injection, cell loss in CA1 and CA3 layers was apparent in both groups of animals, although it became more intense in the KA-injected group. Remarkably, by 9 d, both CA1 and CA3 regions of the hippocampus of NP031112-injected rats were almost completely normal, compared with KA-injected cells, which still presented a significant neuronal loss and a disorganization of both regions of the hippocampus.

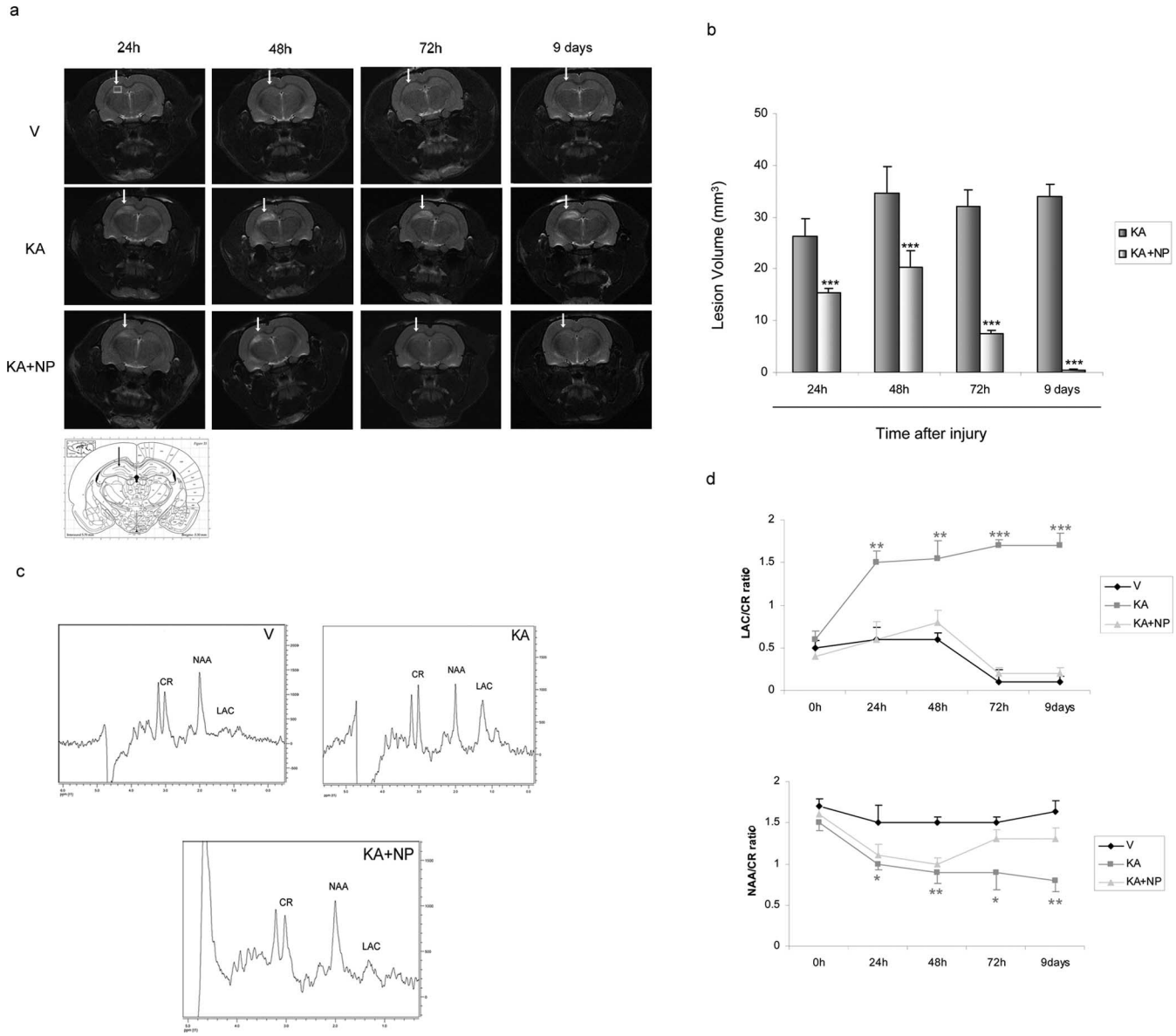

Figure 2. Effect of NP031112 on KA-induced brain edema as detected by MRI. T_2-weighted imaging was performed at 7 tesla as described in Materials and Methods at different times after KA injection. ***a***, Representative coronal images of rat brain injected with vehicle (top), KA (middle), and KA plus NP031112 (bottom). Hyperintensity areas in T_2-weighted MRIs reveal regions of edema after KA injection. Hyperintense areas were reduced in the NP031112-treated rats compared with the KA-injected rats, demonstrating a decrease in the injured area. No hyperintensity was found in the vehicle-injected rats. Arrows indicate the injection site. An anatomic diagram (Paxinos, 1998) showing (arrow) the precise localization of the microinjection in the rat hippocampus is shown. ***b***, Quantitative analysis of total lesion volumes of KA- and KA plus NP031112-injected rats. The volume of the edemas was significantly lower in NP031112-treated rats, compared with KA-treated group at all of the times studied. Values represent the mean ± SD from five different animals and five independent sections per animal. ***$p \leq 0.001$. ***c***, Representative point-resolved spatially spectra acquired from the hippocampal region (white box) with resonances from NAA, lactate (Lac), and creatine (Cr) 9 d after treatment. ***d***, Time course of variation of NAA or lactate values (mean ± SD) in the ipsilateral hemisphere of control-, KA-, and KA plus NP031112-treated animals during 9 d, normalized to the creatine peak. V, Vehicle; NP, NP031112. *$p \leq 0.05$; **$p \leq 0.01$; ***$p \leq 0.001$, versus vehicle-injected animals at each time point.

Quantitative studies (Fig. 3*b*) showed a decrease of 85, 96, and 94%, compared with the vehicle-injected rats, in the number of neurons in the CA3 subfield of the hippocampus 1, 3, and 9 d, respectively, after KA injection. In contrast, in the NP031112-treated group, only a moderate decrease (47%) in cell number was observed 3 d after KA injection. These results extend the observations made *in vitro* and suggest that treatment of KA-injected animals with NP031112 results in an almost complete recovery of the regions more affected by the injury.

One of the events that take place in the hippocampus after excitotoxic injury is the sequential activation of microglia and astroglia. Concerning astrogliosis, resting astrocytes were distributed mostly in the stratum lacunosum-moleculare layer of the hippocampus (LMol) of vehicle-injected animals (Fig. 4*a*). Twenty-four hours after KA injection, the highest GFAP immunoreactive signal intensity was not only observed in the LMol but also in the hilus of the dentate gyrus (data not shown). Nine days after injury, a dramatic increased in GFAP immunoreactivity was detected in all regions of the hippocampus (Fig. 4*a*). This strong astrogliosis was completely absent in the animals treated with NP031112, and the pattern of GFAP immunostaining in these animals was indistinguishable from that of control animals.

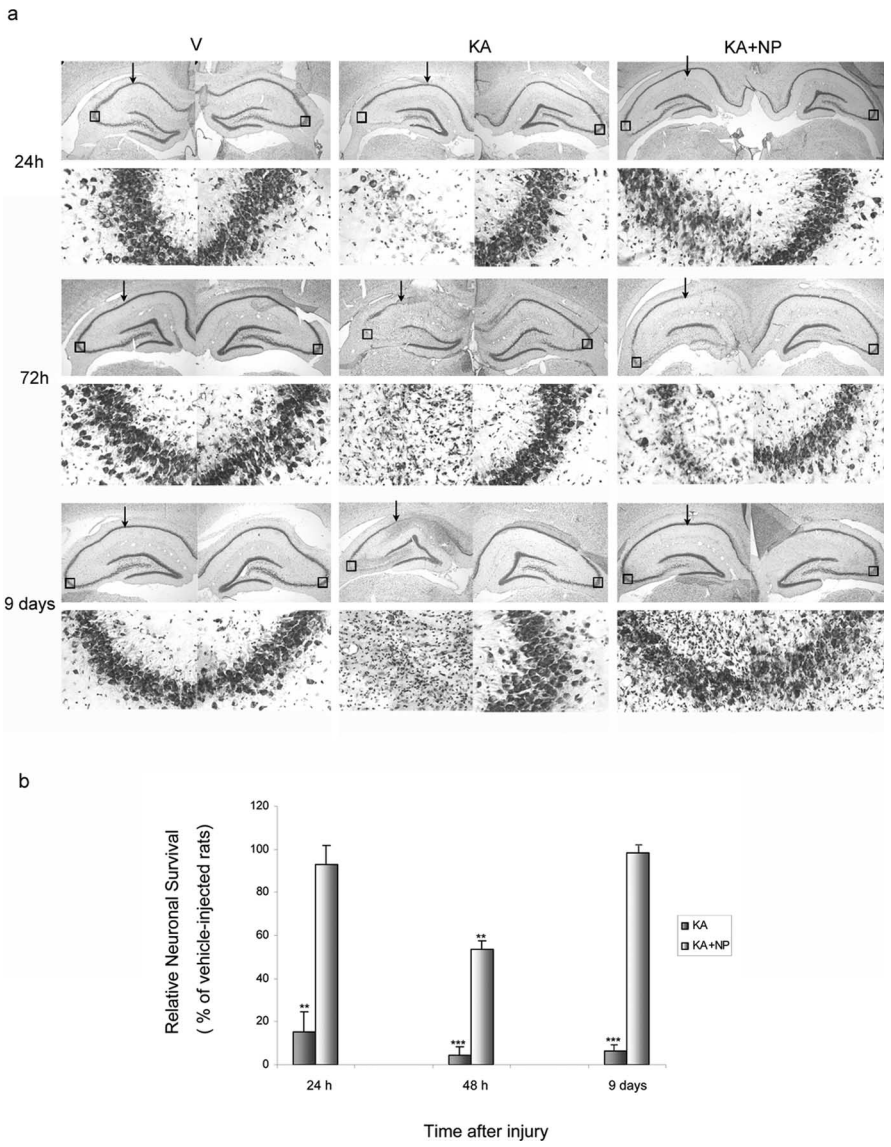

Figure 3. Neuroprotective effects of NP031112 on KA-induced excitotoxicity. ***a***, Rats were injected with saline, KA, or KA plus NP031112 and killed at different times after injection. Neuronal cell loss was assessed in coronal brain sections, using a Nissl stain. Arrows indicate the injection site. Insets, 400× magnifications of Nissl-stained CA3 cells (boxed areas). No apparent cell loss was observed in control animals. Three days after KA, cell loss was apparent on the CA3 and CA1 subfields of the hippocampus in both KA and KA plus NP031112-injected rats. By day 9, cell loss was more prominent in KA-injected animals, whereas animals treated with NP031112 showed no cell loss. V, Vehicle; NP, NP031112. ***b***, The extent of neuronal damage in the CA3 area of the hippocampus was quantified as described in Materials and Methods. Data were normalized against the mean values given by vehicle-injected rats. Values represent the mean ± SD from five different animals and five independent sections per animal. $^{**}p \leq 0.01$; $^{***}p \leq 0.001$, versus vehicle-injected animals at each time point.

Quantification of the data revealed a 6.7- and 2.2-fold decrease in both the number of strongly GFAP$^+$ astrocytes and staining intensity, respectively, in the NP031112-treated animals, compared with the KA-injected group (Fig. 4*b*). Microglial activation in the contralateral hippocampus of kainic-injected rats, as well as in the hippocampus of vehicle-injected animals, was at almost undetectable levels in all regions of the hippocampus (Fig. 4*c*). After KA injection, numerous reactive microglial cells appeared in the ipsilateral part of all regions of the hippocampus. KA treatment resulted in morphological changes in microglial cells, which included swelling of the cell somas and thickening and retraction of the cell processes, two characteristic features of reactive microglia (Jorgensen et al., 1993; Ladeby et al., 2005). Coadministration of NP031112 together with KA completely blocked microglial activation. Quantitative analysis of OX-42$^+$ cells from KA- and KA plus NP031112-injected animals shows a 40-fold decrease in the number of microglial cells 9 d after KA injection in the NP031112 group (Fig. 4*d*).

Double immunofluorescence staining of the rat hippocampus 9 d after injection of KA revealed an induction of the TNF-α cytokine, both in astrocytes and microglial cells (Fig. 4*e*), whereas the expression of this cytokine was almost completely absent in the neuronal population. Injection of KA in the presence of NP031112 significantly decreased TNF-α-positive staining both in astrocytes and microglia.

Subsequently, in view of the *in vitro* results described above, which suggested an implication of the nuclear receptor PPARγ in the action of NP031112, we next examined the possible involvement of this receptor on NP031112 actions *in vivo*. To this end, some rats were injected with the PPARγ antagonist GW9662 together with KA and NP031112 and killed 24 h later for histological evaluation. As expected, KA injection induced a substantial loss of hippocampal CA3 neurons and, once more, NP031112 treatment afforded robust neuroprotection (Fig. 5*a*,*c*). The PPARγ antagonist GW9662 alone did not modify the number of surviving neurons in vehicle-injected rats but abrogated NP031112-elicited neuroprotection. These findings suggest that NP031112 acts via activation of PPARγ to elicit protection of hippocampal neurons. Treatment of rats with GW9662 also inhibited the blocking effects of NP031112 on activation of microglia in the hippocampus, as shown in Figure 5, *b* and *d*. Overall, these findings indicate that NP031112 acts via PPARγ to protect hippocampal neurons from KA-induced cell death and inflammation. Next, we analyzed the neuroprotective effect of the GSK-3β inhibitor LiCl. For this purpose, two additional groups of rats were injected either with KA or with KA plus LiCl, and the number of CA3 neurons and activated microglial cells were determined in the hippocampus 24 h later. As expected, LiCl alone does not alter any of the parameters analyzed (data not shown). In contrast, LiCl administration caused a moderate neuroprotective effect against KA-induced injury (Fig. 5*a*,*c*) that was much lower than the one observed in NP031112-treated animals. Correspondingly, the number of OX-42-positive cells was slightly reduced in animals treated with LiCl, compared with the KA-injected group (Fig. 5*b*,*d*). These data further suggest that the effects of NP031112 are mediated mainly through PPARγ activation, although some effects because of its inhibition of GSK-3β cannot be discarded.

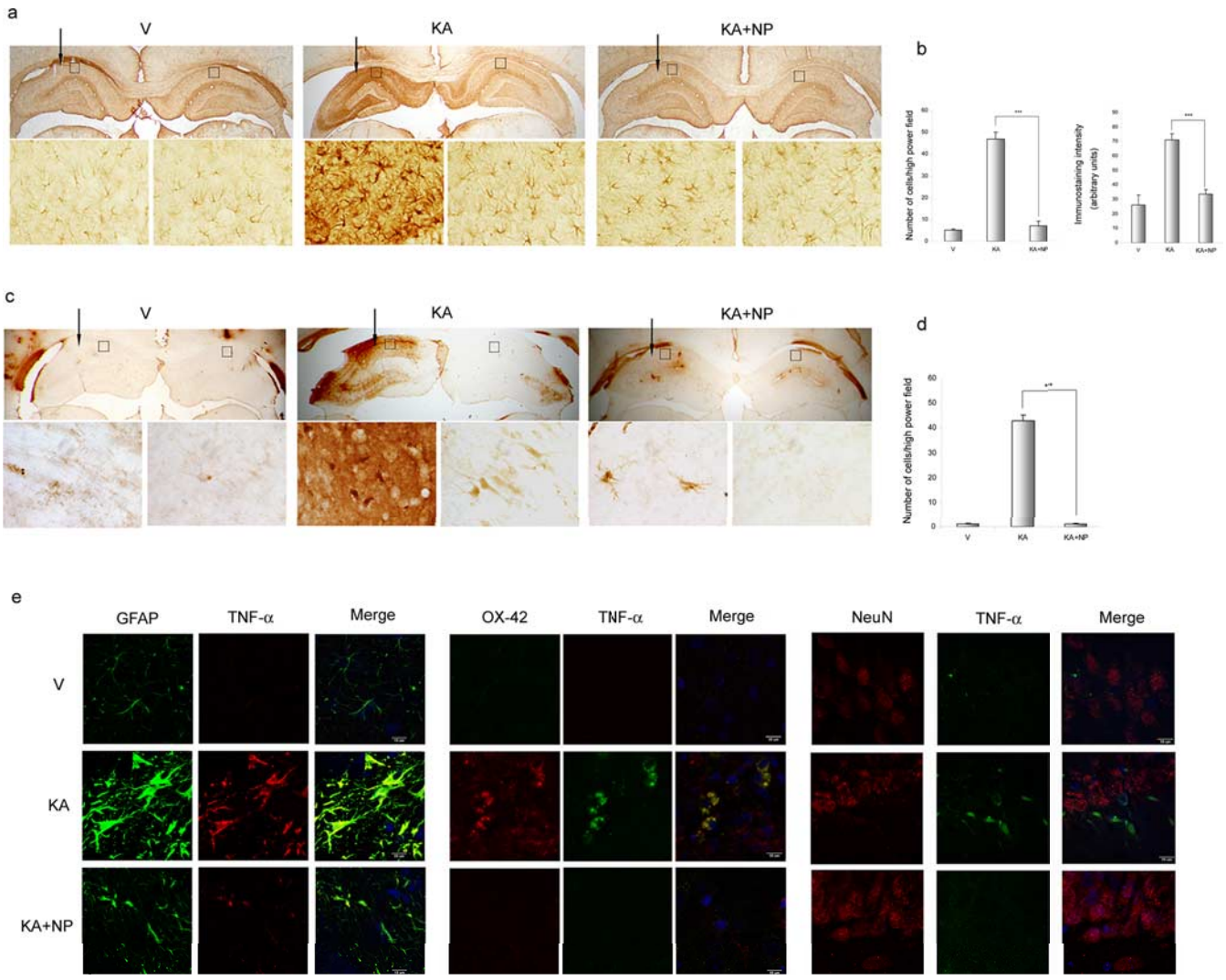

Figure 4. Effect of NP031112 administration on KA-induced glial activation. ***a–d***, GFAP- and OX-42-positive cells in the hippocampus. Rats were injected with saline, KA, or KA plus NP031112 and killed 9 d after injection. Arrows indicate the injection site. Coronal sections (30 μm) were stained with mouse monoclonal antibodies directed against either GFAP (***a***) or cd11b (OX-42; ***c***) to detect astrocytes or microglial cells, respectively, as described in Materials and Methods. Insets, 400× magnifications of GFAP- and OX-42-stained cells (boxed regions). A significant increase in gliosis is observed after KA injection, which is prevented in the animals treated with NP031112. ***b***, Quantification of the number of reactive astrocytes and their mean immunostaining intensity evaluated in the molecular layer of the hippocampus. Values represent the mean ± SD from five different animals and five independent sections per animal. $^{***}p \leq 0.001$. ***d***, Quantification of the number of reactive microglial cells analyzed in the molecular layer of the hippocampus. Values represent the mean ± SD from five different animals and five independent sections per animal. $^{***}p \leq 0.001$. ***e***, Induction of TNF-α in astrocytes, microglia, and neurons after KA injection is abrogated by NP031112. Coronal sections were double stained with a polyclonal antibody directed against TNF-α and with mouse monoclonal antibodies directed against NeuN, GFAP, or cd11b (OX-42) and examined by confocal microscopy. Photomicrographs showing representative CA3 fields for each group are shown. Scale bars, 10 μm. DAPI was used as a counterstain.

Susceptibility of NP031112-treated rats to KA-induced seizures

KA administered intraperitoneally at a dose of 10 mg/kg caused the entrance in SE in 80% of rats (Fig. 6*a*). Intragastrical administration of NP031112 1 h before KA injection had no effect on the percentage of rats reaching SE (80%), and only a small delay in the entrance of SE could be observed [126 ± 8.9 min in the NP031112-treated rats, compared with 104 ± 5.5 min ($p < 0.01$) in the control animals]. During the latency period, KA-injected rats displayed approximately the same number of WDS than NP031112-treated rats (Fig. 6*b*). We next evaluated neuronal damage in coronal brain sections of surviving rats 72 h after KA administration (Fig. 6*c*). Low-power images of the Nissl-stained hippocampus revealed extensive damage, evident in the CA1 and CA3 regions, which was substantially attenuated by orally administered NP031112. Together, these results suggest that the neuroprotective effects of NP031112 cannot be attributed to an anticonvulsant action.

Discussion

Collectively, our data clearly show that administration of the TDZD NP031112 in a rat model of excitotoxicity markedly induces neuroprotection and attenuates the production of proinflammatory cytokines and activation of astrocytes and microglial cells. Additionally, NP031112 actions appear to be mediated mainly through activation of the nuclear receptor PPARγ within the hippocampal cells, although part of its effects could be attributable to its inhibitory action of GSK-3β activity, because a modest neuroprotective effect of LiCl was observed *in vivo*. These results suggest that NP031112 can be a therapeutic agent in neu-

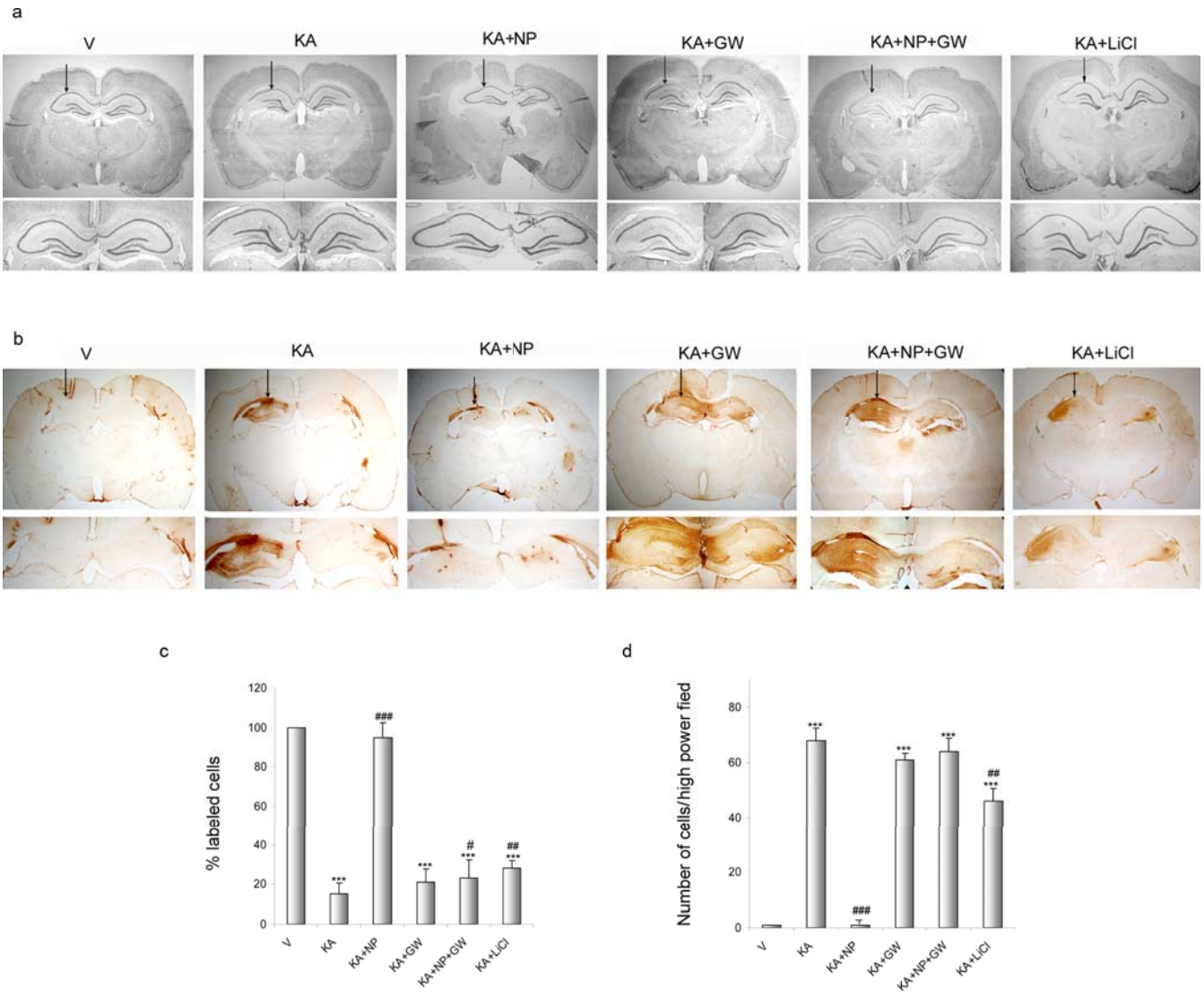

Figure 5. The PPARγ antagonist GW9662 abolishes NP031112 neuroprotection after KA injection. Rats were injected with saline (V), KA, KA plus NP031112 (NP), or KA plus LiCl and killed 24 h after injection. Some animals were also injected with 0.7 μg GW9662 (GW). Arrows indicate the injection site. ***a***, Neuronal cell loss was assessed in coronal brain sections using a Nissl stain. NP031112 treatment affords robust neuroprotection in the CA3 regions of the hippocampus 24 h after KA injection, whereas LiCl administration only had a small effect on the decrease in CA3 neurons elicited by KA injection. Injection of the PPARγ antagonist GW9662 after NP031112 and KA treatment abolished this neuroprotection. Treatment with the PPARγ antagonist did not affect the number of surviving neurons in any of the other treatment groups. ***b***, Gliosis was assessed in similar brain sections by staining with a mouse monoclonal antibody directed against cd11b (OX-42) to detect microglial cells. Treatment with GW9662 blocked the anti-inflammatory effect of NP031112. ***c***, Quantification of neuronal damage in the CA3 area of the hippocampus. ***d***, Quantification of the number of reactive microglial cells analyzed in the molecular layer of the hippocampus. Values represent the mean ± SD from five different animals and five independent sections per animal. $^{***}p \leq 0.001$ versus vehicle-injected animals; $^{\#}p \leq 0.05$; $^{\#\#}p \leq 0.01$; $^{\#\#\#}p \leq 0.001$ versus KA-injected animals.

rodegenerative disorders in which excitotoxic neuronal cell death and inflammation processes are involved.

We initially analyzed the anti-inflammatory and neuroprotective effects of NP031112 in an *in vitro* model of excitotoxicity, using primary cultures of astrocytes, microglia, and neurons. We show that NP031112 attenuates glutamate-induced excitotoxic glial activation and neuronal damage. NP031112 appears to be an extremely potent agent, because its effects were achieved at much lower concentrations than the two other TDZD compounds previously examined (Luna-Medina et al., 2005). The mechanism of action of all of these TDZD compounds in the neuroprotection experiments *in vitro* seems to be the activation of the nuclear receptor PPARγ, as suggested by the activation of a reporter gene containing a PPARγ response element and the blocking effect of the PPARγ antagonist GW9662 of their anti-inflammatory and neuroprotective actions. Although the TDZD compounds have been identified previously as ATP-noncompetitive inhibitors of GSK-3β activity (Martinez et al., 2002a,b), and it has been shown that inactivation of GSK-3β protects against KA-induced neurotoxicity *in vivo* (Goodenough et al., 2004), it is unlikely that a direct inhibition of this enzyme by TDZDs represents the major mechanism for their anti-inflammatory and neuroprotective effects *in vitro*, because these effects were not entirely mimicked by LiCl, a selective inhibitor of GSK-3β activity.

In the present study, we focused on the study of the anti-inflammatory and neuroprotective effects of NP031112, in an *in vivo* experimental model of excitotoxicity. Excitotoxicity is a concept of neuronal cell death caused by overactivation of excitatory

amino-acid receptors and it is thought to represent a common biochemical pathway, which plays an important role in the pathogenesis of many acute and chronic neurodegenerative disorders such as stroke, traumatic brain injury, amyotrophic lateral sclerosis, and Parkinson's, Huntington's, and Alzheimer's diseases (Dirnagl et al., 1999; Doble, 1999; Nicotera et al., 1999). Also, and as pointed out in the Introduction, one of the events associated to many brain neurodegenerative diseases is an inflammation response, which has long been linked to neuronal cell death (Barone and Feuerstein, 1999; del Zoppo et al., 2000). Inhibition of this process could then protect against neurodegeneration and expansion of brain injury. This view is further supported by epidemiological data showing that long-term treatment with NSAIDs may protect against Alzheimer's and Parkinson's diseases (Chen et al., 2003; Hald and Lotharius, 2005; Townsend and Pratico, 2005).

Here, we show that NP031112 has a potent anti-inflammatory effect *in vivo* after KA-induced excitotoxicity. In the MRI studies, we analyzed the effect of NP031112 on the inflammatory process induced by KA at different times after injection. NP031112 treatment reduced the extension and intensity of the inflammation in the hippocampus and completely abrogated the reduction in NAA, which has been widely used as an indicator of brain pathology and of disease progression (Demougeot et al., 2004). NP031112 also reduced the increase in lactate observed in the KA-injected animals. Increases of lactate concentration are often related to pathologies, which enhance the anaerobic pathway (Choi et al., 2005; Moller et al., 2005; Williams et al., 2005). In agreement with these findings, our results also demonstrate that NP031112 significantly reduces other inflammatory parameters, such as the accumulation of reactive astrocytes and microglia in the hippocampus. The underlying mechanisms of this anti-inflammatory effect of NP031112 may involve the suppression of certain cytokines [e.g., TNF-α, because it has been shown that the production of this cytokine can predispose to local inflammation and contribute to brain injury initiation and progression (Chao et al., 1995; Rizzi et al., 2003)]. Indeed, our results show that administration of NP031112 significantly decreased TNF-α levels *in vitro* and in astrocytes and microglial cells *in vivo* after KA injection. Together, these data clearly indicate that NP031112 plays an important role in neuroinflammation and it is able to efficiently block this process when locally injected at very low concentrations in the damaged hippocampus.

In addition to this potent anti-inflammatory action of NP031112, the administration of this compound also causes a significant delay of neuronal cell loss in the CA1 and CA3 subregions of the hippocampus. Twenty-four hours after intrahippocampal injection, KA causes a prominent decrease in the number of neurons in the CA3 field of the hippocampus, which is blocked by NP031112 administration (Fig. 3). These *in vivo* data, together with the observed neuroprotective action *in vitro* against glutamate-induced neurotoxicity, suggest that, in addition to its anti-inflammatory effects, NP031112 could exert a more direct neuroprotective action. Notably, 9 d after NP031112 injection, both areas of the hippocampus were almost completely recovered. As expected, intraperitoneal injection of KA induced typical behavioral activity and histopathological changes in the hippocampus (loss of pyramidal cells in CA1 and CA3 areas). NP031112 acute administration had no effect on the behavioral seizures; however, it inhibited hippocampal damage, suggesting that the neuroprotective effects of this compound are not exerted through an inhibition of seizure activity.

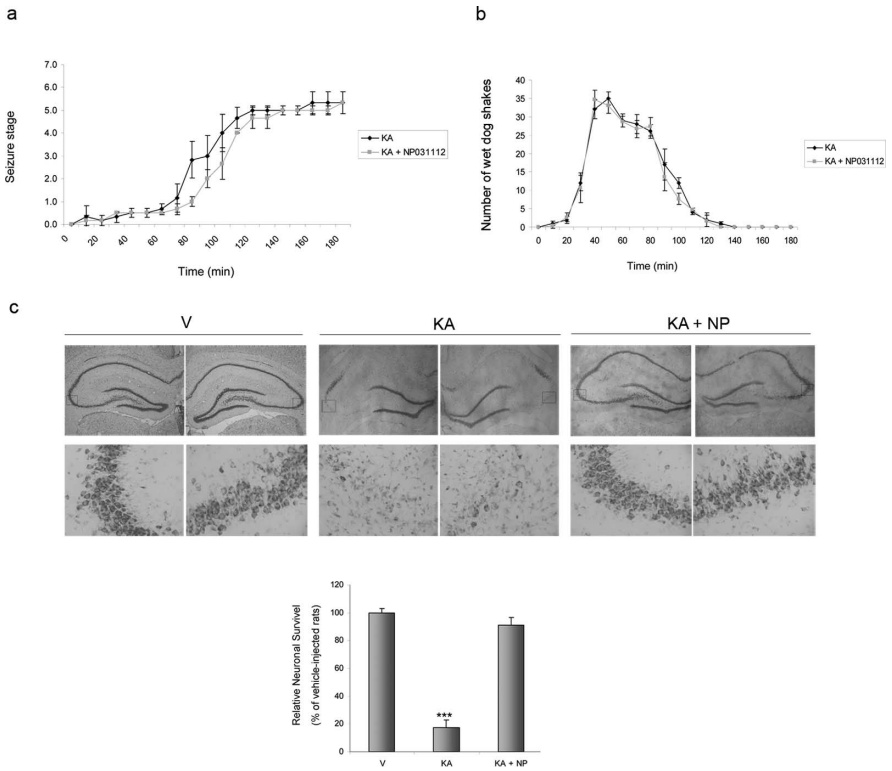

Figure 6. Effect of NP031112 administered orally on behavioral activity and neuronal loss after injection of KA. ***a***, ***b***, NP031112 (50 mg/kg) was administered intragastrically 1 h before intraperitoneal injection of KA (10 mg/kg), and the behavioral activity was analyzed. NP031112 has no significant effects on behavioral seizures induced by KA. Each value represents the mean ± SEM from at least nine animals. ***c***, The data correspond to animals that entered SE. Animals were treated as in ***a***, and 72 h after KA injections, animals were killed and coronal hippocampal sections were stained with Nissl. NP031112-treated rats exhibited a diminished loss of neurons in the CA1 and CA3 regions, when compared with KA-injected rats. V, Vehicle; NP, NP031112. Values represent the mean ± SD from five different animals and five independent sections per animal. ***$p \leq 0.001$ versus vehicle-injected animals.

Regarding the molecular mechanisms underlying the effects of NP031112, the present data are consistent with PPARγ playing a major role on its action. Our results demonstrate that NP031112 is able to strongly activate a consensus PPARγ response element in primary astrocytes in culture and that blocking this activation with a known PPARγ antagonist results in a prevention of the NP031112 neuroprotective effects *in vitro* as well as *in vivo*. These results, together with the *in vitro* and *in vivo* experiments using the GSK-3β inhibitor LiCl, suggest that, although TDZDs were originally identified as GSK-3β inhibitors, the mechanisms by which NP031112 exerts its neuroprotective and anti-inflammatory effects in excitotoxic injury involve mainly the activation of the nuclear receptor PPARγ. In agreement with these results, an anti-inflammatory and neuroprotective effect has been suggested for other PPARγ agonists (for review, see

Landreth and Heneka, 2001; Townsend and Pratico, 2005). Epidemiological studies have shown that the long-term use of NSAIDs reduces the risk of developing and delays the onset of both Alzheimer's and Parkinson's diseases (Chen et al., 2003). Ibuprofen, an NSAID, reduces microglial activation induced by β-amyloid peptide (Combs et al., 2000) and amyloid plaque load in an animal model of Alzheimer's disease (Yan et al., 2003). PPARγ agonists of the TZD family, including rosiglitazone, pioglitazone, and troglitazone, have also been shown to have anti-inflammatory and neuroprotective effects (Diab et al., 2002; Camacho et al., 2004; Kiaei et al., 2005). Additionally, 15-deoxy-$\Delta^{12,14}$-prostaglandin J_2, the most potent natural ligand of PPARγ, reduces *in vitro* microglial activation (Bernardo et al., 2000) and T cell activity in an animal model of human multiple sclerosis (Diab et al., 2002). More recently, a protective role of PPARγ agonists against ischemic brain injury has been demonstrated (Shimazu et al., 2005; Sundararajan et al., 2005; Zhao et al., 2006).

In conclusion, we show that one single intrahippocampal injection of the TDZD compound NP031112 affords robust neuroprotection of hippocampal neurons against excitotoxic injury in adult rats. Our findings also suggest that the nuclear receptor PPARγ participates in this NP031112-induced neuroprotection. Hence, NP031112 may hold promise for preventing permanent neurological impairment in adults after a brain injury.

References

Barone FC, Feuerstein GZ (1999) Inflammatory mediators and stroke: new opportunities for novel therapeutics. J Cereb Blood Flow Metab 19:819–834.

Ben-Ari Y, Tremblay E, Ottersen OP (1980) Injections of kainic acid into the amygdaloid complex of the rat: an electrographic, clinical and histological study in relation to the pathology of epilepsy. Neuroscience 5:515–528.

Bernardo A, Levi G, Minghetti L (2000) Role of the peroxisome proliferator-activated receptor-gamma (PPAR-gamma) and its natural ligand 15-deoxy-Delta12, 14-prostaglandin J2 in the regulation of microglial functions. Eur J Neurosci 12:2215–2223.

Bottomley PA (1987) Spatial localization in NMR spectroscopy in vivo. Ann NY Acad Sci 508:333–348.

Camacho IE, Serneels L, Spittaels K, Merchiers P, Dominguez D, De Strooper B (2004) Peroxisome-proliferator-activated receptor γ induces a clearance mechanism for the amyloid-β peptide. J Neurosci 24:10908–10917.

Chao CC, Hu S, Ehrlich L, Peterson PK (1995) Interleukin-1 and tumor necrosis factor-alpha synergistically mediate neurotoxicity: involvement of nitric oxide and of N-methyl-D-aspartate receptors. Brain Behav Immun 9:355–365.

Chen H, Zhang SM, Hernan MA, Schwarzschild MA, Willett WC, Colditz GA, Speizer FE, Ascherio A (2003) Nonsteroidal anti-inflammatory drugs and the risk of Parkinson disease. Arch Neurol 60:1059–1064.

Choi CB, Kim HY, Han DY, Kang YW, Han YM, Jeun SS, Choe BY (2005) In vivo 1H MR spectroscopic findings in traumatic contusion of ICR mouse brain induced by fluid percussion injury. Eur J Radiol 55:96–101.

Choi DW (1988) Glutamate neurotoxicity and diseases of the nervous system. Neuron 1:623–634.

Combs CK, Johnson DE, Karlo JC, Cannady SB, Landreth GE (2000) Inflammatory mechanisms in Alzheimer's disease: inhibition of β-amyloid-stimulated proinflammatory responses and neurotoxicity by PPARγ agonists. J Neurosci 20:558–567.

Coyle JT (1983) Neurotoxic action of kainic acid. J Neurochem 41:1–11.

del Zoppo G, Ginis I, Hallenbeck JM, Iadecola C, Wang X, Feuerstein GZ (2000) Inflammation and stroke: putative role for cytokines, adhesion molecules and iNOS in brain response to ischemia. Brain Pathol 10:95–112.

Demougeot C, Marie C, Giroud M, Beley A (2004) N-acetylaspartate: a literature review of animal research on brain ischaemia. J Neurochem 90:776–783.

Diab A, Deng C, Smith JD, Hussain RZ, Phanavanh B, Lovett-Racke AE, Drew PD, Racke MK (2002) Peroxisome proliferator-activated receptor-gamma agonist 15-deoxy-δ(12,14)-prostaglandin J(2) ameliorates experimental autoimmune encephalomyelitis. J Immunol 168:2508–2515.

Dirnagl U, Iadecola C, Moskowitz MA (1999) Pathobiology of ischaemic stroke: an integrated view. Trends Neurosci 22:391–397.

Doble A (1999) The role of excitotoxicity in neurodegenerative disease: implications for therapy. Pharmacol Ther 81:163–221.

Goodenough S, Conrad S, Skutella T, Behl C (2004) Inactivation of glycogen synthase kinase-3beta protects against kainic acid-induced neurotoxicity in vivo. Brain Res 1026:116–125.

Hald A, Lotharius J (2005) Oxidative stress and inflammation in Parkinson's disease: is there a causal link? Exp Neurol 193:279–290.

Hennig J, Nauerth A, Friedburg H (1986) RARE imaging: a fast imaging method for clinical MR. Magn Reson Med 3:823–833.

Jorgensen MB, Finsen BR, Jensen MB, Castellano B, Diemer NH, Zimmer J (1993) Microglial and astroglial reactions to ischemic and kainic acid-induced lesions of the adult rat hippocampus. Exp Neurol 120:70–88.

Kiaei M, Kipiani K, Chen J, Calingasan NY, Beal MF (2005) Peroxisome proliferator-activated receptor-gamma agonist extends survival in transgenic mouse model of amyotrophic lateral sclerosis. Exp Neurol 191:331–336.

Kielian T, Drew PD (2003) Effects of peroxisome proliferator-activated receptor-gamma agonists on central nervous system inflammation. J Neurosci Res 71:315–325.

Ladeby R, Wirenfeldt M, Garcia-Ovejero D, Fenger C, Dissing-Olesen L, Dalmau I, Finsen B (2005) Microglial cell population dynamics in the injured adult central nervous system. Brain Res Brain Res Rev 48:196–206.

Landreth GE, Heneka MT (2001) Anti-inflammatory actions of peroxisome proliferator-activated receptor gamma agonists in Alzheimer's disease. Neurobiol Aging 22:937–944.

Lipton SA, Nicotera P (1998) Calcium, free radicals and excitotoxins in neuronal apoptosis. Cell Calcium 23:165–171.

Luna-Medina R, Cortes-Canteli M, Alonso M, Santos A, Martinez A, Perez-Castillo A (2005) Regulation of inflammatory response in neural cells in vitro by thiadiazolidinones derivatives through peroxisome proliferator-activated receptor {gamma} activation. J Biol Chem 280:21453–21462.

Martinez A, Castro A, Dorronsoro I, Alonso M (2002a) GSK-3 inhibitors as promising drugs for the treatment of Alzheimer disease, cancer, diabetes, and inflammation. Med Res Rev 22:373–384.

Martinez A, Alonso M, Castro A, Perez C, Moreno FJ (2002b) First non-ATP competitive glycogen synthase kinase 3 beta (GSK-3beta) inhibitors: thiadiazolidinones (TDZD) as potential drugs for the treatment of Alzheimer's disease. J Med Chem 45:1292–1299.

Moller HE, Kurlemann G, Putzler M, Wiedermann D, Hilbich T, Fiedler B (2005) Magnetic resonance spectroscopy in patients with MELAS. J Neurol Sci 229–230:131–139.

Nicotera P, Leist M, Manzo L (1999) Neuronal cell death: a demise with different shapes. Trends Pharmacol Sci 20:46–51.

Paxinos G, Watson C (1998) The rat brain in stereotaxic coordinates, Ed 4. San Diego: Academic.

Petrova TV, Akama KT, Van Eldik LJ (1999) Cyclopentenone prostaglandins suppress activation of microglia: down-regulation of inducible nitric-oxide synthase by 15-deoxy-Delta12,14-prostaglandin J2. Proc Natl Acad Sci USA 96:4668–4673.

Racine RJ (1972) Modification of seizure activity by electrical stimulation. II. Motor seizure. Electroencephalogr Clin Neurophysiol 32:281–294.

Ricote M, Huang JT, Welch JS, Glass CK (1999) The peroxisome proliferator-activated receptor (PPARgamma) as a regulator of monocyte/macrophage function. J Leukoc Biol 66:733–739.

Rizzi M, Perego C, Aliprandi M, Richichi C, Ravizza T, Colella D, Veliskova J, Moshe SL, De Simoni MG, Vezzani A (2003) Glia activation and cytokine increase in rat hippocampus by kainic acid-induced status epilepticus during postnatal development. Neurobiol Dis 14:494–503.

Shimazu T, Inoue I, Araki N, Asano Y, Sawada M, Furuya D, Nagoya H, Greenberg JH (2005) A peroxisome proliferator-activated receptor-gamma agonist reduces infarct size in transient but not in permanent ischemia. Stroke 36:353–359.

Sperk G (1994) Kainic acid seizures in the rat. Prog Neurobiol 42:1–32.

Sperk G, Lassmann H, Baran H, Seitelberger F, Hornykiewicz O (1985) Kainic acid-induced seizures: dose-relationship of behavioural, neurochemical and histopathological changes. Brain Res 338:289–295.

Sundararajan S, Gamboa JL, Victor NA, Wanderi EW, Lust WD, Landreth GE

(2005) Peroxisome proliferator-activated receptor-gamma ligands reduce inflammation and infarction size in transient focal ischemia. Neuroscience 130:685–696.

Tauck DL, Nadler JV (1985) Evidence of functional mossy fiber sprouting in hippocampal formation of kainic acid-treated rats. J Neurosci 5:1016–1022.

Tkac I, Starcuk Z, Choi IY, Gruetter R (1999) In vivo 1H NMR spectroscopy of rat brain at 1 ms echo time. Magn Reson Med 41:649–656.

Townsend KP, Pratico D (2005) Novel therapeutic opportunities for Alzheimer's disease: focus on nonsteroidal anti-inflammatory drugs. FASEB J 19:1592–1601.

Wang Q, Yu S, Simonyi A, Sun GY, Sun AY (2005) Kainic acid-mediated excitotoxicity as a model for neurodegeneration. Mol Neurobiol 31:3–16.

Williams K, Westmoreland S, Greco J, Ratai E, Lentz M, Kim WK, Fuller RA, Kim JP, Autissier P, Sehgal PK, Schinazi RF, Bischofberger N, Piatak M, Lifson JD, Masliah E, Gonzalez RG (2005) Magnetic resonance spectroscopy reveals that activated monocytes contribute to neuronal injury in SIV neuroAIDS. J Clin Invest 115:2534–2545.

Yan Q, Zhang J, Liu H, Babu-Khan S, Vassar R, Biere AL, Citron M, Landreth G (2003) Anti-inflammatory drug therapy alters β-amyloid processing and deposition in an animal model of Alzheimer's disease. J Neurosci 23:7504–7509.

Zhao Y, Patzer A, Herdegen T, Gohlke P, Culman J (2006) Activation of cerebral peroxisome proliferator-activated receptors gamma promotes neuroprotection by attenuation of neuronal cyclooxygenase-2 overexpression after focal cerebral ischemia in rats. FASEB J 20:1162–1175.